Catalytically active inclusion bodies: A novel enzyme immobilization method for biocatalysis

Inaugural-Dissertation

zur Erlangung des Doktorgrades
der Mathematisch-Naturwissenschaftlichen Fakultät
der Heinrich-Heine-Universität Düsseldorf

vorgelegt von

Ramona Kloß
aus Görlitz

Jülich, Juni 2018

aus dem Institut für Bio- und Geowissenschaften 1:
Biotechnologie des Forschungszentrum Jülich GmbH
der Heinrich-Heine Universität Düsseldorf

Gedruckt mit der Genehmigung der
Mathematisch-Naturwissenschaftlichen Fakultät der
Heinrich-Heine-Universität Düsseldorf

Referent: Prof. Dr. Martina Pohl
Korreferent: Prof. Dr. Karl-Erich Jäger
Tag der mündlichen Prüfung: 12.07.2018

Abstract

In the last decades, biocatalysis gained in importance for the production of valuable fine chemicals and pharmaceuticals due to high regio-, chemo-, and stereoselectivity. The demands on biocatalysts for application in organic synthesis and technical processes are high in terms of handling, productivity and stability. These requirements can be fulfilled by immobilization of the enzyme, which furthermore enables the easy separation and recycling of the biocatalyst. Many immobilization methods require previous (chromatographic) enzyme purification steps followed by additional steps e.g. to fix the enzyme on the surface of a carrier. As generic methods are missing, a case-to-case optimization is necessary, making immobilization methods often time-consuming and laborious. As an alternative, an easy, carrier-free and generic method would be desirable.

In this thesis catalytically active inclusion bodies (CatIBs) were investigated as an alternative carrier-free and cell-free immobilization strategy and tested for the application in biocatalysis. Since enzyme production is combined with immobilization directly in the bacterial production cell, only few steps are necessary to obtain the lyophilized biocatalyst. The CatIBs were created by fusion of the respective target enzyme to aggregation-inducing tags containing an aggregation-prone part. Two of these tags, forming a coiled-coil domain, were comparatively studied, namely one from the cell-surface protein tetrabrachion (TDoT) from hyperthermophilic archaeon *Staphylothermus marinus* and the 3HAMP domain (Histidine kinases, Adenylyl cyclases, Methyl-accepting chemotaxis proteins (MCPs), and Phosphatases) from *P. aeruginosa* soluble receptor Aer2. The easy production of different CatIBs was enabled by using a modular expression vector and a simple isolation protocol including only cell disruption and one washing step. CatIBs were shown to be generally applicable to a broad spectrum of enzymes of different complexity. In this thesis, the CatIB toolbox was successfully enlarged by two NADPH-dependent alcohol dehydrogenases from *Ralstonia sp.* (*R*ADH) and from *L. brevis* (*Lb*ADH), two thiamine diphosphate (ThDP)-dependent enzymes, benzaldehyde lyase from *P. fluorescens* Biovar I (*Pf*BAL) and benzoyl-formate decarboxylase from *P. putida* (*Pp*BFD), and the pyridoxal 5'-phosphate-dependent constitutive lysine decarboxylase from *E. coli* (*Ec*LDC). The CatIBs produced by fusion to either the TDoT-domain or the 3HAMP-domain differed concerning compactness of the particles, solubility, yield, activity, lipid, and protein content. Their morphology in *E. coli* cells differed between compact-packed or diffuse particles as observed in the microscope in phase-contrast. By means of molecular biological methods, the efficiency to produce CatIBs

could be improved, such as changing the fusion site and using a different coiled-coil domain, which enables the fine-tuning of the CatIB properties for the required application.

Both kinds of CatIBs showed differences in their applicability and stability in biocatalytic reaction systems. CatIBs could be successfully applied in different reactions systems such as (repetitive) batch and a continuously operated enzyme membrane reactor (EMR) in buffer, as well as in monophasic and biphasic aqueous-organic reaction systems. They showed a good reusability and stability under several reaction conditions.

Finally, CatIBs were successfully applicable for the production of high valuable products under technical conditions in culture supernatants of a *C. glutamicum* L-lysine producer strain at L-lysine concentrations of up to 1 M in repetitive batch as well as batch experiments. Furthermore, *Pf*BAL-CatIBs could be used for the carboligation of up to 85 mM benzaldehyde and derivatives in biphasic reaction system as well as for the continuous production of 30 mM (*R*)-2-hydroxy-1-phenylpropanone, a valuable precursor and building block for pharmaceuticals.

Zusammenfassung

In den letzten Jahrzehnten hat die Biokatalyse aufgrund der hohen Regio-, Chemo- und Stereoselektivität an Bedeutung für die Herstellung wertvoller Feinchemikalien und Pharmazeutika gewonnen. Die Anforderungen an Biokatalysatoren für den Einsatz in der organischen Synthese und in technischen Prozessen sind hoch in Bezug auf Handhabung, Produktivität und Stabilität. Durch die Enzymimmobilisierung können diese Anforderungen erfüllt werden, was zudem eine einfache Trennung und Wiederverwertung des Biokatalysators ermöglicht. Viele Immobilisierungsmethoden erfordern vorherige (chromatographische) Enzymreinigungsschritte, gefolgt von zusätzlichen Schritten, z. B. das Enzym auf der Oberfläche eines Trägers zu fixieren. Da generische Methoden fehlen, ist eine individuelle Optimierung notwendig, was die Immobilisierung oft zeit- und arbeitsaufwändig macht. Als Alternative wäre eine einfache, trägerfreie und generische Methode wünschenswert.

In dieser Arbeit wurden katalytisch aktive Einschlusskörper (CatIBs) als alternative träger- und zellfreie Immobilisierungsstrategie untersucht und für den Einsatz in der Biokatalyse getestet. Da die Enzymproduktion mit der Immobilisierung direkt in der bakteriellen Produktionszelle kombiniert wird, sind nur wenige Schritte notwendig, um den lyophilisierten Biokatalysator zu erhalten. Die CatIBs wurden durch Fusion des jeweiligen Ziel-Enzyms mit einem Aggregations-induzierenden Protein erstellt. Zwei dieser *Tags*, die eine *coiled-coil* Domäne bilden, wurden vergleichend untersucht, nämlich das Zelloberflächenprotein Tetrabrachion (TDoT) aus dem hyperthermophilen Archäon *S. marinus* und die 3HAMP-Domäne (Histidin-Kinasen, Adenylyl-Cyclasen, Methyl-akzeptierende Chemotaxis-Proteine (MCPs) und Phosphatasen) des löslichen Rezeptors Aer2 von *P. aeruginosa*. Die einfache Herstellung verschiedener CatIBs wurde durch die Verwendung eines modularen Expressionsvektors und eines einfachen Isolationsprotokolls ermöglicht, das neben dem Zellaufschluss nur einen Waschschritt umfasst. CatIBs erwiesen sich als allgemein anwendbar für ein breites Spektrum von Enzymen unterschiedlicher Komplexität. In dieser Arbeit wurde die CatIB-Toolbox erfolgreich um zwei NADPH-abhängige Alkoholdehydrogenasen aus *Ralstonia sp.* (*R*ADH) und aus *L. brevis* (*Lb*ADH), zwei Thiamindiphosphat (ThDP)-abhängige Enzymen, Benzaldehydlyase aus *P. fluorescens* Biovar I (*Pf*BAL) und Benzoylformiatdecarboxylase aus *P. putida* (*Pp*BFD) und die Pyridoxal-5'-phosphat-abhängige, konstitutive Lysindecarboxylase aus *E. coli* (*Ec*LDC) erweitert. Die durch Fusion zur TDoT-Domäne oder zur 3HAMP-Domäne erzeugten CatIBs unterschieden sich

hinsichtlich Kompaktheit der Partikel, Unlöslichkeit, Ausbeute, Aktivität, Lipid- und Proteingehalt. Ihre Morphologie in *E. coli* Zellen variiert zwischen kompakt gepackten oder diffusen Partikeln, wie im Mikroskop im Phasenkontrast beobachtet wurde. Mit Hilfe molekularbiologischer Methoden konnte die Effizienz bei der Herstellung von CatIBs verbessert werden, z. B. durch Änderung der Fusionsstelle und Verwendung einer anderen *coiled-coil* Domäne, was die Feinanpassung der CatIB-Eigenschaften für die gewünschte Anwendung ermöglicht.

Beide Arten von CatIBs zeigten Unterschiede in ihrer Anwendbarkeit und Stabilität in biokatalytischen Reaktionssystemen. CatIBs konnten erfolgreich in verschiedenen Reaktionssystemen wie (repetitiven) *batch* und einem kontinuierlich betriebenen Enzym-Membranreaktor (EMR) im Puffer sowie in monophasischen und biphasischen wässrig-organischen Reaktionssystemen eingesetzt werden. Sie zeigten eine gute Wiederverwendbarkeit und Stabilität unter verschiedenen Reaktionsbedingungen.

Schließlich wurden CatIBs für die Herstellung von hochwertigen Produkten unter technischen Bedingungen in Kulturüberständen eines *C. glutamicum* L-Lysin Produzentenstammes bei L-Lysin-Konzentrationen von bis zu 1 M in repetitiven *batch* und *batch* Experimenten erfolgreich eingesetzt. Darüber hinaus konnten *Pf*BAL-CatIBs zur Carboligation von bis zu 85 mM Benzaldehyd und dessen Derivaten in biphasischen Reaktionssystemen sowie zur kontinuierlichen Herstellung von 30 mM (*R*)-2-Hydroxy-1-phenylpropanon, einem wertvollen Vorläufer und Baustein für Arzneimittel, eingesetzt werden.

Publications

Poster presentations

R. Lamm, V. D. Jäger, R. Kloss, M. Pohl, U. Krauss, K.-E. Jäger, J. Büchs. Catalytically-active inclusion bodies: Application of high-throughput cultivation technologies to study innovative enzyme aggregates, 2018, DECHEMA-Himmelfahrtstagung, Madgeburg.

V. D. Jäger, S. Longerich, R. Kloß, A. Grünberger, M. Pohl, K.-E. Jaeger, U. Krauss. Towards the realization of an enzyme cascade in Catalytically-active Inclusion Bodies, 2017, Biotrans Budapest.

R. Kloß, V. D. Jäger, M. Diener, U. Krauß, M. Pohl. Catalytically active Inclusion Bodies: A new Carrier-free Enzyme Immobilisation Method, 2016, ProcessNet Aachen (Posterpreis).

V. D. Jäger, R. Kloß, M. Diener, M. Dietrich, M. Pohl, K.-E. Jaeger, U. Krauss. Catalytically-active Inclusion Bodies (CatIBs) New Carrier-free Enzyme Immobilizates for Biocatalysis, 2016, Biocat Hamburg (Posterpreis).

Talks

R. Kloß, M. Limberg, V. D. Jäger, U. Mackfeld, T. Karmainski, A. Grünberger, U. Krauß, M. Pohl. Catalytically active inclusion bodies: A novel carrier-free enzyme immobilisation method, 2017, Biotrans Budapest.

R. Kloß, V. D. Jäger, M. Diener, U. Krauß, M. Pohl. Catalytically active Inclusion Bodies: A new Carrier-free Enzyme Immobilisation Method, 2016, ProcessNet Aachen.

D. Rother; D. Johannes; R. Kloß; V. Jäger; U. Krauß; M. Pohl. Enzyme toolboxes & reaction engineering – Solutions for applied biocatalysis, 2016, ProcessNet Aachen.

Publications

R. Kloss, M. H. Limberg, U. Mackfeld, D. Hahn, A. Grünberger, V. D. Jäger, U. Krauss, M. Oldiges, M. Pohl. Catalytically active inclusion bodies of L-lysine decarboxylase from *E. coli* for 1,5-diaminopentane production, Scientific Reports, 2018, 8(1), p. 5856.

V. D. Jäger, R. Lamm, R. Kloß, E. Kaganovitch, A. Grünberger, M. Pohl, J. Büchs, K.-E. Jaeger, U. Krauss. A synthetic reaction cascade implemented by colocalization of two proteins within catalytically-active inclusion bodies, ASC Synthetic Biology, 2018, 7(9), p. 2282.

R. Kloss, T. Karmainski, V. D. Jäger, D. Hahn, A. Grünberger, M. Baumgart, U. Krauss, K.-E. Jaeger, W. Wiechert, and M. Pohl. Tailor-made catalytically active inclusion bodies for different applications in biocatalysis. Catalysis Science & Technology, 2018, 8(22), p. 5816.

V. D. Jäger, R. Kloss, A. Grünberger, S. Seide, D. Hahn, T. Karmainski, M. Piqueray, J. Embruch, S. Longerich, U. Mackfeld, K.-E. Jaeger, W. Wiechert, M. Pohl, and U. Krauss. Tailoring the properties of (catalytically)-active inclusion bodies. Microbial Cell Factories, 2019, 18(33), p. 1

So remember to look at the stars and not down at your feet. Try to make sense of what you see and wonder about what makes the universe exist. Be curious. And however difficult life may seem, there is always something you can do and succeed at.

Stephen Hawking's Last Speech to Humanity, March, 2018

Table of contents

Abbreviations

(*R*)-2-HPP	(*R*)-2-hydroxy-1-phenylpropanone
(*R,R*)-PPD	(1*R*,2*R*)-1-phenylpropan-1,2-diol
(*S*)-2-HPP	(*S*)-2-hydroxy-1-phenylpropanone
3HAMP	*h*istidinkinases, *a*denylylcyclases, *m*ethyl accepting chemotaxis proteins and *p*hosphatases
ADH	alcohol dehydrogenase
AdiA	inducible arginine decarboxylase
Amp	ampillicin
*At*HNL	hydroxynitrile lyase from *Arabidopsis thaliana*
BAL	benzaldehyde lyase
BFD	benzoylformate decarboxylase
BSA	bovine serum albumin
*Bs*LA	lipase A from *Bacillus subtilis*
C. glutamicum	*Corynebacterium glutamicum*
cadA	gene encoding for inducible lysine decarboxylase
CadB	cadaverine antiporter
cadBA	operon encoding for inducible lysine decarboxylase and cadaverine antiporter CadB
CadC	transcription activator for the cadBA
CatIBs	catalytically active inclusion bodies
CLEA	cross-linked enzyme aggregates
CLEC	cross-linked enzyme crystals
Da	Dalton
DAP	1,5-diaminopentane, cadaverine
DMBA	3,5-dimethoxybenzaldehyde
DMSO	dimethyl sulfoxide
DNA	deoxyribonucleic acid
E	extinction
E. coli	*Escherichia coli*
EC	enzyme commission
Ec	*E. coli*
*Ec*LDC	lysine decarboxylase from *E. coli*
*Ec*MenD	2-succinyl-5-enol-pyruvyl-6-hydroxy-3-cyclohexene-1-carboxylate synthase from *E. coli*
ee	enantiomeric excess
EMR	enzyme membrane reactor
FIBs	functional inclusion bodies
GadA/GadB	glutamic acid decarboxylases
GC	gas chromatography
HL-ADH	horse liver alcohol dehydrogenase
HPLC	high pressure liquid chromatography
Ibp	inclusion body associated protein
IBs	inclusion bodies
IPTG	isopropyl-β-D-thiogalactoside, isopropyl β-D-1-thiogalactopyranoside
k	rate constant
Kan	kanamycin
k_{cat}	turnover number
kDa	kilo Dalton
l	liter
LB	lysogeny broth
Lb	*L.actobacillus brevis*
*Lb*ADH	alcohol dehydrogenase from *L. brevis*
LDC	lysine decarboxylase
ldcC	gene encoding for constitutive lysine decarboxylase
ldcI	gene encoding for inducible lysine decarboxylase
mCherry	monomeric Cherry fluorophore
MTBE	methyl *tert*-butyl ether
NAD(P)H / $NAD(P)^+$	nicotinamide adenine dinucleotide (phosphate)
NTA	Nitrilotriacetic acid
OD	optical density
omp	outer membrane protein
PA	polyamide
PAGE	pPolyacrylamide gel electrophoresis
Pf	*Pseudomonas fluorescens*
*Pf*BAL	Benzaldehyde lyase from *Pseudomonas fluorescens*
pH	negative decadic logarithm of the H+ ion concentration
PLP	pyridoxal 5'-phosphate
Pp	*Pseudomonas putida*
*Pp*BFD	benzoylformate decarboxylase from *Pseudomonas putida* ATCC 12633
R	*Ralstonia sp*
*R*ADH	*Ralstonia* sp alcohol dehydrogenase
rpm	revolutions per minute
RT	room temperature
s	second
SDS	sodiumdodecylsufate
SEM	scanning electron microscopy
STY	space-time yield
TB	terrific broth
TDoT	*te*tramerization *do*main of the cell-surface protein *t*etrabrachion
ThDP	thiamine-diphosphate
TMBZ	(*R*)-(3,3´,5,5´)-tetramethoxybenzoin
U	units
UV	ultraviolet
v/v	volume per volume
vol%	volume per volume in percent
w/v	weight per volume
WT	wild type
YFP	yellow fluorescent protein

1 Introduction

1.1 Biocatalysis

1.1.1 Definition of biocatalysis

Generally, biocatalysis is defined as the conversion of organic compounds by living organisms, cell extracts or isolated enzymes. Enzymes as catalysts are the driving force and accelerate the conversion of substances by reducing the activation energy. Since ancient times, biocatalytic processes have been used by mankind, being of great importance for the production and preservation of beverages and food, like beer, bread, and cheese, without knowing the molecular processes [1,2]. The systematic study of enzymes as driving force for biocatalysis was started in the nineteenth century by Louis Pasteur and other researchers as was summarized in several reviews [3,4]. They studied the fermentation of alcohol and lactic acid and figured out that fermentation is correlated to the presence of yeast cells. In the same time, Eduard Buchner studied the cell-free sugar fermentation by the enzyme “zymase”, which was more likely a mixture of several enzymes derived from yeast [5]. Kühne named these not cellularly organized enzymes “Fermente”, which are characterized as compounds that enable fermentation outside or in the absence of microorganisms [6]. These new insights paved the way for modern biocatalysis.

1.1.2 Application of biocatalysis in the 20th century

Biotechnological discoveries and inventions in the 20th century, above all the improvements in molecular biology, enabled the application of modern biocatalysis in industry. By means of genetic modification techniques recombinant cells could be created, which are able to overproduce natural primary and secondary metabolites, but also non-naturally occurring products by introduction of the respective genetic information. Examples of naturally- and non- naturally-occurring products are amino acids, vitamins, solvents (e.g. acetone, butanol, ethanol), and organic acids as well as biopharmaceuticals like antibiotics, insulin, antitumor agents, or cholesterol-lowering agents [7–10]. Besides microbial biotechnology, isolated enzymes are used in industry for the production of food and feed, pulp and paper, textiles, cosmetics, fine chemicals and pharmaceuticals [11,12]. The use of isolated enzymes was enabled by recombinant DNA technologies [13]. However, the industrial application of enzymes is often hampered by insufficient stability and catalytic efficiency of the biocatalysts,

besides of specificity issues [12]. The main challenge of limited enzyme stability was overcome by the development of various immobilization strategies during a so-called “first wave of biocatalysis” [13]. Protein engineering technologies, like random mutagenesis followed to adapt the enzymes’ substrate range towards non-natural substrates in a “second wave” [12]. In the “third wave of biocatalysis”, the stability, substrate specificity, and enantioselectivity of the enzyme was improved by directed evolution, which was enabled by several developments, e.g. gene synthesis, sequence analysis, bioinformatics tools, and computer modelling [13]. All these scientific and technological advances can enable the realization of enzymatic catalysis as an environmentally friendly alternative to chemical synthesis [13].

1.1.3 Advantages of enzymes

The application of enzymes in industry is rapidly growing, since enzymes catalyze reactions regio-, chemo-, and stereoselectively under mild reaction conditions, which is specifically useful for the production of chiral fine chemicals and pharmaceuticals [14]. Synthetic routes can often be shortened compared to chemical processes, since protection groups are not necessary [12]. There are several other advantages of enzymes for the application in organic synthesis:

- Enzymes can accelerate a reaction by a factor of 10^8-10^{10} compared to a non-catalyzed reaction, which mostly exceeds the performance of chemical catalysts [14].
- Many enzymes are catalytically promiscuous, since they accept a broad range of different substrates [14,15].
- Enzymes work in aqueous reaction systems under similar conditions (except for e.g. lipases). Thus, a multi-enzyme cascade reaction can be realized, thereby shifting unfavorable equilibria and avoiding the isolation of unstable reaction intermediates [14].
- Besides aqueous reaction systems, some enzymes show activity also in organic solvents by choosing an appropriate environment [16,17]. This enables the application of enzymes in reactions with higher poorly water-soluble substrate concentrations, as it is often applied in industrial processes. However, several isolated enzymes lose their activity and stability in organic solvents due to denaturation effects [17–19], which can be overcome by using enzymes entrapped in whole cells [20].

All these properties of enzymes are beneficial to apply them in technical processes and to replace chemical process steps by biocatalytic ones. This replacement is one way to realize the aims of green chemistry [21,22], which has the objective of a long-term, sustainable and environmentally friendly world-wide development of processes, which are less hazardous to humans and the environment [23]. In this context, bioeconomy, as a political vision, aims at a knowledge-based sustainable production of compounds based on renewable resources and at the implementation of environmentally friendly, green economy. This can be *inter alia* realized by implementation of biocatalytic processes or process steps into current industrial processes [24,25].

1.2 General immobilization techniques

In order to establish biocatalytic processes that are competitive with their chemical alternative, cost reduction for the biocatalyst are key. Of utmost importance in that respect is the improvement of stability for long-term use [26], especially as harsh reaction conditions often prevail in biocatalytic processes such as high salt concentrations, organic solvents, unfavorable pH-values, and mechanical shear stress [27,28]. Hence, there is a high demand for stable biocatalysts for the application in biocatalytic processes, which can be attained by enzyme engineering techniques or immobilization of the enzyme. The latter enables additionally the reuse and recycling of biocatalysts at the same time [29,30].

Enzyme immobilization represents the easiest stabilization method, which can be applied to all enzymes, since structure information is often not required with a few exceptions for targeted immobilization techniques. The easiest way of immobilization can be realized by using resting whole cells. There are several reports of successful application of lyophilized recombinant whole cells containing for example the benzaldehyde lyase from *Pseudomonas fluorescens* (*Pf*BAL) in aqueous-organic and micro-aqueous solvent systems [20,31,32]. The application of whole cells is advantageous since no time consuming and expensive enzyme purification is needed and cofactors can be easily recycled by other enzymes naturally present in the whole cell biocatalyst. The enzymes inside the cells are protected against the reaction environment, which increases the enzyme stability. However, the cell membrane may cause mass transfer limitations, which decreases the reaction rate [33]. Furthermore, the whole cell approach could result in undesired side reactions due to the cellular enzymes. Further, safety issues can hamper the application of this approach, since the handling of genetically modified organisms (GMO) requires a respective permission for application in chemical industry [14].

These disadvantages can be overcome by the use of immobilized enzymes. Generally, there are three concepts described for the immobilization of isolated enzymes (Figure 1-1): i. by binding on a support (carrier), ii. entrapment into a carrier-material, and iii. carrier-free by direct cross-linking of the enzymes [29,30,34,35]. However, no immobilization method is generic, which makes the individual adaptation to the respective enzyme in a trial and error process necessary [36]. Rodrigues *et al*. report on the creation of a biocatalysts library by using different immobilization strategies to find the conditions where enzyme properties improved best with respect to selectivity, activity, and the product yields [37]. However, this strategy is very time-consuming and expensive. Some progress to a more generic immobilization method was made by using carrier materials with tailorable pore size and functionality on the surface [36]. Generally, the immobilization method should be chosen according to parameters providing not only the highest stabilization and activity of the enzyme, but also enable the best performance in the specific reaction environment [36]. An overview of recommendations for the selection of an appropriate immobilization method is given in the review of Hanefeld [36].

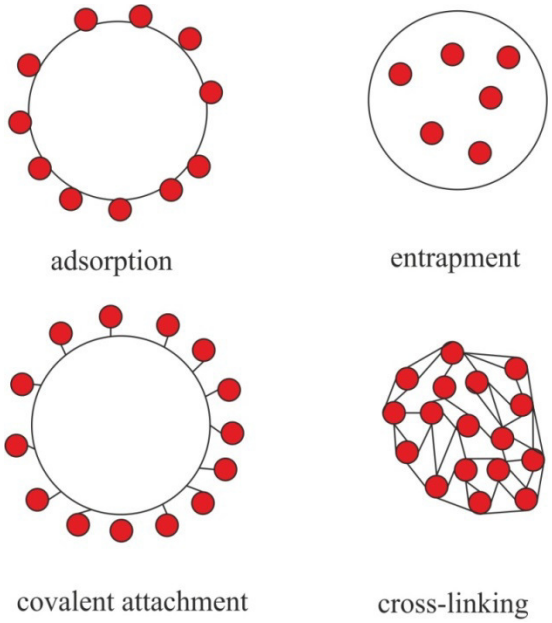

Figure 1-1 Enzymes (red dots) can be immobilized in different ways: by binding on a support (carrier) via adsorption or covalent binding, entrapment into a carrier-material or by cross-linking. The illustration was adapted from Adlercreutz, Sheldon and van Pelt [30,35].

Despite the advantages of immobilization, the main drawback of several techniques is a lower activity due to partial enzyme inactivation and mass transfer limitations [38,39]. The advantages and disadvantages of all techniques were discussed in the following chapters.

1.2.1 Immobilization on a carrier

The enzyme can be bound to a support by non-covalent or covalent interactions. Biopolymers, synthetic polymers or materials on silica basis are frequently used carriers [30].

Adsorption by non-covalent interactions is a simple and cheap method, with the enzyme being not chemically modified [38]. Since such interactions are weak, enzyme leakage can be a problem, especially in aqueous solution. Thus, such immobilizates should be applied in organic solvents [29]. Generally, lipases were immobilized by this method for example *Candida antarctica* lipase B (CaL-B), which is commercial available as Novozyme 435 (Novozymes) and Chirazyme (Roche Molecular Biochemicals) and is usually applied in organic solvents [29,35].

Ionic interactions or affinity adsorption are another possibility to bind the enzyme on a carrier. Enzymes can be attached by ionic interaction to poly-saccharide biopolymers e.g, dextran, agarose and chitosan or macroporous acrylic polymer resins, which could be also functionalized [29]. Affinity adsorption is usually realized by a matrix-bound ligand with affinity to a peptide or protein genetically fused to the enzyme [40] (Table 1-1). Generally affinity adsorption via such a fusion-tag based approach is used to purify proteins, but it can be also used to couple purification and enzyme immobilization in a single step [41]. Affinity ligand binding by the so-called His-Tag is the easiest way, where the enzyme could be absorbed, *inter alia*, to superparamagnetic solid support [42] or on a nickel(II)–nitrilotriacetic acid derivatized carriers (Kurlemann 2003). Besides Ni^{2+}, other chelated metal-ions are available such as Co^{2+}, Cu^{2+}, Zn^{2+}, and also Fe^{3+}. The latter is used by the EziG-technology, which is supposed to have the advantage that enzyme binding is more stable thus minimizing enzyme leakage [43,44]. Furthermore, there is a broad range of fusion proteins with affinity towards carrier materials, such as cellulose binding-domains, but also maltose-, calmodulin- or chitin-binding domains [41,43]. Affinity binding can be also realized via antigen and monoclonal antibody interactions, such as the FLAG-tag or using enzymes, like the glutathione S-transferases (GSTs) with a strong binding affinity to a glutathione resin [43]. In most cases, the binding via affinity or ionic interactions is reversible, so that enzyme leakage is a common problem for these enzyme immobilization methods [38]. However, there are methods with a higher stability such as the streptavidin-tag, which is reported to be more thermostable as biotin-streptavidin/avidin complex [27]. Furthermore, some affinity tags form covalent bonds being more stable and thus diminishing enzyme leakage. One of these covalent immobilization tags is the novel HaloTag™ technology [45], which uses a modified

dehalogenase as a fusion tag. A covalent bond is provided upon binding to a terminal chloroalkane ligand, which is exposed on the surface of Sepharose® beads or magnetic particles [45]. This method is advantageous since it also enables a site-oriented covalent binding of the enzyme on the carrier.

Table 1-1 A selection of common affinity tags taken from Malhotra, Barbosa *et al.,* and Rehm *et al.* [41,43,46]

tag	**size**	**affinity matrix**	**mode of interaction**
His-tag	6–10 His	immobilized metal ions: Ni, Co, Cu, Zn, Fe (EziG)[1]	metal coordination
GST (glutathione-S-transferase)	211 aa	glutathione resin	affinitiy
FLAG-tag	8 aa (DYKDDDDK) (22 aa for 3xFLAG)	anti-FLAG monoclonal antibody	affinitiy
Strepdavidin (Strep)	8 aa (WSHPQFEK)	engineered avidin	affinitiy
Protein A (staphylococcal Protein A)	280 aa	immobilized IgG	affinitiy
CBD (cellulose binding domain)	-[2]	cellulose	affinitiy
MBP (maltose-binding protein)	396 aa	cross-linked amylose	affinitiy
CBP (calmodulin-binding protein)	26 aa	immobilized calmodulin	affinitiy
CBD (chitin-binding domain)	51 aa	chitin	affinitiy
HaloTag	approx. 300 aa	chloroalkane	covalent

[1]Engelmark Cassimjee and Federsel [44]

[2]CBDs differ in size and pattern [47]

In contrast, there are several covalent immobilization methods, which do not work site-oriented but target amino acids displayed at the surface of the enzyme randomly. Covalent binding is often realized by reaction of epoxide groups on the carrier with ε-amino group of L-lysine residues on the enzyme surface [29]. The usage of epoxide groups is advantageous, since the linkage is stable and the attachment is realized under mild reaction conditions [48,49]. Carriers can be, *inter alia*, chelate-epoxy modified magnetic nanoparticles [50], functionalized mesoporous silicates [51], electrospun polymer nanofibers [29], the commercial available co-polymer Eupergit (Evonik), and polymethylacrylate-based Sepabeads (Resindion) [48]. Furthermore resins with multiple reactive functional groups were developed to improve the enzyme binding [41,48]. To functionalize the particles for enzyme binding, glutaraldehyde can be used for covalent binding of the enzymatic amino-groups to the amino-functionalized Sepabeads [52]. Furthermore, the usage of glutaraldehyde to cross-link the enzyme on the support can enhance the enzyme load, the stability and activity of some enzyme immobilizates [29,48]. Further functional groups are, for example glyoxyl groups on e.g. glyoxyl agerose [48]. However, the activity can be decreased by covalent attachment

technique due to the mode of chemical modification and carrier properties, which can vary depending on the respective enzyme [29]. The random covalent attachment and binding of the enzyme to a carrier can negatively influence the activity, since the carrier can block the accessibility to the active site, which results in steric hindrance. By site-oriented covalent binding, the binding site on the enzyme surface can be selected, so that the substrate channel is not blocked by binding to the carrier. Thus, the targeted immobilization using affinity tags can be considered as a more efficient enzyme immobilization.

1.2.2 Enzyme entrapment

Besides adsorption on a carrier, enzymes can be entrapped in usually hydrophilic polymer networks, such as polymer matrices (e.g. polyacrylamide, N-isopropylacrylamide, N-isopropylmethacrylamide, poly-vinyl alcohol, or silica-cased sol-gels) natural hydrogels (agarose, chitosan and alginate) or membrane devices (hollow fibers or microcapsule) [29,30,46,53]. Partially dried PVA hydrogels revealed improved mechanical stability and are commercially available as Lentikats®. They were employed for entrapment of whole cell as well as enzymes. This method is, however, hampered by enzyme leakage, which could be overcome by increasing the enzymes size by e.g. cross-linking [30]. Some microgels are reported to stabilize emulsions, so that the entrapped enzyme can be used in a biphasic reaction system [53].

Entrapment can be advantageous as the entrapped enzyme is protected against inactivating influences like sheer stress or hydrophobic solvents, since the matrix provides an aqueous micro-environment. However, the mass transfer can be limited for larger molecules [29], whereas low molecular weight substances can be transported through the semi-permeable membrane [38].

1.2.3 Enzyme cross-linking

To enhance the enzyme loading and to avoid the use of expensive carrier materials, a carrier-free immobilization method would be desirable, which can be realized by cross-linking the enzymes with bifunctional reagents. Typical examples are cross-linked enzyme crystals (CLECs) and cross-linked enzyme aggregates (CLEAs) [30].

CLECs are prepared from crystallized enzymes by cross-linking with glutaraldehyde, which results in robust particles that can be employed in organic solvents. In 1990s, this method was commercialized by Altus Biologics, which, however, nowadays no longer distribute CLECs.

The method is hampered by the requirement to crystallize the enzymes of high purity. Crystallization is an often laborious, time-consuming and thus expensive procedure, so that this method is not applied so often anymore [30]. Furthermore not every enzyme can be easily crystallized.

The production of CLEAs is easier and less expensive and occurs in two steps. In the first step, the enzyme, dissolved in aqueous solution, is precipitated by the addition of salts, water miscible organic solvents or non-ionic polymers, which results in the formation active enzyme aggregates. This step is followed by cross-linking of the aggregated enzyme. Surface amino-groups of the enzyme react with a bi-functional chemical cross-linker, e.g. glutaraldehyde, which results in the formation of a Schiff-base. To establish stable covalent imine bonds, the Schiff-bases must be reduced by e.g. sodium borohydride. CLEAs can be formed from purified enzymes or from cell-free crude cell extracts containing the target enzyme [30]. To adjust the physical properties, CLEAs can be combined with other materials, like polymers or nanoparticles. A CLEA-silica composite was produced by addition of siloxanes during the cross-linking step [30]. Magnetic CLEAs enable the easy separation from the reaction. To increase rigidity, CLEA immobilization can be combined with Lentikats [29]. Spherical carrier-free enzyme particles (Spherezymes) were generated by addition of a precipitant and a cross-linker to a water-in-oil emulsion, which was successfully done especially for lipases. Combi-CLEAs were evolved for catalytic cascade processes [30]. The CLEA method was commercialized by CLEA Technologies (Netherlands) in 2002, which however, declared bankrupt in 2017.

The CLEA immobilization method has several disadvantages. General drawbacks can be a decrease in activity [38,54] due to reduction of flexibility, which in turn could be advantageous for an improved stability [55]. The active site can be impaired by the crosslinking agent, resulting in a complete loss of activity, as reported for e.g. an alcohol dehydrogenase from *L. brevis* and a nitrilase from *P. fluorescence* [56] (compare Table 1-2). Glutaraldehyde is assumed to easily penetrate into the active site so that it can react with amino acid residues essential for catalysis. By choosing an appropriate macro-molecular cross-linking agent, e.g. dextran polyaldehyde, the activity of the respective enzymes could be recovered to 10% and 50%, since dextran polyaldehyde is larger than glutaraldehyde and cannot access the active site that easily [56]. An overview about the residual activities of several enzymes immobilized as CLEAs is given in Table 1-2 and in the paper of Schoevaart [57]. The examples in Table 1 demonstrate that the activity recovery varies depending on the enzyme, the precipitants and the cross-linking agents.

Table 1-2 Selected examples of activity recoveries of enzymes immobilized as CLEAs. Activity was compared to the initial activity of the soluble enzyme solution, which was precipitated and cross-linked. *Activity recovery refers to the total activity before and after CLEA formation.

enzyme class	enzyme	origin	activity recovery* [%]	activity assay	comments on CLEA preparation	refer-ence
1	ADH	*Lactobacillus brevis*	0 or 10	UV-based, acetophenone as substrate	crosslinker: glutaraldehyde or dextran polyaldehyde	[56]
1	laccase	*Tinea versicolor*	32	UV-based, 2,2′-azino-bis(3-ethylbenzothia-zoline-6-sulfonic acid) (ABTS) as substrate	magnetic cross-linked aggregates	[58]
1	tyrosinase	*mushroom*	100	UV-based, catechol oxidation		[59]
3	Penicillin G acylase	*Escherichia coli*	48 or 85-90	titration, penicillin G potassium salt as substrate	crosslinker: glutaraldehyde or dextran polyaldehyde	[56]
3	α-l-rhamnosidase	*Brevundimonas sp.*	0, 35, or 82	HPLC-based, 4-nitrophenyl-α-L-rhamnopyranoside as substrate	usage of different precipitants and concentrations	[60]
3	lipase	*Pencilluim notatum*	24 or 52	HPLC-based, hydrolytic activity of nitrophenyl palmitate (p-NPP) as a susbtrate	crosslinker: glutaraldehyde (GLA) and ethylene glycol-bis [succinic acid N-hydroxysuccinimide] (EG-NHS)	[61]
3	α-amylase	*Bacillus amyloliquefaciens*	100	reducing sugar (estimated as maltose) released from starch was measured using 3,5-dinitrosalicylic acid		[62]
4	hydroxynitrile lyase	*Manihot esculenta*	11-35	UV-based, mandelonitrile as a substrate	usage of different precipitants and glutaraldehyde concentrations	[54]
4	hydroxynitrile lyase	*Manihot esculenta*	6-93	HPLC-based, hydrocyanation of cinnamic aldehyde	usage of different precipitants and glutaraldehyde concentrations	[54]
4	hydroxynitrile lyase	*Prunus amygdalus*	10	UV-based, mandelonitrile as a substrate	crosslinker: glutaraldehyde or dextran polyaldehyde	[56]
4	nitrilase	*Pseudomonas fluorescens*	0 or 50	HPLC-based, mandelonitrile as a substrate	crosslinker: glutaraldehyde or dextran polyaldehyde	[56]
4	phenylalanine ammonia lyase	*Rhodotorula glutinis*	10-36	UV-based, L-phenylalanine as a substrate	usage of different co-aggregation additives	[63]
4	nitrile hydratase	*Escherichia coli*	14 or 50	HPLC-based, acrylonitrile as a substrate	crosslinker: glutaraldehyde or dextran polyaldehyde	[64]
4	nitrile hydratase	*Haloalkaliphilic actinobacterium*	21	HPLC-based, hexanenitrile as a substrate		[65]
4	lysine decarboxylase	*Escherichia coli*	8	HPLC-based, L-lysine as a substrate		[66]

Another drawback of this method is the necessity of fine-tuning the steps to prepare CLEAs, which is time-consuming and laborious. Several parameters have to be adapted, like protein concentration, the choice of the precipitant and cross-linking agent as well as their appropriate concertation and the duration of the precipitation and cross-linking step [29,54,57,67–69]. Most frequently, the activity recovery is reduced if the parameters are not properly adjusted [54,56] (Table 1-2). Furthermore, the ratio of cross-linking agent can influence enantioselectivity and an excess can impair the stability and productivity [29].

As the ε-amino groups of the lysine residues on the enzyme surface are the main targets for crosslinking, it can be expected that not every enzyme molecule is cross-linked in the same manner. The distribution and the number of lysine residues on the surface vary between the different enzymes, which hampers the methodological transfer. This problem can be overcome by co-precipitation of the target enzyme with a polymer, which contains free amino groups, e.g. poly-L-lysine, or a second protein, e.g. bovine serum albumin (BSA) [30].

Despite the usage of poly-L-lysine or BSA as co-precipitant, all these examples show that the CLEAs cannot be used as a generic immobilization method, since the method has to be adapted individually to the respective enzyme by fine-tuning of the parameters mentioned above.

1.3 Catalytically active inclusion bodies

1.3.1 An overview about catalytically active inclusion bodies

As pointed out in the previous chapters, despite affinity-based method most immobilization methods are not generic, which requires individual adaptation of the chosen strategy to the target enzyme. To reduce the costs to a level comparable to crude cell extracts, the immobilization *in vivo* would be advantageous [70]. A simple way for simultaneous enzyme production and immobilization could be the usage of inclusion bodies.

Inclusion bodies are naturally produced and accumulate in the cytosol of some bacteria. In this thesis, only the protein containing inclusion bodies (IB) are studied in detail. An overview about other inclusion bodies is given by Shively [71].

IBs can be formed during recombinant protein production as a result of mutations, stress conditions and high rates of protein biosynthesis [72]. IB formation is regulated by several cellular genes, encoding for proteases and chaperones. IBs are fully biocompatible, mechanically stable, and contain particular amyloid-like structures [73], which can be

visualized by amyloid specific dyes like Congo red and thioflavin T [74]. Generally, IBs were assumed to consist of misfolded protein. In several cases they are used for the easy production of recombinant proteins, which are refolded to the native conformation after denaturation [75–77]. For instance, the production of enzymes as IBs represents a simple chromato-graphy-free protein purification method [78,79] or IBs were used as beneficial strategy to produce proteins, which are difficult to express and/or are even toxic for the host cell [80]. However, recent studies have shown that these enzyme aggregates can maintain at least part of their biological activity under certain conditions [72]. These active IBs are called catalytically active inclusion bodies (CatIBs).

CatIBs can be naturally produced by self-aggregation of the enzyme, which was first reported for a β-galactosidase and an endoglucanase G from *Clostridium thermocellum* [81,82]. These enzyme aggregates were proven to be active although produced as IBs. Since the widespread opinion of inactive aggregates withstood, activity was assumed to be a result of contamination [83]. The first detailed characterization and investigations of CatIBs was started by García-Fruitós *et al.* [84]. This study proved that the human dihydrofolate reductase is functionally produced as IBs. Furthermore, it could be shown that CatIB formation can also be induced by fusion to self-assembling tags, which contain an aggregation-prone part. *E. coli* β-galactosidase and two fluorescent proteins were successfully produced as functional IBs by fusion to the FMDV VP1 capsid protein or the human Aβ-amyloid peptide [84].

Meanwhile, various examples for self-assembling tags inducing CatIB formation are known. Among these are cellulose binding domains [85–88], pyruvate oxidase (PoxB) of *Paenibacillus polymyxa* [89], the viral capsid protein VP1 [84], coiled-coil domains [90,91] or various self-assembling peptides [78,92–94]. Furthermore, enzymes can be bound on inclusion body particles as for example on polyhydroxyalkanoate (PHA) inclusion bodies, which are surrounded by a protein shell, where among others PHA synthase and PHA granule-binding proteins are attached to [95]. A comprehensive overview about CatIB formation and application was published by Krauss *et al.* [96].

These examples demonstrate that IBs can be catalytically active, since they probably contain correctly folded protein. However, there still exists only a small number of studies dealing with CatIBs. Since they were still regarded as inactive aggregates, activity was presumably not tested for all observed IBs [97]. On the other hand, there are studies about IBs, which did not show any activity [96,98,99]. Therefore, it is not clear, under which circumstances proteins retain functionality in IBs. The variety of different enzymes forming CatIBs indicates

that not only the enzyme's properties have an influence on the formation of active IBs, but also the conditions during gene expression. There is up to now no rule that can predict the CatIB formation, as not all influences are known [96]. First attempts have been made to predict the formation of aggregates induced by fusion tags with web tools like TANGO [100], AGGRESCAN [101] and ZYGGREGATOR [102]. These softwares can only give a first hint, but cannot predict the formation of active IBs, since the calculations are based on the unfolded state of the peptides and proteins. Furthermore, several other influences, like sequence and structure of the target protein and fusion tag as well as the linker polypeptide have to be considered [96].

1.3.2 CatIB application

The combination of mechanical stability together with biological activity renders IBs beneficial for biomedical application [103–105]. They could be applied, for example, as carrier nanoparticles for therapeutic peptides, which are e.g. able to accumulate in tumor [106]. Another field is tissue engineering, where the IBs could act as scaffold material for the regeneration of damaged tissue [103].

Biocatalysis is another field for the application of CatIBs. Generally, CatIBs have several benefits for biocatalytic application compared to other immobilization methods. They represent a cheap and simple alternative to generally applied immobilization methods as they are carrier-free immobilizates comparable to CLEAs (see chapter 1.2.3). They can be biologically produced in *E. coli* cells [81,96,107,108] as well as in the yeast *Pichia pastoris* [105]. CatIBs can be easily isolated from cells by mechanical methods, whereas high-pressure homogenization is the method of choice [109]. This step can be followed by a simple centrifugation step for IB separation from the soluble fraction and further washing steps [97]. Further steps, like chromatographic purification or crosslinking-steps, are not needed [96]. Furthermore, CatIBs can be produced free of genetically modified organisms (GMO-free) by inactivating and separating any remaining vital recombinant *E. coli* cells during the production process [110].

The application of CatIBs in biocatalysis was demonstrated by Nahalka *et al.* for e.g. sialic acid aldolase, which was N-terminally fused to a cellulose-binding module (CBM) resulting in CatIBs, which were entrapped in alginate beads and cross-linked by glutaraldehyde. Repetitive batch experiments for the production of sialic acid revealed a good stability of these so-called cross-linked inclusion bodies (CLIB) [108]. A recently published study reports

about protein crystalline inclusions using the protein-tags CipA and CipB for the immobilization of *inter alia* several enzymes of the violacein biosynthetic pathway in a single IB [111]. Other studies dealt with the CatIB application of maltodextrin phosphorylase from *Pyrococcus furiosus* for starch degradation or with polyphosphate kinase immobilized in agar/TiO_2 beads for adenosine 5'-triphosphate (ATP) supply, both in repetitive batch mode [112,113]. However, only a few other reports focus on the application of CatIBs in biocatalysis [85,90,107,114].

Most studies concerning CatIBs do not go beyond measuring activity, as for example studies about new self-assembling enzymes, e.g. nitrilase PpL19 from *Pseudomonas psychrotolerans* [115] or a loop-deletion variant of the green fluorescent protein (GFP) [116]. Furthermore, a recently published study focused on the improvement of CatIB production fused to an aggregation-inducing tag [117]. However, all of these studies omitted the application of CatIBs in biocatalysis.

1.3.3 Formation of CatIBs induced by coiled-coil domains

A recently published study focused on the systematic evaluation of the CatIB concept for biocatalysis [90,91]. The group of Ulrich Krauss reported on the successful production of CatIBs by fusion to a coiled-coil domain: the cell-surface protein tetrabrachion (TDoT) from hyperthermophilic archaeon *Staphylothermus marinus* [118–120]. The formation of CatIBs by fusion to the TDoT domain was discovered accidentally, since the initial aim was the stabilization of enzymes by using oligomerization domains. Diener generated CatIBs of three different enzymes, the lipase A from *Bacillus subtilis* (*Bs*LA), hydroxynitrile lyase from *Arabidopsis thaliana* (*At*HNL), and the thiamine-diphosphate (ThDP)-dependent enzyme MenD (2-succinyl-5-enol-pyruvyl-6-hydroxy-3-cyclohexene-1-carboxylate synthase) from *E. coli* (*Ec*MenD) by fusion to the TDoT domain [90,91]. Furthermore, the formation and production of CatIBs in *E. coli* cells were analyzed by functional IBs of the yellow fluorescent protein (YFP) CatIBs [91]. *At*HNL-CatIBs were successfully applied for the production of chiral cyanohydrines in a mono-phasic micro-aqueous reaction system consisting of buffer-saturated methyl *tert*-butyl ether (MTBE) as a solvent. These CatIBs revealed a two orders of magnitude higher stability towards acidic pH values compared to the soluble enzyme and could be recycled several times. Furthermore, recycling of MenD CatIBs could be also demonstrated in buffer without significant loss of activity [90,91]. The TDoT domain as self-assembling tag induced in all cases the formation of active and stable CatIBs.

As this approach is very promising to reduce the costs for the preparation of immobilized biocatalyst, the CatIB formation induced by coiled-coil domains was patented [121].

One monomer of TDoT is composed of 52 amino acids and is assembled in its physiological structure to a parallel homo-tetramer forming the coiled-coil structure motif, a so-called tetramerization domain [118–120] (see Figure 1-2A). Another oligomerization domain used in this thesis is the 3HAMP domain (Histidine kinases, Adenylyl cyclases, Methyl-accepting chemotaxis proteins (MCPs), and Phosphatases) from *P. aeruginosa* soluble receptor Aer2, which is part of a prokaryotic signaling module [122]. It forms a stable dimeric coiled-coil structure of parallel homo-dimers and is composed of 172 amino acids for each monomer (see Figure 1-2B). It has a special structure of 3 alpha helices, which form a chain.

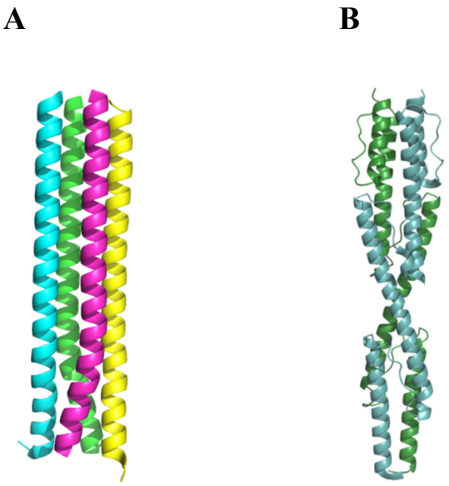

Figure 1-2 Superhelical structures of A) TDoT (PDB: 1fe6) and B) 3HAMP (PDB: 3lnr) coiled-coil domains. One TDoT monomer is composed of 52 amino acids and is assembled to a parallel homo-tetramer. 3HAMP forms a parallel homo-dimer and is composed of 172 amino acids for each monomer.

Superhelical structures are formed by coiled-coil motifs, which generally consist of at least two right-handed α-helices twisted around each other with a slight left turn [123]. The structure of a coiled-coil was first postulated by Crick and Pauling independent of each other [124,125]. Generally, the coiled-coil primary structure consists of a heptad repeat $(abcdefg)_n$ of seven amino acids. The amino acid residues in positions **a** and **d** are commonly hydrophobic and positions **e** and **g** contain mainly charged residues [126,127]. The residues in positions **b, c,** and **f** are variable adapted to the respective environment of the protein. The hydrophobic as well as the charged amino acid residues are involved in the formation of the stable coiled-coil structure, as they form the interactions between the α-helices [128] (Figure 1-3A). The hydrophobic side chains form a densely packed hydrophobic core within the coiled-coil structure [127], exemplarily shown for the leucine zipper (Figure 1-3B). Charged

amino acid residues are arranged laterally and interact with each other, thus contributing to the stabilization of the structure. The hydrophobic residues are not positioned exactly on top of each other, which results in the formation of a twisted, superhelical structure. Thus, the amino acid residues act as a kind of zipper so that the strands are arranged like in a rope [129,130].

A

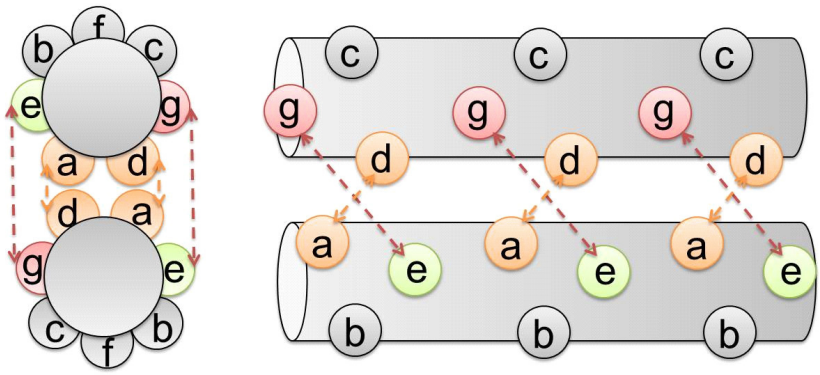

B

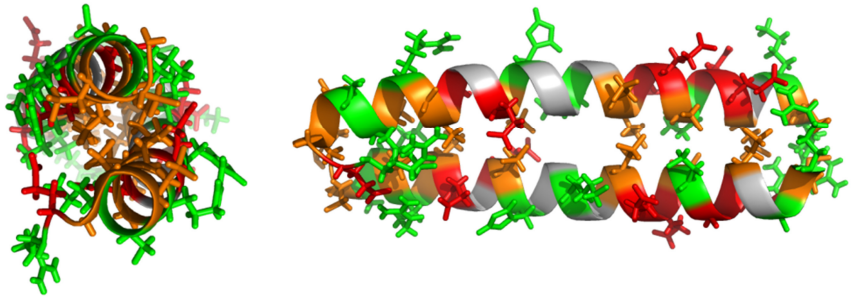

Figure 1-3 The heptad repeat of coiled-coil structure is exemplarily demonstrated by the structure of GCN4 leucine zipper. (A) A schematic illustration of the heptad repeat adapted from Alber; Oshaben *et al.*; and Diener, 2014 [91,131,132] (B) The side chains of the GCN4 leucine zipper (PDB: 4dmd [132] were colored respectively: Charged side chains at position e and g are marked in green (positive side chains) or red (negative side chains). Hydrophobic side chains in position a and d are labeled in orange. The remaining chains are marked in grey. The hydrophobic side chains form a hydrophobic core within the coiled-coil structure, which is very tightly packed, so that the coiled-coil forms a stable and fixed structure. The hydrophobic residues are not positioned exactly on top of each other, which results in the formation of a twisted, superhelical structure. Charged amino acid residues are arranged laterally and interact with each other, thus contributing to the stabilization of the structure. The outer amino acids in position b, c, f are adapted to the respective environment of the protein and can be charged or uncharged, as can be seen for GCN4 leucine zipper.

The superhelical structure can be explained by the architecture of the coiled-coil. The periodicity of seven amino acids results in 3.5 amino acid residues per turn. However, in α-helix without distortion, one turn consist of 3.63 residues on average, which results in a drift of 0.13 residues per turn for amino acid residues in a coiled-coil structure. To achieve a uniform packing, the coiled-coil strands bend to reduce their periodicity to 3.5 relative to their central axis. Since the α-helices are right-handed, the resulting supercoil turns left [133]. There are also exceptions for the left-handed supercoil, like the right-handed coiled-coil

tetramer of TDoT with 11-residue repeats [119,120]. This structure results in an extremely thermostable protein with hydrophobic water-filled cavities [120].

The simplest coiled-coil structures are composed of parallel or antiparallel oriented homodimers. The oligomerization varies between two and up to five α-helices. Homo-oligomers are composed of monomers with the same α-helical sequence, whereas hetero-oligomers consist of different α-helical monomers [127,134]. Due to this variety of different coiled-coil structures, their natural functions are divers. They comprise for example stabilization of the cell structure, a dynamic function as the motor proteins like myosin, dynein and kinesin, and molecular recognition by inter- or intramolecular binding, like the leucine zipper proteins for DNA binding [130,133,135]

The here presented CatIB immobilization strategy was applied to the following enzymes by fusion to two different coiled-coil domains (TDoT and 3HAMP): namely the thiamine diphosphate (ThDP)-dependent enzymes benzaldehyde lyase from *P. fluorescens* Biovar I (*Pf*BAL) and benzoylformate decarboxylase from *Pseudomonas. putida* (*Pp*BFD), the NADPH-dependent alcohol dehydrogenases from *Ralstonia sp.* (*R*ADH) and from *L. brevis* (*Lb*ADH), and the PLP-dependent (pyridoxal 5'-phosphate), constitutive lysine decarboxylase from *E. coli* (*Ec*LDC).

1.4 Thiamine diphosphate-dependent enzymes

ThDP-dependent enzymes are found in several steps of the metabolism of all organisms and catalyze the cleavage and formation of C-C, C-N, C-S, C-P and C-O [136,137]. As ThDP-dependent enzymes enable the stereoselective formation of a variety of different linkages like the synthesis of acyloins, they present a promising biocatalyst for asymmetric synthesis [138]. There are nine superfamilies with a diverse sequence and domain organization, among them α-ketoacid decarboxylases, transketolases, α-ketoacid dehydrogenases [139], which are listed in the ThDP-dependent Enzymes Engineering Database (TEED, https://teed.biocatnet.de/) [140] as a part of the BioCatNet [141]. The TEED database aims to analyze systematically the relation between sequence and structure [140]. Generally, all ThDP-dependent enzymes consist of two to four subunits containing the following domains each, which feature α/β-topology namely the PYR- (pyrimidine) and the PP- (pyrophosphate) with a high tertiary structural similarity [142]. Additionally these domains are flanked or connected by other domains like the middle domain [143], which varies between the enzyme ThDP-superfamilies. The domains can be arranged differently and can vary in their sequence with a

low sequence similarity of usually less than 20% [136]. In this work the focus was on the decarboxylase (DC) superfamily. The active site of the DC family is formed between the PYR- and the PP- domain of dimers. Thus enzymes from this structural family belong to the inter-monomer PYR-PP-type [139].

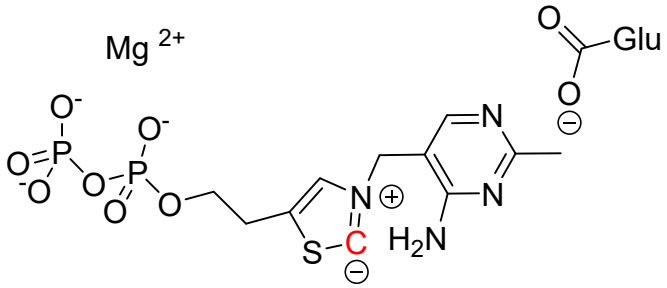

Figure 1-4 The chemical structure of thiamine diphosphate (ThDP) in the activated form. It appears in the typical V-conformation in the active site of ThDP-dependent enzymes, which brings the C2 atom (red) of thiazolium close to the N4 atom of the pyrimidine unit. ThDP is bound in the ThDP-binding pocket via the diphosphate residue to a divalent magnesium ion., which is coordinated in the active site via the aspartate side chain of the highly conserved binding motif Gly-Asp-Gly. ThDP is deprotonated at C2 to the active ylide form by a conserved glutamate residue next to the N1-atom of the pyrimidine ring (in the PYR-domain of the enzyme). Structure is adapted from Frank *et al.* [136].

The reaction mechanism of ThDP-dependent enzymes is highly similar and can be divided into two classes: enzymes with decarboxylase or transferase activity [136]. A central role is taken by ThDP, which is the active form of vitamin B1 (thiamine) and is composed of a diphosphate, a pyrimidine and a thiazolium ring (Figure 1-4). ThDP is bound in the ThDP-binding pocket via the diphosphate residue to a divalent magnesium or calcium cation, respectively. This cation is coordinated in the active site via the aspartate side chain of the highly conserved binding motif Gly-Asp-Gly [144]. ThDP is bound in a V-conformation, which brings the C2 atom of thiazolium close to the N4 atom of the pyrimidine unit (Figure 1-4) [136,145,146]. The catalytic activity originates from the C2 atom of the thiazolium ring. In a first step, the ThDP deprotonated at C2 to the active ylide form, which is mediated by a conserved glutamate residue next to the N1-atom of the pyrimidine ring (Figure 1-4, Figure 1-5A, first step). This induces the formation of an 1',4'-imino tautomer in the pyrimidine ring. The proximity of the N4-atom of the pyrimidine ring to the C2 atom of the thiazolium ring is essential for the proton transfer, so that a nucleophilic anion is formed at C2 [136,147]. Exemplarily, the carboligation (C-C bond formation) of benzaldehyde and acetaldehyde towards (*R*)-2-HPP ((*R*)-2-hydroxy-1-phenylpropanone) by benzaldehyde lyase from *Pseudomonas putida* (*Pf*BAL) is described, which proceeds presumably in the proposed mechanism as described earlier [148–151] based on the general mechanistic description for ThDP-dependent enzymes [137,145,152]. The C2 carbanion attacks the carbonyl carbon of the donor benzaldehyde forming a covalent ThDP-hydroxybenzyl intermediate (Figure 1-5A).

An enamine-carbanion is formed by deprotonation. The former electrophilic carbonyl carbon of benzaldehyde is now nucleophilic. Thus activated, the ThDP- bound benzaldehyde can nucleophilically attack an acceptor aldehyde, here acetaldehyde, so that a (*R*)-2-HPP-ThDP intermediate is formed (Figure 1-5B). After release of the product from the active site, ThDP is regenerated to the active ylide form. Principally all steps of the reaction cycle are reversibel [148]. Generally, ThDP and magnesium ions must be added to the buffer, since they are not covalently bound, but are necessary for activity maintenance, which was shown for *Pf*BAL [153]. As CatIBs of this enzyme were studied in this thesis, *Pf*BAL is described in more detail in the following.

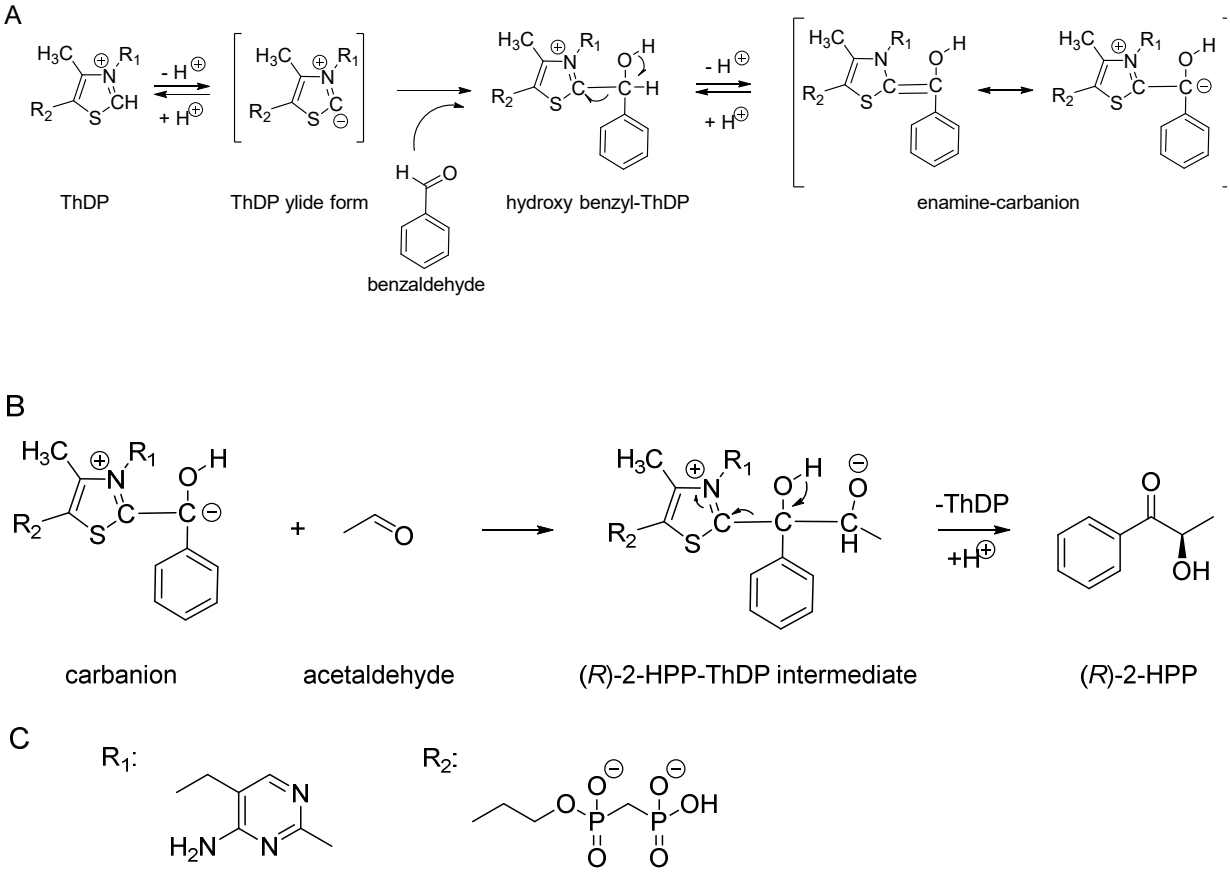

Figure 1-5 Proposed mechanism for the carboligation of benzaldehyde and acetaldehyde to (*R*)-2-HPP ((*R*)-2-hydroxy-1-phenylpropanone) by benzaldehyde lyase from *Pseudomonas putida* (*Pf*BAL) , which proceeds presumably as described earlier [148–151]. (A) In a first step the ThDP is transferred into the active ylide form by deprotonation at its C2. This induces the formation of an 1',4'-imino tautomer in the pyrimidine ring. The proximity of N4-atom of the pyrimidine unit to the C2 atom is essential for the proton transfer, so that a nucleophilic C2 atom is formed. For details see text. (B) This activated aldehyde can mediate a nucleophilic attack to an acceptor aldehyde, here acetaldehyde, so that a (*R*)-2-HPP-ThDP intermediate is formed. After release of the product from the active site, ThDP is regenerated to the ylide form. All reaction steps are principally reversible. This model is adapted from Pohl *et al.* [148].

1.4.1 Benzaldehyde lyase from *P. fluorescens*

*Pf*BAL (EC 4.1.2.38) was isolated from *P. fluorescens* Biovar I, which is able to grow on lignin-derived compounds like anisoin and benzoin presumably due to the lyase activity of *Pf*BAL [154,155]. The resulting aldehydes are metabolized most probably in the β-ketoadipate pathway [156]. As described above, *Pf*BAL belongs to the superfamily of decarboxylases and is a homo-tetramer with a size of 60 kDa per subunit [157,158].

*Pf*BAL is able to catalyze the C-C-bond formation between an aromatic aldehyde donor and an aromatic or aliphatic aldehyde acceptor strictly (*R*)-selectively [153,159–162]. Furthermore, *Pf*BAL catalyzes the cleavage of a broad range of benzoins and α-hydroxy ketones [153,154,159] with a high activity of e.g. 74 U/mg for the cleavage of (*rac*)-benzoin (K_M of 0.05 mM) [153,163]. *Pf*BAL is currently the only yet known ThDP-dependent decarboxylase with such a high C-C bond cleavage activity [164]. Compared to other lyases, *Pf*BAL has also a higher specific ligase activity, especially for the ligation of benzaldehyde towards (*R*)-benzoin with an activity of 320 U/mg [153]. Unlike other ThDP-dependent enzymes, *Pf*BAL exhibits no [165] or only a very low decarboxylase activity (<0.02 U/mg for benzoylformate) [163]. *Pf*BAL accepts a broad substrate spectrum of *ortho-, meta-* und *para*-substituted benzaldehydes as well as different aliphatic aldehydes and catalyzes mixed carboligation reactions [159,166]. In order to realize efficient reactions catalyzed by *Pf*BAL with a high substrate load and thus a high yield, several reaction engineering approaches are reported to be tackled and applied, which are presented in the following chapter.

1.4.1.1 Reaction engineering for *Pf*BAL-catalyzed reactions

*Pf*BAL is an important enzyme for the production of chiral α-hydroxy ketones, which can be used as building blocks for chiral 1,2-diols or 1,2-amino-alcohols with the appropriate alcohol dehydrogenase (see chapter 1.5) or ω-transaminase [167,168]. The mixed carboligation of benzaldehyde and acetaldehyde to (*R*)-2-HPP is well-characterized. However, (*R*)-benzoin is formed as an intermediate during this reaction in batch mode, which is observed especially at the beginning of the reaction, since the formation of (*R*)-benzoin is faster compared to (*R*)-2-HPP [150]. The reaction equilibrium can be shifted by an excess of acetaldehyde to (*R*)-2-HPP-formation [45,150,159,169,170].

Different reaction engineering approaches to improve the production of (*R*)-2-HPP were studied in the last decade; *inter alia*, different reaction modes (fed-batch, continuous) and the addition of organic solvents in mono- or biphasic reaction systems. In this thesis only a small

overview is given, focusing on results relevant for the application of *Pf*BAL CatIBs (chaps. 2.2, 3.2). A major challenge is the low stability of *Pf*BAL in aqueous buffer. Domínguez de María *et al.* observed a half-life of about 7 h in 50 mM potassium phosphate buffer (pH 8.0) at 20 °C [170] and Mikolajek *et al.* observed a half-life of 16 h in 50 mM potassium phosphate buffer (pH 6.5) at 30 °C [171]. Another challenge are inactivating effects caused by the aliphatic and aromatic aldehydes [171–173].

Several reaction engineering studies were performed to improve the enzyme stability and (*R*)-2-HPP productivity and thus the space-time yield of the process. First, organic solvents were added to counteract the precipitation of (*R*)-benzoin, which is poorly water-soluble [150]. Dimethylsulfoxide (DMSO, 20-30 vol%) was identified as a useful co-solvent since it increased the solubility of benzaldehydes and benzoins [166] and stabilizes the enzyme up to a concentration of 30 vol% [174], which, however, is concomitant with a reduced activity [170,175]. Other successfully tested more hydrophobic organic solvents were methyl-*tert*-butyl ether (MTBE, 5 vol%) [172,174,176], and 2-methyltetrahydrofuran (5 vol%) [177].

In order to shift the reaction equilibrium to the (*R*)-2-HPP product site instead of (*R*)-benzoin, the reaction mode can be selected appropriately. This can be realized especially in continuous reaction mode in an enzyme membrane reactor EMR, which is equipped with a semi-permeable membrane for enzyme retention [150]. For the synthesis of different (*R*)-2-hydroxy ketones, the continuous reaction mode was preferably used to prevent inactivation by low concentrations of the aliphatic and aromatic aldehydes [171–173]. Carboligation reactions were successfully conducted under the thus optimized reaction conditions with 30 vol% DMSO in buffer [150,169,172]. A continuous reaction was also realized in a plug-flow reactor [169,178].

Another possibility to circumvent the inactivation by aldehydes could be realized by separating the reagents from the enzyme in a two-phase system consisting of a not water-miscible organic phase containing the substrate and a buffer phase containing the enzyme [179]. A two-phase system ensures high substrate loads, as well as high buffer content. Several organic solvents were tested so far for *Pf*BAL: besides MTBE, which was most often used [176,178,180], studies using 2-octanone and toluene [180], as well as hexane were described [181,182]. In such aqueous-organic two-phase systems, *Pf*BAL can be inactivated at the interphase, which is, however, less distinct than the inactivation caused by the aldehyde substrates [180]. Improved stabilization and productivity in a two-phase system was reported for immobilized *Pf*BAL, entrapped in cryogel beads consisting of polyvinyl alcohol and

applied in batch or continuous reaction mode for the synthesis of furoin and its derivatives [178,181].

Whole cells were used to apply *Pf*BAL under biphasic [31] or micro-aqueous reaction conditions enabling a higher substrate load of 0.5 M benzaldehyde [20,32]. Because of stability reasons, acetaldehyde pulsing was mandatory in a fed-batch mode to ensure an excess of acetaldehyde and thus suppress the formation of (*R*)-benzoins as a site product [20,32]. Further immobilization strategies were realized by immobilization on carriers for example via the His-Tag on superparamagnetic solid support [42], on the respective sepharose material (Kurlemann 2003), via adsorption on non-porous glass beads [183], via covalent binding on chelate-epoxy modified magnetic nanoparticles [50] as well as on Sepharose® beads via the HaloTag^{TM} technology [45]. Immobilization enables the enzyme application in plug-flow reactor [169,178] or in repetitive batch [42,45,50].

1.4.2 Benzoylformate decarboxylase from *P. putida*

Another decarboxylase used in this thesis is the benzoylformate decarboxylase from *Pseudomonas putida* ATCC 12633 (*Pp*BFD, EC 4.1.1.7), which was first described in 1966 by Hegeman [184–186]. *P. putida* was able to grow on (*R*)-mandelic acid as a sole carbon source. As part of the mandelate catabolism of *P. putida*, *Pp*BFD catalyzes the decarboxylation of benzoylformate to benzaldehyde and CO_2 [185], which is then metabolized to benzoic acid. This is followed by a conversion in the β-ketoadipate pathway and the citrate acid cycle [156]. Up to now, six other BFDs with benzoylformate cleaving activity were identified [187–189], where two are also originated from *P. putida* ATCC12633 [187]. The first identified *Pp*BFD represents the most potent enzyme for biocatalysis and was well characterized [190–192]. The crystal structure of *Pp*BFD shows a homo-tetramer with a size of 56 kDa per subunit [193,194]. This *Pp*BFD showed a high decarboxylation activity for benzoylformate (V_{max}: 400 U/mg, K_M: 0.37 mM) [192], but poorly accepted substrates with aliphatic or sterically demanding substituents as small aliphatic or larger aromatic 2-keto acids [190].

Besides the decarboxylation activity, also carboligation activity is described for *Pp*BFD, which is able to catalyze the formation of C-C-bonds between several aromatic, hetero-aromatic, cyclic aliphatic or olefinic donor aldehydes and acetaldehyde as acceptor [190,195]. *Pp*BFD exhibits a smaller substrate range regarding sterically demanding substituents compared to *Pf*BAL [161], but it is the only yet known ThDP-dependent wild type

decarboxylase, which catalyzes the formation of (*S*)-2-HPP (V_{max}: 7 U/mg, 92% *ee*) [164]. It revealed a so-called *S*-pocket in the active site that enables the binding of small acceptor aldehydes e.g. acetaldehyde [192,196], in contrast to *Pf*BAL, where no *S*-pocket exists.

The self-ligation of benzaldehyde, however, yields (*R*)-benzoin (V_{max}: 0.25 U/mg, 99% *ee*) in the absence of acetaldehyde. To optimize the selectivity, activity and stability of *Pp*BFD, reaction engineering approaches have been used [164]. To enhance the selectivity, low benzaldehyde concentrations in a continuous reactor were realized, since *Pp*BFD is inactivated by high benzaldehyde concentrations [190]. Generally, the carboligase activity is low, compared to the decarboxylation activity and could be enhanced by exchange of the histidine at position 281 to alanine by side-directed mutagenesis [193,196], resulting in an increased carboligase activity towards benzoin (50 U/mg) [196] and its derivatives [161]. The exchange of leucine at positon 461 towards alanine and glycine revealed the possibility to produce a variety of different (*S*)-hydroxy ketones with high enantioselectivity by addition of larger acceptor aldehydes e.g. propanal [192]. This variant exhibits an enlarged active site at the acceptor binding site (*S*-pocket) [193,196]. Furthermore, the enantiomeric excess (*ee*) was increased compared to the wild type enzyme to 98% and the undesired side-product (*R*)-benzoin was reduced for the variant L461A. By directed evolution and site-directed mutagenesis approaches the stability against organic solvents was improved and the donor substrate range was increased to *ortho*-substituted benzaldehyde derivatives as donor [197,198]. This studies yielded the variant L476Q with an enhanced carboligation activity for (*S*)-2-HPP formation (28 U/mg; 95% *ee*) [198]. This variant was used in this thesis.

Besides protein engineering, the enzyme was stabilized by immobilization, such as adsorption on Sephabeads [199] or on non-porous glass beads [183], by covalent binding on magnetic epoxy silica nanoparticles [200,201], and on Sepharose® beads via the HaloTag™ technology [202]. Another option was the encapsulation in whole cells [31]. By reaction engineering approaches, the *ee* for (*S*)-2-HPP could be increase to 94% with an isolated yield of 60%, within 20 h in a biphasic reaction medium with MTBE and aqueous buffer containing 0.4 M benzaldehyde and 0.9 M acetaldehyde [31].

1.5 Alcohol dehydrogenases

Alcohol dehydrogenases (ADH, EC 1.1.1.1) can be found in many organisms and were first discovered in yeast, where they catalyze the oxidation of alcohol to acetaldehyde under NAD^+ reduction as fermentation process under anaerobic conditions [203]. Generally, ADHs catalyze reversible oxidoreduction reactions, where the reducing equivalents are transferred between the acceptor and donor molecules. Reducing equivalents are often hydride ions, provided by the cofactor nicotinamide adenine dinucleotide (phosphate) (NAD(P)(H)) (Figure 1-6) [204]. As an example, the reduction of an aldehyde/ketone (acceptor) is realized by a hydride transfer from the cofactor (NAD(P)(H)), which acts as donor (see Figure 1-7). This reaction is highly stereospecific [205,206]. Whether oxidation and reduction reaction occurs, can be influenced by appropriate adjustment of the reaction parameters [204].

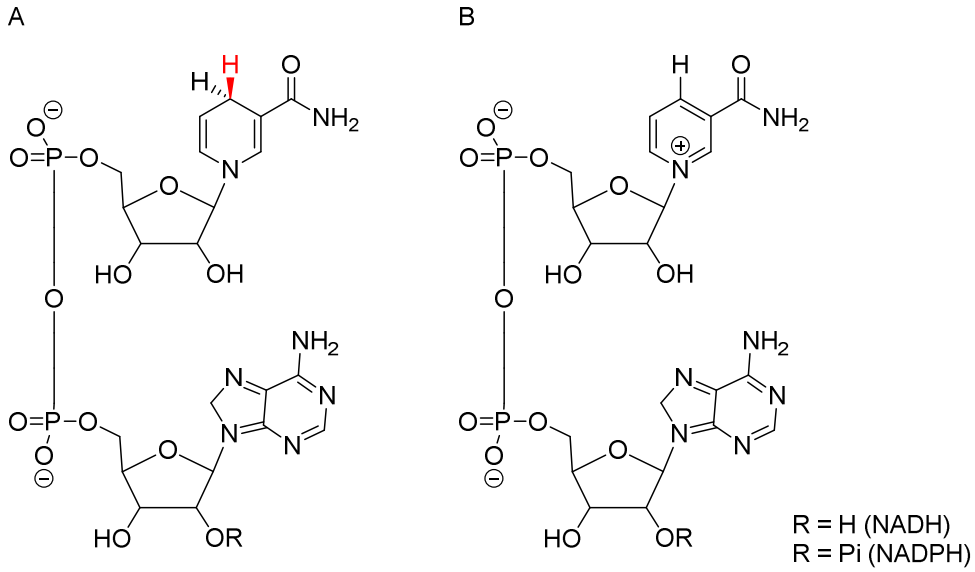

Figure 1-6 The cofactor nicotinamide adenine dinucleotide (phosphate) (NAD(P)(H)) (A) reduced form, (B) oxidized form. The structure was adapted from Patel [204].

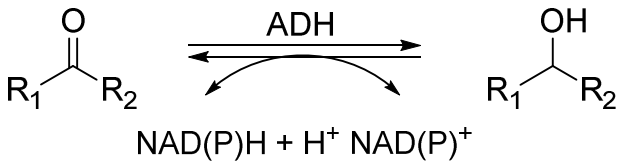

Figure 1-7 Reversible oxidoreduction reaction of alcohol dehydrogenases (ADH) under the hydride transfer from the cofactor nicotinamide adenine dinucleotide (phosphate) (NAD(P)(H))

To enable cofactor-binding, the structure of ADHs contain the typical Rossmann fold [207]. Besides the structural diversity of the active site, there exist some conserved structures that determine the preference for one cofactor. In NADPH-preferring ADHs, the negatively

charged phosphomonoester is coordinated by a largely conserved, positively charged arginine or hydrogenbond donating residues. In NADH-preferring ADHs, a carboxylate side chain interacts with the diol group at the ribose near the adenine [208]. Due to this specificity, the cell is able to separately regulate the different enzyme classes, which belong to different pathways. ADHs, which are part of the anabolism often use NADP(H) for reductive biosynthesis, whereas enzymes from the catabolism reqiure NAD(H) for oxidative degradations.

In this work, the focus was on the two alcohol dehydrogenases from *Ralstonia sp.* (*R*ADH) and from *L. brevis* (*Lb*ADH) that both prefer NADPH and belong to the short chain ADHs [209–213]. ADHs can be dived into the following groups: medium-chain, zinc-containing ADHs, "iron-activated" long-chain ADHs and short chain ADHs that do not require any metal atom for activity. Short chain ADHs are usually composed of approx. 250 amino acids [213]. Although the sequence similarity between the different short chain ADHs is 10-30%, the tertiary structure shows a highly similar α/β folding pattern. Highly conserved residues were found in the active site of several short chain ADHs, which form a catalytic tetrad of Asn–Ser–Tyr–Lys residues [214]. They were assumed to constitute a proton relay system together with the 2′-OH of the nicotinamide ribose, probably similar to the mechanism found in horse liver ADH [215].

1.5.1 Cofactor regeneration

Due to economic reasons, the cofactor NAD(P)H is applied in catalytic amounts and thus has to be regenerated [14]. Cofactor regeneration can be realized in different ways [216,217], whereas the regeneration via enzymes is the most favorable route [216–218]. Two concepts are possible: the co-substrate- or coenzyme-coupled approach. The enzyme-coupled approach is realized by addition of a second oxidoreductase, which requires also an additional co-substrate, for example glucose dehydrogenase for the regeneration of NADPH [219,220] and formate dehydrogenases for regeneration of NADH [221,222].

The substrate-coupled approach is usually realized via a large excess of a cheap co-substrate, generally isopropanol or ethanol, which enables the reduction of the target substrate with high conversion [223]. The effect can be combined with co-product removal, which also minimizes potential toxic effects of the co-product towards the enzyme [224]. Furthermore, smart bifunctional co-substrates like 1,4-butandiol enhance the reaction rates. 1,4-Butandiol is

converted to a kinetically inert lactone and thus enables an irreversible regeneration reaction, which lowers the required molar excess for the co-substrate [225].

To maximize the atom-efficiency, redox equivalents can be recycled within the cascade in a biocatalytic hydrogen-borrowing cascade. Within this cascade, the steps are combined in such a way that the oxidized cofactor is regenerated and reduced in the following reaction step, which is generally similar to redox networks in metabolic pathways [226,227]. The advantages of this cascade are that no additional co-substrate is required and no by-product is formed, which usually has to be separated from the target product. The coupling of the steps, however, can be challenging and must work; otherwise the redox cofactor gets oxidized by other enzymes that are present. As an example for a hydrogen-borrowing cascade, the production of amines can be performed in a cascade with alcohol dehydrogenase and transaminase, which are coupled by an alanine dehydrogenase that regenerates NADH and alanine as the co-substrate for the transaminase reaction. Here, it could be demonstrated that especially primary alcohols could be converted to the respective amines by this method, e.g. with full conversion of 50 mM 1-hexanol after 24 h [227].

Another possibility to minimize the costs by using cofactor recycling can be realized by the combined production of two valuable products. The reduction of a ketone can be combined with the oxidation of a racemic alcohol to obtain finally two enantiopure alcohols. This was demonstrated to work for a variety of different substituted ketones and racemic alcohols with a high conversion and enantiomeric excess (*ee*) [228].

In the following chapter, the two ADHs are presented that are of particular interest for this thesis: *R*ADH and *Lb*ADH.

1.5.2 Alcohol dehydrogenases from *Ralstonia sp.*

*R*ADH from *Ralstonia sp.* DSM 6428 was first described by the group of Kroutil in 2008 [209]. *R*ADH is composed of homotetrameres, each subunit has a size of 27 kDa, so that it is part of the a short-chain dehydrogenases family [209,210]. One monomer consists of the typical Rossmann fold of 7 β-sheets surrounded by 6 α-helices, whereby the α6 helix was assumed to act as lid over the active site as the cofactor is bound [210]. The active site is formed within one monomer. NADPH is preferred due to interactions of the phosphate group of NADPH with two arginine residues (Arg38 and Arg39) and one residue of asparagine (Asn15) located within the active site [229]. The highly conserved residues for short chain ADHs were found at position Ser137 and Tyr150 and are involved in catalysis [210,214].

*R*ADH accepts bulky-bulky ketones. The highest specific activity was obtained for the reduction of araliphatic 2-hydroxy ketones with up to 363 U/mg for (*R*)-2-hydroxy-1-phenyl-propan-1-one ((*R*)-2-HPP) [230]. The product (1*R*,2*R*)-1-phenylpropane-1,2-diol ((1*R*,2*R*)-PPD) can be further converted to important pharmaceutical building blocks e.g. the calicum channel blocker diltiazem [231]. Generally, reductions are catalyzed with high selectivity [210] following Prelog's rule [205]. Furthermore, enantiomerically pure (*R*)- and (*S*)-2-hydroxy ketones were converted with high diastereoselectivities to the corresponding 1,2-diols [230], which makes the enzyme interesting for applications in cascade reactions.

Cofactor regeneration was realized by the substrate-coupled cofactor approach using bulky co-substrates like cyclohexanol [232] or benzyl alcohol [229] amongst others such as ethanol or isopropanol [223]. A higher efficiency than for isopropanol is reported for the enzyme-coupled approach by using a glucose dehydrogenase to recycle the cofactor, which resulted in similar *ee*-values but higher activities [209]. The pH-optimum for the reduction activity is between pH 6 and 9.5 and for the oxidation between pH 10 and 11.5. Stability studies revealed a good stability of *R*ADH with half-lives of 60–70 h between pH 5.5 and 8 at room temperature, whereas the storage stability could be enhanced by addition of 0.8 mM $CaCl_2$ during the purification procedure and in the reaction medium [232]. The reason for this could not yet be elucidated, since a respective Ca^{2+}-binding site is missing in the crystal structure [210].

The application of *R*ADH in biocatalytic reactions with higher substrate concentrations was studied only in a few cases [233]. To stabilize the enzyme, *R*ADH had to be immobilized in *E. coli* whole cells for the conversion of high concentrations of (*R*)-2-HPP, which is formed from benzaldehyde (0.5 M) and 0.18 M acetaldehyde catalyzed by *Pf*BAL in a two-step cascade reaction in micro-aqueous reaction system [32]. Additional immobilization of the whole cell biocatalyst in teabags showed a good recyclability for five batches [20]

1.5.3 Alcohol dehydrogenases from *L. brevis*

*Lb*ADH belongs to the short chain ADHs and was first characterized by the Hummel group [211–213] *Lb*ADH catalyzes oxidoreduction reactions using the cofactor NADP(H) and is *R*-selective [211,234,235]. due to the anti-Prelog selectivity [205]. Usually ketoreductases exhibit Prelog selectivity, so that anti-Prelog selectivity is rare [236].

The homotetramer *Lb*ADH contains two Mg^{2+} ion binding sites and one active site in each monomer. Mg^{2+} was demonstrated to be important for activity and structural integrity

maintenance of the enzyme, since it couples the putative C-terminal hinge of the substrate-binding loop to some side-chains thus forming the substrate binding region [234]. The subunits (subunit size 27 kDa) are composed of the typical Rossmann-fold for cofactor binding. The catalytic triad was found at position Ser142, Tyr155, Lys159, together with the conserved Asn113 [211,234].

*Lb*ADH shows a broad substrate scope, accepting aliphatic and sterically demanding araliphatic as well as aromatic ketones, keto ester, diketones, cyclohexanone derivatives, and 2-hydroxy ketones with high stereoselectivity [211,230,237,238]. A high specific activity was observed for the reduction of acetophenone to (*R*)-phenylethanol with 113 U/mg [239], which is hardly accepted by any other ADH [211], except for *R*ADH [209]. The conversion of acetophenone is industrially relevant, since acetophenone is part of synthetic routes as starting material or intermediate [240,241]. Therefore, *Lb*ADH is an interesting enzyme for preparative applications towards enantiopure alcohols [237]. *Lb*ADH can be also used in cascade reactions to reduce α-hydroxy ketones yielding the (*S*)-products. The reduction of (*R*)-2-HPP to (1*R*,2*S*)-PPD was catalyzed with 1 U/mg (K_m = 7.5 mM) [242]. In contrast to *R*ADH, the pH-optima for reduction (pH 6.8-8.5) and oxidation (pH 6.2-10) reaction clearly overlap for *Lb*ADH [239].

Cofactor regeneration was often performed with inexpensive isopropanol as co-substrate in a substrate-coupled cofactor regeneration approach [237,238,243–245], since *Lb*ADH is stable in the presence of higher alcohol concentrations as well as other organic solvents [237]. The isolated enzyme [177,246] as well as immobilized *Lb*ADH was applied in biocatalytic reactions. Immobilization of *Lb*ADH was for example realized by using the CLEA technology with a 7-10% activity recovery by using dextran polyaldehyde as cross-linking agent [56]. There are several examples for the application of immobilized *Lb*ADH in reactions that showed either a higher stability, could be applied in plug-flow or could be reused for several batches. The immobilization on Sepabeads® [247] increased the operational stability 60-times compared to the soluble enzyme. During a plug-flow reaction, a constant conversion of 60% was obtained for more than 10 weeks with an *ee* > 99.5% and a space-time yield of 30 g/(L × day) [247]. Furthermore, *Lb*ADH was immobilized by using whole recombinant *E. coli* cells [245,248], which were used for continuous production of (2*R*,5*R*)-hexanediol or (*S*)-2-butanol under full conversion and with excellent space-time yields of >170 g/(L × d) and 2,278 ± 29 g/(L × d), respectively. *Lb*ADH was adsorbed on glass beads for application in gas-phase reactions and showed an half-life of 40 days for the production of (*R*)-1-phenylethanol in continuous mode [249]. The application of *Lb*ADH on superabsorbing

polymers [250] resulted in (nearly) full conversion and high *ee* for the reduction of several prochiral ketones (acetophenone, 4-acetylpyridine and ethyl acetoacetate) in isopropanol as solvent within 18–48 h. The batch could be repeated four-times without lost in activity. Furthermore, *Lb*ADH was covalent bound on Sepharose® beads via the HaloTag™ technology for application in plug-flow reactor [202,251], which could be used in a cascade reaction together with *Pp*BFD. The cascade reaction revealed a high operational stability of the single cascade steps up to several weeks and resulted in a high conversion (up to 99%) with high stereoselectivities (*ee*/*ic*) (up to 96%) for the production of (1*S*,2*S*)-1-phenylpropane-1,2-diol and space–time yields of up to 1,850 g/(L × d) [202].

1.6 Lysine decarboxylase from *E. coli*

1.6.1 General overview

In contrast to the aforementioned ThDP-dependent decarboxylases catalyzing *inter alia* α-keto-acids, lysine decarboxylase from *E. coli* (*Ec*LDC, EC 4.1.1.18) catalyzes the decarboxylation of α-amino acids, namely L-lysine to 1,5-diaminopentane (DAP, trivial name: cadaverine) under CO_2 release. Pyridoxal 5'-phosphate (PLP) is used as a cofactor (Figure 1-8). Two coding genes were reported to be expressed in *E. coli:* the inducible lysine decarboxylase (*Ec*LDCi, encoded by ldcI or cadA) and the constitutive lysine decarboxylase (*Ec*LDCc, encoded by ldcC) [252,253]. The *Ec*LDCi enables *E. coli* to grow under acidic conditions [254,255] as one of the acid stress-induced amino-acid decarboxylases, acting as biodegradative enzymes. These decarboxylases enable stress protection over a wide pH range, since they were induced at different pH values: pH 2 for induction of GadA/GadB glutamic acid decarboxylases [256] and the inducible arginine decarboxylase AdiA [257], pH 5 for the inducible ornithine decarboxylase SpeF [258] and *Ec*LDCi [259]. The gene cadA encoding *Ec*LDCi is induced at pH 5, under anaerobic conditions and in the presence of excess L-lysine [254,255]. The acidic medium is neutralized by excretion of the produced cadaverine into the medium by an inner membrane lysine-cadaverine antiporter CadB, which is encoded in the cadBA operon [260]. *Ec*LDCi was furthermore found to protect against phosphate starvation [261].

In contrast to *Ec*LDCi, the constitutive *Ec*LDC (*Ec*LDCc, encoded by ldcC) is a biosynthetic, weakly expressed LDC being part of the polyamine synthesis pathway of *E. coli.* In this pathway, cadaverine is converted to aminopropyl cadaverine, which is essential for the vegetative cellular growth [252,262,263].

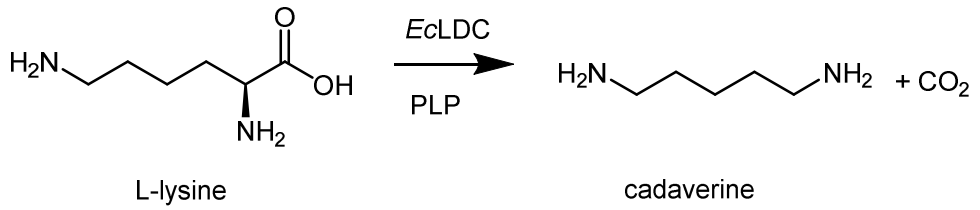

Figure 1-8 Decarboxylation of L-lysine catalyzed by lysine decarboxylase from *E.coli* (*Ec*LDC) to 1,5-diaminopentane (DAP, trivial name: cadaverine) under CO_2 release and pyridoxal 5'-phosphate (PLP) as a cofactor.

Both *Ec*LDC enzymes show a high sequence similarity of 69% identical and 84% similar residues [253], with an identical homo-decameric structure, resolved for both enzymes from X-ray crystallography [264] and cryo-electron microscopy [265]. *Ec*LDC oligomers are formed by the association of five symmetric dimers, which results in a homodecameric enzyme [264–266]. Dimerization is required for the formation of the active site, which is located between two dimers [264,265]. The subunits of both enzymes are composed in the same manner and consist of three domains: an N-terminal wing domain; a core domain and the C-terminal domain. The core domain contains a short linker region, a large PLP-binding subdomain with the conserved lysine forming the "internal" aldimine with PLP, and a subdomain 4 [264,265]. Differences in structural characteristics allow distinguishing between LDCc and LDCi. Consensus sequences were found for each type in the highly conserved C-terminal beta-sheet especially the RavA interaction domain binding motif (regulatory ATPase variant A, stress response protein) [265]. In contrast to *Ec*LDCi, *Ec*LDCc does not interact with RavA, thus missing this binding site [265,267]. Furthermore, the pH optima differ: *Ec*LDCi shows an optimum at weakly acidic pH of 5.7, whereas *Ec*LDCc has a broader pH-optimum (pH 6.2-8) [252].

As *Ec*LDC belongs to the α-family of PLP-dependent enzymes [268,269], the decarboxylation takes place at the Cα-position of L-lysine. PLP is bound covalently to the ε-amino group of a highly conserved lysine residue in the active site via an imine bond, which results in an "internal aldimine" bond (Schiff base) that protects the aldehyde of PLP as a covalent enzyme-PLP complex. In the next step, an "external aldimine" intermediate is formed by reaction of the enzyme-PLP complex with the α-amino group of the substrate via transamination (see Figure 1-9). The decarboxylation (CO_2 release) is realized by placement of the imine electron-removal group β to the releasing CO_2, so that the carbanion is resonance stabilized. The resulting carbanion is then protonated. To release the final decarboxylated product, the prior transamination reaction with the conserved lysine is reversed, so that again the "internal aldimine" is formed [270].

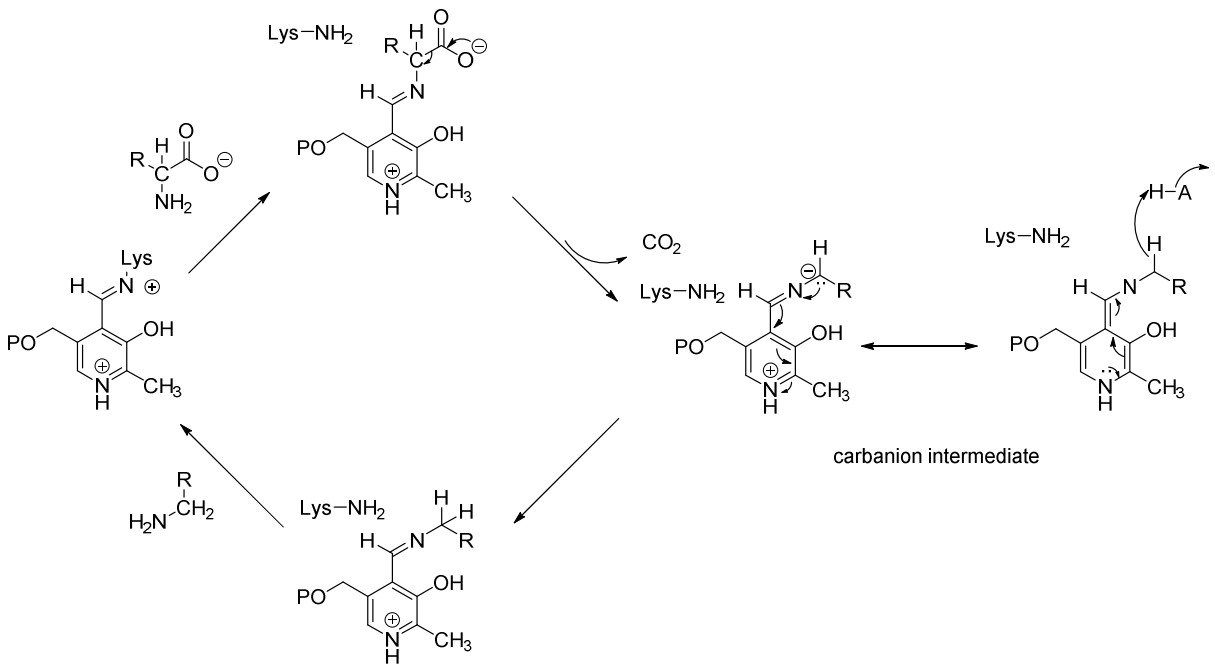

Figure 1-9 Reaction mechanism of PLP-dependent decarboxylases adapted from Jordan and Patel [270]. For details see text.

1.6.2 Application of *Ec*LDC for cadaverine production

Biotechnological cadaverine production was studied intensively in the last decade. In the chemical industry, cadaverine is an important building block for bio-based polyamides like PA5.10 and PA5.4, which are produced by poly-condensation with dicarboxylic acids such as succinate [271,272] or sebacic acid [273], thus enabling the replacement of petroleum-based polyamide PA6 [274,275]. Research into cadverine production is economically viable, as there is a prosperous industry of millions of tons for plastic [275] and the raw material L-lysine [276].

Cadaverine production was realized either by microbial production or by bioconversion. In a microbial production, the metabolism of an organism is used to produce the target products, so that the production is combined with the fermentation and growth of the microorganism. Therefore, a growth medium is required, which contains the nutrients necessary for microbial growth such as a water, carbon- and a nitrogen-sources, mineral salts, and sometimes vitamins. In contrast to this, in a bioconversion, the fermentation is separated from the production step. The enzymes are overproduced in microorganisms and were then used for the production step as single catalyst with the substrate as starting material. An overview about the respective cadaverine production ways is given in the recently published review from Ma *et al.* [277], whereby it is here shortened to some examples.

Industrial workhorses such as *C. glutamicum* [278–282] and *E. coli* [283] were designed by metabolic engineering to convert the overproduced L-lysine to cadaverine by introduction of the LDC genes derived from *E. coli* and/or optimizing existing pathways. The strains had to be optimized, to increase the tolerance of the microorganism towards higher cadaverine concentrations (0.5 M) [284]. Furthermore, the enzyme *Ec*LDCc is inhibited by cadaverine [285]. Both challenges could be overcome by realizing product export by co-expression of *cadB* from *E. coli* [286] and by overexpression of the major facilitator permease Cg2893 [285]. Furthermore, the production of by-products such as N-acetyl-1,5-diaminopentane were reduced by deletion of the N-acetyltransferase NCgl1469 [287]. Deletion of the lysine exporter (lysE) [288] increased the L-lysine concentration in the cells [279]. These optimizations resulted in the production of 88 g L^{-1} cadaverine in 50 h, with a productivity of 2.2 g·(L h)$^{-1}$ and a yield of 0.29 $g_{(cadaverine)}/g_{(glucose)}$ with a molar yield of 50% [279], which represents the highest productivity reported so far. However, most of the yields are far below industrial relevant concentrations, which can be explained by the following facts. The theoretical obtainable value of L-lysine by *C. glutamicum* can maximally reach 0.81 $mol_{(lysine)}/mol_{(glucose)}$ [276], which was not reached so far. The highest yield obtained was 120 g L^{-1} L-lysine with a productivity of 4 g $(L \cdot h)^{-1}$ and a yield of 0.55 $g_{(lysine)}/g_{(glucose)}$ in a fed-batch culture within 30 h [280]. Since the maximal yield for cadaverine (0.29 $g_{(cadaverine)}/g_{(glucose)}$) was half as high as the maximal yield for L-lysine (0.55 $g_{(lysine)}/g_{(glucose)}$), it can be concluded that the produced L-lysine is not fully converted to cadaverine although the strains were intensively optimized.

Higher cadaverine yields can be obtained from bioconversion performed with immobilized LDC. Immobilization was necessary, since the pure *Ec*LDCc enzyme is inhibited by the product cadaverine losing 50% activity at 30 mM (3 g l^{-1}) cadaverine [285]. Most studies concerned the application of *E. coli* whole cells overexpressing the gene encoding *Ec*LDCi [284,289], *Ec*LDCc [290] or lysine decarboxylase from *Klebsiella oxytoca* [291] or *Klebsiella pneumoniae* [292]. Furthermore, *E. coli* whole cells were immobilized in alginate beads [293,294]. The pure *Ec*LDCi enzyme was immobilized on poly(3-hydroxybutyrate) (P(3HB) biopolymer [295] or crosslinked as CLEAs [66]. *Ec*LDCi CLEAs showed 100% conversion of 100 mM L-lysine after 2 h. However, *Ec*LDCi CLEAs gave only 31% immobilization yield and 8% residual activity. The highest productivity of 221 g l^{-1} cadaverine was obtained using a fed-batch strategy with 344 g l^{-1} (2.35 M) L-lysine and *E. coli* whole cells overexpressing *Ec*LDCi, which however, resulted in a maximum conversion of only 92%. To overcome mass transfer limitations caused by the cell membrane, the lysine transporter CadB was

coexpressed in these whole cells [284]. Nearly 100% conversion was obtained with lower L-lysine concentrations of 200 g/L (1.37 M) yielding 133.7 g L^{-1} (1.3 M) cadaverine within 120 h [290]. In general, the bioconversions were carried out in buffer and only in a few cases in culture supernatants of L-lysine producers [289,290].

1.7 Aim of the thesis

To meet the high demands of biocatalysis, which requires stable and reusable biocatalyst, CatIBs represent a new, cell-free, and carrier-free immobilization method. Based on initial previous studies, the goal of this thesis was to increase the CatIB toolbox by further enzymes, to test the generic concept of the approach, and, most importantly, to study their properties and their application in different biocatalytic reaction systems.

Five complex, cofactor-dependent enzymes were selected: two NADPH-dependent alcohol dehydrogenases from *Ralstonia* sp. (*R*ADH) and from *Lactobacillus brevis* (*Lb*ADH), two ThDP-dependent lyases: benzaldehyde lyase from *Pseudomonas fluorescence* (*Pf*BAL) and benzoylformate decarboxylase from *Pseudomonas putida* (*Pp*BFD variant L476Q), and the PLP-dependent constitutive lysine decarboxylase from *E. coli* (*Ec*LDC).

All enzymes should be prepared as CatIBs using two different coiled-coil domains (TDoT and 3HAMP) as aggregation-inducing tags. The effects of the different CatIBs should be studied with respect to morphology, compactness and solubility of the particles, composition, residual activity, stability and applicability in different reaction systems.

Relating to their application in biocatalysis, CatIBs will be systematically evaluated compared to their soluble counterpart concerning long-term stability and recycling experiments. Stability studies will be performed under various process conditions, such as the variation of pH or the addition of solvents. As some of the selected soluble enzymes had a low stability, as for example *R*ADH and *Pf*BAL, a potential stabilization as CatIBs should be studied. Two examples of enzymes will be studied in-depth: i. *Pf*BAL CatIBs in batch and continuous reaction mode in a mono- and biphasic solvent system in comparison to the soluble enzyme, and ii. *Ec*LDC CatIBs under technical conditions in culture supernatants of a *C. glutamicum* L-lysine producer strain.

The doctoral thesis is part of the BioSc “CatIB - Catalytically active inclusion bodies: New carrier-free enzyme immobilisates for biocatalysis” project funded by the Ministry of Innovation, Science and Research of the German State of North Rhine-Westphalia.

2 Results

2.1 Tailoring the properties of (catalytically)-active inclusion bodies

V. D. Jäger[+], R. Kloss[+], A. Grünberger, S. Seide, D. Hahn, T. Karmainski, M. Piqueray, J. Embruch, S. Longerich, U. Mackfeld, K.-E. Jaeger, W. Wiechert, M. Pohl, and U. Krauss[*]

[+] These authors contributed equally to this work

[*] Corresponding author

published in Microbial Cell Factories, 2019, 18(33), p. 1

https://microbialcellfactories.biomedcentral.com/articles/10.1186/s12934-019-1081-5

Context:

The established CatIB toolbox in the BioSc cooperation project was analyzed in-depth regarding differences in CatIB formation efficiency, which included activity in the pellet, the overall activity, lyophilizate yield and the morphology of the CatIBs. This was studied empirically and optimized on the molecular biological level by exchanging the linker, the coiled-coil domain and the fusion site to the enzyme. The influence of the fusion tag on the morphology and aggregation propensity (relative activity in the pellet compared to the crude cell extract) was analyzed and a correlation was found between the empirically observed aggregation tendency and the size of hydrophobic surface patches of the respective enzyme structure. The latter is a first step to predict the aggregation propensity of the respective enzymes.

Contributions:

R. Kloss and V. D. Jäger contributed equally: they wrote the manuscript, planed, supervised, analyzed and assisted the experiments. V. D. Jäger optimized the plasmid, created the fusion proteins and characterized the fluorescence proteins and activity of *R*ADH and *Pf*BAL CatIBs

and optimized the *R*ADH activity assays. R. Kloss and U. Krauss planned the genetic construct of the C-terminal fusion. R. Kloss optimized the activity assays for *Pf*BAL, *Pp*BFD, and *Lb*ADH, and supervised the characterization of these enzymes and *Ec*LDC. S. Seide, D. Hahn, T. Karmainski, M. Piqueray, S. Longerich, U. Mackfeld, and J. Embruch performed experiments planned and supervised by R. Kloss and V. D. Jäger under the coordination and supervision of M. Pohl and U. Krauss. A. Grünberger performed live-cell imaging with the assistance of R. Kloss and V. D. Jäger and contributed respective parts to the manuscript. U. Krauss performed the prediction of the aggregation propensity. W. Wiechert, K.-E. Jaeger, M. Pohl and U. Krauss planned the CatIB project and corrected the manuscript.

Jäger *et al. Microb Cell Fact* (2019) 18:33
https://doi.org/10.1186/s12934-019-1081-5

Microbial Cell Factories

RESEARCH Open Access

Tailoring the properties of (catalytically)-active inclusion bodies

V. D. Jäger[1,4†], R. Kloss[2,4†], A. Grünberger[2,3], S. Seide[2], D. Hahn[2], T. Karmainski[2], M. Piqueray[1], J. Embruch[2], S. Longerich[1], U. Mackfeld[2], K.-E. Jaeger[1,2,4], W. Wiechert[2,4], M. Pohl[2,4] and U. Krauss[1,4*]

Abstract

Background: Immobilization is an appropriate tool to ease the handling and recycling of enzymes in biocatalytic processes and to increase their stability. Most of the established immobilization methods require case-to-case optimization, which is laborious and time-consuming. Often, (chromatographic) enzyme purification is required and stable immobilization usually includes additional cross-linking or adsorption steps. We have previously shown in a few case studies that the molecular biological fusion of an aggregation-inducing tag to a target protein induces the intracellular formation of protein aggregates, so called inclusion bodies (IBs), which to a certain degree retain their (catalytic) function. This enables the combination of protein production and immobilization in one step. Hence, those biologically-produced immobilizates were named catalytically-active inclusion bodies (CatIBs) or, in case of proteins without catalytic activity, functional IBs (FIBs). While this strategy has been proven successful, the efficiency, the potential for optimization and important CatIB/FIB properties like yield, activity and morphology have not been investigated systematically.

Results: We here evaluated a CatIB/FIB toolbox of different enzymes and proteins. Different optimization strategies, like linker deletion, C- versus N-terminal fusion and the fusion of alternative aggregation-inducing tags were evaluated. The obtained CatIBs/FIBs varied with respect to formation efficiency, yield, composition and residual activity, which could be correlated to differences in their morphology; as revealed by (electron) microscopy. Last but not least, we demonstrate that the CatIB/FIB formation efficiency appears to be correlated to the solvent-accessible hydrophobic surface area of the target protein, providing a structure-based rationale for our strategy and opening up the possibility to predict its efficiency for any given target protein.

Conclusion: We here provide evidence for the general applicability, predictability and flexibility of the CatIB/FIB immobilization strategy, highlighting the application potential of CatIB-based enzyme immobilizates for synthetic chemistry, biocatalysis and industry.

Keywords: Immobilization, Biocatalysis, Inclusion bodies, Protein aggregates, Protein engineering, Structure–function relations, Enzymes

*Correspondence: u.krauss@fz-juelich.de
†V. D. Jäger and R. Kloss contributed equally to this work
[1] Institut für Molekulare Enzymtechnologie, Heinrich-Heine-Universität Düsseldorf, Forschungszentrum Jülich, 52425 Jülich, Germany
Full list of author information is available at the end of the article

Background

For sustainable application, enzyme preparations have to face several requirements, such as long-term stability under process conditions and the possibility of recycling [1]. In order to stabilize enzymes, e.g. towards organic solvents or harsh reaction conditions, immobilization is often the preferred strategy, for which a variety of methods are available [2–5]. Enzymes can be bound onto a carrier material by non-covalent adsorption with the risk of enzyme leakage, or by covalent binding, which mostly requires chemical modification using crosslinking agents. An example are cross-linked enzyme aggregates (CLEAs) [6], which do not require any carrier material and stabilize precipitated enzyme aggregates using glutaraldehyde as a crosslinking agent. Another method is encapsulation of the biocatalyst in polymeric matrices, e.g. in a highly porous sol–gel [7]. All of these methods, however, need case-to-case optimization, since at present no general-purpose strategy for immobilization is available. Moreover, most of the presented immobilization methods require previous (chromatographic) purification of the biocatalyst, which may raise production costs enormously and thus hampers industrial application [8].

We and others have previously shown that the molecular biological fusion of coiled-coil domains [9–11], small artificial peptides [12–15] and aggregation-prone proteins and domains [16–22] to a target protein, induces the intracellular formation of protein aggregates, so called inclusion bodies (IBs) [23], which, in contrast to the long held view of IBs as inactive intracellular waste deposits [24], can to a certain degree retain their function or, in case of enzymes, their catalytic activity (reviewed recently in [2, 11]. This strategy enables the combination of protein production and immobilization, resulting in (in situ) biologically-produced immobilizates, which we coined catalytically-active IBs (CatIBs) [9–11] or in case of proteins without catalytic activity, functional IBs (FIBs) [25]. Like IBs, CatIBs/FIBs contain predominantly the recombinant target protein [26]. Furthermore, they can be produced fast and cost-efficiently, because any previous purification and subsequent cross-linking steps are dispensable. These properties render the resulting particles beneficial for the application in synthetic chemistry, biocatalysis [9, 16, 27], and biomedicine [28–30].

In contrast to most of the above-mentioned strategies that employed artificial peptides or aggregation-prone proteins, our recently presented strategy relies on the fusion of a naturally-occurring coiled-coil domain for the targeted production of CatIBs/FIBs [9–11]. In these studies the tetrameric coiled-coil domain of the cell-surface protein tetrabrachion (tetramerization domain of tetrabrachion; TDoT) from *Staphylothermus marinus* [31] was fused to a variety of different target enzymes with different complexity: the lipase A from *Bacillus subtilis* (*Bs*LA), a hydroxynitrile lyase from *Arabidopsis thaliana* (*At*HNL), the thiamine-diphosphate (ThDP)-dependent enzyme MenD (2-succinyl-5-enol-pyruvyl-6-hydroxy-3-cyclohexene-1-carboxylate synthase) from *E. coli* (*Ec*MenD), and the pyridoxal 5′-phosphate (PLP)-dependent lysine decarboxylase from *E. coli* (*Ec*LDC), as well as the yellow fluorescent protein (YFP) [9–11]. Thus, we already demonstrated that the fusion strategy is applicable to a broad spectrum of enzymes as well as fluorescent proteins of the GFP family. In these recent studies, the application of CatIBs in biocatalysis was addressed in more detail, e.g. it could be demonstrated that *At*HNL–CatIBs revealed a higher stability at acidic pH values compared to the soluble enzyme, and could be recycled several times for the production of chiral cyanohydrins in a mono-phasic micro-aqueous reaction system consisting of the buffer-saturated organic solvent, methyl *tert*-butyl ether (MTBE) [9]. CatIBs of the constitutive L-lysine decarboxylase of *E. coli* were employed for the efficient biocatalytic production of 1,5-diaminopentane (trivial name: cadaverine) [10]. Moreover, very recently we employed the CatIB strategy for the coimmobilization of two enzymes, namely a benzaldehyde lyase from *Pseudomonas fluorescens* (*Pf*BAL) and an alcohol dehydrogenase from *Ralstonia* sp. (*R*ADH), to facilitate the realization of an integrated enzymatic two-step cascade for the production of (1*R*,2*R*)-1-phenylpropane-1,2-diol, a building block of the calcium channel blocker diltiazem [25]. The resulting *Pf*BAL/*R*ADH Co-CatIBs showed improved stability in the cascade reaction as compared to the soluble enzymes [25]. Improved stability, compared to soluble, purified *Pf*BAL, was also demonstrated for the isolated *Pf*BAL-CatIBs, while additionally it could be shown that, depending on the employed coiled-coil domain, CatIBs can be tailored for the application in different reaction systems [32]. For example, the use of the 3HAMP coiled coil, which was derived from the oxygen sensor protein Aer2 from *Pseudomonas aeruginosa*, as aggregation-inducing tag, resulted in CatIBs that were better suited for the use in biphasic aqueous-organic reaction systems, e.g. with cyclopentyl methyl ether (CPME) as organic phase [32]. In contrast, TDoT-*Pf*BAL CatIBs appeared to be better suited for the use in monophasic buffer/dimethyl sulfoxide (DMSO) mixtures [32]. While demonstrating the application potential of CatIBs, these studies did not fully address differences in aggregation (CatIB/FIB formation) efficiency and characteristics, such as the overall activity compared to the soluble purified enzyme, the composition of the particles, the final yield, or their morphology. Moreover, the flexibility of the approach,

i.e. in terms of optimization potential by fusion–protein redesign, and the structural basis for CatIB/FIB formation remain unaddressed.

To fill this gap, in the present contribution we applied our fusion strategy to different fluorescent reporter proteins and various differently complex enzymes and empirically analyzed the properties of already established CatIBs. Using this strategy, for three out of seven target proteins, CatIB/FIB formation was successful, revealing variable CatIB/FIB formation efficiency. Based on this initial success, we set out to evaluate the optimization potential for our strategy by generating redesigned fusion constructs by (i) deleting intradomain linkers, (ii) considering C-terminal instead of N-terminal TDoT fusion and (iii) by employing an alternative coiled-coil domain as aggregation-inducing tag. Employing those simple genetic optimization steps, all of the target proteins that initially failed to produce active aggregates or only did so inefficiently, could successfully be produced as CatIBs/FIBs. Using this wealth of different CatIBs/FIBs, we systematically characterized biotechnologically-relevant properties like residual activities compared to the soluble purified enzyme, yield, particle composition, and morphology. Interestingly, (electron) microscopic studies revealed differences in particle/immobilizate morphology, which could be correlated to different CatIB/FIB properties such as activity retention, yield and composition. Last but not least, we show evidence that aggregation (CatIB/FIB formation) efficiency appears to be correlated to the solvent-accessible hydrophobic surface area of the target enzyme, providing a structure-based rationale for our strategy and opening up the possibility to predict its efficacy for any given target protein.

Results and discussion

The toolbox strategy

As outlined in the introduction, our previously presented immobilization strategy relies on the molecular biological fusion of a tetrameric coiled-coil domain to a target enzyme, which induces the formation of catalytically-active inclusion bodies (CatIBs) that in case of non-catalytically-active target proteins, such as fluorescent proteins (FPs), are called functional inclusion bodies (FIBs). In its physiological context, this coiled-coil domain forms a strong superhelix [33, 34] and induces the formation of CatIBs/FIBs by a currently unknown mechanism [11]. The initial gene-fusion-containing expression plasmid was constructed from separate modules so that every part could be easily exchanged or deleted (Additional file 1: Figure S5, A). In all previous constructs the fusion protein contained an N-terminal hexahistidine (His_6) tag, followed by the TDoT domain fused N-terminally to the target enzyme, via a linker region consisting of a flexible $(GGGS)_3$-motif and a protease Factor Xa cleavage site. In contrast to our initial study [9], the starting vector used in this study did not possess the coding sequence for an N-terminal His_6 tag, as also described recently [10]. To rule out any effect of His_6-tag removal on the aggregation behaviour, quantified here as the efficiency of CatIB/FIB formation, we compared FIB formation for a TDoT-L-YFP construct with and without N-terminal His_6-tag (Additional file 1: Figure S1). CatIB/FIB formation efficiency is hereby defined as the activity, or in case of FPs, fluorescence, of the insoluble IB-containing pellet fraction (P) relative to the activity/fluorescence of the crude cell extract (CCE, set to 100%). For both constructs, similar fluorescence was detected in the insoluble IB-containing fraction of the corresponding lysates, suggesting that the His_6 tag has no influence on the aggregation inducing behaviour of the TDoT domain (Additional file 1: Figure S1). Therefore, to simplify the previous vector design, all further constructs were generated without His_6 tag.

To further validate the broad applicability of our CatIB/FIB strategy, we here employed simple FPs, for easy detection and microscopic observation of FIB formation, and generated CatIBs of various differently complex target enzymes to enable catalytic characterization. As target FPs we selected a monomeric version of the enhanced yellow fluorescent protein [35, 36] (YFP; 27.1 kDa) (for details regarding the employed YFP version see "Methods") and mCherry (26.7. kDa), a monomeric red fluorescent protein [37]. As target enzymes, two alcohol dehydrogenases (*R*ADH from *Ralstonia* sp. and *Lb*ADH from *Lactobacillus brevis*) and two ThDP-dependent enzymes [benzoylformate decarboxylase from *Pseudomonas putida* (*Pp*BFD) and benzaldehyde lyase from *Pseudomonas fluorescence* (*Pf*BAL)] were added to the CatIB toolbox. *R*ADH and *Lb*ADH are NADPH-dependent tetrameric enzymes with a subunit size of about 27 kDa [38–40]. *R*ADH requires Ca^{2+}-ions for its stability [41], whereas Mg^{2+}-ions are important for *Lb*ADH to maintain its structural integrity and catalytic activity [42]. *Pf*BAL [43] and *Pp*BFD [44–47] are thiamine-diphosphate (ThDP) and Mg^{2+}-ion dependent tetrameric enzymes with a subunit size of 60 kDa (*Pf*BAL) and 56 kDa (*Pp*BFD). CatIBs of *Pf*BAL as well as *R*ADH have recently been described [25]. For *Pp*BFD, we used the variant L476Q with enhanced carboligation activity [48]. The by far biggest enzyme tested as CatIBs is *Ec*LDC, the constitutive lysine decarboxylase from *Escherichia coli* [49]. This pyridoxal 5′-phosphate (PLP)-dependent enzyme forms a decamer that comprises five dimers with a subunit size of 80.6 kDa. The biocatalytic application of *Ec*LDC-CatIBs was recently demonstrated [10].

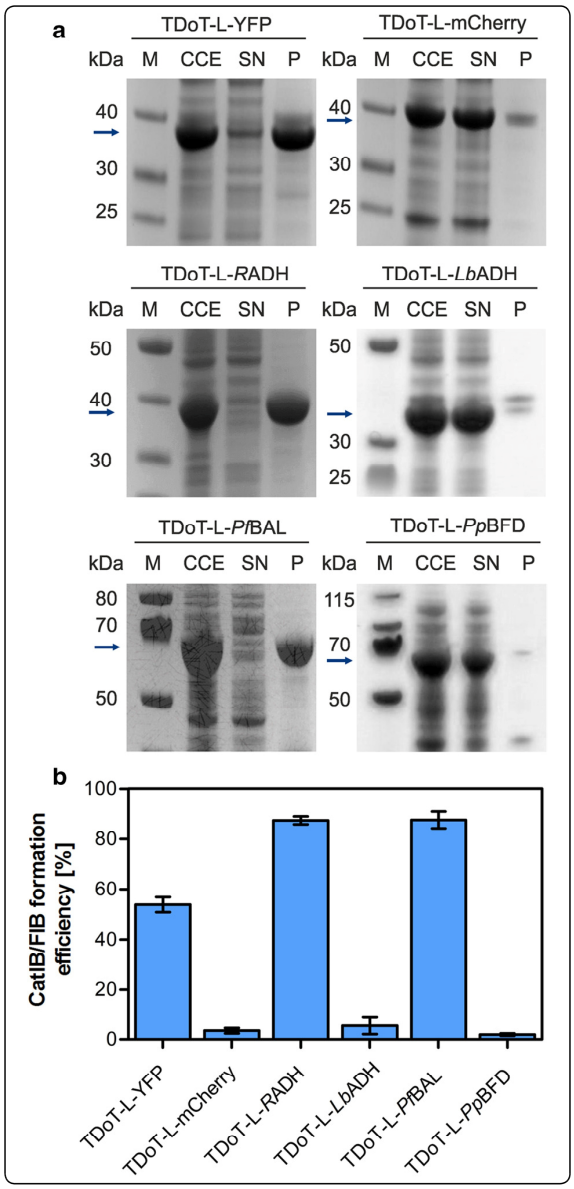

Fig. 1 Evaluation of the CatIB/FIB strategy by **a** SDS-PAGE analysis of CatIB/FIB-production and **b** CatIB/FIB formation efficiency for TDoT-L-YFP (Data taken from [25]), TDoT-L-mCherry, TDoT-L-*R*ADH (Data taken from [25]), TDoT-L-*Lb*ADH, TDoT-L-*Pf*BAL (Data taken from [25]), and TDoT-L-*Pp*BFD. After cell disruption, the crude cell extract (CCE) was separated by centrifugation into the soluble protein containing supernatant (SN) and the insoluble IB-containing pellet (P) fractions. **a** SDS-PAGE analysis of the respective protein/enzyme fractions: CCE, SN, and P. The molecular mass of the respective fusion proteins is indicated by arrows (TDoT-L-YFP: 34.6 kDa, TDoT-L-mCherry: 34.3 kDa, TDoT-L-*R*ADH: 34.3 kDa, TDoT-L-*Lb*ADH: 34.3 kDa, TDoT-L-*Pf*BAL: 66.5 kDa, TDoT-L-*Pp*BFD: 65.3 kDa). The protein content in the SN was measured using the Bradford method [87]. **b** CatIB/FIB formation efficiency quantified as the activity/fluorescence in P fractions expressed relative to the activity/fluorescence of the CCE (set to 100%). The complete datasets illustrating the distribution of activity/fluorescence in the CCE, SN and P fractions can be found in Additional file 1: Figure S2. Note: the P fraction was washed once with water and centrifuged again before the activity/fluorescence measurement. The initial rate activities of the ADHs were measured by reduction of 1-phenylethanol (TDoT-L-*Lb*ADH) or cyclohexanone (TDoT-L-*R*ADH) under the consumption of NADPH (Additional file 1: Figure S13a and b). Initial rate activities of the TDoT-L-*Pf*BAL CatIBs and the TDoT-L-*Pp*BFD CatIBs were measured by following the carboligation of 3,5-dimethoxybenzaldehyde (DMBA) to the respective benzoin or by following the decarboxylation of benzoylformate to benzaldehyde (Additional file 1: Figure S13c and d). Error bars correspond to the standard deviation of the mean derived from at least three biological replicates

Formation of CatIBs/FIBs by N-terminal TDoT fusion

Our previous design concept for immobilization of additional target proteins was validated by fusing the TDoT-domain N-terminally to the above described target proteins following the fusion strategy depicted in Additional file 1: Figure S5a. CatIBs/FIBs were produced and purified using a standardized protocol [9, 10]. This protocol included standardized expression of the gene fusions in *E. coli* BL21(DE3), cell disruption and fractionation of the resulting crude cell extract (CCE) by centrifugation to separate the soluble protein containing fraction (supernatant, SN) from the insoluble, CatIB/FIB-containing fraction (pellet, P). To remove any eventually present soluble protein from the IB pellet, the pellet was resuspended in water, and subsequently centrifuged to separate again the supernatant from the CatIB/FIB containing pellet. All fractions were analyzed by SDS-PAGE (Fig. 1a) and CatIB/FIB formation efficiency was quantified as the activity, or in case of FPs the fluorescence of the once washed IB-containing pellet faction (P) relative to the activity/fluorescence of the CCE (set to 100%) (Fig. 1b). For clarity, only the relative activity in the washed CatIB/FIB-containing pellet fraction is shown in Fig. 1b. The complete datasets illustrating the distribution of activity/fluorescence in the CCE, SN and P fractions can be found in Additional file 1: Figure S2).

Whereas for both TDoT-L-*R*ADH and TDoT-L-*Pf*BAL > 80% of the CCE activity was found in the pellet fraction, only 40% of the YFP fluorescence was detected in the pellet, indicating that, our strategy works less efficient for YFP (Fig. 1b). For TDoT-L-mCherry, TDoT-L-*Lb*ADH, and TDoT-L-*Pp*BFD, this effect was even more pronounced, as for these fusions barely any activity/fluorescence could be detected in the IB-containing pellet fraction (Fig. 1b), whereas the majority of the CCE activity was present in the soluble (SN) fraction (Additional

file 1: Figure S2). The same overall trend was also seen in the corresponding SDS-PAGE analyses. The TDoT-L-*Ec*LDC fusion formed large amounts of insoluble aggregates (Additional file 1: Figure S6), which, however, did barely possess any detectable activity ($k_{cat} = 6.2*10^{-7}\ s^{-1}$). In conclusion, our previously presented fusion strategy, relying on the N-terminal fusion of the TDoT coiled-coil domain, was successful for three out of seven of the tested target proteins/enzymes. To evaluate the potential for optimization, we modified our initial strategy generating redesigned fusion constructs by (i) deleting intra-domain linkers, (ii) considering C-terminal instead of N-terminal TDoT fusion and (iii) by employing an alternative coiled-coil domain as aggregation inducing tag.

Concepts to improve the CatIB/FIB formation efficiency

Deletion of the linker region

From previous studies it is known that the linker employed for fusion protein design can have a large impact on fusion protein functionality [50, 51]. Therefore, as a first optimization approach, the influence of deleting the linker polypeptide that in our fusion proteins connect the TDoT coiled-coil domain with the target enzyme/protein, was exemplarily tested for the TDoT-L-mCherry fusion protein, which almost exclusively remained in the supernatant (SN) after cell disruption (96.8%) (Additional file 1: Figure S2a) and barely any fluorescence was detectable in the insoluble FIB-containing pellet (Fig. 1b). Additionally, the same optimization strategy was tested for TDoT-L-YFP, for which only 40% of the total fluorescence of the CCE was found in the pellet fraction (Fig. 1b and Additional file 1: Figure S2a). Therefore, the fusion variants TDoT-YFP and TDoT-mCherry were generated, which lack the $(GGGS)_3$ linker motif as well as the Factor Xa cleavage site (Additional file 1: Figure S5a). Deletion of the linker resulted in about 10% increased fluorescence in the FIB-containing pellet fraction (P) of TDoT-YFP. The improvement was more pronounced for TDoT-mCherry. Here, the fluorescence in the pellet fraction increased by almost 30% (Fig. 2), which is also apparent from the corresponding SDS-PAGE analysis (Fig. 2a; compare to Fig. 1a; TDoT-L-mCherry).

This improvement of the FIB-formation efficiency might hereby be related to a higher rigidity of the fusion protein, due to deletion of the linker. In conclusion, linker deletion appears to be one suitable strategy to improve the CatIB/FIB formation efficiency for difficult target proteins.

C-terminal TDoT-domain fusion

When designing N-terminal or C-terminal fusion proteins of multimeric proteins, it is instrumental to consider

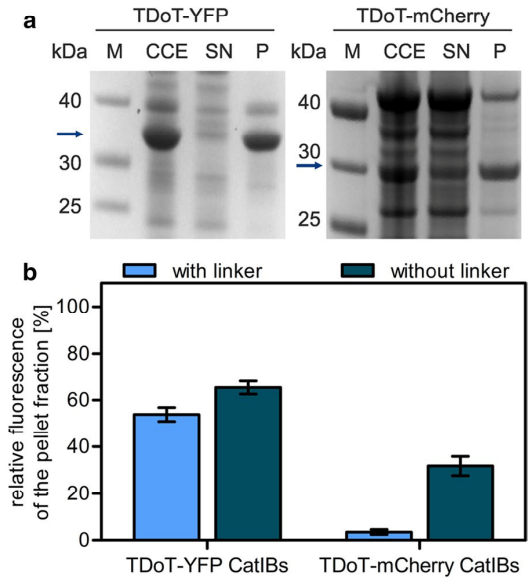

Fig. 2 Optimization of the CatIB strategy by excision of the linker region. CatIB formation was evaluated by **a** SDS-PAGE analysis and **b** FIB formation efficiency for TDoT-YFP and TDoT-mCherry (Data taken from [25]) without linker (dark blue bars) compared to TDoT-L-YFP (Data taken from [25]) and TDoT-L-mCherry with linker (light blue bars). After cell disruption, the crude cell extract (CCE) was separated by centrifugation into the soluble protein containing supernatant (SN) and the insoluble FIB-containing pellet (P) fraction. Sample preparation for SDS-PAGE analysis and determination of the FIB formation efficiency was carried out as described in Fig. 1. **a** SDS-PAGE analysis of the respective protein fractions: CCE, SN, and P. The molecular mass of the target fusion proteins is indicated by arrows (TDoT-YFP: 33.1 kDa, TDoT-mCherry: 32.7 kDa). **b** FIB formation efficiency quantified as the fluorescence in P fractions expressed relative to the fluorescence of the CCE (set to 100%). The complete datasets illustrating the distribution of fluorescence in the CCE, SN and P fractions can be found in Additional file 1: Figure S3. Error bars correspond to the standard deviation of the mean derived from at least three biological replicates

steric constrains imposed by the quaternary structure, i.e. with regard to the location of the termini. We therefore analyzed the structures of all our multimeric target proteins (*R*ADH, *Lb*ADH, *Pf*BAL, *Pp*BFD and *Ec*LDC) for the accessibility of the N- and C-terminus (Additional file 1: Figure S4). For *R*ADH, *Lb*ADH, *Pf*BAL and *Pp*BFD, the N-termini are localized at the protein surface facing outwards and should thus be accessible for TDoT fusion (Additional file 1: Figure S4a–d) without impacting the formation of the multimer. Thus, C-terminal TDoT fusion was not considered in these cases. In contrast, in *Ec*LDC, the N-termini are buried within the decameric structure of the *Ec*LDC multimer, whereas the C-terminus is located at the protein surface [52] (Additional file 1: Figure S4e). Therefore, N-terminal fusion of the TDoT tag appears not

Table 1 Characteristics of CatIBs/FIBs All constructs were characterized regarding CatIB/FIB formation efficiency, quantified as the relative activity of the insoluble CatIB/FIB-containing pellet fraction compared to the crude cell extract (set to 100%), the initial rate activity (k_{cat}; $\mu mol_{Product}$ s^{-1}, per subunit) of the lyophilized CatIB preparation, activity retention compared to the soluble enzyme, the relative protein and lipid content based on the initial weight of the lyophilizate and the yield of CatIBs obtained from 100 g wet *E. coli* cells

Construct	CatIB/FIB formation efficiency [%]	Activity k_{cat} [s^{-1}]	Residual activity [%][d]	Rel. protein content lyophilizate [%]	Yield $\frac{g_{lyophilizate}}{100 g_{cells}}$ g	Lipid content [%]
Constructs showing robust CatIB/FIB formation efficiency						
TDoT fusions						
TDoT-L-YFP	53.8 ± 7.4 (6)[b]	na	na	70.0 ± 5.3 (4)	4.9 ± 0.6 (3)	nd
TDoT-YFP	65.4 ± 4.9 (3)	na	na	69.2 ± 6.8 (2)	5.5 (1)	nd
TDoT-mCherry	31.8 ± 8.2 (4)[b]	na	na	85.7 ± 8.3 (2)	3.2 (1)	nd
TDoT-L-*Bs*LA[a]	114.1 ± 3.1 (1)	nd	nd	79 (1)	8.6 (1)	nd
TDoT-L-*At*HNL[a]	76.4 ± 3.5 (1)	4.3 ± 0.2 (1)	11.1	85 (1)	7.3 (1)	nd
TDoT-L-*Ec*MenD[a]	90.3 ± 0.2 (1)	nd	nd	93 (1)	12.2 (1)	nd
TDoT-L-*R*ADH	87.5 ± 3.2 (4)[b]	0.054 ± 0.008 (3)[b]	2.0[b]	84.6 ± 3.9 (3)[b]	9.7 ± 1.7 (4)[b]	14.3 ± 0.3 (1)
TDoT-L-*Pf*BAL	87.7 ± 6.8 (4)[b]	0.77 ± 0.12 (4)[b,c]	1.0[b,c]	71.9 ± 4.5 (4)[b,c]	8.8 ± 1.0 (8)[b]	16.4 ± 1.0 (1)[c]
TDoT-*Ec*LDC	nd	$6.2*10^{-7}$ (1)	nd	nd	nd	nd
*Ec*LDC-L-TDoT	nd	0.71 (1)[e]	nd	67.9 ± 5.9 (3)[e]	12.4 ± 3.0 (3)	12.9 ± 3.2 (1)
3HAMP fusions						
3HAMP-L-*R*ADH	75.4 ± 3.7 (4)	0.33 ± 0.02 (3)	12.0	50.9 ± 7.6 (3)	3.8 ± 0.5 (3)	30.6 ± 8.3 (1)
3HAMP-L-*Pf*BAL	75.8 ± 8.0 (5)	13.9 ± 2.9 (3)[c]	18.1[c]	33.8 ± 5.2 (3)[c]	3.3 ± 0.5 (4)	30.1 ± 4.7 (1)[c]
3HAMP-L-*Lb*ADH	67.0 ± 21.7 (3)	0.60 ± 0.20 (3)	1.0	54.6 ± 8.0 (3)	8.1 ± 1.3 (3)	34.7 ± 1.36 (1)
3HAMP-L-*Pp*BFD	61.3 ± 35.4 (3)	23.4 ± 6.1 (4)	10.3	35.5 ± 6.7 (4)	6.6 ± 1.4 (3)	27.9 ± 3.7 (1)
*Ec*LDC-L-3HAMP	nd	0.80 (1)	nd	56.5 ± 6.5 (2)	7.5 ± 6.5 (4)	17.7 ± 0.6 (1)
Constructs showing low CatIB/FIB formation efficiency						
TDoT-L-mCherry	3.5 ± 1.9 (3)	na	na	15.8 ± 0.5 (1)	2.8 (1)	nd
TDoT-L-*Lb*ADH	5.4 ± 5.9 (3)	3.63 ± 0.90 (3)	5.8	43.4 ± 5.5 (3)	2.5 ± 0.4 (3)	25.2 ± 0.73 (1)
TDoT-L-*Pp*BFD	1.2 ± 0.6 (3)	9.2 ± 4.7 (4)	4.1	26.9 ± 4.1 (4)	1.6 ± 0.7 (3)	19.1 ± 0.8 (1)
3HAMP-L-YFP	6.3 ± 3.2 (4)	na	na	49.0 ± 5.7 (3)	5.4 ± 1.0 (3)	nd
3HAMP-L-mCherry	5.5 ± 0.2 (5)	na	na	36.4 ± 4.1 (4)	3.0 ± 0.9 (4)	nd

[a] Data taken from [9]

[b] Data taken from [25]

[c] Data taken from [32]

[d] Residual activity (k_{ca}, µmol product, per subunit) relative to the activity of the corresponding soluble purified enzyme: (*R*ADH: $k_{cat} = 2.76 \pm 0.04\ s^{-1}$; *Pf*BAL: $k_{cat} = 76.7 \pm 2.3\ s^{-1}$; *Lb*ADH: $k_{cat} = 62.2 \pm 6.7\ s^{-1}$; *Pp*BFD: $k_{cat} = 226 \pm 40\ s^{-1}$)

[e] Data given in or derived from [10]. Numbers in brackets refer to the numbers of the biological replicates that were used to obtain error estimates. na: not applicable; nd: not determined

to be feasible for *Ec*LDC, which is corroborated by the observation that the resulting TDoT-L-*Ec*LDC CatIBs, although formed in large amounts, showed barely any activity ($k_{cat} = 6.2*10^{-7}\ s^{-1}$; vide infra, Table 1). At least dimerization of *Ec*LDC is necessary to form the active site [52, 53]. Thus, it is likely that the N-terminal fusion of the TDoT domain impairs the formation of a correctly folded active site. To improve activity and potentially the CatIB-formation efficiency, we modified our initial TDoT-L-*Ec*LDC construct (Additional file 1: Figure S5a) by shifting the TDoT domain from the N-terminus to the C-terminus of *Ec*LDC (Additional file 1: Figure S5b), resulting in *Ec*LDC-L-TDoT. SDS-PAGE analysis of the resulting *Ec*LDC-L-TDoT CatIBs revealed, similar to the N-terminal fusion, large amounts of protein in the insoluble IB-containing pellet fraction (Additional file 1: Figure S6). However, in contrast to the N-terminal fusion, the activity of the final *Ec*LDC-L-TDoT-CatIB lyophilizate was increased by six orders of magnitude ($k_{cat} = 0.71\ s^{-1}$). In conclusion, for target proteins for which structural information is available, the position and accessibility of the N- and C-termini should be considered when generating TDoT fusion proteins to induce CatIB formation, whereas

for target proteins with unknown structure both, N-and C-terminal fusions may be considered.

Fusion to a different coiled-coil domain

To improve the CatIB/FIB formation efficiency, the exchange of the TDoT-domain by another coiled-coil domain was considered as further optimization option. As an alternative to TDoT, the 3HAMP-domain [HAMP: histidine kinases, adenylyl cyclases, methyl-accepting chemotaxis proteins (MCPs), and phosphatases], which is part of the soluble oxygen sensor Aer2 of *P. aeruginosa* [54], was selected. The 3HAMP domain was chosen because of its larger size (172 amino acids) compared to the rather short TDoT coiled-coil domain (52 amino acids), with the rationale in mind that for larger target proteins larger coiled-coils might be needed to facilitate efficient CatIB/FIB formation. Therefore, as the next logical optimization step, we generated fusion proteins for *Lb*ADH and *Pp*BFD, which instead of TDoT were fused to the 3HAMP domain. As in case of our initial fusion strategy and in light of the above described structure analyses (Additional file 1: Figure S4; see chapter "*C-terminal TDoT-domain fusion*"), the 3HAMP domain was fused to the N-terminus of the respective target enzyme, resulting in the constructs 3HAMP-L-*Lb*ADH and 3HAMP-L-*Pp*BFD. Interestingly, for both target enzymes N-terminal 3HAMP-fusion drastically increased the CatIB-formation efficiency, as evidenced by both SDS-PAGE analysis (Fig. 3a; compare to TDoT-L-*Lb*ADH and TDoT-L-*Pp*BFD in Fig. 1a) and activity measurements of the CatIB-containing pellet fraction after fractionation of the corresponding crude cell extracts (Fig. 3b). Compared to the corresponding TDoT fusions (see also Fig. 1b), the CatIB-formation efficiency was increased 12- and 51-fold for 3HAMP-L-*Lb*ADH and 3HAMP-L-*Pp*BFD, respectively.

Prompted by these results, we also generated 3HAMP fusions of the remaining target proteins and quantified CatIB formation efficiency (Fig. 3c, d). While for YFP and mCherry the FIB formation efficiency was low, i.e. compared to the corresponding best performing TDoT construct (Fig. 2), clear CatIB formation was observed for 3HAMP-L-*Pf*BAL and 3HAMP-L-*R*ADH (Fig. 3c, d). In conclusion, the 3HAMP domain apparently can replace TDoT as a tag to induce CatIB/FIB formation and appears to be a valid alternative for difficult targets, for which the TDoT fusion approach fails.

Comparative characterization of TDoT and 3HAMP CatIBs/FIBs

As shown above, we were able to successfully produce CatIBs/FIBs for all of the seven tested target enzymes/proteins by optimizing our initial TDoT fusion strategy. To elucidate potential differences between CatIBs/FIBs produced by TDoT and 3HAMP fusion, we characterized all obtained CatIBs and FIBs with regard to yield ($g_{lyophilizate}$ per 100 g wet *E. coli* cells), composition (relative protein and lipid content), specific activity (k_{cat}), and residual activity compared to the respective soluble purified target enzymes, where possible. The corresponding data is summarized in Table 1 (see also Additional file 1: Figure S8 for details). Some of this data has been presented before, e.g. as part of CatIB application studies [10, 25, 32]. For comparison we also included the respective values (if available) from our first CatIB study, in which we demonstrated CatIB formation by TDoT fusion to the lipase A from *Bacillus subtilis* (*Bs*LA), a hydroxynitrile lyase from *Arabidopsis thaliana* (*At*HNL), and the thiamine-diphosphate (ThDP)-dependent enzyme MenD (2-succinyl-5-enol-pyruvyl-6-hydroxy-3-cyclohexene-1-carboxylate synthase) from *E. coli* (*Ec*MenD) [9].

To provide a better overview, we grouped the different constructs into two categories (i) TDoT and 3HAMP fusion constructs showing robust CatIB/FIB formation and (ii) constructs that only showed low CatIB/FIB formation efficiency (< 10%), irrespective of whether they were fused with TDoT or 3HAMP. The latter category contained constructs of the initial round of experiments, where the TDoT domain was fused N-terminally to the target protein/enzyme (TDoT-L-mCherry, TDoT-L-*Lb*ADH, TDoT-L-*Pp*BFD; see chapter "*Formation of CatIBs/FIBs by N-terminal TDoT fusion*") as well as constructs fused with the 3HAMP domain (3HAMP-L-YFP and 3HAMP-L-mCherry; see chapter "*Fusion to a different coiled-coil domain*"). Compared to the constructs with robust CatIB/FIB formation efficiency those preparations showed low to moderate protein content (16–49%) and lyophilizate yields (1.6–5.4 g lyophilizate per 100 g wet cells) as well as low lipid content (19–25%). In terms of yield and composition those values likely derive from cellular constituents, which remain in the insoluble pellet after cell lysis and centrifugation, i.e. non-lysed cells, cell debris, membrane proteins, and membrane lipids. Surprisingly, the CatIB preparations of TDoT-L-*Lb*ADH and TDoT-L-*Pp*BFD, for which we only observe low CatIB formation efficiency (1.2–5.4% of the overall crude cell extract activity), still showed activities that correspond to 5.8% (TDoT-L-*Lb*ADH) and 4.1% (TDoT-L-*Pp*BFD) of the activity of the corresponding soluble purified enzymes. Several explanations could account for this phenomenon. First, the observed activities result from intact non-lysed cells, containing the respective soluble produced fusion protein, which would require that the substrates used for the activity assays can be taken up by these cells. Likewise, those intact cells could become

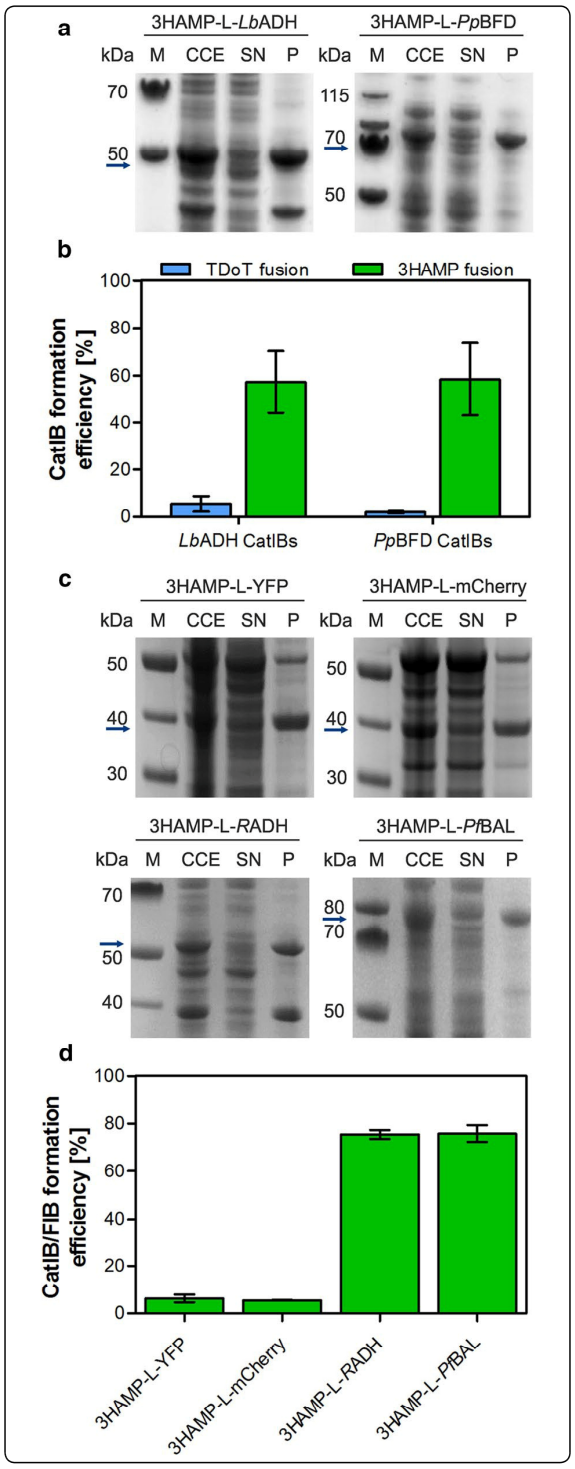

Fig. 3 Optimization of the CatIB strategy by variation of coiled-coil domains using 3HAMP instead of TDoT fusions. CatIB formation was evaluated by **a** SDS-PAGE analysis and **b** CatIB formation efficiency for 3HAMP-L-*Lb*ADH- and 3HAMP-L-*Pp*BFD (green bars) compared to TDoT-L-*Lb*ADH and TDoT-L-*Pp*BFD (blue bars). Panels c) and d) contain the equivalent data for 3HAMP-L-YFP, 3HAMP-L-mCherry, 3HAMP-L-*Pf*BAL and 3HAMP-L-*R*ADH. After cell disruption, the crude cell extract (CCE) was separated by centrifugation into the soluble protein containing supernatant (SN) and the insoluble IB containing pellet (P) fraction. Sample preparation for SDS-PAGE analysis and the determination of the CatIB/FIB formation efficiency was carried out as described in Fig. 1. **a**, **c** SDS-PAGE analysis of the respective protein fractions: CCE, SN, and P. The molecular mass of the target fusion proteins is indicated by arrows (3HAMP-L-*Lb*ADH: 47.1 kDa; 3HAMP-L-*Pp*BFD: 77.0 kDa, 3HAMP-L-YFP: 47.4 kDa, 3HAMP-L-mCherry: 47.1 kDa, 3HAMP-L-*R*ADH: 47.1 kDa and 3HAMP-L-*Pf*BAL: 79.3 kDa). **b**, **d** CatIB/FIB formation efficiency determined as described in Fig. 1. The complete datasets illustrating the distribution of activity in the CCE, SN and P fractions can be found in Additional file 1: Figure S7. Initial rate activities were measured as described in Fig. 1

(partially) lysed during lyophilization of the washed pellet, which would result in the release of the soluble produced fusion protein and hence could account for the observed activity. Secondly, those constructs might indeed form intracellular CatIBs, which, however, disintegrate or are solubilized during the washing step of the CatIB preparation procedure. The latter hypothesis should be observable by SDS-PAGE analyses, i.e. by the appearance of target fusion protein bands in the soluble wash fractions retrieved during the CatIB preparation procedure. Indeed, compared to TDoT-L-*Pf*BAL (Additional file 1: Figure S9c), increased solubilization/leakage of the fusion proteins is observed during the preparation of the TDoT-L-*Lb*ADH and TDoT-L-*Pp*BFD CatIBs (Additional file 1: Figure S9a and b).

Among the constructs showing robust CatIB/FIB formation, all CatIBs/FIBs produced by TDoT fusion, with the exception of the FPs, which showed FIB formation efficiencies between approx. 32% (TDoT-mCherry) and 65% (TDoT-YFP), showed higher CatIB/FIB formation efficiencies [between 76% (TDoT-L-*At*HNL) and 114% (TDoT-L-*Bs*LA)] compared to the 3HAMP fusions [between 61% (3HAMP-L-*Pp*BFD) and 76% (3HAMP-L-*Pf*BAL)]. Here, either less efficient CatIB/FIB formation or partial solubilization/leakage of the fusion protein during the CatIB/FIB preparation procedure might be potential causes. The latter is supported by SDS-PAGE analysis (Additional file 1: Figure S10), where for both 3HAMP-L-*Lb*ADH as well as 3HAMP-L-*Pp*BFD increased leakage/solubilization is observed during the washing steps performed for CatIB/FIB preparation (Additional file 1: Figure S10, compare to TDoT-*L*-*Pf*BAL, Additional file 1: Figure S9c).

Interestingly, in terms of activity (expressed as k_{cat} to account for the differences in molecular mass between the TDoT and 3HAMP fusions and the respective soluble purified enzymes) and residual activity (compared to the respective soluble enzyme), the 3HAMP CatIBs generally seem to outperform the TDoT CatIBs. With the exception of TDoT-L-*At*HNL the TDoT CatIBs showed residual activities of 1–2% of the respective soluble purified enzyme, while the 3HAMP CatIBs possessed residual activities between 10% (3HAMP-L-*Pp*BFD) and 18% (3HAMP-L-*Pf*BAL). For example, the direct comparison between equivalent TDoT and 3HAMP fusions revealed a 6- and 18-fold increase in k_{cat} and residual activity for the 3HAMP-*R*ADH and 3HAMP-*Pf*BAL CatIBs, respectively (Table 1).

The observed differences in activity between TDoT and 3HAMP CatIBs are also manifested in differences in CatIB/FIB composition. Here, the relative protein content of the respective lyophilizates was higher for the TDoT CatIBs/FIBs (between 66% [*Ec*LDC-L-TDoT) and 93% (TDoT-L-*Ec*MenD)] compared to the corresponding 3HAMP CatIBs/FIBs [between 34% (3HAMP-L-*Pf*BAL) and 57% (*Ec*LDC-L-3HAMP)]. The lower protein content of the 3HAMP CatIBs/FIBs, however, was accompanied by increased lipid content (approx. 2-fold higher than for the tested TDoT CatIBs/FIBs).

With the exception of the FPs, in terms of yield we routinely obtain 7.3–12.2 g of CatIB lyophilizate per 100 g wet cells of TDoT CatIBs, while for the 3HAMP CatIBs somewhat lower yields of 3.3–8.1 g of CatIB lyophilizate per 100 g wet cells were obtained.

In conclusion, CatIBs/FIBs derived from TDoT or 3HAMP fusion appear to possess different characteristics. Most interestingly the here described 3HAMP CatIBs showed much higher residual activities than the TDoT-derived CatIBs, which would be advantageous for application. This might be related to a less dense packing of the 3HAMP CatIBs, which would enable better substrate access and could result in higher activities. This hypothesis is supported by the observation that 3HAMP CatIBs more easily disintegrate during CatIB preparation (vide supra, see Additional file 1: Figure S10). As a carrier-free immobilization method, CatIBs can be best compared to cross-linked enzyme aggregates (CLEAs), which showed residual activities of 6–100% based on the initial activity of the enzyme preparation (usually crude cell extracts) before immobilization [55–63]. In the case of CatIBs, as in situ produced immobilizates, we cannot determine the initial total activity before the immobilization process but can only refer to k_{cat} of the purified soluble enzyme. Although a direct comparison of residual activities is not possible, it can be concluded that 3HAMP CatIBs possess residual activities that are at least comparable to certain CLEA preparations. However, compared to CLEAs, CatIBs can be produced more easily and more straightforward involving only cell lysis, centrifugation, and washing steps, i.e. not requiring tedious and expensive enzyme purification, precipitation, and/or cross-linking.

Morphology of the CatIBs

The distinct characteristics observed here for the TDoT and 3HAMP CatIBs/FIBs hint at distinct molecular differences, which might be observable as different CatIB/FIB morphologies. We therefore comparatively investigated the morphology of the different CatIBs/FIBs by conventional (fluorescence) microscopy and scanning electron microscopy (SEM). Hereby, IBs are known to form dense refractive particles at the cell poles in *E. coli*, which can be observed by conventional microscopy [64]. Previous SEM studies of isolated IBs revealed round or barrel like shapes with a size between 300 nm and 1 µm [9, 30, 65, 66].

As a first step, microscopic images of *E. coli* cells after production of different CatIBs/FIBs were taken (Fig. 4). Phase-contrast images were acquired for all preparations and fluorescence detection was used to directly visualize FIB formation for the YFP and mCherry FIBs (Fig. 4a–f); the latter providing additional insight into the localization and morphology of the resulting IB particles. Therefore, we first focused on the different FIB producing constructs. For all TDoT-fusions of YFP and mCherry (with or without the linker region), defined particles were visible at the cell poles, in both phase-contrast and fluorescence images. Interestingly, the construct TDoT-L-mCherry, which showed only low FIB formation efficiency (Fig. 1; Table 1), still shows intracellular FIB formation (Fig. 4d), indicating that the particles are less stable/compact and thus disintegrate more or less completely during cell lysis or later CatIB preparation steps. The same, although to a lesser degree, might be the case for TDoT-L-YFP, as also lower than average FIB formation efficiencies were observed here (Fig. 1, Table 1). In contrast, the 3HAMP-FIBs of YFP and mCherry show no distinct cell-pole localized IB particles in phase-contrast. The corresponding fluorescence images, however, reveal that the fusion proteins are partly distributed throughout the cytoplasm and are partly membrane associated (Fig. 4c, f). In a few cells, less well-defined bright fluorescent spots are found at the cell poles. This is in accordance to the low FIB formation efficiency observed for 3HAMP-L-YFP and 3HAMP-L-mCherry (Fig. 3), and indicates that, indeed, the 3HAMP-derived CatIBs/FIBs might possess a different morphology.

To address this issue, we next acquired phase-contrast images for the remaining 3HAMP and TDoT fusion

constructs (Fig. 4g–k). Here, only the TDoT-fusion of *R*ADH (g), *Pf*BAL (i), and *Ec*LDC (k) as well as the 3HAMP-fusion of *Ec*LDC (k), which also showed robust CatIB formation efficiencies (Fig. 1, Table 1), gave visible CatIB formation. With the exception of the *Ec*LDC-L-3HAMP fusion, which clearly showed intracellular IB formation, all 3HAMP fusions did not show distinct IB particles in the corresponding phase-contrast images.

At the first glance, this appears contradictory to the robust CatIB formation efficiency and the high specific activity (Table 1) observed for e.g. 3HAMP-L-*R*ADH and 3HAMP-L-*Pf*BAL (Fig. 3, Table 1). In principle, two explanations could account for this discrepancy. First, although unlikely, the respective 3HAMP CatIBs are not formed inside the cell and only aggregate into particles after cell disruption. Secondly, the particles are formed within the cell but possess a less dense and more diffuse structure, so that they are not detectable as refractive particles in phase-contrast images. The observed membrane association and the presence of bright fluorescent spots at the cell poles of the 3HAMP mCherry and YFP fusions (Fig. 4c, f) would support the latter possibility. A more diffuse, less densely packed structure would also account for the higher activities observed for the 3HAMP CatIBs, as such particles would enable better substrate accessibility. Likewise, partial membrane association would also explain the increased lipid content of the 3HAMP CatIBs, as membrane lipids might become co-purified together with the CatIBs.

Further, more detailed insight into those morphological features might be gained by scanning SEM. Therefore, we exemplarily acquired SEM images for a set of TDoT and 3HAMP CatIBs (Fig. 5).

As expected, the TDoT-YFP and the TDoT-L-*Pf*BAL CatIBs form classical IBs with round or barrel-like shapes and a size between 500 nm and about 1 µm (Fig. 5a, c). Interestingly, the structures of the corresponding 3HAMP CatIBs appear less well ordered, forming sheets of micrometer-sized flakes, which, however, appear to consist of smaller substructures (Fig. 5b, d).

In conclusion, the TDoT and 3HAMP CatIBs, which possess different characteristics such as residual activity

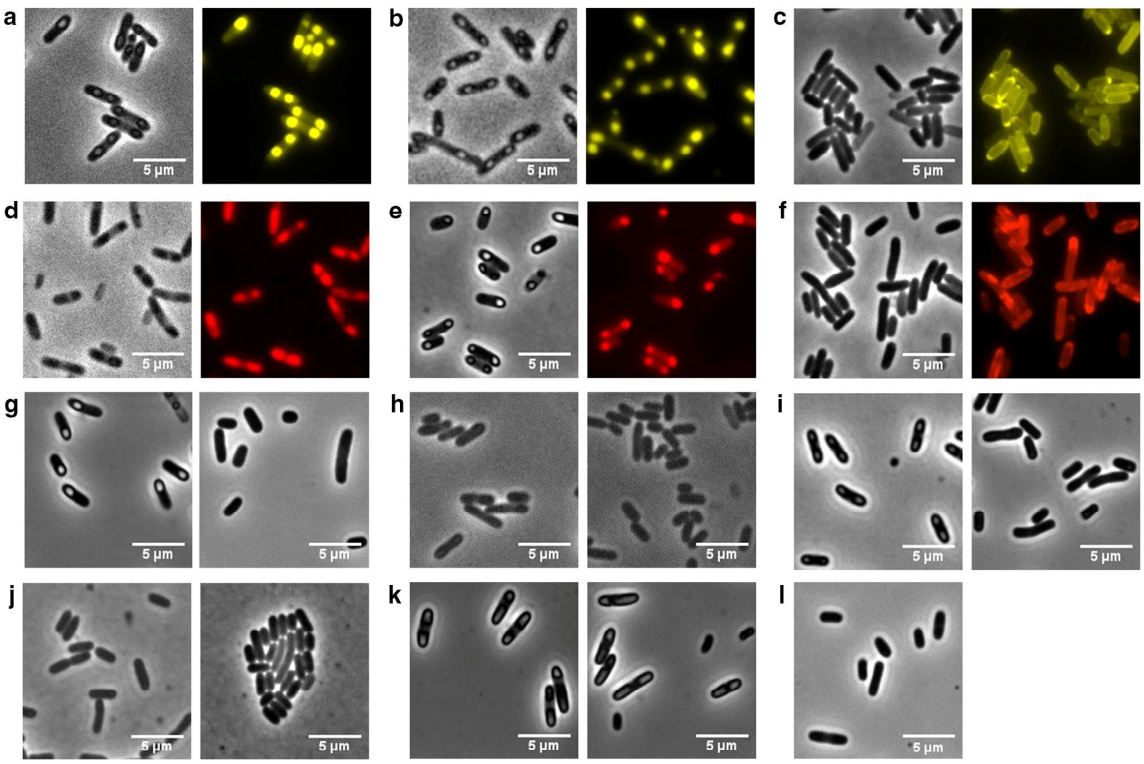

Fig. 4 Microscopy images illustrating CatIB/FIB formation in *E. coli*. **a**–**f** Phase-contrast and fluorescence images of *E. coli* cells expressing **a** TDoT-L-YFP, **b** TDoT-YFP, **c** 3HAMP-L-YFP, **d** TDoT-L-mCherry, **e** TDoT-mCherry, and **f** 3HAMP-mCherry. **g**–**k** phase-contrast images of TDoT fusion (left) and 3HAMP fusion (right) expressing *E. coli* cells containing **g** *R*ADH, **h** *Lb*ADH, **i** *Pf*BAL, **j** *Pp*BFD, **k** *Ec*LDC (here, the coiled-coil domain is fused C-terminally), and **l** *E. coli* BL21(DE3) with empty pET-28a vector. All strains were grown under standard growth conditions as described in "Methods" section

and composition, also show clearly distinct morphology. Moreover, the more diffuse, less densely packed structure of the 3HAMP CatIBs could account for the improved activity compared to the compact, well ordered TDoT CatIBs. To the best of our knowledge this morphological distinction has not been observed before.

Relationship between target sequence, structure, and CatIB formation

The fact that fusing the TDoT coiled-coil domain to certain target proteins resulted in low CatIB/FIB formation efficiencies (Fig. 1, Table 1), while others showed robust aggregate formation (although with variable efficacy), indicates that certain sequence- or structural-features are a prerequisite for CatIB/FIB formation and/or determine the efficiency of the aggregation process. This rationale includes the observation that certain CatIBs/FIBs appear to more easily disintegrate during CatIB/FIB preparation, as this phenomenon likewise results in lower apparent CatIB/FIB formation efficiencies.

We therefore initially analyzed the here employed target proteins as well as the corresponding TDoT fusions for their propensity to aggregate using sequenced-based predictions, as recent studies have indicated that the propensity for IB formation is linked to certain aggregation-prone sequence stretches [11, 67–69]. Hereby, the aggregation propensity of unfolded polypeptide chains appears to be correlated to physicochemical properties like hydrophobicity, secondary structure propensity and charge [70], which can be inferred from the amino acid sequence of both the target protein and the fusion [71]. We here used AGGRESCAN, one of the more widely employed tools for the prediction of aggregation hot spots [72]. In Fig. 6a, the CatIB/FIB formation efficiency (Table 1) of all TDoT fusions was plotted against the AGGRESCAN-derived Na^4vSS score (for further explanations see "Methods"; Additional file 1: Table S1). With the exception of *Lb*ADH and the *Pp*BFD (which both did not form classical, compact CatIBs when fused to the TDoT domain; Fig. 4h, j), there seems to be a weak linear relationship between the Na^4vSS values of the target proteins and the CatIB-formation propensity (outliers were *Lb*ADH and *Pp*BFD; $R^2 = 0.735$ when excluding outliers and $R^2 = 0.353$ when including outliers). Here, target proteins that yield low Na^4vSS values (mCherry, YFP; Additional file 1: Table S1) also yield lower activities/fluorescence in the insoluble fraction. Such low aggregation propensities (i.e. high negative Na^4vSS values) have been for example inferred for intrinsically disordered proteins (IDPs) [72], which are generally very resistant to aggregation and often remain soluble even after boiling [73, 74]. In contrast, the majority of the here employed target proteins showing robust CatIB-formation yield Na^4vSS values between −5 and +5 (Additional file 1: Table S1). Thus, they show aggregation propensities well within the range reported for globular, soluble, and IB-forming polypeptides [72].

We next tried to address the influence of fusing the TDoT coiled-coil domain to any given target by calculating the relative change of the Na^4vSS value due to

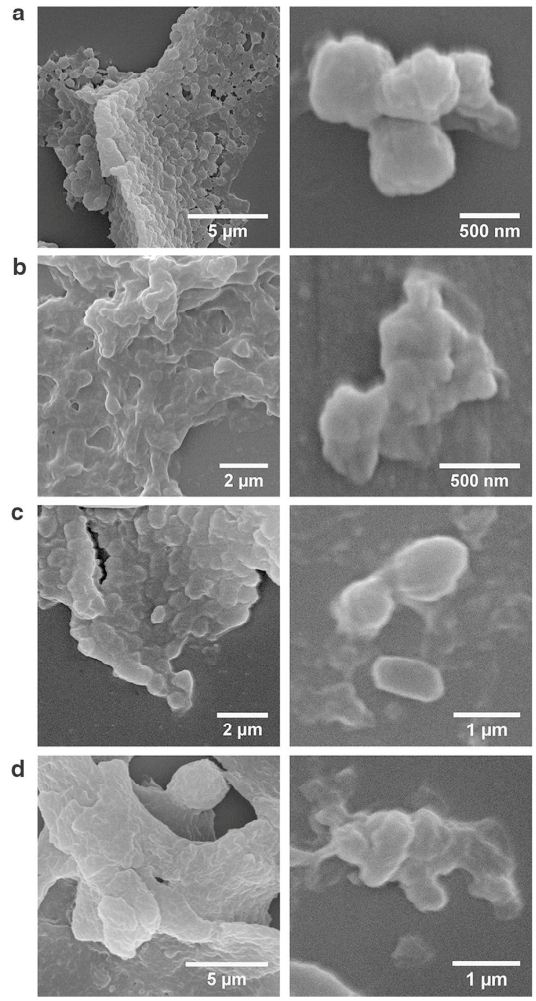

Fig. 5 SEM images of **a** TDoT-YFP, **b** 3HAMP-L-YFP, **c** TDoT-L-*Pf*BAL, and **d** 3HAMP-L-*Pf*BAL CatIBs/FIBs at different magnification. Overview images are shown on the left and detailed images at higher magnification illustrating the smallest particles found in the corresponding preparations are shown on the right. SEM samples were prepared from the final lyophilized CatIB/FIB preparations. Samples were prepared and SEM images were acquired as described in "Methods" section

addition of the TDoT domain (ΔNa^4vSS) (Fig. 6b; Additional file 1: Table S1). Here, no clear trend was observed. On the contrary, while some of the targets that show little aggregation or no classical compact CatIBs (mCherry, *Lb*ADH, *Pp*BFD, YFP) exhibit low positive or low negative ΔNa^4vSS values, the *Bs*LA and *At*HNL fusions, which display robust CatIB formation, show the most prominent (−275% and −51%) change in Na^4vSS by addition of the TDoT domain. This suggests that the TDoT fusion should increase their solubility, which however was not observed experimentally (Additional file 1: Table S1). In conclusion sequence-based predictions can be used in a first approximation to predict the aggregation propensity of a given target protein, however, the consequences of TDoT fusion (i.e. the efficacy of the resulting CatIB-formation process) cannot be directly inferred or understood only based on those predictions.

Since CatIBs/FIBs, in contrast to conventional IBs, retain a certain degree of activity, it seems reasonable to assume that the corresponding enzymes/proteins retain their native (quaternary) structure in CatIBs/FIBs (at least to some extend). Therefore, it seems likely that in CatIBs/FIBs aggregation does not solely occur from the unfolded state (as the previous sequence-based predictions assume) but also involves the aggregation or co-aggregation of already folded (i.e. native) protein species. Hereby, the presence/absence of hydrophobic surface patches on a given target could determine the efficiency of aggregation. To address this issue, we evaluated the available target protein structures for the presence of large hydrophobic surface patches by using the Rosetta protein design software (see "Methods" for details; Additional file 1: Figure S11, Table S2) [75, 76]. For five out of nine of the target proteins, the plot of the CatIB/FIB formation efficiency against the percentage of the hydrophobic patch area on the overall solvent accessible surface area (SASA) yielded a good linear relation (excluding outliers: $R^2 = 0.995$; including *Ec*MenD, *R*ADH, YFP, and *Lb*ADH: $R^2 = 0.286$) (Additional file 1: Figure S12). When we consider the presence of alternative oligomeric assemblies (inferred by using the PISA webserver; see "Methods"; Additional file 1: Table S2), the correlation is significantly improved for *R*ADH and YFP (excluding outliers: $R^2 = 0.975$; including *Ec*MenD and *Lb*ADH: $R^2 = 0.837$) (Fig. 6c). Here, it appears that the presence of large hydrophobic surface patches clearly relates to the efficacy of CatIB formation, thus providing a structural rationale, why certain highly soluble proteins like mCherry fail to form insoluble FIBs or form only FIBs that disintegrate during cell lysis or are solubilized during CatIB/FIB preparation.

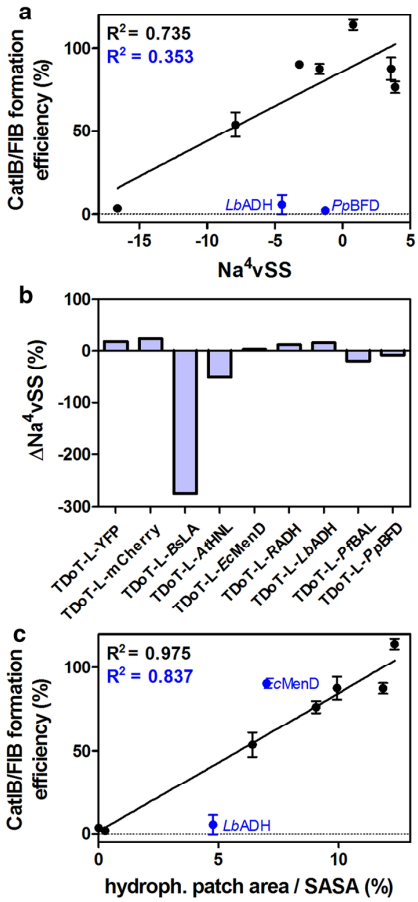

Fig. 6 Computational analysis of the **a**, **b** sequence-based and **c** structural determinants of CatIB/FIB formation analyzed based on the TDoT dataset. **a** Sequence-based aggregation propensities were inferred using the AGGRESCAN webserver [72] and the average aggregation-propensity values per amino acid (a^4v) normalized to a 100-residue protein (Na^4vSS) were used as indicator for aggregation. Low (negative) Na^4vSS are an indicator for low aggregation propensity as for example demonstrated for intrinsically disordered proteins (IDPs) [72]. **b** The relative change of the Na^4vSS value due to addition of the TDoT domain $\left(\Delta Na^4vSS = \left(\frac{(Na^4vSS_{fusion} - Na^4vSS_{target})}{|Na^4vSS_{target}|}\right) \times 100\right)$ has in the past been used for the computation of the effects of point mutations on aggregation [72]. Positive values suggest increased and negative values decreased aggregation due to addition of the TDoT domain. **c** The presence/absence of large hydrophobic surface patches for the corresponding target protein structures was quantified using the hpatch tool implemented in Rosetta [75, 76, 94]. Surface areas were quantified using Pymol 1.7.0.0 (Schrödinger, LCC, New York, NY, USA). In a and c CatIB-formation was plotted as the relative activity in the insoluble fraction (Additional file 1: Table S1). Coefficient of determination (R^2) values are always given excluding the blue-highlighted outliers (black) and including the outliers (blue)

Conclusions

The generation of catalytically-active inclusion bodies (CatIBs) represents a recently developed, promising strategy for the solely biological production of carrier-free enzyme immobilizates. This strategy relies on the molecular biological fusion of a coiled-coil domain to target enzymes/proteins to induce the formation of intracellular aggregates (inclusion bodies, IBs) which retain a certain degree of activity. While this strategy has already been proven successful in multiple cases, the efficiency, the potential for optimization, and important CatIB properties like yield, activity, and morphology have not been investigated systematically. In this contribution, different optimization strategies, like linker deletion, C- versus N-terminal fusion, and the fusion of alternative aggregation-inducing tags have been evaluated. While linker deletion and C-terminal instead of N-terminal fusion successfully yielded CatIBs/FIBs for certain target proteins for which our initial N-terminal fusion strategy failed, the use of the 3HAMP coiled-coil domain as alternative aggregation-inducing tag resulted in CatIBs with superior activity and altered composition. Using conventional microscopy and scanning electron microscopy, we provide evidence for the distinct morphology of 3HAMP-derived CatIBs. The latter appears moreover to be linked to their superior performance. Last but not least, we demonstrated that CatIB formation efficiency can be correlated to the solvent-accessible hydrophobic surface area of the target enzyme, providing a structure-based rationale for our strategy and opening up the possibility to predict its efficiency for any given target protein. In conclusion, we here provide evidence for the general applicability, predictability, and flexibility of the CatIB immobilization strategy, highlighting its application potential for synthetic chemistry and industry.

Methods

Reagents and chemicals

Chemicals were purchased from Sigma-Aldrich, Fluka, Roth, KMF, Biosolve, Alfa Aesar, AppliChem, and Merck. Enzymes for molecular biology were purchased from Thermo Scientific (Waltham, MA, USA). Enantiopure (*R*)-(3,3‘,5,5‘)-tetramethoxy benzoin (TMBZ) for the calibration of HPLC analysis was taken from a stock prepared as described elsewhere [10, 25, 77].

Construction of expression plasmids

The general design strategy for the construction of the respective TDoT gene fusions has been described before [9] (Additional file 1: Figure S5a). If not stated otherwise, all gene fusions consisted of gene fragments coding for a coiled-coil domain (here TDoT or 3HAMP), a linker polypeptide, consisting of a protease Factor Xa cleavage site and a triple $(GGGS)_3$ and the respective target proteins/enzymes cloned into a pET-28a vector (Novagen, Merck KGaA, Frankfurt, Germany). As target FPs YFP (27.1 kDa), a monomeric version of the enhanced yellow fluorescent protein (eYFP) from *Aequorea victoria* was used. This YFP contains the A206K exchange for the monomerization [36] but lacks the Q69K substitution, which renders it less sensitive in the neutral pH [78, 79]. As a second FP target, the monomeric red fluorescent protein mCherry from *Discosoma striata* (26.7 kDa) [37] was chosen. As target enzymes, two alcohol dehydrogenases (*R*ADH from *Ralstonia* sp. and *Lb*ADH from *Lactobacillus brevis* [38–40]) and two ThDP-dependent enzymes [benzoylformate decarboxylase from *Pseudomonas putida* (*Pp*BFD) [43] and benzaldehyde lyase from *Pseudomonas fluorescence* (*Pf*BAL)] [46, 47] were used. To simplify the toolbox vector, the N-terminal His_6-tag was removed from pTDoT-Linker-YFP [9], resulting in the pTDoT-L-YFP vector, as described before [25]. All in the following described constructs were based on this simplified toolbox vector and hence lacked the N-terminal His_6 tag.

The pTDoT-YFP and pTDoT-mCherry vectors lacking the linker polypeptide, consisting of the Factor Xa protease cleavage site and the triple $(GGGS)_3$ motif, were created as described before [25]. For the exchange of the coiled-coil domain, the pTDoT-L-YFP plasmid was digested with *Nde*I and *Spe*I to release the *tdot* fragment. A codon-optimized *3hamp* gene fragment, containing 5′-*Nde*I and 3′-*Spe*I restriction sites, was synthesized and supplied on a plasmid (pEX-A-3HAMP-Linker, Eurofins Genomics, Ebersberg, Germany). After restriction, the corresponding *3hamp* gene fragment was ligated into the initial plasmid, lacking the *tdot* gene fragment, to attain the p3HAMP-L-YFP vector. Genes coding for mCherry, *R*ADH, *Lb*ADH, *Pf*BAL, *Pp*BFD, and *Ec*LDC were amplified by standard PCR utilizing oligonucleotide primers containing a 5′-*BamH*I and a 3′-*Sal*I (mCherry, *R*ADH, *Lb*ADH, *Ec*LDC) or 3′-*Not*I (*Pf*BAL, *Pp*BFD) site. PCR products were digested with respective restriction endonucleases and ligated into similarly hydrolyzed pTDoT-L-YFP or p3HAMP-L-YFP. The vectors containing the TDoT-L-*R*ADH and TDoT-L-*Pf*BAL fusion as well as the vector containing the 3HAMP-L-*Pf*BAL fusion has been constructed as described in [25] and [32], respectively. The construction of the plasmid p*Ec*LDC-L-TDoT, for C-terminal fusion of TDoT to *Ec*LDC, has also been described before [10]. The plasmid containing the gene fusion encoding for the C-terminal *Ec*LDC-L-3HAMP fusion (p*Ec*LDC-L-3HAMP) was constructed similarly to the N-terminal 3HAMP-vectors by digesting p*Ec*LCD-L-TDoT with *Bam*HI and *Not*I and ligating the resulting linear DNA with a PCR amplified *3hamp* gene fragment

utilizing oligonucleotide primers containing a 5′-*BamH*I and a 3′-*Not*I restriction site, originated from the pEX-A-3HAMP-Linker vector. All sequences were verified by sequencing (Seqlab GmbH, Göttingen, Germany and LGC genomics, Berlin, Germany). For information about all plasmids and oligonucleotide primers see Additional file 1.

Production and purification of inclusion bodies (IBs)

The target gene fusions were heterologously expressed in *E. coli* BL21(DE3) using autoinduction medium [80] for 69 h at 15 °C as described recently [9, 10, 25]. Cell disruption was performed from a 10% (w/v) suspension in lysis buffer (50 mM sodium phosphate buffer, 100 mM NaCl, pH 8.0) with an Emulsiflex-C5 high-pressure homogenizer (Avestin Europe GmbH, Mannheim, Germany) as described before [10, 25]. To separate the IB-containing pellet from the soluble supernatant, the crude cell extract was centrifuged (30 min at 4 °C and 15,000×*g*) and frozen at − 20 °C in a freezer. The pellet was washed once with the initial volume of MilliQ water and was again centrifuged. The obtained pellet was lyophilized for 72 h from a frozen (− 80 °C) 10% (w/v) suspension in MilliQ water (Christ ALPHA 1-3 LD Plus, Martin Christ Gefriertrocknungsanlagen GmbH, Osterode, Germany). The dried CatIBs were grounded and stored as a fine powder at − 20 °C until further use [10, 25].

Production and purification of soluble enzymes

Soluble *R*ADH, encoded on a pET-22b vector [81], was produced in *E. coli* BL21(DE3) according to the expression protocol used for the CatIB production. Soluble *Lb*ADH, encoded on a pET-21a vector, was produced in *E. coli* BL21(DE3) as described elsewhere [82, 83]. Soluble *Pf*BAL was fused to a C-terminal hexahistidine tag and was encoded on a pkk233_2 vector [84]. The protein was produced in *E. coli* SG 13009 according to a protocol described elsewhere [77, 84] using a 40 l Techfors fermenter (Infors AG, Bottmingen, Swiss) at 30 °C in fed-batch mode [85]. Soluble *Pp*BFD-L476Q (fused to a C-terminal hexahistidine tag) encoded on the pkk233_2 vector was produced in *E. coli* SG 13009 according to a protocol described elsewhere [48].

Cells were harvested, centrifuged and the remaining pellet was frozen at − 20 °C. The frozen cells were suspended in a 25% (w/v) suspension in the respective equilibration buffer used for purification. Cell disruption was performed on ice by sonication (UP200 s, Hielscher Ultrasonics GmbH, Teltow, Germany) 10-times for 1 min at an amplitude of 70% and a cycle of 0.5, followed by a 1 min break. The soluble enzyme was separated from the cell debris by centrifugation for 30 min (18,000×*g*, 4 °C).

Purification of soluble *R*ADH was performed by anion exchange chromatography according to the protocol described previously [81]. The first step included a desalting by gel filtration with a Sephadex-G25 (GE Healthcare, Little Chalfont, United Kingdom) column with 10 mM TEA-buffer (pH 7.5, 0.8 mM $CaCl_2$). In the second step the desalted protein fraction was purified via anion exchanger (Q-Sepharose Fast Flow column, GE Healthcare, Little Chalfont, United Kingdom) starting with equilibration buffer (50 mM TEA, pH 7.5, 0.8 mM $CaCl_2$), followed by an application of a linear NaCl-gradient up to 200 mM NaCl (50 mM TEA, pH 7.5, 0.8 mM $CaCl_2$, 200 mM NaCl) within 150 min at a flow of 1 ml min^{-1}. Desalting was performed again by gel filtration on a Sephadex-G25 (GE Healthcare, Little Chalfont, United Kingdom) column with 10 mM TEA-buffer (pH 7.5, 0.8 mM $CaCl_2$).

Soluble *Lb*ADH was purified by anion-exchange chromatography [82, 83] by an anion exchanger (Q-Sepharose Fast Flow column, GE Healthcare, Little Chalfont, United Kingdom) starting with equilibration buffer (50 mM TEA, pH 7.2, 1 mM $MgCl_2$). This was followed by an application of a linear NaCl-gradient up to 1 M NaCl (50 mM TEA, pH 7.2, 1 mM $MgCl_2$, 1 M NaCl) within 150 min at a flow of 1 ml min^{-1}. Desalting was performed by gel filtration on a Sephadex-G25 (GE Healthcare, Little Chalfont, United Kingdom) column with 10 mM TEA-buffer (pH 7.5, 1 mM $MgCl_2$).

The soluble *Pf*BAL was purified by metal ion affinity chromatography as described earlier [46, 86]. For the purification with the Ni–NTA-Sepharose column (QIAGEN, Hilden, Germany) the following buffers were used: equilibration buffer (50 mM TEA, pH 7.5, 2.5 mM $MgSO_4$, 0.5 mM ThDP, 300 mM NaCl), washing buffer (50 mM TEA, pH 7.5, 50 mM imidazole, 300 mM NaCl), elution buffer (50 mM TEA, pH 7.5, 250 mM imidazole, 300 mM NaCl). For the final desalting step with Sephadex-G25 (GE Healthcare, Little Chalfont, United Kingdom) column, 10 mM TEA-buffer (pH 7.5, 2.5 mM $MgSO_4$, 0.1 mM ThDP) was employed.

The soluble *Pp*BFD-L476Q was purified by metal ion affinity chromatography as described earlier [45, 46, 48]. For the purification with Ni–NTA-Sepharose column (QIAGEN, Hilden, Germany) the following buffers were used: equilibration buffer (50 mM KPi, pH 7.0, 2.5 mM $MgSO_4$, 0.1 mM ThDP), washing buffer (50 mM TEA, pH 7.0, 50 mM imidazole), elution buffer (50 mM TEA, pH 7.5, 250 mM imidazole). For the final desalting step with Sephadex-G25 (GE Healthcare, Little Chalfont, United Kingdom) column, 10 mM TEA-buffer (pH 6.5, 2.5 mM $MgSO_4$, 0.1 mM ThDP) was employed.

The enzyme solutions were lyophilized (Christ ALPHA 1-3 LD Plus, Martin Christ Gefriertrocknungsanlagen GmbH, Osterode, Germany) from frozen (− 20 °C), maximal 2 mg ml^{-1} protein solutions (in the respective storage buffer) and stored at − 20 °C until further use.

Sodium dodecyl sulfate-polyacrylamide gel electrophoresis (SDS-PAGE) and determination of protein concentration

The distribution of the recombinant fusion proteins in *E. coli* cell extract fractions, crude cell extract (CCE), soluble supernatant (SN), and insoluble IB-containing pellet (P), as well as the success of the IB-purification was analyzed by SDS-PAGE as described recently [10, 25]. For SDS-PAGE NuPAGE™ 4–12% Bis–Tris Protein Gels with MES SDS running buffer (50 mM MES, 50 mM TRIS, 0.1% SDS, 1 mM EDTA, pH 7.3) and PageRuler Prestained Protein ladders or PageRuler Plus Prestained Protein ladders (both: ThermoFisher Nunc, Waltham, MA, USA) were used. The total protein content in the supernatant was determined, using the Bradford assay [87]. SDS-PAGE samples of the supernatant fraction contained 10 µg protein, all other samples were prepared relative to the supernatant fractions by using the same sample volume [10, 25].

The protein content of lyophilized CatIBs was determined by the absorption at 280 nm. Therefore, lyophilized CatIBs were dissolved in 6 M guanidine hydrochloride, incubated for 30 min at 30 °C under constant shaking at 1000 rpm (Thermomixer comfort, Eppendorf, Germany), and centrifuged for 20 min at 4 °C and 16,060×*g*. The absorption of the protein solution was measured at 280 nm. The protein content was estimated using the molar extinction coefficient as calculated based on the amino acid composition using the ProtParam Tool (http://web.expasy.org/protparam [88] (Additional file 1: Table S6).

Cell fractionation and determination of the CatIB/FIB formation efficiency

Inclusion body production was evaluated by determining the distribution of functional recombinant fusion proteins in different *E. coli* cell extract fractions. Therefore, the fluorescence or activity of the respective target protein was measured in all fractions: crude cell extract (CCE), supernatant (SN), and pellet (P) as described before [25]. Suitable dilutions of the CCE in lysis buffer (50 mM sodium phosphate buffer, 100 mM sodium chloride, pH 8.0) were separated into the soluble supernatant (SN) fraction and insoluble IB-containing pellet fraction (P) by centrifugation (2 min, 7697×*g*, room temperature). The P fraction was washed once with lysis buffer and was resuspended in the initial volume of lysis buffer before measuring. The fluorescence/activity in P (IBs) and SN (soluble protein) was expressed relative to the activity of the crude cell extract (set to 100%). CatIB/FIB formation efficiency was defined as the relative activity, or in case of FPs fluorescence, of the insoluble IB-containing pellet fraction.

For the fluorescent proteins YFP and mCherry distribution in different fractions [crude cell extract (CCE), soluble protein-containing supernatant (SN), and IB-containing pellet (P)] was determined by fluorescence spectroscopy, as described recently [25].

The distribution of the enzymes *R*ADH, *Lb*ADH, *Pf*BAL, and *Pp*BFD in different cell fractions was determined by continuous photometric activity assays in 10 × 4 mm quartz-glass cuvettes with a volume of 1 ml (4 mm light path in excitation) using a Fluorolog3-22 spectrofluorometer (Horiba Jobin–Yvon, Bensheim, Germany) in front-face angle according to the *Pf*BAL initial rate activity assay developed by Schwarz [77].

*R*ADH activity was measured by following the reduction of cyclohexanone to cyclohexanol (Additional file 1: Figure S13a) by detecting the consumption of the cofactor NADPH. The reaction was monitored for 90 s at 30 °C by excitation at λ_{ex} 350 nm and emission at λ_{em} 460 nm (bandwidth 1.4 nm in excitation and emission) using TEA-buffer (50 mM TEA, 0.8 mM CaCl2, pH 7.5) with 100 mM cyclohexanone, 0.2 mM NADPH, and 200 µl sample suspension in suitable dilutions. Measurements of all distributions were performed at least as four technical replicates of biological triplicates.

*Pf*BAL activity was measured using the carboligation of 3,5-dimethoxybenzaldehyde (DMBA) to (*R*)-(3,3′,5,5′)-tetramethoxy benzoin (TMBZ) (Additional file 1: Figure S13c). DMBA consumption was monitored for 90 s at 25 °C by excitation at λ_{ex} 350 nm and emission at λ_{em} 460 nm (bandwidth 1.3 nm in excitation and emission) in TEA-buffer (50 mM TEA, 0.5 mM ThDP, 2.5 mM $MgSO_4$, pH 8.0) with 3 mM DMBA [in DMSO, final concentration 20% (v/v)] and 200 µl sample suspension in suitable dilutions.

The *Lb*ADH and *Pp*BFD activity distribution in different *E. coli* cell extract fractions was measured as described in the activity assays section below.

Phase-contrast and fluorescence image acquisition

Microscopy imaging was performed as described before [25]. After cultivation of *E. coli* BL21(DE3) containing CatIBs/FIBs, a culture volume of 1 ml was removed and the cells were harvested by centrifugation for 2 min at 15,800×*g*. The resulting cell pellet was suspended in lysis buffer (50 mM sodium phosphate buffer, 100 mM NaCl, pH 8) to an OD_{600} of approx. 10. A volume of 1.5 µl was

applied on a microscope slide with a 1% (w/v) agarose base, covered with a coverslip and placed in the microscope setup for imaging. An inverted Nikon Eclipse Ti microscope (Nicon GmbH, Düsseldorf, Germany) was used, equipped with an Apo TIRF 100× Oil DIC N objective (ALA OBJ-Heater, Ala Scientific Instruments, USA), an ANDOR Zyla CMOS camera (Andor Technology plc., Belfast, UK), and an Intensilight (Nicon GmbH, Düsseldorf, Germany) light source for fluorescence excitation, and fluorescence filters for YFP (excitation: 520/60 nm, dichroic mirror: 510 nm, emission: 540/40 nm) and mCherry (excitation: 575/15 nm, dichroic mirror: 593 nm, emission: 629/56 nm) (AHF Analysentechnik, Tübingen, Germany). The filter spectra are given in nm as peak/peak width. The dichroic mirror serves as longpass filter for wavelengths larger than the given value. Fluorescence and camera exposure was 200 ms for both filters at 25 or 12.5% lamp intensity. Analysis of cell images were performed with Fiji [89].

Lipid content determination

For the gravimetric determination of the lipid content [90] approx. 100 mg lyophilized CatIBs were weighted and transferred into a 50 ml falcon tube. After mixing with 14 ml chloroform and 7 ml methanol, the suspension was incubated for 2 h at 60 °C and 750 rpm in a thermomixer (Thermomixer comfort, Eppendorf, Hamburg, Germany). After incubation, the complete suspension was transferred to a 50 ml separating funnel for washing with 5.6 ml 0.73% (w/v) NaCl solution. After collecting the lower organic phase, the remaining aqueous phase was extracted with 14 ml chloroform. The organic phase was pooled, dried over $MgSO_4$, and concentrated by a rotating evaporator (Rotavapor R-100, Büchi Labortechnik GmbH, Essen, Germany). The remaining liquid was transferred to a glass vessel and organic solvent was removed by evaporation first under the hood and then under high vacuum (0.2 mbar) over 24 h. The lipid amount was gravimetrically determined. The lipid content was calculated based on the initial weight. All measurements were performed in three technical replicates of one biological sample.

Activity assays

The initial rate activity of *R*ADH and *R*ADH-CatIBs was measured by using a discontinuous photometric assay in which the consumption of the cofactor NADPH was measured at 340 nm, during the enzyme-catalyzed reduction of cyclohexanone to cyclohexanol (Additional file 1: Figure S13a). The reaction was performed in a polypropylene reaction tube (2 ml safe-lock tube) in a reaction volume of 1750 µl containing 100 mM cyclohexanone and 0.4 mM NADPH in TEA-buffer (50 mM, pH 7.5, 0.8 mM $CaCl_2$) which was pre-incubated at 30 °C. The reaction was started with 300–500 µg ml^{-1} *R*ADH-CatIBs or 10–20 µg ml^{-1} soluble *R*ADH (pre-incubated for 5 min at 30 °C). Reactions were performed for 5 min at 30 °C and 1000 rpm in a thermomixer (Thermomixer comfort, Eppendorf, Germany). Every minute (0–5 min) samples of 250 µl were taken and diluted 1:3 in MeOH to stop the reaction. Samples were centrifuged for 5 min (7697×*g*, room temperature) and measured in standard disposable cuvettes. The amount consumption of NADPH was quantified employing a molar extinction coefficient of $\varepsilon_{340nm} = 1.975\ M^{-1}\ cm^{-1}$ as determined in the reaction system.

For initial rate activity determination of *Pf*BAL-CatIBs and soluble *Pf*BAL, the carboligation of 3,5-dimethoxy benzaldehyde (DMBA) to (*R*)-(3,3‘,5,5‘)-tetramethoxy benzoin (TMBZ) (Additional file 1: Figure S13c) was followed to a conversion of 10% by a discontinuous HPLC assay. The reaction was carried out in polypropylene reaction tubes in 1 ml reaction volume comprised of 80% (v/v) TEA-buffer (50 mM, pH 7.5, 2.5 mM $MgSO_4$, 0.1 mM ThDP), 20% (v/v) DMSO and 10 mM DMBA, This solution was incubated at 30 °C before the reaction was started by addition of the enzyme (0.017–0.30 mg ml^{-1} *Pf*BAL-CatIBs, 3–6 µg ml^{-1} soluble *Pf*BAL, initial protein weight) The reaction was performed for 5 min at 30 °C and 1000 rpm in a thermomixer (Thermomixer comfort, Eppendorf, Germany) under sampling (20 µl) every minute. Subsequently, the sample was diluted 1:10 with 180 µl methanol (incl. 0.1‰ (v/v) *p*-methoxy benzaldehyde as internal standard) to stop the reaction and to prepare the sample for HPLC analysis (see below).

The initial rate activity of *Ec*LDC-CatIBs was measured for the decarboxylation of 10 mM L-lysine in potassium phosphate buffer (50 mM, pH 8.0) containing 0.1 mM PLP at 30 °C and 1000 rpm by a discontinuous HPLC-based assay according to the protocol described previously [10].

*Lb*ADH and *Pp*BFD initial rate activities were measured by continuous photometric activity assays in 10 × 4 mm quartz-glass cuvettes with a volume of 1 ml (4 mm light path in excitation) using a Fluorolog3-22 spectrofluorometer (Horiba Jobin–Yvon, Bensheim, Germany) in front-face angle [77].

*Lb*ADH activity was measured for the reduction of acetophenone to 1-phenylethanol (Additional file 1: Figure S13b) under the consumption of the cofactor NADPH [83], which was detected by excitation at λ_{ex} 350 nm and emission at λ_{em} 460 nm (bandwidth 1.5 nm in excitation and emission). The reaction was started by addition of 500 µl sample suspension in suitable dilutions (protein amount of approx. 0.07–0.4 mg ml^{-1} soluble

*Lb*ADH and 2–25 mg ml^{-1} *Lb*ADH-CatIBs) to the preheated TEA-buffer (50 mM pH 7.0, 0.8 mM $MgCl_2$) containing 10.7 mM acetophenone, and 0.2 mM NADPH, and was followed for 90 s at 30 °C. For NADPH calibration, NADPH, in concentrations between 0.1 mM and 0.20 mM, was dissolved in TEA-buffer and measured under the same conditions.

*Pp*BFD activity was followed by a coupled two-step assay reaction beginning with *Pp*BFD-catalyzed decarboxylation of phenylglyoxylic acid (PGA) to benzaldehyde, which was followed by the reduction to benzyl alcohol by horse liver (HL-)ADH under the oxidation of NADH (Additional file 1: Figure S13d). The reaction was started by the addition of 500 µl sample suspension in suitable dilutions (protein amount of approx. 0.05–0.35 mg ml^{-1} soluble *Pp*BFD and 0.4–2.5 mg ml^{-1} *Pp*BFD-CatIBs) to the preheated reaction solution containing TEA-buffer (50 mM TEA, 0.5 mM ThDP, 2.5 mM $MgSO_4$, pH 6.5) with 5 mM PGA, 0.25 mM NADH, and 0.25 U ml^{-1} HL-ADH. NADH consumption was monitored for 90 s at 30 °C by excitation at λ_{ex} 350 nm and emission at λ_{em} 460 nm (bandwidth 1.4 nm in excitation and emission). For NADPH calibration, NADPH concentrations between 0.1 mM and 0.25 mM were dissolved in TEA-buffer and measured under the same conditions.

Measurements of the initial rate activities were performed at least as three technical replicates of the respective biological triplicates. Activity was calculated as turn over number k_{cat} [s^{-1}] referring to the amount of enzyme (in µmol and referring to one subunit, calculated based on the protein content) which catalyzes the formation of 1 µmol product per second from the respective substrate under the applied reaction conditions.

HPLC analysis

For *Ec*LDC activity determinations the concentration of L-lysine and 1,5-diaminopentane (DAP) was determined as described recently [10].

The concentration of DMBA and TMBZ, the substrate and reaction product of the *Pf*BAL activity assay, were determined by high performance liquid chromatography (HPLC). The samples were prepared for HPLC analysis by centrifugation at 15,800×*g* for 1 min. Subsequently, the supernatant was transferred to HPLC vials equipped with inlets. For analysis, 10 µl of samples were injected into a Thermo Scientific Dionex Ultimate 3000 HPLC system containing a diode-array detector DAD-3000 (ThermoFisher Scientific, Waltham, MA, USA). As stationary phase, a Chiralpak® IE column was used (4,6 µm × 250 mm, 5 µm particle size column, Daicel, Tokyo, Japan), which was combined with a pre-column of the same material (Chiralpak® IE 4 mm x 10 mm; Daicel, Tokyo, Japan). The columns were tempered to 20 °C. Separation was achieved under isocratic elution (flow rate 1 ml min^{-1}) using a binary mobile phase consisting of 50% (v/v) dd H_2O and 50% (v/v) acetonitrile. The analytes eluted at retention times of 6.1 min for *p*-MBA (270 nm), 7.6 min for DMBA (215 nm); and 9.4 min for (*R*)-TMBZ (215 nm). To quantify substrate and product, a calibration of DMBA and TMBZ was performed [32].

Scanning electron microscopy

Scanning electron microscopy images of CatIBs were taken by Steffen Köhler from the Center for Advanced Imaging (CAi) at the Heinrich-Heine University Düsseldorf with a Leo 1430 VP scanning electron microscopy (Carl Zeiss AG, Oberkochen, Germany). For sample preparation, 2 mg ml^{-1} lyophilized TDoT-CatIBs or 4 mg ml^{-1} 3HAMP-CatIBs were used. CatIB solutions (2.5 µl) were fixed on a silicon disk (VWR, Radnor, Pennsylvania, USA) with 2.5% (v/v) glutaraldehyde in 100 mM sodium phosphate buffer, pH 7.2 for 2 h at 25 °C and 250 rpm and rinsed three times for 10 min with buffer [91]. Afterwards, the samples were dehydrated through a graded ethanol series (30, 50, 70, 95, and 100%) for 15 min, respectively. Samples were dried by critical point method and coated with gold at the CAi before images were taken at an accelerating voltage of 15 or 19 kV.

Computational analysis of sequence-based and structural determinants of CatIB formation

The aggregation propensity of the target proteins, as well as of the corresponding TDoT fusions, was inferred from their amino acid sequence by using the AGGRESCAN tool (http://bioinf.uab.es/aggrescan) [72] (see Additional file 1: Table S1). Implementation tests and details about the algorithm employed by AGGRESCAN have been provided elsewhere [11, 72]. The program provides several parameters that serve as a global indicator for the aggregation propensity of a given amino acid sequence. The average aggregation-propensity values per amino acid (a^4v) normalized to a 100-residue protein (Na^4vSS) were employed as quantitative descriptors for aggregation propensity. Those values have previously been shown to be good indicators for changes in aggregation properties, due to the introduction of point mutations, and have also been employed for the differentiation of soluble, unfolded, amyloid- and IB-forming proteins [72].

Alternatively, the presence/absence of large hydrophobic surface patches was considered as structural proxy for the aggregation propensity of a given target protein. Therefore, for each target protein, the pdb coordinates representing the most likely native oligomer were obtained from the pdb data bank (https://www.rcsb.org) [92]. Alternative oligomeric assemblies were derived using the PISA webserver ['Protein interfaces, surfaces

and assemblies' service PISA at the European Bioinformatics Institute (http://www.ebi.ac.uk/pdbe/prot_int/pistart.html)] [93]. All solvent molecules and heteroatoms were removed before surface calculations were performed. The surface properties of the target proteins were evaluated by using the Rosetta protein design software [75, 76] by employing the hpatch tool [94]. The hpatch tool identifies surface localized clusters of hydrophobic atoms (hydrophobic patches) and provides a Pymol selection term for visualization of each identified patch. The overall patch area was calculated by summation over all identified patches. Patch areas and the overall solvent accessible surface area (SASA) were calculated with Pymol 1.7.0.0 (Schrödinger, LCC, New York, NY, USA). PDB-IDs and additional information about the employed structures and assemblies is provided in Additional file 1: Table S2.

Additional file

Additional file 1. Additional information containing Additional Results, Methods, DNA and amino acid sequences of the fusion proteins and Additional references.

Abbreviations

IBs: inclusion bodies; CatIBs: catalytically-active inclusion bodies; FIBs: functional inclusion bodies; *E. coli*: *Escherichia coli*; CLEAs: cross-linked enzyme aggregates; FPs: fluorescent proteins; TDoT: coiled-coil tetramerization domain of tetrabrachion; HAMP: histidine kinases, adenylyl cyclases, methyl-accepting chemotaxis proteins, and phosphatases; 3HAMP: coiled-coil HAMP domain of the Aer2 oxygen sensor; SEM: scanning electron microscopy; SASA: solvent accessible surface area.

Authors' contributions

VDJ and RK contributed equally: both wrote the manuscript, planed, supervised, analyzed, and assisted the experiments. VDJ optimized the plasmids constructs, generated the different expression vectors and created the fusion proteins. RK, assisted by UK, planned and generated the genetic construct for the C-terminal fusion. VDJ characterized the fluorescent proteins, measured the distributions and activities for *R*ADH and *Pf*BAL, optimized the *R*ADH activity assays and performed scanning electron microscopy. RK optimized the activity assays for *Pf*BAL, *Pp*BFD, and *Lb*ADH, and supervised the characterization of these enzymes and *Ec*LDC. VDJ, RK, and AG performed live-cell imaging. UK performed bioinformatic and computational structural analyses. SS, DH, TK, M. Piqueray, UM, JM, and SL performed experiments, that were planned and supervised by RK and VDJ under the coordination and supervision of M. Pohl and UK. WW, KE-J, M. Pohl, and UK planned the CatIB project and corrected the manuscript. All authors commented on the manuscript. All authors read and approved the final manuscript.

Author details

[1] Institut für Molekulare Enzymtechnologie, Heinrich-Heine-Universität Düsseldorf, Forschungszentrum Julich, 52425 Julich, Germany. [2] IBG-1: Biotechnology, Forschungszentrum Jülich GmbH, 52425 Jülich, Germany. [3] Multiscale Bioengineering, Bielefeld University, Universitätsstraße 25, 33615 Bielefeld, Germany. [4] Bioeconomy Science Center (BioSC), c/o, Forschungszentrum Jülich, 52425 Jülich, Germany.

Acknowledgements

The scientific activities of the Bioeconomy Science Center were financially supported by the Ministry of Innovation, Science and Research within the framework of the NRW Strategieprojekt BioSC (No. 313/323-400-002 13). BioSC is a research cluster of RWTH Aachen University, the universities of Düsseldorf and Bonn, and Forschungszentrum Jülich. The authors thank the Institute for Bioorganic Chemistry (IBOC, Heinrich-Heine University/FZ Jülich) for performing ^{1}H-NMR analysis, Steffen Köhler of the Center for Advanced Imaging (Heinrich-Heine University Düsseldorf) for the scanning electron microscopy pictures, and Christoph Westerwalbesloh and Eugen Kaganovitch from the Microscale Bioengineering Group (IBG-1, Forschungszentrum Jülich) for taking phase-contrast and fluorescence images of *E. coli* cells containing CatIBs/FIBs.

Competing interests

The authors declare that they have no competing interests.

Availability of data and materials

All data generated or analyzed during this study are included in this article and it's Additional file 1.

Consent for publication

Not applicable.

Ethics approval and consent to participate

Not applicable.

Funding

This research was funded by the Ministry of Innovation, Science and Research within the framework of the NRW Strategieprojekt BioSC (No. 313/323-400-002 13).

Publisher's Note

Received: 4 December 2018 Accepted: 30 January 2019
Published online: 07 February 2019

References

1. Castro GR, Knubovets T. Homogeneous biocatalysis in organic solvents and water-organic mixtures. Crit Rev Biotechnol. 2003;23:195–231.
2. Rehm FB, Chen S, Rehm BH. Enzyme engineering for in situ immobilization. Molecules. 2016;21:1370. https://doi.org/10.3390/molecules211013 70.
3. Hanefeld U, Gardossi L, Magner E. Understanding enzyme immobilisation. Chem Soc Rev. 2009;38(453–46):8.
4. Sheldon RA, van Pelt S. Enzyme immobilisation in biocatalysis: why, what and how. Chem Soc Rev. 2013;42:6223–35.
5. Es I, Vieira JD, Amaral AC. Principles, techniques, and applications of biocatalyst immobilization for industrial application. Appl Microbiol Biotechnol. 2015,99.2065–82.
6. Sheldon RA. Characteristic features and biotechnological applications of cross-linked enzyme aggregates (CLEAs). Appl Microbiol Biotechnol. 2011;92:467–77.
7. Pierre AC. The sol-gel encapsulation of enzymes. Biocatal Biotransform. 2004;22:145–70.
8. Tufvesson P, Lima-Ramos J, Nordblad M, Woodley JM. Guidelines and cost analysis for catalyst production in biocatalytic processes. Org Process Res Dev. 2011;15:266–74.
9. Diener M, Kopka B, Pohl M, Jaeger KE, Krauss U. Fusion of a coiled-coil domain facilitates the high-level production of catalytically active enzyme inclusion bodies. Chemcatchem. 2016;8:142–52.
10. Kloss R, Limberg MH, Mackfeld U, Hahn D, Grünberger A, Jäger VD, Krauss U, Oldiges M, Pohl M. Catalytically active inclusion bodies of L-lysine decarboxylase from *E. coli* for 1,5-diaminopentane production. Sci Rep. 2018;8:5856.

11. Krauss U, Jäger VD, Diener M, Pohl M, Jaeger KE. Catalytically-active inclusion bodies—carrier-free protein immobilizates for application in biotechnology and biomedicine. J Biotechnol. 2017;258:136–47.
12. Zhou B, Xing L, Wu W, Zhang X-E, Lin Z. Small surfactant-like peptides can drive soluble proteins into active aggregates. Microb Cell Fact. 2012;11:10.
13. Lin Z, Zhou B, Wu W, Xing L, Zhao Q. Self-assembling amphipathic alpha-helical peptides induce the formation of active protein aggregates in vivo. Faraday Discuss. 2013;166:243–56.
14. Wu W, Xing L, Zhou B, Lin Z. Active protein aggregates induced by terminally attached self-assembling peptide ELK16 in *Escherichia coli*. Microbial Cell Fact. 2011;10:9.
15. Wang X, Zhou B, Hu W, Zhao Q, Lin Z. Formation of active inclusion bodies induced by hydrophobic self-assembling peptide GFIL8. Microb Cell Fact. 2015;14:88.
16. Nahálka J, Nidetzky B. Fusion to a pull-down domain: a novel approach of producing *Trigonopsis variabilis* D-amino acid oxidase as insoluble enzyme aggregates. Biotechnol Bioeng. 2007;97:454–61.
17. Nahálka J, Patoprstý V. Enzymatic synthesis of sialylation substrates powered by a novel polyphosphate kinase (PPK3). Org Biomol Chem. 2009;7:1778–80.
18. Choi S-L, Lee SJ, Ha J-S, Song JJ, Rhee YH, Lee S-G. Generation of catalytic protein particles in *Escherichia coli* cells using the cellulose-binding domain from *Cellulomonas fimi* as a fusion partner. Biotechnol Bioprocess Eng. 2011;16:1173–9.
19. García-Fruitós E, González-Montalbán N, Morell M, Vera A, Ferraz RM, Arís A, Ventura S, Villaverde A. Aggregation as bacterial inclusion bodies does not imply inactivation of enzymes and fluorescent proteins. Microb Cell Fact. 2005;4:27.
20. Hrabárová E, Achbergerová L, Nahálka J. Insoluble protein applications: the use of bacterial inclusion bodies as biocatalysts. Methods Mol Biol. 2015;1258:411–22.
21. Nahálka J, Mislovicová D, Kavcová H. Targeting lectin activity into inclusion bodies for the characterisation of glycoproteins. Mol BioSyst. 2009;5:819–21.
22. Park S-Y, Park S-H, Choi S-K. Active inclusion body formation using *Paenibacillus polymyxa* PoxB as a fusion partner in *Escherichia coli*. Anal Biochem. 2012;426:63–5.
23. Kopito RR. Aggresomes, inclusion bodies and protein aggregation. Trends Cell Biol. 2000;10:524–30.
24. Baneyx F, Mujacic M. Recombinant protein folding and misfolding in *Escherichia coli*. Nat Biotechnol. 2004;22:1399–408.
25. Jäger VD, Lamm R, Kloss R, Kaganovitch E, Grünberger A, Pohl M, Büchs J, Jaeger K-E, Krauss U. A synthetic reaction cascade implemented by co-localization of two proteins within catalytically-active inclusion bodies. ACS Synth Biol. 2018;7:2282-95. https://doi.org/10.1021/acssynbio.8b00274.
26. Steinmann B, Christmann A, Heiseler T, Fritz J, Kolmar H. In vivo enzyme immobilization by inclusion body display. Appl Environ Microbiol. 2010;76:5563–9.
27. Li S, Lin K, Pang H, Wu Y, Xu J. Production, characterization, and application of an organic solvent-tolerant lipase present in active inclusion bodies. Appl Biochem Biotechnol. 2013;169:612–23.
28. Ratera I, Peternel S, Seras-Franzoso J, Cano-Garrido O, García-Fruitós E, Cubarsí R, Vazquez E, Corchero JL, Rodríguez-Carmona E, Veciana J, Villaverde A. Biomedical applications of bacterial inclusion bodies. In Doglia SM, editor. Protein Aggregation in Bacteria: Functional and structural properties of inclusion bodies in bacterial cells. Lotti M2014. p. 203–20.
29. Rueda F, Gasser B, Sánchez-Chardi A, Roldán M, Villegas S, Puxbaum V, Ferrer-Miralles N, Unzueta U, Vázquez E, Garcia-Fruitós E, et al. Functional inclusion bodies produced in the yeast *Pichia pastoris*. Microb Cell Fact. 2016;15:166.
30. Vázquez E, Corchero JL, Burgueño JF, Seras-Franzoso J, Kosoy A, Bosser R, Mendoza R, Martínez-Láinez JM, Rinas U, Fernández E, et al. Functional inclusion bodies produced in bacteria as naturally occurring nanopills for advanced cell therapies. Adv Mater. 2012;24:1742–7.
31. Stetefeld J, Jenny M, Schulthess T, Landwehr R, Engel J, Kammerer RA. Crystal structure of a naturally occurring parallel right-handed coiled coil tetramer. Nat Struct Biol. 2000;7:772–6.
32. Kloss R, Karmainski T, Jäger VD, Hahn D, Grünberger A, Baumgart M, Krauss U, Jaeger K-E, Wiechert W, Pohl M. Tailor-made catalytically active inclusion bodies for different applications in biocatalysis. Catal Sci Technol. 2018;8:5816–26.
33. Lupas AN, Gruber M. The structure of α-helical coiled coils. Adv Protein Chem. 2005;70:37–78.
34. Woolfson DN, Bartlett GJ, Bruning M, Thomson AR. New currency for old rope: from coiled-coil assemblies to α-helical barrels. Curr Opin Struct Biol. 2012;22:432–41.
35. Wachter RM, Elsliger MA, Kallio K, Hanson GT, Remington SJ. Structural basis of spectral shifts in the yellow-emission variants of green fluorescent protein. Structure. 1998;6:1267–77.
36. Zacharias DA, Violin JD, Newton AC, Tsien RY. Partitioning of lipid-modified monomeric GFPs into membrane microdomains of live cells. Science. 2002;296:913–6.
37. Shaner NC, Campbell RE, Steinbach PA, Giepmans BN, Palmer AE, Tsien RY. Improved monomeric red, orange and yellow fluorescent proteins derived from *Discosoma* sp. red fluorescent protein. Nat Biotechnol. 2004;22:1567–72.
38. Hummel W. Large-scale applications of NAD(P)-dependent oxidoreductases: recent developments. Trends Biotechnol. 1999;17:487–92.
39. Schlieben NH, Niefind K, Muller J, Riebel B, Hummel W, Schomburg D. Atomic resolution structures of *R*-specific alcohol dehydrogenase from *Lactobacillus brevis* provide the structural bases of its substrate and cosubstrate specificity. J Mol Biol. 2005;349:801–13.
40. Lavandera I, Kern A, Ferreira-Silva B, Glieder A, de Wildeman S, Kroutil W. Stereoselective bioreduction of bulky-bulky ketones by a novel ADH from *Ralstonia* sp. J Org Chem. 2008;73:6003–5.
41. Kulig J, Frese A, Kroutil W, Pohl M, Rother D. Biochemical characterization of an alcohol dehydrogenase from *Ralstonia* sp. Biotechnol Bioeng. 2013;110:1838–48.
42. Niefind K, Muller J, Riebel B, Hummel W, Schomburg D. The crystal structure of *R*-specific alcohol dehydrogenase from *Lactobacillus brevis* suggests the structural basis of its metal dependency. J Mol Biol. 2003;327:317–28.
43. Gonzalez B, Vicuna R. Benzaldehyde lyase, a novel thiamine PPi-requiring enzyme, from *Pseudomonas fluorescens* biovar I. J Bacteriol. 1989;171:2401–5.
44. Tsou AY, Ransom SC, Gerlt JA, Buechter DD, Babbitt PC, Kenyon GL. Mandelate pathway of *Pseudomonas putida*: sequence relationships involving mandelate racemase, (*S*)-mandelate dehydrogenase, and benzoylformate decarboxylase and expression of benzoylformate decarboxylase in *Escherichia coli*. Biochemistry. 1990;29:9856–62.
45. Iding H, Dünnwald T, Greiner L, Liese A, Muller M, Siegert P, Grotzinger J, Demir AS, Pohl M. Benzoylformate decarboxylase from *Pseudomonas putida* as stable catalyst for the synthesis of chiral 2-hydroxy ketones. Chemistry. 2000;6:1483–95.
46. Gocke D, Walter L, Gauchenova E, Kolter G, Knoll M, Berthold CL, Schneider G, Pleiss J, Muller M, Pohl M. Rational protein design of ThDP-dependent enzymes-engineering stereoselectivity. ChemBioChem. 2008;9:406–12.
47. Hegeman GD. Benzoylformate decarboxylase (*Pseudomonas putida*). In: Methods in Enzymology, vol 17. Academic Press; 1970. p. 674–8.
48. Lingen B, Kolter-Jung D, Dünkelmann P, Feldmann R, Grötzinger J, Pohl M, Müller M. Alteration of the substrate specificity of benzoylformate decarboxylase from *Pseudomonas putida* by directed evolution. ChemBioChem. 2003;4:721–6.
49. Kind S, Jeong WK, Schroder H, Wittmann C. Systems-wide metabolic pathway engineering in *Corynebacterium glutamicum* for bio-based production of diaminopentane. Metab Eng. 2010;12:341–51.
50. Arai R, Ueda H, Kitayama A, Kamiya N, Nagamune T. Design of the linkers which effectively separate domains of a bifunctional fusion protein. Protein Eng. 2001;14:529–32.
51. Chen X, Zaro JL, Shen WC. Fusion protein linkers: property, design and functionality. Adv Drug Deliv Rev. 2013;65:1357–69.
52. Kandiah E, Carriel D, Perard J, Malet H, Bacia M, Liu K, Chan SW, Houry WA, Ollagnier de Choudens S, Elsen S, Gutsche I. Structural insights into the Escherichia coli lysine decarboxylases and molecular determinants of interaction with the AAA + ATPase RavA. Sci Rep. 2016;6:24601.
53. Kanjee U, Gutsche I, Alexopoulos E, Zhao B, El Bakkouri M, Thibault G, Liu K, Ramachandran S, Snider J, Pai EF, Houry WA. Linkage between the bacterial acid stress and stringent responses: the structure of the inducible lysine decarboxylase. EMBO J. 2011;30:931–44.

54. Airola MV, Watts KJ, Bilwes AM, Crane BR. Structure of concatenated HAMP domains provides a mechanism for signal transduction. Structure. 2010;18:436–48.
55. Alvarenga AE, Amoroso MJ, Illanes A, Castro GR. Cross-linked α-l-rhamnosidase aggregates with potential application in food industry. Eur Food Res Technol. 2014;238:797–801.
56. Chmura A, van der Kraan GM, Kielar F, van Langen LM, van Rantwijk F, Sheldon RA. Cross-linked aggregates of the hydroxynitrile lyase from *Manihot esculenta*: highly active and robust biocatalysts. Adv Synth Catal. 2006;348:1655–61.
57. Cui J, Zhao Y, Feng Y, Lin T, Zhong C, Tan Z, Jia S. Encapsulation of spherical cross-linked phenylalanine ammonia lyase aggregates in mesoporous biosilica. J Agric Food Chem. 2017;65:618–25.
58. Cui JD, Sun LM, Li LL. A simple technique of preparing stable CLEAs of phenylalanine ammonia lyase using co-aggregation with starch and bovine serum albumin. Appl Biochem Biotechnol. 2013;170:1827–37.
59. Kumar VV, Sivanesan S, Cabana H. Magnetic cross-linked laccase aggregates—bioremediation tool for decolorization of distinct classes of recalcitrant dyes. Sci Total Environ. 2014;487:830–9.
60. Mateo C, Palomo JM, van Langen LM, van Rantwijk F, Sheldon RA. A new, mild cross-linking methodology to prepare cross-linked enzyme aggregates. Biotechnol Bioeng. 2004;86:273–6.
61. Park SH, Soetyono F, Kim HK. Cadaverine production by using cross-linked enzyme aggregate of *Escherichia coli* lysine decarboxylase. J Microbiol Biotechnol. 2017;27:289–96.
62. Talekar S, Waingade S, Gaikwad V, Patil S, Nagavekar N. Preparation and characterization of cross linked enzyme aggregates (CLEAs) of *Bacillus amyloliquefaciens* alpha amylase. J Biochem Technol. 2012;3:349–53.
63. Zhou LY, Mou HX, Gao J, Ma L, He Y, Jiang YJ. Preparation of cross-linked enzyme aggregates of nitrile hydratase ES-NHT-118 from *E coli* by macromolecular cross-linking agent. Chin J Chem Eng. 2017;25:487–92.
64. Rokney A, Shagan M, Kessel M, Smith Y, Rosenshine I, Oppenheim ABE. *E. coli* transports aggregated proteins to the poles by a specific and energy-dependent process. J Mol Biol. 2009;392:589–601.
65. Cano-Garrido O, Sánchez-Chardi A, Parés S, Giró I, Tatkiewicz WI, Ferrer-Miralles N, Ratera I, Natalello A, Cubarsi R, Veciana J, et al. Functional protein-based nanomaterial produced in microorganisms recognized as safe: a new platform for biotechnology. Acta Biomater. 2016;43:230–9.
66. Wang L. Towards revealing the structure of bacterial inclusion bodies. Prion. 2009;3:139–45.
67. Lopez de la Paz M, Serrano L. Sequence determinants of amyloid fibril formation. Proc Natl Acad Sci USA. 2004;101:87–92.
68. Esteras-Chopo A, Serrano L, Lopez de la Paz M. The amyloid stretch hypothesis: recruiting proteins toward the dark side. Proc Natl Acad Sci USA. 2005;102:16672–7.
69. Teng PK, Eisenberg D. Short protein segments can drive a non-fibrillizing protein into the amyloid state. Protein Eng Des Sel. 2009;22:531–6.
70. Chiti F, Stefani M, Taddei N, Ramponi G, Dobson CM. Rationalization of the effects of mutations on peptide and protein aggregation rates. Nature. 2003;424:805–8.
71. Hamodrakas SJ. Protein aggregation and amyloid fibril formation prediction software from primary sequence: towards controlling the formation of bacterial inclusion bodies. FEBS J. 2011;278:2428–35.
72. Conchillo-Sole O, de Groot NS, Aviles FX, Vendrell J, Daura X, Ventura S. AGGRESCAN: a server for the prediction and evaluation of "hot spots" of aggregation in polypeptides. BMC Bioinform. 2007;8:65.
73. Tompa P. Intrinsically unstructured proteins. Trends Biochemical. Science. 2002;27:527–33.
74. Kalthoff C. A novel strategy for the purification of recombinantly expressed unstructured protein domains. J Chromatogr B Anal Technol Biomed Life Sci. 2003;786:247–54.
75. Kuhlman B, Baker D. Native protein sequences are close to optimal for their structures. Proc Natl Acad Sci. 2000;97:10383.
76. Rohl CA, Strauss CE, Misura KM, Baker D. Protein structure prediction using Rosetta. Methods Enzymol. 2004;383:66–93.
77. Schwarz M. Einflussfaktoren auf die Stabilität und Aktivität der Benzaldehydlyase aus *Pseudomonas fluorescens* in Carboligasereaktionen mit aromatischen Aldehyden. Forschungszentrum Jülich GmbH, IBG-1, Forschungszentrum Jülich; 2010.
78. Miyawaki A, Griesbeck O, Heim R, Tsien RY. Dynamic and quantitative Ca^{2+} measurements using improved cameleons. Proc Natl Acad Sci USA. 1999;96:2135–40.
79. Shaner NC, Steinbach PA, Tsien RY. A guide to choosing fluorescent proteins. Nat Methods. 2005;2:905–9.
80. Studier FW. Protein production by auto-induction in high density shaking cultures. Protein Expr Purif. 2005;41:207–34.
81. Kulig J, Simon RC, Rose CA, Husain SM, Hackh M, Ludeke S, Zeitler K, Kroutil W, Pohl M, Rother D. Stereoselective synthesis of bulky 1,2-diols with alcohol dehydrogenases. Catal Sci Technol. 2012;2:1580–9.
82. Kulishova L, Dimoula K, Jordan M, Wirtz A, Hofmann D, Santiago-Schübel B, Fitter J, Pohl M, Spiess AC. Factors influencing the operational stability of NADPH-dependent alcohol dehydrogenase and an NADH-dependent variant thereof in gas/solid reactors. J Mol Catal B Enzym. 2010;67:271–83.
83. Kulishova L. Analysis of factors influencing enzyme activity and stability in the solid state Heinrich-Heine Universität Düsseldorf, Institut für Molekulare Enzymtechnologie; 2010.
84. Janzen E, Muller M, Kolter-Jung D, Kneen MM, McLeish MJ, Pohl M. Characterization of benzaldehyde lyase from *Pseudomonas fluorescens*: a versatile enzyme for asymmetric C-C bond formation. Bioorg Chem. 2006;34:345–61.
85. Korz DJ, Rinas U, Hellmuth K, Sanders EA, Deckwer WD. Simple fed-batch technique for high cell density cultivation of *Escherichia coli*. J Biotechnol. 1995;39:59–65.
86. Pohl M, Müller M, Demir AS. Nucleotide sequence encoding a benzaldehyde lyase, and process for stereoselectively synthesizing 2-hydroxyketones. vol. US 7,045,334 B2 2006.
87. Bradford MM. A rapid and sensitive method for the quantitation of microgram quantities of protein utilizing the principle of protein-dye binding. Anal Biochem. 1976;72:248–54.
88. Gasteiger E, Hoogland C, Gattiker A, Duvaud SE, Wilkins MR, Appel RD, Bairoch A. Protein identification and analysis tools on the ExPASy server. In: Walker JM, editor. The proteomics protocols handbook. Totowa: Humana Press; 2005. p. 571–607.
89. Schneider CA, Rasband WS, Eliceiri KW. NIH Image to ImageJ: 25 years of image analysis. Nat Methods. 2012;9:671–5.
90. Morschett H, Wiechert W, Oldiges M. Automation of a Nile red staining assay enables high throughput quantification of microalgal lipid production. Microb Cell Fact. 2016;15:34.
91. White SL, Wise RR. Anatomy and ultrastructure of *Wolffia columbiana* and *Wolffia borealis*, two nonvascular aquatic angiosperms. Int J Plant Sci. 1998;159:297–304.
92. Berman HM, Westbrook J, Feng Z, Gilliland G, Bhat TN, Weissig H, Shindyalov IN, Bourne PE. The protein data bank. Nucleic Acids Res. 2000;28:235–42.
93. Krissinel E, Henrick K. Inference of macromolecular assemblies from crystalline state. J Mol Biol. 2007;372:774–97.
94. Jacak R, Leaver-Fay A, Kuhlman B. Computational protein design with explicit consideration of surface hydrophobic patches. Proteins. 2012;80:825–38.

Supporting Information

Tailoring the properties of (catalytically)-active inclusion bodies

V. D. Jäger[1,5+], R. Kloss[2,5+], A. Grünberger[2,4], S. Seide[2], D. Hahn[2], T. Karmainski[2], M. Piqueray[1], J. Embruch[2], S. Longerich[1], U. Mackfeld[2], K.-E. Jaeger[1,2,5], W. Wiechert[2,5], M. Pohl[2,5], and U. Krauss[1,5*]

[1]Institut für Molekulare Enzymtechnologie, Heinrich-Heine-Universität Düsseldorf, Forschungszentrum Jülich, 52425 Jülich, Germany

[2] Forschungszentrum Jülich GmbH, IBG-1: Biotechnology, 52425 Jülich, Germany

[4] Multiscale Bioengineering, Bielefeld University, Universitätsstraße 25, 33615 Bielefeld, Germany

[5] Bioeconomy Science Center (BioSC), c/o, Forschungszentrum Jülich, 52425 Jülich, Germany

*Corresponding author

+Both authors contributed equally

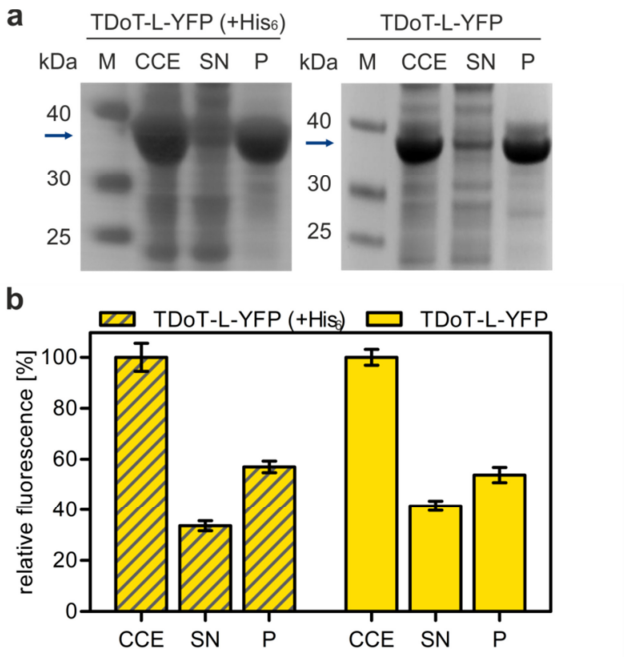

Figure S1: Improving the CatIB strategy by deleting the Hexahistidine-tag (His_6-tag) from the original vector [1]. Evaluation by (a) SDS-PAGE analysis and (b) fluorescence distribution for TDoT-L-YFP (+His) (36.8 kDa) and TDoT-L-YFP (34.6). After cell disruption, the crude cell extract (CCE) was separated by centrifugation into the soluble protein containing supernatant (SN) and the insoluble IB containing pellet (P) fraction. (a) SDS-PAGE analysis of the respective protein fractions: CCE, SN, and P. The molecular mass of the respective fusion protein is indicated by arrows. The protein content in the SN was measured according to Bradford [2]. (b) Normalized fluorescence in the CCE, SN, and P fractions of the respective proteins. Note, that the P fraction was washed once with water and centrifuged again before the fluorescence measurement. The fluorescence in CCE, SN, and P fractions was calculated relative to the activity in the CCE, which was set to 100%. Error bars correspond to the standard deviation of the mean derived from at least three technical replicates.

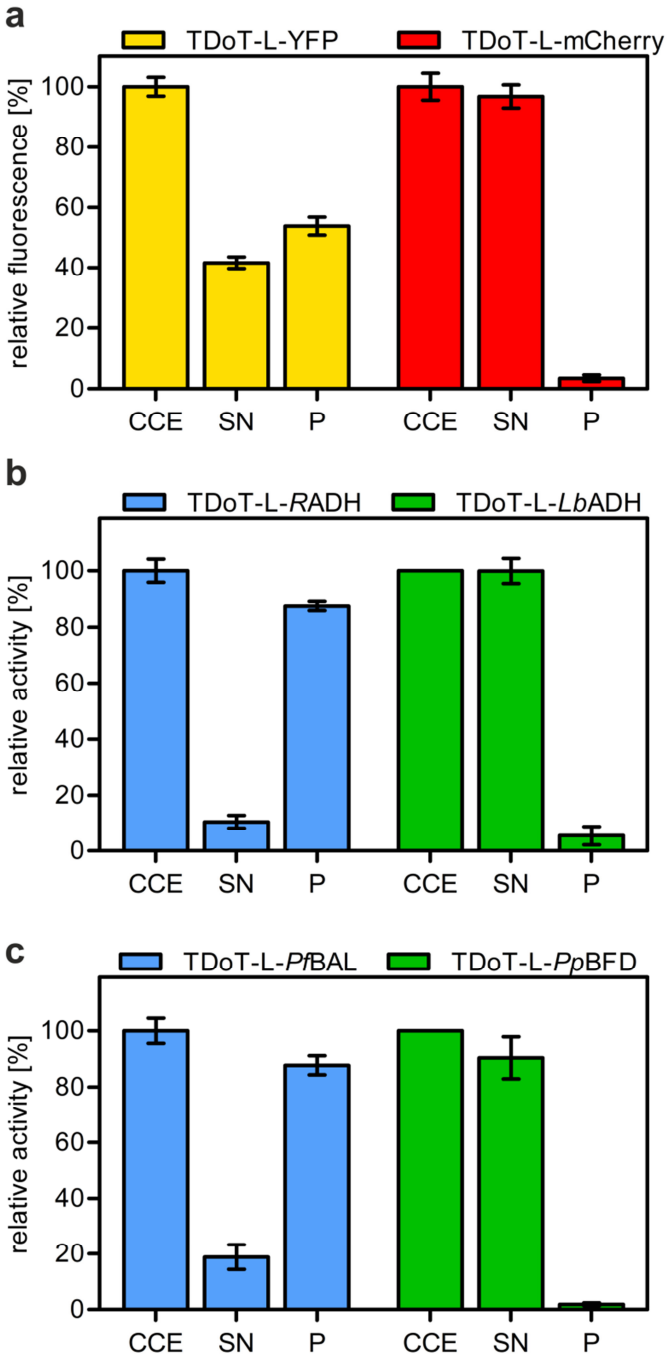

Figure S2: The fluorescence/activity distribution of (a) TDoT-L-YFP-, TDoT-L-mCherry-, (b) TDoT-L-*R*ADH-, TDoT-L-*Lb*ADH-, (c) TDoT-L-*Pf*BAL- and TDoT-L-*Pp*BFD-CatIB. Sample preparation was done as in Figure S1. Initial rate activities were measured by carboligation of 3,5-dimethoxybenzaldehyde (DMBA) to the respective benzoin catalyzed by TDoT-L-*Pf*BAL-CatIBs and decarboxylation of benzoylformate to benzaldehyde by TDoT-L-*Pp*BFD-CatIBs, which was followed by the reduction to benzyl alcohol by horse liver HL-ADH under the oxidation of NADH. Initial rate activities of the ADH enzymes were measured by reduction of 1-phenylethanol (TDoT-L-*Lb*ADH) or cyclohexaone (TDoT-L-*R*ADH) under the consumption of NADPH. For reaction equations see Figure S13. Error bars correspond to the standard deviation of the mean derived from at least three biological replicates. Controls expressing the corresponding soluble versions of YFP, mCherry, *R*ADH, and *Pf*BAL (with TDoT tag) have been presented before [3].

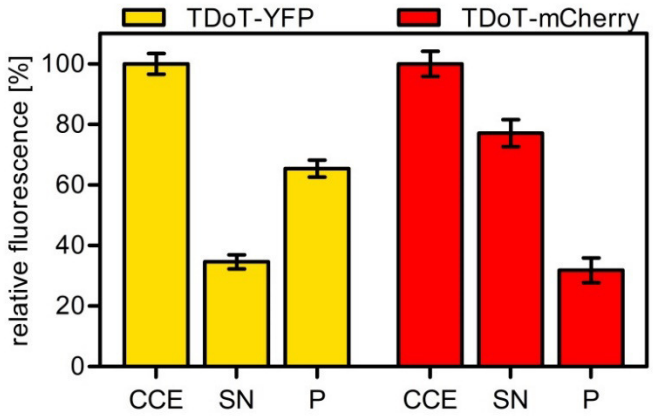

Figure S3: The fluorescence distribution of the linker-free variants TDoT-YFP- and TDoT-mCherry-FIBs. Sample preparation was done as in Figure S1. Error bars correspond to the standard deviation of the mean derived from at least three biological replicates.

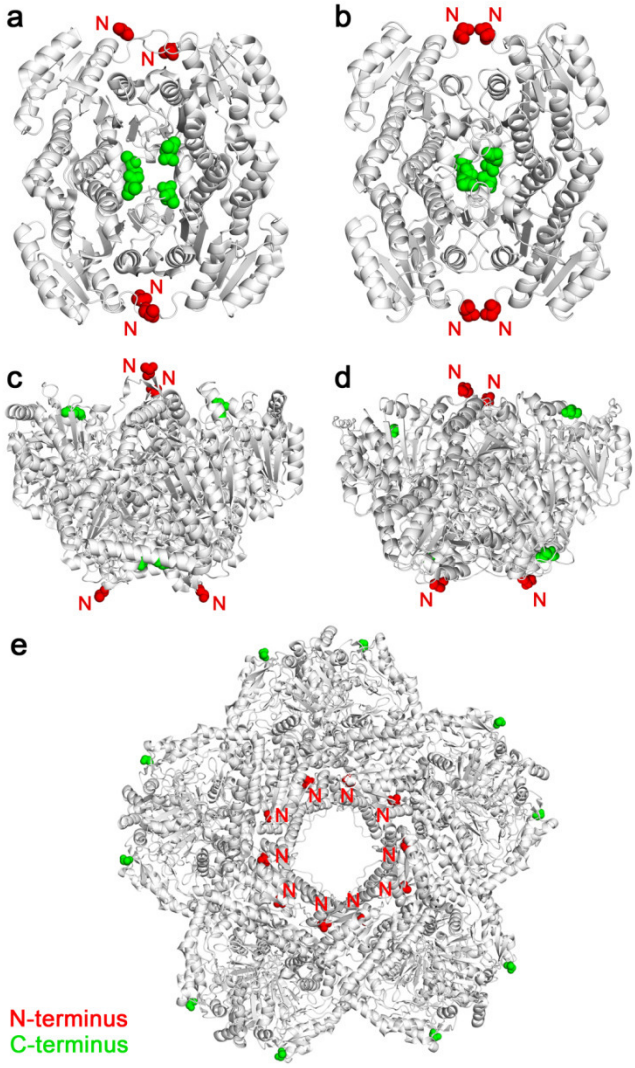

Figure S4: Structures of the multimeric target enzymes of this study: (a) *R*ADH (PDB: 4BMN), (b) *Lb*ADH (PDB: 1ZK4), (c) *Pf*BAL (PDB: 2UZ1), (d) *Pp*BFD (PDB: 5DEI) and (e) *Ec*LDC (PDB: 5FKZ). All subunits are shown in grey cartoon representation, while the N- and C-terminal amino acids are shown as spheres in red (N-terminus) and green (C-terminus). For clarity, only the N-terminus is labelled in each panel. The N-terminus is accessible in *R*ADH, *Lb*ADH, *Pf*BAL, and *Pp*BFD. In contrast, it is buried within the decameric structure in the N-terminal wing domain of the *Ec*LDC multimer, whereas the C-terminus is located at the outer part in the C-terminal domain [4] and hence should be accessible for tag fusion.

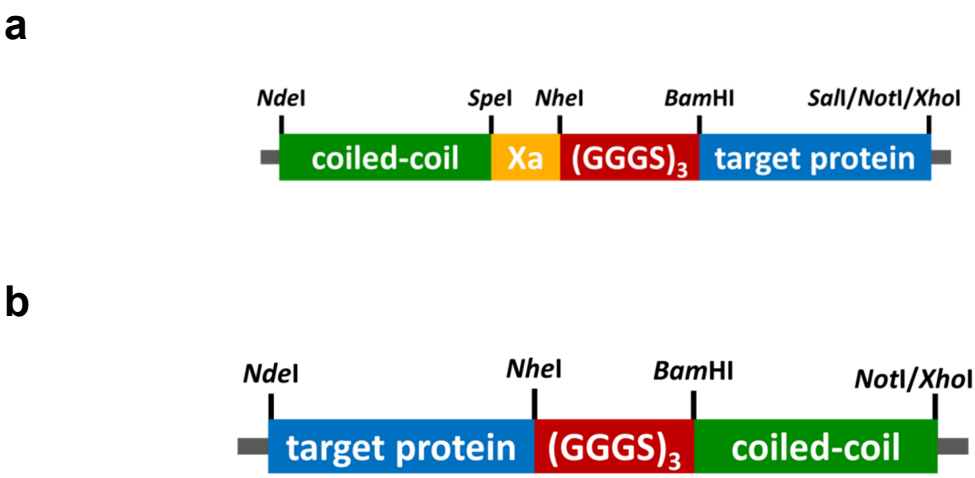

Figure S5: Schematic illustration of the N-terminal (a) and C-terminal (b) fusion strategy employed for the generation of CatIBs/FIBs. All expression vectors/gene fusions are constructed modularly, so that every element can be easily exchanged or deleted, by the use of the depicted restriction sites. Gene fusions consist of coding sequences for: the respective target protein (blue), a coiled-coil domain (green), for which we used the TDoT coiled-coil domain (52 amino acids) of the cell-surface protein tetrabrachion of *Staphylothermus marinus* [5] or the 3HAMP coiled coil (172 amino acids) of the soluble oxygen sensor Aer2 of *Pseudomonas aeruginosa* [6]. Whenever mentioned gene fusions additionally contained a linker region, comprising a cleavage site of the Factor Xa protease (orange, 4 amino acids) and a $(GGGS)_3$-motif (red, 12 amino acids). The gene fusion design shown in (b) was chosen only for the enzyme *Ec*LDC [4].

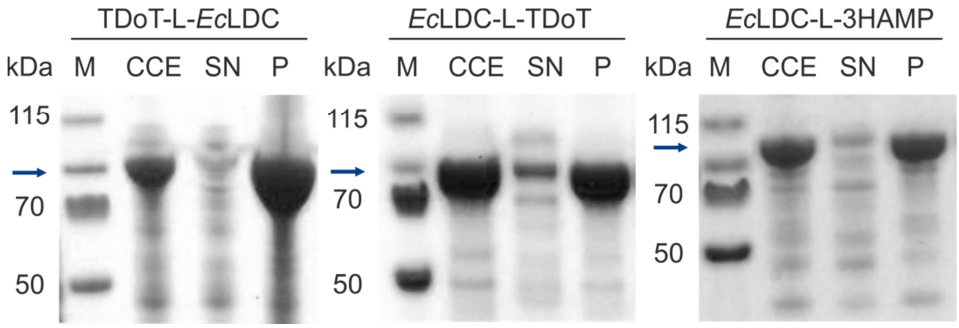

Figure S6: SDS-PAGE analysis of the respective protein fractions of TDoT-L-*Ec*LDC-CatIBs (90.3 kDa), *Ec*LDC-L-TDoT-CatIBs (87.5 kDa) and *Ec*LDC-L-3HAMP-CatIBs (100.5 kDa): crude cell extract (CCE), supernatant (SN), and pellet (P). The target protein is indicated by arrows. Sample preparation was done as in Figure S1.

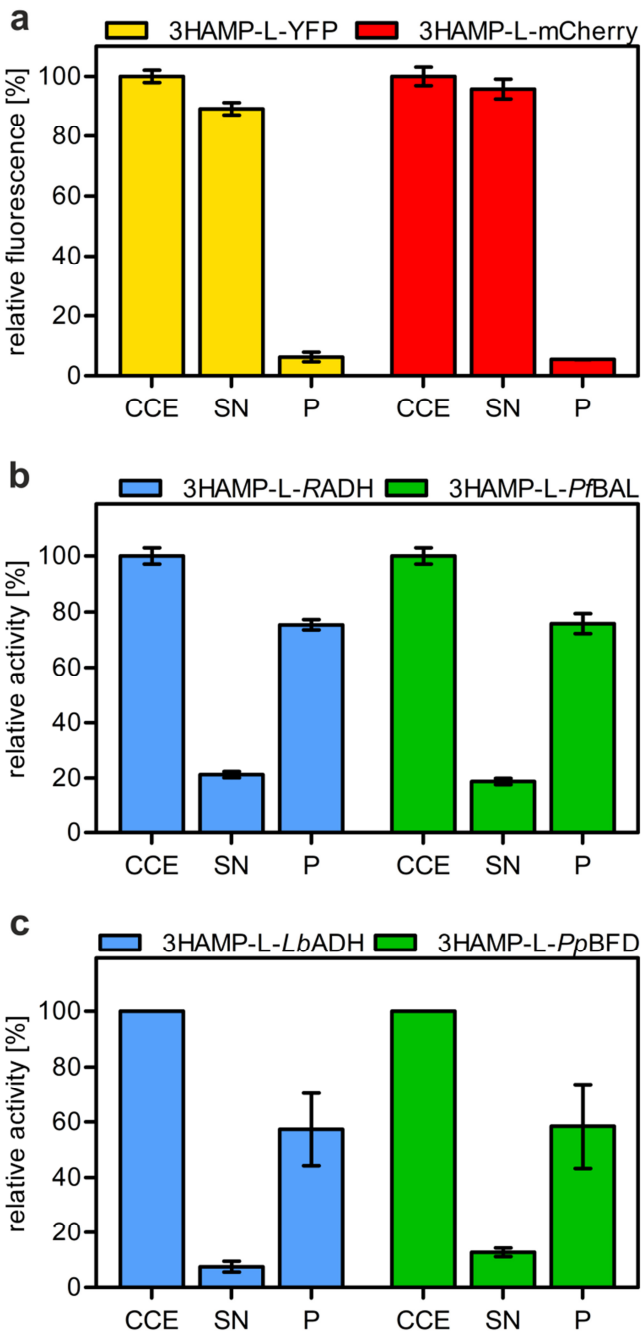

Figure S7: The fluorescence/activity distribution of (a) 3HAMP-L-YFP-, 3HAMP-L-mCherry-, (b) 3HAMP-L-*R*ADH-, 3HAMP-L-*Pf*BAL-, (c) 3HAMP-L-*Lb*ADH-, and 3HAMP-L-*Pp*BFD-CatIBs.. Sample preparation was done as in Figure S1. Initial rate activities were measured by carboligation of 3,5-dimethoxybenzaldehyde (DMBA) to the respective benzoin catalyzed by 3HAMP-L-*Pf*BAL-CatIBs and decarboxylation of benzoylformate to benzaldehyde by 3HAMP-L-*Pp*BFD-CatIBs, which was followed by the reduction to benzyl alcohol by horse liver HL-ADH under the oxidation of NADH. The initial rate activities of the ADH enzymes were measured by reduction of 1-phenylethanol (3HAMP-L-*Lb*ADH) or cycloheaxone (3HAMP-L-*R*ADH) under the consumption of NADPH. For reaction equations see Figure S13. Error bars correspond to the standard deviation of the mean derived from at least three biological replicates.

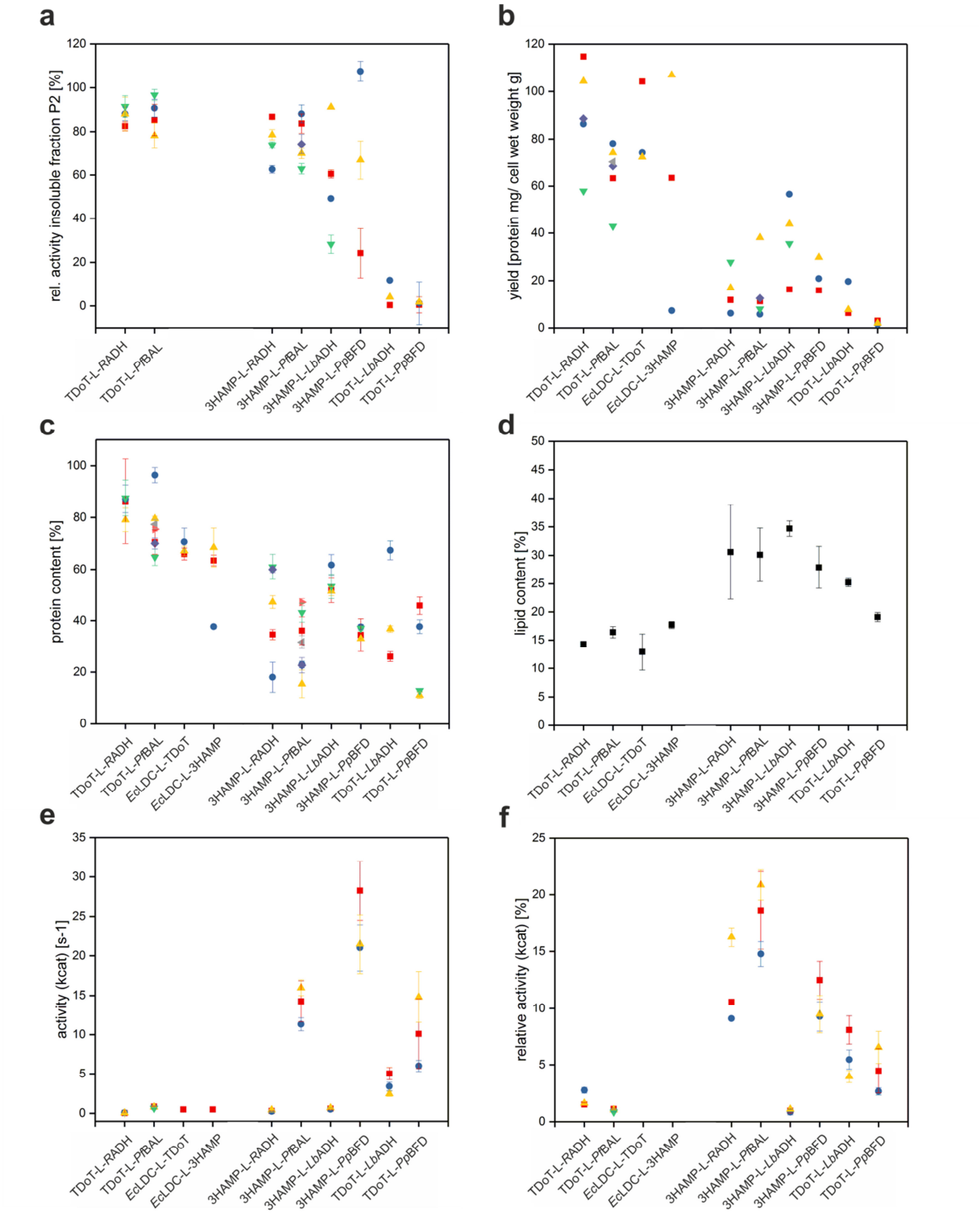

Figure S8: Mean values for each biological replicate with standard deviation (A) for the activity in the pellet compared to CCE, (B) yield (mg protein for 1 g wet cell weight), (C) protein content, and (D) lipid content, based on the dry weight of lyophilized CatIBs, (E) initial rate activity (k_{cat}) and (F) residual activity compared to the soluble enzyme.

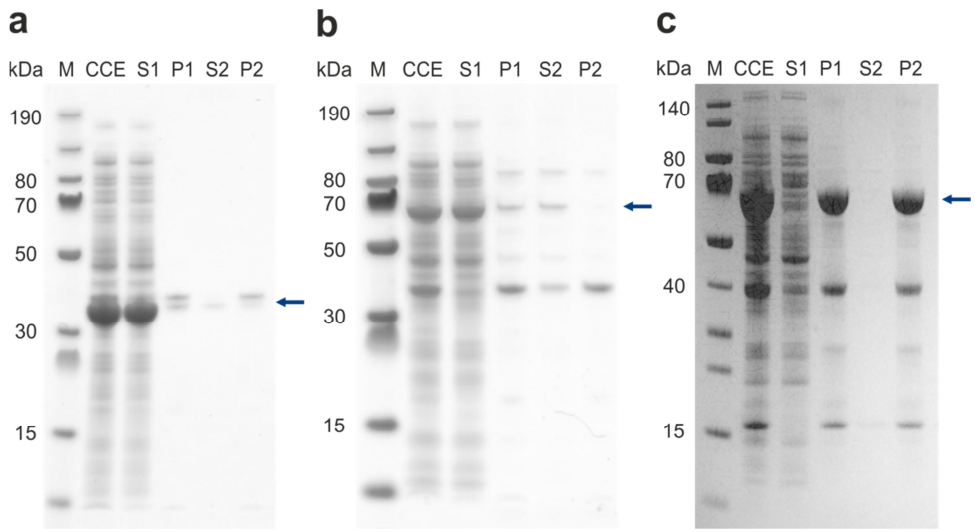

Figure S9: Evaluation of the CatIB strategy by SDS-PAGE analysis of the respective protein fractions of (a) TDoT-L-*Lb*ADH (34.3 kDa), (b) TDoT-L-*Pp*BFD (64.2 kDa) and (c) TDoT-L-*Pf*BAL CatIBs (66.5 kDa): crude cell extract (CCE), supernatant (SN), and pellet (P). The target protein is indicated by arrows. Sample preparation was done as in Figure S1.

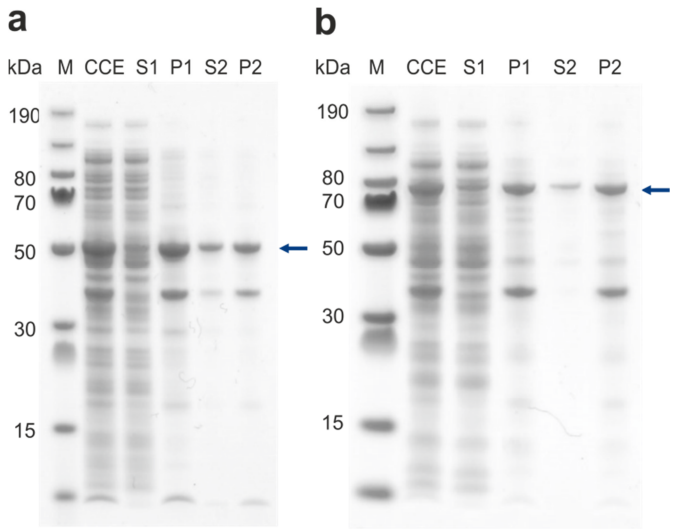

Figure S10: Evaluation of the CatIB strategy by SDS-PAGE analysis of the respective protein fractions of (a) 3HAMP-L-*Lb*ADH- (47.1 kDa), (b) 3HAMP-L-*Pp*BFD-CatIBs (77.0 kDa): crude cell extract (CCE), supernatant (SN), and pellet (P). The target protein is indicated by arrows. Sample preparation was done as in Figure S1.

Table S1: Sequence-based aggregation-propensity prediction for each target protein and the corresponding TDoT fusion. All predictions were carried out using the AGGRESCAN web server (http://bioinf.uab.es/aggrescan) [7]. Displayed are the average aggregation-propensity values per amino acid (a^4v) normalized to a 100 residue protein (Na^4vSS) and the relative change in Na^4vSS (ΔNa^4vSS) due to fusion of the TDoT domain.

target protein	Na^4vSS	TDoT-target-protein fusion	Na^4vSS	ΔNa^4vSS*
YFP	-7.9	TDoT-L-YFP	-6.5	17.7
mCherry	-16.6	TDoT-L-mCherry	-12.6	24.1
*Bs*LA	0.8	TDoT-L-*Bs*LA	-1.4	-275.0
*At*HNL	3.9	TDoT-L-*At*HNL	1.9	-51.3
*Ec*MenD	-3.2	TDoT-L-*Ec*MenD	-3.1	3.1
*R*ADH	-1.7	TDoT-L-*R*ADH	-1.5	11.8
*Lb*ADH	-4.5	TDoT-L-*Lb*ADH	-3.8	15.6
*Pf*BAL	3.6	TDoT-L-*Pf*BAL	2.9	-19.4
*Pp*BFD	-1.3	TDoT-L-*Pp*BFD	-1.4	-7.7

*calculated according to: $\Delta Na^4vSS = \left(\frac{(Na^4vSS_{fusion} - Na^4vSS_{target})}{|Na^4vSS_{target}|}\right) \times 100\right)$ [7].

Table S2: Surface properties of the target proteins used in this study. The presence/absence of large hydrophobic surface patches for the corresponding target protein structures was quantified using the hpatch tool implemented in Rosetta [8-10]. Surface areas were quantified using Pymol 1.7.0.0 (Schrödinger, LCC, New York, NY, USA).

target protein	PDB-ID	comments	hydrophobic patch area [A^2]	solvent accessible surface area (SASA) [A^2]	hydrophob. patch area / overall SASA [%]
YFP	1YFP	asu, monomer, chain A and B	1000	9467	10.6
YFP*	1YFP	1st PISA dimer	1085	16914	6.4
mCherry*	2H5Q	asu, monomer	0	9493	0
*Bs*LA*	1ISP	asu, monomer	972	7867	12.4
*At*HNL*	3DQZ	asu, dimer, chain A and B	1692	18662	9.1
*Ec*MenD	2JLC	asu, dimer	1566	34022	4.6
*Ec*MenD*	2JLC	1st PISA tetramer	3797	54278	7.0
*R*ADH	4BMN	tetramer	1183	27318	4.3
*R*ADH*	4BMN	1st PISA dimer	2068	17423	11.9
*Lb*ADH	1ZK4	1st PISA tetramer	2748	27590	9.9
*Lb*ADH*	1ZK4	2nd PSIA dimer	874	18316	4.8
*Pf*BAL*	2UZ1	asu, tetramer	5194	52235	9.9
*Pp*BFD*	5DEI	asu, tetramer	185	69766	0.27

* final data used in Figure 6c; main paper; asu: the pdb coordinates present in the asymmetric unit were used for surface calculations.

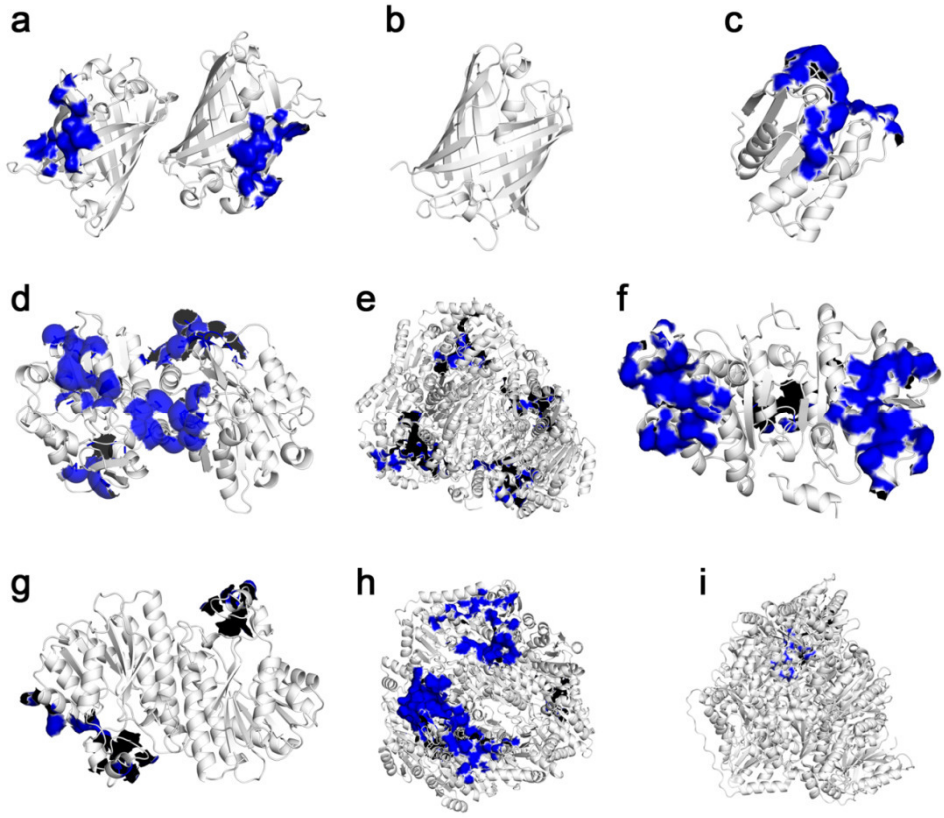

Figure S11: Hydrophobic patch analysis of (a) YFP, (b) mCherry, (c) *Bs*LA, (d) *At*HNL, (e) *Ec*MenD, (f) *R*ADH, (g) *Lb*ADH, (h) *Pf*BAL, and (i) *Pp*BFD. Structures are shown in cartoon representation in grey with the Rossetta-identified hydrophobic surface patches shown as blue surfaces [9, 10]. PDB-IDs were as follows YFP (1YFP), mCherry (2H5Q), *Bs*LA (1ISP), *At*HNL (3DWZ), *Ec*MenD (2JLC), *R*ADH (4BMN), *Lb*ADH (1ZK4), *Pf*BAL (2UZ1) and *Pp*BFD (5DEI).

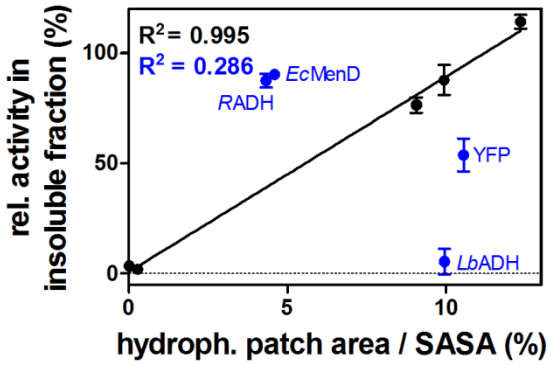

Figure S12: Computational analysis of the structural determinants of CatIB formation. The presence/absence of large hydrophobic surface patches for the corresponding target protein structures was quantified using the hpatch tool implemented in Rosetta [8-10]. Surface areas were quantified using Pymol 1.7.0.0 (Schrödinger, LCC, New York, NY, USA). CatIB-formation was plotted as the relative activity in the insoluble fraction (Table S6). Coefficient of determination (R^2) values are always given excluding the blue-highlighted outliers (black) and including the outliers (blue).

Table S3: Plasmids used in this study. DNA and amino acid sequences of all gene fusions are given in the annex.

Vector	Genotyp	Description
pET28a	*ColE1 lacZ'* Kan^R P_{T7} P_{lac}	Merck (Darmstadt, Germany)
pTDoT-Linker-YFP	pET-28a, P_{T7}, gene fusion [*His-tag- tdot*-factor Xa recognition site- *(GGGS)$_3$ linker-yfp*]	[11]
pTDoT-L-YFP	pET-28a, P_{T7}, gene fusion [*tdot*-factor Xa recognition site-*(GGGS)$_3$ linker-yfp*]	pTDoT-Linker-YFP derivative, insertion of a 40 bp *Xba*I/*Nde*I RBS containing fragment of pET28a in pTDoT-Linker-YFP; without the 99 bp fragment containing RBS and *His-tag* [3]
pTDoT-YFP	pET-28a, P_{T7}, gene fusion [*tdot-yfp*]	pTDoT-L-YFP derivative, insertion of a 155 bp *Nde*I/*Bam*HI *tdot*-containing fragment in pTDoT-L-YFP; without the 215 bp fragment containing *tdot*, factor Xa recognition site and *(GGGS)$_3$ linker*
p3HAMP-L-YFP	pET-28a, P_{T7}, gene fusion [*3hamp*-factor Xa recognition site-*(GGGS)$_3$ linker-yfp*]	pTDoT-L-YFP derivative, insertion of a 518 bp *Nde*I/*Spe*I *3hamp*-containing fragment in pTDoT-L-YFP; without the 155 bp fragment containing *tdot*,
pTDoT-L-mCherry	pET-28a, P_{T7}, gene fusion [*tdot*-factor Xa recognition site-*(GGGS)$_3$ linker- mcherry*]	pTDoT-L-YFP derivative, insertion of 717 bp PCR-amplified *Bam*HI/*Sal*I *mcherry* fragment in pTDoT-L-YFP; without the 726 bp fragment containing *yfp* [3]
pTDoT-mCherry	pET-28a, P_{T7}, gene fusion [*tdot- mcherry*]	pTDoT-L-mCherry derivative, insertion of 155 bp *Nde*I/*Bam*HI *tdot*-containing fragment in pTDoT-L-mCherry; without the 215 bp fragment containing *tdot*, factor Xa recognition site and *(GGGS)$_3$ linker* [3]
p3HAMP-L-mCherry	pET-28a, P_{T7}, gene fusion [*3hamp*-factor Xa recognition site-*(GGGS)$_3$ linker-mcherry*]	pTDoT-L-mCherry derivative, insertion of a 518 bp *Nde*I/*Spe*I *3hamp*-containing fragment in pTDoT-L-mCherry; without the 155 bp fragment containing *tdot*,
pET22b-*R*ADH	pET22b, P_{T7}, *radh* gene	[12]
pTDoT-L-*R*ADH	pET-28a, P_{T7}, gene fusion [*tdot*- factor Xa recognition site-*(GGGS)$_3$ linker-radh*]	pTDoT-L-YFP derivative, insertion of 756 bp PCR-amplified *Bam*HI/*Sal*I *radh* fragment in pTDoT-L-YFP; without the 726 bp fragment containing *yfp* [3]
p3HAMP-L-*R*ADH	pET-28a, P_{T7}, gene fusion [*3hamp*-factor Xa recognition site-*(GGGS)$_3$ linker-radh*]	pTDoT-L-*R*ADH derivative, insertion of a 518 bp *Nde*I/*Spe*I *3hamp*-containing fragment in pTDoT-L-*R*ADH; without the 155 bp fragment containing *tdot*
pET21a-*Lb*ADH	pET21a, P_{T7}, *lbadh* gene	[13]
pTDoT-L-*Lb*ADH	pET-28a, P_{T7}, gene fusion [*tdot*-factor Xa recognition site-*(GGGS)$_3$ linker-lbadh*]	pTDoT-L-YFP derivative, insertion of 766 bp PCR-amplified *Bam*HI/*Sal*I *lbadh* fragment in pTDoT-L-YFP; without the 726 bp fragment containing *yfp*
p3HAMP-L-*Lb*ADH	pET-28a, P_{T7}, gene fusion [*3hamp*-factor Xa recognition site-*(GGGS)$_3$ linker-lbadh*]	p3HAMP-L-*R*ADH derivative, insertion of 766 bp PCR-amplified *Bam*HI/*Sal*I *lbadh* fragment in p3HAMP-L-*R*ADH; without the 756 bp fragment containing *radh*
pKK233_2-*Pf*BAL-*His*	pKK233_2 P_{trc}, gene fusion [*pfbal, His-tag]*	[14]
pTDoT-L-*Pf*BAL	pET-28a, P_{T7}, gene fusion [*tdot*-factor Xa recognition site-*(GGGS)$_3$ linker- pfbal*]	pTDoT-L-YFP derivative, insertion of 1699 bp PCR-amplified *Bam*HI/*Not*I *pfbal* fragment in pTDoT-L-YFP; without the 739 bp fragment containing *yfp* [3, 15]
p3HAMP-L-*Pf*BAL	pET-28a, P_{T7}, gene fusion [*3hamp*-factor Xa recognition site-*(GGGS)$_3$ linker-pfbal*]	pTDoT-L-*Pf*BAL derivative, insertion of a 518 bp *Nde*I/*Spe*I *3hamp*-containing fragment in pTDoT-L-*Pf*BAL; without the 155 bp fragment containing *tdot* [15]
pKK233_2-*Pp*BFD *L476Q-His*	pKK233_2 P_{trc}, gene fusion [*ppbfd, His-tag]*	[16]
pTDoT-L-*Pp*BFD *L476Q*	pET-28a, P_{T7}, gene fusion [*tdot*-factor Xa recognition site-*(GGGS)$_3$ linker-ppbfd*]	pTDoT-L-YFP derivative, insertion of 1600 bp PCR-amplified *Bam*HI/*Not*I *ppbfd* fragment in pTDoT-L-YFP; without the 739 bp fragment containing *yfp*
p3HAMP-L-*Pp*BFD *L476Q*	pET-28a, P_{T7}, gene fusion [*3hamp*-factor Xa recognition site-*(GGGS)$_3$ linker-ppbfd*]	p3HAMP-L-*Pf*BAL derivative, insertion of 766 bp PCR-amplified *Bam*HI/*Not*I *ppbfd* fragment in p3HAMP-L-*Pf*BAL; without the 1699 bp fragment containing *pfbal*
pTDoT-L-*Ec*LDC	pET-28a, P_{T7}, gene fusion [*tdot*-factor Xa recognition site-*(GGGS)$_3$ linker-ecldc*]	pTDoT-L-YFP derivative, insertion of 2148 bp PCR-amplified *Bam*HI/*Sal*I *ecldc* fragment in pTDoT-L-YFP; without the 726 bp fragment containing *yfp*
p*Ec*LDC-L-TDoT	pET-28a, P_{T7}, gene fusion [*ecldc-(GGGS)$_3$ linker-tdot*]	pTDoT-L-*Pf*BAL derivative, i) insertion of 2144 bp PCR-amplified *Nde*I/*Nhe*I *ecld* fragment in pTDoT-L-*Pf*BAL; without the 173 bp fragment containing *tdot-Xa*, ii) insertion of 160 bp PCR-amplified *Bam*HI/*Not*I *tdot* fragment in p*Ec*LDC-L-*Pf*BAL, without the 1699 bp fragment containing *bfbal* [17]
p*Ec*LDC-L-3HAMP	pET-28a, P_{T7}, gene fusion [*ecldc-(GGGS)$_3$ linker-3hamp*]	p*Ec*LDC-L-TDoT derivative, insertion of 526 bp PCR-amplified *Bam*HI/*Not*I *3hamp* fragment in p*Ec*LDC-L-TDoT; without the 160 bp fragment containing *tdot*

Table S4: Oligonucleotide primers used in this study. Restriction endonuclease cleavage sites are underlined.

Name	Sequence (5' - 3')	Application
*Bam*HI_YFP_fw	ATATATGGATCCATGGTGAGCAAGGGCGAG	PCR amplification of *yfp*
YFP_*Sal*I_rv	ATATATGTCGACTTACTTGTACAGCTCGTCCATG	
*Bam*HI_mCherry_fw	ATATATGGATCCATGGTGAGCAAGGGCGAGGAGG	PCR amplification of *mcherry*
mCherry_*Sal*I_rv	ATATATGTCGACTTACTTGTACAGCTCGTCCATGCCGC	
*Bam*HI_*Pf*BAL_fw	ATATATGGATCCATGGCGATGATTACAGGCGGCGAAC	PCR amplification of *pfbal*
*Pf*BAL_*Not*I_rv	ATATATGCGGCCGCTTATGCGAAGGGGTCCATG	
*Bam*HI_*R*ADH_fw	ATATATGGATCCATGTATCGTCTGCTGAATAAAACCGC	PCR amplification of *radh*
*R*ADH_*Sal*I_rv	ATATATGTCGACTTAAACCTGGGTCAGACCACCATC	
*Nde*I_ TDoT_fw	ATATATCATATGATCATTAACGAAACTGCCGATGAC	Removal of factor Xa recognition site and $(GGGS)_3$ linker
TDoT_*Bam*HI_rv	TATATAGGATCCAATGCTCGCGAGAATGGTG	
RBS_Oligo_fw	CTAGAAATAATTTTGTTTAACTTTAAGAAGGAGATATACA	Removal of His-Tag
RBS_Oligo_rv	TATGTATATCTCCTTCTTAAAGTTAAACAAAATTATTT	
*Bam*HI_*Lb*ADH_fw	ATATATGGATCCATGTCTAACCGTTTGGATGGTAAGGTAG	PCR amplification of *lbadh*
*Lb*ADH_*Sal*I_rev	ATATATGTCGACTCTATTGAGCAGTGTAGCCACCG	
*Bam*HI_BFD_fw	ATATATGGATCCATGGCTTCGGTACACGGCACCAC	PCR amplification of *ppbfd*
BFD_*Not*I_rev	ATATATGCGGCCGCTTAAGATCTCTTCACCGGGCTTAC	
*Bam*HI_LDC_fwd	ATATATGGATCCATGAACATCATCGCTATCATGGGCCC	PCR amplification of *ecldc*
LDC_*Sal*I_rev	ATATATGTCGACTTAGCCTGCCATCTTAAGGACGCG	
*Nde*I_LDC_fw	ATATATCATATGATGAACATCATCGCTATCATGGGCCC	PCR amplification of *ecldc*
LDC_*Nhe*I_rv	ATATATGCTAGCGCCTGCCATCTTAAGGACG	
*Bam*HI_TDot_fw	ATATATGGATCCATCATTAACGAAACTGCCGATGACATCG	PCR amplification of *tdot*
TDot_*Not*I_rv	ATATATGCGGCCGCTTAAATGCTCGCGAGAATG	
*Bam*HI_3HAMP_fw	ACGTATGGATCCATGGGCCTGTTTAACGCCCATGCAGTTG	PCR amplification of *3hamp*
3HAMP_*Not*I_rev	ACATATGCGGCCGCTTAATTGTAGGCGGCTGTGGCCAGC	

Table S5: The used strains are given with genotype and reference or source.

strains	genotype	reference or source
E. coli BL21 (DE3)	*F⁻ ompT hsdSB(rB⁻ mB⁻) gal dcm (λIts857ind1 Sam7 nin5 lacUV5-T7 gene1)*	[18] Invitrogen (Carlsbad, USA)
E. coli DH5α	*supE44 ΔlacU169 (Φ80lacZDM15) hsdR17 recA1 endA1 gyrA96 thi-1 relA1*	Invitrogen (Carlsbad, USA)
E. coli SG 13009	*F⁻ ompT hsdS$_B$ (rB⁻mB⁻) dcm gal* (DE3)	Qiagen (Hilden Germany)

Table S6: Extinction coefficient and molecular weight of all used enzymes and proteins in soluble and CatIB form calculated with ExPASy ProtParam Tool (http://expasy.org/tools/protparam [19]).

Protein	Extinction coefficient [$L \cdot mol^{-1} \cdot cm^{-1}$]	Molecular weight [kDa]
TDoT-L-YFP-CatIBs	26 485	34.6
TDoT-YFP-CatIBs	26 485	33.1
3HAMP-L-YFP-CatIBs	34 965	47.4
TDoT-L-mCherry-CatIBs	37 360	34.3
TDoT-mCherry-CatIBs	37 360	32.7
3HAMP-L-mCherry-CatIBs	45 840	47.1
soluble *R*ADH	14 440	26.7
TDoT-L-*R*ADH-CatIBs	17 420	34.3
3HAMP-L-*R*ADH-CatIBs	25 900	47.1
soluble *Lb*ADH	19 940	26.8
TDoT-L-*Lb*ADH-CatIBs	22 920	34.3
3HAMP-L-*Lb*ADH-CatIBs	31 400	47.1
soluble *Pf*BAL	52 160	60.0
TDoT-L-*Pf*BAL-CatIBs	55 140	66.5
3HAMP-L-*Pf*BAL-CatIBs	63 620	79.3
soluble *Pp*BFD	62 340	57.4
TDoT-L- *Pp*BFD-CatIBs	65 320	64.2
3HAMP- *L-Pp*BFD-CatIBs	73 800	77.0
TDoT- L-*Ec*LDC-CatIBs	109 210	90.3
*Ec*LDC-L-TDoT-CatIBs	109 210	87.5
*Ec*LDC-L-3HAMP-CatIBs	117 690	100.5

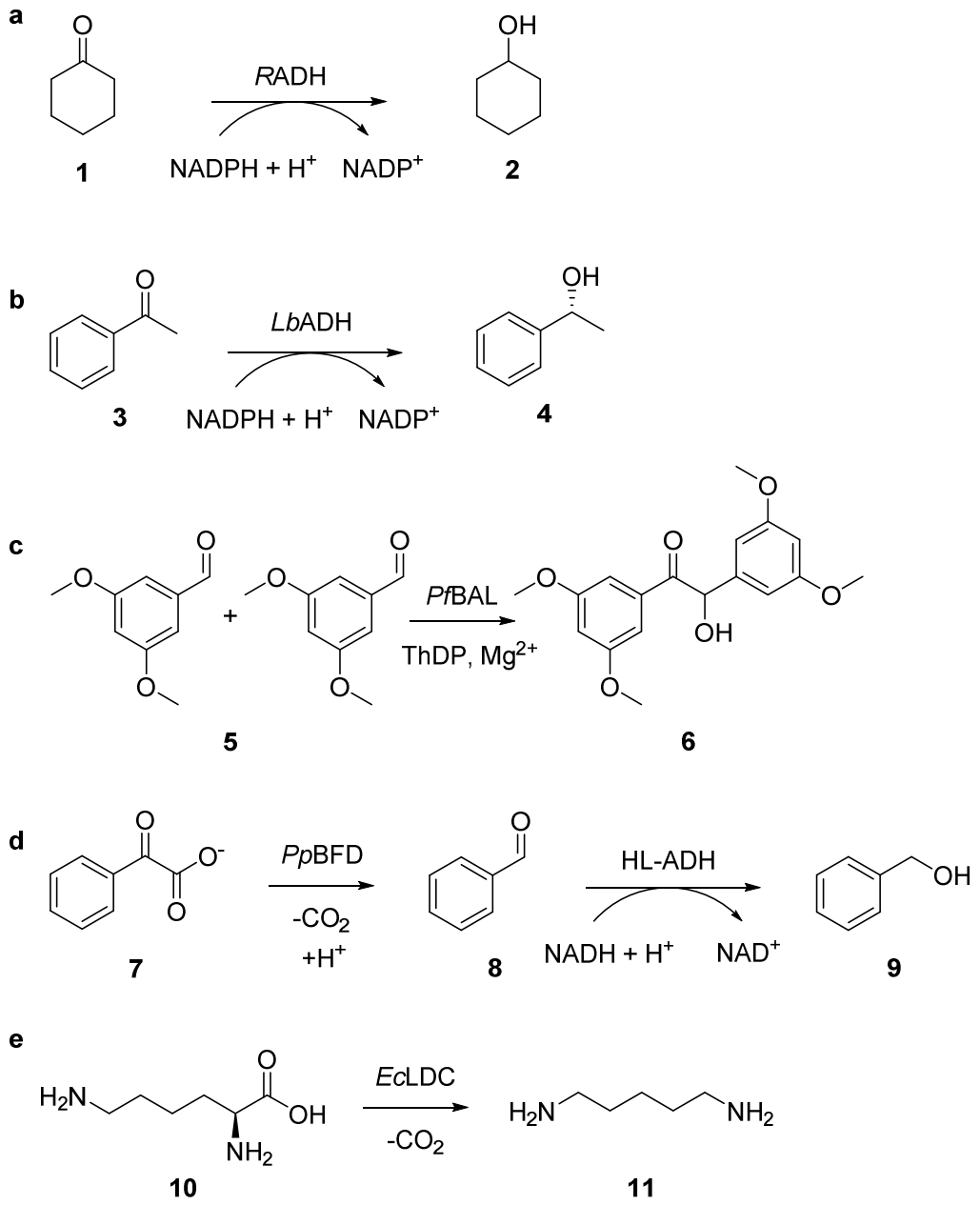

Figure S13: Reactions to measure the initial rate activities of the enzymes used in this study. (a) *R*ADH-CatIBs catalyze the reduction of cyclohexanone 1 to cyclohexanol 2 under the consumption of NADPH. (b) *Lb*ADH-CatIBs catalyze the reduction of acetophenone 3 to (*R*)-1-phenylethanol 4 under the consumption of NADPH. (c) *Pf*BAL-CatIBs catalyze the carboligation of 3,5-dimethoxybenzaldehyde (DMBA, 5) to the respective benzoin (*R*)-(3,3´,5,5´)-tetramethoxybenzoin (TMBZ, 6). (d) *Pp*BFD-CatIBs catalyze the decarboxylation of benzoylformate 7 to benzaldehyde 8 followed by the reduction to benzyl alcohol 9 by horse liver (HL-)ADH under the oxidation of NADH. (e) *Ec*LDC-CatIBs catalyze the decarboxylation of L-lysine 10 to cadaverine (1,5-diaminopentane, 11).

DNA and amino acid sequence of the fusion constructs

The here employed variant of the yellow fluorescent protein (YFP) was derived from introducing the A206K mutation into enhanced YFP (eYFP). In contrast to mYFP [20] this variant lacks the Q69K mutation, which renders YFP less pH-sensitive in the neutral pH range [21]. The here used *Pp*BFD variant L476Q was derived from error-prone PCR and is described elsewhere [16].

TDoT-L-YFP

```
   M  I  I  N  E  T  A  D  D  I  V  Y  R  L  T  V  I  I  D  D  R  Y  E  S
CATATGATCATTAACGAAACTGCCGATGACATCGTTTATCGCCTGACAGTCATTATCGATGATCGCTACGAATCG
NdeI          TDoT
L  K  N  L  I  T  L  R  A  D  R  L  E  M  I  I  N  D  N  V  S  T  I  L  A
CTGAAAAACCTGATTACCTTACGTGCAGATCGCTTGGAGATGATCATCAATGACAATGTGTCCACCATTCTCGCG

S  I  T  S  I  E  G  R  A  S  G  G  G  S  G  G  G  S  G  G  G  S  G  S  M
AGCATTACTAGTATTGAAGGCCGTGCTAGCGGCGGTGGGTCTGGAGGCGGCTCAGGTGGTGGGTCGGGATCCATG
   SpeI      Xa          NheI      3xGGGS-Linker                    BamHI
V  S  K  G  E  E  L  F  T  G  V  V  P  I  L  V  E  L  D  G  D  V  N  G  H
GTGAGCAAGGGCGAGGAGCTGTTCACCGGGGTGGTGCCCATCCTGGTCGAGCTGGACGGCGACGTAAACGGCCAC
YFP
K  F  S  V  S  G  E  G  E  G  D  A  T  Y  G  K  L  T  L  K  F  I  C  T  T
AAGTTCAGCGTGTCCGGCGAGGGCGAGGGCGATGCCACCTACGGCAAGCTGACCCTGAAGTTCATCTGCACCACC

G  K  L  P  V  P  W  P  T  L  V  T  T  F  G  Y  G  L  Q  C  F  A  R  Y  P
GGCAAGCTGCCCGTGCCCTGGCCCACCCTCGTGACCACCTTCGGCTACGGCCTGCAGTGCTTCGCCCGCTACCCC

D  H  M  K  Q  H  D  F  F  K  S  A  M  P  E  G  Y  V  Q  E  R  T  I  F  F
GACCACATGAAGCAGCACGACTTCTTCAAGTCCGCCATGCCCGAAGGCTACGTCCAGGAGCGCACCATCTTCTTC

K  D  D  G  N  Y  K  T  R  A  E  V  K  F  E  G  D  T  L  V  N  R  I  E  L
AAGGACGACGGCAACTACAAGACCCGCGCCGAGGTGAAGTTCGAGGGCGACACCCTGGTGAACCGCATCGAGCTG

K  G  I  D  F  K  E  D  G  N  I  L  G  H  K  L  E  Y  N  Y  N  S  H  N  V
AAGGGCATCGACTTCAAGGAGGACGGCAACATCCTGGGGCACAAGCTGGAGTACAACTACAACAGCCACAACGTC

Y  I  M  A  D  K  Q  K  N  G  I  K  V  N  F  K  I  R  H  N  I  E  D  G  S
TATATCATGGCCGACAAGCAGAAGAACGGCATCAAGGTGAACTTCAAGATCCGCCACAACATCGAGGACGGCAGC

V  Q  L  A  D  H  Y  Q  Q  N  T  P  I  G  D  G  P  V  L  L  P  D  N  H  Y
GTGCAGCTCGCCGACCACTACCAGCAGAACACCCCCATCGGCGACGGCCCCGTGCTGCTGCCCGACAACCACTAC

L  S  Y  Q  S  K  L  S  K  D  P  N  E  K  R  D  H  M  V  L  L  E  F  V  T
CTGAGCTACCAGTCCAAACTGAGCAAAGACCCCAACGAGAAGCGCGATCACATGGTCCTGCTGGAGTTCGTGACC

A  A  G  I  T  L  G  M  D  E  L  Y  K  *
GCCGCCGGGATCACTCTCGGCATGGACGAGCTGTACAAGTAAGTCGACAAGCTTGCGGCCGCACTCGAG
                                          SalI          NotI     XhoI
```

TDoT-YFP

```
   M  I  I  N  E  T  A  D  D  I  V  Y  R  L  T  V  I  I  D  D  R  Y  E  S
CATATGATCATTAACGAAACTGCCGATGACATCGTTTATCGCCTGACAGTCATTATCGATGATCGCTACGAATCG
NdeI          TDoT
L  K  N  L  I  T  L  R  A  D  R  L  E  M  I  I  N  D  N  V  S  T  I  L  A
CTGAAAAACCTGATTACCTTACGTGCAGATCGCTTGGAGATGATCATCAATGACAATGTGTCCACCATTCTCGCG

S  I  G  S  M  V  S  K  G  E  E  L  F  T  G  V  V  P  I  L  V  E  L  D  G
AGCATTGGATCCATGGTGAGCAAGGGCGAGGAGCTGTTCACCGGGGTGGTGCCCATCCTGGTCGAGCTGGACGGC
    BamHI  YFP
D  V  N  G  H  K  F  S  V  S  G  E  G  E  G  D  A  T  Y  G  K  L  T  L  K
GACGTAAACGGCCACAAGTTCAGCGTGTCCGGCGAGGGCGAGGGCGATGCCACCTACGGCAAGCTGACCCTGAAG

F  I  C  T  T  G  K  L  P  V  P  W  P  T  L  V  T  T  F  G  Y  G  L  Q  C
TTCATCTGCACCACCGGCAAGCTGCCCGTGCCCTGGCCCACCCTCGTGACCACCTTCGGCTACGGCCTGCAGTGC

F  A  R  Y  P  D  H  M  K  Q  H  D  F  F  K  S  A  M  P  E  G  Y  V  Q  E
TTCGCCCGCTACCCCGACCACATGAAGCAGCACGACTTCTTCAAGTCCGCCATGCCCGAAGGCTACGTCCAGGAG

R  T  I  F  F  K  D  D  G  N  Y  K  T  R  A  E  V  K  F  E  G  D  T  L  V
CGCACCATCTTCTTCAAGGACGACGGCAACTACAAGACCCGCGCCGAGGTGAAGTTCGAGGGCGACACCCTGGTG
```

```
N  R  I  E  L  K  G  I  D  F  K  E  D  G  N  I  L  G  H  K  L  E  Y  N  Y
AACCGCATCGAGCTGAAGGGCATCGACTTCAAGGAGGACGGCAACATCCTGGGGCACAAGCTGGAGTACAACTAC

N  S  H  N  V  Y  I  M  A  D  K  Q  K  N  G  I  K  V  N  F  K  I  R  H  N
AACAGCCACAACGTCTATATCATGGCCGACAAGCAGAAGAACGGCATCAAGGTGAACTTCAAGATCCGCCACAAC

I  E  D  G  S  V  Q  L  A  D  H  Y  Q  Q  N  T  P  I  G  D  G  P  V  L  L
ATCGAGGACGGCAGCGTGCAGCTCGCCGACCACTACCAGCAGAACACCCCCATCGGCGACGGCCCCGTGCTGCTG

P  D  N  H  Y  L  S  Y  Q  S  K  L  S  K  D  P  N  E  K  R  D  H  M  V  L
CCCGACAACCACTACCTGAGCTACCAGTCCAAACTGAGCAAAGACCCCAACGAGAAGCGCGATCACATGGTCCTG

L  E  F  V  T  A  A  G  I  T  L  G  M  D  E  L  Y  K  *
CTGGAGTTCGTGACCGCCGCCGGGATCACTCTCGGCATGGACGAGCTGTACAAGTAAGTCGACAAGCTTGCGGCC
                                                        SalI          NotI
GCACTCGAGCACCACCACCACCACCACTGAGATCCGGCT
  XhoI
```

3HAMP-L-YFP

```
   M  G  L  F  N  A  H  A  V  A  Q  Q  R  A  D  R  I  A  T  L  L  Q  S  F
CATATGGGCCTGTTTAACGCCCATGCAGTTGCGCAGCAACGCGCGGATCGCATTGCGACTCTCCTGCAGTCCTTT
NdeI          3HAMP
A  D  G  Q  L  D  T  A  V  G  E  A  P  A  P  G  Y  E  R  L  Y  D  S  L  R

GCGGATGGTCAGTTGGACACCGCCGTGGGTGAAGCGCCAGCACCTGGTTACGAACGCCTGTATGACTCGCTTCGC
A  L  Q  R  Q  L  R  E  Q  R  A  E  L  Q  Q  V  E  S  L  E  A  G  L  A  E

GCCCTTCAGCGCCAACTGCGCGAACAACGTGCGGAGTTACAACAGGTTGAGAGCCTGGAAGCAGGCTTGGCTGAA
M  S  R  Q  H  E  A  G  W  I  D  Q  T  I  P  A  E  R  L  E  G  R  A  A  R

ATGAGTCGGCAGCATGAAGCAGGGTGGATTGACCAGACGATTCCGGCTGAACGGTTAGAGGGCCGTGCAGCACGT
I  A  K  G  V  N  E  L  V  A  A  H  I  A  V  K  M  K  V  V  S  V  V  T  A

ATCGCCAAAGGCGTGAATGAGCTGGTTGCTGCGCACATTGCGGTGAAAATGAAAGTCGTGAGCGTAGTCACCGCG
Y  G  Q  G  N  F  E  P  L  M  D  R  L  P  G  K  K  A  Q  I  T  E  A  I  D

TATGGCCAAGGGAACTTCGAACCGCTCATGGATCGCCTGCCGGGTAAGAAAGCCCAGATCACGGAGGCCATTGAT
G  V  R  E  R  L  R  G  A  A  E  A  T  S  A  Q  L  A  T  A  A  Y  N  T  S

GGCGTACGTGAACGCCTGCGTGGAGCTGCTGAAGCGACCTCTGCGCAGCTGGCCACAGCCGCCTACAATACTAGT
                                                                        SpeI
I  E  G  R  A  S  G  G  G  S  G  G  G  S  G  G  G  S  G  S  M  V  S  K  G
ATTGAAGGCCGTGCTAGCGGCGGTGGGTCTGGAGGCGGCTCAGGTGGTGGGTCGGGATCCATGGTGAGCAAGGGC
Xa          NheI    3xGGGS-Linker                                BamHI   YFP
E  E  L  F  T  G  V  V  P  I  L  V  E  L  D  G  D  V  N  G  H  K  F  S  V
GAGGAGCTGTTCACCGGGGTGGTGCCCATCCTGGTCGAGCTGGACGGCGACGTAAACGGCCACAAGTTCAGCGTG

S  G  E  G  E  G  D  A  T  Y  G  K  L  T  L  K  F  I  C  T  T  G  K  L  P
TCCGGCGAGGGCGAGGGCGATGCCACCTACGGCAAGCTGACCCTGAAGTTCATCTGCACCACCGGCAAGCTGCCC

V  P  W  P  T  L  V  T  T  F  G  Y  G  L  Q  C  F  A  R  Y  P  D  H  M  K
GTGCCCTGGCCCACCCTCGTGACCACCTTCGGCTACGGCCTGCAGTGCTTCGCCCGCTACCCCGACCACATGAAG

Q  H  D  F  F  K  S  A  M  P  E  G  Y  V  Q  E  R  T  I  F  F  K  D  D  G
CAGCACGACTTCTTCAAGTCCGCCATGCCCGAAGGCTACGTCCAGGAGCGCACCATCTTCTTCAAGGACGACGGC

N  Y  K  T  R  A  E  V  K  F  E  G  D  T  L  V  N  R  I  E  L  K  G  I  D
AACTACAAGACCCGCGCCGAGGTGAAGTTCGAGGGCGACACCCTGGTGAACCGCATCGAGCTGAAGGGCATCGAC

F  K  E  D  G  N  I  L  G  H  K  L  E  Y  N  Y  N  S  H  N  V  Y  I  M  A
TTCAAGGAGGACGGCAACATCCTGGGGCACAAGCTGGAGTACAACTACAACAGCCACAACGTCTATATCATGGCC

D  K  Q  K  N  G  I  K  V  N  F  K  I  R  H  N  I  E  D  G  S  V  Q  L  A
GACAAGCAGAAGAACGGCATCAAGGTGAACTTCAAGATCCGCCACAACATCGAGGACGGCAGCGTGCAGCTCGCC
```

```
D  H  Y  Q  Q  N  T  P  I  G  D  G  P  V  L  L  P  D  N  H  Y  L  S  Y  Q
GACCACTACCAGCAGAACACCCCCATCGGCGACGGCCCCGTGCTGCTGCCCGACAACCACTACCTGAGCTACCAG

S  K  L  S  K  D  P  N  E  K  R  D  H  M  V  L  L  E  F  V  T  A  A  G  I
TCCAAACTGAGCAAAGACCCCAACGAGAAGCGCGATCACATGGTCCTGCTGGAGTTCGTGACCGCCGCCGGGATC

T  L  G  M  D  E  L  Y  K  *
ACTCTCGGCATGGACGAGCTGTACAAGTAAGTCGACAAGCTTGCGGCCGCACTCGAG
                               SalI          NotI    XhoI
```

TDoT-L-mCherry

```
   M  I  I  N  E  T  A  D  D  I  V  Y  R  L  T  V  I  I  D  D  R  Y  E  S
CATATGATCATTAACGAAACTGCCGATGACATCGTTTATCGCCTGACAGTCATTATCGATGATCGCTACGAATCG
NdeI        TDoT
L  K  N  L  I  T  L  R  A  D  R  L  E  M  I  I  N  D  N  V  S  T  I  L  A
CTGAAAAACCTGATTACCTTACGTGCAGATCGCTTGGAGATGATCATCAATGACAATGTGTCCACCATTCTCGCG

S  I  T  S  I  E  G  R  A  S  G  G  G  S  G  G  G  S  G  G  G  S  G  S  M
AGCATTACTAGTATTGAAGGCCGTGCTAGCGGCGGTGGGTCTGGAGGCGGCTCAGGTGGTGGGTCGGGATCCATG
      SpeI     Xa        NheI     3xGGGS-Linker                    BamHI
V  S  K  G  E  E  D  N  M  A  I  I  K  E  F  M  R  F  K  V  H  M  E  G  S
GTGAGCAAGGGCGAGGAGGATAACATGGCCATCATCAAGGAGTTCATGCGCTTCAAGGTGCACATGGAGGGCTCC
mCherry
V  N  G  H  E  F  E  I  E  G  E  G  E  G  R  P  Y  E  G  T  Q  T  A  K  L
GTGAACGGCCACGAGTTCGAGATCGAGGGCGAGGGCGAGGGCCGCCCCTACGAGGGCACCCAGACCGCCAAGCTG

K  V  T  K  G  G  P  L  P  F  A  W  D  I  L  S  P  Q  F  M  Y  G  S  K  A
AAGGTGACCAAGGGTGGCCCCCTGCCCTTCGCCTGGGACATCCTGTCCCCTCAGTTCATGTACGGCTCCAAGGCC

Y  V  K  H  P  A  D  I  P  D  Y  L  K  L  S  F  P  E  G  F  K  W  E  R  V
TACGTGAAGCACCCCGCCGACATCCCCGACTACTTGAAGCTGTCCTTCCCCGAGGGCTTCAAGTGGGAGCGCGTG

M  N  F  E  D  G  G  V  V  T  V  T  Q  D  S  S  L  Q  D  G  E  F  I  Y  K
ATGAACTTCGAGGACGGCGGCGTGGTGACCGTGACCCAGGACTCCTCCTTGCAGGACGGCGAGTTCATCTACAAG

V  K  L  R  G  T  N  F  P  S  D  G  P  V  M  Q  K  K  T  M  G  W  E  A  S
GTGAAGCTGCGCGGCACCAACTTCCCCTCCGACGGCCCCGTAATGCAGAAGAAGACCATGGGCTGGGAGGCCTCC

S  E  R  M  Y  P  E  D  G  A  L  K  G  E  I  K  Q  R  L  K  L  K  D  G  G
TCCGAGCGGATGTACCCCGAGGACGGCGCCCTGAAGGGCGAGATCAAGCAGAGGCTGAAGCTGAAGGACGGCGGC

H  Y  D  A  E  V  K  T  T  Y  K  A  K  K  P  V  Q  L  P  G  A  Y  N  V  N
CACTACGACGCTGAGGTCAAGACCACCTACAAGGCCAAGAAGCCCGTGCAGCTGCCCGGCGCCTACAACGTCAAC

I  K  L  D  I  T  S  H  N  E  D  Y  T  I  V  E  Q  Y  E  R  A  E  G  R  H
ATCAAGTTGGACATCACCTCCCACAACGAGGACTACACCATCGTGGAACAGTACGAACGCGCCGAGGGCCGCCAC

S  T  G  G  M  D  E  L  Y  K  *
TCCACCGGCGGCATGGACGAGCTGTACAAGTAAGTCGACAAGCTTGCGGCCGCACTCGAG
                               SalI          NotI    XhoI
```

TDoT-mCherry

```
   M  I  I  N  E  T  A  D  D  I  V  Y  R  L  T  V  I  I  D  D  R  Y  E  S
CATATGATCATTAACGAAACTGCCGATGACATCGTTTATCGCCTGACAGTCATTATCGATGATCGCTACGAATCG
NdeI        TDoT
L  K  N  L  I  T  L  R  A  D  R  L  E  M  I  I  N  D  N  V  S  T  I  L  A
CTGAAAAACCTGATTACCTTACGTGCAGATCGCTTGGAGATGATCATCAATGACAATGTGTCCACCATTCTCGCG

S  I  G  S  M  V  S  K  G  E  E  D  N  M  A  I  I  K  E  F  M  R  F  K  V
AGCATTGGATCCATGGTGAGCAAGGGCGAGGAGGATAACATGGCCATCATCAAGGAGTTCATGCGCTTCAAGGTG
      BamHI  mCherry
```

```
H  M  E  G  S  V  N  G  H  E  F  E  I  E  G  E  G  E  G  R  P  Y  E  G  T
CACATGGAGGGCTCCGTGAACGGCCACGAGTTCGAGATCGAGGGCGAGGGCGAGGGCCGCCCCTACGAGGGCACC

Q  T  A  K  L  K  V  T  K  G  G  P  L  P  F  A  W  D  I  L  S  P  Q  F  M
CAGACCGCCAAGCTGAAGGTGACCAAGGGTGGCCCCCTGCCCTTCGCCTGGGACATCCTGTCCCCTCAGTTCATG

Y  G  S  K  A  Y  V  K  H  P  A  D  I  P  D  Y  L  K  L  S  F  P  E  G  F
TACGGCTCCAAGGCCTACGTGAAGCACCCCGCCGACATCCCCGACTACTTGAAGCTGTCCTTCCCCGAGGGCTTC

K  W  E  R  V  M  N  F  E  D  G  G  V  V  T  V  T  Q  D  S  S  L  Q  D  G
AAGTGGGAGCGCGTGATGAACTTCGAGGACGGCGGCGTGGTGACCGTGACCCAGGACTCCTCCTTGCAGGACGGC

E  F  I  Y  K  V  K  L  R  G  T  N  F  P  S  D  G  P  V  M  Q  K  K  T  M
GAGTTCATCTACAAGGTGAAGCTGCGCGGCACCAACTTCCCCTCCGACGGCCCCGTAATGCAGAAGAAGACCATG

G  W  E  A  S  S  E  R  M  Y  P  E  D  G  A  L  K  G  E  I  K  Q  R  L  K
GGCTGGGAGGCCTCCTCCGAGCGGATGTACCCCGAGGACGGCGCCCTGAAGGGCGAGATCAAGCAGAGGCTGAAG

L  K  D  G  G  H  Y  D  A  E  V  K  T  T  Y  K  A  K  K  P  V  Q  L  P  G
CTGAAGGACGGCGGCCACTACGACGCTGAGGTCAAGACCACCTACAAGGCCAAGAAGCCCGTGCAGCTGCCCGGC

A  Y  N  V  N  I  K  L  D  I  T  S  H  N  E  D  Y  T  I  V  E  Q  Y  E  R
GCCTACAACGTCAACATCAAGTTGGACATCACCTCCCACAACGAGGACTACACCATCGTGGAACAGTACGAACGC

A  E  G  R  H  S  T  G  G  M  D  E  L  Y  K  *
GCCGAGGGCCGCCACTCCACCGGCGGCATGGACGAGCTGTACAAGTAAGTCGACAAGCTTGCGGCCGCACTCGAG
                                                 SalI          NotI    XhoI
```

3HAMP-L-mCherry

```
   M  G  L  F  N  A  H  A  V  A  Q  Q  R  A  D  R  I  A  T  L  L  Q  S  F
CATATGGGCCTGTTTAACGCCCATGCAGTTGCGCAGCAACGCGCGGATCGCATTGCGACTCTCCTGCAGTCCTTT
NdeI          3HAMP
A  D  G  Q  L  D  T  A  V  G  E  A  P  A  P  G  Y  E  R  L  Y  D  S  L  R

GCGGATGGTCAGTTGGACACCGCCGTGGGTGAAGCGCCAGCACCTGGTTACGAACGCCTGTATGACTCGCTTCGC
A  L  Q  R  Q  L  R  E  Q  R  A  E  L  Q  Q  V  E  S  L  E  A  G  L  A  E

GCCCTTCAGCGCCAACTGCGCGAACAACGTGCGGAGTTACAACAGGTTGAGAGCCTGGAAGCAGGCTTGGCTGAA
M  S  R  Q  H  E  A  G  W  I  D  Q  T  I  P  A  E  R  L  E  G  R  A  A  R

ATGAGTCGGCAGCATGAAGCAGGGTGGATTGACCAGACGATTCCGGCTGAACGGTTAGAGGGCCGTGCAGCACGT
I  A  K  G  V  N  E  L  V  A  A  H  I  A  V  K  M  K  V  V  S  V  V  T  A

ATCGCCAAAGGCGTGAATGAGCTGGTTGCTGCGCACATTGCGGTGAAAATGAAAGTCGTGAGCGTAGTCACCGCG
Y  G  Q  G  N  F  E  P  L  M  D  R  L  P  G  K  K  A  Q  I  T  E  A  I  D

TATGGCCAAGGGAACTTCGAACCGCTCATGGATCGCCTGCCGGGTAAGAAAGCCCAGATCACGGAGGCCATTGAT
G  V  R  E  R  L  R  G  A  A  E  A  T  S  A  Q  L  A  T  A  A  Y  N  T  S

GGCGTACGTGAACGCCTGCGTGGAGCTGCTGAAGCGACCTCTGCGCAGCTGGCCACAGCCGCCTACAATACTAGT
                                                                      SpeI
I  E  G  R  A  S  G  G  G  S  G  G  G  S  G  G  G  S  G  S  M  V  S  K  G
ATTGAAGGCCGTGCTAGCGGCGGTGGGTCTGGAGGCGGCTCAGGTGGTGGGTCGGGATCCATGGTGAGCAAGGGC
Xa            NheI    3xGGGS-Linker                          BamHI   mCherry
E  E  D  N  M  A  I  I  K  E  F  M  R  F  K  V  H  M  E  G  S  V  N  G  H
GAGGAGGATAACATGGCCATCATCAAGGAGTTCATGCGCTTCAAGGTGCACATGGAGGGCTCCGTGAACGGCCAC

E  F  E  I  E  G  E  G  E  G  R  P  Y  E  G  T  Q  T  A  K  L  K  V  T  K
GAGTTCGAGATCGAGGGCGAGGGCGAGGGCCGCCCCTACGAGGGCACCCAGACCGCCAAGCTGAAGGTGACCAAG

G  G  P  L  P  F  A  W  D  I  L  S  P  Q  F  M  Y  G  S  K  A  Y  V  K  H
GGTGGCCCCCTGCCCTTCGCCTGGGACATCCTGTCCCCTCAGTTCATGTACGGCTCCAAGGCCTACGTGAAGCAC

P  A  D  I  P  D  Y  L  K  L  S  F  P  E  G  F  K  W  E  R  V  M  N  F  E
CCCGCCGACATCCCCGACTACTTGAAGCTGTCCTTCCCCGAGGGCTTCAAGTGGGAGCGCGTGATGAACTTCGAG
```

```
D  G  G  V  V  T  V  T  Q  D  S  S  L  Q  D  G  E  F  I  Y  K  V  K  L  R
GACGGCGGCGTGGTGACCGTGACCCAGGACTCCTCCTTGCAGGACGGCGAGTTCATCTACAAGGTGAAGCTGCGC

G  T  N  F  P  S  D  G  P  V  M  Q  K  K  T  M  G  W  E  A  S  S  E  R  M
GGCACCAACTTCCCCTCCGACGGCCCCGTAATGCAGAAGAAGACCATGGGCTGGGAGGCCTCCTCCGAGCGGATG

Y  P  E  D  G  A  L  K  G  E  I  K  Q  R  L  K  L  K  D  G  G  H  Y  D  A

TACCCCGAGGACGGCGCCCTGAAGGGCGAGATCAAGCAGAGGCTGAAGCTGAAGGACGGCGGCCACTACGACGCT

E  V  K  T  T  Y  K  A  K  K  P  V  Q  L  P  G  A  Y  N  V  N  I  K  L  D
GAGGTCAAGACCACCTACAAGGCCAAGAAGCCCGTGCAGCTGCCCGGCGCCTACAACGTCAACATCAAGTTGGAC

I  T  S  H  N  E  D  Y  T  I  V  E  Q  Y  E  R  A  E  G  R  H  S  T  G  G
ATCACCTCCCACAACGAGGACTACACCATCGTGGAACAGTACGAACGCGCCGAGGGCCGCCACTCCACCGGCGGC

M  D  E  L  Y  K  *
ATGGACGAGCTGTACAAGTAAGTCGACAAGCTTGCGGCCGCACTCGAG
                      SalI      NotI      XhoI
```

*R*ADH

```
catatgtatcgtctgctgaataaaaccgcagttattaccggtggtaatagcggtattggt
 H  M  Y  R  L  L  N  K  T  A  V  I  T  G  G  N  S  G  I  G
 NdeI
ctggcaaccgcaaaacgttttgttgccgaaggtgcctatgtttttattgttggtcgtcgt
 L  A  T  A  K  R  F  V  A  E  G  A  Y  V  F  I  V  G  R  R

cgtaaagaactggaacaggcagcagcagaaattggtcgtaatgttaccgcagttaaagcc
 R  K  E  L  E  Q  A  A  A  E  I  G  R  N  V  T  A  V  K  A

gatgttaccaaactggaagatctggatcgtctgtatgcaattgttcgtgaacagcgtggt
 D  V  T  K  L  E  D  L  D  R  L  Y  A  I  V  R  E  Q  R  G

agcattgatgttctgtttgcaaatagcggtgccattgaacagaaaaccctggaagaaatt
 S  I  D  V  L  F  A  N  S  G  A  I  E  Q  K  T  L  E  E  I

acaccggaacattatgatcgcacctttgatgttaatgtgcgtggtctgatttttaccgtt
 T  P  E  H  Y  D  R  T  F  D  V  N  V  R  G  L  I  F  T  V

cagaaagcactgccgctgctgcgtgatggtggtagcgttattctgaccagcagcgttgcc
 Q  K  A  L  P  L  L  R  D  G  G  S  V  I  L  T  S  S  V  A

ggtgttctgggtctgcaggcacatgatacctatagcgcagcaaaagcagcagttcgtagc
 G  V  L  G  L  Q  A  H  D  T  Y  S  A  A  K  A  A  V  R  S

ctggcacgtacctggaccaccgaactgaaaggtcgtagcattcgtgttaatgcagttagt
 L  A  R  T  W  T  T  E  L  K  G  R  S  I  R  V  N  A  V  S

ccgggtgcaattgataccccgattattgaaaatcaggttagcacccaggaagaagcagac
 P  G  A  I  D  T  P  I  I  E  N  Q  V  S  T  Q  E  E  A  D

gaactgcgcgcaaaatttgcagcagcaacaccgctgggtcgtgttggtcgtccggaagaa
 E  L  R  A  K  F  A  A  A  T  P  L  G  R  V  G  R  P  E  E

ctggcagcagccgttctgtttctggcaagtgatgatagcagctatgttgcaggtattgaa
 L  A  A  A  V  L  F  L  A  S  D  D  S  S  Y  V  A  G  I  E

ctgtttgttgatggtggtctgacccaggtttaataactcgag
 L  F  V  D  G  G  L  T  Q  V  -  -  L  E
                                  XhoI
```

TDoT-L-*R*ADH

```
   M  I  I  N  E  T  A  D  D  I  V  Y  R  L  T  V  I  I  D  D  R  Y  E  S
CATATGATCATTAACGAAACTGCCGATGACATCGTTTATCGCCTGACAGTCATTATCGATGATCGCTACGAATCG
NdeI          TDoT
L  K  N  L  I  T  L  R  A  D  R  L  E  M  I  I  N  D  N  V  S  T  I  L  A
CTGAAAAACCTGATTACCTTACGTGCAGATCGCTTGGAGATGATCATCAATGACAATGTGTCCACCATTCTCGCG

S  I  T  S  I  E  G  R  A  S  G  G  G  S  G  G  G  S  G  G  G  S  G  S  M
AGCATTACTAGTATTGAAGGCCGTGCTAGCGGCGGTGGGTCTGGAGGCGGCTCAGGTGGTGGGTCGGGATCCATG
   SpeI        Xa        NheI   3xGGGS-Linker                          BamHI
Y  R  L  L  N  K  T  A  V  I  T  G  G  N  S  G  I  G  L  A  T  A  K  R  F
TATCGTCTGCTGAATAAAACCGCAGTTATTACCGGTGGTAATAGCGGTATTGGTCTGGCAACCGCAAAACGTTTT
RADH
V  A  E  G  A  Y  V  F  I  V  G  R  R  R  K  E  L  E  Q  A  A  A  E  I  G
GTTGCCGAAGGTGCCTATGTTTTTATTGTTGGTCGTCGTCGTAAAGAACTGGAACAGGCAGCAGCAGAAATTGGT

R  N  V  T  A  V  K  A  D  V  T  K  L  E  D  L  D  R  L  Y  A  I  V  R  E
CGTAATGTTACCGCAGTTAAAGCCGATGTTACCAAACTGGAAGATCTGGATCGTCTGTATGCAATTGTTCGTGAA

Q  R  G  S  I  D  V  L  F  A  N  S  G  A  I  E  Q  K  T  L  E  E  I  T  P
CAGCGTGGTAGCATTGATGTTCTGTTTGCAAATAGCGGTGCCATTGAACAGAAAACCCTGGAAGAAATTACACCG

E  H  Y  D  R  T  F  D  V  N  V  R  G  L  I  F  T  V  Q  K  A  L  P  L  L
GAACATTATGATCGCACCTTTGATGTTAATGTGCGTGGTCTGATTTTTACCGTTCAGAAAGCACTGCCGCTGCTG

R  D  G  G  S  V  I  L  T  S  S  V  A  G  V  L  G  L  Q  A  H  D  T  Y  S
CGTGATGGTGGTAGCGTTATTCTGACCAGCAGCGTTGCCGGTGTTCTGGGTCTGCAGGCACATGATACCTATAGC

A  A  K  A  A  V  R  S  L  A  R  T  W  T  T  E  L  K  G  R  S  I  R  V  N
GCAGCAAAAGCAGCAGTTCGTAGCCTGGCACGTACCTGGACCACCGAACTGAAAGGTCGTAGCATTCGTGTTAAT

A  V  S  P  G  A  I  D  T  P  I  I  E  N  Q  V  S  T  Q  E  E  A  D  E  L
GCAGTTAGTCCGGGTGCAATTGATACCCCGATTATTGAAAATCAGGTTAGCACCCAGGAAGAAGCAGACGAACTG

R  A  K  F  A  A  A  T  P  L  G  R  V  G  R  P  E  E  L  A  A  A  V  L  F
CGCGCAAAATTTGCAGCAGCAACACCGCTGGGTCGTGTTGGTCGTCCGGAAGAACTGGCAGCAGCCGTTCTGTTT

L  A  S  D  D  S  S  Y  V  A  G  I  E  L  F  V  D  G  G  L  T  Q  V  *
CTGGCAAGTGATGATAGCAGCTATGTTGCAGGTATTGAACTGTTTGTTGATGGTGGTCTGACCCAGGTTTAAGTC
                                                                  SalI

GACAAGCTTGCGGCCGCACTCGAG
         NotI     XhoI
```

3HAMP-L-*R*ADH

```
   M  G  L  F  N  A  H  A  V  A  Q  Q  R  A  D  R  I  A  T  L  L  Q  S  F
CATATGGGCCTGTTTAACGCCCATGCAGTTGCGCAGCAACGCGCGGATCGCATTGCGACTCTCCTGCAGTCCTTT
NdeI          3Hamp
A  D  G  Q  L  D  T  A  V  G  E  A  P  A  P  G  Y  E  R  L  Y  D  S  L  R
GCGGATGGTCAGTTGGACACCGCCGTGGGTGAAGCGCCAGCACCTGGTTACGAACGCCTGTATGACTCGCTTCGC

A  L  Q  R  Q  L  R  E  Q  R  A  E  L  Q  Q  V  E  S  L  E  A  G  L  A  E
GCCCTTCAGCGCCAACTGCGCGAACAACGTGCGGAGTTACAACAGGTTGAGAGCCTGGAAGCAGGCTTGGCTGAA

M  S  R  Q  H  E  A  G  W  I  D  Q  T  I  P  A  E  R  L  E  G  R  A  A  R
ATGAGTCGGCAGCATGAAGCAGGGTGGATTGACCAGACGATTCCGGCTGAACGGTTAGAGGGCCGTGCAGCACGT

I  A  K  G  V  N  E  L  V  A  A  H  I  A  V  K  M  K  V  V  S  V  V  T  A
ATCGCCAAAGGCGTGAATGAGCTGGTTGCTGCGCACATTGCGGTGAAAATGAAAGTCGTGAGCGTAGTCACCGCG

Y  G  Q  G  N  F  E  P  L  M  D  R  L  P  G  K  K  A  Q  I  T  E  A  I  D
TATGGCCAAGGGAACTTCGAACCGCTCATGGATCGCCTGCCGGGTAAGAAAGCCCAGATCACGGAGGCCATTGAT
```

```
G  V  R  E  R  L  R  G  A  A  E  A  T  S  A  Q  L  A  T  A  A  Y  N  T  S
GGCGTACGTGAACGCCTGCGTGGAGCTGCTGAAGCGACCTCTGCGCAGCTGGCCACAGCCGCCTACAATACTAGT
                                                                    SpeI
I  E  G  R  A  S  G  G  G  S  G  G  G  S  G  G  G  S  G  S  M  Y  R  L  L
ATTGAAGGCCGTGCTAGCGGCGGTGGGTCTGGAGGCGGCTCAGGTGGTGGGTCGGGATCCATGTATCGTCTGCTG
     Xa        NheI    3xGGGS-Linker                        BamHI
N  K  T  A  V  I  T  G  G  N  S  G  I  G  L  A  T  A  K  R  F  V  A  E  G
AATAAAACCGCAGTTATTACCGGTGGTAATAGCGGTATTGGTCTGGCAACCGCAAAACGTTTTGTTGCCGAAGGT
RADH
A  Y  V  F  I  V  G  R  R  R  K  E  L  E  Q  A  A  A  E  I  G  R  N  V  T
GCCTATGTTTTTATTGTTGGTCGTCGTCGTAAAGAACTGGAACAGGCAGCAGCAGAAATTGGTCGTAATGTTACC

A  V  K  A  D  V  T  K  L  E  D  L  D  R  L  Y  A  I  V  R  E  Q  R  G  S
GCAGTTAAAGCCGATGTTACCAAACTGGAAGATCTGGATCGTCTGTATGCAATTGTTCGTGAACAGCGTGGTAGC

I  D  V  L  F  A  N  S  G  A  I  E  Q  K  T  L  E  E  I  T  P  E  H  Y  D
ATTGATGTTCTGTTTGCAAATAGCGGTGCCATTGAACAGAAAACCCTGGAAGAAATTACACCGGAACATTATGAT

R  T  F  D  V  N  V  R  G  L  I  F  T  V  Q  K  A  L  P  L  L  R  D  G  G
CGCACCTTTGATGTTAATGTGCGTGGTCTGATTTTTACCGTTCAGAAAGCACTGCCGCTGCTGCGTGATGGTGGT

S  V  I  L  T  S  S  V  A  G  V  L  G  L  Q  A  H  D  T  Y  S  A  A  K  A
AGCGTTATTCTGACCAGCAGCGTTGCCGGTGTTCTGGGTCTGCAGGCACATGATACCTATAGCGCAGCAAAAGCA

A  V  R  S  L  A  R  T  W  T  T  E  L  K  G  R  S  I  R  V  N  A  V  S  P
GCAGTTCGTAGCCTGGCACGTACCTGGACCACCGAACTGAAAGGTCGTAGCATTCGTGTTAATGCAGTTAGTCCG

G  A  I  D  T  P  I  I  E  N  Q  V  S  T  Q  E  E  A  D  E  L  R  A  K  F
GGTGCAATTGATACCCCGATTATTGAAAATCAGGTTAGCACCCAGGAAGAAGCAGACGAACTGCGCGCAAAATTT

A  A  A  T  P  L  G  R  V  G  R  P  E  E  L  A  A  A  V  L  F  L  A  S  D
GCAGCAGCAACACCGCTGGGTCGTGTTGGTCGTCCGGAAGAACTGGCAGCAGCCGTTCTGTTTCTGGCAAGTGAT

D  S  S  Y  V  A  G  I  E  L  F  V  D  G  G  L  T  Q  V  *
GATAGCAGCTATGTTGCAGGTATTGAACTGTTTGTTGATGGTGGTCTGACCCAGGTTTAAGTCGACAAGCTTGCG
                                                        SalI
GCCGCACTCGAG
NotI  XhoI
```

*Lb*ADH

```
CATATGTCTAACCGTTTGGATGGTAAGGTAGCAATCATTACAGGTGGTACGTTGGGTATCGGTTTAGCTATCGCC
    M  S  N  R  L  D  G  K  V  A  I  I  T  G  G  T  L  G  I  G  L  A  I  A
NdeI
ACGAAGTTCGTTGAAGAAGGGGCTAAGGTCATGATTACCGGCCGGCACAGCGATGTTGGTGAAAAAGCAGCTAAG
 T  K  F  V  E  E  G  A  K  V  M  I  T  G  R  H  S  D  V  G  E  K  A  A  K

AGTGTCGGCACTCCTGATCAGATTCAATTTTTCCAACATGATTCTTCCGATGAAGACGGCTGGACGAAATTATTC
 S  V  G  T  P  D  Q  I  Q  F  F  Q  H  D  S  S  D  E  D  G  W  T  K  L  F

GATGCAACGGAAAAAGCCTTTGGCCCAGTTTCTACATTAGTTAATAACGCTGGGATCGCGGTTAACAAGAGTGTC
 D  A  T  E  K  A  F  G  P  V  S  T  L  V  N  N  A  G  I  A  V  N  K  S  V

GAAGAAACCACGACTGCTGAATGGCGTAAATTATTAGCCGTCAACCTTGATGGTGTCTTCTTCGGTACCCGATTA
 E  E  T  T  T  A  E  W  R  K  L  L  A  V  N  L  D  G  V  F  F  G  T  R  L

GGGATTCAACGGATGAAGAACAAAGGCTTAGGGGCTTCCATCATCAACATGTCTTCGATCGAAGGCTTTGTGGGT
 G  I  Q  R  M  K  N  K  G  L  G  A  S  I  I  N  M  S  S  I  E  G  F  V  G

GATCCTAGCTTAGGGGCTTACAACGCATCTAAAGGGGCCGTACGGATTATGTCCAAGTCAGCTGCCTTAGATTGT
 D  P  S  L  G  A  Y  N  A  S  K  G  A  V  R  I  M  S  K  S  A  A  L  D  C

GCCCTAAAGGACTACGATGTTCGGGTAAACACTGTTCACCCTGGCTACATCAAGACACCATTGGTTGATGACCTA
 A  L  K  D  Y  D  V  R  V  N  T  V  H  P  G  Y  I  K  T  P  L  V  D  D  L
```

```
CCAGGGGCCGAAGAAGCGATGTCACAACGGACCAAGACGCCAATGGGCCATATCGGTGAACCTAACGATATTGCC
 P  G  A  E  E  A  M  S  Q  R  T  K  T  P  M  G  H  I  G  E  P  N  D  I  A

TACATCTGTGTTTACTTGGCTTCTAACGAATCTAAATTTGCAACGGGTTCTGAATTCGTAGTTGACGGTGGCTAC
 Y  I  C  V  Y  L  A  S  N  E  S  K  F  A  T  G  S  E  F  V  V  D  G  G  Y

ACTGCTCAATAGTAGCGCGGATCCGAATTCGAGCTCCGTCGACAAGCTTGCGGCCGC
 T  A  Q  *  *  R  G  S  E  F  E  L  R  R  Q  A  C  G  R
                  BamHI                 SalI           NotI
```

TDoT-L-*Lb*ADH

```
CATATGATCATTAACGAAACTGCCGATGACATCGTTTATCGCCTGACAGTCATTATCGATGATCGCTACGAATCG
     M  I  I  N  E  T  A  D  D  I  V  Y  R  L  T  V  I  I  D  D  R  Y  E  S
NdeI          TDoT
CTGAAAAACCTGATTACCTTACGTGCAGATCGCTTGGAGATGATCATCAATGACAATGTGTCCACCATTCTCGCG
 L  K  N  L  I  T  L  R  A  D  R  L  E  M  I  I  N  D  N  V  S  T  I  L  A

AGCATTACTAGTATTGAAGGCCGTGCTAGCGGCGGTGGGTCTGGAGGCGGCTCAGGTGGTGGGTCGGGATCCATG
 S  I  T  S  I  E  G  R  A  S  G  G  G  S  G  G  G  S  G  G  G  S  G  S  M
       SpeI     Xa        NheI           3xGGGS-Linker                 BamHI
TCTAACCGTTTGGATGGTAAGGTAGCAATCATTACAGGTGGTACGTTGGGTATCGGTTTAGCTATCGCCACGAAG
 S  N  R  L  D  G  K  V  A  I  I  T  G  G  T  L  G  I  G  L  A  I  A  T  K
 LbADH
TTCGTTGAAGAAGGGGCTAAGGTCATGATTACCGGCCGGCACAGCGATGTTGGTGAAAAAGCAGCTAAGAGTGTC
 F  V  E  E  G  A  K  V  M  I  T  G  R  H  S  D  V  G  E  K  A  A  K  S  V

GGCACTCCTGATCAGATTCAATTTTTCCAACATGATTCTTCCGATGAAGACGGCTGGACGAAATTATTCGATGCA
 G  T  P  D  Q  I  Q  F  F  Q  H  D  S  S  D  E  D  G  W  T  K  L  F  D  A

ACGGAAAAAGCCTTTGGCCCAGTTTCTACATTAGTTAATAACGCTGGGATCGCGGTTAACAAGAGTGTCGAAGAA
 T  E  K  A  F  G  P  V  S  T  L  V  N  N  A  G  I  A  V  N  K  S  V  E  E

ACCACGACTGCTGAATGGCGTAAATTATTAGCCGTCAACCTTGATGGTGTCTTCTTCGGTACCCGATTAGGGATT
 T  T  T  A  E  W  R  K  L  L  A  V  N  L  D  G  V  F  F  G  T  R  L  G  I

CAACGGATGAAGAACAAAGGCTTAGGGGCTTCCATCATCAACATGTCTTCGATCGAAGGCTTTGTGGGTGATCCT
 Q  R  M  K  N  K  G  L  G  A  S  I  I  N  M  S  S  I  E  G  F  V  G  D  P

AGCTTAGGGGCTTACAACGCATCTAAAGGGGCCGTACGGATTATGTCCAAGTCAGCTGCCTTAGATTGTGCCCTA
 S  L  G  A  Y  N  A  S  K  G  A  V  R  I  M  S  K  S  A  A  L  D  C  A  L

AAGGACTACGATGTTCGGGTAAACACTGTTCACCCTGGCTACATCAAGACACCATTGGTTGATGACCTACCAGGG
 K  D  Y  D  V  R  V  N  T  V  H  P  G  Y  I  K  T  P  L  V  D  D  L  P  G

GCCGAAGAAGCGATGTCACAACGGACCAAGACGCCAATGGGCCATATCGGTGAACCTAACGATATTGCCTACATC
 A  E  E  A  M  S  Q  R  T  K  T  P  M  G  H  I  G  E  P  N  D  I  A  Y  I

TGTGTTTACTTGGCTTCTAACGAATCTAAATTTGCAACGGGTTCTGAATTCGTAGTTGACGGTGGCTACACTGCT
 C  V  Y  L  A  S  N  E  S  K  F  A  T  G  S  E  F  V  V  D  G  G  Y  T  A

CAATAGAGTCGACAAGCTTGCGGCCGCACTCGA
 Q  *  S  R  Q  A  C  G  R  T  R
       SalI           NotI
```

3HAMP-L-*Lb*ADH

```
CATATGGGCCTGTTTAACGCCCATGCAGTTGCGCAGCAACGCGCGGATCGCATTGCGACTCTCCTGCAGTCCTTT
     M  G  L  F  N  A  H  A  V  A  Q  Q  R  A  D  R  I  A  T  L  L  Q  S  F
NdeI                                   3HAMP
```

```
GCGGATGGTCAGTTGGACACCGCCGTGGGTGAAGCGCCAGCACCTGGTTACGAACGCCTGTATGACTCGCTTCGC
 A  D  G  Q  L  D  T  A  V  G  E  A  P  A  P  G  Y  E  R  L  Y  D  S  L  R

GCCCTTCAGCGCCAACTGCGCGAACAACGTGCGGAGTTACAACAGGTTGAGAGCCTGGAAGCAGGCTTGGCTGAA
 A  L  Q  R  Q  L  R  E  Q  R  A  E  L  Q  Q  V  E  S  L  E  A  G  L  A  E

ATGAGTCGGCAGCATGAAGCAGGGTGGATTGACCAGACGATTCCGGCTGAACGGTTAGAGGGCCGTGCAGCACGT
 M  S  R  Q  H  E  A  G  W  I  D  Q  T  I  P  A  E  R  L  E  G  R  A  A  R

ATCGCCAAAGGCGTGAATGAGCTGGTTGCTGCGCACATTGCGGTGAAAATGAAAGTCGTGAGCGTAGTCACCGCG
 I  A  K  G  V  N  E  L  V  A  A  H  I  A  V  K  M  K  V  V  S  V  V  T  A

TATGGCCAAGGGAACTTCGAACCGCTCATGGATCGCCTGCCGGGTAAGAAAGCCCAGATCACGGAGGCCATTGAT
 Y  G  Q  G  N  F  E  P  L  M  D  R  L  P  G  K  K  A  Q  I  T  E  A  I  D

GGCGTACGTGAACGCCTGCGTGGAGCTGCTGAAGCGACCTCTGCGCAGCTGGCCACAGCCGCCTACAATACTAGT
 G  V  R  E  R  L  R  G  A  A  E  A  T  S  A  Q  L  A  T  A  A  Y  N  T  S
                                                                    SpeI

ATTGAAGGCCGTGCTAGCGGCGGTGGGTCTGGAGGCGGCTCAGGTGGTGGGTCGGGATCCATGTCTAACCGTTTG
 I  E  G  R  A  S  G  G  G  S  G  G  G  S  G  G  G  S  G  S  M  S  N  R  L
    Xa          NheI  3xGGGS-Linker                       BamHI          LbADH

GATGGTAAGGTAGCAATCATTACAGGTGGTACGTTGGGTATCGGTTTAGCTATCGCCACGAAGTTCGTTGAAGAA
 D  G  K  V  A  I  I  T  G  G  T  L  G  I  G  L  A  I  A  T  K  F  V  E  E

GGGGCTAAGGTCATGATTACCGGCCGGCACAGCGATGTTGGTGAAAAAGCAGCTAAGAGTGTCGGCACTCCTGAT
 G  A  K  V  M  I  T  G  R  H  S  D  V  G  E  K  A  A  K  S  V  G  T  P  D

CAGATTCAATTTTTCCAACATGATTCTTCCGATGAAGACGGCTGGACGAAATTATTCGATGCAACGGAAAAAGCC
 Q  I  Q  F  F  Q  H  D  S  S  D  E  D  G  W  T  K  L  F  D  A  T  E  K  A

TTTGGCCCAGTTTCTACATTAGTTAATAACGCTGGGATCGCGGTTAACAAGAGTGTCGAAGAAACCACGACTGCT
 F  G  P  V  S  T  L  V  N  N  A  G  I  A  V  N  K  S  V  E  E  T  T  T  A

GAATGGCGTAAATTATTAGCCGTCAACCTTGATGGTGTCTTCTTCGGTACCCGATTAGGGATTCAACGGATGAAG
 E  W  R  K  L  L  A  V  N  L  D  G  V  F  F  G  T  R  L  G  I  Q  R  M  K

AACAAAGGCTTAGGGGCTTCCATCATCAACATGTCTTCGATCGAAGGCTTTGTGGGTGATCCTAGCTTAGGGGCT
 N  K  G  L  G  A  S  I  I  N  M  S  S  I  E  G  F  V  G  D  P  S  L  G  A

TACAACGCATCTAAAGGGGCCGTACGGATTATGTCCAAGTCAGCTGCCTTAGATTGTGCCCTAAAGGACTACGAT
 Y  N  A  S  K  G  A  V  R  I  M  S  K  S  A  A  L  D  C  A  L  K  D  Y  D

GTTCGGGTAAACACTGTTCACCCTGGCTACATCAAGACACCATTGGTTGATGACCTACCAGGGGCCGAAGAAGCG
 V  R  V  N  T  V  H  P  G  Y  I  K  T  P  L  V  D  D  L  P  G  A  E  E  A

ATGTCACAACGGACCAAGACGCCAATGGGCCATATCGGTGAACCTAACGATATTGCCTACATCTGTGTTTACTTG
 M  S  Q  R  T  K  T  P  M  G  H  I  G  E  P  N  D  I  A  Y  I  C  V  Y  L

GCTTCTAACGAATCTAAATTTGCAACGGGTTCTGAATTCGTAGTTGACGGTGGCTACACTGCTCAATAGAGTCGA
 A  S  N  E  S  K  F  A  T  G  S  E  F  V  V  D  G  G  Y  T  A  Q  *  S  R
                                                                    SalI

CAAGCTTGCGGCCGCACTCGA
 Q  A  C  G  R  T  R
       NotI
```

*Pf*BAL-His$_6$

```
ATGGCGATGATTACAGGCGGCGAACTGGTTGTTCGCACCCTAATAAAGGCTGGGGTCGAACATCTGTTCGGCCTG
 M  A  M  I  T  G  G  E  L  V  V  R  T  L  I  K  A  G  V  E  H  L  F  G  L
```

CACGGCGCGCATATCGATACGATTTTTCAAGCCTGTCTCGATCATGATGTGCCGATCATCGACACCCGCCATGAG
H G A H I D T I F Q A C L D H D V P I I D T R H E

GCCGCCGCAGGGCATGCGGCCGAGGGCTATGCCCGCGCTGGCGCCAAGCTGGGCGTGGCGCTGGTCACGGCGGGC
A A A G H A A E G Y A R A G A K L G V A L V T A G

GGGGGATTTACCAATGCGGTCACGCCCATTGCCAACGCTTGGCTGGATCGCACGCCGGTGCTCTTCCTCACCGGA
G G F T N A V T P I A N A W L D R T P V L F L T G

TCGGGCGCGCTGCGTGATGATGAAACCAACACGTTGCAGGCGGGGATTGATCAGGTCGCCATGGCGGCGCCCATT
S G A L R D D E T N T L Q A G I D Q V A M A A P I

ACCAAATGGGCGCATCGGGTGATGGCAACCGAGCATATCCCACGGCTGGTGATGCAGGCGATCCGCGCCGCGTTG
T K W A H R V M A T E H I P R L V M Q A I R A A L

AGCGCGCCACGCGGGCCGGTGTTGCTGGATCTGCCGTGGGATATTCTGATGAACCAGATTGATGAGGATAGCGTC
S A P R G P V L L D L P W D I L M N Q I D E D S V

ATTATCCCCGATCTGGTCTTGTCCGCGCATGGGGCCAGACCCGACCCTGCCGATCTGGATCAGGCTCTCGCGCTT
I I P D L V L S A H G A R P D P A D L D Q A L A L

TTGCGCAAGGCGGAGCGGCCGGTCATCGTGCTCGGCTCAGAAGCCTCGCGGACAGCGCGCAAGACGGCGCTTAGC
L R K A E R P V I V L G S E A S R T A R K T A L S

GCCTTCGTGGCGGCGACTGGCGTGCCGGTGTTTGCCGATTATGAAGGGCTAAGCATGCTCTCGGGGCTGCCCGAT
A F V A A T G V P V F A D Y E G L S M L S G L P D

GCTATGCGGGGCGGGCTGGTGCAAAACCTCTATTCTTTTGCCAAAGCCGATGCCGCGCCAGATCTCGTGCTGATG
A M R G G L V Q N L Y S F A K A D A A P D L V L M

CTGGGGGCGCGCTTTGGCCTTAACACCGGGCATGGATCTGGGCAGTTGATCCCCCATAGCGCGCAGGTCATTCAG
L G A R F G L N T G H G S G Q L I P H S A Q V I Q

GTCGACCCTGATGCCTGCGAGCTGGGACGCCTGCAGGGCATCGCTCTGGGCATTGTGGCCGATGTGGGTGGGACC
V D P D A C E L G R L Q G I A L G I V A D V G G T

ATCGAGGCTTTGGCGCAGGCCACCGCGCAAGATGCGGCTTGGCCGGATCGCGGCGACTGGTGCGCCAAAGTGACG
I E A L A Q A T A Q D A A W P D R G D W C A K V T

GATCTGGCGCAAGAGCGCTATGCCAGCATCGCTGCGAAATCGAGCAGCGAGCATGCGCTCCACCCCTTTCACGCC
D L A Q E R Y A S I A A K S S S E H A L H P F H A

TCGCAGGTCATTGCCAAACACGTCGATGCAGGGGTGACGGTGGTAGCGGATGGTGCGCTGACCTATCTCTGGCTG
S Q V I A K H V D A G V T V V A D G A L T Y L W L

TCCGAAGTGATGAGCCGCGTGAAACCCGGCGGTTTTCTCTGCCACGGCTATCTAGGCTCGATGGGCGTGGGCTTC
S E V M S R V K P G G F L C H G Y L G S M G V G F

GGCACGGCGCTGGGCGCGCAAGTGGCCGATCTTGAAGCAGGCCGCCGCACGATCCTTGTGACCGGCGATGGCTCG
G T A L G A Q V A D L E A G R R T I L V T G D G S

GTGGGCTATAGCATCGGTGAATTTGATACGCTGGTGCGCAAACAATTGCCGCTGATCGTCATCATCATGAACAAC
V G Y S I G E F D T L V R K Q L P L I V I I M N N

CAAAGCTGGGGGGCGACATTGCATTTCCAGCAATTGGCCGTCGGCCCCAATCGCGTGACGGGCACCCGTTTGGAA
Q S W G A T L H F Q Q L A V G P N R V T G T R L E

AATGGCTCCTATCACGGGGTGGCCGCCGCCTTTGGCGCGGATGGCTATCATGTCGACAGTGTGGAGAGCTTTTCT
N G S Y H G V A A A F G A D G Y H V D S V E S F S

GCGGCTCTGGCCCAAGCGCTCGCCCATAATCGCCCCGCCTGCATCAATGTCGCGGTCGCGCTCGATCCGATCCCG

```
 A  A  L  A  Q  A  L  A  H  N  R  P  A  C  I  N  V  A  V  A  L  D  P  I  P

CCCGAAGAACTCATTCTGATCGGCATGGACCCCTTCGGATCTCATCACCATCACCATCACTAAGCTTCT
 P  E  E  L  I  L  I  G  M  D  P  F  G  S  H  H  H  H  H  H  *  A  S
                                          His-tag              HindIII
```

TDoT-L-*Pf*BAL

```
    M  I  I  N  E  T  A  D  D  I  V  Y  R  L  T  V  I  I  D  D  R  Y  E  S
CATATGATCATTAACGAAACTGCCGATGACATCGTTTATCGCCTGACAGTCATTATCGATGATCGCTACGAATCG
NdeI                TDoT
 L  K  N  L  I  T  L  R  A  D  R  L  E  M  I  I  N  D  N  V  S  T  I  L  A
CTGAAAAACCTGATTACCTTACGTGCAGATCGCTTGGAGATGATCATCAATGACAATGTGTCCACCATTCTCGCG

 S  I  T  S  I  E  G  R  A  S  G  G  G  S  G  G  G  S  G  G  G  S  G  S  M
AGCATTACTAGTATTGAAGGCCGTGCTAGCGGCGGTGGGTCTGGAGGCGGCTCAGGTGGTGGGTCGGGATCCATG
     SpeI          Xa          NheI     3xGGGS-Linker                BamHI
 A  M  I  T  G  G  E  L  V  V  R  T  L  I  K  A  G  V  E  H  L  F  G  L  H
GCGATGATTACAGGCGGCGAACTGGTTGTTCGCACCCTAATAAAGGCTGGGGTCGAACATCTGTTCGGCCTGCAC
PfBAL
 G  A  H  I  D  T  I  F  Q  A  C  L  D  H  D  V  P  I  I  D  T  R  H  E  A
GGCGCGCATATCGATACGATTTTTCAAGCCTGTCTCGATCATGATGTGCCGATCATCGACACCCGCCATGAGGCC

 A  A  G  H  A  A  E  G  Y  A  R  A  G  A  K  L  G  V  A  L  V  T  A  G  G
GCCGCAGGGCATGCGGCCGAGGGCTATGCCCGCGCTGGCGCCAAGCTGGGCGTGGCGCTGGTCACGGCGGGCGGG

 G  F  T  N  A  V  T  P  I  A  N  A  W  L  D  R  T  P  V  L  F  L  T  G  S
GGATTTACCAATGCGGTCACGCCCATTGCCAACGCTTGGCTGGATCGCACGCCGGTGCTCTTCCTCACCGGATCG

 G  A  L  R  D  D  E  T  N  T  L  Q  A  G  I  D  Q  V  A  M  A  A  P  I  T
GGCGCGCTGCGTGATGATGAAACCAACACGTTGCAGGCGGGGATTGATCAGGTCGCCATGGCGGCGCCCATTACC

 K  W  A  H  R  V  M  A  T  E  H  I  P  R  L  V  M  Q  A  I  R  A  A  L  S
AAATGGGCGCATCGGGTGATGGCAACCGAGCATATCCCACGGCTGGTGATGCAGGCGATCCGCGCCGCGTTGAGC

 A  P  R  G  P  V  L  L  D  L  P  W  D  I  L  M  N  Q  I  D  E  D  S  V  I
GCGCCACGCGGGCCGGTGTTGCTGGATCTGCCGTGGGATATTCTGATGAACCAGATTGATGAGGATAGCGTCATT

 I  P  D  L  V  L  S  A  H  G  A  R  P  D  P  A  D  L  D  Q  A  L  A  L  L
ATCCCCGATCTGGTCTTGTCCGCACATGGGGCCAGACCCGACCCTGCCGATCTGGATCAGGCTCTCGCGCTTTTG

 R  K  A  E  R  P  V  I  V  L  G  S  E  A  S  R  T  A  R  K  T  A  L  S  A
CGCAAGGCGGAGCGGCCGGTCATCGTGCTCGGCTCAGAAGCCTCGCGGACAGCGCGCAAGACGGCGCTTAGCGCA

 F  V  A  A  T  G  V  P  V  F  A  D  Y  E  G  L  S  M  L  S  G  L  P  D  A
TTCGTGGCGGCGACTGGCGTGCCGGTGTTTGCCGATTATGAAGGGCTAAGCATGCTCTCGGGGCTGCCCGATGCT

 M  R  G  G  L  V  Q  N  L  Y  S  F  A  K  A  D  A  A  P  D  L  V  L  M  L
ATGCGGGGCGGGCTGGTGCAAAACCTCTATTCTTTTGCCAAAGCCGATGCCGCGCCAGATCTCGTGCTGATGCTG

 G  A  R  F  G  L  N  T  G  H  G  S  G  Q  L  I  P  H  S  A  Q  V  I  Q  V
GGGGCGCGCTTTGGCCTTAACACCGGGCATGGATCTGGGCAGTTGATCCCCCATAGCGCGCAGGTCATTCAGGTC

 D  P  D  A  C  E  L  G  R  L  Q  G  I  A  L  G  I  V  A  D  V  G  G  T  I
GACCCTGATGCCTGCGAGCTGGGACGCCTGCAGGGCATCGCTCTGGGCATTGTGGCCGATGTGGGTGGGACCATC

 E  A  L  A  Q  A  T  A  Q  D  A  A  W  P  D  R  G  D  W  C  A  K  V  T  D
GAGGCTTTGGCGCAGGCCACCGCGCAAGATGCGGCTTGGCCGGATCGCGGCGACTGGTGCGCCAAAGTGACGGAT

 L  A  Q  E  R  Y  A  S  I  A  A  K  S  S  S  E  H  A  L  H  P  F  H  A  S
CTGGCGCAAGAGCGCTATGCCAGCATCGCTGCGAAATCGAGCAGCGAGCATGCGCTCCACCCCTTTCACGCCTCG

 Q  V  I  A  K  H  V  D  A  G  V  T  V  V  A  D  G  A  L  T  Y  L  W  L  S
CAGGTCATTGCCAAACACGTCGATGCAGGGGTGACGGTGGTAGCGGATGGTGCGCTGACCTATCTCTGGCTGTCC
```

```
E  V  M  S  R  V  K  P  G  G  F  L  C  H  G  Y  L  G  S  M  G  V  G  F  G
GAAGTGATGAGCCGCGTGAAACCCGGCGGTTTTCTCTGCCACGGCTATCTAGGCTCGATGGGCGTGGGCTTCGGC

T  A  L  G  A  Q  V  A  D  L  E  A  G  R  R  T  I  L  V  T  G  D  G  S  V
ACGGCGCTGGGCGCGCAAGTGGCCGATCTTGAAGCAGGCCGCCGCACGATCCTTGTGACCGGCGATGGCTCGGTG

G  Y  S  I  G  E  F  D  T  L  V  R  K  Q  L  P  L  I  V  I  I  M  N  N  Q
GGCTATAGCATCGGTGAATTTGATACGCTGGTGCGCAAACAATTGCCGCTGATCGTCATCATCATGAACAACCAA

S  W  G  A  T  L  H  F  Q  Q  L  A  V  G  P  N  R  V  T  G  T  R  L  E  N
AGCTGGGGGGGCGACATTGCATTTCCAGCAATTGGCCGTCGGCCCCAATCGCGTGACGGGCACCCGTTTGGAAAAT

G  S  Y  H  G  V  A  A  A  F  G  A  D  G  Y  H  V  D  S  V  E  S  F  S  A
GGCTCCTATCACGGGGTGGCCGCCGCCTTTGGCGCGGATGGCTATCATGTCGACAGTGTGGAGAGCTTTTCTGCG

A  L  A  Q  A  L  A  H  N  R  P  A  C  I  N  V  A  V  A  L  D  P  I  P  P
GCTCTGGCCCAAGCGCTCGCCCATAATCGCCCCGCCTGCATCAATGTCGCGGTCGCGCTCGATCCGATCCCGCCC

E  E  L  I  L  I  G  M  D  P  F  A  *
GAAGAACTCATTCTGATCGGCATGGACCCCTTCGCATAAGCGGCCGCACTCGAG
                                        NotI     XhoI
```

3HAMP-L-*Pf*BAL

```
   M  G  L  F  N  A  H  A  V  A  Q  Q  R  A  D  R  I  A  T  L  L  Q  S  F
CATATGGGCCTGTTTAACGCCCATGCAGTTGCGCAGCAACGCGCGGATCGCATTGCGACTCTCCTGCAGTCCTTT
NdeI          3HAMP
A  D  G  Q  L  D  T  A  V  G  E  A  P  A  P  G  Y  E  R  L  Y  D  S  L  R

GCGGATGGTCAGTTGGACACCGCCGTGGGTGAAGCGCCAGCACCTGGTTACGAACGCCTGTATGACTCGCTTCGC
A  L  Q  R  Q  L  R  E  Q  R  A  E  L  Q  Q  V  E  S  L  E  A  G  L  A  E

GCCCTTCAGCGCCAACTGCGCGAACAACGTGCGGAGTTACAACAGGTTGAGAGCCTGGAAGCAGGCTTGGCTGAA
M  S  R  Q  H  E  A  G  W  I  D  Q  T  I  P  A  E  R  L  E  G  R  A  A  R

ATGAGTCGGCAGCATGAAGCAGGGTGGATTGACCAGACGATTCCGGCTGAACGGTTAGAGGGCCGTGCAGCACGT
I  A  K  G  V  N  E  L  V  A  A  H  I  A  V  K  M  K  V  V  S  V  V  T  A

ATCGCCAAAGGCGTGAATGAGCTGGTTGCTGCGCACATTGCGGTGAAAATGAAAGTCGTGAGCGTAGTCACCGCG
Y  G  Q  G  N  F  E  P  L  M  D  R  L  P  G  K  K  A  Q  I  T  E  A  I  D

TATGGCCAAGGGAACTTCGAACCGCTCATGGATCGCCTGCCGGGTAAGAAAGCCCAGATCACGGAGGCCATTGAT
G  V  R  E  R  L  R  G  A  A  E  A  T  S  A  Q  L  A  T  A  A  Y  N  T  S

GGCGTACGTGAACGCCTGCGTGGAGCTGCTGAAGCGACCTCTGCGCAGCTGGCCACAGCCGCCTACAATACTAGT
                                                                      SpeI
I  E  G  R  A  S  G  G  G  S  G  G  G  S  G  G  G  S  G  S  M  A  M  I  T
ATTGAAGGCCGTGCTAGCGGCGGTGGGTCTGGAGGCGGCTCAGGTGGTGGGTCGGGATCCATGGCGATGATTACA
Xa          NheI   3xGGGS-Linker                                BamHI  PfBAL
G  G  E  L  V  V  R  T  L  I  K  A  G  V  E  H  L  F  G  L  H  G  A  H  I
GGCGGCGAACTGGTTGTTCGCACCCTAATAAAGGCTGGGGTCGAACATCTGTTCGGCCTGCACGGCGCGCATATC

D  T  I  F  Q  A  C  L  D  H  D  V  P  I  I  D  T  R  H  E  A  A  A  G  H
GATACGATTTTTCAAGCCTGTCTCGATCATGATGTGCCGATCATCGACACCCGCCATGAGGCCGCCGCAGGGCAT

A  A  E  G  Y  A  R  A  G  A  K  L  G  V  A  L  V  T  A  G  G  G  F  T  N
GCGGCCGAGGGCTATGCCCGCGCTGGCGCCAAGCTGGGCGTGGCGCTGGTCACGGCGGGCGGGGGGATTTACCAAT

A  V  T  P  I  A  N  A  W  L  D  R  T  P  V  L  F  L  T  G  S  G  A  L  R
GCGGTCACGCCCATTGCCAACGCTTGGCTGGATCGCACGCCGGTGCTCTTCCTCACCGGATCGGGCGCGCTGCGT

D  D  E  T  N  T  L  Q  A  G  I  D  Q  V  A  M  A  A  P  I  T  K  W  A  H
GATGATGAAACCAACACGTTGCAGGCGGGGATTGATCAGGTCGCCATGGCGGCGCCCATTACCAAATGGGCGCAT

R  V  M  A  T  E  H  I  P  R  L  V  M  Q  A  I  R  A  A  L  S  A  P  R  G
CGGGTGATGGCAACCGAGCATATCCCACGGCTGGTGATGCAGGCGATCCGCGCCGCGTTGAGCGCGCCACGCGGG
```

```
P  V  L  L  D  L  P  W  D  I  L  M  N  Q  I  D  E  D  S  V  I  I  P  D  L
CCGGTGTTGCTGGATCTGCCGTGGGATATTCTGATGAACCAGATTGATGAGGATAGCGTCATTATCCCCGATCTG

V  L  S  A  H  G  A  R  P  D  P  A  D  L  D  Q  A  L  A  L  L  R  K  A  E
GTCTTGTCCGCACATGGGGCCAGACCCGACCCTGCCGATCTGGATCAGGCTCTCGCGCTTTTGCGCAAGGCGGAG

R  P  V  I  V  L  G  S  E  A  S  R  T  A  R  K  T  A  L  S  A  F  V  A  A
CGGCCGGTCATCGTGCTCGGCTCAGAAGCCTCGCGGACAGCGCGCAAGACGGCGCTTAGCGCATTCGTGGCGGCG

T  G  V  P  V  F  A  D  Y  E  G  L  S  M  L  S  G  L  P  D  A  M  R  G  G
ACTGGCGTGCCGGTGTTTGCCGATTATGAAGGGCTAAGCATGCTCTCGGGGCTGCCCGATGCTATGCGGGGCGGG

L  V  Q  N  L  Y  S  F  A  K  A  D  A  A  P  D  L  V  L  M  L  G  A  R  F
CTGGTGCAAAACCTCTATTCTTTTGCCAAAGCCGATGCCGCGCCAGATCTCGTGCTGATGCTGGGGGCGCGCTTT

G  L  N  T  G  H  G  S  G  Q  L  I  P  H  S  A  Q  V  I  Q  V  D  P  D  A
GGCCTTAACACCGGGCATGGATCTGGGCAGTTGATCCCCCATAGCGCGCAGGTCATTCAGGTCGACCCTGATGCC

C  E  L  G  R  L  Q  G  I  A  L  G  I  V  A  D  V  G  G  T  I  E  A  L  A
TGCGAGCTGGGACGCCTGCAGGGCATCGCTCTGGGCATTGTGGCCGATGTGGGTGGGACCATCGAGGCTTTGGCG

Q  A  T  A  Q  D  A  A  W  P  D  R  G  D  W  C  A  K  V  T  D  L  A  Q  E
CAGGCCACCGCGCAAGATGCGGCTTGGCCGGATCGCGGCGACTGGTGCGCCAAAGTGACGGATCTGGCGCAAGAG

R  Y  A  S  I  A  A  K  S  S  S  E  H  A  L  H  P  F  H  A  S  Q  V  I  A
CGCTATGCCAGCATCGCTGCGAAATCGAGCAGCGAGCATGCGCTCCACCCCTTTCACGCCTCGCAGGTCATTGCC

K  H  V  D  A  G  V  T  V  V  A  D  G  A  L  T  Y  L  W  L  S  E  V  M  S
AAACACGTCGATGCAGGGGTGACGGTGGTAGCGGATGGTGCGCTGACCTATCTCTGGCTGTCCGAAGTGATGAGC

R  V  K  P  G  G  F  L  C  H  G  Y  L  G  S  M  G  V  G  F  G  T  A  L  G
CGCGTGAAACCCGGCGGTTTTCTCTGCCACGGCTATCTAGGCTCGATGGGCGTGGGCTTCGGCACGGCGCTGGGC

A  Q  V  A  D  L  E  A  G  R  R  T  I  L  V  T  G  D  G  S  V  G  Y  S  I
GCGCAAGTGGCCGATCTTGAAGCAGGCCGCCGCACGATCCTTGTGACCGGCGATGGCTCGGTGGGCTATAGCATC

G  E  F  D  T  L  V  R  K  Q  L  P  L  I  V  I  I  M  N  N  Q  S  W  G  A
GGTGAATTTGATACGCTGGTGCGCAAACAATTGCCGCTGATCGTCATCATCATGAACAACCAAAGCTGGGGGGCG

T  L  H  F  Q  Q  L  A  V  G  P  N  R  V  T  G  T  R  L  E  N  G  S  Y  H
ACATTGCATTTCCAGCAATTGGCCGTCGGCCCCAATCGCGTGACGGGCACCCGTTTGGAAAATGGCTCCTATCAC

G  V  A  A  A  F  G  A  D  G  Y  H  V  D  S  V  E  S  F  S  A  A  L  A  Q
GGGGTGGCCGCCGCCTTTGGCGCGGATGGCTATCATGTCGACAGTGTGGAGAGCTTTTCTGCGGCTCTGGCCCAA

A  L  A  H  N  R  P  A  C  I  N  V  A  V  A  L  D  P  I  P  P  E  E  L  I
GCGCTCGCCCATAATCGCCCCGCCTGCATCAATGTCGCGGTCGCGCTCGATCCGATCCCGCCCGAAGAACTCATT

L  I  G  M  D  P  F  A  *
CTGATCGGCATGGACCCCTTCGCATAAGCGGCCGCACTCGAG
                           NotI   XhoI
```

*Pp*BFD *L476Q* –His_6

```
ATGGCTTCGGTACACGGCACCACATACGAACTCTTGCGACGTCAAGGCATCGATACGGTCTTCGGCAATCCTGGC
 M  A  S  V  H  G  T  T  Y  E  L  L  R  R  Q  G  I  D  T  V  F  G  N  P  G

TCGAACGAGCTCCCGTTTTTGAAGGACTTTCCAGAGGACTTTCGATACATCCTGGCTTTGCAGGAAGCGTGTGTG
 S  N  E  L  P  F  L  K  D  F  P  E  D  F  R  Y  I  L  A  L  Q  E  A  C  V

GTGGGCATTGCAGACGGCTATGCGCAAGCCAGTCGGAAGCCGGCTTTCATTAACCTGCATTCTGCTGCTGGTACC
 V  G  I  A  D  G  Y  A  Q  A  S  R  K  P  A  F  I  N  L  H  S  A  A  G  T
```

```
GGCAATGCTATGGGTGCACTCAGTAACGCCTGGAACTCACATTCCCCGCTGATCGTCACTGCCGGCCAGCAGACC
 G  N  A  M  G  A  L  S  N  A  W  N  S  H  S  P  L  I  V  T  A  G  Q  Q  T

AGGGCGATGATTGGCGTTGAAGCTCTGCTGACCAACGTCGATGCCGCCAACCTGCCACGACCACTTGTCAAATGG
 R  A  M  I  G  V  E  A  L  L  T  N  V  D  A  A  N  L  P  R  P  L  V  K  W

AGCTACGAGCCCGCAAGCGCAGCAGAAGTCCCTCATGCGATGAGCAGGGCTATCCATATGGCAAGCATGGCGCCA
 S  Y  E  P  A  S  A  A  E  V  P  H  A  M  S  R  A  I  H  M  A  S  M  A  P

CAAGGCCCTGTCTATCTTTCGGTGCCATATGACGATTGGGATAAGGATGCTGATCCTCAGTCCCACCACCTTTTT
 Q  G  P  V  Y  L  S  V  P  Y  D  D  W  D  K  D  A  D  P  Q  S  H  H  L  F

GATCGCCATGTCAGTTCATCAGTACGCCTGAACGACCAGGATCTCGATATTCTGGTGAAAGCTCTCAACAGCGCA
 D  R  H  V  S  S  S  V  R  L  N  D  Q  D  L  D  I  L  V  K  A  L  N  S  A

TCCAACCCGGCGATCGTCCTGGGCCCGGACGTCGACGCAGCAAATGCGAACGCAGACTGCGTCATGTTGGCCGAA
 S  N  P  A  I  V  L  G  P  D  V  D  A  A  N  A  N  A  D  C  V  M  L  A  E

CGCCTCAAAGCTCCGGTTTGGGTTGCGCCATCCGCTCCACGCTGCCCATTCCCTACCCGTCATCCTTGCTTCCGT
 R  L  K  A  P  V  W  V  A  P  S  A  P  R  C  P  F  P  T  R  H  P  C  F  R

GGATTGATGCCAGCTGGCATCGCAGCGATTTCTCAGCTGCTCGAAGGTCACGATGTGGTTTTGGTAATCGGCGCT
 G  L  M  P  A  G  I  A  A  I  S  Q  L  L  E  G  H  D  V  V  L  V  I  G  A

CCAGTGTTCCGTTACCACCAATACGACCCAGGTCAATATCTCAAACCTGGCACGCGATTGATTTCGGTGACCTGC
 P  V  F  R  Y  H  Q  Y  D  P  G  Q  Y  L  K  P  G  T  R  L  I  S  V  T  C

GACCCGCTCGAAGCTGCACGCGCGCCAATGGGCGATGCGATCGTGGCAGACATTGGTGCGATGGCTAGCGCTCTT
 D  P  L  E  A  A  R  A  P  M  G  D  A  I  V  A  D  I  G  A  M  A  S  A  L

GCCAACTTGGTTGAAGAGAGCAGCCGCCAGCTCCCAACTGCAGCTCCGGAACCCGCGAAGGTTGACCAAGACGCT
 A  N  L  V  E  E  S  S  R  Q  L  P  T  A  A  P  E  P  A  K  V  D  Q  D  A

GGCCGACTTCACCCAGAGACAGTGTTCGACACACTGAACGACATGGCCCCGGAGAATGCGATTTACCTGAACGAG
 G  R  L  H  P  E  T  V  F  D  T  L  N  D  M  A  P  E  N  A  I  Y  L  N  E

TCGACTTCAACGACCGCCCAAATGTGGCAGCGCCTGAACATGCGCAACCCTGGTAGCTACTACTTCTGTGCAGCT
 S  T  S  T  T  A  Q  M  W  Q  R  L  N  M  R  N  P  G  S  Y  Y  F  C  A  A

GGCGGACTGGGCTTCGCCCTGCCTGCAGCAATTGGCGTTCAACTCGCAGAACCCGAGCGACAAGTCATCGCCGTC
 G  G  L  G  F  A  L  P  A  A  I  G  V  Q  L  A  E  P  E  R  Q  V  I  A  V

ATTGGCGACGGATCGGCGAACTACAGCATTAGTGCGTTGTGGACTGCAGCTCAGTACAACATCCCCACTATCTTC
 I  G  D  G  S  A  N  Y  S  I  S  A  L  W  T  A  A  Q  Y  N  I  P  T  I  F

GTGATCATGAACAACGGCACCTACGGTGCGTTGCGATGGTTTGCCGGCGTTCTCGAAGCAGAAAACGTTCCTGGG
 V  I  M  N  N  G  T  Y  G  A  L  R  W  F  A  G  V  L  E  A  E  N  V  P  G

CAGGATGTGCCAGGGATCGACTTCCGCGCACTCGCCAAGGGCTATGGGGTCCAAGCGCTGAAAGCCGACAACCTT
 Q  D  V  P  G  I  D  F  R  A  L  A  K  G  Y  G  V  Q  A  L  K  A  D  N  L

GAGCAGCTCAAGGGTTCGCTACAAGAAGCGCTTTCTGCCAAAGGCCCGGTACTTATCGAAGTAAGCACCGTAAGC
 E  Q  L  K  G  S  L  Q  E  A  L  S  A  K  G  P  V  L  I  E  V  S  T  V  S

CCGGTGAAGAGATCTCATCACCATCACCATCACTAAGCTTCTAGAGGATCC
 P  V  K  R  S  H  H  H  H  H  H  *  A  S  R  G  S
                                   HindIII
```

TDoT-L-*Pp*BFD *L476Q*

```
CATATGATCATTAACGAAACTGCCGATGACATCGTTTATCGCCTGACAGTCATTATCGATGATCGCTACGAATCG
     M  I  I  N  E  T  A  D  D  I  V  Y  R  L  T  V  I  I  D  D  R  Y  E  S
NdeI                                                                    TDoT
CTGAAAAACCTGATTACCTTACGTGCAGATCGCTTGGAGATGATCATCAATGACAATGTGTCCACCATTCTCGCG
 L  K  N  L  I  T  L  R  A  D  R  L  E  M  I  I  N  D  N  V  S  T  I  L  A

AGCATTACTAGTATTGAAGGCCGTGCTAGCGGCGGTGGGTCTGGAGGCGGCTCAGGTGGTGGGTCGGGATCCATG
 S  I  T  S  I  E  G  R  A  S  G  G  G  S  G  G  G  S  G  G  G  S  G  S  M
       SpeI     Xa        NheI     3xGGGS-Linker                    BamHI
GCTTCGGTACACGGCACCACATACGAACTCTTGCGACGTCAAGGCATCGATACGGTCTTCGGCAATCCTGGCTCG
 A  S  V  H  G  T  T  Y  E  L  L  R  R  Q  G  I  D  T  V  F  G  N  P  G  S
 PpBFD L476Q
AACGAGCTCCCGTTTTTGAAGGACTTTCCAGAGGACTTTCGATACATCCTGGCTTTGCAGGAAGCGTGTGTGGTG
 N  E  L  P  F  L  K  D  F  P  E  D  F  R  Y  I  L  A  L  Q  E  A  C  V  V

GGCATTGCAGACGGCTATGCGCAAGCCAGTCGGAAGCCGGCTTTCATTAACCTGCATTCTGCTGCTGGTACCGGC
 G  I  A  D  G  Y  A  Q  A  S  R  K  P  A  F  I  N  L  H  S  A  A  G  T  G

AATGCTATGGGTGCACTCAGTAACGCCTGGAACTCACATTCCCCGCTGATCGTCACTGCCGGCCAGCAGACCAGG
 N  A  M  G  A  L  S  N  A  W  N  S  H  S  P  L  I  V  T  A  G  Q  Q  T  R

GCGATGATTGGCGTTGAAGCTCTGCTGACCAACGTCGATGCCGCCAACCTGCCACGACCACTTGTCAAATGGAGC
 A  M  I  G  V  E  A  L  L  T  N  V  D  A  A  N  L  P  R  P  L  V  K  W  S

TACGAGCCCGCAAGCGCAGCAGAAGTCCCTCATGCGATGAGCAGGGCTATCCATATGGCAAGCATGGCGCCACAA
 Y  E  P  A  S  A  A  E  V  P  H  A  M  S  R  A  I  H  M  A  S  M  A  P  Q

GGCCCTGTCTATCTTTCGGTGCCATATGACGATTGGGATAAGGATGCTGATCCTCAGTCCCACCACCTTTTTGAT
 G  P  V  Y  L  S  V  P  Y  D  D  W  D  K  D  A  D  P  Q  S  H  H  L  F  D

CGCCATGTCAGTTCATCAGTACGCCTGAACGACCAGGATCTCGATATTCTGGTGAAAGCTCTCAACAGCGCATCC
 R  H  V  S  S  S  V  R  L  N  D  Q  D  L  D  I  L  V  K  A  L  N  S  A  S

AACCCGGCGATCGTCCTGGGCCCGGACGTCGACGCAGCAAATGCGAACGCAGACTGCGTCATGTTGGCCGAACGC
 N  P  A  I  V  L  G  P  D  V  D  A  A  N  A  N  A  D  C  V  M  L  A  E  R

CTCAAAGCTCCGGTTTGGGTTGCGCCATCCGCTCCACGCTGCCCATTCCCTACCCGTCATCCTTGCTTCCGTGGA
 L  K  A  P  V  W  V  A  P  S  A  P  R  C  P  F  P  T  R  H  P  C  F  R  G

TTGATGCCAGCTGGCATCGCAGCGATTTCTCAGCTGCTCGAAGGTCACGATGTGGTTTTGGTAATCGGCGCTCCA
 L  M  P  A  G  I  A  A  I  S  Q  L  L  E  G  H  D  V  V  L  V  I  G  A  P

GTGTTCCGTTACCACCAATACGACCCAGGTCAATATCTCAAACCTGGCACGCGATTGATTTCGGTGACCTGCGAC
 V  F  R  Y  H  Q  Y  D  P  G  Q  Y  L  K  P  G  T  R  L  I  S  V  T  C  D

CCGCTCGAAGCTGCACGCGCGCCAATGGGCGATGCGATCGTGGCAGACATTGGTGCGATGGCTAGCGCTCTTGCC
 P  L  E  A  A  R  A  P  M  G  D  A  I  V  A  D  I  G  A  M  A  S  A  L  A

AACTTGGTTGAAGAGAGCAGCCGCCAGCTCCCAACTGCAGCTCCGGAACCCGCGAAGGTTGACCAAGACGCTGGC
 N  L  V  E  E  S  S  R  Q  L  P  T  A  A  P  E  P  A  K  V  D  Q  D  A  G

CGACTTCACCCAGAGACAGTGTTCGACACACTGAACGACATGGCCCCGGAGAATGCGATTTACCTGAACGAGTCG
 R  L  H  P  E  T  V  F  D  T  L  N  D  M  A  P  E  N  A  I  Y  L  N  E  S

ACTTCAACGACCGCCCAAATGTGGCAGCGCCTGAACATGCGCAACCCTGGTAGCTACTACTTCTGTGCAGCTGGC
 T  S  T  T  A  Q  M  W  Q  R  L  N  M  R  N  P  G  S  Y  Y  F  C  A  A  G

GGACTGGGCTTCGCCCTGCCTGCAGCAATTGGCGTTCAACTCGCAGAACCCGAGCGACAAGTCATCGCCGTCATT
 G  L  G  F  A  L  P  A  A  I  G  V  Q  L  A  E  P  E  R  Q  V  I  A  V  I
```

```
GGCGACGGATCGGCGAACTACAGCATTAGTGCGTTGTGGACTGCAGCTCAGTACAACATCCCCACTATCTTCGTG
 G  D  G  S  A  N  Y  S  I  S  A  L  W  T  A  A  Q  Y  N  I  P  T  I  F  V

ATCATGAACAACGGCACCTACGGTGCGTTGCGATGGTTTGCCGGCGTTCTCGAAGCAGAAAACGTTCCTGGGCAG
 I  M  N  N  G  T  Y  G  A  L  R  W  F  A  G  V  L  E  A  E  N  V  P  G  Q

GATGTGCCAGGGATCGACTTCCGCGCACTCGCCAAGGGCTATGGGGTCCAAGCGCTGAAAGCCGACAACCTTGAG
 D  V  P  G  I  D  F  R  A  L  A  K  G  Y  G  V  Q  A  L  K  A  D  N  L  E

CAGCTCAAGGGTTCGCTACAAGAAGCGCTTTCTGCCAAAGGCCCGGTACTTATCGAAGTAAGCACCGTAAGCCCG
 Q  L  K  G  S  L  Q  E  A  L  S  A  K  G  P  V  L  I  E  V  S  T  V  S  P

GTGAAGAGATCTTAAGCGGCCGCACTCGAG
 V  K  R  S  *  A  A  A  L  E
                NotI
```

3HAMP-L-*Pp*BFD *L476Q*

```
CATATGGGCCTGTTTAACGCCCATGCAGTTGCGCAGCAACGCGCGGATCGCATTGCGACTCTCCTGCAGTCCTTT
    M  G  L  F  N  A  H  A  V  A  Q  Q  R  A  D  R  I  A  T  L  L  Q  S  F
NdeI                                                                  3HAMP
GCGGATGGTCAGTTGGACACCGCCGTGGGTGAAGCGCCAGCACCTGGTTACGAACGCCTGTATGACTCGCTTCGC
 A  D  G  Q  L  D  T  A  V  G  E  A  P  A  P  G  Y  E  R  L  Y  D  S  L  R

GCCCTTCAGCGCCAACTGCGCGAACAACGTGCGGAGTTACAACAGGTTGAGAGCCTGGAAGCAGGCTTGGCTGAA
 A  L  Q  R  Q  L  R  E  Q  R  A  E  L  Q  Q  V  E  S  L  E  A  G  L  A  E

ATGAGTCGGCAGCATGAAGCAGGGTGGATTGACCAGACGATTCCGGCTGAACGGTTAGAGGGCCGTGCAGCACGT
 M  S  R  Q  H  E  A  G  W  I  D  Q  T  I  P  A  E  R  L  E  G  R  A  A  R

ATCGCCAAAGGCGTGAATGAGCTGGTTGCTGCGCACATTGCGGTGAAAATGAAAGTCGTGAGCGTAGTCACCGCG
 I  A  K  G  V  N  E  L  V  A  A  H  I  A  V  K  M  K  V  V  S  V  V  T  A

TATGGCCAAGGGAACTTCGAACCGCTCATGGATCGCCTGCCGGGTAAGAAAGCCCAGATCACGGAGGCCATTGAT
 Y  G  Q  G  N  F  E  P  L  M  D  R  L  P  G  K  K  A  Q  I  T  E  A  I  D

GGCGTACGTGAACGCCTGCGTGGAGCTGCTGAAGCGACCTCTGCGCAGCTGGCCACAGCCGCCTACAATACTAGT
 G  V  R  E  R  L  R  G  A  A  E  A  T  S  A  Q  L  A  T  A  A  Y  N  T  S
                                                                      SpeI
ATTGAAGGCCGTGCTAGCGGCGGTGGGTCTGGAGGCGGCTCAGGTGGTGGGTCGGGATCCATGGCTTCGGTACAC
 I  E  G  R  A  S  G  G  G  S  G  G  G  S  G  G  G  S  G  S  M  A  S  V  H
    Xa          NheI  3xGGGS-Linker                    BamHI          PpBFD
L476Q
GGCACCACATACGAACTCTTGCGACGTCAAGGCATCGATACGGTCTTCGGCAATCCTGGCTCGAACGAGCTCCCG
 G  T  T  Y  E  L  L  R  R  Q  G  I  D  T  V  F  G  N  P  G  S  N  E  L  P

TTTTTGAAGGACTTTCCAGAGGACTTTCGATACATCCTGGCTTTGCAGGAAGCGTGTGTGGTGGGCATTGCAGAC
 F  L  K  D  F  P  E  D  F  R  Y  I  L  A  L  Q  E  A  C  V  V  G  I  A  D

GGCTATGCGCAAGCCAGTCGGAAGCCGGCTTTCATTAACCTGCATTCTGCTGCTGGTACCGGCAATGCTATGGGT
 G  Y  A  Q  A  S  R  K  P  A  F  I  N  L  H  S  A  A  G  T  G  N  A  M  G

GCACTCAGTAACGCCTGGAACTCACATTCCCCGCTGATCGTCACTGCCGGCCAGCAGACCAGGGCGATGATTGGC
 A  L  S  N  A  W  N  S  H  S  P  L  I  V  T  A  G  Q  Q  T  R  A  M  I  G

GTTGAAGCTCTGCTGACCAACGTCGATGCCGCCAACCTGCCACGACCACTTGTCAAATGGAGCTACGAGCCCGCA
 V  E  A  L  L  T  N  V  D  A  A  N  L  P  R  P  L  V  K  W  S  Y  E  P  A

AGCGCAGCAGAAGTCCCTCATGCGATGAGCAGGGCTATCCATATGGCAAGCATGGCGCCACAAGGCCCTGTCTAT
 S  A  A  E  V  P  H  A  M  S  R  A  I  H  M  A  S  M  A  P  Q  G  P  V  Y
```

```
CTTTCGGTGCCATATGACGATTGGGATAAGGATGCTGATCCTCAGTCCCACCACCTTTTTGATCGCCATGTCAGT
 L  S  V  P  Y  D  D  W  D  K  D  A  D  P  Q  S  H  H  L  F  D  R  H  V  S

TCATCAGTACGCCTGAACGACCAGGATCTCGATATTCTGGTGAAAGCTCTCAACAGCGCATCCAACCCGGCGATC
 S  S  V  R  L  N  D  Q  D  L  D  I  L  V  K  A  L  N  S  A  S  N  P  A  I

GTCCTGGGCCCGGACGTCGACGCAGCAAATGCGAACGCAGACTGCGTCATGTTGGCCGAACGCCTCAAAGCTCCG
 V  L  G  P  D  V  D  A  A  N  A  N  A  D  C  V  M  L  A  E  R  L  K  A  P

GTTTGGGTTGCGCCATCCGCTCCACGCTGCCCATTCCCTACCCGTCATCCTTGCTTCCGTGGATTGATGCCAGCT
 V  W  V  A  P  S  A  P  R  C  P  F  P  T  R  H  P  C  F  R  G  L  M  P  A

GGCATCGCAGCGATTTCTCAGCTGCTCGAAGGTCACGATGTGGTTTTGGTAATCGGCGCTCCAGTGTTCCGTTAC
 G  I  A  A  I  S  Q  L  L  E  G  H  D  V  V  L  V  I  G  A  P  V  F  R  Y

CACCAATACGACCCAGGTCAATATCTCAAACCTGGCACGCGATTGATTTCGGTGACCTGCGACCCGCTCGAAGCT
 H  Q  Y  D  P  G  Q  Y  L  K  P  G  T  R  L  I  S  V  T  C  D  P  L  E  A

GCACGCGCGCCAATGGGCGATGCGATCGTGGCAGACATTGGTGCGATGGCTAGCGCTCTTGCCAACTTGGTTGAA
 A  R  A  P  M  G  D  A  I  V  A  D  I  G  A  M  A  S  A  L  A  N  L  V  E

GAGAGCAGCCGCCAGCTCCCAACTGCAGCTCCGGAACCCGCGAAGGTTGACCAAGACGCTGGCCGACTTCACCCA
 E  S  S  R  Q  L  P  T  A  A  P  E  P  A  K  V  D  Q  D  A  G  R  L  H  P

GAGACAGTGTTCGACACACTGAACGACATGGCCCCGGAGAATGCGATTTACCTGAACGAGTCGACTTCAACGACC
 E  T  V  F  D  T  L  N  D  M  A  P  E  N  A  I  Y  L  N  E  S  T  S  T  T

GCCCAAATGTGGCAGCGCCTGAACATGCGCAACCCTGGTAGCTACTACTTCTGTGCAGCTGGCGGACTGGGCTTC
 A  Q  M  W  Q  R  L  N  M  R  N  P  G  S  Y  Y  F  C  A  A  G  G  L  G  F

GCCCTGCCTGCAGCAATTGGCGTTCAACTCGCAGAACCCGAGCGACAAGTCATCGCCGTCATTGGCGACGGATCG
 A  L  P  A  A  I  G  V  Q  L  A  E  P  E  R  Q  V  I  A  V  I  G  D  G  S

GCGAACTACAGCATTAGTGCGTTGTGGACTGCAGCTCAGTACAACATCCCCACTATCTTCGTGATCATGAACAAC
 A  N  Y  S  I  S  A  L  W  T  A  A  Q  Y  N  I  P  T  I  F  V  I  M  N  N

GGCACCTACGGTGCGTTGCGATGGTTTGCCGGCGTTCTCGAAGCAGAAAACGTTCCTGGGCAGGATGTGCCAGGG
 G  T  Y  G  A  L  R  W  F  A  G  V  L  E  A  E  N  V  P  G  Q  D  V  P  G

ATCGACTTCCGCGCACTCGCCAAGGGCTATGGGGTCCAAGCGCTGAAAGCCGACAACCTTGAGCAGCTCAAGGGT
 I  D  F  R  A  L  A  K  G  Y  G  V  Q  A  L  K  A  D  N  L  E  Q  L  K  G

TCGCTACAAGAAGCGCTTTCTGCCAAAGGCCCGGTACTTATCGAAGTAAGCACCGTAAGCCCGGTGAAGAGATCT
 S  L  Q  E  A  L  S  A  K  G  P  V  L  I  E  V  S  T  V  S  P  V  K  R  S

TAAGCGGCCGCACTCGAG
 *  A  A  A  L  E
     NotI
```

TDoT-L-*Ec*LDC

```
CATATGATCATTAACGAAACTGCCGATGACATCGTTTATCGCCTGACAGTCATTATCGATGATCGCTACGAATCG
      M  I  I  N  E  T  A  D  D  I  V  Y  R  L  T  V  I  I  D  D  R  Y  E  S
NdeI                                                                    TDoT
CTGAAAAACCTGATTACCTTACGTGCAGATCGCTTGGAGATGATCATCAATGACAATGTGTCCACCATTCTCGCG
 L  K  N  L  I  T  L  R  A  D  R  L  E  M  I  I  N  D  N  V  S  T  I  L  A

AGCATTACTAGTATTGAAGGCCGTGCTAGCGGCGGTGGGTCTGGAGGCGGCTCAGGTGGTGGGTCGGGATCCATG
 S  I  T  S  I  E  G  R  A  S  G  G  G  S  G  G  G  S  G  G  G  S  G  S  M
     SpeI     Xa     NheI     3xGGGS-Linker                    BamHI
```

AACATCATCGCTATCATGGGCCCTCACGGTGTTTTCTACAAGGATGAGCCAATCAAGGAGCTGGAATCCGCACTA
N I I A I M G P H G V F Y K D E P I K E L E S A L

*Ec*LDC

GTTGCACAGGGCTTTCAGATCATCTGGCCCCAGAACTCCGTTGACCTTCTCAAATTCATCGAGCACAATCCTCGC
V A Q G F Q I I W P Q N S V D L L K F I E H N P R

ATTTGTGGTGTGATTTTTGACTGGGACGAGTACTCTCTTGATTTATGCTCCGACATCAACCAGCTCAACGAGTAC
I C G V I F D W D E Y S L D L C S D I N Q L N E Y

CTGCCACTCTACGCATTCATCAACACTCACTCCACCATGGACGTTTCCGTGCAGGACATGCGTATGGCACTCTGG
L P L Y A F I N T H S T M D V S V Q D M R M A L W

TTCTTTGAATACGCTCTGGGCCAGGCTGAGGACATCGCGATCCGCATGCGTCAGTACACCGACGAGTACCTGGAC
F F E Y A L G Q A E D I A I R M R Q Y T D E Y L D

AACATCACCCCTCCATTCACCAAGGCTCTCTTCACCTACGTAAAGGAACGCAAGTACACTTTCTGCACCCCAGGC
N I T P P F T K A L F T Y V K E R K Y T F C T P G

CACATGGGCGGCACCGCCTACCAGAAGTCCCCAGTCGGATGCCTCTTCTACGACTTCTTCGGCGGTAACACTCTT
H M G G T A Y Q K S P V G C L F Y D F F G G N T L

AAGGCAGATGTCTCCATTTCCGTCACCGAGTTGGGCTCTCTGCTGGACCACACCGGCCCTCACCTGGAGGCAGAA
K A D V S I S V T E L G S L L D H T G P H L E A E

GAGTACATCGCTCGTACCTTCGGTGCTGAACAGTCCTACATCGTCACCAACGGTACTTCCACCAGCAACAAGATC
E Y I A R T F G A E Q S Y I V T N G T S T S N K I

GTTGGTATGTACGCAGCTCCTTCTGGCTCCACCCTGTTGATCGACCGCAACTGTCACAAGTCCCTCGCGCATCTT
V G M Y A A P S G S T L L I D R N C H K S L A H L

CTTATGATGAACGATGTGGTCCCTGTATGGCTGAAGCCAACCCGTAACGCTCTGGGCATCCTTGGCGGTATCCCC
L M M N D V V P V W L K P T R N A L G I L G G I P

CGTCGCGAGTTCACCCGTGATTCCATCGAGGAAAAGGTTGCAGCCACTACCCAGGCACAGTGGCCTGTCCACGCT
R R E F T R D S I E E K V A A T T Q A Q W P V H A

GTCATTACCAACTCGACCTACGACGGCCTGCTCTACAACACCGATTGGATCAAGCAGACCCTAGATGTTCCTTCC
V I T N S T Y D G L L Y N T D W I K Q T L D V P S

ATTCACTTCGACAGCGCATGGGTTCCTTACACTCACTTCCACCCAATCTACCAGGGTAAGTCCGGAATGTCCGGC
I H F D S A W V P Y T H F H P I Y Q G K S G M S G

GAGCGTGTCGCTGGCAAGGTTATCTTCGAAACCCAATCAACCCACAAGATGCTGGCTGCTCTCTCCCAGGCTTCT
E R V A G K V I F E T Q S T H K M L A A L S Q A S

CTGATCCACATCAAGGGCGAGTACGACGAGGAAGCTTTCAACGAGGCTTTCATGATGCACACCACCACCTCCCCA
L I H I K G E Y D E E A F N E A F M M H T T T S P

TCCTACCCTATCGTCGCGTCCGTCGAGACTGCTGCCGCAATGCTTCGCGGTAACCCAGGTAAGCGCCTCATCAAC
S Y P I V A S V E T A A A M L R G N P G K R L I N

CGTTCCGTTGAGCGCGCTCTTCACTTCCGTAAGGAAGTGCAGCGCCTGCGTGAGGAATCTGACGGTTGGTTCTTC
R S V E R A L H F R K E V Q R L R E E S D G W F F

GACATTTGGCAGCCACCTCAGGTTGATGAGGCCGAGTGCTGGCCAGTTGCTCCAGGTGAACAGTGGCACGGATTC
D I W Q P P Q V D E A E C W P V A P G E Q W H G F

AACGATGCAGATGCTGACCACATGTTTTTGGACCCGGTCAAGGTCACCATTCTTACTCCTGGTATGGATGAGCAG
N D A D A D H M F L D P V K V T I L T P G M D E Q

GGCAACATGTCTGAGGAGGGTATCCCAGCTGCTCTGGTTGCAAAGTTCCTCGACGAACGTGGCATCGTTGTTGAG
G N M S E E G I P A A L V A K F L D E R G I V V E

```
AAGACCGGACCATACAACCTGCTGTTCCTGTTCAGCATCGGCATCGACAAAACCAAGGCAATGGGTCTGCTGCGC
 K  T  G  P  Y  N  L  L  F  L  F  S  I  G  I  D  K  T  K  A  M  G  L  L  R

GGCCTTACCGAGTTCAAGCGCTCCTACGACCTGAACCTTCGCATCAAGAATATGCTGCCGGACCTGTACGCTGAA
 G  L  T  E  F  K  R  S  Y  D  L  N  L  R  I  K  N  M  L  P  D  L  Y  A  E

GATCCTGATTTCTACCGCAACATGCGCATCCAGGACCTCGCACAGGGCATCCACAAGCTCATTCGCAAGCACGAC
 D  P  D  F  Y  R  N  M  R  I  Q  D  L  A  Q  G  I  H  K  L  I  R  K  H  D

CTGCCAGGCCTTATGCTCCGTGCATTCGATACCCTCCCAGAGATGATCATGACCCCTCACCAGGCTTGGCAGCGC
 L  P  G  L  M  L  R  A  F  D  T  L  P  E  M  I  M  T  P  H  Q  A  W  Q  R

CAGATCAAGGGCGAGGTGGAAACCATCGCACTGGAGCAGCTGGTTGGTCGTGTCTCCGCCAACATGATCCTGCCA
 Q  I  K  G  E  V  E  T  I  A  L  E  Q  L  V  G  R  V  S  A  N  M  I  L  P

TATCCACCTGGCGTTCCGCTGCTGATGCCAGGCGAGATGCTCACCAAGGAGTCCCGCACCGTATTGGACTTCCTT
 Y  P  P  G  V  P  L  L  M  P  G  E  M  L  T  K  E  S  R  T  V  L  D  F  L

CTCATGTTGTGCTCTGTTGGCCAGCACTACCCAGGCTTCGAGACCGACATCCACGGCGCTAAGCAAGATGAAGAC
 L  M  L  C  S  V  G  Q  H  Y  P  G  F  E  T  D  I  H  G  A  K  Q  D  E  D

GGCGTTTACCGCGTTCGCGTCCTTAAGATGGCAGGCTAAGTCGACAAGCTTGCGGCCGCACTCGAG
 G  V  Y  R  V  R  V  L  K  M  A  G  *  V  D  K  L  A  A  A  L  E
                                       SalI           NotI
```

***Ec*LDC-L-TDoT**

```
CATATGATGAACATCATCGCTATCATGGGCCCTCACGGTGTTTTCTACAAGGATGAGCCAATCAAGGAGCTGGAA
 H  M  M  N  I  I  A  I  M  G  P  H  G  V  F  Y  K  D  E  P  I  K  E  L  E
 NdeI                                                                  EcLDC
TCCGCACTAGTTGCACAGGGCTTTCAGATCATCTGGCCCCAGAACTCCGTTGACCTTCTCAAATTCATCGAGCAC
 S  A  L  V  A  Q  G  F  Q  I  I  W  P  Q  N  S  V  D  L  L  K  F  I  E  H

AATCCTCGCATTTGTGGTGTGATTTTTGACTGGGACGAGTACTCTCTTGATTTATGCTCCGACATCAACCAGCTC
 N  P  R  I  C  G  V  I  F  D  W  D  E  Y  S  L  D  L  C  S  D  I  N  Q  L

AACGAGTACCTGCCACTCTACGCATTCATCAACACTCACTCCACCATGGACGTTTCCGTGCAGGACATGCGTATG
 N  E  Y  L  P  L  Y  A  F  I  N  T  H  S  T  M  D  V  S  V  Q  D  M  R  M

GCACTCTGGTTCTTTGAATACGCTCTGGGCCAGGCTGAGGACATCGCGATCCGCATGCGTCAGTACACCGACGAG
 A  L  W  F  F  E  Y  A  L  G  Q  A  E  D  I  A  I  R  M  R  Q  Y  T  D  E

TACCTGGACAACATCACCCCTCCATTCACCAAGGCTCTCTTCACCTACGTAAAGGAACGCAAGTACACTTTCTGC
 Y  L  D  N  I  T  P  P  F  T  K  A  L  F  T  Y  V  K  E  R  K  Y  T  F  C

ACCCCAGGCCACATGGGCGGCACCGCCTACCAGAAGTCCCCAGTCGGATGCCTCTTCTACGACTTCTTCGGCGGT
 T  P  G  H  M  G  G  T  A  Y  Q  K  S  P  V  G  C  L  F  Y  D  F  F  G  G

AACACTCTTAAGGCAGATGTCTCCATTTCCGTCACCGAGTTGGGCTCTCTGCTGGACCACACCGGCCCTCACCTG
 N  T  L  K  A  D  V  S  I  S  V  T  E  L  G  S  L  L  D  H  T  G  P  H  L

GAGGCAGAAGAGTACATCGCTCGTACCTTCGGTGCTGAACAGTCCTACATCGTCACCAACGGTACTTCCACCAGC
 E  A  E  E  Y  I  A  R  T  F  G  A  E  Q  S  Y  I  V  T  N  G  T  S  T  S

AACAAGATCGTTGGTATGTACGCAGCTCCTTCTGGCTCCACCCTGTTGATCGACCGCAACTGTCACAAGTCCCTC
 N  K  I  V  G  M  Y  A  A  P  S  G  S  T  L  L  I  D  R  N  C  H  K  S  L

GCGCATCTTCTTATGATGAACGATGTGGTCCCTGTATGGCTGAAGCCAACCCGTAACGCTCTGGGCATCCTTGGC
 A  H  L  L  M  M  N  D  V  V  P  V  W  L  K  P  T  R  N  A  L  G  I  L  G
GGTATCCCCCGTCGCGAGTTCACCCGTGATTCCATCGAGGAAAAGGTTGCAGCCACTACCCAGGCACAGTGGCCT
 G  I  P  R  R  E  F  T  R  D  S  I  E  E  K  V  A  A  T  T  Q  A  Q  W  P
```

```
GTCCACGCTGTCATTACCAACTCGACCTACGACGGCCTGCTCTACAACACCGATTGGATCAAGCAGACCCTAGAT
 V  H  A  V  I  T  N  S  T  Y  D  G  L  L  Y  N  T  D  W  I  K  Q  T  L  D

GTTCCTTCCATTCACTTCGACAGCGCATGGGTTCCTTACACTCACTTCCACCCAATCTACCAGGGTAAGTCCGGA
 V  P  S  I  H  F  D  S  A  W  V  P  Y  T  H  F  H  P  I  Y  Q  G  K  S  G

ATGTCCGGCGAGCGTGTCGCTGGCAAGGTTATCTTCGAAACCCAATCAACCCACAAGATGCTGGCTGCTCTCTCC
 M  S  G  E  R  V  A  G  K  V  I  F  E  T  Q  S  T  H  K  M  L  A  A  L  S

CAGGCTTCTCTGATCCACATCAAGGGCGAGTACGACGAGGAAGCTTTCAACGAGGCTTTCATGATGCACACCACC
 Q  A  S  L  I  H  I  K  G  E  Y  D  E  E  A  F  N  E  A  F  M  M  H  T  T

ACCTCCCCATCCTACCCTATCGTCGCGTCCGTCGAGACTGCTGCCGCAATGCTTCGCGGTAACCCAGGTAAGCGC
 T  S  P  S  Y  P  I  V  A  S  V  E  T  A  A  A  M  L  R  G  N  P  G  K  R

CTCATCAACCGTTCCGTTGAGCGCGCTCTTCACTTCCGTAAGGAAGTGCAGCGCCTGCGTGAGGAATCTGACGGT
 L  I  N  R  S  V  E  R  A  L  H  F  R  K  E  V  Q  R  L  R  E  E  S  D  G

TGGTTCTTCGACATTTGGCAGCCACCTCAGGTTGATGAGGCCGAGTGCTGGCCAGTTGCTCCAGGTGAACAGTGG
 W  F  F  D  I  W  Q  P  P  Q  V  D  E  A  E  C  W  P  V  A  P  G  E  Q  W

CACGGATTCAACGATGCAGATGCTGACCACATGTTTTTGGACCCGGTCAAGGTCACCATTCTTACTCCTGGTATG
 H  G  F  N  D  A  D  A  D  H  M  F  L  D  P  V  K  V  T  I  L  T  P  G  M

GATGAGCAGGGCAACATGTCTGAGGAGGGTATCCCAGCTGCTCTGGTTGCAAAGTTCCTCGACGAACGTGGCATC
 D  E  Q  G  N  M  S  E  E  G  I  P  A  A  L  V  A  K  F  L  D  E  R  G  I

GTTGTTGAGAAGACCGGACCATACAACCTGCTGTTCCTGTTCAGCATCGGCATCGACAAAACCAAGGCAATGGGT
 V  V  E  K  T  G  P  Y  N  L  L  F  L  F  S  I  G  I  D  K  T  K  A  M  G

CTGCTGCGCGGCCTTACCGAGTTCAAGCGCTCCTACGACCTGAACCTTCGCATCAAGAATATGCTGCCGGACCTG
 L  L  R  G  L  T  E  F  K  R  S  Y  D  L  N  L  R  I  K  N  M  L  P  D  L

TACGCTGAAGATCCTGATTTCTACCGCAACATGCGCATCCAGGACCTCGCACAGGGCATCCACAAGCTCATTCGC
 Y  A  E  D  P  D  F  Y  R  N  M  R  I  Q  D  L  A  Q  G  I  H  K  L  I  R

AAGCACGACCTGCCAGGCCTTATGCTCCGTGCATTCGATACCCTCCCAGAGATGATCATGACCCCTCACCAGGCT
 K  H  D  L  P  G  L  M  L  R  A  F  D  T  L  P  E  M  I  M  T  P  H  Q  A

TGGCAGCGCCAGATCAAGGGCGAGGTGGAAACCATCGCACTGGAGCAGCTGGTTGGTCGTGTCTCCGCCAACATG
 W  Q  R  Q  I  K  G  E  V  E  T  I  A  L  E  Q  L  V  G  R  V  S  A  N  M

ATCCTGCCATATCCACCTGGCGTTCCGCTGCTGATGCCAGGCGAGATGCTCACCAAGGAGTCCCGCACCGTATTG
 I  L  P  Y  P  P  G  V  P  L  L  M  P  G  E  M  L  T  K  E  S  R  T  V  L

GACTTCCTTCTCATGTTGTGCTCTGTTGGCCAGCACTACCCAGGCTTCGAGACCGACATCCACGGCGCTAAGCAA
 D  F  L  L  M  L  C  S  V  G  Q  H  Y  P  G  F  E  T  D  I  H  G  A  K  Q

GATGAAGACGGCGTTTACCGCGTTCGCGTCCTTAAGATGGCAGGCGCTAGCGGCGGTGGGTCTGGAGGCGGCTCA
 D  E  D  G  V  Y  R  V  R  V  L  K  M  A  G  A  S  G  G  G  S  G  G  G  S
                                              NheI        3xGGGS-Linker
GGTGGTGGGTCGGGATCCATCATTAACGAAACTGCCGATGACATCGTTTATCGCCTGACAGTCATTATCGATGAT
 G  G  G  S  G  S  I  I  N  E  T  A  D  D  I  V  Y  R  L  T  V  I  I  D  D
             BamHI       TDoT
CGCTACGAATCGCTGAAAAACCTGATTACCTTACGTGCAGATCGCTTGGAGATGATCATCAATGACAATGTGTCC
 R  Y  E  S  L  K  N  L  I  T  L  R  A  D  R  L  E  M  I  I  N  D  N  V  S

ACCATTCTCGCGAGCATTTAAGCGGCCGCACTCGAG
 T  I  L  A  S  I  *  A  A  A  L  E
                    NotI
```

***Ec*LDC-L-3HAMP**

```
CATATGATGAACATCATCGCTATCATGGGCCCTCACGGTGTTTTCTACAAGGATGAGCCAATCAAGGAGCTGGAA
 H  M  M  N  I  I  A  I  M  G  P  H  G  V  F  Y  K  D  E  P  I  K  E  L  E
 NdeI                                                                EcLDC
TCCGCACTAGTTGCACAGGGCTTTCAGATCATCTGGCCCCAGAACTCCGTTGACCTTCTCAAATTCATCGAGCAC
 S  A  L  V  A  Q  G  F  Q  I  I  W  P  Q  N  S  V  D  L  L  K  F  I  E  H

AATCCTCGCATTTGTGGTGTGATTTTTGACTGGGACGAGTACTCTCTTGATTTATGCTCCGACATCAACCAGCTC
 N  P  R  I  C  G  V  I  F  D  W  D  E  Y  S  L  D  L  C  S  D  I  N  Q  L

AACGAGTACCTGCCACTCTACGCATTCATCAACACTCACTCCACCATGGACGTTTCCGTGCAGGACATGCGTATG
 N  E  Y  L  P  L  Y  A  F  I  N  T  H  S  T  M  D  V  S  V  Q  D  M  R  M

GCACTCTGGTTCTTTGAATACGCTCTGGGCCAGGCTGAGGACATCGCGATCCGCATGCGTCAGTACACCGACGAG
 A  L  W  F  F  E  Y  A  L  G  Q  A  E  D  I  A  I  R  M  R  Q  Y  T  D  E

TACCTGGACAACATCACCCCTCCATTCACCAAGGCTCTCTTCACCTACGTAAAGGAACGCAAGTACACTTTCTGC
 Y  L  D  N  I  T  P  P  F  T  K  A  L  F  T  Y  V  K  E  R  K  Y  T  F  C

ACCCCAGGCCACATGGGCGGCACCGCCTACCAGAAGTCCCCAGTCGGATGCCTCTTCTACGACTTCTTCGGCGGT
 T  P  G  H  M  G  G  T  A  Y  Q  K  S  P  V  G  C  L  F  Y  D  F  F  G  G

AACACTCTTAAGGCAGATGTCTCCATTTCCGTCACCGAGTTGGGCTCTCTGCTGGACCACACCGGCCCTCACCTG
 N  T  L  K  A  D  V  S  I  S  V  T  E  L  G  S  L  L  D  H  T  G  P  H  L

GAGGCAGAAGAGTACATCGCTCGTACCTTCGGTGCTGAACAGTCCTACATCGTCACCAACGGTACTTCCACCAGC
 E  A  E  E  Y  I  A  R  T  F  G  A  E  Q  S  Y  I  V  T  N  G  T  S  T  S

AACAAGATCGTTGGTATGTACGCAGCTCCTTCTGGCTCCACCCTGTTGATCGACCGCAACTGTCACAAGTCCCTC
 N  K  I  V  G  M  Y  A  A  P  S  G  S  T  L  L  I  D  R  N  C  H  K  S  L

GCGCATCTTCTTATGATGAACGATGTGGTCCCTGTATGGCTGAAGCCAACCCGTAACGCTCTGGGCATCCTTGGC
 A  H  L  L  M  M  N  D  V  V  P  V  W  L  K  P  T  R  N  A  L  G  I  L  G

GGTATCCCCCGTCGCGAGTTCACCCGTGATTCCATCGAGGAAAAGGTTGCAGCCACTACCCAGGCACAGTGGCCT
 G  I  P  R  R  E  F  T  R  D  S  I  E  E  K  V  A  A  T  T  Q  A  Q  W  P

GTCCACGCTGTCATTACCAACTCGACCTACGACGGCCTGCTCTACAACACCGATTGGATCAAGCAGACCCTAGAT
 V  H  A  V  I  T  N  S  T  Y  D  G  L  L  Y  N  T  D  W  I  K  Q  T  L  D

GTTCCTTCCATTCACTTCGACAGCGCATGGGTTCCTTACACTCACTTCCACCCAATCTACCAGGGTAAGTCCGGA
 V  P  S  I  H  F  D  S  A  W  V  P  Y  T  H  F  H  P  I  Y  Q  G  K  S  G

ATGTCCGGCGAGCGTGTCGCTGGCAAGGTTATCTTCGAAACCCAATCAACCCACAAGATGCTGGCTGCTCTCTCC
 M  S  G  E  R  V  A  G  K  V  I  F  E  T  Q  S  T  H  K  M  L  A  A  L  S

CAGGCTTCTCTGATCCACATCAAGGGCGAGTACGACGAGGAAGCTTTCAACGAGGCTTTCATGATGCACACCACC
 Q  A  S  L  I  H  I  K  G  E  Y  D  E  E  A  F  N  E  A  F  M  M  H  T  T

ACCTCCCCATCCTACCCTATCGTCGCGTCCGTCGAGACTGCTGCCGCAATGCTTCGCGGTAACCCAGGTAAGCGC
 T  S  P  S  Y  P  I  V  A  S  V  E  T  A  A  A  M  L  R  G  N  P  G  K  R

CTCATCAACCGTTCCGTTGAGCGCGCTCTTCACTTCCGTAAGGAAGTGCAGCGCCTGCGTGAGGAATCTGACGGT
 L  I  N  R  S  V  E  R  A  L  H  F  R  K  E  V  Q  R  L  R  E  E  S  D  G

TGGTTCTTCGACATTTGGCAGCCACCTCAGGTTGATGAGGCCGAGTGCTGGCCAGTTGCTCCAGGTGAACAGTGG
 W  F  F  D  I  W  Q  P  P  Q  V  D  E  A  E  C  W  P  V  A  P  G  E  Q  W

CACGGATTCAACGATGCAGATGCTGACCACATGTTTTTGGACCCGGTCAAGGTCACCATTCTTACTCCTGGTATG
 H  G  F  N  D  A  D  A  D  H  M  F  L  D  P  V  K  V  T  I  L  T  P  G  M
```

```
GATGAGCAGGGCAACATGTCTGAGGAGGGTATCCCAGCTGCTCTGGTTGCAAAGTTCCTCGACGAACGTGGCATC
 D  E  Q  G  N  M  S  E  E  G  I  P  A  A  L  V  A  K  F  L  D  E  R  G  I

GTTGTTGAGAAGACCGGACCATACAACCTGCTGTTCCTGTTCAGCATCGGCATCGACAAAACCAAGGCAATGGGT
 V  V  E  K  T  G  P  Y  N  L  L  F  L  F  S  I  G  I  D  K  T  K  A  M  G

CTGCTGCGCGGCCTTACCGAGTTCAAGCGCTCCTACGACCTGAACCTTCGCATCAAGAATATGCTGCCGGACCTG
 L  L  R  G  L  T  E  F  K  R  S  Y  D  L  N  L  R  I  K  N  M  L  P  D  L

TACGCTGAAGATCCTGATTTCTACCGCAACATGCGCATCCAGGACCTCGCACAGGGCATCCACAAGCTCATTCGC
 Y  A  E  D  P  D  F  Y  R  N  M  R  I  Q  D  L  A  Q  G  I  H  K  L  I  R

AAGCACGACCTGCCAGGCCTTATGCTCCGTGCATTCGATACCCTCCCAGAGATGATCATGACCCCTCACCAGGCT
 K  H  D  L  P  G  L  M  L  R  A  F  D  T  L  P  E  M  I  M  T  P  H  Q  A

TGGCAGCGCCAGATCAAGGGCGAGGTGGAAACCATCGCACTGGAGCAGCTGGTTGGTCGTGTCTCCGCCAACATG
 W  Q  R  Q  I  K  G  E  V  E  T  I  A  L  E  Q  L  V  G  R  V  S  A  N  M

ATCCTGCCATATCCACCTGGCGTTCCGCTGCTGATGCCAGGCGAGATGCTCACCAAGGAGTCCCGCACCGTATTG
 I  L  P  Y  P  P  G  V  P  L  L  M  P  G  E  M  L  T  K  E  S  R  T  V  L

GACTTCCTTCTCATGTTGTGCTCTGTTGGCCAGCACTACCCAGGCTTCGAGACCGACATCCACGGCGCTAAGCAA
 D  F  L  L  M  L  C  S  V  G  Q  H  Y  P  G  F  E  T  D  I  H  G  A  K  Q

GATGAAGACGGCGTTTACCGCGTTCGCGTCCTTAAGATGGCAGGCGCTAGCGGCGGTGGGTCTGGAGGCGGCTCA
 D  E  D  G  V  Y  R  V  R  V  L  K  M  A  G  A  S  G  G  G  S  G  G  G  S
                                   NheI          3xGGGS-Linker

GGTGGTGGGTCGGGATCCATGGGCCTGTTTAACGCCCATGCAGTTGCGCAGCAACGCGCGGATCGCATTGCGACT
 G  G  G  S  G  S  M  G  L  F  N  A  H  A  V  A  Q  Q  R  A  D  R  I  A  T
             BamHI        3HAMP

CTCCTGCAGTCCTTTGCGGATGGTCAGTTGGACACCGCCGTGGGTGAAGCGCCAGCACCTGGTTACGAACGCCTG
 L  L  Q  S  F  A  D  G  Q  L  D  T  A  V  G  E  A  P  A  P  G  Y  E  R  L

TATGACTCGCTTCGCGCCCTTCAGCGCCAACTGCGCGAACAACGTGCGGAGTTACAACAGGTTGAGAGCCTGGAA
 Y  D  S  L  R  A  L  Q  R  Q  L  R  E  Q  R  A  E  L  Q  Q  V  E  S  L  E

GCAGGCTTGGCTGAAATGAGTCGGCAGCATGAAGCAGGGTGGATTGACCAGACGATTCCGGCTGAACGGTTAGAG
 A  G  L  A  E  M  S  R  Q  H  E  A  G  W  I  D  Q  T  I  P  A  E  R  L  E

GGCCGTGCAGCACGTATCGCCAAAGGCGTGAATGAGCTGGTTGCTGCGCACATTGCGGTGAAAATGAAAGTCGTG
 G  R  A  A  R  I  A  K  G  V  N  E  L  V  A  A  H  I  A  V  K  M  K  V  V

AGCGTAGTCACCGCGTATGGCCAAGGGAACTTCGAACCGCTCATGGATCGCCTGCCGGGTAAGAAAGCCCAGATC
 S  V  V  T  A  Y  G  Q  G  N  F  E  P  L  M  D  R  L  P  G  K  K  A  Q  I

ACGGAGGCCATTGATGGCGTACGTGAACGCCTGCGTGGAGCTGCTGAAGCGACCTCTGCGCAGCTGGCCACAGCC
 T  E  A  I  D  G  V  R  E  R  L  R  G  A  A  E  A  T  S  A  Q  L  A  T  A

GCCTACAATTAAGCGGCCGCACTCGAG
 A  Y  N  *  A  A  A  L  E
                NotI
```

References

1. Diener M, Kopka B, Pohl M, Jaeger KE, Krauss U. Fusion of a coiled-coil domain facilitates the high-level production of catalytically active enzyme inclusion bodies. Chemcatchem 2016; 8;142-152.
2. Bradford MM. A rapid and sensitive method for the quantitation of microgram quantities of protein utilizing the principle of protein-dye binding. Analytical Biochemistry 1976; 72;248-254.

3. Jäger VD, Lamm R, Kloss R, Kaganovitch E, Grünberger A, Pohl M, Büchs J, Jaeger K-E, Krauss U. A synthetic reaction cascade implemented by co-localization of two proteins within catalytically-active inclusion bodies. ACS Synthetic Biology 2018; [Epub ahead of print] doi: 10.1021/acssynbio.8b00274.
4. Kandiah E, Carriel D, Perard J, Malet H, Bacia M, Liu K, Chan SW, Houry WA, Ollagnier de Choudens S, Elsen S, Gutsche I. Structural insights into the *Escherichia coli* lysine decarboxylases and molecular determinants of interaction with the AAA+ ATPase RavA. Scientific Reports 2016; 6;24601.
5. Stetefeld J, Jenny M, Schulthess T, Landwehr R, Engel J, Kammerer RA. Crystal structure of a naturally occurring parallel right-handed coiled coil tetramer. Nature Structural Biology 2000; 7;772-776.
6. Airola MV, Watts KJ, Bilwes AM, Crane BR. Structure of concatenated HAMP domains provides a mechanism for signal transduction. Structure 2010; 18;436-448.
7. Conchillo-Sole O, de Groot NS, Aviles FX, Vendrell J, Daura X, Ventura S. AGGRESCAN: a server for the prediction and evaluation of "hot spots" of aggregation in polypeptides. BMC Bioinformatics 2007; 8;65.
8. Jacak R, Leaver-Fay A, Kuhlman B. Computational protein design with explicit consideration of surface hydrophobic patches. Proteins 2012; 80;825-838.
9. Kuhlman B, Baker D. Native protein sequences are close to optimal for their structures. Proceedings of the National Academy of Sciences 2000; 97;10383.
10. Rohl CA, Strauss CE, Misura KM, Baker D. Protein structure prediction using Rosetta. Methods Enzymol 2004; 383;66-93.
11. Diener M. Von gezielter Oligomerisierung zu katalytisch aktiven inclusion bodies – Eine alternative Strategie zur Stabilisierung und Immobilisierung von Biokatalysatoren. Heinrich-Heine University Düsseldorf, Institut für Molekulare Enzymtechnologie; 2014.
12. Kulig J, Simon RC, Rose CA, Husain SM, Hackh M, Ludeke S, Zeitler K, Kroutil W, Pohl M, Rother D. Stereoselective synthesis of bulky 1,2-diols with alcohol dehydrogenases. Catalysis Science & Technology 2012; 2;1580-1589.
13. Weckbecker A, Hummel W. Cloning, expression, and characterization of an (*R*)-specific alcohol dehydrogenase from *Lactobacillus kefir*. Biocatalysis and Biotransformation 2006; 24;380-389.
14. Janzen E, Muller M, Kolter-Jung D, Kneen MM, McLeish MJ, Pohl M. Characterization of benzaldehyde lyase from *Pseudomonas fluorescens*: A versatile enzyme for asymmetric C-C bond formation. Bioorganic Chemistry 2006; 34;345-361.
15. Kloss R, Karmainski T, Jäger VD, Hahn D, Grünberger A, Baumgart M, Krauss U, Jaeger K-E, Wiechert W, Pohl M. Tailor-made catalytically active inclusion bodies for different applications in biocatalysis. Catalysis Science & Technology, 2018, 8(22), p. 5816.
16. Lingen B, Kolter-Jung D, Dünkelmann P, Feldmann R, Grötzinger J, Pohl M, Müller M. Alteration of the substrate specificity of benzoylformate decarboxylase from *Pseudomonas putida* by directed evolution. ChemBioChem 2003; 4;721-726.
17. Kloss R, Limberg MH, Mackfeld U, Hahn D, Grünberger A, Jäger VD, Krauss U, Oldiges M, Pohl M. Catalytically active inclusion bodies of L-lysine decarboxylase from *E. coli* for 1,5-diaminopentane production. In Scientific reports, vol. 8. pp. 58562018; 5856.
18. Studier FW, Moffatt BA. Use of bacteriophage T7 RNA polymerase to direct selective high-level expression of cloned genes. J Mol Biol 1986; 189;113-130.
19. Gasteiger E, Hoogland C, Gattiker A, Duvaud Se, Wilkins MR, Appel RD, Bairoch A. Protein identification and analysis tools on the ExPASy server. In The Proteomics Protocols Handbook. Edited by Walker JM. Totowa, NJ: Humana Press; 2005: 571-607.
20. Shaner NC, Steinbach PA, Tsien RY. A guide to choosing fluorescent proteins. Nature Methods 2005; 2;905-909.
21. Miyawaki A, Griesbeck O, Heim R, Tsien RY. Dynamic and quantitative Ca^{2+} measurements using improved cameleons. Proceedings of the National Academy of Sciences of the United States of America 1999; 96;2135-2140.

2.2 Tailor-made catalytically active inclusion bodies for different applications in biocatalysis

R. Kloss, T. Karmainski, V. D. Jäger, D. Hahn, A. Grünberger, M. Baumgart, U. Krauss, K.-E. Jaeger, W. Wiechert and M. Pohl*

* Corresponding author

published in Catalysis Science & Technology, 2018, 8(22), p. 5816

https://pubs.rsc.org/en/content/articlelanding/2018/cy/c8cy01891j#!divAbstract

Context:

Two different *Pf*BAL-CatIBs were tested for biocatalytic application in batch and continuous reaction mode in a mono- and biphasic solvent system in comparison to the soluble enzyme. We could show that the aggregation-inducing domain had a pronounced effect on the stability and activity of the *Pf*BAL-CatIBs in the different reaction systems. Thereby both kinds of *Pf*BAL CatIBs were shown to be a suitable alternative for the soluble enzyme. TDoT-*Pf*BAL-CatIBs worked best in a monophasic aqueous-organic solvent system, whereas 3HAMP-*Pf*BAL-CatIBs gave best results in a biphasic reaction system.

Contributions:

V. D. Jäger, R. Kloss and T. Karmainski performed the construction of plasmids. V. D. Jäger, T. Karmainski, D. Hahn and R. Kloss performed production, purification, and characterization of the CatIBs. M. Baumgart did the MALDI-TOF analysis with the assistance of R. Kloss and V. D. Jäger. The obtained data were analyzed with the assistance of R. Kloss. A. Grünberger performed live-cell imaging with the assistance of V. D. Jäger and R. Kloss. R. Kloss and M. Pohl wrote the manuscript with input from A. Grünberger and M. Baumgart. M. Pohl, U. Krauss, K.-E. Jaeger, and W. Wiechert planned the CatIB project and corrected the manuscript.

Catalysis Science & Technology

PAPER

View Article Online
View Journal

Check for updates

Cite this: DOI: 10.1039/c8cy01891j

Tailor-made catalytically active inclusion bodies for different applications in biocatalysis†

Ramona Kloss, [ad] Tobias Karmainski, [a] Vera D. Jäger, [bd] Doris Hahn,[a] Alexander Grünberger, [ac] Meike Baumgart, [a] Ulrich Krauss, [bd] Karl-Erich Jaeger, [abd] Wolfgang Wiechert[ad] and Martina Pohl *[ad]

Received 10th September 2018,
Accepted 12th October 2018

DOI: 10.1039/c8cy01891j

rsc.li/catalysis

We have recently demonstrated that fusions of different target enzymes to the coiled-coil domain TDoT induced the formation of catalytically active inclusion bodies (CatIBs) in *E. coli* (doi:10.1016/j.jbiotec.2017.04.033). Here we show that the CatIB properties can be tailored to the requirements of different reaction systems using two different coiled-coil domains as fusion tags: TDoT and 3HAMP. As an example the benzaldehyde lyase from *Pseudomonas fluorescens* (*Pf*BAL) was chosen, which catalyzes the formation of 2-hydroxy ketones and benzoins from aromatic donor aldehydes and aromatic or aliphatic acceptor aldehydes. Using these fusion tags two different kinds of *Pf*BAL-CatIBs were successfully produced that differ in morphology, solubility during washing steps, initial rate activity, protein and lipid content. TDoT-*Pf*BAL and 3HAMP-*Pf*BAL CatIBs were studied relative to the soluble enzyme concerning their application in biocatalysis in continuous reaction mode and in batch using a mono- and biphasic solvent system. Both CatIBs outperformed the soluble enzyme with respect to stability under reaction conditions. In the buffer/DMSO system used for the continuous synthesis of (*R*)-2-hydroxy-1-phenylpropanone, TDoT-*Pf*BAL was superior to the soluble enzyme. Besides, 3HAMP-*Pf*BAL was more suitable in a biphasic reaction system for the synthesis of (*R*)-benzoins and revealed an up to 3-fold higher activity compared to the soluble enzyme.

1. Introduction

For the realization of cost-efficient and eco-efficient biocatalytic processes, high space–time yields and productivities are needed.[1,2a] To achieve this goal, biocatalysts should be easy to produce, should show a high stability specifically under technical reaction conditions and should be easily separable from the reaction mixture for recycling. All these properties can in principle be obtained with appropriate immobilization methods. Although immobilization goes often at the expense of activity, the gain in stability can compensate for this loss.

In this study, we have used a novel method for biocatalyst immobilization. We compare the properties of two different catalytically-active inclusion bodies (CatIBs) of benzaldehyde lyase from *Pseudomonas fluorescens* (*Pf*BAL). CatIBs represent a recently developed, cheap and simple alternative to generally applied immobilization methods, which comprise often time-consuming, laborious and expensive purification and immobilization steps.[2,3] CatIBs are a cell-free and carrier-free immobilizate which can easily be produced as insoluble protein fraction from *E. coli* cells,[4–7] and can directly be used as a cheap enzyme preparation for biotransformations, which is essential to operate biocatalytic steps economically.[2a,8] In the past, inclusion bodies were either regarded as waste or were produced prior to obtain the native target protein upon denaturation and refolding. However, recent studies showed that enzymes can retain some activity as inclusion bodies. Despite their accidental production,[7,9] active inclusion bodies can be produced by fusion of aggregation-inducing tags, such as cellulose binding domains,[10] natural and artificial peptides likes small surfactant-like peptides,[11] amphipathic[12a,b] and hydrophobic self-assembling peptides,[12c] and amyloidogenic peptides like Aβ.[13a] Further options are the fusion of aggregation-prone proteins and protein domains, amongst others, the viral capsid protein VP1 of the foot-and-mouth disease virus[13a] and a pyruvate oxidase.[13b] A detailed overview about the state of the art was recently published.[4]

[a] Forschungszentrum Jülich GmbH, IBG-1: Biotechnology, 52425 Jülich, Germany. E-mail: ma.pohl@fz-juelich.de
[b] Institut für Molekulare Enzymtechnologie, Heinrich-Heine-Universität Düsseldorf, Forschungszentrum Jülich, 52425 Jülich, Germany
[c] Multiscale Bioengineering, Bielefeld University, Universitätsstraße 25, 33615 Bielefeld, Germany
[d] Bioeconomy Science Center (BioSC), c/o, Forschungszentrum Jülich, 52425 Jülich, Germany

† Electronic supplementary information (ESI) available: Additional results, experimental and sequences. See DOI: 10.1039/c8cy01891j

*Pf*BAL represents a promising enzyme for industrial application, since it catalyses the strictly (*R*)-selectively C–C-bond formation between an aromatic donor aldehyde and an aromatic or aliphatic acceptor aldehyde.[14–18] Additionally, *Pf*BAL catalyses also the reverse reaction, *i.e.* the cleavage of α-hydroxy ketones.[18–20] A well-studied reaction is the carboligation of benzaldehyde and acetaldehyde to (*R*)-2-hydroxy-1-phenylpropanone ((*R*)-HPP). Further biocatalytic reduction using appropriate alcohol dehydrogenases yields the important pharmaceutical building block (1*R*,2*R*)-1-phenylpropane-1,2-diol (PPD), *e.g.* for the calcium channel blocker diltiazem.[21] During this reaction in batch mode, (*R*)-benzoin occurs as an intermediate, especially at the beginning due to differences in reaction speed for the formation of (*R*)-benzoin and (*R*)-HPP, respectively.[22] In the presence of excess acetaldehyde, the reaction can be shifted to the preferred formation of (*R*)-HPP.[14,22–25]

The application of *Pf*BAL was broadly studied using aqueous,[18,26] monophasic[18,22–25,27–31] or biphasic[32–37] aqueous-organic solvents as well as micro-aqueous reaction systems[38,39] using the purified enzyme,[14,18,20,22,27,31,33,37] as whole cell biocatalyst,[36,38,39] and immobilized on or in different carriers.[23,24,29,30,32,34,35] Preferred water-miscible cosolvents for the enzyme are dimethyl sulfoxide (DMSO, 20–30 vol%),[18,20,22–25,27–30] methyl-*tert*-butyl ether (MTBE, 5 vol%),[26,28,33] and 2-methyltetrahydrofuran (5 vol%).[31] Different reactors were tested with *Pf*BAL. Besides batch[18,20,22,24,27–31,33,35,37] and fed-batch systems,[33,36,38,39] continuous reaction systems such as plug-flow reactors[23,34] and enzyme-membrane reactors were applied.[22,28] With whole cells also biphasic micro-aqueous as well as monophasic micro-aqueous reaction systems were successfully tested, which enable a significantly higher substrate concentration and thus a higher productivity.[36,38,39] Besides whole cells, which constitute the simplest way of immobilization, *Pf*BAL was entrapped in cryogel beads.[34,35] Further, immobilizations *via* the His-tag on a superparamagnetic solid support[29] as well as on the respective Sepharose® material were described.[23] Covalent binding was realized on chelate-epoxy modified magnetic nanoparticles[30] as well as on Sepharose® beads *via* the HaloTag® technology directly from crude cell extracts.[24] These carrier-based immobilization methods enabled efficient retention and recycling of the enzyme. However, there is only limited data available concerning potential stabilizing effects resulting from immobilization of this enzyme. This aspect is specifically relevant for *Pf*BAL, because the enzyme is known to be inactivated by aldehydes, which is only partly reversible.[40] Thus, soluble *Pf*BAL can usually not be reused. Using the HaloTag® technology, we could recently demonstrate that repetitive batch reactions were possible over seven cycles, most probably because the immobilizate was intensively washed in between the reaction steps.[24]

Here, we study the application of two different *Pf*BAL-CatIB constructs in batch and continuous reaction mode in a mono- and biphasic solvent system relative to the soluble enzyme using different carboligation reactions. CatIBs were obtained by fusion with two different coiled-coil domains. We previously evaluated the targeted production of CatIBs by fusion of the tetramerization domain of the cell-surface protein tetrabrachion (known as TDoT) from *Staphylothermus marinus* to different target enzymes as well as fluorescent proteins which resulted in the targeted formation of functional inclusion bodies.[4,41,42,55] Besides the TDoT-domain, the 3HAMP-domain was evaluated as an aggregation-inducing element. In its native context, the domain 3HAMP (Histidine kinases, Adenylyl cyclases, Methyl-accepting chemotaxis proteins (MCPs), and Phosphatases) is part of the soluble oxygen sensor Aer2 of *Pseudomonas aeruginosa*, which is an element of a prokaryotic signalling module.[43] Our results show that the kind of the fusion tag has a strong effect not only on the morphology but also on the stability and the activity of the resulting CatIBs. Depending on the reaction system, both evaluated *Pf*BAL-CatIBs exhibited properties superior to those of the soluble enzyme.

2. Results and discussion

2.1 Characteristics of two different kinds of CatIBs

Two different *Pf*BAL-CatIBs were generated by a genetic fusion of the genes encoding *Pf*BAL and the two different coiled-coil domains, 3HAMP and TDoT, yielding the respective N-terminal fusions of the coiled-coil domain to the *Pf*BAL.[41] The formation of inclusion bodies in *E. coli* cells was imaged using an inverted epifluorescence microscope.[44,45] As demonstrated in Fig. 1, the live cell images showed that the coiled-coil fusions determined the morphology of the inclusion bodies. While TDoT-*Pf*BAL forms typically dense and compact particles in *E. coli*,[46] 3HAMP-*Pf*BAL yields rather diffuse particles located at the cell poles, which are less clearly visible in unmodified phase-contrast images (Fig. 1B). The corresponding particles can however be clearly detected after local image equalization (see ESI,† Fig. S1). To distinguish between the different kinds of CatIBs, we called the TDoT-*Pf*BAL "compact CatIBs" and the 3HAMP-*Pf*BAL "diffuse CatIBs". To the best of our knowledge, such

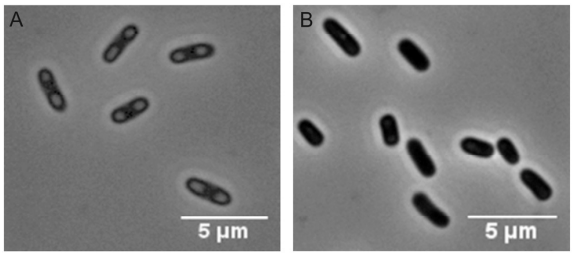

Fig. 1 Phase contrast microscopic images of *E. coli* BL21(DE3) cells containing *Pf*BAL-CatIBs. (A) TDoT-*Pf*BAL, (B) 3HAMP-*Pf*BAL. While TDoT-*Pf*BAL forms dense and compact particles in *E. coli*, 3HAMP-*Pf*BAL yields rather diffuse particles. Images were recorded by an inverted epifluorescence microscope in phase-contrast mode (see sect. 4.5). For a better visualization the pictures were modified by image equalization, as shown in the ESI,† Fig. S1.

morphology distinctions of inclusion bodies have not been described so far.

For a detailed comparative characterization, both CatIB types were extracted from the cells by cell disruption, followed by centrifugation and two washing steps using a previously developed standardised protocol.[41,42] Sodium dodecyl sulfate-polyacrylamide gel electrophoresis (SDS-PAGE) analysis of the purification steps demonstrated that TDoT-*Pf*BAL was only present in the insoluble cell fraction and was barely dissolved during the washing steps of the pellet, as expected (Fig. 2).[41]

In contrast, the diffuse 3HAMP-*Pf*BAL CatIBs are partially soluble, which results in progressive disintegration of the pellet during washing. As a consequence, the yield of lyophilised CatIBs obtained from 1 g of wet *E. coli* cells is about 4-fold higher for TDoT-*Pf*BAL (72 ± 8 mg) compared to 3HAMP-*Pf*BAL (18 ± 17 mg), whereas the yield of 3HAMP-*Pf*BAL could not be reproduced so well resulting in a high standard deviation (Table 1). Both CatIB variants differ enzymatic activity, protein content, and lipid content. TDoT-*Pf*BAL revealed a high protein content of 72 ± 5%, which is typical for inclusion bodies.[41,42] In contrast, 3HAMP-*Pf*BAL CatIBs contained only 34 ± 5% protein (Table 1). Inclusion bodies can contain phospholipids, membrane proteins and, depending on the purification procedure, also nucleic acids besides the target proteins.[47] A similar pattern of contaminating bands was observed for different TDoT-fusion-based CatIBs using SDS-PAGE.[41,42] Here, these accompanying proteins for TDoT-*Pf*BAL- (band #1) and 3HAMP-*Pf*BAL-CatIBs (band #2) were analysed by MALDI-TOF analysis. We identified the prominent additional bands as chaperones (IbpA and IbpB[48–50] at 15 kDa, band #4), membrane proteins (OmpA and OmpF[51] at 40 kDa, band #3), and murein lipoprotein (8 kDa, band #3). Remarkably, for 3HAMP-*Pf*BAL-CatIBs the band corresponding to OmpA and OmpF at about 40 kDa is as prominent as the target enzyme (Fig. 2). However, no proteins with reported enzymatic activity were identified, which could interfere with the reaction.

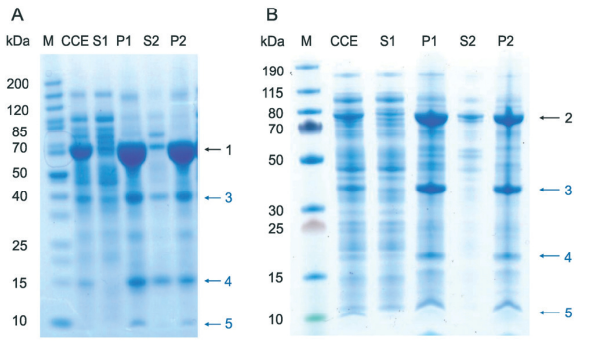

Fig. 2 SDS-PAGE analysis of the *Pf*BAL-CatIB preparations: TDoT-*Pf*BAL (A, band # 1), 3HAMP-*Pf*BAL (B, band # 2) (calculated molecular weight: 66.5 kDa and 79.3 kDa); CCE = crude cell extract, which was centrifuged for supernatant (S1) and pellet (P1) separation. P1 was washed once with MilliQ water by resuspension and subsequent centrifugation, which results in S2 and P2; the protein concentration in solution was measured using the Bradford assay (sect. 4.4). For SDS-PAGE (sect. 4.4) samples were diluted with water to obtain a protein concentration of 1 mg ml^{-1} (CCE, S1, P1, P2) except for S2, P2 of 3HAMP-*Pf*BAL (0.3 mg ml^{-1}) and S2 of TDoT-*Pf*BAL (0.4 mg ml^{-1}). By MALDI-TOF analysis the following accompanying proteins were identified: membrane proteins OmpA and OmpF (band # 3) at 40 kDa, chaperones IbpA and IbpB at 15 kDa (band # 4) and murein lipoprotein at 8 kDa (band # 5). M = marker (PageRuler Plus Unstained (A) or Prestained (B) Protein *ladder*, ThermoFisher Scientific).

Due to the co-purification of cellular proteins in the CatIB preparation, it was expected that membrane lipids such as phospholipids could also be associated with the CatIBs.[47] Therefore, the lipid content was determined gravimetrically upon extraction with methanol and chloroform (see sect. 4.6) and showed about double the amount for 3HAMP-*Pf*BAL (30%) compared to TDoT-*Pf*BAL-CatIBs (16%) based on the dry weight (Table 1). Finally, comparison of the initial rate activities revealed a 17-fold higher turnover number (k_{cat}) for 3HAMP-*Pf*BAL-CatIBs of 13.9 s^{-1} compared to 0.8 s^{-1} for TDoT-*Pf*BAL-CatIBs (Table 1). This is in line with the diffuse nature of the 3HAMP-*Pf*BAL-CatIBs. The less dense packing of the CatIB particles most probably results in smaller particles with a larger surface which enables better access of the substrate molecules and thus higher activity.

The protein yield obtained from 1 g of wet *E. coli* cells was comparable for the soluble *Pf*BAL, which was purified using metal ion affinity chromatography,[52,53] and 3HAMP-*Pf*BAL but four-times higher for TDoT-*Pf*BAL. Compared to the highly active soluble *Pf*BAL, TDoT-*Pf*BAL CatIBs reached approx. 1% and 3HAMP-*Pf*BAL-CatIBs 18% of its activity (k_{cat}) (Table 1). Generally, a reduction of activity relative to the soluble enzyme has been reported for several immobilised enzymes[54] due to lower flexibility, steric hindrance and diffusion limitations caused by the aggregation of the enzyme molecules.

In order to study the properties of the *Pf*BAL-CatIB variants under reaction conditions, they were analysed in buffer, in the absence and presence of DMSO as a cosolvent using an enzyme membrane reactor as well as in batch using a biphasic aqueous-organic solvent system.

2.2 Reactivity of *Pf*BAL-CatIBs and soluble enzyme in buffer in the absence and presence of DMSO

Stability in buffer. The stabilities of the two *Pf*BAL-CatIB variants were first measured in buffer relative to the soluble enzyme. For this purpose, the same protein concentration of each enzyme variant was incubated in triethanol amine (TEA)-buffer (50 mM, pH 7.5, supplemented with ThDP and magnesium sulfate) in polypropylene reaction tubes at 30 °C and 1000 rpm (see ESI,† sect. 2.11). These conditions resemble those chosen for subsequent biotransformations but did not contain any substrate or product. Residual activities were measured over 72 hours (see sect. 4.7). Half-lives decreased in the order TDoT-*Pf*BAL (57 h) > soluble *Pf*BAL (36 h) > 3HAMP-*Pf*BAL (23 h), which were estimated based on the course of the deactivation curve. This initial experiments showed different stabilities of the three *Pf*BAL variants

Table 1 Characteristics of TDoT-*Pf*BAL and 3HAMP-*Pf*BAL-CatIBs compared to the soluble *Pf*BAL. The yield indicates the protein content in the lyophilisate obtained from 1 g wet cells after cell disruption and purification by washing and centrifugation steps (for CatIBs) or metal ion affinity chromatography (for soluble *Pf*BAL) (sect. 4.3). The protein content was determined by measuring the absorption at 280 nm after solubilization with guanidine hydrochloride (sect. 4.4). This value was calculated based on the weight of the dry CatIB lyophilisate (1–2 mg ml^{-1}). The lipid content was measured as described in sect. 4.6. The activity (k_{cat}) was determined for the carboligation of 3,5-dimethoxybenzaldehyde (DMBA) to (*R*)-(3,3′,5,5′)-tetramethoxybenzoin (TMBZ) (sect. 4.7). The employed protein concentration to determine k_{cat} was 0.12–0.30 mg ml^{-1} for TDoT-*Pf*BAL, 0.017–0.044 mg ml^{-1} for 3HAMP-*Pf*BAL, and 3–6 μg ml^{-1} for soluble *Pf*BAL. Errors correspond to the standard deviation of the mean obtained from a biological triplicate, except for lipid content and the data of soluble *Pf*BAL (n = 1, 3 technical replicates)

Variant	Yield [mg protein per g wet cells]	Protein content of the lyophilisate [%]	Lipid content [%]	k_{cat} [s^{-1}]	Residual activity^b [%]
Soluble *Pf*BAL	20 ± 14	74.9 ± 0.3^a	—	76.7 ± 2.3^a	100^a
TDoT-*Pf*BAL	72 ± 8	72 ± 5^a	16.4 ± 1.0	0.8 ± 0.1^a	1.0^a
3HAMP-*Pf*BAL	18 ± 17	34 ± 5	30.1 ± 4.7	13.9 ± 2.9	18.1

^{a} Data taken from ref. 55. ^{b} Compared to soluble enzyme.

already upon incubation in buffer, with TDoT-*Pf*BAL showing the highest stability.

Stability under continuous reaction conditions in buffer and buffer/DMSO. Subsequently, the stability under reaction conditions in the absence of DMSO was studied using a continuous enzyme membrane reactor (EMR).[56] The mixed carboligation of benzaldehyde and acetaldehyde towards (*R*)-2-hydroxy-1-phenylpropan-1-one ((*R*)-HPP) was chosen as a test reaction. The EMR was equipped with a membrane (cut-off 10 kDa) to retain the soluble enzyme with a size of 240 kDa. The results in Fig. 3A show that the presence of substrates and products in the absence of DMSO affected the enzyme stability. The highest stability was found for TDoT-*Pf*BAL (half-life 49 h), followed by 3HAMP-*Pf*BAL-CatIBs (half-life 10 h) and the soluble *Pf*BAL (half-life 7 h) (see ESI,† Table S4). TDoT-*Pf*BAL showed a 2–5-fold higher stability than 3HAMP-*Pf*BAL-CatIBs under these reaction conditions in the absence of DMSO.

The addition of DMSO (20–30 vol%) to the aqueous buffer is not only beneficial for the solubility of aromatic aldehydes and benzoins, it can also positively affect the stability of the soluble enzyme.[22,25] Therefore, the effect of 30 vol% DMSO on all *Pf*BAL-variants was tested under continuous reaction conditions. As demonstrated in Fig. 3B the stability of all variants was significantly increased in the presence of DMSO, with a 5.9-fold increase in half-life for 3HAMP-*Pf*BAL-CatIBs (59 h), a 2.7-fold increase for TDoT-*Pf*BAL (131 h), and even a 13-fold increase for the soluble *Pf*BAL (92 h) (see Fig. 3B and ESI,† Table S4).

Deactivation kinetics. In buffer and without substrates and products the soluble *Pf*BAL and the *Pf*BAL-CatIBs showed an unusual deactivation behaviour, which could not be described by a typical first-order deactivation (see ESI,† Fig. S2). Under continuous reaction conditions without DMSO, the course of deactivation of TDoT-*Pf*BAL follows a bi-phasic deactivation mechanism, with a slower initial part followed by a

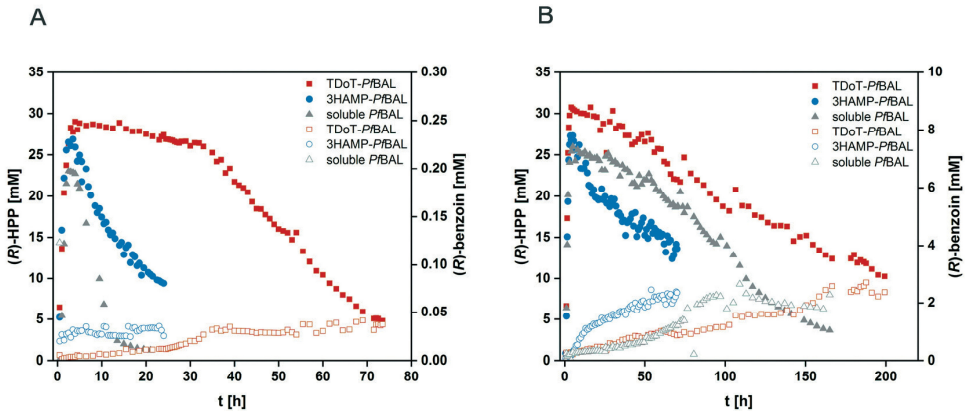

Fig. 3 Carboligation of benzaldehyde and acetaldehyde to (*R*)-HPP and (*R*)-benzoin by *Pf*BAL, TDoT-*Pf*BAL-, and 3HAMP-*Pf*BAL-CatIBs, respectively, in a continuous EMR in the absence (A) and presence (B) of 30 vol% DMSO. Filled symbols refer to (*R*)-HPP and empty symbols to the concentration of (*R*)-benzoin, which is formed as a by-product. Half-life was deduced from the point in time where 50% conversion to (*R*)-HPP (approx. 15 mM) was reached. Reaction conditions: 30 mM benzaldehyde, 90 mM acetaldehyde, TEA-buffer (50 mM, pH 7.5, 2.5 mM $MgSO_4$, 0.5 mM ThDP), 30 vol% DMSO (B); 28 U ml^{-1} protein concentrations of the enzymes: TDoT-*Pf*BAL (A: 50 mg ml^{-1}; B: 56.8 mg ml^{-1}), 3HAMP-*Pf*BAL (A: 3.8 mg ml^{-1}; B: 5.9 mg ml^{-1}), *Pf*BAL (0.94 mg ml^{-1}), 300 rpm, 30 °C, $V_{reactor}$ = 3 ml, residence time: 30 min, flow: 0.1 ml min^{-1}, PEEK (polyether ether ketone) – enzyme membrane reactor (EMR) with regenerated cellulose membrane (YM10 Milipore, 10 kDa cut-off), n = 1.

faster second part. The reason for the biphasic inactivation process is currently unclear. However, as the deactivation behaviour of the TDoT-*Pf*BAL-CatIBs in batch in the absence of substrates and products is similar (see ESI,† Fig. S2) to the deactivation in the EMR in the presence of these reaction components, effects caused by the reactor material, the membrane, substrates and products, as well as enzyme leakage from the EMR can be ruled out. The latter was additionally tested by SDS-PAGE analysis of the reactor efflux (data not shown). Besides, in the presence of 30 vol% DMSO the conversion curves of all three variants show the same form (Fig. 3B).

Accumulation of the reaction intermediate (*R*)-benzoin. In both reaction systems the concentration of (*R*)-benzoin in the efflux increased with progressive inactivation of the *Pf*BAL variants. Due to the presence of DMSO in the reaction buffer, the concentration of dissolved (*R*)-benzoin was higher compared to the experiments in the absence of DMSO (Fig. 3). In all cases, (*R*)-benzoin precipitated in the reaction chamber, which was observed when the reactor was opened at the end of the experiment and quantified in some cases (see ESI,† Table S4).

Absorption phenomena. The continuous reactions in the EMR revealed a maximum conversion of about 80% in the absence of DMSO and 90–95% with 30 vol% DMSO (Fig. 3). The reason, why full conversion could not be achieved was partially deduced to the absorption of benzaldehyde and (*R*)-HPP by the reactor material (polyether ether ketone = PEEK) (see ESI,† Fig. S3) and by the polypropylene (PP) reaction tubes (see ESI,† sect. 3.3.2 and Table S5), which were used for HPLC sample preparation. Furthermore, evaporation of benzaldehyde occurred from the open glass test tubes in the HPLC sampling device over longer storage time (see ESI,† Fig. S4). The evaporation of benzaldehyde and absorption of benzaldehyde and (*R*)-HPP resulted in an apparent lower conversion. Since the PEEK-reactor gave much better results compared to a stainless-steel reactor with respect to enzyme stability (data not shown), only the PP reaction tubes were exchanged by glass vials in the following experiments to minimize this error.

pH-effect. Besides DMSO as a cosolvent, the stability and activity of soluble *Pf*BAL is influenced by the pH of the aqueous reaction system. Based on earlier studies, the stability optimum is at pH 7, whereas the activity optimum was found between pH 8.5–9.5 in similar reaction systems.[22,25,27] However, these studies were not performed in an EMR and were carried out in the absence of substrates and products. To study the influence of the pH on the *Pf*BAL-CatIBs and the soluble enzyme under reaction conditions, respective experiments were additionally performed in the EMR at pH 9 as an option to increase the activity relative to the data obtained at pH 7.5 (Fig. 3). For this purpose, all parameters were kept constant and the pH of the TEA-buffer was adjusted after addition of DMSO and the aldehyde substrates. As demonstrated in Fig. S5 (ESI†), the stability decreased in all cases by a factor of 5 to 43 (compare ESI,† Table S4). Interestingly, at

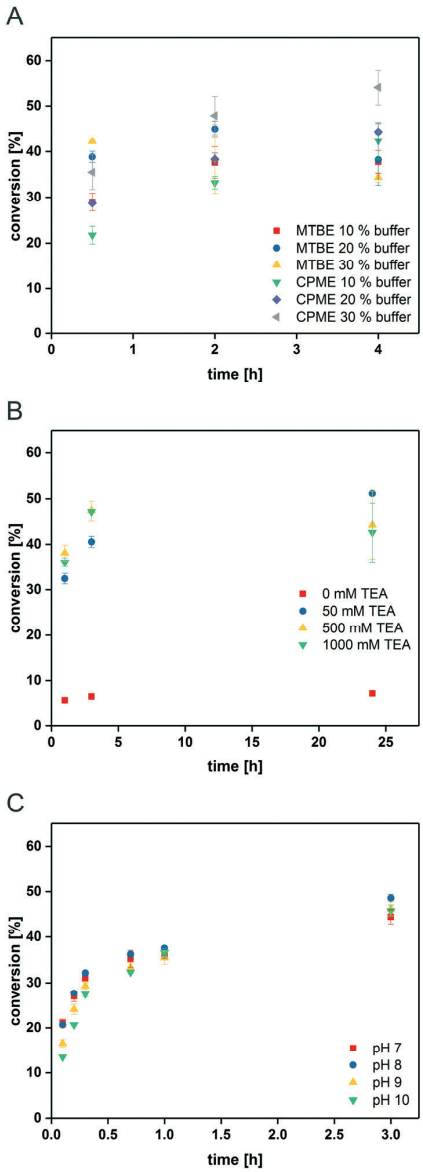

Fig. 4 Optimisation of (A) the buffer content, (B) the buffer salt concentration, and (C) the pH in an aqueous-organic two-phase system for the carboligation of DMBA to TMBZ, catalysed by 3HAMP-*Pf*BAL-CatIBs. (A) Reaction solutions contained a different buffer volume (10–30 vol% TEA-buffer, 1 M, pH 8, 2.5 mM $MgSO_4$, 0.1 mM ThDP) in CPME or MTBE, respectively, and 50 mM DMBA as the substrate. (B) Reaction solutions contained different buffer salt concentrations and were performed in CPME with 30 vol% TEA-buffer in different concentrations (0 mM, 50 mM, 500 mM or 1 M, pH 8, 2.5 mM $MgSO_4$, 0.1 mM ThDP) and 70 mM DMBA. (C) Reactions were performed in CPME with 30 vol% TEA-buffer with varying pH (50 mM, pH 7, 8, 9, or 10, 2.5 mM $MgSO_4$, 0.1 mM ThDP) and 85 mM DMBA as a substrate. All reactions were conducted with the following parameters: 6 U ml^{-1} 3HAMP-*Pf*BAL (1.1 mg ml^{-1} protein concentration) in 2 ml glass vials at 30 °C, 1400 rpm, V = 1 ml, in a thermomixer, n = 2. For experimental details see sect. 4.9.

pH 9 the deactivation curves for all variants show a typical first order exponential decay.

The results demonstrated the very different impact of the reaction conditions on the *Pf*BAL-variants. Whereas the addition of 30 vol% DMSO increased the stability of all variants in a similar manner (Fig. 3B), the pH change altered the stabilities unpredictably. At pH 9, 3HAMP-*Pf*BAL showed a similar half-life to the soluble enzyme and TDoT-*Pf*BAL, which is most stable at pH 7.5, showed the lowest stability (Fig. S5, Table S4 in ESI†).

In summary, TDoT-*Pf*BAL-CatIBs showed the best performance in 30 vol% DMSO in TEA-buffer at pH 7.5 with a half-life of 131 h, which presents a clearly increased stability compared to the soluble enzyme (7 h).

2.3 3HAMP-*Pf*BAL-CatIBs can be used in a biphasic reaction system

Carboligations of aldehydes, which are less soluble than benzaldehyde and acetaldehyde in an aqueous reaction system, were carried out in a biphasic aqueous-organic system with more than 50 vol% organic solvent. As a model reaction, the carboligation of 3,5-dimethoxybenzaldehyde (DMBA) to (*R*)-(3,3′,5,5′)-tetramethoxy benzoin (TMBZ) was optimised regarding solvent, buffer content, buffer concentration, and pH. Preliminary studies revealed CPME (cyclopentyl methyl ether) and MTBE (methyl *tert*-butyl ether) as optimal organic solvents for the carboligation reaction with TDoT-*Pf*BAL-CatIBs (see ESI,† Fig. S6). Both solvents were first tested in the monophasic micro-aqueous mode. As the activity of the *Pf*BAL-CatIBs was too low under these conditions, the volume of the TEA-buffer (1 M, pH 8) was increased to 20 vol% (ESI,† Fig. S7). However, this study showed that TDoT-*Pf*BAL-CatIBs formed emulsions in the biphasic system upon shaking (ESI,† Fig. S8), which made the sample preparation and handling quite difficult. Since emulsion formation was less pronounced for 3HAMP-*Pf*BAL in MTBE resulting in a higher conversion of about 50% (Fig. 4A), these CatIBs were used for all subsequent experiments to optimise the reaction conditions.

A concentration of 3HAMP-*Pf*BAL corresponding to 6 U ml^{-1} was sufficient to increase the conversion of 50–85 mM DMBA up to 50%. In contrast to MTBE no emulsion formation was observed in CPME (ESI,† Fig. S9). Hence, this solvent was used in all subsequent experiments. Furthermore, CPME is regarded as a green solvent in contrast to MTBE.[57,58] The optimization experiments showed that 30 vol% of 50 mM TEA-buffer in CPME were optimal (Fig. 4A and B). Concerning the optimal pH range, 3HAMP-*Pf*BAL-CatIBs showed a very similar activity between pH 7–9 (Fig. 4C). However, in all cases the conversion did not exceed 50%, because the reaction equilibrium was reached (K_{eq} = 0.02 mM) (ESI,† Fig. S10 and Table S6). The higher substrate concentrations (50–85 mM DMBA), which could be applied in the biphasic system, yielded TMBZ concentrations much higher than K_M (5 mM)[40] which favours the *Pf*BAL-catalysed back reaction.

For the subsequent experiments 30 vol% buffer (50 mM TEA, pH 8) in CPME were chosen. Under these conditions, the carboligation reactions of DMBA to TMBZ (Fig. 5A) and of benzaldehyde to (*R*)-benzoin (Fig. 5B) were followed and compared using the soluble *Pf*BAL and the 3HAMP-*Pf*BAL-CatIBs, respectively. The formation of TMBZ catalysed by 3HAMP-*Pf*BAL is with 4.1 s^{-1} almost twice as fast as the formation of (*R*)-benzoin (2.6 s^{-1}). For the soluble *Pf*BAL, the formation of (*R*)-benzoin (2.0 s^{-1}) is slightly faster than the TMBZ formation (1.4 s^{-1}) (ESI,† Table S7). Thus, in the biphasic system the initial rate activity of 3HAMP-*Pf*BAL is up to 3-fold higher compared to the soluble enzyme. The latter

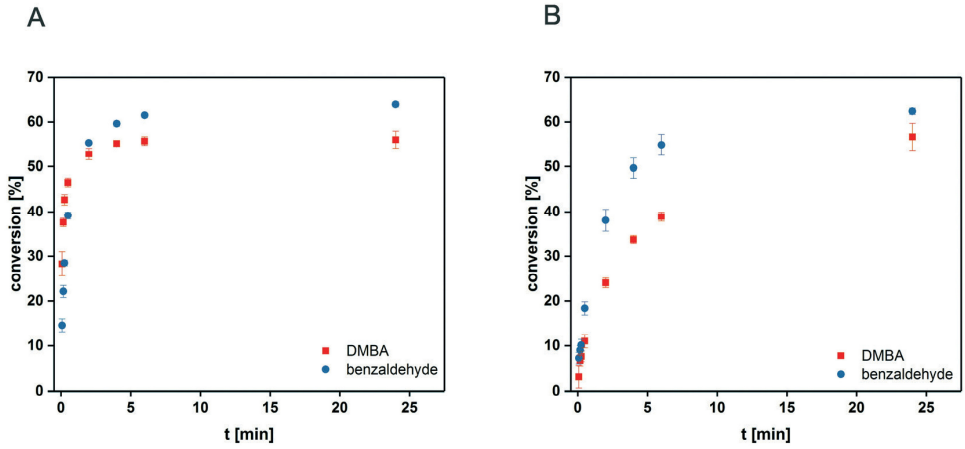

Fig. 5 Carboligation of benzaldehyde or DMBA (3,5-dimethoxybenzaldehyde) to the respective (*R*)-benzoin catalysed by (A) 3HAMP-*Pf*BAL or (B) soluble *Pf*BAL in the biphasic reaction system. Reaction conditions: 6 U ml^{-1} 3HAMP-*Pf*BAL (0.84 mg ml^{-1} protein concentration) and 2.6 U ml^{-1} *Pf*BAL (0.34 mg ml^{-1} protein concentration), 70 mM benzaldehyde or 70 mM DMBA in 1 ml reaction volume composed of 30 vol% TEA-buffer (50 mM, 2.5 mM $MgSO_4$, 0.5 mM ThDP, pH 7.5); 70 vol% CPME, 1400 rpm, 30 °C, *n* = 3. For experimental details see sect. 4.10.

will most probably be more affected by interphase inactivation as well as deactivation by the aldehyde substrates, which diminishes the stability of the soluble *Pf*BAL under these conditions.[32] Thus, 3HAMP-*Pf*BAL-CatIBs provide a viable alternative to the soluble *Pf*BAL in a biphasic system with CPME as an organic solvent.

3. Conclusions

In this study, we demonstrate that catalytically active inclusion bodies (CatIBs) represent an attractive immobilization strategy for benzaldehyde lyase from *Pseudomonas fluorescens* (*Pf*BAL). Two different kinds of CatIBs were produced by genetic fusion of *Pf*BAL with two different coiled-coil domains, namely TDoT and 3HAMP. The resulting TDoT-*Pf*BAL- and 3HAMP-*Pf*BAL-CatIBs differed in morphology, initial rate activity, protein and lipid content. TDoT-*Pf*BAL-CatIBs showed the typical characteristics of dense inclusion bodies, located at the cell poles in the *E. coli* production strain: a high protein (72%) and low lipid (16%) content, insolubility during the washing steps resulting in a high yield (72 mg dry TDoT-*Pf*BAL-CatIBs from 1 g wet cells), but a low initial rate activity (0.8 s^{-1}: approx. 1% residual activity compared to soluble *Pf*BAL). In contrast, 3HAMP-*Pf*BAL-CatIBs behaved completely different and formed diffuse particles in *E. coli*, which partially dissolved during the washing steps. This resulted in a lower yield (18 mg dry 3HAMP-*Pf*BAL-CatIBs from 1 g wet cells). Compared to the TDoT-CatIBs, the protein content was two-fold lower (34%) concomitant with two-fold higher lipid content (30%). Most probably as a result of the less dense packing of the particles, the activity of the 3HAMP-*Pf*BAL-CatIBs was 18-times higher than for TDoT-*Pf*BAL-CatIBs (18% relative to the soluble *Pf*BAL).

The application of both kinds of CatIBs was studied in a mono- and biphasic solvent system in comparison to the soluble *Pf*BAL in continuous reaction mode and in batch, respectively. Using the mono-phasic aqueous-organic solvent system, a continuous reaction mode for the carboligation of benzaldehyde and acetaldehyde towards (*R*)-HPP was realised using an EMR. This reactor enables constant reaction conditions for the enzyme and allows the direct determination of the inactivation processes from the conversion curve. For this reaction, TDoT-*Pf*BAL showed the highest stability in TEA-buffer at pH 7.5 with 30 vol% DMSO. The half-life was 1.4-fold higher compared to the soluble *Pf*BAL. Thus, the TDoT-*Pf*BAL represents a suitable alternative or the soluble enzyme in this monophasic continuous reaction mode.

In order to dissolve poorly water-soluble substrates, an aqueous-organic biphasic reaction system with CPME as an organic solvent was established. In this system, 3HAMP-*Pf*BAL CatIBs were more suitable than TDoT-*Pf*BAL CatIBs, since the latter formed emulsions, which impaired sample preparation and handling. The conversion of DMBA and benzaldehyde to the respective benzoins was followed under optimised reaction conditions (CPME with 30% TEA-buffer (pH 8, 50 mM)) and was compared to the soluble enzyme. 3HAMP-*Pf*BAL revealed a 3-fold higher activity than the soluble *Pf*BAL, indicating a higher stability in this biphasic reaction system, since high aldehyde concentrations as well as the interphase were reported to deactivate the soluble *Pf*BAL.[32] It can be concluded that 3HAMP-*Pf*BAL-CatIBs are a suitable alternative to the soluble enzyme in the biphasic reaction system.

In summary, we have demonstrated that different coiled-coil domains as aggregation-inducing tag significantly affect CatIB properties including enzymatic activity, stability, protein content, and emulsion-forming tendency. Our results thus suggest an experimental strategy to produce tailor-made CatIB immobilizates with activity under various reaction conditions prevailing in aqueous, micro aqueous, or biphasic systems.

4. Experimental

4.1 Materials

Chemicals were purchased from Sigma-Aldrich, Fluka, Roth, KMF, Biosolve, Alfa Aesar, AppliChem, and Merck. Enzymes for molecular biology were purchased from Thermo Scientific (Waltham, USA). Enantiopure (*R*)-2-hydroxy-1-phenylpropanone ((*R*)-HPP) for HPLC calibration was taken from a stock prepared as described elsewhere.[39]

4.2 Cloning

The fusion proteins TDoT-*Pf*BAL and 3HAMP-*Pf*BAL were constructed as recently described[41] by cloning of the *pf*bal gene into a modified pET28a vector already containing the 3HAMP- or TDoT-domain, so that the final vector consisted of the TDoT-domain or 3HAMP-domain, a linker containing a Factor Xa protease recognition site and 3xGGGS linker (L), and the *Pf*BAL enzyme (from N- to C-terminus). For a detailed description of the cloning strategy, the employed oligonucleotide primers, DNA- and protein sequences as well as used strains see ESI,† Table S1–S3 and section 2.1–2.10.

4.3 Enzyme production, cell disruption and protein purification

*Pf*BAL-CatIBs were produced in *E. coli* BL21(DE3). For cell disruption, cells were treated 3-times at 1000 bar using a high-pressure homogenizer (EmulsiFlex-C5, Avestin Europe GmbH, Mannheim, Germany). Subsequently, CatIBs were purified as recently described elsewhere.[41,42]

Soluble *Pf*BAL with a C-terminal hexahistidine tag, encoded on a pkk233_2 vector, was produced in *E. coli* SG 13009 according to protocol described elsewhere[18,40] in a 40 L Techfors fermenter (Infors AG, Swiss) at 30 °C in fed-batch mode.[59] The cell pellet was stored at −20 °C after harvesting and centrifugation. For purification, the cells were suspended in a 25% (w/v) of the equilibration buffer and disrupted on ice by sonication (UP200s, Hielscher Ultrasonics GmbH, Teltow, Germany) 10-times for 1 min at 70% amplitude and a cycle of 0.5, followed by a 1 min break. The soluble components containing the target enzyme were separated from the cell

debris by centrifugation for 30 min (18 000 × *g*, 4 °C). The enzyme was purified as described earlier by metal ion affinity chromatography[52,53] using a Ni-NTA-sepharose column (Qiagen, Hilden, Germany) with the following buffers: equilibration buffer (50 mM TEA, pH 7.5, 2.5 mM $MgSO_4$, 0.5 mM ThDP, 300 mM NaCl), washing buffer (50 mM TEA, pH 7.5, 50 mM imidazole, 300 mM NaCl), elution buffer (50 mM TEA, pH 7.5, 250 mm imidazole, 300 mM NaCl); and for the final desalting step using a Sephadex-G25 (GE Healthcare, Little Chalfont, United Kingdom) column: 10 mM TEA buffer, pH 7.5, 2.5 mM $MgSO_4$, 0.1 mM ThDP. The TEA-HCl solution was adjusted by sodium hydroxide solution.

4.4 SDS-PAGE, MALDI-TOF analysis and protein assay

SDS-PAGE analysis of the purification steps was performed using the NuPAGE® Kit (ThermoFisher Scientific, Waltham, USA) by the protocol described recently.[42] For the preparation of SDS-PAGE samples, the protein concentration in the soluble fraction was determined *via* the Bradford assay.[60]

The protein content of the lyophilised CatIBs and soluble *Pf*BAL was determined at 280 nm after solubilisation with guanidine hydrochloride using a recently described protocol.[42] The protein content was estimated using the molar extinction coefficient (Table 2) which was calculated based on the amino acid composition by the ProtParam Tool (http://web.expasy.org/protparam).[61]

MALDI-TOF mass spectrometry was performed to identify the accompanying protein bands apparent on SDS-PAGE gel which had been stained with colloidal Coomassie.[62] The protein bands were excised and digested in-gel with trypsin as described previously.[63] Samples were analysed by mass spectrometry measurement as described earlier.[64]

4.5 Phase contrast image acquisition

Images were obtained as described recently by inverted epi-fluorescence microscope in phase-contrast.[42,44,45]

4.6 Lipid content determination

The gravimetric lipid determination was adapted from Morschett *et al.*[65] About 100 mg lyophilised CatIBs were weighed into a 50 ml falcon tube, mixed with 14 ml chloroform and 7 ml methanol and incubated for 2 h at 60 °C and 750 rpm in a thermomixer (Thermomixer comfort, Eppendorf, Hamburg, Germany). The mixture was transferred to a 50 ml separating funnel and washed with 5.6 ml NaCl solution (0.73% w/v). The lower organic phase containing the lipids was collected and the aqueous phase was extracted with 14 ml chloroform. The organic phases were pooled, dried over $MgSO_4$ and concentrated by a rotating evaporator (Rotavapor R-100, Büchi Labortechnik GmbH, Essen, Germany). The remaining liquid was transferred to a dry, pre-weighted glass vessel and dried first under the hood and then under high vacuum (0.2 mbar) over 24 h. The remaining lipid amount was determined gravimetrically and the lipid content was calculated based on the initial weight. All measurements were performed in triplicate for one batch of the respective CatIBs.

Table 2 Extinction coefficient of soluble *Pf*BAL, TDoT-*Pf*BAL and 3HAMP-*Pf*BAL calculated with ExPASy ProtParam Tool (http://expasy.org/tools/protparam)[61]

Protein	Molar extinction coefficient [L mol^{-1} cm^{-1}]
Soluble *Pf*BAL	52 160
TDoT-*Pf*BAL	55 140
3HAMP-*Pf*BAL	63 620

4.7 Activity assay

In order to determine the initial rate activity of soluble *Pf*BAL and *Pf*BAL-CatIBs, the carboligation of 3,5-dimethoxy benzaldehyde (DMBA) to (*R*)-(3,3′,5,5′)-tetramethoxy benzoin (TMBZ) was measured up to a conversion of 10% by a discontinuous HPLC assay (see sect. 4.13). The reaction was performed in a polypropylene reaction tube (1.5 ml safe-lock tube, Eppendorf, Germany) in 1 ml reaction volume containing 80 vol% TEA-buffer (50 mM, pH 7.5, 2.5 mM $MgSO_4$, 0.1 mM ThDP) and 20 vol% DMSO with 10 mM DMBA, which was incubated at 30 °C prior to reaction. The reaction was started by addition of the enzyme (protein concentration of approx. 0.12–0.30 mg ml^{-1} for TDoT-*Pf*BAL, 0.017–0.044 mg ml^{-1} for 3HAMP-*Pf*BAL, and 3–6 μg ml^{-1} for soluble *Pf*BAL) and was performed for 5 min at 30 °C and 1000 rpm in a thermomixer (Thermomixer comfort, Eppendorf, Germany). Sampling was performed every minute by taking 20 μl samples from the tubes, which were diluted (1:10) with 180 μl methanol (incl. 4.7 mM toluol or 0.1 vol‰ 4-methoxy benzaldehyde (4-MBA) as internal standard) to stop the reaction and to prepare the sample for HPLC analysis (see sect. 4.13). Activity was calculated as turnover number k_{cat} [s^{-1}] referring to the amount of enzyme (in μmol, calculated based on the protein content, and referring to one subunit) which catalyses the formation of 1 μmol TMBZ per second from the respective DMBA concentration under the applied reaction conditions. Activity was determined for three technical replicates of the respective biological triplicates.

4.8 Continuous reaction using an EMR

The EMR was developed in-house to realise a continuous reaction mode under constant reaction conditions and membrane-assisted enzyme retention. The EMR consists of PEEK (polyether ether ketone) with a 3 ml reaction chamber and a Teflon plate with integrated magnetic stirrer bar that fits right there. The EMR was equipped with a membrane with 10 kDa cut-off (regenerated cellulose, diameter = 44.5 mm, YM10 Millipore Amicon, Germany). Initial loading of the EMR was performed either by pumping a solution of the soluble enzyme (28.3 U ml, in TEA-buffer, 50 mM, pH 7.5 or 9.0, 2.5 mM $MgSO_4$, 0.5 mM ThDP) into the reactor using an Asia Syringe Pump (Syrris, Royston, United Kingdom) or by placing the lyophilised CatIBs directly into the reaction

chamber, which was then filled with buffer solution. Subsequently, the buffer system including substrates (30 mM distilled benzaldehyde and 90 mM acetaldehyde) required for the respective experiment was pumped through the reactor at 30 °C and 300 rpm. Prior, 30 vol% DMSO had been added to the buffer according to the required reaction conditions and the pH-value of the reaction solution was controlled and adjusted if necessary after the addition of the aldehydes and DMSO. The flow was adjusted to 100 μl min^{-1} which corresponds to a residence time of 30 min. A fraction collector (Pharmacia LKB Frac-100, Amersham Biosciences, United Kingdom) was applied to collect samples of 3 ml or 6 ml volume in open glass test tubes of 9.5 ml volume (3 cm filling height) or of 15 ml volume (3.8 cm filling height), respectively. The 20 μl sample was 1:20 diluted with acetonitrile (incl. 0.822 mM 4-methoxybenzaldehyde (4-MBA) as internal standard) and analysed by HPLC (see sect. 4.13). Continuous reactions were performed in single measurements. Half-lives were taken from the curve at 50% conversion in each case.

4.9 Optimization of the reaction conditions in the biphasic reaction system

In order to optimise the reaction conditions in the biphasic reaction system in batch, the buffer content, the buffer concentration and the pH were optimized for the carboligation reaction 3,5-dimethoxybenzaldehyde (DMBA) catalysed by 3HAMP-*Pf*BAL-CatIBs. The buffer content was optimised between 1–30 vol% TEA-buffer (1 M, pH 8, 2.5 mM $MgSO_4$, 0.1 mM ThDP) added to either MTBE or CPME and contained 50 mM DMBA. The buffer concentration was optimised between 0 mM and 1 M TEA-buffer (0 mM, 50 mM, 500 mM or1 M, pH 8, 2.5 mM $MgSO_4$, 0.1 mM ThDP). 30 vol% buffer were added to 70 vol% CPME and contained 70 mM DMBA. The pH optimum was measured between pH 7–10 in TEA-buffer (50 mM, pH 7, 8, 9, or 10, 2.5 mM $MgSO_4$, 0.1 mM ThDP). 30 vol% buffer were added to 70 vol% CPME and contained 85 mM DMBA. In each case 6 U ml^{-1} 3HAMP-*Pf*BAL (1.1 mg ml^{-1} protein concentration) were suspended in buffer and then the organic solvent containing the substrate was added. The reaction was performed in a volume of 1 ml in 2 ml glass reaction tubes (G1 clear, CS-Chromatographie Service GmbH, Germany) at 30 °C und 1400 rpm in a thermomixer (Thermomixer comfort, Eppendorf, Germany). Samples (20 μl) were taken from the organic phase after different points in time and were diluted 1 : 10 in 180 μl 2-methyltetrahydrofuran, thoroughly mixed and centrifuged at 15 800 × *g* for 1 min. Subsequently, a 20 μl sample from the supernatant was 1 : 10 diluted in 180 μl *n*-heptane (incl. 4.3 mM acetophenone as internal standard), which was analysed by HPLC (see sect. 4.13). These reactions were performed in duplicate.

4.10 Carboligation of benzaldehyde and DMBA in a biphasic reaction system

The carboligation reaction of 70 mM DMBA or 70 mM benzaldehyde to the respective benzoins was catalysed by 2.6 U ml^{-1} soluble *Pf*BAL (0.15 mg ml^{-1} protein concentration) or 6 U ml^{-1} 3HAMP-*Pf*BAL (0.83 mg ml^{-1} protein concentration), respectively. Therefore, biphasic reaction systems were prepared by mixing 30 vol% TEA-buffer (50 mM, pH 8, 2.5 mM $MgSO_4$, 0.1 mM ThDP) with 70 vol% CPME. First the CatIBs were suspended in buffer and then the organic solvent containing the substrate was added. The reaction was performed in 2 ml glass reaction tubes (G1 clear, CS-Chromatographie Service GmbH, Germany) in a total volume of 1 ml at 30 °C und 1400 rpm in a thermomixer (Thermomixer comfort, Eppendorf, Germany). Samples (20 μl) were taken from the organic phase after 5 min, 10 min, 15 min, 30 min, 2 h, 4 h, 6 h and 24 h, were prepared as described in sect. 4.9 and analysed by HPLC (see sect. 4.13). To analyse evaporation effects, control samples were prepared in the same manner without CatIBs. Each carboligation reaction was performed in technical triplicate.

4.11 Synthesis of TMBZ

TMBZ was synthesised by an enzymatic approach[40] and was used for HPLC calibration. *E. coli* whole cells containing *Pf*BAL (25 mg ml^{-1}) were transferred into 6 ml reaction solution consisting of MTBE, 150 μl TEA-buffer (1 M, pH 10, 0.5 mM $MgSO_4$, 0.1 mM ThDP), and 500 mM DMBA. The reaction was performed in an 8 ml glass vial and stirred at 1000 rpm and 30 °C overnight. The reaction was followed by thin-layer chromatography (TLC Plates Polygram® SIL G/UV_{254}, Macherey-Nagel, Düren, Germany). As full conversion of DMBA was not achieved, the reaction solution was chromatographically purified. For this purpose, the reaction solution was filtered and extracted two-times with MTBE. The MTBE phases were pooled, dried over $MgSO_4$, and concentrated by a rotating evaporator (Rotavapor R-100, Büchi Labortechnik GmbH, Essen, Germany). The TMBZ was separated from the DMBA by a chromatographic step with ethyl acetate and petroleum ether in a 4 : 6 mixture as the mobile phase and silica gel (0.04–0.063 mm (400–230 mesh), Roth, Karlsruhe, Germany) as the stationary phase. The TMBZ containing fractions were pooled and the solvent evaporated using a rotating evaporator (Rotavapor R-100, Büchi Labortechnik GmbH, Essen, Germany). After evaporation of residual organic solvents under high vacuum overnight, the purity of the product was determined by ^{1}H-NMR analysis (sect. 4.12). 292.5 mg of purified TMBZ was obtained with a purity of 80.8–82.0%. TMBZ was used for further calibration by HPLC (see sect. 4.13).

4.12 ^{1}H-NMR analysis

For ^{1}H-NMR analysis, 20 mg ml^{-1} TMBZ was dissolved in deuterated $CDCl_3$, which was supplemented with 0.03 vol% tetramethylsilane. The analysis was performed by a 600 MHz Avance DPX-600 (Bruker, Billerica, USA) spectrometer. The NMR-spectrum was analysed by MestReNova (Mestrelab Research, Santiago de Compostela, Spain) and was in-line with published data:[66,67] δ_H 7.06 (2 H, s,), 6.61 (1 H, s,), 6.47 (2 H,

s,), 6.36 (1 H, s,), 5.79 (1 H, d, *J* 6.5), 4.46 (1 H, d, *J* 6.2), 3.78 (6 H, s), 3.75 (6 H, s) (compare ESI,† Fig. S11). Ethyl acetate (18.0–19.2 vol%) was included.

4.13 HPLC analysis

Prior to high performance liquid chromatography (HPLC) analysis, the samples were centrifuged at 15 800 × *g* for 1 min and the supernatant was transferred into HPLC vials with inlet. Subsequently, 10 μl of the prepared samples were analysed using either a Thermo Scientific Dionex Ultimate 3000 HPLC system containing a diode-array detector DAD-3000 (ThermoFisher Scientific, Waltham, MA, USA), or an HPLC system from Agilent Series 1100 (Agilent Technologies Santa Clara, USA) equipped with DAD. All samples were separated on a Chiralpak® IE column (4.6 μm × 250 mm, 5 μm particle size column, Daicel, Tokyo, Japan) combined with a pre-column (Chiralpak® IE 4 mm × 10 mm; Daicel, Tokyo, Japan), which was tempered to 20 °C. The HPLC conditions are given in Table S8 and S9 (ESI†) to quantify substances for the respective experiments. Calibration curves are given in Fig. S12–S14 in ESI.†

Conflicts of interest

There are no conflicts to declare.

Acknowledgements

The scientific activities of the Bioeconomy Science Center were financially supported by the Ministry of Innovation, Science and Research within the framework of the NRW Strategieprojekt BioSC (No. 313/323-400-002 13). BioSC is a research cluster of RWTH Aachen University, the universities of Düsseldorf and Bonn, and Forschungszentrum Jülich. The authors thank the Institute for Bioorganic Chemistry (HHU Düsseldorf and Forschungszentrum Jülich) for performing ^{1}H-NMR analysis.

References

1 R. Birner, in *Bioeconomy*, Springer International Publishing, Cham, 2018, pp. 17–38.
2 (*a*) A. Pellis, S. Cantone, C. Ebert and L. Gardossi, *New Biotechnol.*, 2018, **40**, 154–169; (*b*) R. A. Sheldon and J. M. Woodley, *Chem. Rev.*, 2018, **118**, 801–838.
3 J. M. Guisan, *Immobilization of Enzymes and Cells*, Humana Press, Totowa, NJ, 2nd edn, 2013, vol. 1051.
4 U. Krauss, V. D. Jäger, M. Diener, M. Pohl and K.-E. Jaeger, *J. Biotechnol.*, 2017, **258**, 136–147.
5 S. Li, K. Lin, H. Pang, Y. Wu and J. Xu, *Appl. Biochem. Biotechnol.*, 2013, **169**, 612–623.
6 J. Nahálka, *J. Ind. Microbiol. Biotechnol.*, 2008, **35**, 219–223.
7 D. M. Worrall and N. H. Goss, *Aust. J. Biotechnol.*, 1989, **3**, 28–32.
8 P. Tufvesson, J. Lima-Ramos, M. Nordblad and J. M. Woodley, *Org. Process Res. Dev.*, 2011, **15**, 266–274.
9 K. Tokatlidis, P. Dhurjati, J. Millet, P. Béguin and J.-P. Aubert, *FEBS Lett.*, 1991, **282**, 205–208.
10 (*a*) J. Nahálka and V. Pätoprstý, *Org. Biomol. Chem.*, 2009, **7**, 1778–1780; (*b*) S. L. Choi, S. J. Lee, J. S. Ha, J. J. Song, Y. H. Rhee and S. G. Lee, *Biotechnol. Bioprocess Eng.*, 2011, **16**, 1173–1179; (*c*) E. Hrabárová, L. Achbergerová and J. Nahálka, in *Insoluble Protein: Methods and protocols*, ed. E. García-Fruitós, Springer New York, 2015, vol. 1258, pp. 411–422.
11 B. Zhou, L. Xing, W. Wu, X. E. Zhang and Z. Lin, *Microb. Cell Fact.*, 2012, **11**, 10.
12 (*a*) Z. Lin, B. Zhou, W. Wu, L. Xing and Q. Zhao, *Faraday Discuss.*, 2013, **166**, 243–256; (*b*) W. Wu, L. Xing, B. Zhou and Z. Lin, *Microb. Cell Fact.*, 2011, **10**, 9; (*c*) X. Wang, B. Zhou, W. Hu, Q. Zhao and Z. Lin, *Microb. Cell Fact.*, 2015, **14**, 88.
13 (*a*) E. García-Fruitós, N. González-Montalbán, M. Morell, A. Vera, R. M. Ferraz, A. Arís, S. Ventura and A. Villaverde, *Microb. Cell Fact.*, 2005, **4**, 27; (*b*) S. Y. Park, S. H. Park and S. K. Choi, *Anal. Biochem.*, 2012, **426**, 63–65.
14 A. S. Demir, Ö. Şeşenoglu, E. Eren, B. Hosrik, M. Pohl, E. Janzen, D. Kolter, R. Feldmann, P. Dünkelmann and M. Müller, *Adv. Synth. Catal.*, 2002, **344**, 96–103.
15 A. S. Demir, O. Seşenoglu, P. Dünkelmann and M. Müller, *Org. Lett.*, 2003, **5**, 2047–2050.
16 P. Dünkelmann, D. Kolter-Jung, A. Nitsche, A. S. Demir, P. Siegert, B. Lingen, M. Baumann, M. Pohl and M. Müller, *J. Am. Chem. Soc.*, 2002, **124**, 12084–12085.
17 M. Sanchez-Gonzalez and J. P. N. Rosazza, *Adv. Synth. Catal.*, 2003, **345**, 819–824.
18 E. Janzen, M. Müller, D. Kolter-Jung, M. M. Kneen, M. J. McLeish and M. Pohl, *Bioorg. Chem.*, 2006, **34**, 345–361.
19 B. González and R. Vicuña, *J. Bacteriol.*, 1989, **171**, 2401–2405.
20 A. S. Demir, M. Pohl, E. Janzen and M. Müller, *J. Chem. Soc., Perkin Trans. 1*, 2001, 633–635.
21 B. M. Choudary, N. S. Chowdari, S. Madhi and M. L. Kantam, *J. Org. Chem.*, 2003, **68**, 1736–1746.
22 T. Stillger, M. Pohl, C. Wandrey and A. Liese, *Org. Process Res. Dev.*, 2006, **10**, 1172–1177.
23 N. Kurlemann and A. Liese, *Tetrahedron: Asymmetry*, 2004, **15**, 2955–2958.
24 J. Döbber and M. Pohl, *J. Biotechnol.*, 2017, **241**, 170–174.
25 P. Domínguez de María, T. Stillger, M. Pohl, S. Wallert, K. Drauz, H. Gröger, H. Trauthwein and A. Liese, *J. Mol. Catal. B: Enzym.*, 2006, **38**, 43–47.
26 T. Stillger, *doctoral thesis*, Rheinische Friedrich-Wilhelms-Universität Bonn, 2004.
27 T. Schmidt, M. Zavrel, A. Spiess and M. B. Ansorge-Schumacher, *Bioorg. Chem.*, 2009, **37**, 84–89.
28 F. Hildebrand, S. Kühl, M. Pohl, D. Vasic-Racki, M. Müller, C. Wandrey, S. Lütz, Đ. Vasić-Rački, M. Müller, C. Wandrey and S. Lütz, *Biotechnol. Bioeng.*, 2007, **96**, 835–843.
29 S. B. Sopaci, I. Simşek, B. Tural, M. Volkan and A. S. Demir, *Org. Biomol. Chem.*, 2009, **7**, 1658–1664.
30 B. Tural, S. Tural, E. Ertaş, İ. Yalınkılıç and A. S. Demir, *J. Mol. Catal. B: Enzym.*, 2013, **95**, 41–47.

31 S. Shanmuganathan, D. Natalia, A. van den Wittenboer, C. Kohlmann, L. Greiner and P. Domínguez de María, *Green Chem.*, 2010, **12**, 2240–2245.

32 A. van den Wittenboer, B. Niemeijer, S. K. Karmee and M. B. Ansorge-Schumacher, *J. Mol. Catal. B: Enzym.*, 2010, **67**, 208–213.

33 S. Kühl, D. Zehentgruber, M. Pohl, M. Müller and S. Lütz, *Chem. Eng. Sci.*, 2007, **62**, 5201–5205.

34 M. B. Ansorge-Schumacher, L. Greiner, F. Schroeper, S. Mirtschin and T. Hischer, *Biotechnol. J.*, 2006, **1**, 564–568.

35 T. Hischer, D. Gocke, M. Fernández, P. Hoyos, A. R. Alcántara, J. V. Sinisterra, W. Hartmeier and M. B. Ansorge-Schumacher, *Tetrahedron*, 2005, **61**, 7378–7383.

36 P. Domínguez de María, T. Stillger, M. Pohl, M. Kiesel, A. Liese, H. Gröger and H. Trauthwein, *Adv. Synth. Catal.*, 2008, **350**, 165–173.

37 A. van den Wittenboer, T. Schmidt, P. Müller, M. B. Ansorge-Schumacher and L. Greiner, *Biotechnol. J.*, 2009, **4**, 44–50.

38 J. Wachtmeister, A. Jakoblinnert, J. Kulig, H. Offermann and D. Rother, *ChemCatChem*, 2014, **6**, 1051–1058.

39 A. Jakoblinnert and D. Rother, *Green Chem.*, 2014, **16**, 3472.

40 M. Schwarz, *doctoral thesis*, Heinrich-Heine University Düsseldorf, 2010.

41 M. Diener, B. Kopka, M. Pohl, K.-E. Jaeger and U. Krauss, *ChemCatChem*, 2016, **8**, 142–152.

42 R. Kloss, M. H. Limberg, U. Mackfeld, D. Hahn, A. Grünberger, V. D. Jäger, U. Krauss, M. Oldiges and M. Pohl, *Sci. Rep.*, 2018, **8**, 5856.

43 M. V. Airola, K. J. Watts, A. M. Bilwes and B. R. Crane, *Structure*, 2010, **18**, 436–448.

44 A. Grünberger, C. Probst, S. Helfrich, A. Nanda, B. Stute, W. Wiechert, E. von Lieres, K. Nöh, J. Frunzke and D. Kohlheyer, *Cytometry, Part A*, 2015, **87**, 1101–1115.

45 A. Grünberger, C. Probst, A. Heyer, W. Wiechert, J. Frunzke and D. Kohlheyer, *J. Visualized Exp.*, 2013, 1–11.

46 A. Rokney, M. Shagan, M. Kessel, Y. Smith, I. Rosenshine and A. B. Oppenheim, *J. Mol. Biol.*, 2009, **392**, 589–601.

47 S. Ventura and A. Villaverde, *Trends Biotechnol.*, 2006, **24**, 179–185.

48 S. P. Allen, J. Polazzi, J. K. Gierse and A. M. Easton, *J. Bacteriol.*, 1992, **174**, 6938–6947.

49 M. M. Carrio and A. Villaverde, *J. Biotechnol.*, 2002, **96**, 3–12.

50 F. Hoffmann and U. Rinas, *Biotechnol. Prog.*, 2000, **16**, 1000–1007.

51 G. Georgiou and P. Valax, *Methods Enzymol.*, 1999, **309**, 48–58.

52 D. Gocke, L. Walter, E. Gauchenova, G. Kolter, M. Knoll, C. L. Berthold, G. Schneider, J. Pleiss, M. Müller and M. Pohl, *ChemBioChem*, 2008, **9**, 406–412.

53 M. Pohl, M. Müller and A. S. Demir, *US* 7045334B2, 2006.

54 C. Mateo, J. M. Palomo, L. M. van Langen, F. van Rantwijk and R. A. Sheldon, *Biotechnol. Bioeng.*, 2004, **86**, 273–276.

55 V. D. Jäger, R. Lamm, R. Kloß, E. Kaganovitch, A. Günberger, M. Pohl, J. Büchs, K.-E. Jaeger and U. Krauss, *ACS Synth. Biol.*, 2018, **7**, 2282–2295.

56 R. Wichmann, C. Wandrey, A. F. Buckmann and M. R. Kula, *Biotechnol. Bioeng.*, 1981, **23**, 2789–2802.

57 D. Prat, A. Wells, J. Hayler, H. Sneddon, C. R. Mcelroy, S. Abou-shehada and P. J. Dunn, *Green Chem.*, 2016, **18**, 288–296.

58 K. Watanabe, *Molecules*, 2013, **18**, 3183–3194.

59 D. J. Korz, U. Rinas, K. Hellmuth, E. A. Sanders and W.-D. Deckwer, *J. Biotechnol.*, 1995, **39**, 59–65.

60 M. M. Bradford, *Anal. Biochem.*, 1976, **72**, 248–254.

61 E. Gasteiger, C. Hoogland, A. Gattiker, S. Duvaud, M. R. Wilkins, R. D. Appel and A. Bairoch, in *The Proteomics Protocols Handbook*, ed. J. M. Walker, Humana Press, Totowa, NJ, 2005, vol. 31, pp. 571–607.

62 D. Kang, Y. S. Gho, M. Suh and C. Kang, *Bull. Korean Chem. Soc.*, 2002, **23**, 1511–1512.

63 S. Schaffer, B. Weil, V. D. Nguyen, G. Dongmann, K. Günther, M. Nickolaus, T. Hermann and M. Bott, *Electrophoresis*, 2001, **22**, 4404–4422.

64 A. Koch-Koerfges, A. Kabus, I. Ochrombel, K. Marin and M. Bott, *Biochim. Biophys. Acta, Bioenerg.*, 2012, **1817**, 370–380.

65 H. Morschett, W. Wiechert and M. Oldiges, *Microb. Cell Fact.*, 2016, **15**, 34.

66 J. E. T. Corrie and D. R. Trentham, *J. Chem. Soc., Perkin Trans. 1*, 1992, 2409–2417.

67 K. Arifin, L. J. Minggu, W. R. W. Daud, B. M. Yamin, R. Daik and M. B. Kassim, *Spectrochim. Acta, Part A*, 2014, **120**, 208–215.

Electronic Supplementary Information

Tailor-made catalytically active inclusion bodies for different applications in biocatalysis

R. Kloss[a,d], T. Karmainski[a], V. D. Jäger[b,d], D. Hahn[a], A. Grünberger[a,c], M. Baumgart[a], U. Krauss[b,d], K.-E. Jaeger[a,b,d], W. Wiechert[a,d], and M. Pohl[a,d*]

[a]Forschungszentrum Jülich GmbH, IBG-1: Biotechnology, 52425 Jülich, Germany

[b]Institut für Molekulare Enzymtechnologie, Heinrich-Heine-Universität Düsseldorf, Forschungszentrum Jülich, 52425 Jülich, Germany

[c]Multiscale Bioengineering, Bielefeld University, Universitätsstraße 25, 33615 Bielefeld, Germany

[d]Bioeconomy Science Center (BioSC), c/o, Forschungszentrum Jülich, 52425 Jülich, Germany

[*]Corresponding author

Martina Pohl (email: ma.pohl@fz juelich.de, tel: +49 2461 61-4388, fax: 61-3870).

1 Table of content

2 Experimental

2.1 Cloning & sequences

The gene encoding for *Pf*BAL was cloned into a pET28a vector containing the gene fragment encoding for the TDoT-domain, a linker region consisting of 3xGGGS linker and the Factor Xa protease recognition site (L), which was performed based on the earlier described cloning strategy.1 In brief, the gene coding for *Pf*BAL was amplified by PCR using the below listed oligonucleotide primers (Table S1), and subsequently inserted into the above described pET28a vector by restriction with BamHI and NotI and ligation, resulting in an N-terminal fusion of the target enzyme to linker and TDoT (pTDoT-Xa-L-*Pf*BAL) (Table S2). To insert the 3HAMP domain into the so generated vector (pTDoT-Xa-L-*Pf*BAL), the 3HAMP gene fragment was codon-optimized, synthesized by Eurofins Genomics (Ebersberg, Germany) and supplied on a plasmid (pEX-A-3HAMP-Linker). The DNA fragment coding for 3HAMP-Linker was subsequently cloned into the above described vector (pTDoT-Xa-L-*Pf*BAL) by restriction with endonucleases *Nde*I and *Spe*I and ligation to obtain a vector consisting of 3HAMP-domain, a linker region consisting of 3xGGGS linker and the Factor Xa protease recognition site (L) and the enzyme *Pf*BAL (p3HAMP-Xa-L-*Pf*BAL). All final constructs were verified by sequencing (LGC genomics, Berlin, Germany). Plasmid amplification was performed in *E. coli* DH5α (Table S3).

Table S1: Primer sequences for amplification of *Pf*BAL gen with *BamH*I and *Not*I cleavage sites (underlined)

name	sequence
BamHI_BAL _fw	5'- ATATATGGATCCATGGCGATGATTACAGGCGGCGAAC -3'
BAL_NotI_rev	5'- ATATAT GCGGCCGCTTATGCGAAGGGGTCCATG -3'

Table S2: The used vectors are given with genotype and cloning description. DNA and amino acid sequences are stated in section 0-0.

vector	genotype	description
pET28a	*ColE1 lacZ'* Kan^R P_{T7} P_{lac}	Merck (Darmstadt, Germany)
BAL*His*/ pKK233_2	pKK233_2 P_{trc}, gene fusion [*pfbal, His-tag]*	Janzen et al. 2006 [2]
pTDoT-L-*Pf*BAL	pET28a, P_{T7}, gene fusion [*tdot*-factor Xa recognition site-*$(GGGS)_3$ linker-pfbal*]	pTDoT-L-*At*HNL derivative, insertion of 1699 bp PCR-amplified *Bam*HI/*Not*I *pfbal* fragment in pTDoT-L-*At*HNL; without the 784 bp fragment containing *hnl* [1]
p3HAMP-L-*Pf*BAL	pET28a, P_{T7}, gene fusion [*3hamp*-factor Xa recognition site-*$(GGGS)_3$ linker-pfbal*]	pTDoT-L-*Pf*BAL derivative, insertion of a 518 bp *Nde*I/*Spe*I *3hamp*-containing fragment in pTDoT-L-*Pf*BAL; without the 155 bp fragment containing *tdot*

Table S3: The used strains are given with genotype and reference or source.

strains	genotype	reference or source
E. coli BL21 (DE3)	*F^- ompT hsdSB(rB^- mB^-) gal dcm (λIts857ind1 Sam7 nin5 lacUV5-T7 gene1)*	Studier & Moffatt, 1986 [3], Invitrogen (Carlsbad, USA)
E. coli DH5α	*supE44 ΔlacU169 (Φ80lacZDM15) hsdR17 recA1 endA1 gyrA96 thi-1 relA1*	Invitrogen (Carlsbad, USA)
E. coli SG 13009	*F^- ompT $hsdS_B$ (rB^-mB^-) dcm gal* (DE3)	Qiagen (Hilden Germany)

2.2 Expression vector of TDoT-*Pf*BAL

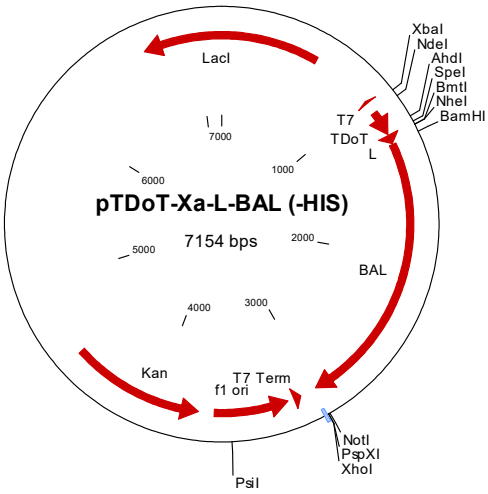

2.3 DNA-sequence of the pET28a vector containing the gene fusion encoding for TDoT-*Pf*BAL

vector DNA (grey), start and stop codon of the *tdot-pfbal*-ORF (red), *Pf*BAL gen (black), linker (green), TDoT (orange), restrictions sites (blue)

CAGCCAGACGCAGACGCGCCGAGACAGAACTTAATGGGCCCGCTAACAGCGCGATTTGCT
GGTGACCCAATGCGACCAGATGCTCCACGCCCAGTCGCGTACCGTCTTCATGGGAGAAAA
TAATACTGTTGATGGGTGTCTGGTCAGAGACATCAAGAAATAACGCCGGAACATTAGTGC
AGGCAGCTTCCACAGCAATGGCATCCTGGTCATCCAGCGGATAGTTAATGATCAGCCCAC
TGACGCGTTGCGCGAGAAGATTGTGCACCGCCGCTTTACAGGCTTCGACGCCGCTTCGTT
CTACCATCGACACCACCACGCTGGCACCCAGTTGATCGGCGCGAGATTTAATCGCCGCGA
CAATTTGCGACGGCGCGTGCAGGGCCAGACTGGAGGTGGCAACGCCAATCAGCAACGACT
GTTTGCCCGCCAGTTGTTGTGCCACGCGGTTGGGAATGTAATTCAGCTCCGCCATCGCCG
CTTCCACTTTTTCCCGCGTTTTCGCAGAAACGTGGCTGGCCTGGTTCACCACGCGGGAAA
CGGTCTGATAAGAGACACCGGCATACTCTGCGACATCGTATAACGTTACTGGTTTCACAT
TCACCACCCTGAATTGACTCTCTTCCGGGCGCTATCATGCCATACCGCGAAAGGTTTTGC
GCCATTCGATGGTGTCCGGGATCTCGACGCTCTCCCTTATGCGACTCCTGCATTAGGAAG
CAGCCCAGTAGTAGGTTGAGGCCGTTGAGCACCGCCGCCGCAAGGAATGGTGCATGCAAG
GAGATGGCGCCCAACAGTCCCCCGGCCACGGGGCCTGCCACCATACCCACGCCGAAACAA
GCGCTCATGAGCCCGAAGTGGCGAGCCCGATCTTCCCCATCGGTGATGTCGGCGATATAG
GCGCCAGCAACCGCACCTGTGGCGCCGGTGATGCCGGCCACGATGCGTCCGGCGTAGAGG
ATCGAGATCTCGATCCCGCGAAATTAATACGACTCACTATAGGGGAATTGTGAGCGGATA
ACAATTCCCCTCTAGAAATAATTTTGTTTAACTTTAAGAAGGAGATATACATATGATCAT
TAACGAAACTGCCGATGACATCGTTTATCGCCTGACAGTCATTATCGATGATCGCTACGA
ATCGCTGAAAAACCTGATTACCTTACGTGCAGATCGCTTGGAGATGATCATCAATGACAA
TGTGTCCACCATTCTCGCGAGCATTACTAGTATTGAAGGCCGTGCTAGCGGCGGTGGGTC
TGGAGGCGGCTCAGGTGGTGGGTCGGGATCCATGGCGATGATTACAGGCGGCGAACTGGT
TGTTCGCACCCTAATAAAGGCTGGGGTCGAACATCTGTTCGGCCTGCACGGCGCGCATAT
CGATACGATTTTTCAAGCCTGTCTCGATCATGATGTGCCGATCATCGACACCCGCCATGA
GGCCGCCGCAGGGCATGCGGCCGAGGGCTATGCCCGCGCTGGCGCCAAGCTGGGCGTGGC
GCTGGTCACGGCGGGCGGGGGATTTACCAATGCGGTCACGCCCATTGCCAACGCTTGGCT
GGATCGCACGCCGGTGCTCTTCCTCACCGGATCGGGCGCGCTGCGTGATGATGAAACCAA
CACGTTGCAGGCGGGGATTGATCAGGTCGCCATGGCGGCGCCCATTACCAAATGGGCGCA
TCGGGTGATGGCAACCGAGCATATCCCACGGCTGGTGATGCAGGCGATCCGCGCCGCGTT

GAGCGCGCCACGCGGGCCGGTGTTGCTGGATCTGCCGTGGGATATTCTGATGAACCAGAT
TGATGAGGATAGCGTCATTATCCCCGATCTGGTCTTGTCCGCACATGGGGCCAGACCCGA
CCCTGCCGATCTGGATCAGGCTCTCGCGCTTTTGCGCAAGGCGGAGCGGCCGGTCATCGT
GCTCGGCTCAGAAGCCTCGCGGACAGCGCGCAAGACGGCGCTTAGCGCATTCGTGGCGGC
GACTGGCGTGCCGGTGTTTGCCGATTATGAAGGGCTAAGCATGCTCTCGGGGCTGCCCGA
TGCTATGCGGGGCGGGCTGGTGCAAAACCTCTATTCTTTTGCCAAAGCCGATGCCGCGCC
AGATCTCGTGCTGATGCTGGGGGCGCGCTTTGGCCTTAACACCGGGCATGGATCTGGGCA
GTTGATCCCCCATAGCGCGCAGGTCATTCAGGTCGACCCTGATGCCTGCGAGCTGGGACG
CCTGCAGGGCATCGCTCTGGGCATTGTGGCCGATGTGGGTGGGACCATCGAGGCTTTGGC
GCAGGCCACCGCGCAAGATGCGGCTTGGCCGGATCGCGGCGACTGGTGCGCCAAAGTGAC
GGATCTGGCGCAAGAGCGCTATGCCAGCATCGCTGCGAAATCGAGCAGCGAGCATGCGCT
CCACCCCTTTCACGCCTCGCAGGTCATTGCCAAACACGTCGATGCAGGGGTGACGGTGGT
AGCGGATGGTGCGCTGACCTATCTCTGGCTGTCCGAAGTGATGAGCCGCGTGAAACCCGG
CGGTTTTCTCTGCCACGGCTATCTAGGCTCGATGGGCGTGGGCTTCGGCACGGCGCTGGG
CGCGCAAGTGGCCGATCTTGAAGCAGGCCGCCGCACGATCCTTGTGACCGGCGATGGCTC
GGTGGGCTATAGCATCGGTGAATTTGATACGCTGGTGCGCAAACAATTGCCGCTGATCGT
CATCATCATGAACAACCAAAGCTGGGGGGCGACATTGCATTTCCAGCAATTGGCCGTCGG
CCCCAATCGCGTGACGGGCACCCGTTTGGAAAATGGCTCCTATCACGGGGTGGCCGCCGC
CTTTGGCGCGGATGGCTATCATGTCGACAGTGTGGAGAGCTTTTCTGCGGCTCTGGCCCA
AGCGCTCGCCCATAATCGCCCCGCCTGCATCAATGTCGCGGTCGCGCTCGATCCGATCCC
GCCCGAAGAACTCATTCTGATCGGCATGGACCCCTTCGCATAAGCGGCCGCACTCGAGCA
CCACCACCACCACCACTGAGATCCGGCTGCTAACAAAGCCCGAAAGGAAGCTGAGTTGGC
TGCTGCCACCGCTGAGCAATAACTAGCATAACCCCTTGGGGCCTCTAAACGGGTCTTGAG
GGGTTTTTTGCTGAAAGGAGGAACTATATCCGGATTGGCGAATGGGACGCGCCCTGTAGC
GGCGCATTAAGCGCGGCGGGTGTGGTGGTTACGCGCAGCGTGACCGCTACACTTGCCAGC
GCCCTAGCGCCCGCTCCTTTCGCTTTCTTCCCTTCCTTTCTCGCCACGTTCGCCGGCTTT
CCCCGTCAAGCTCTAAATCGGGGGCTCCCTTTAGGGTTCCGATTTAGTGCTTTACGGCAC
CTCGACCCCAAAAAACTTGATTAGGGTGATGGTTCACGTAGTGGGCCATCGCCCTGATAG
ACGGTTTTTCGCCCTTTGACGTTGGAGTCCACGTTCTTTAATAGTGGACTCTTGTTCCAA
ACTGGAACAACACTCAACCCTATCTCGGTCTATTCTTTTGATTTATAAGGGATTTTGCCG
ATTTCGGCCTATTGGTTAAAAAATGAGCTGATTTAACAAAAATTTAACGCGAATTTTAAC
AAAATATTAACGTTTACAATTTCAGGTGGCACTTTTCGGGGAAATGTGCGCGGAACCCCT
ATTTGTTTATTTTTCTAAATACATTCAAATATGTATCCGCTCATGAATTAATTCTTAGAA
AAACTCATCGAGCATCAAATGAAACTGCAATTTATTCATATCAGGATTATCAATACCATA
TTTTTGAAAAAGCCGTTTCTGTAATGAAGGAGAAAACTCACCGAGGCAGTTCCATAGGAT
GGCAAGATCCTGGTATCGGTCTGCGATTCCGACTCGTCCAACATCAATACAACCTATTAA
TTTCCCCTCGTCAAAAATAAGGTTATCAAGTGAGAAATCACCATGAGTGACGACTGAATC
CGGTGAGAATGGCAAAAGTTTATGCATTTCTTTCCAGACTTGTTCAACAGGCCAGCCATT
ACGCTCGTCATCAAAATCACTCGCATCAACCAAACCGTTATTCATTCGTGATTGCGCCTG
AGCGAGACGAAATACGCGATCGCTGTTAAAAGGACAATTACAAACAGGAATCGAATGCAA
CCGGCGCAGGAACACTGCCAGCGCATCAACAATATTTTCACCTGAATCAGGATATTCTTC
TAATACCTGGAATGCTGTTTTCCCGGGGATCGCAGTGGTGAGTAACCATGCATCATCAGG
AGTACGGATAAAATGCTTGATGGTCGGAAGAGGCATAAATTCCGTCAGCCAGTTTAGTCT
GACCATCTCATCTGTAACATCATTGGCAACGCTACCTTTGCCATGTTTCAGAAACAACTC
TGGCGCATCGGGCTTCCCATACAATCGATAGATTGTCGCACCTGATTGCCCGACATTATC
GCGAGCCCATTTATACCCATATAAATCAGCATCCATGTTGGAATTTAATCGCGGCCTAGA
GCAAGACGTTTCCCGTTGAATATGGCTCATAACACCCCTTGTATTACTGTTTATGTAAGC
AGACAGTTTTATTGTTCATGACCAAAATCCCTTAACGTGAGTTTTCGTTCCACTGAGCGT
CAGACCCCGTAGAAAAGATCAAAGGATCTTCTTGAGATCCTTTTTTTCTGCGCGTAATCT
GCTGCTTGCAAACAAAAAAACCACCGCTACCAGCGGTGGTTTGTTTGCCGGATCAAGAGC
TACCAACTCTTTTTCCGAAGGTAACTGGCTTCAGCAGAGCGCAGATACCAAATACTGTCC
TTCTAGTGTAGCCGTAGTTAGGCCACCACTTCAAGAACTCTGTAGCACCGCCTACATACC
TCGCTCTGCTAATCCTGTTACCAGTGGCTGCTGCCAGTGGCGATAAGTCGTGTCTTACCG
GGTTGGACTCAAGACGATAGTTACCGGATAAGGCGCAGCGGTCGGGCTGAACGGGGGGTT

CGTGCACACAGCCCAGCTTGGAGCGAACGACCTACACCGAACTGAGATACCTACAGCGTG
AGCTATGAGAAAGCGCCACGCTTCCCGAAGGGAGAAAGGCGGACAGGTATCCGGTAAGCG
GCAGGGTCGGAACAGGAGAGCGCACGAGGGAGCTTCCAGGGGGAAACGCCTGGTATCTTT
ATAGTCCTGTCGGGTTTCGCCACCTCTGACTTGAGCGTCGATTTTTGTGATGCTCGTCAG
GGGGGCGGAGCCTATGGAAAAACGCCAGCAACGCGGCCTTTTTACGGTTCCTGGCCTTTT
GCTGGCCTTTTGCTCACATGTTCTTTCCTGCGTTATCCCCTGATTCTGTGGATAACCGTA
TTACCGCCTTTGAGTGAGCTGATACCGCTCGCCGCAGCCGAACGACCGAGCGCAGCGAGT
CAGTGAGCGAGGAAGCGGAAGAGCGCCTGATGCGGTATTTTCTCCTTACGCATCTGTGCG
GTATTTCACACCGCATATATGGTGCACTCTCAGTACAATCTGCTCTGATGCCGCATAGTT
AAGCCAGTATACACTCCGCTATCGCTACGTGACTGGGTCATGGCTGCGCCCCGACACCCG
CCAACACCCGCTGACGCGCCCTGACGGGCTTGTCTGCTCCCGGCATCCGCTTACAGACAA
GCTGTGACCGTCTCCGGGAGCTGCATGTGTCAGAGGTTTTCACCGTCATCACCGAAACGC
GCGAGGCAGCTGCGGTAAAGCTCATCAGCGTGGTCGTGAAGCGATTCACAGATGTCTGCC
TGTTCATCCGCGTCCAGCTCGTTGAGTTTCTCCAGAAGCGTTAATGTCTGGCTTCTGATA
AAGCGGGCCATGTTAAGGGCGGTTTTTTCCTGTTTGGTCACTGATGCCTCCGTGTAAGGG
GGATTTCTGTTCATGGGGGTAATGATACCGATGAAACGAGAGAGGATGCTCACGATACGG
GTTACTGATGATGAACATGCCCGGTTACTGGAACGTTGTGAGGGTAAACAACTGGCGGTA
TGGATGCGGCGGGACCAGAGAAAAATCACTCAGGGTCAATGCCAGCGCTTCGTTAATACA
GATGTAGGTGTTCCACAGGGTAGCCAGCAGCATCCTGCGATGCAGATCCGGAACATAATG
GTGCAGGGCGCTGACTTCCGCGTTTCCAGACTTTACGAAACACGGAAACCGAAGACCATT
CATGTTGTTGCTCAGGTCGCAGACGTTTTGCAGCAGCAGTCGCTTCACGTTCGCTCGCGT
ATCGGTGATTCATTCTGCTAACCAGTAAGGCAACCCCGCCAGCCTAGCCGGGTCCTCAAC
GACAGGAGCACGATCATGCGCACCCGTGGGGCCGCCATGCCGGCGATAATGGCCTGCTTC
TCGCCGAAACGTTTGGTGGCGGGACCAGTGACGAAGGCTTGAGCGAGGGCGTGCAAGATT
CCGAATACCGCAAGCGACAGGCCGATCATCGTCGCGCTCCAGCGAAAGCGGTCCTCGCCG
AAAATGACCCAGAGCGCTGCCGGCACCTGTCCTACGAGTTGCATGATAAAGAAGACAGTC
ATAAGTGCGGCGACGATAGTCATGCCCCGCGCCCACCGGAAGGAGCTGACTGGGTTGAAG
GCTCTCAAGGGCATCGGTCGAGATCCCGGTGCCTAATGAGTGAGCTAACTTACATTAATT
GCGTTGCGCTCACTGCCCGCTTTCCAGTCGGGAAACCTGTCGTGCCAGCTGCATTAATGA
ATCGGCCAACGCGCGGGGAGAGGCGGTTTGCGTATTGGGCGCCAGGGTGGTTTTTCTTTT
CACCAGTGAGACGGGCAACAGCTGATTGCCCTTCACCGCCTGGCCCTGAGAGAGTTGCAG
CAAGCGGTCCACGCTGGTTTGCCCCAGCAGGCGAAAATCCTGTTTGATGGTGGTTAACGG
CGGGATATAACATGAGCTGTCTTCGGTATCGTCGTATCCCACTACCGAGATATCCGCACC
AACGCGCAGCCCGGACTCGGTAATGGCGCGCATTGCGCCCAGCGCCATCTGATCGTTGGC
AACCAGCATCGCAGTGGGAACGATGCCCTCATTCAGCATTTGCATGGTTTGTTGAAAACC
GGACATGGCACTCCAGTCGCCTTCCCGTTCCGCTATCGGCTGAATTTGATTGCGAGTGAG
ATATTTATGCCAGC

2.4 Amino acid sequence of TDoT-*Pf*BAL

***Pf*BAL gen (black), linker (green), TDoT (orange), restrictions sites (blue)**

M I I N E T A D D I V Y R L T V I I D D R Y E S L K N L I T L R A D R L E M
I I N D N V S T I L A S I T S I E G R A S G G G S G G G S G G G S G S M A M
I T G G E L V V R T L I K A G V E H L F G L H G A H I D T I F Q A C L D H D
V P I I D T R H E A A A G H A A E G Y A R A G A K L G V A L V T A G G G F T
N A V T P I A N A W L D R T P V L F L T G S G A L R D D E T N T L Q A G I D
Q V A M A A P I T K W A H R V M A T E H I P R L V M Q A I R A A L S A P R G
P V L L D L P W D I L M N Q I D E D S V I I P D L V L S A H G A R P D P A D
L D Q A L A L L R K A E R P V I V L G S E A S R T A R K T A L S A F V A A T
G V P V F A D Y E G L S M L S G L P D A M R G G L V Q N L Y S F A K A D A A

P D L V L M L G A R F G L N T G H G S G Q L I P H S A Q V I Q V D P D A C E
L G R L Q G I A L G I V A D V G G T I E A L A Q A T A Q D A A W P D R G D W
C A K V T D L A Q E R Y A S I A A K S S S E H A L H P F H A S Q V I A K H V
D A G V T V V A D G A L T Y L W L S E V M S R V K P G G F L C H G Y L G S M
G V G F G T A L G A Q V A D L E A G R R T I L V T G D G S V G Y S I G E F D
T L V R K Q L P L I V I I M N N Q S W G A T L H F Q Q L A V G P N R V T G T
R L E N G S Y H G V A A A F G A D G Y H V D S V E S F S A A L A Q A L A H N
R P A C I N V A V A L D P I P P E E L I L I G M D P F A

2.5 Expression vector of 3HAMP-*Pf*BAL

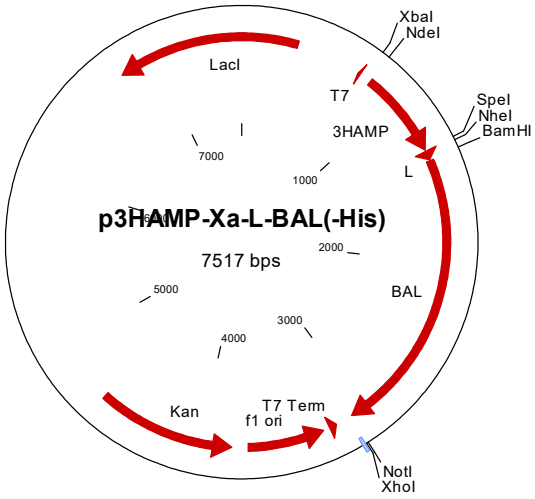

2.6 DNA-sequence of the pET28a vector containing the gene fusion encoding for 3HAMP-*Pf*BAL

vector DNA (grey), start and stop codon of the *3hamp-pfbal*-ORF (red), *Pf*BAL gen (black), linker (green), 3HAMP (orange), restrictions sites (blue)

GCACCGCCGCTTTACAGGCTTCGACGCCGCTTCGTTCTACCATCGACACCACCACGCTGG
CACCCAGTTGATCGGCGCGAGATTTAATCGCCGCGACAATTTGCGACGGCGCGTGCAGGG
CCAGACTGGAGGTGGCAACGCCAATCAGCAACGACTGTTTGCCCGCCAGTTGTTGTGCCA
CGCGGTTGGGAATGTAATTCAGCTCCGCCATCGCCGCTTCCACTTTTTCCCGCGTTTTCG
CAGAAACGTGGCTGGCCTGGTTCACCACGCGGGAAACGGTCTGATAAGAGACACCGGCAT
ACTCTGCGACATCGTATAACGTTACTGGTTTCACATTCACCACCCTGAATTGACTCTCTT
CCGGGCGCTATCATGCCATACCGCGAAAGGTTTTGCGCCATTCGATGGTGTCCGGGATCT
CGACGCTCTCCCTTATGCGACTCCTGCATTAGGAAGCAGCCCAGTAGTAGGTTGAGGCCG
TTGAGCACCGCCGCCGCAAGGAATGGTGCATGCAAGGAGATGGCGCCCAACAGTCCCCCG
GCCACGGGGCCTGCCACCATACCCACGCCGAAACAAGCGCTCATGAGCCCGAAGTGGCGA
GCCCGATCTTCCCCATCGGTGATGTCGGCGATATAGGCGCCAGCAACCGCACCTGTGGCG
CCGGTGATGCCGGCCACGATGCGTCCGGCGTAGAGGATCGAGATCTCGATCCCGCGAAAT
TAATACGACTCACTATAGGGGAATTGTGAGCGGATAACAATTCCCCTCTAGAAATAATTT
TGTTTAACTTTAAGAAGGAGATATACATATGGGCCTGTTTAACGCCCATGCAGTTGCGCA
GCAACGCGCGGATCGCATTGCGACTCTCCTGCAGTCCTTTGCGGATGGTCAGTTGGACAC
CGCCGTGGGTGAAGCGCCAGCACCTGGTTACGAACGCCTGTATGACTCGCTTCGCGCCCT
TCAGCGCCAACTGCGCGAACAACGTGCGGAGTTACAACAGGTTGAGAGCCTGGAAGCAGG

CTTGGCTGAAATGAGTCGGCAGCATGAAGCAGGGTGGATTGACCAGACGATTCCGGCTGA
ACGGTTAGAGGGCCGTGCAGCACGTATCGCCAAAGGCGTGAATGAGCTGGTTGCTGCGCA
CATTGCGGTGAAAATGAAAGTCGTGAGCGTAGTCACCGCGTATGGCCAAGGGAACTTCGA
ACCGCTCATGGATCGCCTGCCGGGTAAGAAAGCCCAGATCACGGAGGCCATTGATGGCGT
ACGTGAACGCCTGCGTGGAGCTGCTGAAGCGACCTCTGCGCAGCTGGCCACAGCCGCCTA
CAATACTAGTATTGAAGGCCGTGCTAGCGGCGGTGGGTCTGGAGGCGGCTCAGGTGGTGG
GTCGGGATCCATGGCGATGATTACAGGCGGCGAACTGGTTGTTCGCACCCTAATAAAGGC
TGGGGTCGAACATCTGTTCGGCCTGCACGGCGCGCATATCGATACGATTTTTCAAGCCTG
TCTCGATCATGATGTGCCGATCATCGACACCCGCCATGAGGCCGCCGCAGGGCATGCGGC
CGAGGGCTATGCCCGCGCTGGCGCCAAGCTGGGCGTGGCGCTGGTCACGGCGGGCGGGGG
ATTTACCAATGCGGTCACGCCCATTGCCAACGCTTGGCTGGATCGCACGCCGGTGCTCTT
CCTCACCGGATCGGGCGCGCTGCGTGATGATGAAACCAACACGTTGCAGGCGGGGATTGA
TCAGGTCGCCATGGCGGCGCCCATTACCAAATGGGCGCATCGGGTGATGGCAACCGAGCA
TATCCCACGGCTGGTGATGCAGGCGATCCGCGCCGCGTTGAGCGCGCCACGCGGGCCGGT
GTTGCTGGATCTGCCGTGGGATATTCTGATGAACCAGATTGATGAGGATAGCGTCATTAT
CCCCGATCTGGTCTTGTCCGCACATGGGGCCAGACCCGACCCTGCCGATCTGGATCAGGC
TCTCGCGCTTTTGCGCAAGGCGGAGCGGCCGGTCATCGTGCTCGGCTCAGAAGCCTCGCG
GACAGCGCGCAAGACGGCGCTTAGCGCATTCGTGGCGGCGACTGGCGTGCCGGTGTTTGC
CGATTATGAAGGGCTAAGCATGCTCTCGGGGCTGCCCGATGCTATGCGGGGCGGGCTGGT
GCAAAACCTCTATTCTTTTGCCAAAGCCGATGCCGCGCCAGATCTCGTGCTGATGCTGGG
GGCGCGCTTTGGCCTTAACACCGGGCATGGATCTGGGCAGTTGATCCCCCATAGCGCGCA
GGTCATTCAGGTCGACCCTGATGCCTGCGAGCTGGGACGCCTGCAGGGCATCGCTCTGGG
CATTGTGGCCGATGTGGGTGGGACCATCGAGGCTTTGGCGCAGGCCACCGCGCAAGATGC
GGCTTGGCCGGATCGCGGCGACTGGTGCGCCAAAGTGACGGATCTGGCGCAAGAGCGCTA
TGCCAGCATCGCTGCGAAATCGAGCAGCGAGCATGCGCTCCACCCCTTTCACGCCTCGCA
GGTCATTGCCAAACACGTCGATGCAGGGGTGACGGTGGTAGCGGATGGTGCGCTGACCTA
TCTCTGGCTGTCCGAAGTGATGAGCCGCGTGAAACCCGGCGGTTTTCTCTGCCACGGCTA
TCTAGGCTCGATGGGCGTGGGCTTCGGCACGGCGCTGGGCGCGCAAGTGGCCGATCTTGA
AGCAGGCCGCCGCACGATCCTTGTGACCGGCGATGGCTCGGTGGGCTATAGCATCGGTGA
ATTTGATACGCTGGTGCGCAAACAATTGCCGCTGATCGTCATCATCATGAACAACCAAAG
CTGGGGGGCGACATTGCATTTCCAGCAATTGGCCGTCGGCCCCAATCGCGTGACGGGCAC
CCGTTTGGAAAATGGCTCCTATCACGGGGTGGCCGCCGCCTTTGGCGCGGATGGCTATCA
TGTCGACAGTGTGGAGAGCTTTTCTGCGGCTCTGGCCCAAGCGCTCGCCCATAATCGCCC
CGCCTGCATCAATGTCGCGGTCGCGCTCGATCCGATCCCGCCCGAAGAACTCATTCTGAT
CGGCATGGACCCCTTCGCATAAGCGGCCGCACTCGAGCACCACCACCACCACCACTGAGA
TCCGGCTGCTAACAAAGCCCGAAAGGAAGCTGAGTTGGCTGCTGCCACCGCTGAGCAATA
ACTAGCATAACCCCTTGGGGCCTCTAAACGGGTCTTGAGGGGTTTTTTGCTGAAAGGAGG
AACTATATCCGGATTGGCGAATGGGACGCGCCCTGTAGCGGCGCATTAAGCGCGGCGGGT
GTGGTGGTTACGCGCAGCGTGACCGCTACACTTGCCAGCGCCCTAGCGCCCGCTCCTTTC
GCTTTCTTCCCTTCCTTTCTCGCCACGTTCGCCGGCTTTCCCCGTCAAGCTCTAAATCGG
GGGCTCCCTTTAGGGTTCCGATTTAGTGCTTTACGGCACCTCGACCCCAAAAAACTTGAT
TAGGGTGATGGTTCACGTAGTGGGCCATCGCCCTGATAGACGGTTTTTCGCCCTTTGACG
TTGGAGTCCACGTTCTTTAATAGTGGACTCTTGTTCCAAACTGGAACAACACTCAACCCT
ATCTCGGTCTATTCTTTTGATTTATAAGGGATTTTGCCGATTTCGGCCTATTGGTTAAAA
AATGAGCTGATTTAACAAAAATTTAACGCGAATTTTAACAAAATATTAACGTTTACAATT
TCAGGTGGCACTTTTCGGGGAAATGTGCGCGGAACCCCTATTTGTTTATTTTTCTAAATA
CATTCAAATATGTATCCGCTCATGAATTAATTCTTAGAAAAACTCATCGAGCATCAAATG
AAACTGCAATTTATTCATATCAGGATTATCAATACCATATTTTTGAAAAAGCCGTTTCTG
TAATGAAGGAGAAAACTCACCGAGGCAGTTCCATAGGATGGCAAGATCCTGGTATCGGTC
TGCGATTCCGACTCGTCCAACATCAATACAACCTATTAATTTCCCCTCGTCAAAAATAAG
GTTATCAAGTGAGAAATCACCATGAGTGACGACTGAATCCGGTGAGAATGGCAAAAGTTT
ATGCATTTCTTTCCAGACTTGTTCAACAGGCCAGCCATTACGCTCGTCATCAAAATCACT
CGCATCAACCAAACCGTTATTCATTCGTGATTGCGCCTGAGCGAGACGAAATACGCGATC
GCTGTTAAAAGGACAATTACAAACAGGAATCGAATGCAACCGGCGCAGGAACACTGCCAG
CGCATCAACAATATTTTCACCTGAATCAGGATATTCTTCTAATACCTGGAATGCTGTTTT
CCCGGGGATCGCAGTGGTGAGTAACCATGCATCATCAGGAGTACGGATAAAATGCTTGAT
GGTCGGAAGAGGCATAAATTCCGTCAGCCAGTTTAGTCTGACCATCTCATCTGTAACATC
ATTGGCAACGCTACCTTTGCCATGTTTCAGAAACAACTCTGGCGCATCGGGCTTCCCATA
CAATCGATAGATTGTCGCACCTGATTGCCCGACATTATCGCGAGCCCATTTATACCCATA
TAAATCAGCATCCATGTTGGAATTTAATCGCGGCCTAGAGCAAGACGTTTCCCGTTGAAT
ATGGCTCATAACACCCCTTGTATTACTGTTTATGTAAGCAGACAGTTTTATTGTTCATGA
CCAAAATCCCTTAACGTGAGTTTTCGTTCCACTGAGCGTCAGACCCCGTAGAAAAGATCA

AAGGATCTTCTTGAGATCCTTTTTTTCTGCGCGTAATCTGCTGCTTGCAAACAAAAAAAC
CACCGCTACCAGCGGTGGTTTGTTTGCCGGATCAAGAGCTACCAACTCTTTTTCCGAAGG
TAACTGGCTTCAGCAGAGCGCAGATACCAAATACTGTCCTTCTAGTGTAGCCGTAGTTAG
GCCACCACTTCAAGAACTCTGTAGCACCGCCTACATACCTCGCTCTGCTAATCCTGTTAC
CAGTGGCTGCTGCCAGTGGCGATAAGTCGTGTCTTACCGGGTTGGACTCAAGACGATAGT
TACCGGATAAGGCGCAGCGGTCGGGCTGAACGGGGGGTTCGTGCACACAGCCCAGCTTGG
AGCGAACGACCTACACCGAACTGAGATACCTACAGCGTGAGCTATGAGAAAGCGCCACGC
TTCCCGAAGGGAGAAAGGCGGACAGGTATCCGGTAAGCGGCAGGGTCGGAACAGGAGAGC
GCACGAGGGAGCTTCCAGGGGGAAACGCCTGGTATCTTTATAGTCCTGTCGGGTTTCGCC
ACCTCTGACTTGAGCGTCGATTTTTGTGATGCTCGTCAGGGGGGCGGAGCCTATGGAAAA
ACGCCAGCAACGCGGCCTTTTTACGGTTCCTGGCCTTTTGCTGGCCTTTTGCTCACATGT
TCTTTCCTGCGTTATCCCCTGATTCTGTGGATAACCGTATTACCGCCTTTGAGTGAGCTG
ATACCGCTCGCCGCAGCCGAACGACCGAGCGCAGCGAGTCAGTGAGCGAGGAAGCGGAAG
AGCGCCTGATGCGGTATTTTCTCCTTACGCATCTGTGCGGTATTTCACACCGCATATATG
GTGCACTCTCAGTACAATCTGCTCTGATGCCGCATAGTTAAGCCAGTATACACTCCGCTA
TCGCTACGTGACTGGGTCATGGCTGCGCCCCGACACCCGCCAACACCCGCTGACGCGCCC
TGACGGGCTTGTCTGCTCCCGGCATCCGCTTACAGACAAGCTGTGACCGTCTCCGGGAGC
TGCATGTGTCAGAGGTTTTCACCGTCATCACCGAAACGCGCGAGGCAGCTGCGGTAAAGC
TCATCAGCGTGGTCGTGAAGCGATTCACAGATGTCTGCCTGTTCATCCGCGTCCAGCTCG
TTGAGTTTCTCCAGAAGCGTTAATGTCTGGCTTCTGATAAAGCGGGCCATGTTAAGGGCG
GTTTTTTCCTGTTTGGTCACTGATGCCTCCGTGTAAGGGGGATTTCTGTTCATGGGGGTA
ATGATACCGATGAAACGAGAGAGGATGCTCACGATACGGGTTACTGATGATGAACATGCC
CGGTTACTGGAACGTTGTGAGGGTAAACAACTGGCGGTATGGATGCGGCGGGACCAGAGA
AAAATCACTCAGGGTCAATGCCAGCGCTTCGTTAATACAGATGTAGGTGTTCCACAGGGT
AGCCAGCAGCATCCTGCGATGCAGATCCGGAACATAATGGTGCAGGGCGCTGACTTCCGC
GTTTCCAGACTTTACGAAACACGGAAACCGAAGACCATTCATGTTGTTGCTCAGGTCGCA
GACGTTTTGCAGCAGCAGTCGCTTCACGTTCGCTCGCGTATCGGTGATTCATTCTGCTAA
CCAGTAAGGCAACCCCGCCAGCCTAGCCGGGTCCTCAACGACAGGAGCACGATCATGCGC
ACCCGTGGGGCCGCCATGCCGGCGATAATGGCCTGCTTCTCGCCGAAACGTTTGGTGGCG
GGACCAGTGACGAAGGCTTGAGCGAGGGCGTGCAAGATTCCGAATACCGCAAGCGACAGG
CCGATCATCGTCGCGCTCCAGCGAAAGCGGTCCTCGCCGAAAATGACCCAGAGCGCTGCC
GGCACCTGTCCTACGAGTTGCATGATAAAGAAGACAGTCATAAGTGCGGCGACGATAGTC
ATGCCCCGCGCCCACCGGAAGGAGCTGACTGGGTTGAAGGCTCTCAAGGGCATCGGTCGA
GATCCCGGTGCCTAATGAGTGAGCTAACTTACATTAATTGCGTTGCGCTCACTGCCCGCT
TTCCAGTCGGGAAACCTGTCGTGCCAGCTGCATTAATGAATCGGCCAACGCGCGGGGAGA
GGCGGTTTGCGTATTGGGCGCCAGGGTGGTTTTTCTTTTCACCAGTGAGACGGGCAACAG
CTGATTGCCCTTCACCGCCTGGCCCTGAGAGAGTTGCAGCAAGCGGTCCACGCTGGTTTG
CCCCAGCAGGCGAAAATCCTGTTTGATGGTGGTTAACGGCGGGATATAACATGAGCTGTC
TTCGGTATCGTCGTATCCCACTACCGAGATATCCGCACCAACGCGCAGCCCGGACTCGGT
AATGGCGCGCATTGCGCCCAGCGCCATCTGATCGTTGGCAACCAGCATCGCAGTGGGAAC
GATGCCCTCATTCAGCATTTGCATGGTTTGTTGAAAACCGGACATGGCACTCCAGTCGCC
TTCCCGTTCCGCTATCGGCTGAATTTGATTGCGAGTGAGATATTTATGCCAGCCAGCCAG
ACGCAGACGCGCCGAGACAGAACTTAATGGGCCCGCTAACAGCGCGATTTGCTGGTGACC
CAATGCGACCAGATGCTCCACGCCCAGTCGCGTACCGTCTTCATGGGAGAAAATAATACT
GTTGATGGGTGTCTGGTCAGAGACATCAAGAAATAACGCCGGAACATTAGTGCAGGCAGC
TTCCACAGCAATGGCATCCTGGTCATCCAGCGGATAGTTAATGATCAGCCCACTGACGCG
TTGCGCGAGAAGATTGT

2.7 Amino acid sequence of 3HAMP-*Pf*BAL

_Pf_BAL gen (black), linker (green), 3HAMP (orange), restrictions sites (blue)

M G L F N A H A V A Q Q R A D R I A T L L Q S F A D G Q L D T A V G E A P A
P G Y E R L Y D S L R A L Q R Q L R E Q R A E L Q Q V E S L E A G L A E M S
R Q H E A G W I D Q T I P A E R L E G R A A R I A K G V N E L V A A H I A V
K M K V V S V V T A Y G Q G N F E P L M D R L P G K K A Q I T E A I D G V R
E R L R G A A E A T S A Q L A T A A Y N T S I E G R A S G G G S G G G S G G

G S G S M A M I T G G E L V V R T L I K A G V E H L F G L H G A H I D T I F
Q A C L D H D V P I I D T R H E A A A G H A A E G Y A R A G A K L G V A L V
T A G G G F T N A V T P I A N A W L D R T P V L F L T G S G A L R D D E T N
T L Q A G I D Q V A M A A P I T K W A H R V M A T E H I P R L V M Q A I R A
A L S A P R G P V L L D L P W D I L M N Q I D E D S V I I P D L V L S A H G
A R P D P A D L D Q A L A L L R K A E R P V I V L G S E A S R T A R K T A L
S A F V A A T G V P V F A D Y E G L S M L S G L P D A M R G G L V Q N L Y S
F A K A D A A P D L V L M L G A R F G L N T G H G S G Q L I P H S A Q V I Q
V D P D A C E L G R L Q G I A L G I V A D V G G T I E A L A Q A T A Q D A A
W P D R G D W C A K V T D L A Q E R Y A S I A A K S S S E H A L H P F H A S
Q V I A K H V D A G V T V V A D G A L T Y L W L S E V M S R V K P G G F L C
H G Y L G S M G V G F G T A L G A Q V A D L E A G R R T I L V T G D G S V G
Y S I G E F D T L V R K Q L P L I V I I M N N Q S W G A T L H F Q Q L A V G
P N R V T G T R L E N G S Y H G V A A A F G A D G Y H V D S V E S F S A A L
A Q A L A H N R P A C I N V A V A L D P I P P E E L I L I G M D P F A

2.8 Expression vector of *Pf*BAL

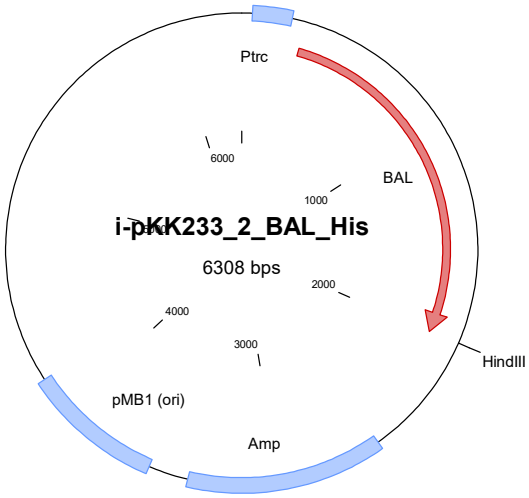

2.9 DNA-sequence of the pKK233_2 vector containing the gene encoding for *Pf*BAL

vector DNA (grey), start and stop codon of the *pfbal*-ORF (red), *Pf*BAL gen (black), His-Tag (brown), restrictions sites (blue)

AATTCTCATGTTTGACAGCTTATCATCGACTGCACGGTGCACCAATGCTTCTGGCGTCAG
GCAGCCATCGGAAGCTGTGGATTGGCTGTGCAGGTCGTAAATCACTGCATAATTCGTGTC
GCTCAAGGCGCACTCCCGTTCTGGATAATGTTTTTTGCGCCGACATATAAACGGTTCTGG
CAAATATTCTGAAATGAGCTGTTGACAATTAATCATCCGGCTCGTATAATGTGTGGAATT
GTGAGCGGATAACAATTTCACACAGGAAACAGACCATGGCGATGATTACAGGCGGCGAAC
TGGTTGTTCGCACCCTAATAAAGGCTGGGGTCGAACATCTGTTCGGCCTGCACGGCGCGC

ATATCGATACGATTTTTCAAGCCTGTCTCGATCATGATGTGCCGATCATCGACACCCGCC
ATGAGGCCGCCGCAGGGCATGCGGCCGAGGGCTATGCCCGCGCTGGCGCCAAGCTGGGCG
TGGCGCTGGTCACGGCGGGCGGGGGATTTACCAATGCGGTCACGCCCATTGCCAACGCTT
GGCTGGATCGCACGCCGGTGCTCTTCCTCACCGGATCGGGCGCGCTGCGTGATGATGAAA
CCAACACGTTGCAGGCGGGGATTGATCAGGTCGCCATGGCGGCGCCCATTACCAAATGGG
CGCATCGGGTGATGGCAACCGAGCATATCCCACGGCTGGTGATGCAGGCGATCCGCGCCG
CGTTGAGCGCGCCACGCGGGCCGGTGTTGCTGGATCTGCCGTGGGATATTCTGATGAACC
AGATTGATGAGGATAGCGTCATTATCCCCGATCTGGTCTTGTCCGCGCATGGGGCCAGAC
CCGACCCTGCCGATCTGGATCAGGCTCTCGCGCTTTTGCGCAAGGCGGAGCGGCCGGTCA
TCGTGCTCGGCTCAGAAGCCTCGCGGACAGCGCGCAAGACGGCGCTTAGCGCCTTCGTGG
CGGCGACTGGCGTGCCGGTGTTTGCCGATTATGAAGGGCTAAGCATGCTCTCGGGGCTGC
CCGATGCTATGCGGGGCGGGCTGGTGCAAAACCTCTATTCTTTTGCCAAAGCCGATGCCG
CGCCAGATCTCGTGCTGATGCTGGGGGCGCGCTTTGGCCTTAACACCGGGCATGGATCTG
GGCAGTTGATCCCCCATAGCGCGCAGGTCATTCAGGTCGACCCTGATGCCTGCGAGCTGG
GACGCCTGCAGGGCATCGCTCTGGGCATTGTGGCCGATGTGGGTGGGACCATCGAGGCTT
TGGCGCAGGCCACCGCGCAAGATGCGGCTTGGCCGGATCGCGGCGACTGGTGCGCCAAAG
TGACGGATCTGGCGCAAGAGCGCTATGCCAGCATCGCTGCGAAATCGAGCAGCGAGCATG
CGCTCCACCCCTTTCACGCCTCGCAGGTCATTGCCAAACACGTCGATGCAGGGGTGACGG
TGGTAGCGGATGGTGCGCTGACCTATCTCTGGCTGTCCGAAGTGATGAGCCGCGTGAAAC
CCGGCGGTTTTCTCTGCCACGGCTATCTAGGCTCGATGGGCGTGGGCTTCGGCACGGCGC
TGGGCGCGCAAGTGGCCGATCTTGAAGCAGGCCGCCGCACGATCCTTGTGACCGGCGATG
GCTCGGTGGGCTATAGCATCGGTGAATTTGATACGCTGGTGCGCAAACAATTGCCGCTGA
TCGTCATCATCATGAACAACCAAAGCTGGGGGGCGACATTGCATTTCCAGCAATTGGCCG
TCGGCCCCAATCGCGTGACGGGCACCCGTTTGGAAAATGGCTCCTATCACGGGGTGGCCG
CCGCCTTTGGCGCGGATGGCTATCATGTCGACAGTGTGGAGAGCTTTTCTGCGGCTCTGG
CCCAAGCGCTCGCCCATAATCGCCCCGCCTGCATCAATGTCGCGGTCGCGCTCGATCCGA
TCCCGCCCGAAGAACTCATTCTGATCGGCATGGACCCCTTCGGATCTCATCACCATCACC
ATCACTAAGCTTCTAGAGGATCCAGCTTGGCTGTTTTGGCGGATGAGAGAAGATTTTCAG
CCTGATACAGATTAAATCAGAACGCAGAAGCGGTCTGATAAAACAGTTTGCCTGGCGGCA
GTAGCGCGGTGGTCCCACCTGACCCCATGCCGAACTCAGAAGTGAAACGCCGTAGCGCCG
ATGGTAGTGTGGGGTCTCCCCATGCGAGAGTAGGGAACTGCCAGGCATCAAATAAAACGA
AAGGCTCAGTCGAAAGACTGGGCCTTTCGTTTTATCTGTTGTTTGTCGGTGAACGCTCTC
CTGAGTAGGACAAATCCGCCGGGAGCGGATTTGAACGTTGCGAAGCAACGGCCCGGAGGG
TGGCGGGCAGGACGCCCGCCATAAACTGCCAGGCATCAAATTAAGCAGAAGGCCATCCTG
ACGGATGGCCTTTTTGCGTTTCTACAAACTCTTTTTGTTTATTTTTCTAAATACATTCAA
ATATGTATCCGCTCATGAGACAATAACCCTGATAAATGCTTCAATAATATTGAAAAAGGA
AGAGTATGAGTATTCAACATTTCCGTGTCGCCCTTATTCCCTTTTTTGCGGCATTTTGCC
TTCCTGTTTTTGCTCACCCAGAAACGCTGGTGAAAGTAAAAGATGCTGAAGATCAGTTGG
GTGCACGAGTGGGTTACATCGAACTGGATCTCAACAGCGGTAAGATCCTTGAGAGTTTTC
GCCCCGAAGAACGTTTTCCAATGATGAGCACTTTTAAAGTTCTGCTATGTGGCGCGGTAT
TATCCCGTGTTGACGCCGGGCAAGAGCAACTCGGTCGCCGCATACACTATTCTCAGAATG
ACTTGGTTGAGTACTCACCAGTCACAGAAAAGCATCTTACGGATGGCATGACAGTAAGAG
AATTATGCAGTGCTGCCATAACCATGAGTGATAACACTGCGGCCAACTTACTTCTGACAA
CGATCGGAGGACCGAAGGAGCTAACCGCTTTTTTGCACAACATGGGGGATCATGTAACTC
GCCTTGATCGTTGGGAACCGGAGCTGAATGAAGCCATACCAAACGACGAGCGTGACACCA
CGATGCCTGTAGCAATGGCAACAACGTTGCGCAAACTATTAACTGGCGAACTACTTACTC
TAGCTTCCCGGCAACAATTAATAGACTGGATGGAGGCGGATAAAGTTGCAGGACCACTTC
TGCGCTCGGCCCTTCCGGCTGGCTGGTTTATTGCTGATAAATCTGGAGCCGGTGAGCGTG
GGTCTCGCGGTATCATTGCAGCACTGGGGCCAGATGGTAAGCCCTCCCGTATCGTAGTTA
TCTACACGACGGGGAGTCAGGCAACTATGGATGAACGAAATAGACAGATCGCTGAGATAG
GTGCCTCACTGATTAAGCATTGGTAACTGTCAGACCAAGTTTACTCATATATACTTTAGA
TTGATTTAAAACTTCATTTTTAATTTAAAAGGATCTAGGTGAAGATCCTTTTTGATAATC
TCATGACCAAAATCCCTTAACGTGAGTTTTCGTTCCACTGAGCGTCAGACCCCGTAGAAA
AGATCAAAGGATCTTCTTGAGATCCTTTTTTTCTGCGCGTAATCTGCTGCTTGCAAACAA
AAAAACCACCGCTACCAGCGGTGGTTTGTTTGCCGGATCAAGAGCTACCAACTCTTTTTC
CGAAGGTAACTGGCTTCAGCAGAGCGCAGATACCAAATACTGTCCTTCTAGTGTAGCCGT
AGTTAGGCCACCACTTCAAGAACTCTGTAGCACCGCCTACATACCTCGCTCTGCTAATCC
TGTTACCAGTGGCTGCTGCCAGTGGCGATAAGTCGTGTCTTACCGGGTTGGACTCAAGAC
GATAGTTACCGGATAAGGCGCAGCGGTCGGGCTGAACGGGGGGTTCGTGCACACAGCCCA
GCTTGGAGCGAACGACCTACACCGAACTGAGATACCTACAGCGTGAGCTATGAGAAAGCG
CCACGCTTCCCGAAGGGAGAAAGGCGGACAGGTATCCGGTAAGCGGCAGGGTCGGAACAG
GAGAGCGCACGAGGGAGCTTCCAGGGGGAAACGCCTGGTATCTTTATAGTCCTGTCGGGT

TTCGCCACCTCTGACTTGAGCGTCGATTTTTGTGATGCTCGTCAGGGGGGCGGAGCCTAT
GGAAAAACGCCAGCAACGCGGCCTTTTTACGGTTCCTGGCCTTTTGCTGGCCTTTTGCTC
ACATGTTCTTTCCTGCGTTATCCCCTGATTCTGTGGATAACCGTATTACCGCCTTTGAGT
GAGCTGATACCGCTCGCCGCAGCCGAACGACCGAGCGCAGCGAGTCAGTGAGCGAGGAAG
CGGAAGAGCGCCTGATGCGGTATTTTCTCCTTACGCATCTGTGCGGTATTTCACACCGCA
TATGGTGCACTCTCAGTACAATCTGCTCTGATGCCGCATAGTTAAGCCAGTATACACTCC
GCTATCGCTACGTGACTGGGTCATGGCTGCGCCCCGACACCCGCCAACACCCGCTGACGC
GCCCTGACGGGCTTGTCTGCTCCCGGCATCCGCTTACAGACAAGCTGTGACCGTCTCCGG
GAGCTGCATGTGTCAGAGGTTTTCACCGTCATCACCGAAACGCGCGAGGCAGCTGCGGTA
AAGCTCATCAGCGTGGTCGTGAAGCGATTCACAGATGTCTGCCTGTTCATCCGCGTCCAG
CTCGTTGAGTTTCTCCAGAAGCGTTAATGTCTGGCTTCTGATAAAGCGGGCCATGTTAAG
GGCGGTTTTTTCCTGTTTGGTCACTTGATGCCTCCGTGTAAGGGGGAATTTCTGTTCATG
GGGGTAATGATACCGATGAAACGAGAGAGGATGCTCACGATACGGGTTACTGATGATGAA
CATGCCCGGTTACTGGAACGTTGTGAGGGTAAACAACTGGCGGTATGGATGCGGCGGGAC
CAGAGAAAAATCACTCAGGGTCAATGCCAGCGCTTCGTTAATACAGATGTAGGTGTTCCA
CAGGGTAGCCAGCAGCATCCTGCGATGCAGATCCGGAACATAATGGTGCAGGGCGCTGAC
TTCCGCGTTTCCAGACTTTACGAAACACGGAAACCGAAGACCATTCATGTTGTTGCTCAG
GTCGCAGACGTTTTGCAGCAGCAGTCGCTTCACGTTCGCTCGCGTATCGGTGATTCATTC
TGCTAACCAGTAAGGCAACCCCGCCAGCCTAGCCGGGTCCTCAACGACAGGAGCACGATC
ATGCGCACCCGTGGCCAGGACCCAACGCTGCCCGAGATGCGCCGCGTGCGGCTGCTGGAG
ATGGCGGACGCGATGGATATGTTCTGCCAAGGGTTGGTTTGCGCATTCACAGTTCTCCGC
AAGAATTGATTGGCTCCAATTCTTGGAGTGGTGAATCCGTTAGCGAGGTGCCGCCGGCTT
CCATTCAGGTCGAGGTGGCCCGGCTCCATGCACCGCGACGCAACGCGGGGAGGCAGACAA
GGTATAGGGCGGCGCCTACAATCCATGCCAACCCGTTCCATGTGCTCGCCGAGGCGGCAT
AAATCGCCGTGACGATCAGCGGTCCAGTGATCGAAGTTAGGCTGGTAAGAGCCGCGAGCG
ATCCTTGAAGCTGTCCCTGATGGTCGTCATCTACCTGCCTGGACAGCATGGCCTGCAACG
CGGGCATCCCGATGCCGCCGGAAGCGAGAAGAATCATAATGGGGAAGGCCATCCAGCCTC
GCGTCGCGAACGCCAGCAAGACGTAGCCCAGCGCGTCGGCCGCCATGCCGGCGATAATGG
CCTGCTTCTCGCCGAAACGTTTGGTGGCGGGACCAGTGACGAAGGCTTGAGCGAGGGCGT
GCAAGATTCCGAATACCGCAAGCGACAGGCCGATCATCGTCGCGCTCCAGCGAAAGCGGT
CCTCGCCGAAAATGACCCAGAGCGCTGCCGGCACCTGTCCTACGAGTTGCATGATAAAGA
AGACAGTCATAAGTGCGGCGACGATAGTCATGCCCCGCGCCCACCGGAAGGAGCTGACTG
GGTTGAAGGCTCTCAAGGGCATCGGTCGACGCTCTCCCTTATGCGACTCCTGCATTAGGA
AGCAGCCCAGTAGTAGGTTGAGGCCGTTGAGCACCGCCGCCGCAAGGAATGGTGCATGCA
AGGAGATGGCGCCCAACAGTCCCCCGGCCACGGGGCCTGCCACCATACCCACGCCGAAAC
AAGCGCTCATGAGCCCGAAGTGGCGAGCCCGATCTTCCCCATCGGTGATGTCGGCGATAT
AGGCGCCAGCAACGGCACCTGTGGCGCCGGTGATGCCGGCCACGATGCGTCCGGCGTAGA
GGATCCGG

2.10 Amino acid sequence of soluble *Pf*BAL

***Pf*BAL** gen (black), His-Tag (brown), restrictions sites (blue)

M A M I T G G E L V V R T L I K A G V E H L F G L H G A H I D T I F Q A C L
D H D V P I I D T R H E A A A G H A A E G Y A R A G A K L G V A L V T A G G
G F T N A V T P I A N A W L D R T P V L F L T G S G A L R D D E T N T L Q A
G I D Q V A M A A P I T K W A H R V M A T E H I P R L V M Q A I R A A L S A
P R G P V L L D L P W D I L M N Q I D E D S V I I P D L V L S A H G A R P D
P A D L D Q A L A L L R K A E R P V I V L G S E A S R T A R K T A L S A F V
A A T G V P V F A D Y E G L S M L S G L P D A M R G G L V Q N L Y S F A K A
D A A P D L V L M L G A R F G L N T G H G S G Q L I P H S A Q V I Q V D P D
A C E L G R L Q G I A L G I V A D V G G T I E A L A Q A T A Q D A A W P D R
G D W C A K V T D L A Q E R Y A S I A A K S S S E H A L H P F H A S Q V I A
K H V D A G V T V V A D G A L T Y L W L S E V M S R V K P G G F L C H G Y L
G S M G V G F G T A L G A Q V A D L E A G R R T I L V T G D G S V G Y S I G

E F D T L V R K Q L P L I V I I M N N Q S W G A T L H F Q Q L A V G P N R V
T G T R L E N G S Y H G V A A A F G A D G Y H V D S V E S F S A A L A Q A L
A H N R P A C I N V A V A L D P I P P E E L I L I G M D P F G S H H H H H H

2.11 Long-term stability measurement in buffer

Stability of the soluble *Pf*BAL and the CatIBs were analyzed after incubation in TEA-buffer (50 mM, pH 7.5, 2.5 mM $MgSO_4$, 0.5 mM ThDP) at 30°C and 1000 rpm. Therefore, 0.6 mg ml^{-1} protein (calculated based on the protein content) of each enzyme (weight: 14.47 mg *Pf*BAL, 9.92 mg TDoT-*Pf*BAL, 41.76 mg 3HAMP-*Pf*BAL) was incubated in 600 µl volume in polypropylene reaction tubes (1.5 ml safe-lock tube, Eppendorf, Germany) and sampled at different points in time (0 h, 4 h, 24 h, 48 h, 72 h) to determine the initial rate activity (see sect. 4.7 in the main paper). Therefore the enzyme solutions were respectively diluted. This stability assay was performed as single measurement.

2.12 Solvent selection for the micro-aqueous reaction system

To select an optimal organic solvent, the conversion of the carboligation reaction of 100 mM 3,5-dimethoxybenzaldehyde (DMBA) by 0.6 U ml^{-1} TDoT-*Pf*BAL was measured (2.89 mg ml^{-1} protein concentration). Therefor micro-aqueous systems were prepared by adding 5 vol% TEA-buffer (1 M, pH 8, 2.5 mM $MgSO_4$, 0.1 mM ThDP) to 5 different organic solvents (cyclopentyl methyl ether (CPME), methyl *tert*-butyl ether (MTBE), cyclohexanone, dimethyl carbonate, 2-methyltetrahydrofuran). First the CatIBs were suspended in buffer and then the organic solvent containing the substrate was added. The reaction was performed in a volume of 1 ml in 2 ml glass reaction tubes (G1 clear, CS-Chromatographie Service GmbH, Germany) at 30 °C und 1400 rpm in a thermomixer (Thermomixer comfort, Eppendorf, Germany). 20 µl samples were taken from the organic phase after 1 h and 17.5 h, and were diluted 1:10 in 180 µl 2-methyltetrahydrofuran, thoroughly mixed and centrifuged at 15800 x *g* for 1 min (Centrifuge 5424, Eppendorf, Germany). Subsequently, 20 µl sample from the supernatant was diluted 1:10 in 180 µl n-heptane (incl. 4.3 mM acetophenone as internal standard), which was analyzed by HPLC (see sect. 4.13 in the main paper). To analyze evaporation effects, control samples were prepared in the same manner without CatIBs. Each solvent was tested once.

2.13 Optimization of the buffer content in the biphasic reaction system

The buffer content was optimized between 1 vol% - 20 vol% TEA-buffer (1 M, pH 8, 2.5 mM MgSO4, 0.1 mM ThDP) added to either MTBE or CPME. The carboligation reaction of 50 mM DMBA was measured catalyzed by 0.6 U ml-1 TDoT-PfBAL (2.9 mg ml-1 protein concentration). The reaction was performed as described in sect. 2.12, 20 µl samples taken at different points in time, were prepared as described in sect. 2.12, and analyzed by HPLC (see sect. 4.13 in the main paper). These reactions were performed in duplicate.

2.14 Determination of the reaction equilibrium in the biphasic reaction system

The reaction equilibrium was measured by the cleavage of 32 mM (R)-3,3′,5,5′-tetramethoxy benzoin (TMBZ) catalyzed by 6 U ml-1 3HAMP-PfBAL (1.1 mg ml-1 protein concentration) in 30 vol% TEA-buffer (50 mM, pH 8, 2.5 mM MgSO4, 0.1 mM ThDP) in CPME. The reaction was performed as described in sect. 2.12. 20 µl

samples taken after 1 h and, were prepared as described in sect. 2.12 , and analyzed by HPLC (see sect. 4.13 in the main paper). These reactions were performed in as single measurement.

3 Results

3.1 Live cell images

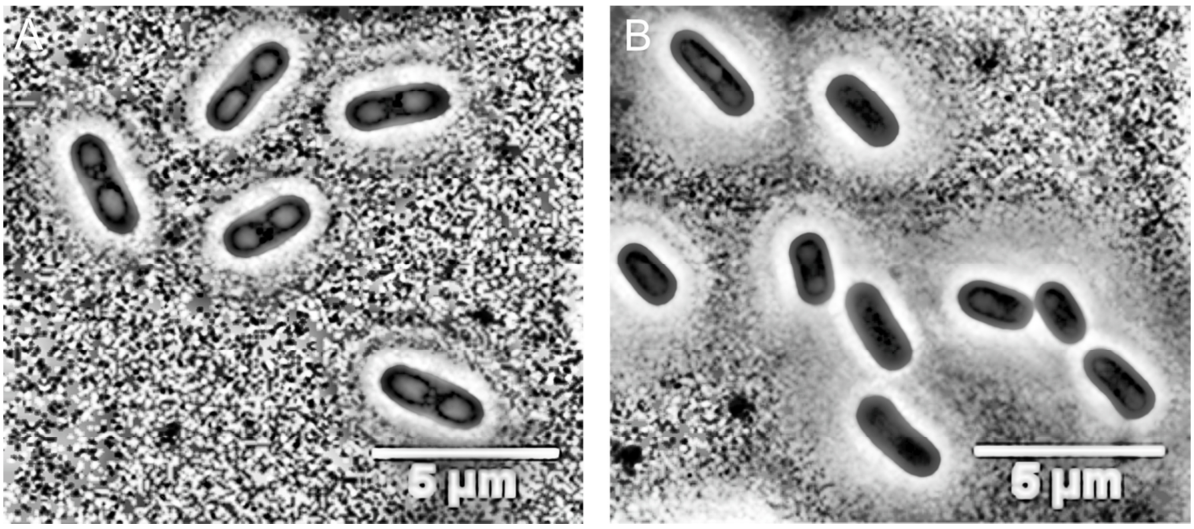

Figure S1: Live cell images of *E. coli* BL21(DE3) cells containing *Pf*BAL-CatIBs. A: TDoT-*Pf*BAL, B: 3HAMP-*Pf*BAL. Images were recorded using an inverted epifluorescence microscope in phase-contrast (see sect. 4.5 in the main paper) For better visualization the pictures were modified by image equalization with CorelDraw X6, version 16.0.0.707. 3HAMP-*Pf*BAL yielded rather diffuse particles at the cell poles, which are less clearly visible in unmodified phase-contrast images (main paper, Figure 1B). The corresponding particles can however be clearly detected after local image equalization (B), which involves increasing the contrast by resetting the darkest and lightest points and then evenly distributing the values across those two points.

3.2 Stability in buffer

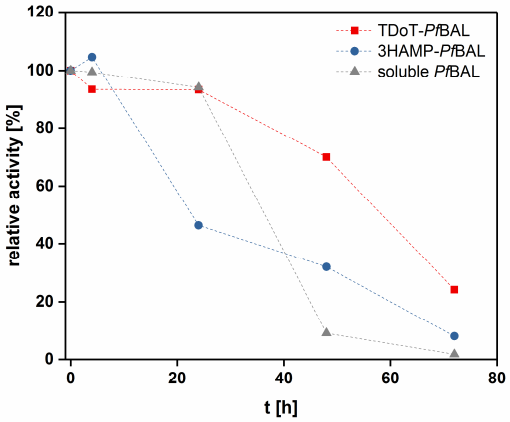

Figure S2: Stability of soluble *Pf*BAL, TDot-*Pf*BAL and 3HAMP-*Pf*BAL incubated in 50 mM TEA-buffer (pH 7.5). Incubation conditions: 50 mM TEA-buffer (pH 7.5, 2.5 mM $MgSO_4$, 0.5 mM ThDP), protein concentration for all enzyme variants: 0.6 mg ml^{-1}, 1000 rpm, T = 30 °C , V = 1 ml; n = 1. After distinct points in time, the initial rate activity was measured. For experimental details see ESI sect.2.11. The half-lives decreased in the order TDoT-*Pf*BAL (57 h) > soluble *Pf*BAL (36 h) > 3HAMP-*Pf*BAL (23 h) and were estimated based on the deactivation curve.

3.3 EMR experiments

3.3.1 Overview of results obtained in EMR experiments

Table S4: Half-life and residual (*R*)-benzoin in the reaction chamber of *Pf*BAL, TDoT-*Pf*BAL, and 3HAMP-*Pf*BAL-CatIBs determined based on the experiments shown in Figure S5, Figure 3 in the main paper. Half-lives were taken from the curve at 50% conversion from benzaldehyde to (*R*)-HPP. For experimental details see sect. 4.8 in the main paper. The residual (*R*)-benzoin was determined by transferring the whole suspension from the reaction chamber into a glass vessel, where methyltetrahydrofuran (m-THF) was added to the water-phase. The water-phase was extracted by m-THF. The reaction chamber was washed with m-THF and pooled with the m-THF phase. Finally the (*R*)-benzoin concentration in the m-THF phase was measured by HPLC and the amount of (*R*)-benzoin was calculated based on the measured concentration and the respective m-THF volume.

pH	reaction system	enzyme	half-life [h]	residual (*R*)-benzoin [mg] in the reaction chamber	(*R*)-benzoin conversion [%] in the reaction chamber calculated based on the total benzaldehyde amount (n/n)
7.5	buffer	TDoT-*Pf*BAL	48	n.d.	n.d.
		3HAMP-*Pf*BAL	10	n.d.	n.d.
		*Pf*BAL	7	7.2	2.5
7.5	30 vol% DMSO in buffer	TDoT-*Pf*BAL	131	n.d.	n.d.
		3HAMP-*Pf*BAL	59	0.036	0.0054
		*Pf*BAL	92	114.3	7.2
9.0	30 vol% DMSO in buffer	TDoT-*Pf*BAL	3	157.3	57.1
		3HAMP-*Pf*BAL	13	n.d.	n.d.
		*Pf*BAL	16	148.0	16.8

3.3.2 Absorption of benzaldehyde and (*R*)-HPP during the EMR experiments

Due to gaps in the mass balance and a maximum conversion of 80% (compare sect. 2.2 in the main paper), the absorption of benzaldehyde and (*R*)-HPP by the PEEK-(polyether ether ketone)-reactor material was tested in the EMR under reaction conditions (30 °C and 300 rpm, 10 kDa membrane) in TEA-buffer or the buffer-DMSO system with 30 vol% DMSO. Therefore, either a benzaldehyde (30 mM) or (*R*)-HPP (30 mM) solution was pumped through the reactor under conditions given in sect. 4.8 in the main paper in the absence of enzyme. After pumping overnight, samples of the efflux (direct at the output, without storage) and the reaction chamber were taken (Figure S3) and analyzed by HPLC (see sect. 4.13 in the main paper). Furthermore, samples were collected in open glass test tubes by a fraction collector, which were stored for the given period under the hood for evaporation analysis (Figure S4). In Figure S3 the relative difference between the initial concentration in the substrate reservoir and in the efflux or reaction chamber are shown in a box plot to visualize the significance of the differences compared to 0 (no difference). The whiskers indicate the minimum and maximum of the data set and the upper and lower quartiles 25% and 75%. Furthermore, outliers, the median and mean are given, whereas the median refers to the middle value of the data set and the mean is calculated by summarizing all values divided by the number of values. If the box (upper and lower quartiles) is on the doted zero line, the difference can be considered as not significant, so that there is no significant absorption of benzaldehyde or (*R*)-HPP by the

reactor material, as can be seen in all cases for the buffer-DMSO system. However, in the buffer system without DMSO, benzaldehyde and (*R*)-HPP were absorbed by the reactor material.

The open glass test tubes containing benzaldehyde or (*R*)-HPP solution were stored over different periods in time under the hood, which results in a more distinct evaporation of benzaldehyde in the buffer system without DMSO (A) than with 30 vol% DMSO (B) (Figure S4). The (*R*)-HPP concentration increased over a longer storage period due to evaporation of the solvent, which is more distinct for the buffer system without DMSO. (*R*)-HPP does not evaporate in both reaction systems.

Table S5 shows the absorption of benzaldehyde by polypropylene (PP) reaction tubes over the time.

Table S5: Absorption of benzaldehyde by polypropylene (PP) reaction tubes (1.5 ml safe-lock tube, Eppendorf, Germany) after different incubation times. Benzaldehyde (33.5 mM) was dissolved in TEA-buffer (50 mM, pH 7.5, 2.5 mM $MgSO_4$, 0.5 mM ThDP) in a glass flask and 500 µl were transferred into a PP reaction tube and incubated with closed lid at room temperature without shaking. Subsequently, the concentration of benzaldehyde in the PP tube was determined by HPLC (sect. 4.13 in the main paper) after 2, 5 and 10 min. Errors correspond to the standard deviation of the mean obtained from technical triplicate.

time (min)	benzaldehyde (mM)	standard deviation (%)
0	33.5	
2	31.0	7.4
5	30.9	7.8
10	30.9	7.8

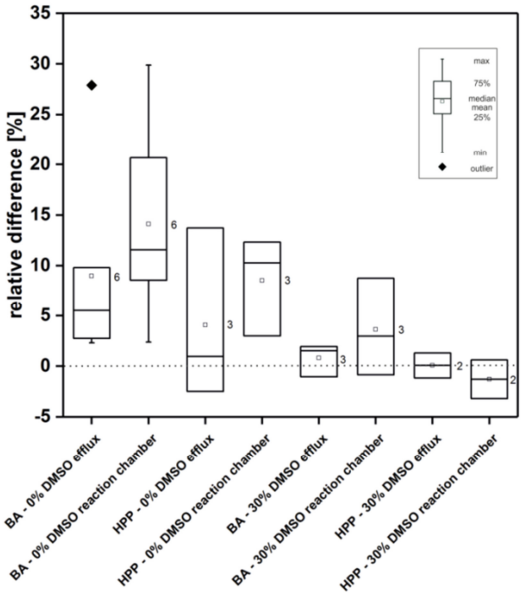

Figure S3: Absorption of benzaldehyde (BA) and (*R*)-2-hydroxy-1-phenylpropanone (HPP) by the PEEK (polyether ether ketone) material of the enzyme membrane reactor. Conditions: 30 mM benzaldehyde or 30 mM (*R*)-HPP in TEA-buffer (50 mM, pH 7.5, 2.5 mM $MgSO_4$, 0.5 mM ThDP), in the presence and absence of 30 vol% DMSO, 300 rpm, T = 30 °C , $V_{reactor}$ = 3 ml, residence time: 30 min, flow: 0.1 ml min^{-1}, membrane: regenerated cellulose (YM10 Milipore, 10 kDa cut-off). The number of repetitions is given next to the box. For experimental details see sect. 4.8 in the main paper.

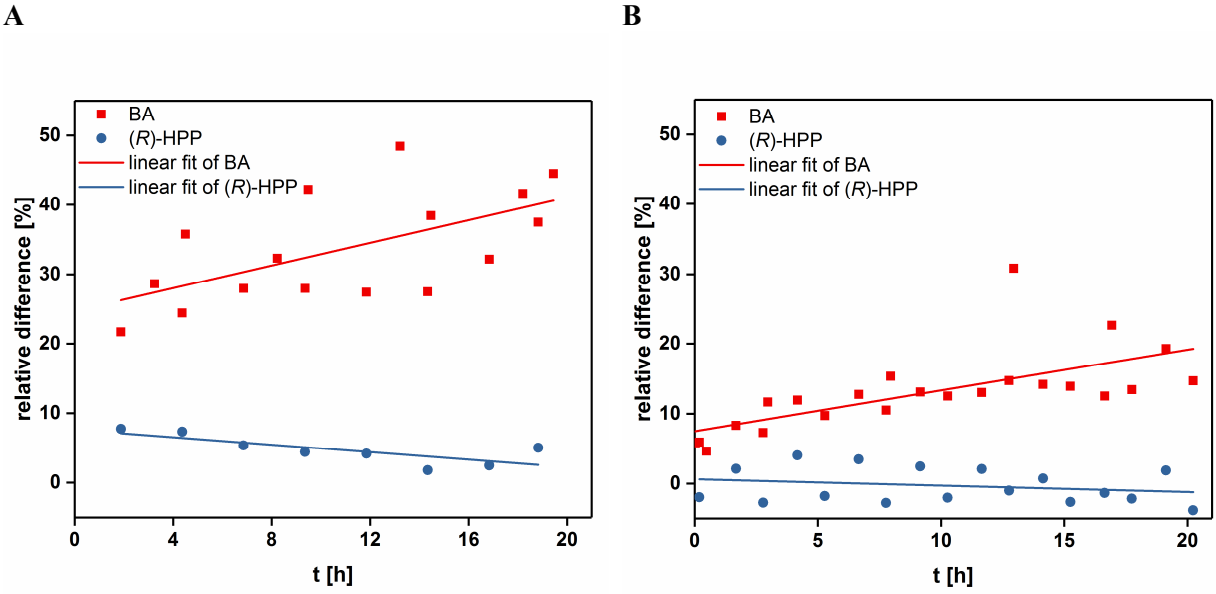

Figure S4: Evaporation of benzaldehyde (BA) and (R)-2-hydroxy-1-phenylpropanone (HPP) dissolved in TEA-buffer (A) without DMSO and (B) with 30 vol% DMSO after being pumped through the enzyme membrane reactor and stored in open glass test tubes over a time period. Conditions: 30 mM benzaldehyde or 30 mM HPP in TEA-buffer (50 mM, pH 7.5, 2.5 mM MgSO4, 0.5 mM ThDP), in the presence and absence of 30 vol% DMSO, 300 rpm, T = 30 °C , Vreactor = 3 ml, residence time: 30 min, flow: 0.1 ml min-1, PEEK (polyether ether ketone) - enzyme membrane reactor (EMR) with regenerated cellulose membrane (YM10 Milipore, 10 kDa cut-off); n = 1-3. For experimental details see sect. 4.8 in the main paper.

3.3.3 EMR experiment in the buffer-DMSO system at pH 9

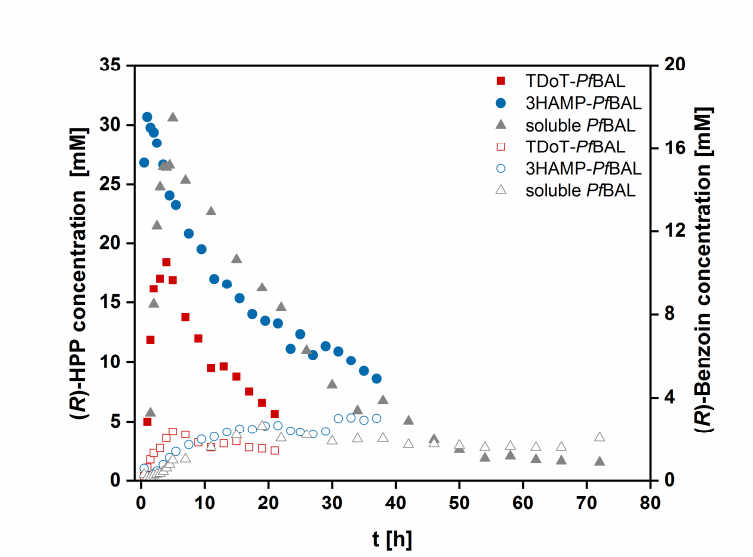

Figure S5: Carboligation of benzaldehyde and acetaldehyde to (*R*)-2-hydroxy-1-phenylpropanone (HPP) in an EMR catalyzed by *Pf*BAL, TDoT-*Pf*BAL, and 3HAMP-*Pf*BAL-CatIBs, respectively. Filled symbols refer to (*R*)-HPP and empty symbols to (*R*)-benzoin concentration. Half-life was deduced from the point in time where 50 % conversion to (*R*)-HPP (approx. 15 mM) was reached. Reaction conditions: 30 mM benzaldehyde, 90 mM acetaldehyde, TEA-buffer (50 mM, pH 9, 2.5 mM $MgSO_4$, 0.5 mM ThDP), 30 vol% DMSO, 28 U ml^{-1} protein concentrations of the enzymes: TDoT-*Pf*BAL (56.8 mg ml^{-1}), 3HAMP-*Pf*BAL (5.9 mg ml^{-1}), *Pf*BAL (0.94 mg ml^{-1}), 300 rpm, T = 30 °C , $V_{reactor}$ = 3 ml, residence time: 30 min, flow: 0.1 ml min^{-1}, PEEK (polyether ether ketone) - enzyme membrane reactor (EMR) with regenerated cellulose membrane (YM10 Milipore, 10 kDa cut-off); n = 1. For experimental details see sect. 4.8 in the main paper. The halve-lives decreased in the order *Pf*BAL (16 h) >3HAMP-*Pf*BAL (13 h) > TDoT-*Pf*BAL (3 h) and were taken from at 50% conversion from benzaldehyde to (*R*)-HPP.

3.4 Results in the biphasic reaction system

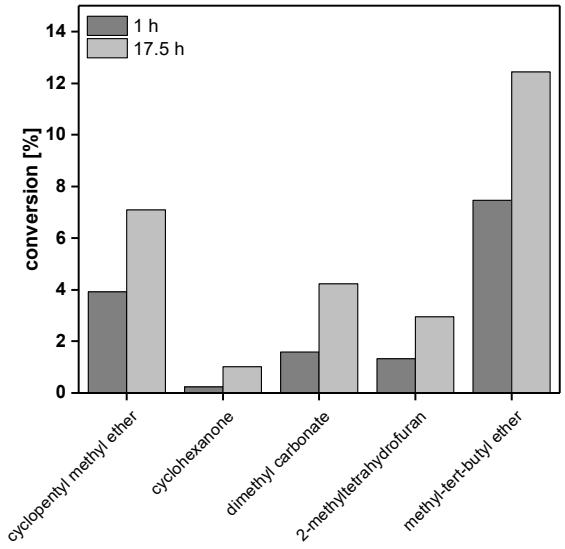

Figure S6: Solvent screening in the micro-aqueous reaction system for the carboligation of DMBA to TMBZ using TDot-*Pf*BAL-CatIBs. Reactions of DMBA to TMBZ were performed in the respective organic solvents (cyclopentyl methyl ether (CPME), cyclohexanone, dimethyl carbonate, 2-methyltetrahydrofuran, methyl *tert*-butyl ether (MTBE)) with 5 vol% TEA-buffer (1 M, pH 8, 2.5 mM $MgSO_4$, 0.1 mM ThDP), 100 mM DMBA, 0.6 U ml^{-1} TDoT-*Pf*BAL (2.9 mg ml^{-1} protein concentration) in 2 ml glass vials at T = 30°C, 1400 rpm, V = 1 ml, in a thermomixer, n = 1. For experimental details see sect. 2.12, n = 1.

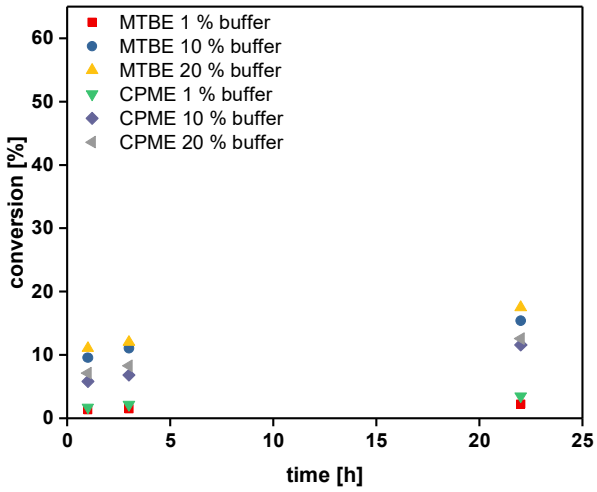

Figure S7: Optimization of the buffer content in MTBE/CPME in the aqueous-organic two-phase system for the carboligation of DMBA to TMBZ using TDoT-*Pf*BAL-CatIBs. Reactions were performed in CPME or MTBE with 1-20 vol% TEA-buffer (1 M, pH 8, 2.5 mM $MgSO_4$, 0.1 mM ThDP), 100 mM DMBA, 0.6 U ml^{-1} TDoT-*Pf*BAL (2.9 mg ml^{-1} protein concentration) in 2 ml glass vials at T = 30°C, 1400 rpm, V = 1 ml, in a thermomixer, n = 1. For experimental details see sect. 2.13. A higher buffer content of 20 vol% is necessary to obtain a higher conversion. Reaction in MTBE with 20 vol% buffer revealed the best results.

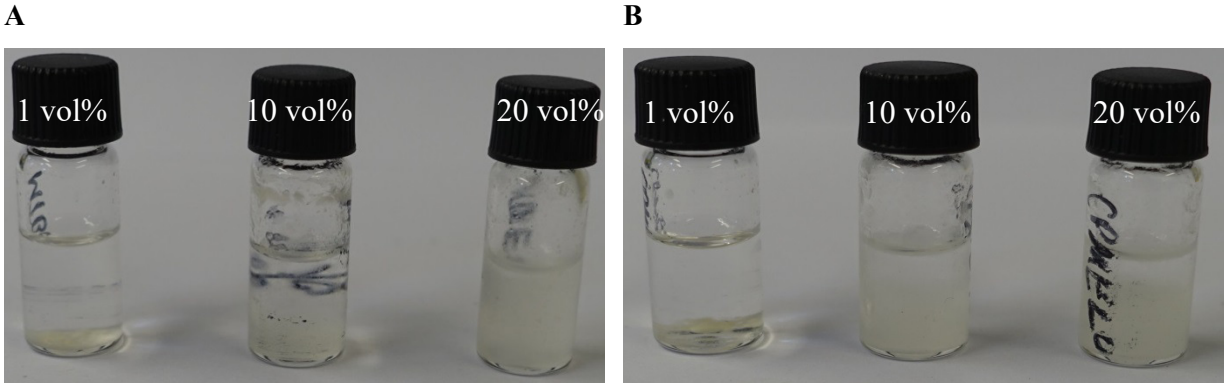

Figure S8: Emulsion formation of TDoT-PfBAL-CatIBs in MTBE (A) or CPME (B) with 1 vol% 10 vol%, or 20 vol% buffer (from left to right) in the aqueous-organic two-phase system after carboligation of DMBA to TMBZ. Reactions were performed in CPME or MTBE with 1-20 vol% TEA-buffer (1 M, pH 8, 2.5 mM MgSO4, 0.1 mM ThDP), 100 mM DMBA, 0.6 U ml-1 TDoT-PfBAL (2.9 mg ml-1 protein concentration) in 2 ml glass vials at T = 30°C, 1400 rpm, V = 1 ml, in a thermomixer, n = 1. For experimental details see sect.2.13.

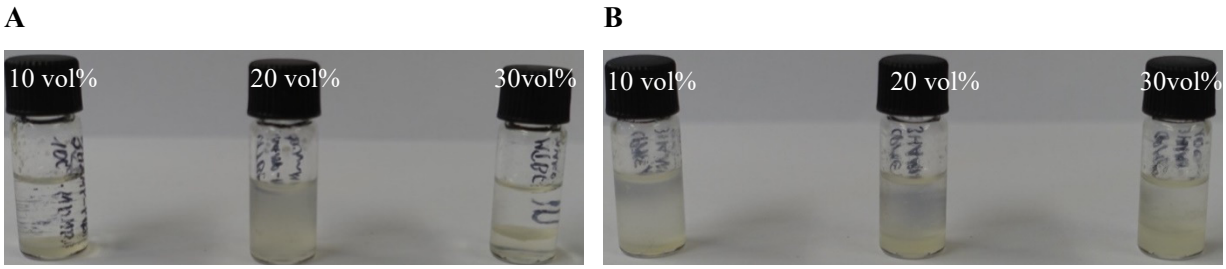

Figure S9: 3HAMP-PfBAL-CatIBs show emulsion formation in (A) MTBE and (B) CPME with 10 vol% 20 vol%, or 30 vol% buffer (from left to right). Carboligation reactions of DMBA to TMBZ were performed in MTBE with 10-30 vol% TEA-buffer (1 M, pH 8, 2.5 mM MgSO4, 0.1 mM ThDP), 50 mM DMBA, 6 U ml-1 3HAMP-PfBAL (1.1 mg ml-1 protein concentration) in 2 ml glass vials at T = 30°C, 1400 rpm, V = 1 ml, in a thermomixer. Image was recorded 24 h after the last measuring point. In between they were stored at room temperature without shaking. At 30 vol% buffer, an emulsion was formed after 0.5 hours of reaction. Since the photo was taken 24 hours later, the 3HAMP-PfBAL accumulated at the interface of the phases. n=1. For experimental details see sect. 2.13.

Table S6: Equilibrium constant K_{eq} for the carboligation of DMBA to TMBZ by 3HAMP-*Pf*BAL-CatIBs in a biphasic system with different DMBA concentrations. K_{eq} was calculated based on data presented in the given figures.

ESI-Figure no.	DMBA		TMBZ		
	start concentration [mM]	end concentration [mM]	start concentration [mM]	end concentration at [mM]	K_{eq} [mM^{-1}]
5A, main paper	50	25.0	0	12.5	0.02
5B, main paper	70	34.2	0	17.9	0.02
5C, main paper	85	46.8	0	19.1	0.01
S10	0	26.0	32	19.0	0.02

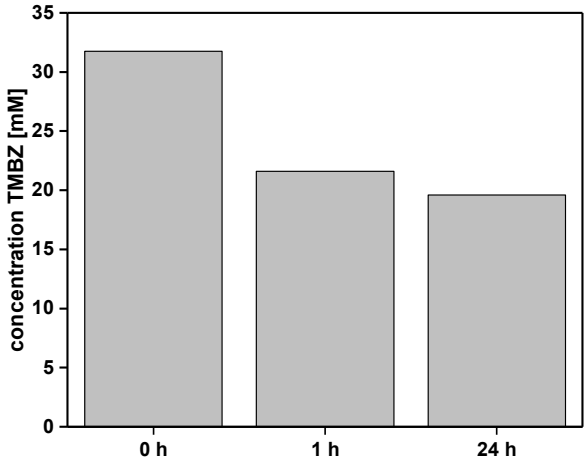

Figure S10: Analysis of the reaction equilibrium of TMBZ synthesis by 3HAMP-*Pf*BAL-CatIBs in the aqueous-organic two-phase system. The reaction equilibrium was determined by the conversion of 32 mM TMBZ to DMBA by 6 U ml^{-1} 3HAMP-*Pf*BAL (1.1 mg ml^{-1} protein concentration) in CPME with 30 vol% TEA-buffer (50 mM, pH 8, 2.5 mM $MgSO_4$, 0.1 mM ThDP), in 2 ml glass vial at T = 30°C, 1400 rpm, V = 1 ml, in a thermomixer, n = 1. For experimental details see sect. 2.14. It could be demonstrated that the reaction equilibrium is at about 50% conversion with a K_{eq} = 0.01 mM (compare Table S7)

Table S7: Initial rate actvitiy of the carboligation of benzaldehyde or DMBA to the respective benzoin catalyzed by 3HAMP-*Pf*BAL or soluble *Pf*BAL in biphasic reaction system. Conditions: 6 U ml^{-1} 3HAMP-PfBAL (0.84 mg ml^{-1} protein concentration), 2.6 U ml^{-1} PfBAL (0.34 mg ml^{-1} protein concentration), 70 mM benzaldehyde or 70 mM DMBA in 1 ml reaction volume composed of 30 vol% TEA-buffer (50 mM, 2.5 mM $MgSO_4$, 0.5 mM ThDP, pH 7.5); 70 vol% CPME, 1400 rpm, 30 °C, n = 3. Calculations are based on Figure 5 in the main paper. SD: standard deviation.

	3HAMP-*Pf*BAL		soluble *Pf*BAL	
	DMBA	benzaldehyde	DMBA	benzaldehyde
k_{cat} [s^{-1}]	4.1	2.6	1.4	2.0
SD	0.1	0.2	0.3	0.3

3.5 ^{1}H-NMR spectrum

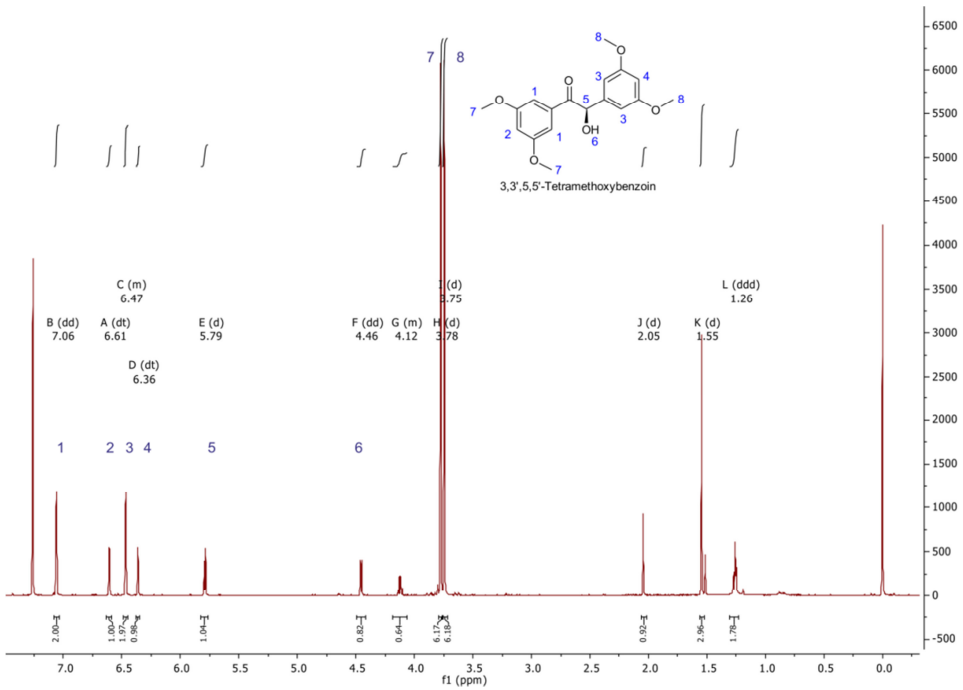

Figure S11: ^{1}H-NMR spectrum (600 MHz, $CDCl_3$) of (*R*)-3,3´,5,5´-tetramethoxy benzoin (TMBZ), which also includes 18.0-19.2 vol% ethyl acetate.

3.6 HPLC calibration curves and analysis

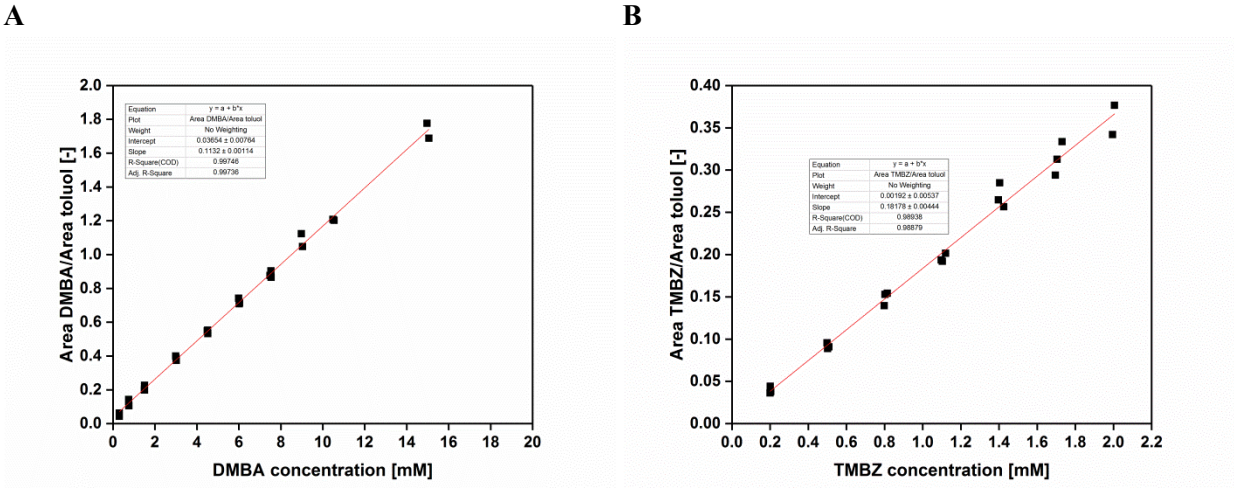

Figure S12: Calibration curve for (A) 3,5-dimethoxybenzaldehyde (DMBA) or (B) (R)-3,3‘,5,5‘-tetramethoxy benzoin (TMBZ) for initial rate determination. Conditions: (A) 4 mg TMBZ, (B) 25 mg DMBA was dissolved in 2 ml DMSO and samples were diluted with TEA-buffer (50 mM, pH 7.5, 2.5 mM MgSO4, 0.1 mM ThDP)and DMSO by the factor of 5, 5.9, 7.1, 9.1, 12.5 20 and 25 to final percentage of 80 vol% TEA-buffer and 20 vol% DMSO. 25 mg DMBA were dissolved in 1 ml DMSO and samples were diluted with TEA-buffer and DMSO by the factor of 5, 7.1, 8.3 10, 12.5, 16.7 25, 50, 100 and 125 to final percentage of 80 vol% TEA-buffer and 20 vol% DMSO Samples were diluted 1:10 with 180 µl methanol (incl. 4.7 mM toluene as internal standard) according to the protocol in sect. 4.7 in the main paper. HPLC analysis was performed with acetonitrile/water as the mobile phase (see sect. 4.13 in the main paper).

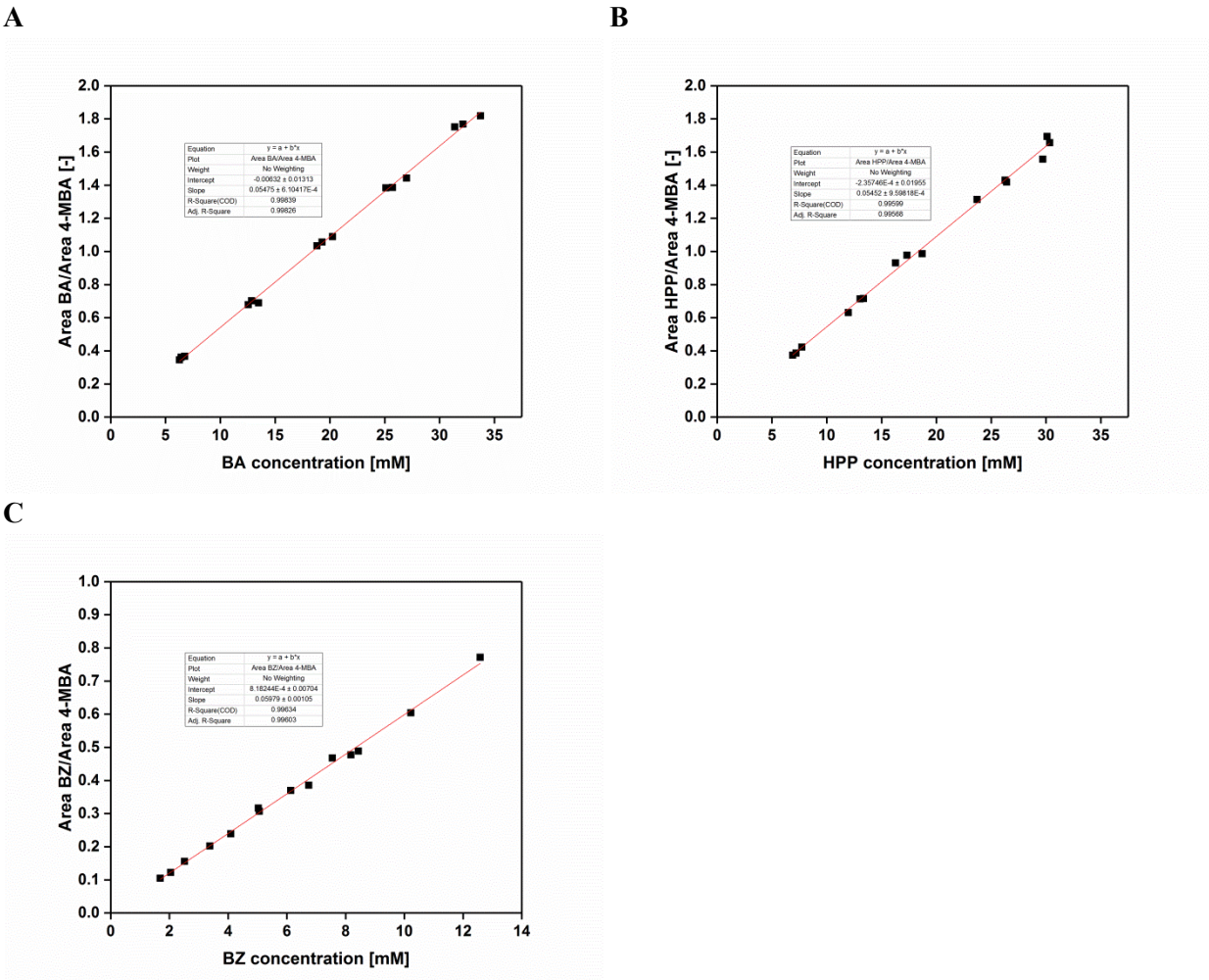

Figure S10: Calibration curve for (A) benzaldehyde (BA), (B) (R)-2-hydroxy-1-phenylpropanone (HPP), and (C) (R)-benzoin (BZ) to determine conversion in the EMR. Conditions: 17-18 mg BZ was dissolved in 5 ml TEA-buffer (50 mM, pH 7.5, 2.5 mM MgSO4, 0.1 mM ThDP) and diluted with TEA-buffer by the factor of 1.25, 1.66, 2.5 and 5. 2-9 mg HPP or 0.7-5.3 mg BZ were dissolved in 2 ml TEA-buffer. All samples werediluted 1:20 according to the protocol in sect. 4.8 in the main paper. HPLC analysis was performed with acetonitrile/water as the mobile phase (see sect. 4.13 in the main paper).

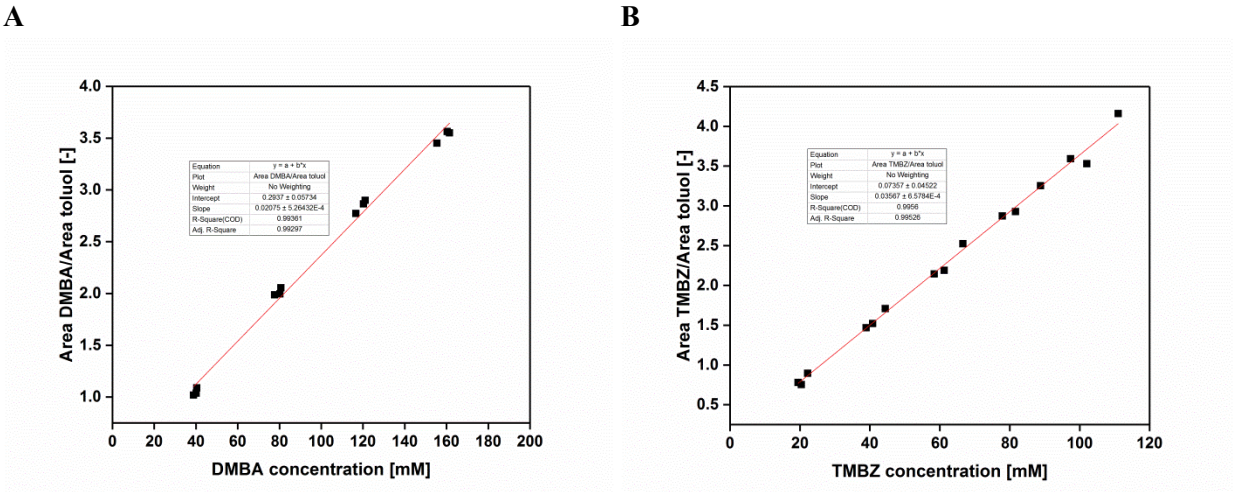

Figure S14: Calibration curve for (A) 3,5-dimethoxybenzaldehyde (DMBA) or B) (R)-(3,3‘,5,5‘)-tetramethoxy benzoin (TMBZ) to determe conversion in the biphasic batch system. Conditions: 33 mg DMBA and 38-44 mg TMBZ were dissolved in 1 ml 2-methyltetrahydrofuran and diluted with 2-methyltetrahydrofuran by the factor of 1.25, 1.66, 2.5 and 5. All amples were diluted 1:10 in 2-methyltetrahydrofuran, and 1:10 diluted in 180 µl n-heptane (incl. 4.3 mM acetophenone as internal standard) according to the protocol in sect. 4.9 in the main paper., HPLC analysis was performed with n-heptane/isopropanol as mobile phase (see sect. 4.13 in the main paper).

Table S8: HPLC conditions to determine substrate and (side-)product concentrations: 3,5-dimethoxybenzaldehyde (DMBA), (*R*)-(3,3‘,5,5‘)-tetramethoxy benzoin (TMBZ), (*R*)-2-hydroxy-1-phenylpropanone (HPP), benzaldehyde (BA) and (*R*)-benzoin (BZ) and the initial standards: toluene, 4-methoxybenzaldehyde (4-MBA), acetophenone. dd: double desalted; ACN: acetonitrile. For the gradient applied in the continuous reaction experiment see Table S10. For HPLC analysis see sect. 4.13 in the main paper)

		initial rate activity determination	**continuous reaction in an EMR**	**reaction in biphasic system**
mobile phase	A	50 vol% (dd) H_2O	gradient of (dd) H_2O	70 vol% *n*-heptane
	B	50 vol% ACN	gradient of ACN	30 vol% 2-propanol
	flow (ml min^{-1})	1.0	0.9	1.5
retention times (min)	DMBA (215 nm)	7.6		4.2
	TMBZ (215 nm)	9.4		11.8
	HPP (245 nm)		7.9	
	BA (245 nm)		9.4	
	BZ (245 nm)		13.8	
	toluol (215 nm)	6.9		
	4-MBA (270 nm)	6.1	11.9	
	acetophenone (215 nm)			3.5

Table S9: Gradient of the mobile phase for HPLC determination and separation of substrates/products during a continuous reaction in an EMR. A is double desalted (dd) H_2O and B acetonitrile (ACN). For HPLC analysis, see sect. 4.13 in the main paper).

time (min)	**A (%)**	**B (%)**
0-7	65	35
7-8	65-40	35-60
8-14	40	60
14-15	40-65	60-35
15-20	65	35

4 References

1. M. Diener, B. Kopka, M. Pohl, K.-E. Jaeger and U. Krauss, ChemCatChem, 2016, 8, 142–152.

2. E. Janzen, M. Müller, D. Kolter-Jung, M. M. Kneen, M. J. McLeish and M. Pohl, Bioorg. Chem., 2006, 34, 345–361.

3. F. W. Studier, Protein Expr. Purif., 2005, 41, 207–234.

2.3 Catalytically active inclusion bodies of L-lysine decarboxylase from *E. coli* for 1,5-diaminopentane production

Ramona Kloss[+], Michael H. Limberg[+], Ursula Mackfeld, Doris Hahn, Alexander Grünberger, Vera D. Jäger, Ulrich Krauss, Marco Oldiges, and Martina Pohl[*]

[+] These authors contributed equally to this work

[*] Corresponding author

published in Scientific Reports, 2018, 8(1), p. 5856,

https://www.nature.com/articles/s41598-018-24070-2

Context:

The application of *Ec*LDC-CatIBs was analyzed under technical conditions in culture supernatants of a *C. glutamicum* L-lysine producer strain at L-lysine concentrations of up to 1 M in (repetitive) batch. *Ec*LDC-CatIBs were proven to be competitive with other processes to produce cadaverine.

Contributions:

D. Hahn performed the construction of plasmids supervised by R. Kloss and U. Krauss, who planned the genetic construct. V. D. Jäger and U. Krauss supported CatIB preparation. U. Mackfeld performed production, purification, and characterization of the CatIBs and analyzed the data with the assistance of R. Kloss and M. H. Limberg, under coordination and supervision of M. Pohl. A. Grünberger performed live-cell imaging with the assistance of V. D. Jäger and R. Kloss. M. H. Limberg and R. Kloss performed microbial L-lysine production under the coordination and supervision of M. Oldiges. R. Kloss, M. H. Limberg, and M. Pohl wrote the manuscript with input from A. Grünberger, U. Krauss, and M. Oldiges.

www.nature.com/scientificreports

SCIENTIFIC REPORTS

OPEN

Catalytically active inclusion bodies of L-lysine decarboxylase from *E. coli* for 1,5-diaminopentane production

Received: 22 November 2017
Accepted: 26 March 2018
Published online: 11 April 2018

Ramona Kloss[1,4], Michael H. Limberg[1], Ursula Mackfeld[1], Doris Hahn[1], Alexander Grünberger[1,5], Vera D. Jäger[2,4], Ulrich Krauss[2,4], Marco Oldiges[1,3] & Martina Pohl[1,4]

Sustainable and eco-efficient alternatives for the production of platform chemicals, fuels and chemical building blocks require the development of stable, reusable and recyclable biocatalysts. Here we present a novel concept for the biocatalytic production of 1,5-diaminopentane (DAP, trivial name: cadaverine) using catalytically active inclusion bodies (CatIBs) of the constitutive L-lysine decarboxylase from *E. coli* (*Ec*LDCc-CatIBs) to process L-lysine-containing culture supernatants from *Corynebacterium glutamicum*. *Ec*LDCc-CatIBs can easily be produced in *E. coli* followed by a simple purification protocol yielding up to 43% dry CatIBs per dry cell weight. The stability and recyclability of *Ec*LDCc-CatIBs was demonstrated in (repetitive) batch experiments starting from L-lysine concentrations of 0.1 M and 1 M. *Ec*LDC-CatIBs exhibited great stability under reaction conditions with an estimated half-life of about 54 h. High conversions to DAP of 87–100% were obtained in 30–60 ml batch reactions using approx. 180–300 mg *Ec*LDCc-CatIBs, respectively. This resulted in DAP titres of up to 88.4 g l^{-1} and space-time yields of up to 660 g_{DAP} l^{-1} d^{-1} per gram dry *Ec*LDCc-CatIBs. The new process for DAP production can therefore compete with the currently best fermentative process as described in the literature.

An interpolation from the current state of the petrochemical industry and fossil-based energy supply to the next century predicts the exhaustion of fossil carbon sources, which can be attributed to an alarmingly rapid exploitation of limited natural deposits[1]. In particular, this applies to crude oil, due to the steadily growing demand[2,3]. Consequently, society will face a notable future price increase for fossil resources, which has already focused public interest on sustainable and eco-efficient alternatives. This has thus encouraged the biotechnology industry to develop processes for the sustainable production of platform chemicals, biofuels[4–6], and in particular bio-based polymers[4,7]. Increasing knowledge about the prokaryotic metabolism and ongoing developments in systems engineering pave the way for the development of microbial hosts also enabling the economic production of intermediates and bulk chemicals. However, to meet economic demand, it is necessary to develop innovative concepts and improved bioprocesses.

Biotechnological workhorses such as *Escherichia coli*, *Saccharomyces cerevisiae* and *Corynebacterium glutamicum* have been engineered to produce ω-amino acids[8], aromatic monomers[9], diamines[10–12], dicarboxylic acids[13–15], diols[16] and hydroxy acids[17], respectively. From this broad spectrum of building blocks for biopolymer production, the linear aliphatic diamine 1,5-diaminopentane (DAP) is probably one of the most attractive options. One reason is its ability to produce fully bio-based polyamides, such as PA 5.4 and PA 5.10, based on DAP and dicarboxylic acids such as succinate[13,18] and sebacic acid[19], respectively. PA 5.10, in particular, exhibits material properties comparable or even superior to the widely used petroleum-based polyamide PA 6[20].

One option for the biotechnological production of DAP is the use of engineered, well-established L-lysine producers, especially *C. glutamicum*[10,21–24] and *E. coli*[12,25–30]. *C. glutamicum* DAP-producer strains are usually created

[1]Forschungszentrum Jülich GmbH, IBG-1: Biotechnology, 52425, Jülich, Germany. [2]Institute of Molecular Enzyme Technology, Heinrich-Heine-Universität Düsseldorf, Forschungszentrum Jülich, 52425, Jülich, Germany. [3]RWTH Aachen University, Institute of Biotechnology, 52074, Aachen, Germany. [4]Bioeconomy Science Center (BioSC), c/o, Forschungszentrum Jülich, 52425, Jülich, Germany. [5]Multiscale Bioengineering, Bielefeld University, Universitätsstraße 25, 33615, Bielefeld, Germany. Ramona Kloss and Michael H. Limberg contributed equally to this work. Correspondence and requests for materials should be addressed to M.P. (email: ma.pohl@fz-juelich.de)

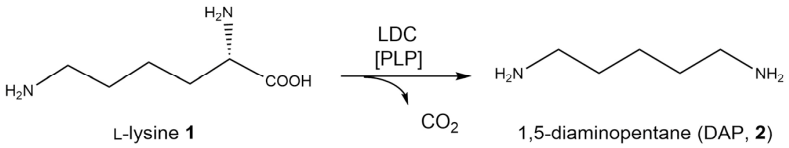

Figure 1. LDC-catalysed decarboxylation of L-lysine to DAP.

by the introduction of one of the L-lysine decarboxylase (LDC) genes from *E. coli* (*cadA*[21] or *ldcC*[10] encoding the acid-inducible enzyme CadA, and the constitutive LDCc, respectively), thus enabling the intracellular decarboxylation of the L-lysine (**1**) to DAP (**2**) (Fig. 1). Both enzymes are very similar (sequence similarity 84%)[31,32], require the cofactor pyridoxal-5′-phosphate (PLP), and appear as decamers composed of five dimers, as was deduced from cryo-electron microscopy[33] and X-ray crystallography[34].

Several constraints need to be tackled for fermentative microbial production, such as the tolerance of the microbial system with respect to DAP[35], the avoidance of by-products such as N-acetyl-1,5-diaminopentane[36] and the management of product export[37], which is no longer possible via the well-engineered lysine exporter LysE[38].

Another option for DAP production is the bioconversion of L-lysine by the addition of LDC to L-lysine containing culture supernatants. Here, immobilisation of the LDC enables easy separation from the reaction medium and recycling of the biocatalyst to decrease process costs. Different concepts have been employed for the immobilisation of LDC, e.g. using whole recombinant *E. coli* cells[25,27,29,39], immobilised recombinant *E. coli* cells in alginate beads[40,41], as well as immobilised LDC on poly(3-hydroxybutyrate) (P(3HB) biopolymer[42] or crosslinked enzyme aggregates (CLEAS) of LDC[43]. Generally, the bioconversions were performed in buffer and only in a few cases directly in culture supernatants of L-lysine producers[25,29].

Catalytically active inclusion bodies (CatIBs) represent biologically produced, cell-free and carrier-free immobilisates that can easily be produced in *E. coli* cells[44–47]. They are a simple and cheap alternative to common immobilisates, which require a case-to-case optimisation of several, often expensive and laborious, steps, including chromatographic purification of the enzyme followed by covalent or non-covalent immobilisation concepts in the presence or absence of carriers[48,49]. The production of immobilised enzymes directly *in vivo* could reduce the production costs of the biocatalyst to the level of crude cell extracts[50], since the insoluble cell fraction can be directly used for biotransformations. Furthermore, CatIB-based biotransformations are free of genetically modified organisms (GMO-free), since any remaining vital recombinant *E. coli* cells can be efficiently inactivated and separated during the production process[51].

Active inclusion bodies can be formed either naturally by self-aggregation of the enzyme[46,52] or by fusion to a tag containing an aggregation-prone part, e.g. cellulose binding domains[53–56], pyruvate oxidase (PoxB) of *Paenibacillus polymyxa*[57], the viral capsid protein VP1, the human Aβ-amyloid peptide[58] or various self-assembling peptides[59,60]. For a detailed overview of the state of the art in this field we refer to a recent review[47]. We previously evaluated the tetramerisation domain of the cell-surface protein tetrabrachion (known as TDoT) from *Staphylothermus marinus*[61] for its potential to induce CatIB formation. The TDoT domain has a rope-like structure forming a stable parallel tetrameric coiled coil[61]. Previous studies have demonstrated that the fusion of the TDoT domain to various enzymes of different complexity resulted in all cases in the formation of CatIBs, which implies that the TDoT-domain is a promising new fusion tag to induce the formation of active inclusion bodies[62].

We here report on an innovative immobilisation approach using CatIBs of the constitutive L-lysine decarboxylase (*Ec*LDCc) and the application of this GMO-free approach to produce DAP in L-lysine-containing culture supernatants. In this study, we demonstrate that this approach also works for the complex PLP-dependent decameric *Ec*LDCc. This enzyme was chosen instead of the frequently used CadA mainly because of the broader pH optimum of *Ec*LDCc (pH 6.2–8) compared to CadA (pH 5.7)[63]. This property makes *Ec*LDCc advantageous for application in L-lysine-containing culture supernatants of the respective *C. glutamicum* producer strains, which exhibit pH values in the range of 6 to 8.5[64,65].

The respective *Ec*LDCc-CatIBs were produced in *E. coli* and successfully applied in culture supernatants of a *C. glutamicum* lysine producer with lysine concentrations of up to 1 M to demonstrate the applicability of this approach on the preparative scale. Under optimised conditions, 74.7–88.4 $g\,l^{-1}$ DAP was produced with 10 $g\,l^{-1}$ dry *Ec*LDCc-CatIBs with a space-time yield of 296–660 $g_{DAP}\,l^{-1}\,d^{-1}$ per gram dry *Ec*LDC-CatIBs (see Table 1).

Results and Discussion

Production of *Ec*LDCc-CatIBs. The gene encoding the constitutive *Ec*LDCc was introduced into a pET28 vector already containing the gene sequences encoding the coiled-coil domain TDoT and an additional 3xGGGS linker region as described elsewhere[62]. Based on the quaternary structure of *Ec*LDCc, the TDoT domain was fused to the C-terminus, since the N-terminus is located within the protein structure[33].

*Ec*LDCc-CatIBs could be easily produced in *E. coli* BL21(DE3) using an auto-induction medium (see Sect. 5.3). The formation of *Ec*LDCc-CatIBs in the respective recombinant *E. coli* cells was demonstrated with inverted epifluorescence microscopy[66,67] showing the CatIBs as bright spots at the cell poles (Fig. 2), which is typical of the deposition of recombinant proteins as inclusion bodies in *E. coli*[68].

A previously developed protocol[62] was further optimised for the purification of *Ec*LDCc-CatIBs (see Fig. 3, left). After two washing steps with water followed by centrifugation, the pellet containing the CatIBs and some cell membrane fractions was lyophilised, yielding 130 ± 37 mg dry CatIBs per gram of wet cells (approx. 13% of

Reference	Present study				Ref[23]
Reaction mode	**repetitive batch**	**repetitive batch**	**batch conversion**		**batch cultivation**
Reaction volume [ml]	$9 \times 60 = 540$	60	30	30	300[2]
Total reaction time [h]	69	4	24	9	50
Temperature [°C]	30	30	30	30	30
PLP [M]	0.0001	0.0001	0.0001	0.0001	—
PLP [mol]	$5.4\ 10^{-5}$	$5.4\ 10^{-5}$	$0.3\ 10^{-5}$	$0.3\ 10^{-5}$	—
L-Lys [M]	0.1	0.1	1	1	—
Total L-Lys [mol]	0.054	0.006	0.03	0.03	—
Total L-Lys [g]	7.89	0.88	4.39	4.39	—
DAP [M]	0.083[1]	0.098	0.87	0.73	0.86
DAP [$g\ l^{-1}$]	8.47	9.99	88.4	74.7	88
Total DAP [g]	4.57[1]	0.599	2.65	2.24	n.d.[2]
Total DAP [mol]	0.0447	0.0059	0.026	0.0219	n.d.[2]
*Ec*LDCc-CatIB [mg ml^{-1}]	3	3	10	10	—
Total amount of dry biocatalyst [mg]	180 (CatIBs)	180 (CatIBs)	300 (CatIBs)	300 (CatIBs)	n.d.[2] (*C. glutamicum)*
Respective WCW of *E. coli* for biocatalyst production [g][3]	1.4	1.4	2.3	2.3	—
Enzymatic productivity $g_{DAP}/g_{biocatalyst}$	25	3.33	8.8	7.5	n.d.[2]
STY [$g\ l^{-1}\ d^{-1}$]	2.94	—	89	198	52.8
STY [$g\ l^{-1}\ d^{-1}$] per g dry CatIBs	16	—	296	660	—
STY [$g\ l^{-1}\ d^{-1}$] per $g_{E.\ coli(WCW)}$	2.1	—	38	86	—
TTN [$mol_{DAP}\ mol_{PLP}^{-1}$]	547–994	978	8,667	7,300	—

Table 1. Productivity measures for the production of DAP. [1]Calculated over all batches. [2]300 ml start volume (no i.nformation concerning final volume available). [3]Refers to previous line.

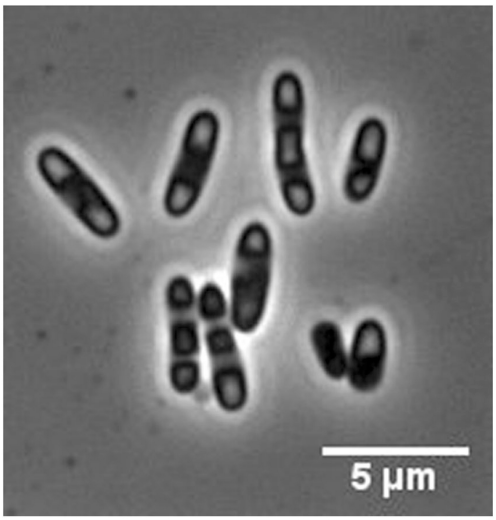

Figure 2. Live cell images of *E. coli* BL21(DE3) cells containing *Ec*LDCc-CatIBs. For details see Supplementary "Live cell imaging."

the wet cell weight, corresponding to 43% dry CatIBs based on dry cell weight). The protein content of the pellet was about 68%, which is comparable to previous results obtained with other CatIB enzymes[62]. The production process was monitored by sodium dodecyl sulfate-polyacrylamide gel electrophoresis (SDS-PAGE, Fig. 3, right) showing that the *Ec*LDCc-TDoT fusion is predominantly present in the pellet. Due to the simple purification protocol (see Methods), further cellular proteins co-purified with the CatIBs were expected, as was also reported for other inclusion body formulations[69].

The activity of the *Ec*LDCc-CatIBs was demonstrated in potassium phosphate buffer (KPi buffer) and cultivation medium (CGXII)[64] (Supplementary Fig. S2). Additionally, the CatIBs were compared to an *E. coli* whole cell biocatalyst containing the overproduced soluble LDCc. The results demonstrate that *Ec*LDCc-CatIBs can compete with the whole cell biocatalyst (for details see Supplementary Fig. S7a,b). Subsequently, the *Ec*LDCc-CatIBs

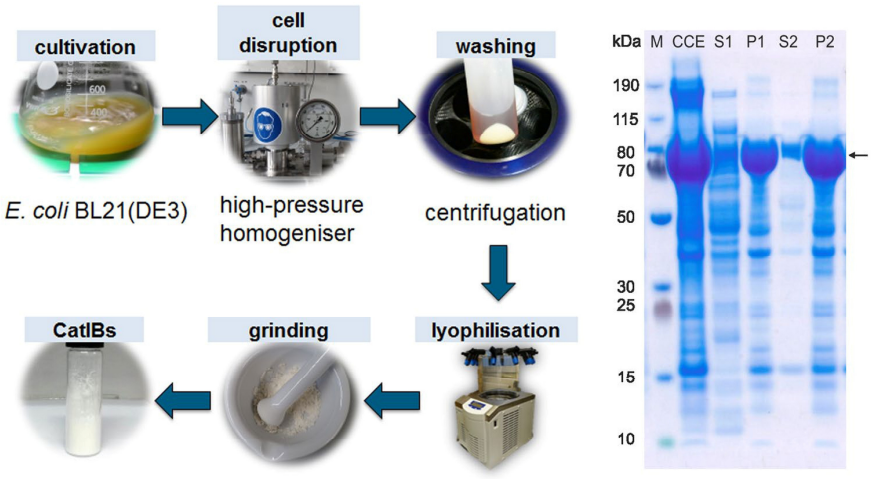

Figure 3. Left: Production and purification of *Ec*LDCc-CatIBs produced in *E. coli* BL21(DE3). Right: SDS-PAGE analysis of the *Ec*LDCc-CatIB preparation (calculated molecular weight: 87.8 kDa, arrow); CCE = crude cell extract, which was centrifuged to separate the supernatant (S1) from the pellet (P1). The pellet P1 was washed once with MilliQ water by resuspension and subsequent centrifugation, resulting in S2 and P2; the protein concentration was measured using the Bradford assay (see Methods). For SDS-PAGE, samples were diluted with water to a protein concentration of 1 mg ml^{-1} by the following dilution factors: 4 for CCE, 2 for S1 and P1, 4.5 for P2; 1 for S2; M = Marker. For details see Methods.

were characterised in CGXII medium and used for a case study under technical conditions in culture supernatants of a *C. glutamicum* L-lysine producer strain.

Characterisation of *Ec*LDCc-CatIBs. *Activity in phosphate buffer.* In a first step, the *Ec*LDCc-CatIBs were characterised in KPi buffer to determine the pH optimum in the pH range of 7–9 and the minimal requirement for PLP.

As already mentioned in the Introduction, the soluble wild-type *Ec*LDCc is active in a relatively broad pH range exhibiting maximal activity between pH 6.2 and pH 8, whereas at pH 8.8 the activity was shown to decrease to 30%[63]. As demonstrated in Fig. 4, *Ec*LDCc-CatIBs showed considerable activity between pH 7.5–9.0 with a clear activity maximum at pH 8. Furthermore, addition of the cofactor PLP was decisive in achieving optimal enzyme activity. Generally, the activity increased by 5–15% in the presence of the cofactor (Fig. 4). Strikingly, at pH 9 the positive PLP effect was approximately 35%. In additional studies, a PLP concentration of 0.05 mM was found to be sufficient for maximal activity of the *Ec*LDCc-CatIBs in buffer (see Supplementary Fig. S3). A similar positive effect of PLP on the LDC activity was recently reported for the second isoenzyme in *E. coli*, the acid-inducible CadA overproduced in recombinant *E. coli*, which was used as a whole-cell biocatalyst. In this case, full conversion of 1 M L-lysine to DAP was observed in the presence of 0.025 mM PLP, whereas without additional PLP only 20% conversion was achieved[29].

Activity in CGXII minimal medium. To verify the applicability of *Ec*LDCc-CatIBs at the preparative scale, DAP production was tested in CGXII cultivation medium providing an experimental setup close to requirements on the technical scale.

First, the optimal pH was determined between pH 7.0–9.0 in fresh CGXII medium with 0.1 mM PLP and 10 mM L-lysine. *Ec*LDCc-CatIBs revealed the highest conversion between pH 8–9, showing a maximum at 8.5 (see Supplementary Fig. S4), which closely corresponds to the pH optimum in KPi buffer (Fig. 4). To ensure comparability, all subsequent experiments were performed at pH 8 providing excellent conditions for *Ec*LDCc-CatIBs in CGXII medium as well as KPi buffer.

In technical processes, L-lysine concentrations of up to 120 g l^{-1} (820 mM) are expected[22]. Therefore, *Ec*LDCc-CatIBs were tested in (repetitive) batch reactions with substrate concentrations of up to 1 M L-lysine. In initial studies with 10–100 mM L-lysine, a concentration of 2 mg ml^{-1} *Ec*LDCc-CatIBs was shown to be sufficient to completely convert 100 mM L-lysine to DAP in 4 h (Fig. 5). Notably, the estimated activity increased from approx. 0.3 U mg^{-1} (10 mM L-lysine) to approx. 0.8 U mg^{-1} (100 mM L-lysine), giving rise to the conclusion that the maximum velocity (V_{max}) of the CatIBs requires a L-lysine concentration of 100 mM or higher. Under the applied conditions, *Ec*LDCc-CatIBs exhibited half-maximum activity at approx. 23 mM L-lysine. This value is much higher compared to the K_M value of 0.84 mM published for the soluble enzyme[70], which was determined under different reaction conditions (soluble *Ec*LDCc in 0.5 M sodium acetate buffer, pH 5.5), which makes a comparison of K_M values meaningless. However, the enormously increased K_M for the CatIBs could indicate a form of mass transport limitation of the substrate or product in the environment of the precipitated protein structure

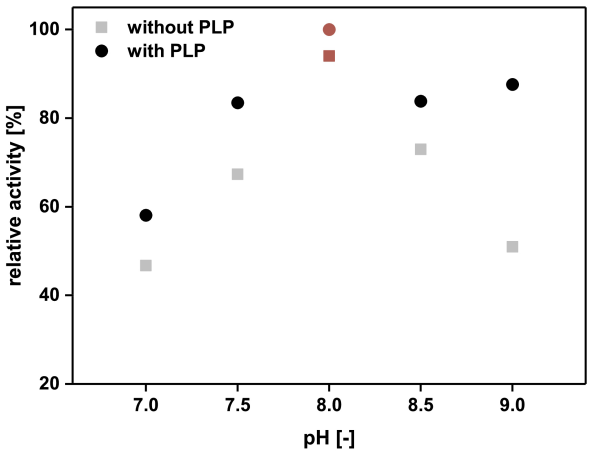

Figure 4. pH optimum of *Ec*LDCc-CatIBs for the decarboxylation of L-lysine in the presence (0.1 mM) and without additional PLP. For assay conditions see Methods. 100% relative activity refers to 0.34 U mg^{-1}_{CatIBs}, which corresponds to 0.52 U $mg^{-1}_{protein}$.

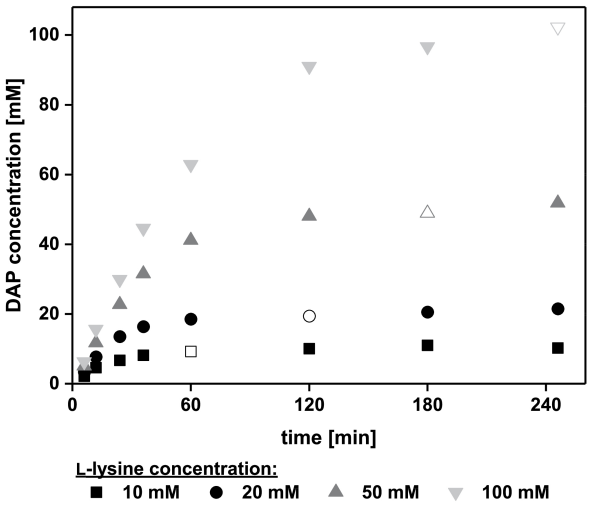

Figure 5. Conversion curves of the *Ec*LDCc-CatIB-catalysed decarboxylation of different L-lysine concentrations to DAP in CGXII medium. Empty symbols indicate the point in time at which full conversion was reached. 2 mg ml^{-1} lyophilised *Ec*LDCc-CatIBs. For details see Methods.

of the CatIBs. The highest enzymatic productivity of 4.9 g_{DAP} $g_{LDC\text{-}CatIBs}{}^{-1}$ (48 $mmol_{DAP}$ $g_{LDC\text{-}CatIBs}{}^{-1}$) was achieved with 100 mM L-lysine in these first studies.

Application of EcLDC-CatIBs for the production of DAP. Subsequently, *Ec*LDC-CatIBs were characterised in CGXII medium containing L-lysine produced by a *C. glutamicum* DM1945 strain[71].

In the first trial, *Ec*LDCc-CatIBs were directly added to the cultivation medium to enable the simultaneous production of L-lysine followed by decarboxylation to DAP in one pot. Surprisingly, only low yields of DAP were obtained, although PLP was added to the cultivation medium. This result could be due to the degradation of PLP by photolysis or oxidation[72] or consumption of the cofactor by *C. glutamicum*, which was earlier reported by Kind *et al.*, who studied the positive effect of adding PLP to the cultivation broth of a *C. glutamicum* DAP producer strain[10]. A further reason could be the low apparent affinity of *Ec*LDCc-CatIBs to L-lysine (K_M approx. 23 mM) as discussed above, which results in low conversion rates at substrate concentrations <100 mM.

In order to circumvent this issue, the lysine-producing cultivation of *C. glutamicum* DM1945 was first completed in CGXII medium. The cell-free culture supernatant was further supplemented with L-lysine to 0.1 M and 0.1 mM PLP.

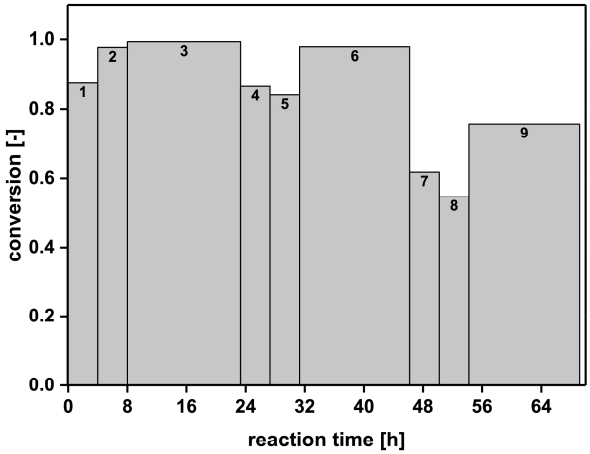

Figure 6. Repetitive batches for the production of DAP with *Ec*LDCc-CatIBs with pH-control. Experimental conditions: 3 mg ml^{-1} lyophilised *Ec*LDCc-CatIBs, 0.1 M L-lysine, 0.1 mM PLP in 60 ml cell-free culture supernatant (CGXII medium, pH 8). Two 4 h batches (batch 1, 2, 4, 5, 7, 8) were followed by 15 h overnight batches (3, 6, 9) on three subsequent days.

The initially performed determination of the stability of *Ec*LDC-CatIBs in this reaction system, as well as their continued application in repetitive batch mode, shows that *Ec*LDCc-CatIBs are fully stable for at least 24 h and can be recycled several times (for details see Supplementary Fig. S5). In repetitive batch mode, the CatIBs were reused after centrifugation and resuspension for five batch cycles, resulting in a productivity of 19.4 g_{DAP} $g_{LDC\text{-}CatIBs}^{-1}$ (190 $mmol_{DAP}$ $g_{LDC\text{-}CatIBs}^{-1}$), which is 4 times higher compared to a single batch (Fig. 5).

Based on these promising results, a repetitive batch on the 60 mL scale with 0.1 M L-lysine was set up in a pH-controlled environment, which was necessary since the reaction products CO_2 and DAP shift the pH. The nine-batch cycles took either 4 or 15 hours. The results of the repetitive batch experiment revealed a constant high conversion of 84–98% during the first 46 h (Fig. 6). The first two repetitive batches (each lasting 4 h) showed almost full conversions of 90–98%. Also the 3rd batch reaction (performed for 15 h) yielded full conversion. After 54 h reaction time (batch 8) the half-life of the *Ec*LDC-CatIBs has almost been achieved, since the conversion decreased to 54%. After 69 h reaction time, the 9th batch (lasting 15 h) only reached 76% conversion, demonstrating that 15 h reaction time was not sufficient to compensate the progressive inactivation. By means of the repetitive batch approach, the enzymatic productivity was increased to 25 $g_{DAP}/g_{LDC\text{-}CatIBs}$ (Table 1), which is 7.5 times higher compared to a single 60 ml batch reaction (e.g. 2nd batch: 3.33 g_{DAP} $g_{LDC\text{-}CatIBs}^{-1}$), yielding a final DAP concentration of 8.47 g l^{-1}, a specific space-time yield (STY) of 16 g_{DAP} l^{-1} d^{-1} per gram *Ec*LDCc-CatIBs, and a total turnover number (ttn) for PLP of up to 994. This experiment showed that the *Ec*LDCc-CatIBs could be reused for several cycles for at least 69 hours under the applied conditions.

To apply the *Ec*LDCc-CatIBs under the requirements on a technical scale, where L-lysine concentrations of up to 1 M are converted to DAP[22,29], the application was next tested in a batch reaction (30 ml) with 1 M L-lysine, which resulted in 87% conversion after approx. 24 h (Fig. 7). The specific activity of 0.75 U mg^{-1}, deduced from conversions $\leq$10%, was comparable to the reaction velocity observed with 100 mM L-lysine (see above), which indicates that there is no substrate inhibition for *Ec*LDCc-CatIBs up to 1 M L-lysine. Although the enzymatic productivity was reduced to 30% (8.8 g_{DAP} g^{-1}_{CatIBs}) compared to the previous repetitive batch experiments with 100 mM L-lysine, due to the higher concentration of CatIBs, the STY was increased 180-fold to 296 g_{DAP} l^{-1} d^{-1} per gram *Ec*LDC-CatIBs. As demonstrated in Fig. 7, the reaction slowed down after a process time of 9 h and between 9 h and 24 h conversion only increased by about 10%. The analysis of the reasons for the slowdown of the reaction requires further investigation. One possibility could be inactivation of the enzyme by negative effects caused by the pH-adjustment with NaOH and HCl or due to high concentrations of DAP, which could be targeted by reaction engineering. If the high DAP concentration is the reason for deactivation of the enzyme, stopping the reaction after 9 h would be a good option (Fig. 7). This would result in a more than twofold higher specific space-time yield of 660 g_{DAP} l^{-1} d^{-1} per gram *Ec*LDC-CatIBs. Accordingly, the ttn for the cofactor PLP was increased by a factor of 10 relative to the repetitive batch with 0.1 M L-lysine (see Table 1). Consequently, a 10 times higher product concentration was reached in one third of the time (24 h) needed for the repetitive batch mode using 0.1 M L-lysine.

Conclusions

The development of cheap, stable, reusable and recyclable biocatalysts is necessary for the prospective creation of competitive sustainable and eco-efficient production processes for platform chemicals, fuels, and polymer building blocks. One promising approach to fulfil industrial demands in terms of productivity, yield, and product titre is the application of whole-cell biotransformation[50] e.g. using resting or metabolically active microbial cells. However, the drawbacks of this approach are productivity issues, e.g. due to undesired side reactions, negative

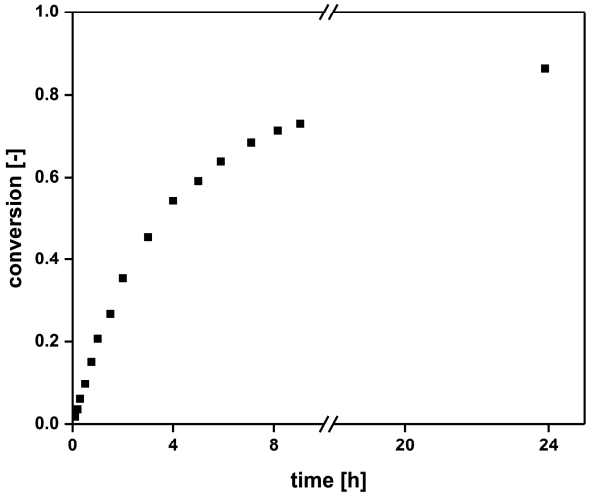

Figure 7. Conversion curve for the production of DAP with *Ec*LDCc-CatIBs in a 30 ml batch reactor with pH control. Experimental conditions: 10 mg ml^{-1} lyophilised *Ec*LDCc-CatIBs, 1 M L-lysine, 0.1 mM PLP, in 30 ml cell-free culture supernatant (CGXII medium, pH 8). For the dosage profile with NaOH and HCl, respectively, to keep the pH constant see Supplementary Fig. S6.

interactions of substrates and products with the microorganism as well as difficulties in downstream processing caused by lysed cells under process conditions. Furthermore, the application of genetically modified organisms (GMO) requires conformity with the respective safety standards. In contrast to whole cells, the preparation of catalytically active inclusion bodies (CatIBs) requires only a few additional steps (cell disruption, solid/liquid separation, washing with water) and thus represents a versatile and cheap GMO-free immobilisation method.

Here we demonstrate the application of CatIBs for the production of 1,5-diaminopentane (DAP) using the constitutive decameric and PLP-dependent lysine decarboxylase from *E. coli* (*Ec*LDCc). Currently, this represents the structurally most complex enzyme in our CatIB toolbox[62].

*Ec*LDCc-CatIBs can be produced with high yields (about 13% dry CatIBs based on the wet cell weight, equivalent to 43% dry CatIBs based on dry cell weight) at low cost comparable to crude cell extract[50]. A two-step process was applied whereby L-lysine is produced first through a *C. glutamicum* producer strain and the culture supernatant is subsequently treated with *Ec*LDCc-CatIBs to produce DAP. Maximal conversion rates were obtained with L-lysine concentrations of 0.1–1 M. As was found for soluble *Ec*LDCc[73] and whole cell catalysts[27,29], the addition of PLP was decisive for optimal CatIB activity. After optimisation of the reaction conditions, a study on a preparative scale demonstrated that *Ec*LDCc-CatIBs are recyclable and stable biocatalysts for DAP production directly applicable in L-lysine-containing culture supernatant. The *Ec*LDCc-CatIBs were successfully reused by simple centrifugation and resuspension steps. Starting from 1 M L-lysine, a maximal DAP concentration of 74.7–88.4 g l^{-1} and a specific STY of up to 296–660 g_{DAP} l^{-1} d^{-1} per gram *Ec*LDC-CatIBs were obtained (see Table 1). This result compares well with the currently best fermentative process using *C. glutamicum*, which also achieved a final titre of 88 g l^{-1} DAP after 50 hours of a combined batch/fed-batch fermentation, but a STY of only 52.8 g l^{-1} d^{-1} (2.2 g l^{-1} h^{-1})[23] (see Table 1). In order to fulfil the technically relevant demands, the usage of *Ec*LDCc CatIBs in batch mode at high substrate concentrations proved to be appropriate in order to obtain high STY.

Methods

Materials. All chemicals were purchased from Sigma-Aldrich, Roth, KMF and Merck. Enzymes for molecular biology were purchased from Thermo Scientific.

Cloning. See Supplementary "Cloning & sequences."

Protein production, cell disruption and protein purification. *Ec*LDCc-CatIBs were produced in *E. coli* BL21(DE3) as recently described elsewhere[62]. Here, a temperature of 15 °C during protein production was decisive for the formation of active *Ec*LDC-CatIBs. Cell disruption was performed with a high-pressure homogeniser (EmulsiFlex-C5, Avestin Europe GmbH, Mannheim, Germany) at 1000 bar using a cooled 10% (w/v) suspension of *E. coli* cells in cell lysis buffer (50 mM sodium phosphate, 100 mM NaCl, pH 8). To ensure thorough cell disruption, the suspension was passed three times through the high-pressure homogeniser under constant cooling. SDS-PAGE (see below) was used to analyse the distribution of the recombinant protein in the *E. coli* cells and during CatIB isolation. After cell disruption, the crude cell extract, and the soluble and insoluble protein fraction were separated by centrifugation at 15,000 × *g* for 30 min. The pellet was washed by suspension in MilliQ water in the initial volume followed by centrifugation. The obtained pellet was frozen overnight at −20 °C and a 10% (w/v) suspension in MilliQ water was prepared for lyophilisation (Christ ALPHA 1–3 LD Plus, Martin Christ Gefriertrocknungsanlagen GmbH, Osterode, Germany). In a mortar the dried pellet was ground to a fine powder, which was weighed and stored at −20 °C for further use.

SDS-PAGE and protein assay. SDS-PAGE analysis was performed using the NuPAGE® Kit (ThermoFisher Scientific), consisting of LDS Sample Buffer (4×) and NuPAGE® Reducing Agent (10×) with a final protein content of 1 mg ml^{-1}. Previously, the soluble protein concentration had been measured using the Bradford assay[74] and bovine serum albumin as a standard. Samples were applied to a NuPAGE™ 4–12% Bis-Tris protein gel, 1.0 mm, with 15 wells together with a protein marker (PageRuler Plus Prestained Protein *ladder*, ThermoFisher Scientific). Gel electrophoresis was performed in NuPAGE® MES SDS running buffer (1×) at 200 V, 100 mA and 15 W.

The protein content of the lyophilised CatIBs was determined by absorption at 280 nm. For this purpose, a defined amount (1–2 mg) of freeze-dried CatIBs was dissolved in 6 M aqueous guanidine hydrochloride solution (1 ml) and incubated at 30 °C for 30 min under constant shaking at 1000 rpm in a thermomixer (Thermomixer comfort, Eppendorf, Germany). The absorption of the protein solution was measured at 280 nm with a spectrophotometer (Shimadzu UV-1800/UV-1600). The protein content was estimated using the molar extinction coefficient (*Ec*LDCc-CatIBs: $\varepsilon = 109{,}210\,l\,mol^{-1}\,cm^{-1}$) as calculated based on the amino acid composition using the ProtParam Tool (http://web.expasy.org/protparam).

Live cell imaging. See Supplementary.

pH optimum of *Ec*LDC-CatIBs in KPi buffer and activity assay. In order to analyse the pH optimum, a reaction with 0.5 mg ml^{-1} lyophilised *Ec*LDCc-CatIBs in a reaction tube (2 ml safe-lock tube, Eppendorf, Germany) in 1 ml KPi buffer (50 mM, pH 7.0, 7.5, 8.0, 8.5, 9.0) containing 10 mM L-lysine, 0.1 mM PLP was performed for 20 min at 30 °C and 1000 rpm in a thermomixer (Thermomixer comfort, Eppendorf, Germany). After different time intervals (5, 10 and 20 min), 20 µl of the samples was taken from one vial. The reaction was stopped by incubation at 90 °C for 2 min and subsequent centrifugation for 2 min at 15,800 × *g*. The samples were then diluted to 1:50 in KPi buffer (50 mM, pH 7.0). The specific activity was calculated based on the DAP formed within the linear range, which was determined by HPLC analysis (see below).

One unit (U) of specific activity is defined as the amount of enzyme (in mg, calculated on the basis of protein content) which catalyses the formation of 1 µmol DAP per minute from the respective L-lysine concentration under the applied reaction conditions. The formation of DAP was monitored using HPLC as described below.

Characterisation of *Ec*LDCc-CatIBs in CGXII medium supplemented with different L-lysine concentrations. To characterise the performance of *Ec*LDCc-CatIBs for the transformation of different L-lysine concentrations from 10–100 mM, reactions of 2 mg ml^{-1} lyophilised *Ec*LDCc-CatIBs each were performed in reaction tubes (2 ml safe-lock tube, Eppendorf, Germany) in 1 ml CGXII medium[64] adjusted to pH 8.0 and containing 10, 20, 50, and 100 mM L-lysine and 0.1 mM PLP for 4 h at 30 °C and 1000 rpm in a thermomixer (Thermomixer comfort, Eppendorf, Germany). After different time intervals (6, 12, 24, 36, 60, 120, 180, and 246 min), 20 µl samples were taken and stopped by 1:5 dilution with methanol. The reaction mixture was then 1:10 diluted in KPi buffer (50 mM, pH 8.0) and subsequently centrifuged for 2 min at 15,800 × *g*. The samples thus obtained were diluted in an appropriate manner to obtain a final DAP concentration suitable for HPLC analysis (see below) between 10 and 100 µM. The specific activity was calculated as described above.

Bioreactor cultivation of *C. glutamicum*. See Supplementary.

Application of *Ec*LDCc-CatIBs in a (repetitive) batch. *Ec*LDCc-CatIBs were characterised in a cell-free culture supernatant (30 or 60 ml), with an adjusted pH of 8.0 and 0.1 mM PLP. Decarboxylation reactions of 100 mM and 1 M L-lysine were performed in repetetive batch and batch experiments, respectively. For the repetitive batch experiment, 3 mg ml^{-1} *Ec*LDCc-CatIBs were used in 60 ml reaction solution. For the single batch reaction, starting from 1 M L-lysine, 10 mg ml^{-1}*Ec*LDCc-CatIBs were added to 30 ml reaction solution. The experiments were performed under pH-control by dosing NaOH (2 M) and HCl (5%), respectively, using a 665 Dosimat, 632 pH meter equipped with a 614 Impulsomat from Metrohm, Germany. For the dosage profile of NaOH and HCl during the batch reaction starting from 1 M L-lysine see Supplementary Fig. S6. Reactions were performed in a doubled-walled 3-neck reactor vessel with two nozzles for the cooling supply to keep the temperature constant at 30 °C. The reaction mixture was stirred with a magnetic stirrer. For the repetitive batch approach, consecutive batch experiments were performed for either 4 h or 15 h. After a batch of 4 h or 15 h, the reaction mixture was transferred to a centrifugal beaker and centrifuged at 30,966 × *g* for 2 min. The pellet was suspended in the fresh reaction solution described above and transferred back into the doubled-walled flask reactor vessel. 20 µl samples were taken from the supernatant of the respective batch (60 ml approach) and the reaction was stopped by 1:5 dilution with methanol. The reaction mixture was then diluted 1:100 in KPi buffer (50 mM, pH 8.0). 5 µl samples were taken from the 30 ml batch experiment after different time intervals (6, 12, 18, 30, 45, 60, 90, 120, 180, 240, 300, 354, 426, 480, 543, and 1434 min) and the reaction was stopped by 1:20 dilution with methanol. The reaction mixture was then diluted (1:250) in KPi buffer (50 mM, pH 8.0). All samples were subsequently centrifuged for 2 min at 15,800 × *g*. The amount of DAP formed was determined by HPLC analysis (see below).The specific activity was calculated as described above.

Quantification of L-lysine and DAP by HPLC. To determine the DAP concentration in cell-free and CatIB-free reaction solutions, a HPLC-system (Agilent 1100 Infinity, Agilent Technologies, Santa Clara, USA) was used, equipped with a fluorescence detector (excitation: 230 nm; emission: 460 nm) and a C18 KinetexEvo column (Phenomenex, Torrence, USA). Prior to injection, samples were diluted 1:2 (v/v) with 100 µM α-aminobutyric acid as the internal standard (Sigma-Aldrich, St. Louis; USA). Analysis of DAP and L-lysine was performed by a method for amino acid quantification[71] including a pre-column derivatisation step at 18 °C using 5 µl *ortho*-phthaldialdehyde (OPA, Sigma-Aldrich) and 5 µl sample (6 mixing iterations). The mobile phase A was

composed of 7.12 g l^{-1} Na_2HPO_4, 6.24 g l^{-1} NaH_2PO_4 and 0.8% (v/v) THF in water, and the mobile phase B contained 50% (v/v) methanol, 45% (v/v) acetonitrile, and 5% (v/v) water. For chromatographic separation, a linear gradient was applied with a flow of 1 ml min^{-1} starting with 0% B, 0–2 min 0–38% B, 2–6 min 38–42% B, 6–7 min 42–70% B, 7–9 min 70–100% B, 9–13 min 100-0% B. Approximate retention times were 8 min for α-aminobutyric acid, 10 min for L-lysine, and 11 min for DAP. In order to correct for possible effects of the analytical matrix on derivatisation efficiency, α-aminobutyric acid (Sigma-Aldrich, St. Louis; USA) was used as an internal standard. The DAP concentration was derived from the linear calibration of five reference solutions (10 µM to 100 µM), included in each measurement run (for the calibration curve see Supplementary Fig. S8).

Data availability. The datasets generated during the current study are available from the corresponding author on reasonable request.

References

1. Kriegler, E. *et al*. Fossil-fueled development (SSP5): An energy and resource intensive scenario for the 21st century. *Glob. Environ. Chang.* **42**, 297–315 (2017).
2. U.S. Energy Information Administration. *International Energy Outlook 2016*. **0484**, (2016).
3. Magnusson, L. U., Gummesson, B., Joksimović, P., Farewell, A. & Nyström, T. Identical, independent, and opposing roles of ppGpp and DksA in *Escherichia coli*. *J. Bacteriol.* **189**, 5193–5202 (2007).
4. Chung, H. *et al*. Bio-based production of monomers and polymers by metabolically engineered microorganisms. *Curr. Opin. Biotechnol.* **36**, 73–84 (2015).
5. Kremer, F., Blank, L. M., Jones, P. R. & Akhtar, M. K. A comparison of the microbial production and combustion characteristics of three alcohol biofuels: Ethanol, 1-butanol, and 1-octanol. *Front. Bioeng. Biotechnol.* **3**, 112 (2015).
6. Wendisch, V. F. Microbial production of amino acids and derived chemicals: Synthetic biology approaches to strain development. *Curr. Opin. Biotechnol.* **30**, 51–58 (2014).
7. Erickson, B., Nelson & Winters, P. Perspective on opportunities in industrial biotechnology in renewable chemicals. *Biotechnol. J.* **7**, 176–185 (2012).
8. Park, S. J. *et al*. Synthesis of nylon 4 from gamma-aminobutyrate (GABA) produced by recombinant *Escherichia coli*. *Bioprocess Biosyst. Eng.* **36**, 885–892 (2013).
9. Meng, D. C. *et al*. Production of poly(3-hydroxypropionate) and poly(3-hydroxybutyrate-co-3-hydroxypropionate) from glucose by engineering *Escherichia coli*. *Metab. Eng.* **29**, 189–195 (2015).
10. Kind, S., Jeong, W. K., Schröder, H. & Wittmann, C. Systems-wide metabolic pathway engineering in *Corynebacterium glutamicum* for bio-based production of diaminopentane. *Metab. Eng.* **12**, 341–351 (2010).
11. Jiang, Y. *et al*. Microbial production of short chain diols. *Microb. Cell Fact.* **13**, 165 (2014).
12. Ma, W. *et al*. Advances in cadaverine bacterial production and its applications. *Engineering* **3**, 308–317 (2017).
13. Litsanov, B., Brocker, M. & Bott, M. Toward homosuccinate fermentation: Metabolic engineering of *Corynebacterium glutamicum* for anaerobic production of succinate from glucose and formate. *Appl. Environ. Microbiol.* **78**, 3325–3337 (2012).
14. Raab, A. M., Gebhardt, G., Bolotina, N., Weuster-Botz, D. & Lang, C. Metabolic engineering of *Saccharomyces cerevisiae* for the biotechnological production of succinic acid. *Metab. Eng.* **12**, 518–525 (2010).
15. Thakker, C., Martínez, I., San, K.-Y. & Bennett, G. N. Succinate production in *Escherichia coli*. *Biotechnol. J.* **7**, 213–24 (2012).
16. Tai, Y.-S. *et al*. Engineering nonphosphorylative metabolism to generate lignocellulose-derived products. *Nat. Chem. Biol.* **12**, 247–253 (2016).
17. Honjo, H., Tsuruno, K., Tatsuke, T., Sato, M. & Hanai, T. Dual synthetic pathway for 3-hydroxypropionic acid production in engineered *Escherichia coli*. *J. Biosci. Bioeng.* **120**, 199–204 (2015).
18. Okino, S. *et al*. An efficient succinic acid production process in a metabolically engineered *Corynebacterium glutamicum* strain. *Appl. Microbiol. Biotechnol.* **81**, 459–464 (2008).
19. Ogunniyi, D. S. Castor oil: A vital industrial raw material. *Bioresour. Technol.* **97**, 1086–1091 (2006).
20. Thielen, M. Bio-polyamides for automotive applications. *Bioplastics Mag.* **5**, 10–11 (2010).
21. Mimitsuka, T., Sawai, H., Hatsu, M. & Yamada, K. Metabolic engineering of *Corynebacterium glutamicum* for cadaverine fermentation. *Biosci. Biotechnol. Biochem.* **71**, 2130–2135 (2007).
22. Becker, J., Zelder, O., Häfner, S., Schröder, H. & Wittmann, C. From zero to hero—Design-based systems metabolic engineering of *Corynebacterium glutamicum* for L-lysine production. *Metab. Eng.* **13**, 159–168 (2011).
23. Kind, S. *et al*. From zero to hero - Production of bio-based nylon from renewable resources using engineered *Corynebacterium glutamicum*. *Metab. Eng.* **25**, 113–123 (2014).
24. Eggeling, L. & Bott, M. A giant market and a powerful metabolism: l-lysine provided by *Corynebacterium glutamicum*. *Appl. Microbiol. Biotechnol.* **99**, 3387–3394 (2015).
25. Oh, Y. H. *et al*. Development of engineered *Escherichia coli* whole-cell biocatalysts for high-level conversion of L-lysine into cadaverine. *J. Ind. Microbiol. Biotechnol.* **42**, 1481–1491 (2015).
26. Liu, P., Zhu, X., Tan, Z., Zhang, X. & Ma, Y. *in Advances in Biochemical Engineering/Biotechnology* **123**, 107–140 (2015).
27. Kim, J.-H. *et al*. Functional study of lysine decarboxylases from *Klebsiella pneumoniae* in *Escherichia coli* and application of whole cell bioconversion for cadaverine production. *J. Microbiol. Biotechnol.* **26**, 1586–1592 (2016).
28. Li, S., Xu, N., Liu, L. & Chen, J. Engineering of carboligase activity reaction in *Candida glabrata* for acetoin production. *Metab. Eng.* **22**, 32–9 (2014).
29. Kim, H. J. *et al*. Optimization of direct lysine decarboxylase biotransformation for cadaverine production with whole-cell biocatalysts at high lysine concentration. *J. Microbiol. Biotechnol.* **25**, 1108–1113 (2015).
30. Qian, Z. G., Xia, X. X. & Lee, S. Y. Metabolic engineering of *Escherichia coli* for the production of cadaverine: A five carbon diamine. *Biotechnol. Bioeng.* **108**, 93–103 (2011).
31. Yamamoto, Y., Miwa, Y., Miyoshi, K., Furuyama, J. & Ohmori, H. The *Escherichia coli* ldcC gene encodes another lysine decarboxylase, probably a constitutive enzyme. *Genes Genet. Syst.* **72**, 167–172 (1997).
32. Snider, J. *et al*. Formation of a distinctive complex between the inducible bacterial lysine decarboxylase and a novel AAA+ ATPase. *J. Biol. Chem.* **281**, 1532–1546 (2006).
33. Kandiah, E. *et al*. Structural insights into the *Escherichia coli* lysine decarboxylases and molecular determinants of interaction with the AAA+ ATPase RavA. *Sci. Rep.* **6**, 24601 (2016).
34. Kanjee, U. *et al*. Linkage between the bacterial acid stress and stringent responses: the structure of the inducible lysine decarboxylase. *EMBO J.* **30**, 931–944 (2011).
35. Ma, W. *et al*. Enhanced cadaverine production from L-lysine using recombinant *Escherichia coli* co-overexpressing CadA and CadB. *Biotechnol. Lett.* **37**, 799–806 (2015).

36. Kind, S., Jeong, W. K., Schröder, H., Zelder, O. & Wittmann, C. Identification and elimination of the competing N-acetyldiaminopentane pathway for improved production of diaminopentane by *Corynebacterium glutamicum*. *Appl. Environ. Microbiol.* **76**, 5175–80 (2010).
37. Li, M. *et al*. Improving the secretion of cadaverine in *Corynebacterium glutamicum* by cadaverine-lysine antiporter. *J. Ind. Microbiol. Biotechnol.* **41**, 701–9 (2014).
38. Vrljic, M., Sahm, H. & Eggeling, L. A new type of transporter with a new type of cellular function: L-lysine export from *Corynebacterium glutamicum*. *Mol. Microbiol.* **22**, 815–26 (1996).
39. Li, N., Chou, H., Yu, L. & Xu, Y. Cadaverine production by heterologous expression of *Klebsiella oxytoca* lysine decarboxylase. *Biotechnol. Bioprocess Eng.* **19**, 965–972 (2014).
40. Bhatia, S. K. *et al*. Biotransformation of lysine into cadaverine using barium alginate-immobilized *Escherichia coli* overexpressing CadA. *Bioprocess Biosyst. Eng.* **38**, 2315–2322 (2015).
41. Kim, J.-H. *et al*. Development of a continuous L-lysine bioconversion system for cadaverine production. *J. Ind. Eng. Chem.* **46**, 44–48 (2016).
42. Seo, H. M. *et al*. *In situ* immobilization of lysine decarboxylase on a biopolymer by fusion with phasin: Immobilization of CadA on intracellular PHA. *Process Biochem.* **51**, 1413–1419 (2016).
43. Park, S. H., Soetyono, F. & Kim, H. K. Cadaverine production by using cross-linked enzyme aggregate of *Escherichia coli* lysine decarboxylase. *J. Microbiol. Biotechnol.* **27**, 289–296 (2017).
44. Li, S., Lin, K., Pang, H., Wu, Y. & Xu, J. Production, characterization, and application of an organic solvent-tolerant lipase present in active inclusion bodies. *Appl. Biochem. Biotechnol.* **169**, 612–623 (2013).
45. Nahálka, J., Vikartovská, A. & Hrabárová, E. A crosslinked inclusion body process for sialic acid synthesis. *J. Biotechnol.* **134**, 146–153 (2008).
46. Worrall, D. M. & Goss, N. H. The formation of biologically active beta-galactosidase inclusion bodies in *Escherichia coli*. *Aust. J. Biotechnol.* **3**, 28–32 (1989).
47. Krauss, U., Jäger, V. D., Diener, M., Pohl, M. & Jaeger, K.-E. Catalytically-active inclusion bodies—Carrier-free protein immobilizates for application in biotechnology and biomedicine. *J. Biotechnol.* **258**, 136–147 (2017).
48. Sheldon, R. A. Enzyme Immobilization: The Quest for Optimum Performance. *Adv. Synth. Catal.* **349**, 1289–1307 (2007).
49. Barbosa, O. *et al*. Strategies for the one-step immobilization–purification of enzymes as industrial biocatalysts. *Biotechnol. Adv.* **33**, 435–456 (2015).
50. Tufvesson, P., Lima-Ramos, J., Nordblad, M. & Woodley, J. M. Guidelines and cost analysis for catalyst production in biocatalytic processes. *Org. Process Res. Dev.* **15**, 266–274 (2011).
51. Rodríguez-Carmona, E., Cano-Garrido, O., Seras-Franzoso, J., Villaverde, A. & García-Fruitós, E. Isolation of cell-free bacterial inclusion bodies. *Microb. Cell Fact.* **9**, 71 (2010).
52. Tokatlidis, K., Dhurjati, P., Millet, J., Béguin, P. & Aubert, J.-P. High activity of inclusion bodies formed in *Escherichia coli* overproducing *Clostridium thermocellum* endoglucanase D. *FEBS Lett.* **282**, 205–208 (1991).
53. Nahálka, J. & Pätoprstý, V. Enzymatic synthesis of sialylation substrates powered by a novel polyphosphate kinase (PPK3). *Org. Biomol. Chem.* **7**, 1778–1780 (2009).
54. Choi, S. L. *et al*. Generation of catalytic protein particles in *Escherichia coli* cells using the cellulose-binding domain from *Cellulomonas fimi* as a fusion partner. *Biotechnol. Bioprocess Eng.* **16**, 1173–1179 (2011).
55. Hrabárová, E., Achbergerová, L. & Nahálka, J. In *Insoluble Protein: Methods and protocols* (ed. García-Fruitós, E.) **1258**, 411–422 (Springer New York, 2015).
56. Nahálka, J., Mislovicová, D. & Kavcová, H. Targeting lectin activity into inclusion bodies for the characterisation of glycoproteins. *Mol. Biosyst.* **5**, 819–21 (2009).
57. Park, S. Y., Park, S. H. & Choi, S. K. Active inclusion body formation using *Paenibacillus polymyxa* PoxB as a fusion partner in *Escherichia coli*. *Anal. Biochem.* **426**, 63–65 (2012).
58. García-Fruitós, E. *et al*. Aggregation as bacterial inclusion bodies does not imply inactivation of enzymes and fluorescent proteins. *Microb. Cell Fact.* **4**, 27 (2005).
59. Wang, X., Zhou, B., Hu, W., Zhao, Q. & Lin, Z. Formation of active inclusion bodies induced by hydrophobic self-assembling peptide GFIL8. *Microb. Cell Fact.* **14**, 88 (2015).
60. Zhou, B., Xing, L., Wu, W., Zhang, X.-E. & Lin, Z. Small surfactant-like peptides can drive soluble proteins into active aggregates. *Microb. Cell Fact.* **11**, 10 (2012).
61. Peters, J. *et al*. Tetrabrachion: A filamentous archaebacterial surface protein assembly of unusual structure and extreme stability. *J. Mol. Biol.* **245**, 385–401 (1995).
62. Diener, M., Kopka, B., Pohl, M., Jaeger, K.-E. & Krauss, U. Fusion of a coiled-coil domain facilitates the high-level production of catalytically active enzyme inclusion bodies. *ChemCatChem* **8**, 142–152 (2016).
63. Kikuchi, Y., Kojima, H., Tanaka, T., Takatsuka, Y. & Kamio, Y. Characterization of a second lysine decarboxylase isolated from *Escherichia coli*. *J. Bacteriol.* **179**, 4486–4492 (1997).
64. Keilhauer, C., Eggeling, L. & Sahm, H. Isoleucine synthesis in *Corynebacterium glutamicum*: molecular analysis of the ilvB-ilvN-ilvC operon. *J. Bacteriol.* **175**, 5595–603 (1993).
65. Follmann, M. *et al*. Functional genomics of pH homeostasis in *Corynebacterium glutamicum* revealed novel links between pH response, oxidative stress, iron homeostasis and methionine synthesis. *BMC Genomics* **10**, 621 (2009).
66. Grünberger, A. *et al*. Microfluidic picoliter bioreactor for microbial single-cell analysis: Fabrication, system setup, and operation. *J. Vis. Exp.* 1–11 https://doi.org/10.3791/50560 (2013).
67. Grünberger, A. *et al*. Spatiotemporal microbial single-cell analysis using a high-throughput microfluidics cultivation platform. *Cytom. Part A* **87**, 1101–1115 (2015).
68. Rokney, A. *et al*. *E. coli* transports aggregated proteins to the poles by a specific and energy-dependent process. *J. Mol. Biol.* **392**, 589–601 (2009).
69. Ventura, S. & Villaverde, A. Protein quality in bacterial inclusion bodies. *Trends Biotechnol.* **24**, 179–185 (2006).
70. Krithika, G., Arunachalam, J., Priyanka, H. & Indulekha, K. The two forms of lysine decarboxylase; Kinetics and effect of expression in relation to acid tolerance response in *E. coli*. *J. Exp. Sci.* **1**, 10–21 (2010).
71. Limberg, M. H. *et al*. Metabolic profile of 1,5-diaminopentane producing *Corynebacterium glutamicum* under scale-down conditions: Blueprint for robustness to bioreactor inhomogeneities. *Biotechnol. Bioeng.* **114**, 560–575 (2017).
72. Reiber, H. Photochemical reactions of vitamin B6 compounds, isolation and properties of products. *Biochem. Biophys. Acta* **279**, 310–315 (1972).
73. Holde, V., Sabo, D. L. & Fischer, E. H. Chemical properties of Escherichia coli lysine decarboxylase including a segment of its pyridoxal 5′-phosphate binding site. *Biochemistry* **13**, 670–676 (1974).
74. Bradford, M. M. A rapid and sensitive method for the quantitation of microgram quantities of protein utilizing the principle of protein-dye binding. *Anal. Biochem.* 248–254 (1976).

Acknowledgements
The scientific activities of the Bioeconomy Science Center were financially supported by the Ministry of Innovation, Science and Research within the framework of the NRW Strategieprojekt BioSC (No. 313/323-400-002 13). BioSC is a research cluster of RWTH Aachen University, the universities of Düsseldorf and Bonn, and Forschungszentrum Jülich. The authors thank the Federal German Ministry of Education and Science for providing funding for the cluster project "Systematic consideration of inhomogeneity at the large scale" (grant no. 031A220A), which is embedded in the ERA-IB framework.

Author Contributions
D.H. performed the construction of plasmids under the direction of R.K. and U.K., who performed structure-based planning of the genetic construct. V.D.J. and U.K. supported CatIB preparation. U.M. performed production, purification, and characterisation of the CatIBs and analysed the data with the assistance of R.K. and M.H.L., and the coordination and supervision of M.P. A.G. performed live-cell imaging with the assistance of V.D.J. and R.K. M.H.L. and R.K. performed microbial L-lysine production under the coordination and supervision of M.O. R.K., M.H.L. and M.P. wrote the manuscript with input from A.G., U.K. and M.O.

Additional Information
Supplementary information accompanies this paper at https://doi.org/10.1038/s41598-018-24070-2.

Competing Interests: The authors declare no competing interests.

Publisher's note: Springer Nature remains neutral with regard to jurisdictional claims in published maps and institutional affiliations.

Supplementary Information

Catalytically active inclusion bodies of lysine decarboxylase from *E. coli* for 1,5-diaminopentane production

Ramona Kloss[1,4+], Michael Limberg[1+], Ursula Mackfeld[1], Doris Hahn[1], Alexander Grünberger[1, 5], Vera D. Jäger[2,4], Ulrich Krauss[2,4], Marco Oldiges[1,3], and Martina Pohl[1,4]

Cloning & sequences

Based on the earlier described cloning strategy[1], the gene encoding *Ec*LDCc was cloned into a pET28a vector containing the gene fragment encoding for i) the TDoT-domain, ii) a 3xGGGS linker (L) and iii) the enzyme *Ec*LDCc. The *Ec*LDCc gen was cloned into the vector by restriction with NdeI and NheI cleavage sites and ligation to attain a construct encoding a C-terminal fusion of the target enzyme to linker and TDoT. Oligonucleotide primer sequences used to amplify *Ec*LDCc gen are shown in the following Table S1. The final plasmid was sequenced by LGC genomics (Berlin, Germany).

Table S1: Primer sequences for amplification of *Ec*LDCc gen with NdeI and NheI cleavage sites (red)

name	sequence
NdeI_LDC_fw	5'- ATATATCATATGATGAACATCATCGCTATCATGGGCCC-3'
LDC_NheI_rv	5'- ATATATGCTAGCGCCTGCCATCTTAAGGACG-3'

Expression vector

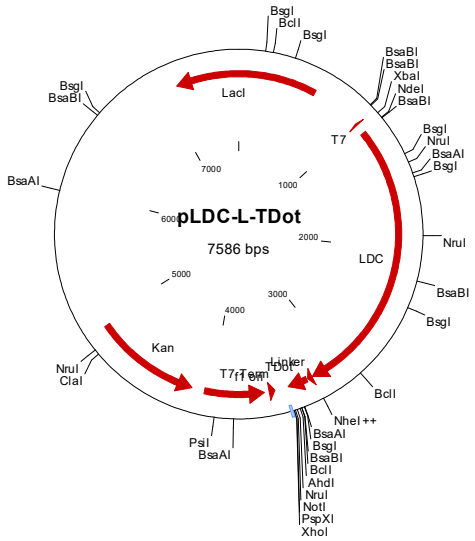

Figure S1: pET28a vector containing the gene fusion encoding for *Ec*LDCc-L-TDoT. The DNA sequence of the vector is shown below.

DNA-sequence of the pET28a vector containing the gene fusion encoding for *Ec*LDCc-L-TDoT

vector DNA (grey), start and stop codon of the *ldcc*-ORF (red), LDCc gen (black), linker (green), TDoT (orange), restrictions sites (blue)

CAGCCAGACGCAGACGCGCCGAGACAGAACTTAATGGGCCCGCTAACAGCGCGATTTGCT
GGTGACCCAATGCGACCAGATGCTCCACGCCCAGTCGCGTACCGTCTTCATGGGAGAAAA
TAATACTGTTGATGGGTGTCTGGTCAGAGACATCAAGAAATAACGCCGGAACATTAGTGC
AGGCAGCTTCCACAGCAATGGCATCCTGGTCATCCAGCGGATAGTTAATGATCAGCCCAC
TGACGCGTTGCGCGAGAAGATTGTGCACCGCCGCTTTACAGGCTTCGACGCCGCTTCGTT
CTACCATCGACACCACCACGCTGGCACCCAGTTGATCGGCGCGAGATTTAATCGCCGCGA
CAATTTGCGACGGCGCGTGCAGGGCCAGACTGGAGGTGGCAACGCCAATCAGCAACGACT
GTTTGCCCGCCAGTTGTTGTGCCACGCGGTTGGGAATGTAATTCAGCTCCGCCATCGCCG
CTTCCACTTTTTCCCGCGTTTTCGCAGAAACGTGGCTGGCCTGGTTCACCACGCGGGAAA
CGGTCTGATAAGAGACACCGGCATACTCTGCGACATCGTATAACGTTACTGGTTTCACAT
TCACCACCCTGAATTGACTCTCTTCCGGGCGCTATCATGCCATACCGCGAAAGGTTTTGC
GCCATTCGATGGTGTCCGGGATCTCGACGCTCTCCCTTATGCGACTCCTGCATTAGGAAG
CAGCCCAGTAGTAGGTTGAGGCCGTTGAGCACCGCCGCCGCAAGGAATGGTGCATGCAAG
GAGATGGCGCCCAACAGTCCCCCGGCCACGGGGCCTGCCACCATACCCACGCCGAAACAA
GCGCTCATGAGCCCGAAGTGGCGAGCCCGATCTTCCCCATCGGTGATGTCGGCGATATAG
GCGCCAGCAACCGCACCTGTGGCGCCGGTGATGCCGGCCACGATGCGTCCGGCGTAGAGG
ATCGAGATCTCGATCCCGCGAAATTAATACGACTCACTATAGGGGAATTGTGAGCGGATA
ACAATTCCCCTCTAGAAATAATTTTGTTTAACTTTAAGAAGGAGATATACATATGATGAA
CATCATCGCTATCATGGGCCCTCACGGTGTTTTCTACAAGGATGAGCCAATCAAGGAGCT
GGAATCCGCACTAGTTGCACAGGGCTTTCAGATCATCTGGCCCCAGAACTCCGTTGACCT
TCTCAAATTCATCGAGCACAATCCTCGCATTTGTGGTGTGATTTTTGACTGGGACGAGTA
CTCTCTTGATTTATGCTCCGACATCAACCAGCTCAACGAGTACCTGCCACTCTACGCATT
CATCAACACTCACTCCACCATGGACGTTTCCGTGCAGGACATGCGTATGGCACTCTGGTT
CTTTGAATACGCTCTGGGCCAGGCTGAGGACATCGCGATCCGCATGCGTCAGTACACCGA
CGAGTACCTGGACAACATCACCCCTCCATTCACCAAGGCTCTCTTCACCTACGTAAAGGA
ACGCAAGTACACTTTCTGCACCCCAGGCCACATGGGCGGCACCGCCTACCAGAAGTCCCC
AGTCGGATGCCTCTTCTACGACTTCTTCGGCGGTAACACTCTTAAGGCAGATGTCTCCAT
TTCCGTCACCGAGTTGGGCTCTCTGCTGGACCACACCGGCCCTCACCTGGAGGCAGAAGA
GTACATCGCTCGTACCTTCGGTGCTGAACAGTCCTACATCGTCACCAACGGTACTTCCAC
CAGCAACAAGATCGTTGGTATGTACGCAGCTCCTTCTGGCTCCACCCTGTTGATCGACCG
CAACTGTCACAAGTCCCTCGCGCATCTTCTTATGATGAACGATGTGGTCCCTGTATGGCT
GAAGCCAACCCGTAACGCTCTGGGCATCCTTGGCGGTATCCCCCGTCGCGAGTTCACCCG
TGATTCCATCGAGGAAAAGGTTGCAGCCACTACCCAGGCACAGTGGCCTGTCCACGCTGT
CATTACCAACTCGACCTACGACGGCCTGCTCTACAACACCGATTGGATCAAGCAGACCCT
AGATGTTCCTTCCATTCACTTCGACAGCGCATGGGTTCCTTACACTCACTTCCACCCAAT
CTACCAGGGTAAGTCCGGAATGTCCGGCGAGCGTGTCGCTGGCAAGGTTATCTTCGAAAC
CCAATCAACCCACAAGATGCTGGCTGCTCTCTCCCAGGCTTCTCTGATCCACATCAAGGG
CGAGTACGACGAGGAAGCTTTCAACGAGGCTTTCATGATGCACACCACCACCTCCCCATC
CTACCCTATCGTCGCGTCCGTCGAGACTGCTGCCGCAATGCTTCGCGGTAACCCAGGTAA
GCGCCTCATCAACCGTTCCGTTGAGCGCGCTCTTCACTTCCGTAAGGAAGTGCAGCGCCT
GCGTGAGGAATCTGACGGTTGGTTCTTCGACATTTGGCAGCCACCTCAGGTTGATGAGGC
CGAGTGCTGGCCAGTTGCTCCAGGTGAACAGTGGCACGGATTCAACGATGCAGATGCTGA
CCACATGTTTTTGGACCCGGTCAAGGTCACCATTCTTACTCCTGGTATGGATGAGCAGGG
CAACATGTCTGAGGAGGGTATCCCAGCTGCTCTGGTTGCAAAGTTCCTCGACGAACGTGG
CATCGTTGTTGAGAAGACCGGACCATACAACCTGCTGTTCCTGTTCAGCATCGGCATCGA
CAAAACCAAGGCAATGGGTCTGCTGCGCGGCCTTACCGAGTTCAAGCGCTCCTACGACCT
GAACCTTCGCATCAAGAATATGCTGCCGGACCTGTACGCTGAAGATCCTGATTTCTACCG
CAACATGCGCATCCAGGACCTCGCACAGGGCATCCACAAGCTCATTCGCAAGCACGACCT
GCCAGGCCTTATGCTCCGTGCATTCGATACCCTCCCAGAGATGATCATGACCCCTCACCA
GGCTTGGCAGCGCCAGATCAAGGGCGAGGTGGAAACCATCGCACTGGAGCAGCTGGTTGG
TCGTGTCTCCGCCAACATGATCCTGCCATATCCACCTGGCGTTCCGCTGCTGATGCCAGG
CGAGATGCTCACCAAGGAGTCCCGCACCGTATTGGACTTCCTTCTCATGTTGTGCTCTGT
TGGCCAGCACTACCCAGGCTTCGAGACCGACATCCACGGCGCTAAGCAAGATGAAGACGG
CGTTTACCGCGTTCGCGTCCTTAAGATGGCAGGCGCTAGCGGCGGTGGGTCTGGAGGCGG
CTCAGGTGGTGGGTCGGGATCCATCATTAACGAAACTGCCGATGACATCGTTTATCGCCT
GACAGTCATTATCGATGATCGCTACGAATCGCTGAAAAACCTGATTACCTTACGTGCAGA
TCGCTTGGAGATGATCATCAATGACAATGTGTCCACCATTCTCGCGAGCATTTAAGCGGC

CGCACTCGAGCACCACCACCACCACCACTGAGATCCGGCTGCTAACAAAGCCCGAAAGGA
AGCTGAGTTGGCTGCTGCCACCGCTGAGCAATAACTAGCATAACCCCTTGGGGCCTCTAA
ACGGGTCTTGAGGGGTTTTTTGCTGAAAGGAGGAACTATATCCGGATTGGCGAATGGGAC
GCGCCCTGTAGCGGCGCATTAAGCGCGGCGGGTGTGGTGGTTACGCGCAGCGTGACCGCT
ACACTTGCCAGCGCCCTAGCGCCCGCTCCTTTCGCTTTCTTCCCTTCCTTTCTCGCCACG
TTCGCCGGCTTTCCCCGTCAAGCTCTAAATCGGGGGCTCCCTTTAGGGTTCCGATTTAGT
GCTTTACGGCACCTCGACCCCAAAAAACTTGATTAGGGTGATGGTTCACGTAGTGGGCCA
TCGCCCTGATAGACGGTTTTTCGCCCTTTGACGTTGGAGTCCACGTTCTTTAATAGTGGA
CTCTTGTTCCAAACTGGAACAACACTCAACCCTATCTCGGTCTATTCTTTTGATTTATAA
GGGATTTTGCCGATTTCGGCCTATTGGTTAAAAAATGAGCTGATTTAACAAAAATTTAAC
GCGAATTTTAACAAAATATTAACGTTTACAATTTCAGGTGGCACTTTTCGGGGAAATGTG
CGCGGAACCCCTATTTGTTTATTTTTCTAAATACATTCAAATATGTATCCGCTCATGAAT
TAATTCTTAGAAAAACTCATCGAGCATCAAATGAAACTGCAATTTATTCATATCAGGATT
ATCAATACCATATTTTTGAAAAAGCCGTTTCTGTAATGAAGGAGAAAACTCACCGAGGCA
GTTCCATAGGATGGCAAGATCCTGGTATCGGTCTGCGATTCCGACTCGTCCAACATCAAT
ACAACCTATTAATTTCCCCTCGTCAAAAATAAGGTTATCAAGTGAGAAATCACCATGAGT
GACGACTGAATCCGGTGAGAATGGCAAAAGTTTATGCATTTCTTTCCAGACTTGTTCAAC
AGGCCAGCCATTACGCTCGTCATCAAAATCACTCGCATCAACCAAACCGTTATTCATTCG
TGATTGCGCCTGAGCGAGACGAAATACGCGATCGCTGTTAAAAGGACAATTACAAACAGG
AATCGAATGCAACCGGCGCAGGAACACTGCCAGCGCATCAACAATATTTTCACCTGAATC
AGGATATTCTTCTAATACCTGGAATGCTGTTTTCCCGGGGATCGCAGTGGTGAGTAACCA
TGCATCATCAGGAGTACGGATAAAATGCTTGATGGTCGGAAGAGGCATAAATTCCGTCAG
CCAGTTTAGTCTGACCATCTCATCTGTAACATCATTGGCAACGCTACCTTTGCCATGTTT
CAGAAACAACTCTGGCGCATCGGGCTTCCCATACAATCGATAGATTGTCGCACCTGATTG
CCCGACATTATCGCGAGCCCATTTATACCCATATAAATCAGCATCCATGTTGGAATTTAA
TCGCGGCCTAGAGCAAGACGTTTCCCGTTGAATATGGCTCATAACACCCCTTGTATTACT
GTTTATGTAAGCAGACAGTTTTATTGTTCATGACCAAAATCCCTTAACGTGAGTTTTCGT
TCCACTGAGCGTCAGACCCCGTAGAAAAGATCAAAGGATCTTCTTGAGATCCTTTTTTTC
TGCGCGTAATCTGCTGCTTGCAAACAAAAAAACCACCGCTACCAGCGGTGGTTTGTTTGC
CGGATCAAGAGCTACCAACTCTTTTTCCGAAGGTAACTGGCTTCAGCAGAGCGCAGATAC
CAAATACTGTCCTTCTAGTGTAGCCGTAGTTAGGCCACCACTTCAAGAACTCTGTAGCAC
CGCCTACATACCTCGCTCTGCTAATCCTGTTACCAGTGGCTGCTGCCAGTGGCGATAAGT
CGTGTCTTACCGGGTTGGACTCAAGACGATAGTTACCGGATAAGGCGCAGCGGTCGGGCT
GAACGGGGGGTTCGTGCACACAGCCCAGCTTGGAGCGAACGACCTACACCGAACTGAGAT
ACCTACAGCGTGAGCTATGAGAAAGCGCCACGCTTCCCGAAGGGAGAAAGGCGGACAGGT
ATCCGGTAAGCGGCAGGGTCGGAACAGGAGAGCGCACGAGGGAGCTTCCAGGGGGAAACG
CCTGGTATCTTTATAGTCCTGTCGGGTTTCGCCACCTCTGACTTGAGCGTCGATTTTTGT
GATGCTCGTCAGGGGGGCGGAGCCTATGGAAAAACGCCAGCAACGCGGCCTTTTTACGGT
TCCTGGCCTTTTGCTGGCCTTTTGCTCACATGTTCTTTCCTGCGTTATCCCCTGATTCTG
TGGATAACCGTATTACCGCCTTTGAGTGAGCTGATACCGCTCGCCGCAGCCGAACGACCG
AGCGCAGCGAGTCAGTGAGCGAGGAAGCGGAAGAGCGCCTGATGCGGTATTTTCTCCTTA
CGCATCTGTGCGGTATTTCACACCGCATATATGGTGCACTCTCAGTACAATCTGCTCTGA
TGCCGCATAGTTAAGCCAGTATACACTCCGCTATCGCTACGTGACTGGGTCATGGCTGCG
CCCCGACACCCGCCAACACCCGCTGACGCGCCCTGACGGGCTTGTCTGCTCCCGGCATCC
GCTTACAGACAAGCTGTGACCGTCTCCGGGAGCTGCATGTGTCAGAGGTTTTCACCGTCA
TCACCGAAACGCGCGAGGCAGCTGCGGTAAAGCTCATCAGCGTGGTCGTGAAGCGATTCA
CAGATGTCTGCCTGTTCATCCGCGTCCAGCTCGTTGAGTTTCTCCAGAAGCGTTAATGTC
TGGCTTCTGATAAAGCGGGCCATGTTAAGGGCGGTTTTTTCCTGTTTGGTCACTGATGCC
TCCGTGTAAGGGGGATTTCTGTTCATGGGGGTAATGATACCGATGAAACGAGAGAGGATG
CTCACGATACGGGTTACTGATGATGAACATGCCCGGTTACTGGAACGTTGTGAGGGTAAA
CAACTGGCGGTATGGATGCGGCGGGACCAGAGAAAAATCACTCAGGGTCAATGCCAGCGC
TTCGTTAATACAGATGTAGGTGTTCCACAGGGTAGCCAGCAGCATCCTGCGATGCAGATC
CGGAACATAATGGTGCAGGGCGCTGACTTCCGCGTTTCCAGACTTTACGAAACACGGAAA
CCGAAGACCATTCATGTTGTTGCTCAGGTCGCAGACGTTTTGCAGCAGCAGTCGCTTCAC
GTTCGCTCGCGTATCGGTGATTCATTCTGCTAACCAGTAAGGCAACCCCGCCAGCCTAGC
CGGGTCCTCAACGACAGGAGCACGATCATGCGCACCCGTGGGGCCGCCATGCCGGCGATA
ATGGCCTGCTTCTCGCCGAAACGTTTGGTGGCGGGACCAGTGACGAAGGCTTGAGCGAGG
GCGTGCAAGATTCCGAATACCGCAAGCGACAGGCCGATCATCGTCGCGCTCCAGCGAAAG
CGGTCCTCGCCGAAAATGACCCAGAGCGCTGCCGGCACCTGTCCTACGAGTTGCATGATA
AAGAAGACAGTCATAAGTGCGGCGACGATAGTCATGCCCCGCGCCCACCGGAAGGAGCTG
ACTGGGTTGAAGGCTCTCAAGGGCATCGGTCGAGATCCCGGTGCCTAATGAGTGAGCTAA
CTTACATTAATTGCGTTGCGCTCACTGCCCGCTTTCCAGTCGGGAAACCTGTCGTGCCAG

CTGCATTAATGAATCGGCCAACGCGCGGGGAGAGGCGGTTTGCGTATTGGGCGCCAGGGT
GGTTTTTCTTTTCACCAGTGAGACGGGCAACAGCTGATTGCCCTTCACCGCCTGGCCCTG
AGAGAGTTGCAGCAAGCGGTCCACGCTGGTTTGCCCCAGCAGGCGAAAATCCTGTTTGAT
GGTGGTTAACGGCGGGATATAACATGAGCTGTCTTCGGTATCGTCGTATCCCACTACCGA
GATATCCGCACCAACGCGCAGCCCGGACTCGGTAATGGCGCGCATTGCGCCCAGCGCCAT
CTGATCGTTGGCAACCAGCATCGCAGTGGGAACGATGCCCTCATTCAGCATTTGCATGGT
TTGTTGAAAACCGGACATGGCACTCCAGTCGCCTTCCCGTTCCGCTATCGGCTGAATTTG
ATTGCGAGTGAGATATTTATGCCAGC

Amino acid sequence of *Ec*LDCc-TDot

***Ec*LDCc gen (black), linker (green), TDoT (orange), restrictions sites (blue)**

M N I I A I M G P H G V F Y K D E P I K E L E S A L V A Q G F Q I I W P Q N
S V D L L K F I E H N P R I C G V I F D W D E Y S L D L C S D I N Q L N E Y
L P L Y A F I N T H S T M D V S V Q D M R M A L W F F E Y A L G Q A E D I A
I R M R Q Y T D E Y L D N I T P P F T K A L F T Y V K E R K Y T F C T P G H
M G G T A Y Q K S P V G C L F Y D F F G G N T L K A D V S I S V T E L G S L
L D H T G P H L E A E E Y I A R T F G A E Q S Y I V T N G T S T S N K I V G
M Y A A P S G S T L L I D R N C H K S L A H L L M M N D V V P V W L K P T R
N A L G I L G G I P R R E F T R D S I E E K V A A T T Q A Q W P V H A V I T
N S T Y D G L L Y N T D W I K Q T L D V P S I H F D S A W V P Y T H F H P I
Y Q G K S G M S G E R V A G K V I F E T Q S T H K M L A A L S Q A S L I H I
K G E Y D E E A F N E A F M M H T T T S P S Y P I V A S V E T A A A M L R G
N P G K R L I N R S V E R A L H F R K E V Q R L R E E S D G W F F D I W Q P
P Q V D E A E C W P V A P G E Q W H G F N D A D A D H M F L D P V K V T I L
T P G M D E Q G N M S E E G I P A A L V A K F L D E R G I V V E K T G P Y N
L L F L F S I G I D K T K A M G L L R G L T E F K R S Y D L N L R I K N M L
P D L Y A E D P D F Y R N M R I Q D L A Q G I H K L I R K H D L P G L M L R
A F D T L P E M I M T P H Q A W Q R Q I K G E V E T I A L E Q L V G R V S A
N M I L P Y P P G V P L L M P G E M L T K E S R T V L D F L L M L C S V G Q
H Y P G F E T D I H G A K Q D E D G V Y R V R V L K M A G A S G G G S G G G
S G G G S G S I I N E T A D D I V Y R L T V I I D D R Y E S L K N L I T L R
A D R L E M I I N D N V S T I L A S I

Live cell imaging

After cultivation of *E. coli* BL21(DE3) containing *Ec*LDCc-CatIBs, 1 ml of the cell suspension in stationary growth phase was harvested by centrifugation at 15,800 xg for 2 min. The cell pellet was frozen at -80°C overnight and suspended in cell lysis buffer (50 mM sodium phosphate buffer, 100 mM NaCl, pH 8) to an OD_{600} of approx. 10. The cell suspension was transferred by a syringe to an in-house developed microfluidic chip, which was prepared for single-cell analysis and cultivation[2,3]. This device comprises hundreds of cultivation chambers for monolayer growth to enable imaging on a plane layer. Images were recorded with a phase contrast inverted epifluorescence microscope (TI-Eclipse, Nikon GmbH, Düsseldorf, Germany), additionally equipped with a CCD camera (Clara DR-3041, Andor Technology Plc., Belfast, UK), an LED light source (pE-100 white,

CoolLed, Andover, UK), a Nikon Plan Apo 100 Ph3 DM Oil objective, and a Nikon Perfect Focus System for thermal drift compensation. Final images were processed by ImageJ (Wayne Rasband, USA).

Bioreactor cultivation of *C. glutamicum*

Bioreactor cultivations of the L-lysine producing *C. glutamicum* DM1945[4] were carried out in a 1 L scale using CGXII minimal medium[5]. For cultivation 1.5 L DASGIP vessels in a DASGIP Bioblock system (DASGIP GmbH, Jülich, Germany) were used as parallel cultivation system. Each bioreactor was equipped with an optical pO_2 sensor (Hamilton, Visiferm DO 225) and a pH electrode (Mettler-Toledo, 405-DPAS-SC-K8S/225/120). The Bioblock controlling platform (DASGIP, DGCS4) was equipped with a monitoring system for pH and pO_2 (DASGIP, PH4PO4), an exhaust gas analyser (DASGIP, GA4), a pumping device for titration (DASGIP, MP8), a gassing system (DASGIP, MF4) and a system for temperature and agitation control (DASGIP, TC4SC4). During cultivation pO_2 was maintained to 30% by controlling the agitation rate (maximum 1200 min^{-1}) and a constant aeration rate of 1 volume air per volume fermentation broth per minute (vvm). The pH of the medium was maintained at pH 7 by the addition of 30% (v/v) aqueous H_3PO_4 and 17.7% (v/v) aqueous NH_3 solution. The temperature during cultivation was set to 30 °C.

Cultivations were directly inoculated from cryo-culture stocks to an initial $OD_{600\ nm}$ = 0.05. Cryo-culture stocks were prepared as described by Unthan *et al.* [6], except that culture medium CGXII containing 20% (v/v) glycerol was used for storage instead of 0.9% (w/v) NaCl. The cell suspension was harvested 6 h after the pO_2 returned to the initial value of 100% saturation. Subsequently, the cell fraction was separated from the liquid culture supernatant by centrifugation (20 min, 12,227 x*g*, 4 ºC) and then stored at -20 ºC.

Optimisation of the reaction system of *Ec*LDCc-CatIBs for the production of DAP from L-lysine

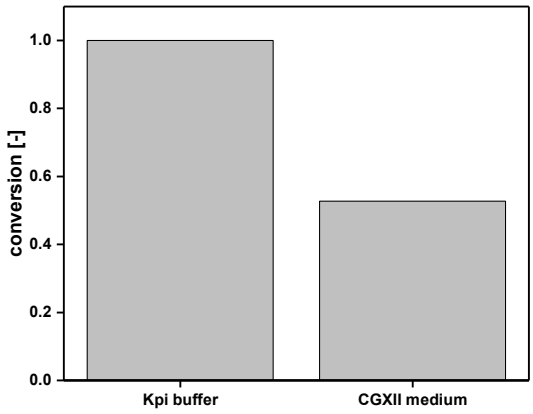

Supplementary Figure S2: Decarboxylation reaction by 1 mg ml-1 *Ec*LDCc-CatIBs with assay conditions: 10 mM L-lysine, 0.1 mM PLP, KPi buffer (50 mM, pH 7.5) or CGXII medium (pH 7.5, 20 g l-1 Glucose, 5 g l-1 urea) for 1 h at 30°C and 1000 rpm; the reaction was stopped by heating at 90°C for 2 min and subsequent centrifugation; Analysis was performed by HPLC analysis (see Methods in the main paper).

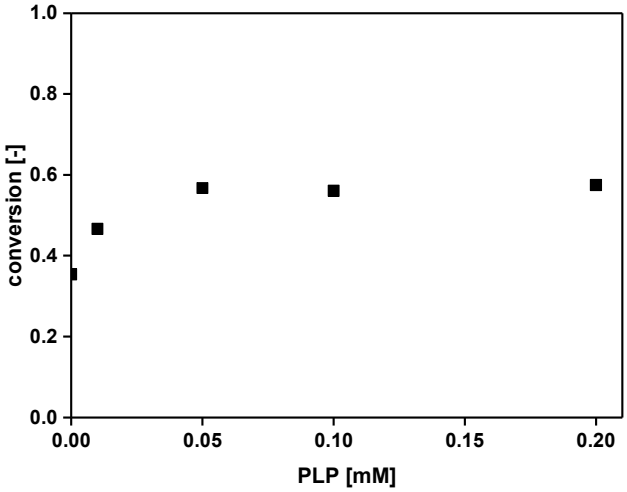

Supplementary Figure S3: Effect of different PLP concentrations (0.0, 0.01, 0.05, 0.1 and 0.2 mM) on the conversion of L-lysine to DAP by 0.5 mg ml^{-1} *Ec*LDCc-CatIBs; experimental conditions: 10 mM L-lysine, KPi buffer (50 mM, pH 8, supplemented with PLP as indicated) for 30 min at 30°C and 1000 rpm; the reaction was stopped by heating at 90°C for 2 min and subsequent centrifugation; Analysis was performed by HPLC analysis (see Methods in the main paper), n = 1.

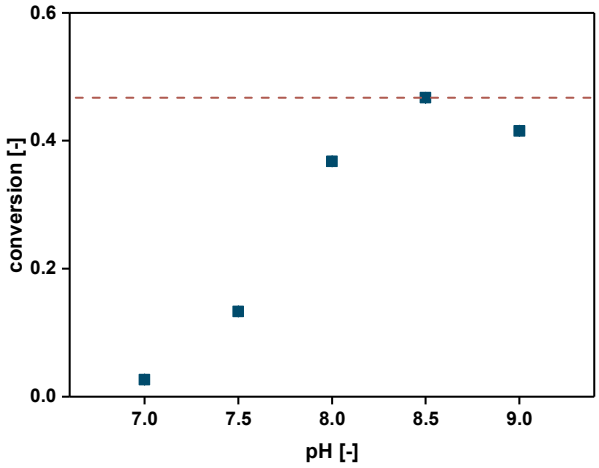

Supplementary Figure S4: Determination of the optimal pH for the *Ec*LDCc-CatIB-catalysed decarboxylation of L-lysine. Experimental conditions: 0.5 mg ml^{-1} lyophilized *Ec*LDCc-CatIBs, 10 mM L-lysine, 0.1 mM PLP, CGXII medium (pH 7, 7.5, 8, 8.5, 9) for 30 min at 30°C and 1000 rpm; the reaction was stopped by 1:5 dilution with methanol and subsequent centrifugation; Analysis was performed by HPLC analysis (see Methods in the main paper), n=3

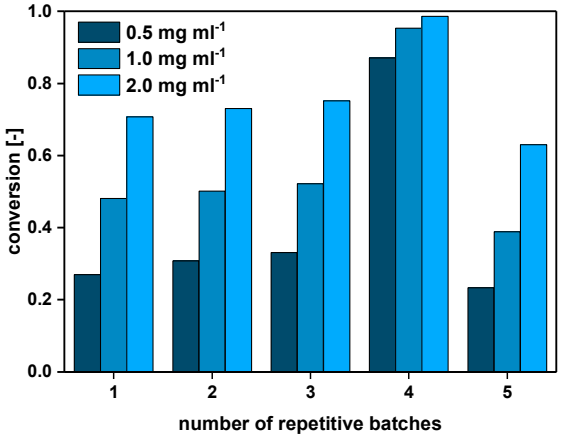

Supplementary Figure S5: Repetitive batch reactions for DAP production catalysed by different concentrations of *Ec*LDCc-CatIBs (0.5, 1 or 2 mg ml^{-1}); Experimental conditions: total volume 1 ml, 100 mM L-lysine, 0.01 mM PLP in cell free culture supernatant (CGXII medium, pH 8) for 2 h at 30°C and 1000 rpm, except batch 4: 16 h overnight. The CatIBs used in the first batch were reused in the next batch after centrifugation and resuspension in a fresh reaction solution. The reaction was stopped by 1:5 dilution with methanol and subsequent centrifugation; HPLC analysis (see Methods in the main paper).

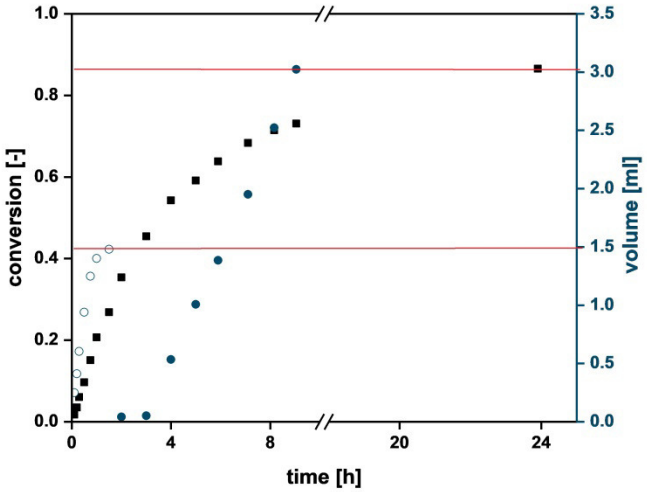

Supplementary Fig. S6: Shows the conversion of 1 M L-lysine in a 30 ml batch reactor (cf. Fig. 7, main paper) supplemented with information on the titration volumes of 2 N NaOH (open circles) and 5% HCl aq. (closed circles). As the reaction is performed in "used" CGXII-medium, the initially included phosphate buffer was metabolised by the growing *C. glutamicum* lysine producer strain. Thus the buffer capacity of the medium was low. The decarboxylation of lysine yields CO_2 and DAP in equimolar concentration. The formation of CO_2 is assumed to decrease pH, which requires titration with NaOH in the beginning of the reaction. With progressive conversion the increasing concentration of DAP led to an increase of pH, which was compensated by addition of HCl.

Control experiments with soluble LDCc in *E. coli*

Preparation of the whole cell biocatalyst: *Ec*LDCc was produced in *E. coli* BL21(DE3) as described in Methods in the main paper. Afterwards the cell pellet was frozen overnight at -20°C and a 10 % (w/v) suspension in MilliQ water was prepared for lyophilisation (Christ ALPHA 1-3 LD Plus, Martin Christ Gefriertrocknungsanlagen GmbH, Osterode, Germany). The dried pellet was weighted and stored at -20°C for further use.

Production of DAP using whole cells with soluble LDCc and *Ec*LDCc-CatIBs: Experimental conditions: lyophilised *E. coli* BL21(DE3) cells containing LDCc (0,01 – 1 mg/ml) or *Ec*LDCc-CatIBs (0.5 mg/ml) were suspended in reaction buffer containing 10 mM L-lysine, 50 mM KPi, pH 8, 0.1 mM PLP, respectively.

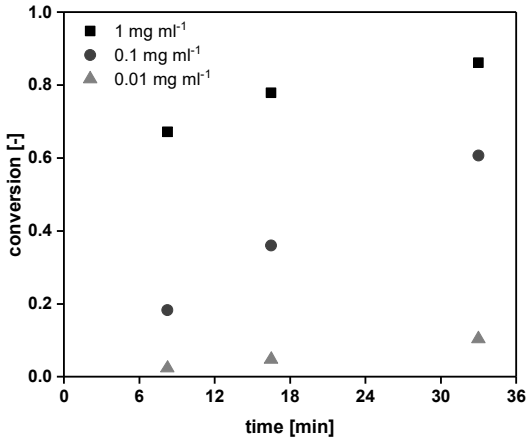

Supplementary Fig. S7a: shows results obtained with the whole cell biocatalyst containing soluble LDCc in 3 different concentrations.

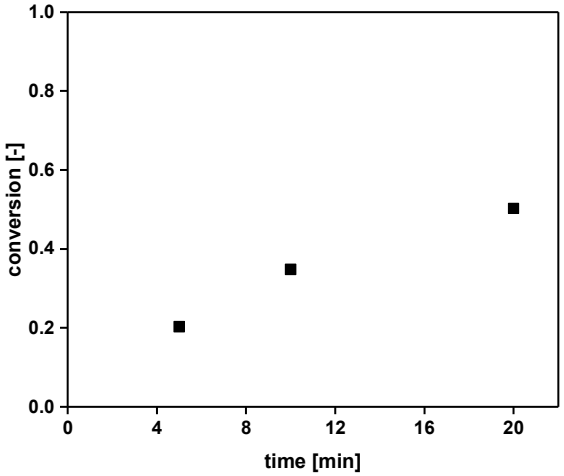

Supplementary Fig. S7b: shows results obtained with 0.5 mg/ml *Ec*LDCc-CatIBs

These studies demonstrate that with 0.1 mg/ml of these whole cell biocatalyst suspended in KPi-buffer 10 mM L-Lys are converted to 50 % in approximately 25 min. The same conversion is achieved with 0.5 mg/ml CatIBs in 20 min. So the *Ec*LDCc-CatIBs perform equally well or even better than the whole cell biocatalyst.

HPLC calibration curves

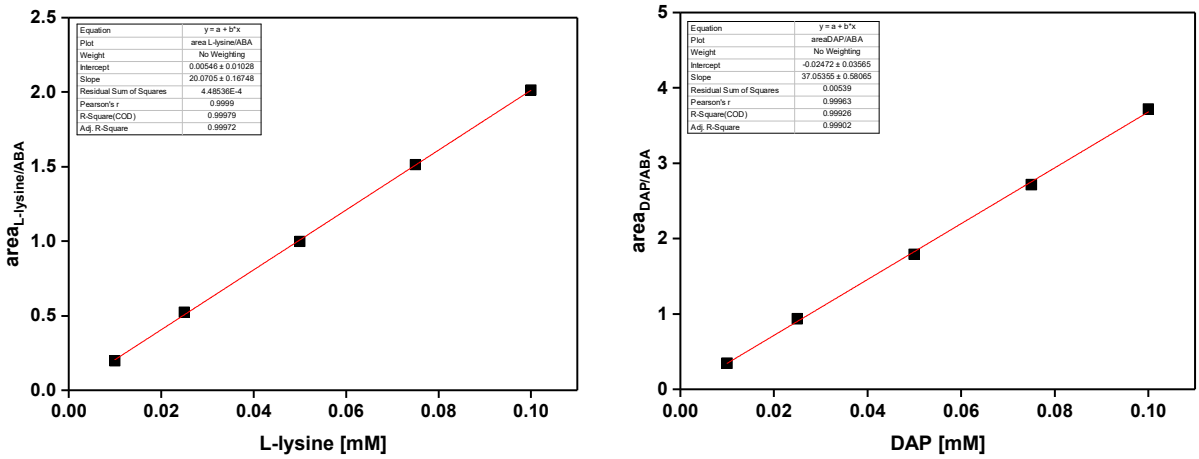

Supplementary Figure S8: **Calibration curve for DAP and L-lysine with the internal standard ABA (alpha-aminobutyric acid), HPLC analysis (see Methods in the main paper).**

References

1. Diener, M., Kopka, B., Pohl, M., Jaeger, K.-E. & Krauss, U. Fusion of a coiled-coil domain facilitates the high-level production of catalytically active enzyme inclusion bodies. *ChemCatChem* **8,** 142–152 (2016).
2. Grünberger, A. *et al.* Microfluidic picoliter bioreactor for microbial single-cell analysis: Fabrication, system setup, and operation. *J. Vis. Exp.* 1–11 (2013). doi:10.3791/50560
3. Grünberger, A. *et al.* Spatiotemporal microbial single-cell analysis using a high-throughput microfluidics cultivation platform. *Cytom. Part A* **87,** 1101–1115 (2015).
4. Limberg, M. H. *et al.* Metabolic profile of 1,5-diaminopentane producing *Corynebacterium glutamicum* under scale-down conditions: Blueprint for robustness to bioreactor inhomogeneities. *Biotechnol. Bioeng.* **114,** 560–575 (2017).
5. Keilhauer, C., Eggeling, L. & Sahm, H. Isoleucine synthesis in *Corynebacterium glutamicum*: molecular analysis of the ilvB-ilvN-ilvC operon. *J. Bacteriol.* **175,** 5595–603 (1993).
6. Unthan, S. *et al.* Beyond growth rate 0.6: What drives *Corynebacterium glutamicum* to higher growth rates in defined medium. *Biotechnol. Bioeng.* **111,** 359–371 (2014).

3 Discussion

3.1 Enlargement of the CatIB toolbox

During this doctoral thesis, the CatIB immobilization method was evaluated as a suitable alternative to already existing immobilization methods, which should include the easy, cost-efficient and finally generic production of enzyme immobilizates. Based on initial studies from a previous thesis [91], were three enzymes were studied, the evaluation of the CatIB strategy was broadened by five further enzyme examples with increasing complexity (Figure 3-1). The construct of the previous thesis contained the following parts (from N- to C-terminus): the TDoT domain, the linker consisting of 3xGGGS and a Factor Xa protease cleavage site and the enzyme, which proved to be useful for all investigated enzymes. The gene encoding for an hexa-histidine tag at the N-terminus [90] was excised as it was a not useful artefact of the commercial pET28a-vector. In chapter 2.1, it was demonstrated that the excision of this His_6-tag had no influence on the CatIB formation efficiency [296]. Not only the enzymes but also the coiled-coil domain could be easily exchanged within the vector construct. Since the efficiency to form CatIBs with a reasonable activity and insolubility was not possible in every case (chap. 2.1), the CatIB formation had to be improved on molecular biological level and is presented in the following chapter.

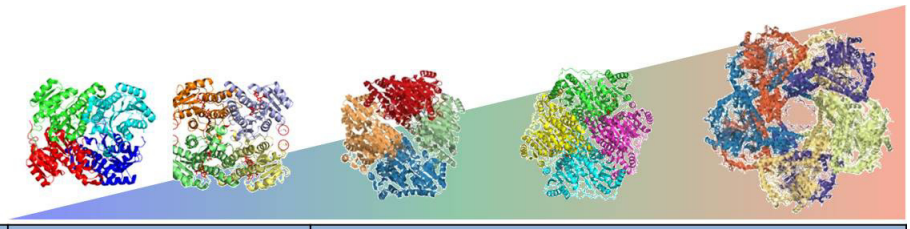

	alcohol dehydrogenases		decarboxylases		
	(*R*ADH)	(*Lb*ADH)	benzaldehyde lyase (*Pf*BAL)	benzoylformate decarboxylase (*Pp*BFD) *L476Q*	lysine decarboxylase (*Ec*LDC)
subunits	4	4	4	4	10
size of subunit	27 kDa	27 kDa	60 kDa	57 kDa	81 kDa
cofactor	NADPH	NADPH	ThDP, Mg^{2+}	ThDP, Mg^{2+}	PLP

Figure 3-1 CatIB toolbox with increasing complexity which consists of the following enzymes: alcohol dehydrogenases from *Ralstonia sp.* (*R*ADH) and from *L. brevis* (*Lb*ADH), ThDP-dependent enzymes benzaldehyde from *P. fluorescens* (*Pf*BAL) and a variant of benzoylformate decarboxylase from *Pseudomona. putida* (*Pp*BFD), and PLP-dependent constitutive lysine decarboxylase from *E. coli* (*Ec*LDC).

3.1.1 Approaches to improve CatIB formation

Since so far no rules exist for the prediction of active IB formation [96], the formation of various CatIBs was empirically studied in chapter 2.1 [296]. Since the molecular structure of the enzyme molecules in the CatIBs cannot be studied directly, yet, their properties must be evaluated based on their solubility, residual activity, morphology, and stability. First of all, all aforementioned enzymes could be successfully produced as CatIBs. To improve the CatIB formation efficiency and characteristics, different molecular biological strategies were applied: the coiled-coil domain or the fusion site to the enzyme was exchanged.

3.1.1.1 Changing the fusion site

The choice of the fusion site was mandatory for the activity of the CatIBs as was shown for *Ec*LDC-CatIBs (chap. 2.1). First, the TDoT-domain and the linker region consisting of 3xGGGS and a Factor Xa protease cleavage site was fused N-terminally to *Ec*LDC (TDoT-*Ec*LDC), which resulted in a poor activity of only $6.2*10^{-7}$ s^{-1} for the final CatIB lyophilizate (see chap. 2.1 Table 1 [296]). Considering the structure of *Ec*LDC, the N-terminus is located within the decameric structure in the N-terminal wing domain of the enzyme, whereas the C-terminus is located at the protein surface (Figure 3-2) [265]. Thus, it can be assumed that the N-terminal fusion of the TDoT domain impairs the formation of a correctly folded active site. Besides, the C-terminal fusion of the TDoT-Linker (without 3xGGGS) construct resulted in a six orders of magnitudes higher activity of 0.71 s^{-1} (see chap. 2.1 Table 1 [296]), confirming the hypothesis that the fusion position influences the activity. Taken together, the fusion site of the enzyme has to be considered, since it could have a great influence on the CatIB activity. Studies on the influences of the fusion position on the protein properties can also be found in literature. The position of the His-Tag was studied for various enzymes, e.g. resulting in a different arrangement of disulfide bonds of a receptor protein [297] or in altered properties and structure of a zinc finger protein [298]. Thus, the position of the fusion protein should be carefully selected having a great influence on the protein properties. However, this generally has to be determined empirically and the protein structure can give a first hint. The CatIBs of all other enzymes studied in this thesis were prepared by N-terminal fusion of the respective coiled-coil domains, since the N-termini were located at the protein surface (see chap. 2.1 Figure S4a-d [296]).

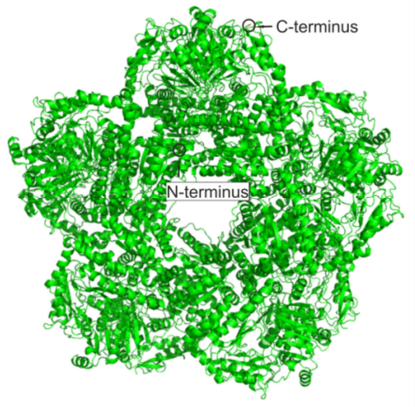

Figure 3-2 Structure of *Ec*LDCc (PDB: 5fkz). The N-terminus is located within the decameric structure in the N-terminal wing domain of the enzyme, whereas the C-terminus is located at the protein surface [265].

3.1.2 Influence of the coiled-coil tag on the CatIB properties

Besides the TDoT-domain, which was already previously tested as a useful aggregation-inducing tag for CatIB formation [90], the CatIB toolbox was broadened by fusion to another self-assembling coiled-coil domain 3HAMP (chap. 1.3.3). 3HAMP was chosen since one monomer is 3-fold larger (172 amino acids) compared to TDoT (52 amino acids). 3HAMP forms dimers and TDoT tetramers, which could also have an influence on the CatIB formation efficiency. The resulting CatIBs showed differences in activity and morphology (chap.. 2.1 [296]), which will be discussed in the following chapter. The following properties were measured and compared: the overall activity compared to the soluble enzyme, the final yield of the CatIB lyophilizate, the solubility, the composition, and the morphology of the particles.

3.1.2.1 The aggregation-inducing tag influences the CatIB morphology

To visualize the formation of CatIBs fused to either TDoT or 3HAMP and produced in *E. coli* BL21(DE3) cells, microscopy images of all CatIB constructs were performed. As some CatIBs were hardly visible in the phase contrast such as 3HAMP-*R*ADH and both *Lb*ADH-CatIBs (Figure 3-3, chap. 2.1 Figure 4 [296]), the monomeric, enhanced yellow fluorescent protein (YFP) from *Aequorea victoria* [299,300] was produced exemplarily as functional inclusion bodies (FIBs) to act as a reporter to visualize the formation of these less visible CatIBs in *E. coli*.

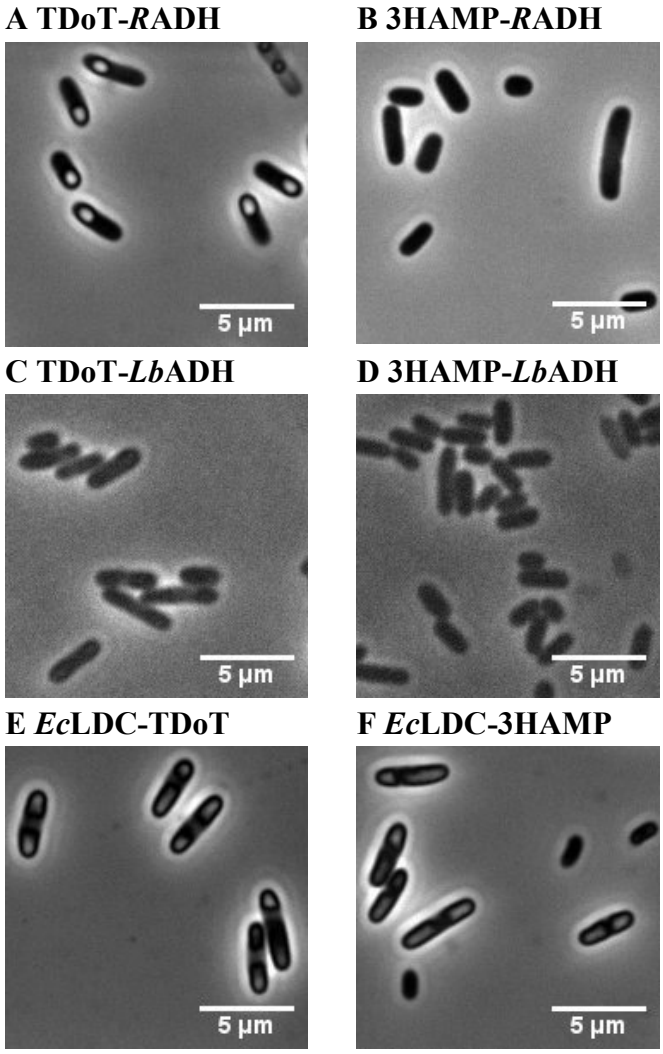

Figure 3-3 Microscopic images of *E. coli* BL21(DE3) cells producing (A) TDoT-*R*ADH, (B) 3HAMP-*R*ADH, (C) TDoT-*Lb*ADH, (D) 3HAMP-*Lb*ADH, (E) *Ec*LDC-TDoT, and (F) *Ec*LDC-3HAMP. Phase contrast images were recorded at the Microscale Bioengineering group at the IBG-1 by an inverted Nikon Eclipse Ti microscope (Nicon GmbH, Düsseldorf, Germany) equipped with an Apo TIRF 100x Oil DIC N objective (ALA OBJ-Heater, Ala Scientific Instruments, USA), and an ANDOR Zyla CMOS camera (Andor Technology plc., Belfast, UK). Pictures were taken from chapter chap. 2.1 Figure 4 [296].

As demonstrated in Figure 3-4 the resulting functional IBs of both fusion proteins TDoT-YFP and 3HAMP-YFP clearly differed similar to the CatIBs seen before (Figure 3-3). The fluorescence images show TDoT-YFP as typically dense and compact particles in *E. coli* (Figure 3-4) [301], which was already observed by Diener [91]. In contrast to this, 3HAMP-YFP accumulates less defined within the cell. These accumulations are only visible on the fluorescence image, but hardly in the phase contrast, indicating a different kind of IBs with lower density than the typically observed ones. The typical IBs, which are clearly visible in the phase contrast as aggregates at the cell poles, were called “compact CatIBs” (like TDoT-YFP). They are clearly morphologically distinct from the “diffuse CatIBs” formed for example by 3HAMP-YFP. The morphology of “diffuse CatIBs” has not been observed so far.

They can be distinguished from soluble proteins, as they can be pelleted similar to the dense CatIBs.

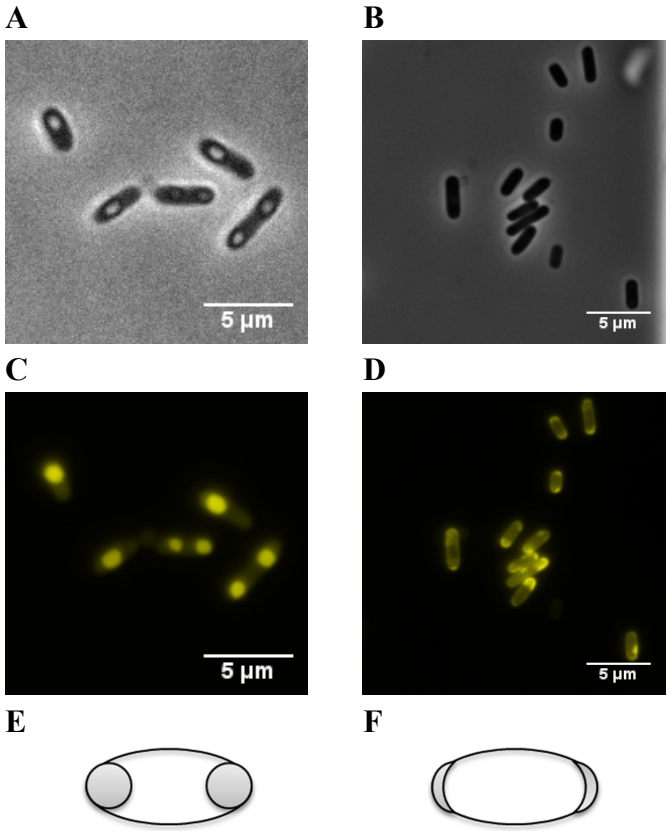

Figure 3-4 Microscopic images of *E. coli* BL21(DE3) cells producing (A, C) TDoT-YFP and (B, D) 3HAMP-YFP. (A, B) phase contrast images, (C, D) fluorescence images using filters (excitation: 520/60 nm, dichroic mirror: 510 nm, emission: 540/40 nm). (E,F) schematic illustration of the cells: (E) refers to the compact and dense inclusion bodies and (F) to the diffuse inclusion bodies. The images were recorded at the Microscale Bioengineering group at the IBG-1 by an inverted Nikon Eclipse Ti microscope (Nicon GmbH, Düsseldorf, Germany) equipped with an Apo TIRF 100x Oil DIC N objective (ALA OBJ-Heater, Ala Scientific Instruments, USA), an ANDOR Zyla CMOS camera (Andor Technology plc., Belfast, UK), an Intensilight (Nicon GmbH, Düsseldorf, Germany) light source for fluorescence excitation. Pictures were taken from the Bachelor thesis of Tobias Karmainski [302] and were provided from Vera D. Jäger.

Similar results were obtained for *Pf*BAL-CatIBs and *R*ADH-CatIBs, which formed compact, clearly visible IBs when fused to TDoT and not or hardly visible aggregates when fused to 3HAMP (Figure 3-3 and chap. 2.1 Figure 4g, 4i [296]). It can be assumed that these poorly visible CatIBs are similar to the 3HAMP-YFP-IBs and thus they were accordingly classified as diffuse CatIBs. *Ec*LDC-CatIBs fused to TDoT and 3HAMP revealed in both cases clearly visible, compact CatIBs, whereas *Lb*ADH and *Pp*BFD showed in both cases the diffuse type (Figure 3-3 and chap. 2.1 Figure 4h, 4j, 4k [296]). These differences in morphology could be also seen in the scanning electron microscope (SEM) images (chap. 2.1 Figure 5 [296]). The compact particles TDoT-YFP (without linker) and TDoT-*Pf*BAL formed distinct particles with a round or barrel-like shape, which had a size of 0.5-1 µm (chap. 2.1 Figure 5a, 5c [296]). These results are in accordance with the previous observed size and structure for TDoT-YFP-CatIBs (with linker) [91]. In contrast, the diffuse particles 3HAMP-YFP (without

linker) and the 3HAMP-*Pf*BAL showed a less ordered structure and seemed to consist of smaller substructures (chap. 2.1 Figure 5b, 5d [296]).

The morphology influenced the solubility behavior as well as the activity and the composition of the CatIBs as will be further discussed in the following. For a survey of all properties see Table 3-1.

3.1.2.2 Compact CatIBs are less soluble than diffuse ones

To characterize the respective CatIBs, their production in *E. coli* was followed by a standardized purification protocol, which was simplified in chapter 2.3 based on the protocol established by Martin Diener [91]. First the enzymes were produced in *E. coli* BL21(DE3), then the obtained cell pellet was suspended in buffer and the cells were disrupted by ultra-homogenizer. Afterwards the obtained crude cell extract was centrifuged and the pellet containing the CatIBs was washed once with water by resuspension and a subsequent centrifugation step. The solubility was analyzed by SDS-PAGE after cell disruption during subsequent washing steps of the pellet. The following fractions were analyzed: the crude cell extract (CCE), which was separated into the soluble protein containing supernatant (SN) and the insoluble, CatIB-containing pellet (P).

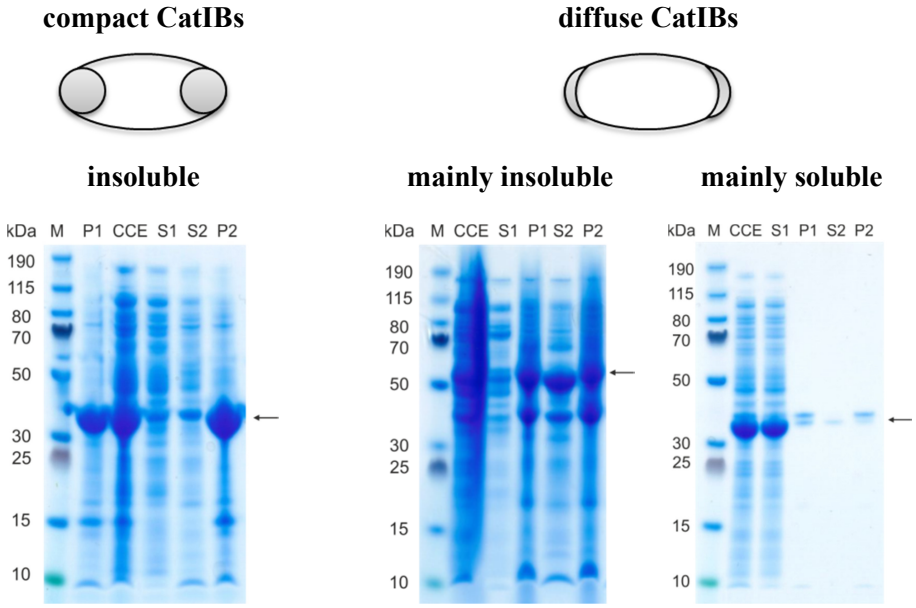

Figure 3-5 SDS-PAGE analysis of the purification steps for compact (TDoT-*R*ADH, 34 kDa), mainly insoluble diffuse CatIBs (3HAMP-*R*ADH, 47 kDa), and mainly soluble diffuse CatIBs (TDoT-*Lb*ADH, 34 kDa). The CCE (crude cell extract) was centrifuged to separate supernatant (S1) and pellet (P1). P1 was washed once with water by resuspension and centrifugation, which results in S2 and P2. The protein concentration in solution was measured using the Bradford assay [303]. For SDS-PAGE, samples were diluted with water to obtain a protein concentration of 1 mg ml^{-1}. Pictures of the SDS-PAGEs were taken from chapter chap. 2.1 Figure S9a [296] and the Master thesis of Selina Seide [304].

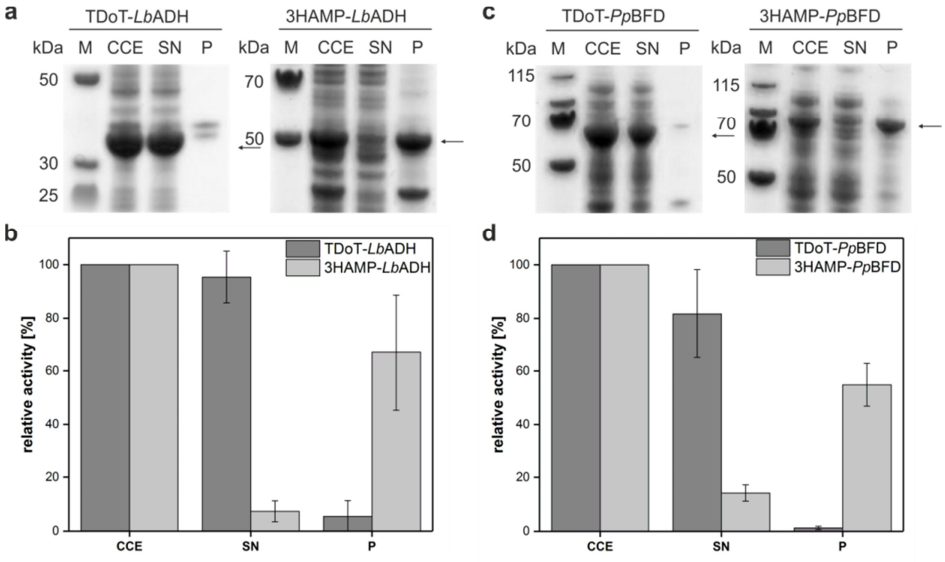

Figure 3-6 Evaluation of 3HAMP-CatIBs by (a) SDS-PAGE analysis of 3HAMP-*Lb*ADH (47 kDa) and 3HAMP-*Pp*BFD (77 kDa) and (b) the relative activity in the pellet of TDoT-*Lb*ADH, 3HAMP-*Lb*ADH, TDoT-*Pp*BFD-CatIBs and 3HAMP-*Pp*BFD-CatIBs during purification. After cell disruption, the crude cell extract (CCE) was separated by centrifugation into the soluble protein containing supernatant (SN) and the insoluble IB containing pellet (P) fraction. (a) SDS-PAGE analysis of the respective enzyme fractions: CCE, SN, and P. The target enzyme is indicated by arrows. The protein content in the SN was measured according to Bradford [303]. (b) Normalized activity in the CCE, SN, and P fractions of the respective enzymes. Note: the P fraction was washed once with water and centrifuged before activity measurement. The activity in the P fraction was calculated relative to the activity in the CCE, which was set to 100%. The initial rate activity of 3HAMP-*Lb*ADH-CatIBs was measured by following the depletion of NADPH upon reduction of acetophenone to 1-phenylethanol (chap. 2.1) [305]. For 3HAMP-*Pp*BFD-CatIBs the decarboxylation of benzoylformate to benzaldehyde was followed in a coupled assay using horse liver ADH, which reduces benzaldehyde to benzyl alcohol under NADH consumption (chap. 2.1) [173]. Results were taken from chapter 2.1 (Figure 3a, 3b [296]).

In Figure 3-5, it can be seen that the washing step did not only remove additional soluble compounds, but also part of the CatIBs from the pellet. Generally, the compact CatIBs were insoluble and did not dissolved during the first washing step in water, which is in accordance to previous results [91]. By contrast, TDoT-*Lb*ADH and TDoT-*Pp*BFD as diffuse CatIBs, also pelletized by centrifugation, dissolved completely during the washing steps (chap. 2.1 Figure S9a, S9b [296]) and thus showed properties between compact CatIBs and soluble enzymes. Here, it is not clear, if the particles are really soluble or are too small to be effectively sedimented at the here applied centrifugation speed of 15,000 *x*g. Exchange of the aggregation-inducing tag to the 3-fold larger 3HAMP domain improved the situation to some extend resulting in more compact CatIBs for *Lb*ADH and *Pp*BFD (Figure 3-6a, c). This larger domain is assumed to enhance the aggregation propensity. As a result, 3HAMP-*Lb*ADH and 3HAMP-*Pp*BFD CatIBs showed a lower solubility and dissolved only progressively in the second washing step (Figure 3-5, Figure 3-6). However, these CatIBs are still diffuse as they were poorly visible in the phase contrast (Figure 3-3, chap. 2.1 Figure 4h, 4j [296]). Thus, they were classified as mainly insoluble, diffuse CatIBs. Interestingly, the fusion of 3HAMP to *Pf*BAL and *R*ADH yielded also this mainly insoluble, diffuse CatIB type and not the

compact one as was obtained by fusion to the TDoT domain (Figure 3-5, chap. 2.1 Figure 4g, 4i [296]).

3.1.2.3 Morphology and properties of CatIBs correlate and are independent of the aggregation-inducing tag

Considering the morphology and the solubility, the CatIBs can be classified and divided in the following order (Table 3-1): Compact CatIBs forms clearly visible particles within the cells and did not dissolve during the washing steps (Figure 3-3, Figure 3-5a and chap. 2.1 Figure 4 [296]). This CatIB category applies to *Ec*LDC, *Pf*BAL, and *R*ADH fused to TDoT as well as *Ec*LDC fused to 3HAMP. The diffuse CatIBs are poorly visible in the phase contrast and dissolved to a lower or higher extent during the washing steps (Figure 3-5b,c, Figure 3-6). Thus, they were classified as mainly insoluble, diffuse and mainly soluble, diffuse CatIBs. Mainly insoluble, diffuse CatIBs were observed for *Lb*ADH, *Pp*BFD, *Pf*BAL and *R*ADH fused to 3HAMP and mainly soluble diffuse CatIBs for *Lb*ADH and *Pp*BFD fused to TDoT. As there is a high structural similarity between *Pp*BFD and *Pf*BAL [157,196], this difference in CatIB morphology is quite astonishing and is further discussed in chapter 3.1.3.

The following parameters were considered for comparative characterization of the CatIBs: the relative activity of the pellet washing fraction compared to the crude cell extract, the yield of the CatIB lyophilizate (and protein content in the lyophilizate) after washing of the pellet, the protein content measured at 280 nm after solubilizing by guanidine hydrochloride, the lipid content after extraction with solvents, and the initial rate activity compared to the soluble enzyme.

The relative activity distribution between soluble fractions (supernatant, SN) and the pellet (P) was measured by initial rate activity measurements relative to the activity in the crude cell extract (CCE). This relative activity distribution is in accordance with the distribution of the target protein seen in the SDS-PAGE (Figure 3-6). Thus, the relative activity of the pellet can be used as an indicator for the solubility of the CatIBs and thus for the efficiency to form those. As the compact CatIBs did not dissolved, they showed a high relative activity of about 88% in the pellet fraction compared to the CCE (for TDoT-*R*ADH and TDoT-*Pf*BAL), whereas the mainly soluble diffuse CatIBs showed a very low relative activity of 2-6% (TDoT-*Lb*ADH and TDoT-*Pp*BFD) (Table 3-1). Due to only progressive dissolving of the mainly insoluble diffuse CatIBs, the relative activity in the pellet fraction was 67-76% (3HAMP-CatIBs), which was higher compared to the mainly soluble diffuse CatIBs but lower than the value for the compact CatIBs.

Table 3-1 Classification of different CatIB types: compact and diffuse CatIBs. The CatIBs were classified as compact and diffuse regarding their morphology in *E. coli* and as insoluble and mainly insoluble and soluble with respect to the SDS-PAGE analysis and the actvities of the pellet fractions compared to the crude cell extract. For each type of CatIBs, the respective mean values such as yield, protein content and lipid content as well as the residual activitiy compared to the soluble enzyme were grouped and evaluated. The classification: high, medium, low refers to the other types of CatIBs. A detailed overview is given in the Appendix, Table 6-1 and chap. 2.1 Table 1 [296]. n.d. refers to not determined

CatIBs types	compact CatIBs 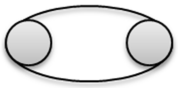		diffuse CatIBs 	
solubility	insoluble		mainly insoluble	mainly soluble
CatIBs	TDoT-*Pf*BAL, TDoT-*R*ADH, *Ec*LDC-TDoT, *Ec*LDC-3HAMP	TDoT-*Bs*LA[1], TDoT-*Ec*MenD[1], TDoT-*At*HNL[1]	3HAMP-*Lb*ADH, 3HAMP-*Pp*BFD, 3HAMP-*Pf*BAL, 3HAMP-*R*ADH	TDoT-*Lb*ADH, TDoT-*Pp*BFD
activity in the pellet fraction compared to CCE	high (88%)	high (76-114%)	medium (67-76%)	low (2-6%)
CatIB yield [$mg_{lyophilizate}$/ $g_{wet\ cells}$]	high (75-124 mg)	high (73-122 mg)	medium (37-81 mg)	low (16-25 mg)
CatIB yield [$mg_{protein}$/ $g_{wet\ cells}$]	high (59-90 mg)	high (62-93 mg)	medium (16-45 mg)	low (5-11 mg)
protein content	high (57-85%)	high (79-93%)	medium (31-55%)	low (27-43%)
lipid content	low (13-18%)	n.d.	high (28-35%)	medium (19-25%)
residual activity compared to soluble enzyme	low (1-2%)	medium (11%) (TDoT-*At*HNL)	medium - high (1-18%)	medium (4-6%)

[1] Diener *et al.* [90]

As the compact CatIBs did not dissolved during the washing steps, a higher yield was obtained (59-90 mg protein/g cell wet weight), compared to the mainly insoluble diffuse CatIBs (16-45 mg protein/g cell wet weight), and the mainly soluble diffuse CatIBs (5-11 mg protein/g cell wet weight) due to a higher loss of target protein during the washing steps. Interestingly, the mainly soluble diffuse CatIBs showed the lowest protein content (27-43%), followed by the mainly insoluble diffuse CatIBs (31-55%). The compact CatIBs showed the highest protein content of 57-85%, which is in line with earlier results [90].

Especially the diffuse CatIB preparations contained contaminations (Figure 3-5), which were identified by MALDI-TOF analysis exemplarily for TDoT-*Pf*BAL- and 3HAMP-*Pf*BAL-CatIBs (for details see chap. 2.2 and Kloss *et al.* [306]). Besides the target protein, the other strong bands were identified as chaperones IbpA and IbpB [307–309] at 15 kDa and membrane proteins OmpA and OmpF [310] at 40 kDa and murein lipoprotein at 8 kDa. Interestingly, the band at 40 kDa is most prominent in the diffuse CatIB preparation (Figure 3-5). The observation of foreign proteins is in line with previous obtained results for inclusion body preparations, where phospholipids, membrane proteins, and nucleic acids were reported as contamination [311]. Since the diffuse CatIBs seemed to accumulate at the cell membrane (Figure 3-4B, D) and contained co-purified cellular proteins to a higher extent, it was assumed that membrane lipids such as phospholipids could be associated with the CatIBs, which was gravimetrically measured for all CatIB preparations by extraction with chloroform and methanol (for details see chaps. 2.1 [296] and 2.2 [306]). The compact CatIBs gave a two-fold lower lipid content (13-18%) compared to the mostly insoluble diffuse CatIBs (28-35%). The mostly soluble compact CatIBs showed lipid contents in between (19-25%). Considering the present data set, it can be assumed that the CatIBs with 3HAMP domain maybe attract lipids to a higher extent (28-35%) than TDoT derived CatIBs (13-25%). The comparison of each biological replicate shows that measurements with diffuse CatIBs show a higher error, which holds especially for the protein content, the total yield and in some cases also for the activity measured in the pellet fraction (3HAMP-*Lb*ADH, 3HAMP-*Pp*BFD) (chap 2.1 Figure S8 [296]). This can be again explained by the diffuse nature of the CatIBs. Since the CatIBs dissolved during the washing steps, the final yield differed depending e.g. on the initial compactness of the pellet, the mixing intensity to achieve suspension of the pellet, and the conditions during the following centrifugation step. Although a standard protocol was followed, the data compared here were produced by different researchers using different CatIB preparations. In summary, the trend between compact and diffuse CatIBs is obviously visible.

3.1.2.4 Diffuse CatIBs show a higher activity

For application in biocatalysis, the residual activity of the CatIBs compared to the soluble enzyme should be ideally high with a high activity recovery. Table 3-2 shows the initial rate activity calculated as total turnover number (k_{cat}) and the relative activity compared to the soluble enzyme. The compact CatIBs TDoT-*R*ADH and TDoT-*Pf*BAL showed a 6-fold to 18-fold lower residual activity compared to the respective counterparts 3HAMP-*R*ADH and

3HAMP-*Pf*BAL, respectively. Generally, the diffuse CatIBs showed higher residual activities (4-18%) compared to the compact CatIBs, except for 3HAMP-*Lb*ADH (1%). This is in accordance with the diffuse nature of these CatIBs, which are less dense packed. These diffuse particles are assumed to be smaller and thus have a better surface to volume ratio for better accessibility of substrates and thus a higher activity. This hypothesis can be confirmed with the SEM images, where the diffuse particles seemed to consist of smaller substructures (chap. 2.1 Figure 5b, 5d [296]).

The highest residual activity of all CatIBs was observed for 3HAMP-*R*ADH with up to 12-27%, which was tested with two substrates (cyclohexanone and (*R*)-2-HPP). Here, it has to be taken into account that the actually measured activity of the soluble *R*ADH for (*R*)-2-HPP was 3-fold lower (116.2 U/mg) than the earlier reported value (362.6 U/mg) [232], probably due to a longer storage time of the *R*ADH (1 year), which could impair the activity [232]. Furthermore, the performed *R*ADH assay differed from the reported continuous photometric assay as it was performed discontinuously. Thus, the higher residual activity of *R*ADH-CatIBs with respect to (*R*)-2-HPP could be a result of the lower activity of soluble *R*ADH due to a longer storage time. Furthermore, it can be assumed that the catalytic properties of the CatIBs, such as accessibility for the substrate could differ, so that K_M or k_{cat} might change differently for the respective substrates. This was also demonstrated for TDoT-*Ec*LDC-CatIBs, which revealed a higher K_M of approx. 23 mM than reported in literature (0.84 mM) [312] (compare chap. 2.3 and Kloss *et al*. [313]).

Besides 3HAMP-*R*ADH, the CatIBs showed relatively low residual activities of 1-10%. Generally, a lower activity is recovered for immobilized enzyme [56] due to a lower flexibility, steric hindrance, mass transfer and diffusion limitations caused by the aggregation of the enzyme [38,39,48]. CatIBs can be best compared to cross-linked enzyme aggregates (CLEAs) as a carrier-free enzyme immobilization method. CLEAs showed activity recovery of 6-100% and in some cases no activity depending on the immobilized enzyme, the precipitants and the cross-linking agents (Table 1-2). Hence, the activity of the CatIBs is in the lower range of CLEAs. The generally low residual activity of all CatIB types was probably obtained, since the activity was calculated based on the whole protein content, so that also not correctly folded enzymes or enzymes in the inner particle were considered for protein determination, although this fraction did not contribute to the activity.

Due to the easy production of CatIBs, the lower activity could be compensated by the higher yield or the easier production protocol, which will be discussed in chapter 3.3.

Table 3-2 Activity (k_{cat}) and residual activity of compact and diffuse CatIBs compared to the respective soluble enzymes. n refers to the number of biological replicates (different batches of separately produced CatIBs). Values were taken from chapter 2.1 [296] and the Master thesis of Selina Seide [304]

	CatIBs	substrate	activity k_{cat} [s^{-1}]			residual activity compared to soluble enzyme [%]
			mean	SD	n	
compact	TDoT-*R*ADH	cyclohexanone[1]	0.054	0.008	3	2
	TDoT-*R*ADH	(*R*)-2-HPP[2]	1.5	0.24	1	3
	TDoT-*Pf*BAL	DMBA[3]	0.77	0.12	4	1
	*Ec*LDC-TDoT	L-lysine[4]	0.71	-	1	n.d.
	*Ec*LDC-3HAMP	L-lysine[4]	0.80	-	1	n.d.
diffuse, mainly insoluble	3HAMP-*R*ADH	cyclohexanone[1]	0.332	0.019	3	12
	3HAMP-*R*ADH	(*R*)-2-HPP[2]	14.11	0.13	1	27
	3HAMP-*Pf*BAL	DMBA[3]	13.9	2.9	3	18.1
	3HAMP-*Lb*ADH	acetophenone[5]	0.6	0.2	3	1
	3HAMP-*Pp*BFD-L476Q	PGA[6]	23.4	6.1	4	10.3
diffuse, mainly soluble	TDoT-*Lb*ADH	acetophenone[5]	3.63	0.9	3	5.8
	TDoT-*Pp*BFD-L476Q	PGA[6]	9.2	4.7	4	4.1

[1] The initial rate activities of *R*ADH-CatIBs was measured by reduction of 100 mM cyclohexanone in TEA-buffer (50 mM, pH 7.5, 0.8 mM $CaCl_2$) under the consumption of 0.4 mM NADPH, which was performed for 5 min at 30 °C and 1000 rpm in a thermomixer (Thermomixer comfort, Eppendorf, Germany). Sampling was performed every minute (250 µl), which were diluted 1:3 in MeOH to stop the reaction and centrifuged for 5 min (7697 *xg*, room temperature). The NADPH decrease was detected in in a discontinuous spectrometry based assay at 340 nm.

[2] The reduction of 10 mM (*R*)-2-HPP by *R*ADH-CatIBs was measured in 50 mM TEA-buffer (0.8 mM $CaCl_2$, pH 7.5) under 3 mM NADPH oxidation and was followed for 5 min at 30°C by a discontinuous HPLC-based assay.

[3] Initial rate activity of *Pf*BAL-CatIBs were measured by carboligation of 3,5-dimethoxybenzaldehyde (DMBA, 10 mM) to the respective benzoin in 80 vol% TEA-buffer (50 mM, pH 7.5, 2.5 mM $MgSO_4$, 0.1 mM ThDP) and 20 vol% DMSO at 30°C and 1000 rpm in a discontinuous assay analyzed by HPLC.

[4] The initial rate activity of *Ec*LDC-CatIBs was measured for the decarboxylation of 10 mM L-lysine in potassium phosphate buffer (50 mM, pH 8.0) containing 0.1 mM PLP at 30°C and 1000 rpm by a discontinuous HPLC-based assay.

[5] The initial rate activities of *Lb*ADH-CatIBs was measured by reduction of 10.7 mM acetophenone in TEA-buffer (50 mM pH 7.0, 0.8 mM $MgCl_2$) under the consumption of 0.2 mM NADPH, which was detected in in a continuous fluorescence spectrometry based assay (details are the same as for *Pp*BFD-CatIBs).

[6] Initial rate activity of *Pp*BFD-CatIBs was measured for the decarboxylation of 5 mM phenylglyoxylic acid (PGA) to benzaldehyde followed by the reduction to benzyl alcohol by 0.25 U ml^{-1} horse liver (HL-)ADH under the oxidation of 0.25 mM NADH in TEA-buffer (50 mM TEA, 0.5 mM ThDP, 2.5 mM $MgSO_4$, pH 6.5), which was detected in in a continuous fluorescence spectrometry based assay (90 s at 30 °C by excitation at λ_{ex} 350 nm and emission at λ_{em} 460 nm, bandwidth 1.4 nm in excitation and emission, 10 x 4 mm quartz-glass cuvettes with a volume of 1 ml (4 mm light path in excitation) using a Fluorolog 3-22 spectrofluorometer (Horiba Jobin Yvon, Bensheim, Germany) in front-face angle.

3.1.3 Can the formation of CatIBs and their morphology be predicted?

There are several computational studies that predict the tendency to form inclusion bodies based on the amino acid sequence. The in chapter 2.1 employed software AGGRESCAN is based on previous discoveries of aggregation "hot spots" [314–316] and indicates that the aggregation propensity of proteins correlates to their conformation, length, function, location, and frequency in occurrence [101]. The prediction correlates the hydrophobicity, secondary structure propensity and charge to the aggregation propensity based on the primary sequence [315]. In chapter 2.1 this tool was applied to establish a correlation of the protein sequence to the aggregation propensity of two fluorescence proteins and eight different enzymes fused to TDoT (Figure 3-7A) [296]. This correlation showed a weak linear relationship between the AGGRESCAN-derived score and the empirically evaluated tendency to form aggregates expressed as relative activity in the pellet compared to the crude cell extract. For this estimation only the protein sequences of the target proteins were considered, without the TDoT sequence. Inclusion of the TDoT sequence impaired the score of this correlation, as the TDoT fusion should theoretically increase the solubility of some enzymes based on the scoring, which did not match with the experimental results. Consequently, the AGGRESCAN tool can be used as a first indicator for aggregation propensity prediction, but cannot be used to correlate the empirical derived data with theoretical structure-based scores for aggregation propensity predication.

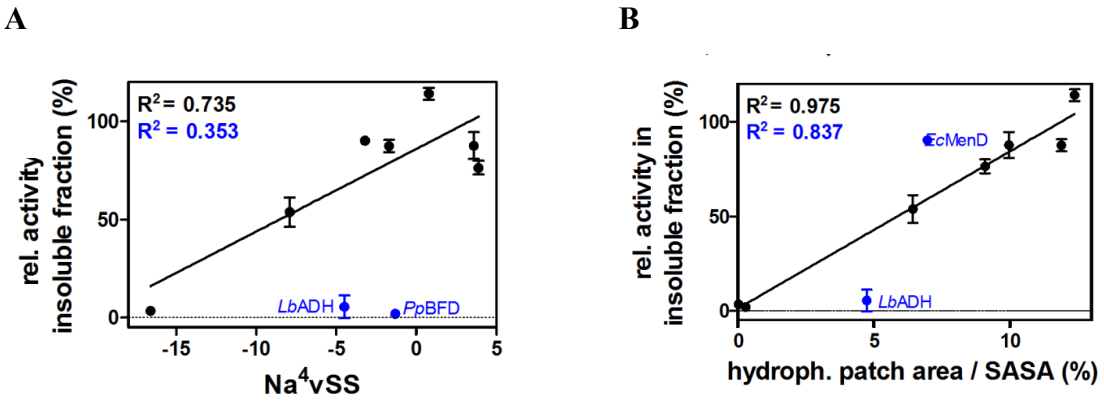

Figure 3-7 Computational analysis of the (A) sequence-based and (B) structural determinants of CatIB formation based upon the TDoT-fusion. (A) Sequence-based aggregation propensities were inferred using the AGGRESCAN webserver [101] and the average aggregation-propensity values per amino acid (a^4v) normalized to a 100-residue protein (Na^4vSS) were used as indicator for aggregation. Low (negative) Na^4vSS are an indicator for low aggregation propensity as for example demonstrated for intrinsically disordered proteins (IDPs) [101]. (B) The presence/absence of large hydrophobic surface patches for the corresponding target protein structures was quantified using the hpatch tool implemented in Rosetta [317–319]. Solvent accessible surface areas (SASA) were quantified using Pymol 1.7.0.0 (Schrödinger, LCC, New York, NY, USA). In (A and B) CatIB-formation was plotted as the relative activity in the insoluble fraction. Coefficient of determination (R^2) values are always given excluding the blue-highlighted outliers (black) and including the outliers (blue). Figures were taken from chapter 2.1 (Figure S12 and Figure 6) [296].

As this tool is based only on the amino acid sequence, it does not consider several other factors influencing the aggregation of proteins, such as temperature and growth rate, fusion to protein tags, specific codon usage, tRNA availability, and optimization of codons in the heterologous expressed sequence [320]. The influence of the temperature on YFP-CatIB formation was shown by the cooperation partner Robin Lamm (Appendix, Figure 6-1). The functionality (fluorescence intensity) of TDoT-YFP FIBs produced in *E. coli* was analyzed at different cultivation temperatures, demonstrating a decrease in fluorescence at temperatures above 15°C. Hence, the cultivation temperature after induction in autoinduction media empirically chosen earlier by Martin Diener was shown to be optimal for the YFP-CatIB production. The result indicates that the temperature during the production of functional IBs is crucial to achieve a high degree of functionality, which correlates with respective observations for the production of soluble recombinant proteins [321]. It can be assumed that 15°C is also the optimal temperature to produce the other enzymes and proteins as CatIBs, which, however, has to be proven in additional experiments.

The program AGGRESCAN considered only the formation of inclusion body aggregates, but not the formation of functional IBs as was addressed in chapter 2.1 [296]. As activity maintenance requires the correct folding of the enzymes, the sequence-based prediction of the aggregation propensity is not sufficient. Activity retention in aggregates requires formation of the native quaternary structure of the protein. Hence, the prediction of aggregation propensity should correlate to properties derived from the quaternary structure of the proteins. As the solvent-accessible hydrophobic surface patches can influence largely the aggregation formation, the empirically derived aggregation propensity data (relative activity in the pellet compared to the crude cell extract) was correlated to the size of hydrophobic surface patches. As demonstrated in Figure 3-7B, both parameters show a good correlation for TDoT-CatIBs. These results suggest that the distribution of hydrophobic surface patches can be used as a parameter to predict the tendency to form functional aggregates. This correlation could explain the difference in aggregation propensity especially of the structural similar ThDP-dependent enzymes *Pf*BAL and *Pp*BFD, which revealed only 24% sequence similarity [157,196]. While *Pf*BAL fused to TDoT formed insoluble CatIBs, respective *Pp*BFD CatIBs dissolved during the washing steps due to a lower distribution of hydrophobic surface patches (chap. 3.1.2.2). The hydrophobic patch area divided by the overall solvent accessible surface area (SASA) was only 0.3% for *Pp*BFD in contrast to 9.9% for *Pf*BAL (Table 3-3). Large hydrophobic surface patches influence the efficacy of CatIB formation. This structural relationship can explain why highly soluble proteins such as mCherry do not form insoluble

IBs when fused to the TDoT domain (chap. 2.1 Figure S2). The relative hydrophobic patch area was zero for mCherry, since there are no hydrophobic patches on the surface. This first trial revealed good results for the correlation between surface patches and the aggregation propensity for TDoT-fused CatIBs but could not explain the differences to 3HAMP-CatIBs, which formed the same type of diffuse CatIBs in all case independently from surface patches.

Therefore, further factors have to be considered as described by de Groot and Ventura, who studied the formation of functional IBs by fusing the green fluorescent protein to an Alzheimer-related peptide as a aggregation-inducing tag [322]. These authors assumed that functionality of IB aggregates is attained by a correct folding of the native protein structure, which should occur prior to aggregation. They demonstrated that the relative rates of folding and aggregation can be fine-tuned using a library of single-point variants of an aggregation-prone protein. They concluded that aggregation competes with correct folding: higher aggregation tendency results in faster aggregation and thus incorrect folding and lower functionality [322].

In our study, we compared CatIBs originated from highly diverse sequences. As discussed above, they all showed more or less functionality using both tested coiled-coil fusion tags. Besides the competition between correct folding and aggregation also the differences in particle density have to be considered in this study, which was not a factor in the study of de Groot and Ventura. The smaller particles of diffuse CatIBs have a larger surface and are easier accessible for substrates, compared to the compact ones, which explains their higher residual activity (Table 3-1, Table 3-2). There is presently no experimental method available to dissect the activity loss caused by the particle density and by misfolded protein, respectively.

An explanation of the differences between 3HAMP CatIBs and TDoT CatIBs, however, can at partly be based on the structural differences of both coiled-coil domains. 3HAMP as part of a soluble receptor is located in the cytosol [122], in contrast to TDoT, which is as cell-surface protein located at the S-layer of the membrane [118–120], thus revealing a 3-fold higher content of hydrophobic surface patches (hydrophobic surface/overall surface for TDoT 14.6% and for 3HAMP 4.7%) (Table 3-3). In its physiological context, 3HAMP forms dimers and consists of 172 amino acids. TDoT forms a tetrameric structure and each subunit is composed of 52 amino acids under physiological conditions. It can be assumed that the TDoT domain will probably not form tetramers within the CatIB aggregates, due to the spatial arrangement and distance of the respective fusion sites in the enzyme. Besides, the formation of

intermolecular coiled-coil is most probable. In contrast, the formation of the dimeric assembly of the 3HAMP domain is more likely to be realized also within the CatIBs.

Thus, it can be assumed that inter- and intramolecular interactions differ, which results in the differences observed for activity, solubility, composition and morphology (Table 3-1). As pointed out above, 3HAMP-CatIBs are to a higher extent associated to membrane lipids (30% lipid content) and membrane proteins (Figure 3-5, Table 3-1) than TDoT-CatIBs. The composition of the CatIBs influences the properties of the particles, which is an important effect that cannot be predicted so far. In order to deduce the efficiency to form the respective CatIB type, several parameters of the coiled-coil domains can be considered.

Table 3-3 Molecular weight of all enzymes and percentage of the coiled-coil domain on the molecular weight of the fusion enzymes. Molecular weights were calculated using the ExPASy ProtParam Tool [323]. The presence/absence of large hydrophobic surface patches for the corresponding target protein structures (without coiled-coil domain) was quantified using the hpatch tool implemented in Rosetta [317–319]. Surface areas were quantified using Pymol 1.7.0.0 (Schrödinger, LCC, New York, NY, USA). Data was taken from chapter 2.1 (Table S2, S6) [296].

Protein	**Molecular weight [kDa] per subunit**	**Percentage coiled-coil domain on the total molecular weight [%]**	**hydrophobic patch area / overall SASA [%]**
TDoT	5.7	-	14.6
3HAMP	18.7	-	4.7
soluble *R*ADH	26.7	-	11.9
TDoT-*R*ADH-CatIBs	34.3	17	n.d.
3HAMP-*R*ADH-CatIBs	47.1	40	n.d.
soluble *Lb*ADH	26.8	-	4.8
TDoT-*Lb*ADH-CatIBs	34.3	17	n.d.
3HAMP-*Lb*ADH-CatIBs	47.1	40	n.d.
soluble *Pf*BAL	60.0	-	9.9
TDoT-*Pf*BAL-CatIBs	66.5	9	n.d.
3HAMP-*Pf*BAL-CatIBs	79.3	24	n.d.
soluble *Pp*BFD	57.4	-	0.27
TDoT- *Pp*BFD-CatIBs	64.2	9	n.d.
3HAMP- *Pp*BFD-CatIBs	77.0	24	n.d.
soluble *Ec*LDC	80.6	-	n.d.
*Ec*LDC-TDoT-CatIBs	87.5	7	n.d.
*Ec*LDC-3HAMP-CatIBs	100.5	19	n.d.

As discussed above, compact CatIBs were observed for *R*ADH and *Pf*BAL fused to TDoT, whereas *Lb*ADH and *Pp*BFD yielded diffuse CatIBs, due to a lower proportion of hydrophobic surface patches on the respective enzyme (Table 3-3). The higher hydrophobicity of the TDoT surface could increase the aggregation propensity of hydrophobic proteins (*R*ADH and *Pf*BAL), thus forming densely packed particles. However, the TDoT domain did not work so well for enzymes with a smaller content of hydrophobic

surface patches (*Lb*ADH and *Pp*BFD), so that these CatIBs dissolved to a higher extent. Since the TDoT domain is 3-fold smaller compared to 3HAMP, the percentage of the domain on the total fusion protein weight is generally lower: 17% for *Lb*ADH and only 9% for *Pp*BFD (Table 3-3). Hence, the influence of this smaller coiled-coil domain is expected to be lower on the aggregation of the protein.

A larger coiled-coil domain was proven to enhance the aggregation propensity for *Lb*ADH- and *Pp*BFD-CatIBs (Figure 3-6), especially for these enzymes with a smaller content of hydrophobic surface patches. 3HAMP is 3-fold larger and thus has a higher percentage on the molecular weight of the fusion protein: 40% for *Lb*ADH and 24% for *Pp*BFD. However, the proposed correlation of hydrophobic surface patches did not work for CatIBs fused to 3HAMP, where all the aforementioned enzymes formed the same type of diffuse but mostly insoluble CatIBs. Furthermore, *Ec*LDC solely yielded compact CatIBs independent from the fusion domain. Here, the decameric structure can be assumed to participate in the formation of compact inclusion body. Since for the constitutive *Ec*LDC only cryo-electron microscopically structural data is available (PDB: 5fkz) lacking information about the surface amino acid residues, the hydrophobic surface patches cannot be calculated.

Taken together, it could be demonstrated that the particle (size), composition, characteristics and dissolving ability can be tuned by means of the coiled-coil domain used as aggregation-inducing tag. A larger coiled-coil domain could enhance the aggregation induced by these tags as it probably increases the aggregation propensity of the enzymes. However, the structure of the respective protein especially the hydrophobic surface patches have to be considered as well.

3.2 Characterization of CatIBs in biocatalysis

One goal of this thesis was to study the different types of CatIBs in biocatalytic reactions, with a special focus on stability, performance, and reusability. Where possible, these studies were performed compared to the soluble enzyme to decide about the usefulness of this approach.

3.2.1 Stability of CatIBs

In order to analyze the stability of the CatIBs, soluble enzymes with a low stability were chosen: *Pf*BAL and *R*ADH.

3.2.1.1 Stability of *R*ADH-CatIB

In previous studies, *R*ADH showed a half-life of 60-70 h between pH 5.5 and 8 at room temperature for the reduction of benzaldehyde [232]. In a long-term stability experiment after incubation in buffer (0.8 mmol l^{-1} $CaCl_2$) without substrate, *R*ADH showed a good half-life of 130 h between 8-15°C.

To analyze the stability, *R*ADH-CatIBs were incubated in buffer at 30°C and under shaking without or in the presence of 5% DMSO or MTBE in comparison to the soluble enzyme, since the addition of co-solvents was reported to enhance the stability of some enzymes [17,324], especially of *Pf*BAL [174]. So far, the stability of *R*ADH in co-solvents was not tested.

In buffer, *R*ADH-CatIBs showed a slight increase in half-life compared to the soluble enzyme (Table 3-4, Figure 3-8). The half-life of all enzymes preparations could be improved about 2-4-times by addition of 5 vol% DMSO and 8-17-fold by addition of 5 vol% MTBE, respectively. In 5 vol% MTBE, CatIBs showed a 4-9-fold higher half-life compared to the soluble enzyme. Both *R*ADH-CatIBs showed an increase in stability compared to the soluble enzyme under this incubation conditions. 3HAMP-*R*ADH-CatIBs showed the highest half-life in each tested incubation system, with an up to 9-fold increase in 5 vol% MTBE. The diffuse 3HAMP-*R*ADH-CatIBs outperformed the soluble *R*ADH as well as the compact TDoT-*R*ADH-CatIBs. Generally, it can be assumed that enzymes in compact particles are more stable compared to less densely-packed particles. This assumption is contradicted by the results of the stability studies, since the diffuse CatIBs have a higher half-life than the compact CatIBs, which was most pronounced in buffer with 5 vol% MTBE. Thus, the reaction system can influence the stability of the enzymes and most probably also the particles, where hydrophobic interactions may change the particle coherence.

An unusual observation was made with the 3HAMP-*R*ADH-CatIBs, which doubled their activity after incubation for 24 h in the buffer/MTBE (5 vol%) system (Appendix, Figure 6-2C). It can be assumed that the particles dissociated into smaller particles upon incubation in the solvent system under shaking. However, also enzyme reactivation has to be considered as a further factor, as was earlier also observed with the lyophilized soluble *R*ADH upon incubation in buffer [232]. Kulig *et al.* observed a reactivation of the soluble *R*ADH of up to 75% of the initial activity measured immediately after dissolving the lyophilisate. The observation was interpreted in terms of refolding of the partially denatured enzyme structure due to the lyophilization process. The same effect could also apply to lyophilized *R*ADH-

CatIBs. Therefore, two contrary effects can be assumed to cause the higher half-life of 3HAMP-*R*ADH-CatIBs compared to the TDoT-*R*ADH-CatIBs. The activity increase due to the previously discussed dissociation of the particles and reactivation of the enzyme contradicts the inactivation of the enzyme, due to temperature and mechanical stress, resulting in an overall apparent stability increase.

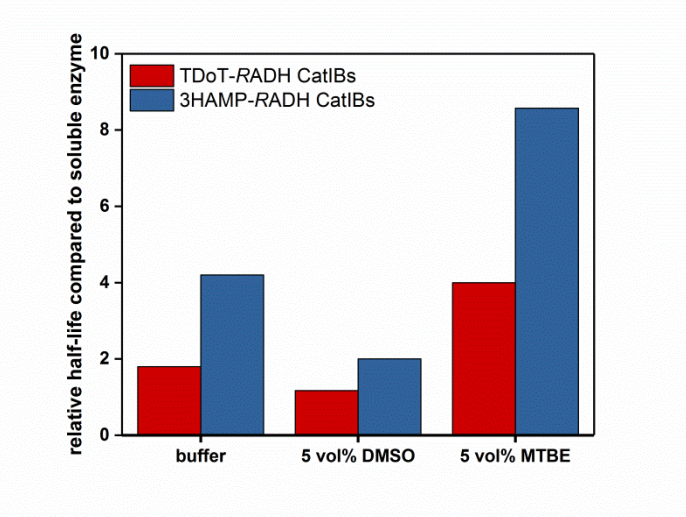

Figure 3-8 Half-lives of TDoT-*R*ADH and 3HAMP-*R*ADH relative to the half-life of soluble *R*ADH (enzyme concentration 0.305 mg ml^{-1}) after incubation in 50 mM TEA-buffer (0.8 mM $CaCl_2$, pH 7.5) in the presence and absence of 5 vol% organic solvent (MTBE or DMSO) in 2 ml total volume over several days at 30°C and 1000 rpm. A relative half-life above 1 refers to a higher stability compared to the soluble enzyme and a value below 1 to a lower stability. After incubation, the initial rate activity was measured via discontinuous activity assay at 30 °C, under constant shaking (1000 rpm) in 1 ml total volume containing 50 mM TEA-buffer (0.8 mM $CaCl_2$, pH 7.5) 2.5 vol% organic solvent (MTBE, DMSO), 10 mM (*R*)-2-HPP, 3 mM NADPH. The enzyme was diluted for the activity assay to the following final concentrations: soluble *R*ADH: 0.305 µg ml^{-1}, TDoT-*R*ADH: 240 µg ml^{-1}, 3HAMP-*R*ADH: 9 µg ml^{-1}. Half-lives were deduced from the point in time where 50% of initial rate activity was reached. Sampling was performed at the beginning of each day. n = 2. Results were taken from the Master thesis of Selina Seide [304].

Table 3-4: Half-lives of soluble *R*ADH, TDoT-*R*ADH and 3HAMP-*R*ADH (enzyme concentration 0.305 mg ml^{-1}) after incubation in 50 mM TEA-buffer (0.8 mM $CaCl_2$, pH 7.5) in the presence and absence of 5 vol% organic solvent (MTBE or DMSO) in 2 ml total volume over several days at 30°C and 1000 rpm. For experimental details see Figure 3-8. Results were taken from the Master thesis of Selina Seide [304].

	Half-life			**Stability compared to soluble enzyme**	
	Soluble *R*ADH	**TDoT-*R*ADH**	**3HAMP-*R*ADH**	**TDoT-*R*ADH**	**3HAMP-*R*ADH**
CatIB type		compact	diffuse, mainly insoluble	compact	diffuse, mainly insoluble
Buffer	20 h	24 h-48 h	48 h-120 h	1.8	4.2
5 vol% DMSO	72 h	48 h-120 h	6 days	1.2	2.0
5 vol% MTBE	168 h	28 days	60 days	4.0	8.6

In summary, a stability increase could be verified for *R*ADH-CatIBs compared to the soluble enzyme, whereby the addition of co-solvents enhanced the stability of all variants tremendously. The diffuse 3HAMP-*R*ADH-CatIBs showed the highest stability in the MTBE-buffer system due to an assumed dissociation of the particles and a reactivation of the enzyme, which counteracted the inactivation process. This experiment was performed in the absence of substrates and is thus only a first indication for the stability of the respective enzyme preparations in biocatalytic applications.

3.2.1.2 Stability of *Pf*BAL-CatIB

In previous experiments, soluble *Pf*BAL revealed a low long-term stability in pure aqueous buffer solution with a half-life of about 7 h in 50 mM potassium phosphate buffer (pH 8.0) at 20 °C [170] or 16 h in same buffer at pH 6.5 and 30 °C [171], which could be enhanced by addition of DMSO (20-30 vol%) or MTBE (5 vol%) [150,170,174]. Therefore, the stabilities of *Pf*BAL-CatIBs were tested in monophasic as well as biphasic aqueous-organic solvent systems.

The incubation in buffer at 30°C under shaking without substrates showed a higher half-life for TDoT-*Pf*BAL (2.5-fold, 57 h) and 3HAMP-*Pf*BAL-CatIBs (1.6-fold, 36 h) compared to the soluble enzyme (23 h) (Figure 3-9, Table 3-5, compare chap. 2.2 Figure S2 [306]). Since *Pf*BAL is inactivated by aliphatic and aromatic aldehydes [171–173], the stability was also tested in a continuously-operated enzyme membrane reactor (EMR) for the production of (*R*)-2-HPP without and in the presence of 30 vol% DMSO at pH 7.5 and pH 9, respectively. Again, TDoT-*Pf*BAL showed the highest half-life (7-fold, 48 h) compared to the soluble enzyme (7 h) (chap. 2.2 Figure 3 [306]). Previously, addition of DMSO was shown to have a positive effect on the stability of the soluble *Pf*BAL [150,170], which could be demonstrated also for the CatIBs. By addition of 30 vol% DMSO, the half-life increased 3-times for TDoT-*Pf*BAL-CatIBs (131 h), 6-times for 3HAMP-*Pf*BAL-CatIBs (59 h) and even 13-times for soluble *Pf*BAL (92 h) at pH 7.5 (chap. 2.2 Figure 4 [306]). Again, TDoT-*Pf*BAL-CatIBs outperformed the soluble enzyme under the applied conditions (pH 7.5, buffer-DMSO system) with a 1.4-fold higher half-life of 131 h. In contrast to this, 3HAMP-*Pf*BAL-CatIBs showed a comparable (in buffer) or 2-times lower half-life (in DMSO-buffer) than the soluble *Pf*BAL. As the stability pH-optimum for the soluble enzyme at pH 6-8 [153] only merely overlaps with the activity optimum between pH 8.5-9.5 in a comparable DMSO-buffer system [150,170,175], all *Pf*BAL variants were tested comparatively at pH 9 in the EMR (chap. 2.2 Figure S5 [306]). However, the higher pH-value impaired the stability of all variants

tremendously. Although TDoT-*Pf*BAL showed the highest stability of all variants at pH 7.5, it revealed the lowest half-life at pH 9.

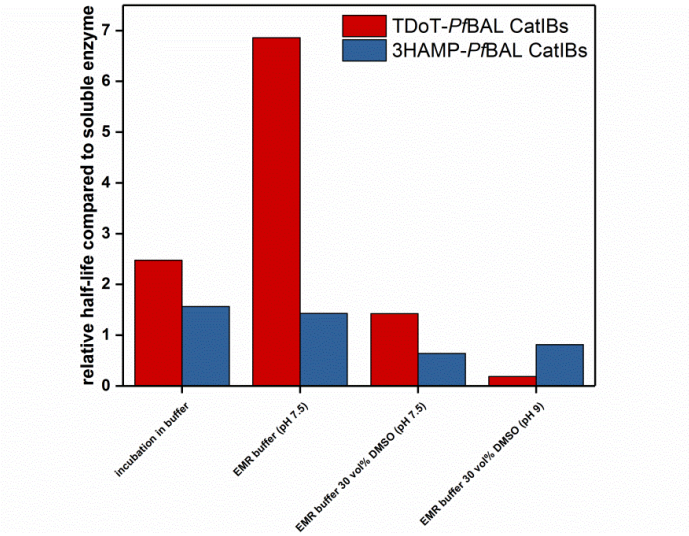

Figure 3-9 Half-lives of TDoT-*Pf*BAL and 3HAMP-*Pf*BAL relative to the half-life of soluble *Pf*BAL after incubation in buffer or in a continuous reaction in an enzyme membrane reactor (EMR). A relative half-life higher than 1 refers to a higher stability compared to the soluble enzyme and a value lower than 1 to a lower stability. Half-lives were deduced from the point in time where 50% conversion to (*R*)-2-HPP was reached. Incubation conditions in buffer: 50 mM TEA-buffer (pH 7.5, 2.5 mM $MgSO_4$, 0.5 mM ThDP) at 30 °C and 1000 rpm, protein concentrations of the enzymes 0.6 mg ml^{-1}, 1000 rpm, T = 30 °C , V = 1 ml; n = 1. After distinct time points, the initial rate activity was measured with a discontinuous activity assay: carboligation of 10 mM 3,5-dimethoxybenzaldehyde (DMBA) 50 mM TEA-buffer (pH 7.5, 2.5 mM MgSO4, 0.5 mM ThDP) and 20 vol% DMSO, n = 1. Continuous EMR conditions: 30 mM benzaldehyde, 90 mM acetaldehyde, TEA-buffer (50 mM, pH 7.5, 2.5 mM $MgSO_4$, 0.5 mM ThDP), 28 U ml^{-1} protein concentrations of the enzymes, 300 rpm, T = 30 °C , $V_{reactor}$ = 3 ml, residence time: 30 min, flow: 0.1 ml min^{-1}, PEEK (polyether ether ketone) - enzyme membrane reactor (EMR) with regenerated cellulose membrane (YM10 Milipore, 10 kDa cut-off), n = 1. Results were taken from chapter 2.2 [306].

In summary, pH 7.5 in a DMSO-buffer system should be applied for continuous reactions in the EMR, where TDoT-*Pf*BAL performed best with a 1.4-fold (131 h half-life) stability increase compared to the soluble enzyme (92 h) and a 2.2-fold higher stability compared to 3HAMP-*Pf*BAL-CatIBs (59 h). In these experiments under reaction conditions, the 3HAMP-*Pf*BAL-CatIBs showed a comparable or even lower stability than the soluble enzyme. Here, the diffuse nature of the not densely-packed particles influences the stability in a negative way, whereas the compact packing of the TDoT-*Pf*BAL-CatIBs is advantageous for the stability under reaction conditions as well as after incubation in buffer at 30°C under shaking. Several effects could impair the stability of the diffuse 3HAMP-*Pf*BAL-CatIBs more pronounced compared to the compact TDoT-CatIBs. These are: the membrane in the EMR, the reactor material and the stirrer. Besides, inactivation could be caused by the aldehyde substrates, which can easier penetrate into the diffuse CatIBs. Since 3HAMP-CatIBs contains a higher lipid content (Table 3-1), it can be assumed that these CatIBs are more hydrophobic and thus interact stronger with hydrophobic surfaces like Teflon® (stirrer) and polyether

ketone (PEEK), of which the EMR was built. Furthermore the stirring by the stir bar could grind the particles to a higher extent, whereby the less densely packed 3HAMP-*Pf*BAL-CatIBs could be disintegrated faster than via shaking. All these effects could impair the stability of 3HAMP-*Pf*BAL-CatIBs, which showed a more pronounced inactivation than TDoT-*Pf*BAL-CatIBs (Table 3-5, Figure 3-9). These assumptions are supported by the results of the incubation studies in buffer at 30°C under shaking, where 3HAMP-*Pf*BAL-CatIBs revealed a higher stability than the soluble enzyme, probably due to an absence of several influences like substrate, mechanical stress due to stirring and the hydrophobic reactor environment (Table 3-5, Figure 3-9).

Table 3-5 Half-lives of soluble *Pf*BAL, TDoT-*Pf*BAL, and 3HAMP-*Pf*BAL upon incubation in buffer and under reaction conditions in a continuously operated enzyme membrane reactor (EMR) for the production of (*R*)-2-HPP. A relative half-life higher than 1 refers to a higher stability compared to the soluble enzyme and a value lower than 1 to a lower stability. Half-lives were deduced from the point in time where 50% conversion to (*R*)-2-HPP was reached. For experimental details see Figure 3-9. Results were taken from chapter 2.2 and Kloss *et al.* [306].

	half-life [h]			**stability compared to soluble enzyme [-]**	
	TDoT-*Pf*BAL	**3HAMP-*Pf*BAL**	**soluble *Pf*BAL**	**TDoT-*Pf*BAL**	**3HAMP-*Pf*BAL**
CatIB type	compact	diffuse, mainly insoluble		compact	diffuse, mainly insoluble
stability after incubation in buffer (pH 7.5) at 30°C under shaking	57	36	23	2.5	1.6
EMR (buffer, pH 7.5)	48	10	7	6.9	1.4
EMR (buffer, 30% DMSO, pH 7.5)	131	59	92	1.4	0.6
EMR (buffer, 30% DMSO, pH 9)	3	13	16	0.2	0.8

3.2.2 Application *Pf*BAL-CatIBs in biphasic organic solvent system

A biphasic system is often employed to enable the biotransformation of poorly water soluble compounds, which are dissolved in the organic phase. Soluble enzymes in the aqueous phase are often sensitive to interphase inactivation, where the exchange of substrates and products occur [17,325]. Immobilization can improve the stability of enzymes in this case, because unfolding at the aqueous-organic interphase can be reduced through a higher conformational stability.

During this thesis, only *Pf*BAL-CatIBs were tested concerning their performance in biphasic reaction systems. Previous studies showed that *Pf*BAL can be inactivated at the interphase, which, however, is less pronounced than the inactivation caused by the aldehyde substrates

that have a greater influence on the stability of the enzyme under reaction conditions [180]. As pointed out in chapter 2.2, CPME (cyclopentyl methyl ether) containing 30 vol% TEA-buffer was best suited for the application of 3HAMP-*Pf*BAL-CatIBs. TDoT-*Pf*BAL-CatIBs could not be used in this system, because they caused the formation of emulsions, which made sample preparation and handling quite difficult. Thus, 3HAMP-*Pf*BAL-CatIBs were applied in carboligation reactions with hydrophobic substrates and products that could benefit from the improved solubility in a biphasic system compared to an aqueous reaction system. Two reactions were tested:

i. the carboligation of 3,5-dimethoxybenzaldehyde (DMBA) to ((*R*)-(3,3′,5,5′)-tetramethoxybenzoin) (TMBZ) and

ii. the carboligation of benzaldehyde to (*R*)-benzoin. 3HAMP-*Pf*BAL-CatIBs outperformed the soluble enzyme as it attained an up to 3-fold higher initial rate activity in this biphasic system compared to the soluble *Pf*BAL (compare chap. 2.2 , Figure 6, Table S7 [306]).

The results showed that the fusion tag has a strong effect on several characteristics of the enzymes. Besides the aforementioned activity, solubility and morphology, the stability and the induction of emulsion formation were different. The compact TDoT-*Pf*BAL-CatIBs tend to form emulsions in MTBE as well as CPME as the particles probably serve as emulsion stabilizer. However, the application of 3HAMP-*Pf*BAL-CatIBs in a biphasic CPME-buffer system worked without emulsion formation and resulted in a better performance than the soluble enzyme. In contrast to that the compact-packing of TDoT-*Pf*BAL-CatIBs was advantageous for the stability in the EMR under reaction conditions whereas the 3HAMP-*Pf*BAL-CatIBs were inactivated faster.

Previously, TDoT-*At*HNL CatIBs were successfully applied in buffer-saturated methyl *tert*-butyl ether (MTBE) and full conversion of 0.5 M benzaldehyde to (*R*)-mandelonitrile could be reached within 10 min [90].

These examples demonstrate that CatIBs are generally useful immobilizates for the application in organic solvents. As demonstrated for *Pf*BAL-CatIBs, their properties can be modulated by different aggregation-inducing tags. This opens up the way for tailor-made CatIBs optimized for the respective enzyme and reaction system.

3.2.3 Reuse of CatIBs

Besides the increased stability, immobilized enzymes can be also easily separated from the reaction mixture and reused to lower the process costs [29,30]. In order to test the recyclability of CatIBs, *Pf*BAL CatIBs as well as *Ec*LDC-CatIBs were applied in repetitive batch experiments (chaps. 2.2 and 2.3) [306,313].

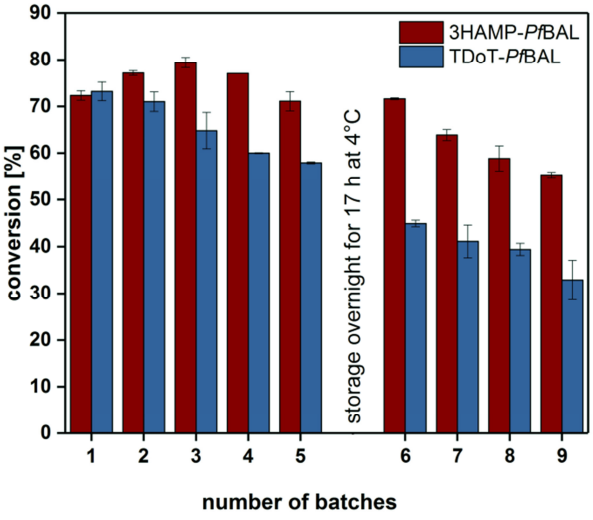

Figure 3-10 Conversion of repetitive batch reactions catalyzed by *Pf*BAL CatIBs for the carboligation of DMBA Batch reaction conditions: 50 mM TEA-HCl (pH 7.5; 2.5 mM $MgSO_4$; 0.5 mM ThDP; 20 vol% DMSO); 4 mM DMBA; T = 30°C, 1000 rpm; protein concentration for TDot-*Pf*BAL-CatIBs; 1.3 mg/ml; and 3HAMP-*Pf*BAL-CatIBs: 86.9 µg/ml ;1.5 ml Eppendorf *safe lock tubes*; one batch lasted 55 min + 3 min centrifugation at 17115 x *g;* V = 1 ml; n = 2; washing steps before the 1st cycle and between every cycle. Results were taken from the Bachelor thesis of Tobias Karmainski [302].

*Pf*BAL-CatIBs showed a good stability and could be reused for at least 9 cycles, with one batch lasting for one hour (Figure 3-10). 3HAMP-*Pf*BAL showed a higher stability in the repetitive batch experiment compared to TDoT-*Pf*BAL and lost only 17% conversion in contrast to TDoT-*Pf*BAL (40% loss in conversion) after the 9th cycle (9 h reaction). Surprisingly, the conversion using 3HAMP-*Pf*BAL as a catalyst increased in the first batches by 7 % and reached the initial conversion of 72% after the 6th cycle again. This result was not expected due to the diffuse nature of the 3HAMP-*Pf*BAL CatIBs, because they were expected to partially dissolve under the repetitive batch conditions including the intermediate washing steps. The results in Fig. 3-10 demonstrate that this did not happen to a great extent. Reasons therefore can be the observed increase of activity, most probably due to the formation of smaller particles and/or reactivation phenomena as observed for *R*ADH (chap. 3.2.1.1), which overcompensated any loss of enzyme during the repeated centrifugation and washing steps between the batch reactions.

The results obtained in the repetitive batch cannot be directly compared to the EMR due to differences in the reaction systems: i. Different carboligation reactions were studied (benzaldehyde and acetaldehyde towards (*R*)-2-HPP in the EMR and DMBA to TMBZ) and a lower DMSO concentration (20 vol%) was employed in the repetitive batch instead of 30 vol% in the EMR. This could explain the lower stability of TDoT-*Pf*BAL compared to 3HAMP-*Pf*BAL in the repetitive batch experiment. ii. A further main difference between a (repetitive) batch and a continuous reaction is the concentration of substrates and products or their respective change over the reaction time. While in the batch reactor the concentration of substrate is high and the product concentration is low at the beginning of the reaction, these concentrations change during the course of the reaction into the opposite direction. Besides, the continuous EMR operates under efflux condition, meaning that the conversion of the substrate can be adjusted by the concentration of the biocatalyst and the retention time. Under ideal conditions (no enzyme inactivation, no equilibrium reaction) the conversion is close to 100 % and the substrate concentration is constantly low with high product concentration. This reactor is specifically useful for enzymes, which are impaired by their substrates through inhibition or inactivation. For soluble *Pf*BAL, a fast inactivation was reported by only low concentrations of aldehydes. *Pf*BAL is inactivated within one hour by only 2 mM of different benzaldehyde derivatives [173]. Thus, it can be assumed that TDoT-*Pf*BAL is inactivated faster by the here employed 4 mM DMBA, but not as fast as it could be assumed for the soluble enzyme. Due to the diffuse nature of the 3HAMP-*Pf*BAL CatIBs, which dissociate into smaller particles, the partial dissolving enhanced the apparent stability. Two opposite effects have an influence on the stability as discussed before for 3HAMP-*R*ADH-CatIBs (chap. 3.2.1.1). The inactivation is counteracted by the dissolving of the particles, which results in a higher activity due to an increased surface-to-volume ratio. Smaller less-compact particles are also better accessible by the solvent during the washing steps between each batch. Schwarz reported the reactivation of inactivated *Pf*BAL by removing the aldehyde substrate via size exclusion chromatography [173], which presumably could be also partially reached by washing the CatIBs between the batch reaction steps. Another hypothesis of Pleiss suggests that the product could inhibit the enzymes, since TMBZ has a 200-fold higher binding affinity to the active site than DMBA, which could maybe block the substrate channel [326]. This binding affinity and the ability of washing out the product could be changed by the solvent accessibility of the respective *Pf*BAL-CatIB. The diffuse 3HAMP-*Pf*BAL-CatIBs showed a higher and increasing activity and, therefore, could probably be better reactivated than TDoT-*Pf*BAL CatIBs.

In summary, 3HAMP-*Pf*BAL-CatIBs performed better in the repetitive batch experiment than TDoT-*Pf*BAL due to their less compact nature, which increased the activity and enabled the washout of inactivating aldehyde substrates and probably also product in between the repetitive batch reactions.

The reuse of CatIBs was also demonstrated successfully for *Ec*LDC-TDoT-CatIBs under technical conditions in culture supernatant of a *C. glutamicum* L-lysine producer strain, demonstrating that these CatIBs are stable for at least 46 h and can be recycled several times (at least 9 cycles) with a half-life of about 56 h (chap. 2.3 Figure 6) [313]. Previously, the reusability of CatIBs was demonstrated in batch in different solvent systems. TDoT-*At*HNL were applied in a water-saturated MTBE and successfully reused in 5 cycles (1 h batches), and TDoT-*Ec*MenD-CatIBs were used in buffer and recycled 7-times (6 h batches) without any loss in activity [90].

3.2.4 Applicability of CatIBs under technical conditions

For *Ec*LDC-TDoT-CatIBs, the application was demonstrated under technical conditions in culture supernatants of a *C. glutamicum* L-lysine producer strain (chap. 2.3) [313], which resulted in a process competitive with the literature (Table 3-6). To lower the process costs, the culture supernatant of a *C. glutamicum* L-lysine producer was directly used without any further purification steps to purify the L-lysine for the next step. This was reported so far only in a few cases [289,290]. *Ec*LDC-TDoT-CatIBs were applied in repetitive batch mode for several cycles for the conversion of 100 mM L-lysine, as discussed above (chap. 3.2.3), and showed still reasonable activity and stability for the conversion 1 M L-lysine (chap. 2.3 Figure 7). However, as the reaction made a continuous pH-adjustment necessary, which most probably partly inactivated the CatIBs through the formation of “hot spots” during the titration process, the final conversion was only 87% after 24 h. A high space-time yield (STY) of 296 $g_{DAP}\ l^{-1}\ d^{-1}$ per g dry CatIBs corresponding to an enzymatic productivity of 8.8 $g_{DAP}\ g^{-1}_{CatIBs}$ was obtained. The STY of 89 $g_{DAP}\ l^{-1}\ d^{-1}$ is in the range of other reported processes for the microbial cadaverine production (52.8 $g_{DAP}\ l^{-1}\ d^{-1}$) [279]. As cadaverine is a valuable product for the chemical industry as building block for bio-based polyamide manufacture of PA5.10 and PA5.4, there exist several studies that address the improvement of the production process. In Table 3-6 the results of chapter 2.3 [313] are compared to several publications describing bioconversions via immobilized LDC. The most common way to immobilize LDC is the application of *E. coli* whole cells, but also alginate beads were employed to further immobilize the whole cells [284,290,293,294]. It can be noticed that

neither the productivity nor the STY (related to the applied catalyst concentration) was calculated in all the here listed reports (Table 3-6), probably due to the fact that the enzyme concentration cannot be that easily determined. Since often neither the activity nor the protein concentration used in the reaction is given in the reports, it is hardly possible to compare the processes. Here, only the conversion, the yield, and the STY could be compared that are not related to the applied catalyst concentration.

The highest yield of 221 g/l DAP (92%) was obtained in a fed-batch process with 1.95 M L-lysine in total using *E. coli* whole cell that co-expressed cadA, encoding for the inducible lysine decarboxylase, and cadB, encoding for the inner membrane lysine-cadaverine antiporter (compare chapter 1.6.1), which results in a STY of 331 $g_{DAP}\ l^{-1}\ d^{-1}$ [284]. The highest STY of 454.8 $g_{DAP}\ l^{-1}\ d^{-1}$ was obtained in batch using barium alginate beads with *E. coli* whole cells (CadA) with 45 U enzyme activity [294] (Table 3-6). Bhatia *et al.* defined 1 unit of activity as "the amount of cells required to produce 1 mmol cadaverine per minute" [294], but did not precisely define the amount of cells. In this thesis, 300 mg *Ec*LDC-TDoT-CatIBs (68% protein content and 0.49 U/mg activity) were used in a 30 ml batch reaction. The calculated activity was 3.33 U/ml and thus 100 U in total. Here, the IUPAC- definition was used: One unit (U) of specific activity is defined as the amount of enzyme (in mg, calculated on the basis of protein content), which catalyzes the formation of 1 µmol DAP per minute (chap. 2.3) [313]. Since the LDC activity in the whole cell catalyst is not given in the report of Bhatia, the activities of both processes cannot be compared.

The employed concentration of L-lysine (0.1-1.95 M) and the achieved final conversion (75-100%) to DAP are different in the reports (Table 3-6). Some processes reached 100% starting from 100 mM L-lysine [66], which is comparable to our repetitive batch process. With up to 1.37 M L-lysine in a batch process, 95.6% conversion was attained with *E. coli* whole cells (LdcC, constitutive *Ec*LDC) in culture supernatant [290] with a STY of 26.7 $g_{DAP}\ l^{-1}\ d^{-1}$ that is lower than the STY achieved in this thesis in the 1 M L-lysine batch. This is due to the fact that our process did last only 24 h [313] instead of 120 h [290]. To achieve a conversion close to 100%, a longer reaction time would be necessary or a higher CatIB concentration.

Interestingly, no publication reports on the necessity to control the pH of the reaction solution, which was mandatory to keep the pH-value constant in our process. For our process, it can be assumed that most of the potassium phosphate-buffer salts of the CGXII medium [327] were consumed by *C. glutamicum* cells during cultivation, so that no buffer components were available anymore for the reaction, which makes the titration necessary. In the reports similar

to our application, where culture supernatant was used as reaction medium, this aspect was not mentioned [289,290]. Here, the medium compostion, however, is not given.

Table 3-6 Productivity measures for the production of DAP (cadaverine) obtained in this thesis compared to literature values * the space-time yield (STY) was calculated based on the given parameters

reference	this thesis [313]		[279]	[294]	[293]	[66]	[290]	[284]	[295]
reaction mode	repetitive batch	batch	batch cultivation	batch	continuous	repetitive batch	batch	fed-batch	repetitive batch
immobilization	CatIBs	CatIBs	no (*C. glutamicum* whole cell cultivation)	barium alginate beads with *E. coli* whole cells (CadA)	alginate beads with *E. coli* whole-cell (CadA) immobilized	CLEAs of CadA	*E.coli* whole cell (LdcC)	*E. coli* whole cell (CadA and CadB)	CadA on intracellular PHA
total reaction time [h]	69	24	50	4	123	no data	120	16	5 x 1
conversion [%]	76-100	87	no data	84	91-94	100	95.6	92	75–80
L-lysine concentration [M]	0.1	1	no data	1	0.91	0.1	1.37	1.95	0.1
DAP [g l^{-1}]	8.47	88.4	88.0	75.8	83.7	n.d.	133.7	221	n.d.
enzymatic productivity [$g_{DAP}/g_{biocatalyst}$]	25	8.8	no data	no data	no data	no data	no data	no data	no data
STY [g l^{-1} d^{-1}]	2.94	89	52.8*	454.8*	16.3*	no data	26.7*	331*	no data
STY [g l^{-1} d^{-1}] per $g_{lyophilized\ CatIBs}$	16	296	no data	no data	no data	no data	no data	no data	no data
STY [g l^{-1} d^{-1}] per $g_{E.\ coli\ (WCW)}$	2.1	38	no data	no data	no data	no data	no data	no data	no data

The reports concerning the usage of immobilized LDC in repetitive batch showed a good stability of the phasin-fused LDC isoenzyme CadA bound to the intracellular P(3HB) granules, for 5 batches (each 1 h) with a conversion of 75–80% of 100 mM L-lysine in 50 mM phosphate buffer [295]. CadA-CLEAs could be also recycled for several batches for the decarboxylation of 100 mM L-lysine in potassium 100 mM phosphate buffer. Until the 10th batch the conversion decreased from 100% to 54% [66]. Here, the duration of one cycle is not given. Since there are several differences to our process (different LDC, reaction medium), the processes can hardly be compared.

In summary, the application of *Ec*LDC-TDoT-CatIBs under technical conditions is in the range of other previously described processes for cadaverine production using immobilized

LDC. However, as several details are not reported in the literature, a detailed comparison is not possible.

3.3 Evaluation of CatIBs as an alternative immobilization method

The aim of this thesis was to evaluate the CatIBs as novel immobilization strategy for biocatalytic application. CatIBs should be ideally a generic method for the simple and cost-efficient production of enzyme immobilizates. In this chapter, the advantages and disadvantage of CatIBs for biocatalysis will be discussed (Table 3-7).

3.3.1 CatIBs as a generic immobilization method

CatIBs as natural carrier-free immobilized enzymes are directly produced in the recombinant *E. coli* cells. No additional immobilization is necessary as well as no time-consuming, laborious and expensive (chromatographic) purification steps. By a standardized protocol all CatIBs could be easily produced and purified. For this purpose, the production and purification protocol was simplified so that after production of CatIBs in *E. coli* cells in auto-induction medium, the cells were disrupted by ultra-homogenizer and subsequently the crude cell extract was centrifuged and the remaining pellet (containing the CatIBs) was washed only once with water and subsequently lyophilized (Figure 3-11). Due to the simple purification protocol, contaminants such as lipids and membrane proteins were co-purified (compare chapter 2.2 and 3.1.2.3), which, however, will not influence the reaction, as these proteins did not exhibit any catalytic activity to the best of our knowledge.

By means of this simple protocol, a CatIB toolbox of different synthetically useful enzymes with different complexity was generated. The modular and generic immobilization method enables the production of every enzyme as CatIBs, which was demonstrated to work for a variety of different enzymes. From the huge variety of different reported coiled-coil domains, currently only two were tested as aggregation-inducing tag. Using the TDoT domain and 3HAMP domain, respectively, two types of CatIBs were obtained, which differed in morphology, solubility, composition (lipids and proteins), activity, and stability. The CatIB properties could be changed and adopted to the requirements of the respective reaction system. However, the respective properties cannot be predicted and have to be evaluated for each case, whereby the morphology has a great influence on the CatIB properties.

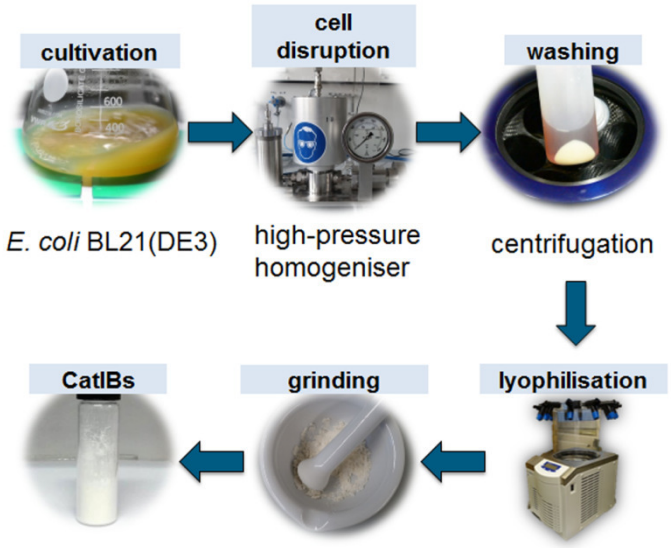

Figure 3-11 Simplified protocol for the production and purification of CatIBs. After cultivation in *E. coli* BL21(DE3) cells in auto-induction medium, the cells were disrupted by ultra-homogenizer and subsequently the crude cell extract was centrifuged and the remaining pellet (containing the CatIBs) was washed only once with water and subsequently lyophilized. Picture was taken from chapter 2.3 [313].

In the cooperation project of this thesis, first steps were done towards the prediction of the CatIB morphology. As was pointed out in chapters 2.1 and 3.1.3, there is a reasonable correlation between the area of hydrophobic patches on the enzyme surfaces and the activity found in the cell pellet, which correlated to the formation of insoluble CatIBs. Whereas this approach worked for TDoT-CatIBs, it could not be transferred to the 3HAMP-CatIBs. Hence, the properties of each CatIB have to be evaluated empirically for each enzyme under the specific reaction conditions. Besides the two already tested coiled-coil domains further candidates could be identified for example from the coiled coil database CC+ (http://coiledcoils.chm. bris.ac.uk/ccplus/search/) [134]. Coiled-coil domains could be tested with different size, numbers of subunits and hydrophobicity.

It was shown that the fusion tag has a strong effect not only on the morphology but also on the stability and the activity of the resulting CatIBs. The diffuse CatIBs revealed a high residual activity of up to 27% compared to the soluble enzyme. This, however, is low compared to other immobilization methods, such as the carrier-free CLEA method; where up to 100% activity recovery could be obtained in some cases (Table 1-2, tyrosinase and α-amylase), whereby the precipitants and the cross-linking agents have to be individually tuned to optimize activity recovery [54,56,60]. As the residual activity strongly depends on the complexity and structure of the enzyme, this high activity recoveries (100%) of the tyrosinase and α-amylase cannot be compared to the here employed enzymes [59,62]. Thus, only the residual activity of *Lb*ADH-CatIBs can be compared to CLEAs, which gave similar results of

approx. 10% residual activity [56] (Table 6-1). In contrast to the CLEAs, CatIBs can be easier produced, since only cell disruption, centrifugation and washing steps are necessary.

Table 3-7 Advantages and disadvantage of CatIBs for biocatalytic application

advantages	**disadvantages**
modular and generic immobilization method: every enzyme can be produced as CatIBs	-
cell-free and carrier-free immobilization method	-
simple and easy production and purification by standardized protocol	CatIBs contain contaminants like lipids and membrane proteins
no time-consuming and expensive purification necessary	-
easy handling	-
properties of CatBs can be fine-tuned by fusion to different coiled-coil domains	depending on the hydrophobicity of the enzyme, CatIBs with different morphology are formed, which can currently only be predicted for TDoT-CatIBs with a certain reliability.
higher stability compared to soluble enzyme depending on reaction conditions	lower activity compared to soluble enzyme depending on reaction conditions
can be applied in aqueous systems (with cosolvents) as well as in biphasic aqueous-organic solvent system	applicability cannot be predicted and has to be tested individually
can be reused and recycled for several batches	-

Another promising covalent immobilization method is the HaloTag^{TM} technology [45], which does not need individual adaption to the respective biocatalyst. By this method, residual activities of up to 65% for HaloTag-*Pp*BFD L476Q were reached, but also 60% for HaloTag-*Pf*BAL and 35% for HaloTag-*Lb*ADH. However, an additional carrier is necessary, but the immobilization step could be combined with the purification step, thus lowering the production costs.

In summary, CatIBs showed a lower residual activity compared to other immobilization methods, which could be explained also by the nature of inclusion body aggregates. It can be assumed that not all the enzyme molecules within these particles are correctly folded and furthermore, there is a diffusion limitation to the enzyme molecules buried inside the particles. The activity of the CatIBs was calculated based on their total protein content, so that also not correctly folded enzymes or enzymes in the inner particle were considered as well as the co-purified membrane proteins and chaperones. This is usually not done for immobilization methods, which use carriers. There, only the amount of enzymes bound on the surface is considered, whereby it is also possible that enzymes bound in superimposed layers, so that enzyme molecules in the lower layer are not accessible for the substrate.

Based on the effect observed with the diffuse CatIBs in this thesis, one way to improve the activity recovery is the generation of smaller particles with a higher surface to volume ratio by fusion to a different coiled-coil domain. These smaller particles, however, will not be useful for all reactor types and reaction conditions, as was shown for 3HAMP-*Pf*BAL-CatIBs in the EMR (chaps. 2.2, [306], and 3.2.1.2).

Furthermore, the activity of the CatIBs can be enhanced by improving the cultivation conditions, as for example the induction temperature was shown to be crucial for a high degree of functionality of YFP-CatIBs (chap. 3.1.3). Other parameters to be tested could be the oxygen supply and different cultivation media, which was started to be analyzed for the production of YFP-CatIBs by the cooperation partner Robin Lamm.

Taken together, the CatIB method can be generic applied to a variety of different enzymes. These CatIBs can be tailored regarding their properties like activity by choosing different coiled-coil domains, which, however, cannot be predicted yet.

3.3.2 Cost-efficiency of CatIBs for biocatalytic application

Finally, the question should be addressed, whether the application of CatIBs in biocatalysis is more cost-efficient than of the soluble enzyme. This question can be answered by considering the yield, the activity and the stability of the CatIBs, as was exemplary done for *Pf*BAL- as well as *R*ADH-CatIBs (Table 3-8, Table 3-10). For this purpose the results of the experiments were chosen, which showed the highest stability of all variants, such as the EMR experiment in buffer with 30 vol% DMSO at pH 7.5 for *Pf*BAL-CatIBs (Table 3-5) and the incubation study in buffer with 5 vol% MTBE for *R*ADH-CatIBs (Table 3-4). The values were compared to the soluble enzyme, which can give a first indication concerning the efficiency of the CatIBs in the biocatalytic application, considering all values as equally important.

Since the yield of the *Pf*BAL-CatIBs is only 3.6-fold higher or comparable to the soluble enzyme and the stability is only up to 1.4-fold higher with a low residual activity (1% or 18%), the *Pf*BAL-CatIB production and biocatalytic application cannot be regarded as more cost-efficient relative to the soluble *Pf*BAL. However, other factors have to be considered, such as the easier reusability of CatIBs and the lower production costs, since no chromatographic purification is necessary. Tufvesson calculated the production costs for different enzymes exemplarily. While whole cell biocatalysts are the cheapest catalyst preparation, the preparation of a crude-cell extract increases the costs by a factor of 2, and for the purified enzyme the costs are 10-fold higher than the whole cell production [70]. The

preparation of CatIBs can be compared to the preparation of the crude cell extract with additional steps of centrifugation, washing, and lyophilization. Here, the costs to prepare CatIBs can be only estimated, but will be lower than for the chromatographic purification but higher than for the preparation of a crude cell extract. Therefore, a factor of 4 was assumed, here (Table 3-9). Calculating the cost-efficiency based on the total activity (unit) obtained from 1 g wet cells and the stability, the relative costs for *Pf*BAL-CatIBs are approx. 100-fold higher compared to the soluble enzyme. The higher stability and the reusability of *Pf*BAL-CatIBs can hardly compensate the higher relative costs. Hence, the *Pf*BAL-CatIBs have to be improved regarding yield, stability and, most important, activity, which could be realized by means of molecular biological methods by exchanging the coiled-coil domain e.g. to get smaller particles with a different morphology. Yield and activity could be further improved by optimizing the production procedure, which was achieved already for YFP-FIBs to some extent (Appendix, Figure 6-1). The optimal temperature during the protein production step is crucial to form functional IBs. In this context, the optimal temperature should be also tested for the production of other CatIBs. Since the diffuse CatIBs generally revealed a lower yield, the washing steps could be reduced to one centrifugation step. Besides, compact CatIBs give higher yields but with lower activity, which will again render the process less cost-efficient compared to the soluble enzyme. All the factors must be balanced to create a cost-efficient process. Last but not least, the investigation of further coiled-coil domains as aggregation-inducing tag should be performed.

Table 3-8 Comparative overviews over the yield, the activity, and the stability of soluble *Pf*BAL, TDoT-*Pf*BAL- and 3HAMP-*Pf*BAL-CatIBs. Data were obtained from three biological replicates. * The activity was measured for the carboligation of 3,5-dimethoxybenzaldehyde to (*R*)-(3,3´,5,5´)-tetramethoxybenzoin (compare chapter 2.1, table 1 [296]).

	soluble *Pf*BAL	**TDoT-*Pf*BAL**	**3HAMP-*Pf*BAL**
yield [$mg_{protein}/g_{wet\ cells}$]	20 ± 14	72 ± 8	18 ± 17
relative yield compared to soluble enzyme [%]		360 (3.6-fold higher)	90
activity (k_{cat}) [s^{-1}]*	76.7 ± 2.26	0.77 ± 0.12	13.9 ± 2.9
relative activity compared to soluble enzyme [%]		1.0%	18.1%
stability (half-life) [h] in EMR (buffer with 30 vol% DMSO, pH 7.5)	92	131	59
relative stability compared to soluble enzyme [%]		143 (1.4-fold higher)	64

Table 3-9 Calculation of the relative costs for biotechnical application of TDoT-*Pf*BAL- and 3HAMP-*Pf*BAL-CatIBs compared to the soluble *Pf*BAL based on the yield, the activity, the stability, and on the cost factors (F) calculated for the production costs for different biocatalyst preparations as whole cells (F=1), crude cell extract from the whole cells (F=2), and chromatographically purified enzyme (F=10) [70]. For CatIB production a cost factor of 4 was assumed. The total activity was calculated based on the activity obtained from 1 g wet cells. Thereof, the relative costs per total activity was calculated, which was related to the stability in the value (F/total activity*half-life).

	soluble *Pf*BAL	**TDoT-*Pf*BAL**	**3HAMP-*Pf*BAL**
yield [$mg_{protein}/g_{wet\ cells}$]	20 ± 14	72 ± 8	18 ± 17
activity (k_{cat}) [s^{-1}]	76.7 ± 2.26	0.77 ± 0.12	13.9 ± 2.9
activity [U mg^{-1}]*	76.7	0.69	10.5
total activity [U]	1 534	49.7	189
cost factor F [-]	10	4	4
cost factor F /total actvitiy [U^{-1}]	$6*10^{-3}$	$80*10^{-3}$	$21*10^{-3}$
stability (half-life) [h] in EMR (buffer with 30 vol% DMSO, pH 7.5)	92	131	59
relative costs (F/total activity/half-life) [$U^{-1}\ h^{-1}$]	$70.8*10^{-6}$	$0.6*10^{-3}$	$0.36*10^{-3}$

* The activity was measured for the carboligation of 3,5-dimethoxybenzaldehyde to (*R*)-(3,3´,5,5´)-tetramethoxybenzoin (compare chapter 2.1 table 1 [296]).

In contrast to *Pf*BAL, the biocatalytic application of *R*ADH-CatIBs seem to be more feasible and cost-efficient compared to the soluble enzyme, especially due to the up to 50-fold higher yield of the TDoT-*R*ADH CatIBs compared to the soluble enzyme (Table 3-10), which was obtained after purification via anion-exchanger (chap. 2.1) [230].

Table 3-10 Comparative overviews over the yield, the activity and the stability of soluble *R*ADH, TDoT-*R*ADH - and 3HAMP-*R*ADH-CatIBs of three biological replicates, except for soluble enzyme * The activity was measured for the reduction of cyclohexanone to cyclohexanol (compare chapter 2.1, table 1 [296]).

	Soluble *R*ADH	**TDoT-*R*ADH**	**3HAMP- *R*ADH**
yield [$mg_{protein}/g_{wet\ cells}$]	2	101 ± 20	9 ± 4
relative yield compared to soluble enzyme [%]		5050 (50-fold higher)	450 (4.5-fold higher)
activity (k_{cat}) [s^{-1}]*	2.77 ± 0.04	0.054 ± 0.008	0.332 ± 0.019
relative activity compared to soluble enzyme [%]		2.0	12.0
stability (half-life) [h] in 5 vol% MTBE	168	672	1440
relative stability compared to soluble enzyme [%]		400 (4-fold higher)	857 (8.6-fold higher)

Furthermore, the stability of *R*ADH-CatIBs is up to 8.6-fold higher. The calculation of the cost-efficiency revealed that the CatIBs are approx. 10-fold cheaper compared to the soluble enzyme in production and for the application in biocatalysis (Table 3-11). This renders the *R*ADH-CatIBs more feasible for biocatalytic application.

Table 3-11 Calculation of the relative costs for biotechnical application of TDoT-*R*ADH- and 3HAMP-*R*ADH-CatIBs compared to the soluble *R*ADH based on the yield, the activity, the stability, and on the cost factors (F) calculated for the production costs for different biocatalyst preparations as whole cells (F=1), crude cell extract from the whole cells (F=2), and chromatographically purified enzyme (F=10) [70]. For CatIB production a cost factor of 4 was assumed. The total activity was calculated based on the activity obtained from 1 g wet cells. Thereof, the relative costs per total activity was calculated, which was related to the stability in the value (F/total activity/half-life).

	Soluble *R*ADH	**TDoT-*R*ADH**	**3HAMP- *R*ADH**
yield [$mg_{protein}/g_{wet\ cells}$]	2	101 ± 20	9 ± 4
activity (k_{cat}) [s^{-1}]	2.77 ± 0.04	0.054 ± 0.008	0.332 ± 0.019
activity [U mg^{-1}]*	6.22	0.094	0.423
total activity [U]	12.44	9.49	3.81
cost factor F [-]	10	4	4
cost factor F /total actvitiy [U^{-1}]	0.80	0.42	1.05
stability (half-life) [h] in 5 vol% MTBE	168 =	672	1440
relative costs (F/total activity/half-life) [U^{-1} h^{-1}]	$4.8*10^{-3}$	$0.63*10^{-3}$	$0.73*10^{-3}$

* The activity was measured for the reduction of cyclohexanone to cyclohexanol (compare chapter 2.1, table 1 [296]).

In summary, the cost-efficiency of CatIBs can be only assumed on basis of the yield, the activity, and stability, which revealed that CatIBs can be competitive to the soluble enzyme in some cases. However, some factors have to be improved, especially the activity, but also the yield and the stability by fusion to different coiled-coil domains or by optimizing the production procedure.

4 Conclusion and Outlook

The aim of this thesis was the evaluation of CatIB as an alternative immobilization strategy, with a special focus on their application in biotransformations. For a systematic evaluation the CatIB toolbox was broadened by five further complex enzymes, with proven application potential in biocatalysis using two different colied-coil domains as fusion tags. An overview on the present CatIB toolbox is shown in Table 4-1. The here presented strategy to produce CatIBs can be generically applied to a variety of different enzymes.

Table 4-1 Status of the CatIB-toolbox obtained by fusion of two different coiled-coil domains as aggregation-inducing domain

enzyme (organism)	**cofactor**	**TDoT-CatIB[1] (CatIB type)**	**3HAMP-CatIB (CatIB type)**	**reference**
hydroxynitrile lyase (*Arabidopsis thaliana*)	no	TDoT-*At*HNL (compact)[2]	-	Diener *et al.* [90]
lipase A (*Bacillus subtilis*)	no	TDoT-*Bs*LA (compact)[2]	-	Diener *et al.* [90]
alcohol dehydrogenase (*Ralstonia sp*)	NADPH	TDoT- *R*ADH (compact)	3HAMP- *R*ADH (diffuse)	chapter 2.1, Jäger *et al.* [296]
alcohol dehydrogenase (*L. brevis*)	NADPH	TDoT- *Lb*ADH (diffuse)	3HAMP- *Lb*ADH (diffuse)	chapter 2.1, Jäger *et al.* [296]
*Ec*MenD (*E. coli*)	ThDP	TDoT-*Ec*MenD (compact)[2]	-	Diener *et al.* [90]
benzaldehyde lyase from (*P. fluorescens*)	ThDP	TDoT-*Pf*BAL (compact)	3HAMP-*Pf*BAL (diffuse)	chapters 2.1, 2.2, Jäger *et al.* [296], Kloss *et al.* [306]
benzoylformate decarboxylase from (*P. putida*)	ThDP	TDoT-*Pp*BFD (diffuse)	3HAMP-*Pp*BFD (diffuse)	chapter 2.1, Jäger *et al.* [296]
lysine decarboxylase (*E. coli*)	PLP	*Ec*LDC-TDoT, TDoT- *Ec*LDC (compact)	*Ec*LDC-3HAMP (compact)	chapters 2.1, 2.3, Jäger *et al.* [296], Kloss *et al.* [313]

[1] If the linker is named in front of the construct, this refers to N-terminal fusion, and if the linker is named in at the end of the construct, it refers to a C-terminal fusion.

[2] The CatIB type was assumed based on the properties of the CatIBs [90], but was not confirmed by microscopy images.

-: not available

The coiled-coil domains TDoT and 3HAMP influenced the morphology and the properties of the CatIBs. The CatIBs varied in several properties: the compactness, the solubility during the washing steps, the yield of the final lyophilizate, the activity and the composition such as protein and lipid content. The morphology of the CatIBs in *E. coli* cells differed between compact-packed or diffuse particles as observed in the microscope in phase-contrast. With the

empirical study of the CatIB types, the differences in the properties could be assigned to the morphology. As the diffuse CatIBs are packed less dense as the compact CatIBs, the diffuse CatIBs showed in some cases a high tendency to dissolve (TDoT-*Lb*ADH- and TDoT-*Pp*BFD) or they dissolved progressively during the washing steps (3HAMP-*Lb*ADH and 3HAMP-*Pp*BFD CatIBs), which both resulted in a lower yield of lyophilizate. The less dense packing, however, resulted in a higher activity than obtained for the compact CatIBs of up to 27% residual activity compared to the soluble enzyme. It was assumed that the less dense packing results in a higher tendency to disintegrate into smaller particles, which have a higher surface to volume ratio and thus a higher activity. Furthermore, the diffuse and compact CatIBs differed in their composition, the compact CatIBs revealed a higher protein content and a lower lipid content, which was vice versa for the diffuse CatIBs. By molecular biological methods, the activity could be enhanced, as was shown for *Ec*LDC-CatIBs for changing the fusion site. By the empirical analysis, it could be demonstrated that the CatIB properties can be fine-tuned by using a different coiled-coil domain.

To predict the formation of CatIBs and their morphology, a correlation was found between the empirically observed aggregation tendency and the size of hydrophobic surface patches of the respective enzyme structure. This prediction worked well for TDoT-CatIBs but not for 3HAMP-CatIBs. This correlation can be used as first indicator to predict the aggregation propensity of a certain enzyme, but the tendency to form CatIBs and their morphology has to be tested empirically.

The applicability of the different CatIB types was analyzed in biocatalytic reactions, where parameters like reusability, stability at 30°C under shaking, and stability under reaction conditions were addressed. *Ec*LDC-TDoT-CatIBs were demonstrated to be applicable under technical conditions in culture supernatants of a *C. glutamicum* L-lysine producer strain in repetitive batch for several cycles for the conversion of 100 mM L-lysine as well as in batch for the conversion of up to 1 M L-lysine. Here, comparable results were obtained to previous reported immobilized *Ec*LDC to produce cadaverine.

*R*ADH-CatIBs were proven to be a suitable alternative for the soluble enzyme after incubation in buffer at 30°C under shaking due to a higher stability, which could be further enhanced by addition of DMSO and MTBE (5 vol%). The diffuse morphology of 3HAMP-*R*ADH-CatIBs was advantageous under these conditions, since they showed the highest stability (half-life of 60 days) due to a dissolving of the particles, which doubled the activity

after incubation for 24 h. Thus, *R*ADH-CatIBs can be probably used for a longer time in a continuous reaction, which has to be tested as it was done for *Pf*BAL CatIBs.

*Pf*BAL-CatIBs were proven to be applicable on a variety of different reaction systems: in buffer, and in monophasic and biphasic aqueous-organic solvent systems. Furthermore, *Pf*BAL-CatIBs can be applied in batch as well as repetitive batch and in a continuous operating EMR and showed a good recyclability for several batches. The different CatIB types showed a different performance under different reaction conditions. The compact TDoT-*Pf*BAL-CatIBs outperformed the diffuse 3HAMP-*Pf*BAL-CatIBs after incubation in buffer and under continuous reaction conditions, whereas the diffuse 3HAMP-*Pf*BAL-CatIBs performed better in repetitive batch with co-solvent and in biphasic reaction system. Thus, the CatIB properties can be adapted to the requirements of different reaction systems using two different coiled-coil domains as fusion tags. In summary, it could be shown that CatIBs can be applied in a variety of different reaction systems, where the performance of the CatIBs strongly depends on their characteristics and has to be tested individually for each reaction system. Furthermore, the performance of the different CatIB type cannot be generalized as the studies were performed only for a few CatIB types.

As an outlook, the CatIB method as alternative immobilization strategy has to be evaluated and analyzed in-depth in the future to be competitive to other immobilization strategies especially regarding residual activity.

First of all, the morphology of the CatIBs could be analyzed in more detail. To confirm the hypothesis that the diffuse CatIBs form smaller particles, the size of the CatIBs could be analyzed as was started for the YFP-FIBs and *Pf*BAL-CatIBs by SEM. A first analysis of the CatIB size in buffer solution by means of dynamic light scattering (DLS) showed that the mixture is highly heterogeneous, which makes the analysis by DLS quite difficult. Thus, only by SEM the particle size of the lyophilized particles can be measured.

During the application analysis, the easy handling of the CatIBs was advantageous, so that it could be assumed that CatIBs could be used as ready-to-use preparation for biocatalysis as well as in chemical synthesis, like other enzyme preparations such as *Candida antarctica* lipase B (Novozyme 435) [29]. Since first studies of our CatIB preparations showed a low vital recombinant *E. coli* cell number, a permission to work with genetically modified organisms (GMO) is required, which has to be applied additionally for the application in chemical industry. The cell-free preparation of CatIBs could be realized by means of an extended purification protocol, where any remaining cells of a IB preparation can be

separated and efficiently inactivated [110]. This protocol could be also tested for the preparation of the CatIBs. Thus, the application of CatIBs in chemical industry can be good alternative to recombinant whole cells, which require GMO-permission.

For a first evaluation of the cost efficiency of CatIBs in biocatalytic application, three parameters were considered: the yield, the activity and the stability, which influences each other. By means of these parameters, the cost-efficiency of the CatIBs compared to the soluble enzyme can be adjusted. The activity was shown to be improved by using a different coiled-coil domain. The resulting less dense packing of the CatIBs, however, impaired the stability in several reaction systems. Here a good balance between stability (given by the compact packing of the particles) and activity has to be found, particularly as it can be assumed that the activity of the CatIBs cannot be enhanced that much. Since the properties of the CatIBs fused to different coiled-coil domains cannot be predicted, a toolbox of CatIBs with several coiled-coil domains has to be established and tested for the desired characteristics. Here, high-throughput methods for the analysis of the CatIB properties would provide a faster selection of the desired CatIBs, whereby the morphology during the formation in the *E. coli* cells could give a first hint. The compact-packed CatIBs could be easily selected from the dense-packed particles by using microscopy in combination with a high-throughput cultivation method, such as the BioLector®. Here, larger coiled-coil domains should be tested, such that their properties can compensate those of the respective enzyme fusion to a great extent. Therewith the properties of CatIBs would be predictable. Such coiled-coil domains can be found in the coiled coil database CC+ (http://coiledcoils.chm.bris.ac.uk/ccplus/search/) [134].

Another possibility to enhance the activity would be the enzyme immobilization on inclusion bodies such as magnetosoms or polyhydroxyalkanoate (PHA), so that the enzymes are not buried within the particle. Both methods do not require additional enzyme purification and immobilization as was also shown for the CatIBs. PHA were naturally used by cells as energy and carbon storage [46,71] and are surrounded by a protein shell. To immobilize enzymes by means of PHA, the PHA-binding PHA synthase or PHA-granule-binding proteins can be fused to the target enzyme, which attach on the PHA inclusion body. These PHA IBs are synthezied *in vivo* by the (co-expressed) PHA synthase [95]. Enzymes can be also bound on magnetosome inclusion bodies, which contain crystallized iron. Magnetosomes are bound by a protein-containing lipid bilayer membrane in magnetite-forming magnetotactic bacteria [328]. Immobilization on these particles is realized by fusion of the target enzyme to magnetosome-anchoring proteins. One advantage of magnetosomes is the easy separation

from the reaction mixture by a magnet [329–331]. So far, CatIBs were separated only by centrifugation or by usage of the tea-bags [90], whereby the latter did not work in aqueous systems.

In summary, the aims of the thesis (chap. 1.7) to evaluate the CatIBs as an alternative immobilization strategy with respect to their application in biocatalysis were attained. It could be demonstrated that the here presented strategy to produce CatIBs can be generically applied to a variety of different enzymes by expanding the CatIB toolbox with further enzymes of different complexities, which were fused to two different coiled-coil domains. By using different coiled-coil domains, the properties of CatIBs can be tuned to the respective reaction system. The applicability of CatIBs was demonstrated in different reaction environments and media, showing a good stability, reusability and handling. Besides some properties that have to be improved such as the activity, the CatIB strategy presents a promising alternative to existing immobilization methods.

5 References

1. Lindström B, Pettersson LJ. A brief history of catalysis. Cattech. 2003;7(4):130–8.
2. Copeland RA. Enzymes: A practical introduction to structure, mechanism, and data analysis. Wiley-VCH Verlag. 2000 Dec;45(25):1–397.
3. Manchester KL. Louis Pasteur (1822-1895) - Chance and the prepared mind. Trends Biotechnol. 1995 Dec;13(12):511–5.
4. Copeland R. A brief history of enzymology. In: Enzymes: A practical introduction to structure, mechanism, and data analysis. 2000. p. 1–10.
5. Büchner E. Alkoholische Gärung ohne Hefezellen. In: Berichte der deutschen chemischen Gesellschaft. 1897. p. 1110–3.
6. Kühne W. Über das Verhalten verschiedener organisierter und sog. ungeformter Fermente. Verhandlungen des naturhistorisch-medicinischen Vereins zu Heidelberg. 1877;1(3):190–3.
7. Adrio J, Demain A. Microbial enzymes: Tools for biotechnological processes. Biomolecules. 2014 Jan;4(1):117–39.
8. Nielsen J. Production of biopharmaceutical proteins by yeast: Advances through metabolic engineering. Bioengineered. 2013;4(4):207–11.
9. Diez B, Mellado E, Rodrıguez M, Fouces R, Barredo J-L. Recombinant microorganisms for industrial production of antibiotics. Biotechnol Bioeng. 1997;55:216–26.
10. Matejczyk M. Environmental and recombinant microorganisms for biopharmaceuticals production. Civ Environ Eng. 2014;5(2007):15–21.
11. Kirk O, Borchert TV, Fuglsang CC. Industrial enzyme applications. Curr Opin Biotechnol. 2002 Aug;13(4):345–51.
12. Choi J-M, Han S-S, Kim H-S. Industrial applications of enzyme biocatalysis: Current status and future aspects. Biotechnol Adv. 2015 Nov;33(7):1443–54.
13. Bornscheuer UT, Huisman GW, Kazlauskas RJ, Lutz S, Moore JC, Robins K. Engineering the third wave of biocatalysis. Nature. 2012 May;485(7397):185–94.
14. Faber K. Biotransformations in organic chemistry. 6th ed. Springer Heidelberg; 2011. 423 p.
15. Arora B, Mukherjee J, Gupta MN. Enzyme promiscuity: Using the dark side of enzyme specificity in white biotechnology. Sustain Chem Process. 2014;2(1):25.
16. Zaks A, Klibanov AM. Enzymatic catalysis in nonaqueous solvents. J Biol Chem. 1988 Mar 5;263(7):3194–201.
17. Doukyu N, Ogino H. Organic solvent-tolerant enzymes. Biochem Eng J. 2010 Feb;48(3):270–82.
18. Khmelnitsky YL, Mozhaev V V, Belova AB, Sergeeva M V, Martinek K. Denaturation capacity: A new quantitative criterion for selection of organic solvents as reaction media in

biocatalysis. Eur J Biochem. 1991 May;198(1):31–41.

19. Castro GR, Knubovets T. Homogeneous biocatalysis in organic solvents and water-organic mixtures. Crit Rev Biotechnol. 2003 Jan 9;23(3):195–231.
20. Wachtmeister J, Jakoblinnert A, Kulig J, Offermann H, Rother D. Whole-cell teabag catalysis for the modularisation of synthetic enzyme cascades in micro-aqueous systems. ChemCatChem. 2014 Apr;6(4):1051–8.
21. Philp JC, Ritchie RJ, Allan JEM. Biobased chemicals: The convergence of green chemistry with industrial biotechnology. Trends Biotechnol. 2013;31(4):219–22.
22. Sheldon RA. Fundamentals of green chemistry: Efficiency in reaction design. Chem Soc Rev. 2012;41(4):1437–51.
23. Anastas PT, Williamson TC. Green chemistry: An overview. In: Green chemistry: Designing chemistry for the environment. 1996. p. 1–17.
24. Aguilar A, Bochereau L, Matthiessen L. Biotechnology as the engine for the knowledge-based bio-economy. Biotechnol Genet Eng Rev. 2009;26(1):371–88.
25. Birner R. Bioeconomy Concepts. In: Bioeconomy. Cham: Springer International Publishing; 2018. p. 17–38.
26. Wilding KM, Schinn S-M, Long EA, Bundy BC. The emerging impact of cell-free chemical biosynthesis. Curr Opin Biotechnol. 2018 Oct 5;53(1):115–21.
27. Liszka MJ, Clark ME, Schneider E, Clark DS. Nature versus nurture: Developing enzymes that function under extreme conditions. Annu Rev Chem Biomol Eng. 2012;3(1):77–102.
28. Bommarius AS, Paye MF. Stabilizing biocatalysts. Chem Soc Rev. 2013;42(15):6534.
29. Brady D, Jordaan J. Advances in enzyme immobilisation. Biotechnol Lett. 2009;31:1639–50.
30. Sheldon RA, van Pelt S. Enzyme immobilisation in biocatalysis: Why, what and how. Chem Soc Rev. 2013 Mar;42(15):6223–35.
31. Domínguez de María P, Stillger T, Pohl M, Kiesel M, Liese A, Gröger H, Trauthwein H. Enantioselective C-C bond ligation using recombinant *Escherichia coli*-whole-cell biocatalysts. Adv Synth Catal. 2008 Jan 4;350(1):165–73.
32. Jakoblinnert A, Rother D. A two-step biocatalytic cascade in micro-aqueous medium: Using whole cells to obtain high concentrations of a vicinal diol. Green Chem. 2014;16(7):3472–82.
33. de Carvalho CCCR. Enzymatic and whole cell catalysis: Finding new strategies for old processes. Biotechnol Adv. 2011;29(1):75–83.
34. Mohamad NR, Marzuki NHC, Buang NA, Huyop F, Wahab RA. An overview of technologies for immobilization of enzymes and surface analysis techniques for immobilized enzymes. Biotechnol Biotechnol Equip. 2015;(May 2015):1–16.
35. Adlercreutz P. Immobilisation and application of lipases in organic media. Chem Soc Rev. 2013;42(15):6406.
36. Hanefeld U, Gardossi L, Magner E. Understanding enzyme immobilisation. Chem Soc Rev.

2009 Feb;38(2):453–68.

37. Rodrigues RC, Ortiz C, Berenguer-Murcia Á, Torres R, Fernández-Lafuente R. Modifying enzyme activity and selectivity by immobilization. Chem Soc Rev. 2013;42(15):6290–307.
38. Eş I, Vieira JDG, Amaral AC. Principles, techniques, and applications of biocatalyst immobilization for industrial application. Appl Microbiol Biotechnol. 2015;99(5):2065–82.
39. Hartmann M, Kostrov X. Immobilization of enzymes on porous silicas – benefits and challenges. Chem Soc Rev. 2013;42(15):6277.
40. Varalakshmi V, Siva rama prasad D. Enzyme immobilization: The fascinating challenge in biotechnology. J Environ Sci , Comput Sci Eng Technol. 2013;2(3):840–53.
41. Barbosa O, Ortiz C, Berenguer-Murcia Á, Torres R, Rodrigues RC, Fernandez-Lafuente R. Strategies for the one-step immobilization–purification of enzymes as industrial biocatalysts. Biotechnol Adv. 2015 Sep;33(5):435–56.
42. Sopaci ŞB, Şimşek İ, Tural B, Volkan M, Demir AS. Carboligation reactions with benzaldehyde lyase immobilized on superparamagnetic solid support. Org Biomol Chem. 2009;7(8):1658.
43. Malhotra A. Tagging for protein expression. In: Methods in enzymology. 1st ed. Elsevier Inc.; 2009. p. 239–58.
44. Engelmark Cassimjee K, Federsel H-J. EziG: A universal platform for enzyme immobilization. In: Biocatalysis: An industrial perspective. The Royal Society of Chemistry; 2017. p. 345–62.
45. Döbber J, Pohl M. HaloTag^{TM}: Evaluation of a covalent one-step immobilization for biocatalysis. J Biotechnol. 2017;241:170–4.
46. Rehm FBH, Chen S, Rehm BHA. Enzyme engineering for *in situ* immobilization. Molecules. 2016 Oct 14;21(10):1370.
47. Levy I, Shoseyov O. Cellulose-binding domains. Biotechnol Adv. 2002 Nov;20(3–4):191–213.
48. Mateo C, Palomo JM, Fernandez-Lorente G, Guisan JM, Fernandez-Lafuente R. Improvement of enzyme activity, stability and selectivity via immobilization techniques. Enzyme Microb Technol. 2007 May;40(6):1451–63.
49. Mateo C, Grazú V, Pessela BCC, Montes T, Palomo JM, Torres R, López-Gallego F, Fernández-Lafuente R, Guisán JM. Advances in the design of new epoxy supports for enzyme immobilization-stabilization. Biochem Soc Trans. 2007 Dec 1;35(Pt 6):1593–601.
50. Tural B, Tural S, Ertaş E, Yalinkiliç I, Demir AS. Purification and covalent immobilization of benzaldehyde lyase with heterofunctional chelate-epoxy modified magnetic nanoparticles and its carboligation reactivity. J Mol Catal B Enzym. 2013;95:41–7.
51. Magner E. Immobilisation of enzymes on mesoporous silicate materials. Chem Soc Rev. 2013;42(15):6213.
52. Basso A, Braiuca P, Cantone S, Ebert C, Linda P, Spizzo P, Caimi P, Hanefeld U, Degrassi G, Gardossi L. *In silico* analysis of enzyme surface and glycosylation effect as a tool for efficient

covalent immobilisation of CalB and PGA on sepabeads. Adv Synth Catal. 2007;349(6):877–86.

53. Wiese S, Spiess AC, Richtering W. Microgel-stabilized smart emulsions for biocatalysis. Angew Chem Int Ed Engl. 2013 Jan 7;52(2):576–9.
54. Chmura A, van der Kraan GM, Kielar F, van Langen LM, van Rantwijk F, Sheldon RA. Cross-linked aggregates of the hydroxynitrile lyase from *Manihot esculenta*: Highly active and robust biocatalysts. Adv Synth Catal. 2006 Aug;348(12–13):1655–61.
55. Cao L. Carrier-bound immobilized enzymes: Principles, application and design. WILEY-VCH Verlag; 2006. 578 p.
56. Mateo C, Palomo JM, Van Langen LM, Van Rantwijk F, Sheldon RA. A new, mild cross-linking methodology to prepare cross-linked enzyme aggregates. Biotechnol Bioeng. 2004;86(3):273–6.
57. Schoevaart R, Wolbers MW, Golubovic M, Ottens M, Kieboom APG, van Rantwijk F, van der Wielen LAM, Sheldon RA. Preparation, optimization, and structures of cross-linked enzyme aggregates (CLEAs). Biotechnol Bioeng. 2004 Sep 20;87(6):754–62.
58. Kumar VV, Sivanesan S, Cabana H. Magnetic cross-linked laccase aggregates - Bioremediation tool for decolorization of distinct classes of recalcitrant dyes. Sci Total Environ. 2014;487(1):830–9.
59. Aytar BS, Bakir U. Preparation of cross-linked tyrosinase aggregates. Process Biochem. 2008;43(2):125–31.
60. Alvarenga AE, Amoroso MJ, Illanes A, Castro GR. Cross-linked α-l-rhamnosidase aggregates with potential application in food industry. Eur Food Res Technol. 2014;238(5):797–801.
61. Rehman S, Bhatti HN, Bilal M, Asgher M. Cross-linked enzyme aggregates (CLEAs) of *Pencilluim notatum* lipase enzyme with improved activity, stability and reusability characteristics. Int J Biol Macromol. 2016;91:1161–9.
62. Talekar S, Waingade S, Gaikwad V, Patil S, Nagavekar N. Preparation and characterization of cross linked enzyme aggregates (CLEAs) of *Bacillus amyloliquefaciens* alpha amylase. J Biochem Technol. 2012;3(4):349–53.
63. Cui JD, Sun LM, Li LL. A simple technique of preparing stable CLEAs of phenylalanine ammonia lyase using co-aggregation with starch and bovine serum albumin. Appl Biochem Biotechnol. 2013 Aug 11;170(8):1827–37.
64. Zhou L, Mou H, Gao J, Ma L, He Y, Jiang Y. Preparation of cross-linked enzyme aggregates of nitrile hydratase ES-NHT-118 from *E. coli* by macromolecular cross-linking agent. Chinese J Chem Eng. 2017 Apr;25(4):487–92.
65. van Pelt S, Quignard S, Kubáč D, Sorokin DY, van Rantwijk F, Sheldon RA. Nitrile hydratase CLEAs: The immobilization and stabilization of an industrially important enzyme. Green Chem. 2008;10(4):395–400.

66. Park SH, Soetyono F, Kim HK. Cadaverine production by using cross-linked enzyme aggregate of *Escherichia coli* lysine decarboxylase. J Microbiol Biotechnol. 2017;27(2):289–96.
67. Kaul P, Stolz A, Banerjee UC. Cross-linked amorphous nitrilase aggregates for enantioselective nitrile hydrolysis. Adv Synth Catal. 2007 Sep 3;349(13):2167–76.
68. Cao L, Langen L van, Sheldon RA. Immobilised enzymes: Carrier-bound or carrier-free? Curr Opin Biotechnol. 2003 Aug;14(4):387–94.
69. Cui JD, Jia SR. Optimization protocols and improved strategies of cross-linked enzyme aggregates technology: Current development and future challenges. Crit Rev Biotechnol. 2013;8551(1):1–14.
70. Tufvesson P, Lima-Ramos J, Nordblad M, Woodley JM. Guidelines and cost analysis for catalyst production in biocatalytic processes. Org Process Res Dev. 2011;15(1):266–74.
71. Shively JM. Inclusions in Prokaryotes. Shively JM, editor. Inclusions in Prokaryotes. Springer-Verlag; 2006. (Microbiology Monographs; vol. 1).
72. Gatti-Lafranconi P, Natalello A, Ami D, Doglia SM, Lotti M. Concepts and tools to exploit the potential of bacterial inclusion bodies in protein science and biotechnology. FEBS J. 2011;278:2408–18.
73. Carrió M, González-Montalbán N, Vera A, Villaverde A, Ventura S. Amyloid-like properties of bacterial inclusion bodies. J Mol Biol. 2005;347:1025–37.
74. Wang L. Towards revealing the structure of bacterial inclusion bodies. Prion. 2009;3(3):139–45.
75. Eiberle MK, Jungbauer A. Technical refolding of proteins: Do we have freedom to operate? Biotechnol J. 2010;5(6):547–59.
76. Singh A, Upadhyay V, Upadhyay AK, Singh SM, Panda AK. Protein recovery from inclusion bodies of *Escherichia coli* using mild solubilization process. Microb Cell Fact. 2015;14(1):1–10.
77. Yamaguchi H, Miyazaki M. Refolding techniques for recovering biologically active recombinant proteins from inclusion bodies. Biomolecules. 2014;4(1):235–51.
78. Li G-Y, Xiao Z-Z, Lu H-P, Li Y-Y, Zhou X-H, Tan X, Zhang X-Y, Xia X-L, Sun H-C. A simple method for recombinant protein purification using self-assembling peptide-tagged tobacco etch virus protease. Protein Expr Purif. 2016 Dec;128:86–92.
79. Lin Z, Zhao Q, Xing L, Zhou B, Wang X. Aggregating tags for column-free protein purification. Biotechnol J. 2015;10(12):1877–86.
80. Jong WSP, Vikström D, Houben D, Berg van Saparoea HB, Gier JW, Luirink J. Application of an *E. coli* signal sequence as a versatile inclusion body tag. Microb Cell Fact. 2017;16(1):1–13.
81. Worrall DM, Goss NH. The formation of biologically active beta-galactosidase inclusion bodies in *Escherichia coli*. Aust J Biotechnol. 1989;3(1):28–32.

82. Tokatlidis K, Dhurjati P, Millet J, Béguin P, Aubert J-P. High activity of inclusion bodies formed in *Escherichia coli* overproducing *Clostridium thermocellum* endoglucanase D. FEBS Lett. 1991 Apr;282(1):205–8.

83. García-Fruitós E, Vázquez E, Díez-Gil C, Corchero JL, Seras-Franzoso J, Ratera I, Veciana J, Villaverde A. Bacterial inclusion bodies: Making gold from waste. Trends Biotechnol. 2012;30(2):65–70.

84. García-Fruitós E, González-Montalbán N, Morell M, Vera A, Ferraz RM, Arís A, Ventura S, Villaverde A. Aggregation as bacterial inclusion bodies does not imply inactivation of enzymes and fluorescent proteins. Microb Cell Fact. 2005;4:27.

85. Nahálka J, Pätoprstý V. Enzymatic synthesis of sialylation substrates powered by a novel polyphosphate kinase (PPK3). Org Biomol Chem. 2009;7(9):1778–80.

86. Choi SL, Lee SJ, Ha JS, Song JJ, Rhee YH, Lee SG. Generation of catalytic protein particles in *Escherichia coli* cells using the cellulose-binding domain from *Cellulomonas fimi* as a fusion partner. Biotechnol Bioprocess Eng. 2011;16:1173–9.

87. Hrabárová E, Achbergerová L, Nahálka J. Insoluble protein applications: The use of bacterial inclusion bodies as biocatalysts. In: García-Fruitós E, editor. Insoluble Protein: Methods and protocols. Springer New York; 2015. p. 411–22. (Methods in Molecular Biology; vol. 1258).

88. Nahálka J, Mislovicová D, Kavcová H. Targeting lectin activity into inclusion bodies for the characterisation of glycoproteins. Mol Biosyst. 2009 Aug;5(8):819–21.

89. Park S-Y, Park S-H, Choi S-K. Active inclusion body formation using *Paenibacillus polymyxa* PoxB as a fusion partner in *Escherichia coli*. Anal Biochem. 2012;426(1):63–5.

90. Diener M, Kopka B, Pohl M, Jaeger K-E, Krauss U. Fusion of a coiled-coil domain facilitates the high-level production of catalytically active enzyme inclusion bodies. ChemCatChem. 2016 Jan;8(1):142–52.

91. Diener M. Von gezielter Oligomerisierung zu katalytisch aktiven inclusion bodies - Eine alternative Stratiegie zu Stabilisierung und Immobilisierung von Biokatalysatoren. Heinrich-Heine-Universität Düsseldorf; 2014.

92. Wang X, Zhou B, Hu W, Zhao Q, Lin Z. Formation of active inclusion bodies induced by hydrophobic self-assembling peptide GFIL8. Microb Cell Fact. 2015;14:88.

93. Zhou B, Xing L, Wu W, Zhang X-E, Lin Z. Small surfactant-like peptides can drive soluble proteins into active aggregates. Microb Cell Fact. 2012;11(1):10.

94. Wu W, Xing L, Zhou B, Lin Z. Active protein aggregates induced by terminally attached self-assembling peptide ELK16 in *Escherichia coli*. Microb Cell Fact. 2011;10(1):9.

95. Roessl U, Nahálka J, Nidetzky B. Carrier-free immobilized enzymes for biocatalysis. Biotechnol Lett. 2010 Mar 27;32(3):341–50.

96. Krauss U, Jäger VD, Diener M, Pohl M, Jaeger K-E. Catalytically-active inclusion bodies—Carrier-free protein immobilizates for application in biotechnology and biomedicine. J

Biotechnol. 2017 Sep;258:136–47.

97. García-Fruitós E. Inclusion bodies: A new concept. Microb Cell Fact. 2010;9:2010–2.

98. Upadhyay AK, Singh A, Mukherjee KJ, Panda AK. Refolding and purification of recombinant L-asparaginase from inclusion bodies of *E. coli* into active tetrameric protein. Front Microbiol. 2014;5(SEP):1–10.

99. Chen J, Yu J, Tang L, Tang M, Shi Y, Pang Y. Comparison of the expression of *Bacillus thuringiensis* full-length and N-terminally truncated vip3A gene in *Escherichia coli*. J Appl Microbiol. 2003;95(2):310–6.

100. Fernandez-Escamilla A-M, Rousseau F, Schymkowitz J, Serrano L. Prediction of sequence-dependent and mutational effects on the aggregation of peptides and proteins. Nat Biotechnol. 2004 Oct;22(10):1302–6.

101. Conchillo-Solé O, de Groot NS, Avilés FX, Vendrell J, Daura X, Ventura S. AGGRESCAN: A server for the prediction and evaluation of "hot spots" of aggregation in polypeptides. BMC Bioinformatics. 2007 Feb 27;8:65.

102. Tartaglia GG, Vendruscolo M. The Zyggregator method for predicting protein aggregation propensities. Chem Soc Rev. 2008 Jul;37(7):1395–401.

103. Ratera I, Peternel S, Seras-Franzoso J, Cano-Garrido O, García-Fruitós E, Cubarsí R, Vazquez E, Corchero JL, Rodríguez-Carmona E, Veciana J, Villaverde A. Biomedical applications of bacterial inclusion bodies. In: Protein aggregation in bacteria:Functional and structural properties of inclusion bodies in bacterial cells. 2016. p. 203–20.

104. Vázquez E, Corchero JL, Burgueño JF, Seras-Franzoso J, Kosoy A, Bosser R, Mendoza R, Martínez-Láinez JM, Rinas U, Fernández E, Ruiz-Avila L, García-Fruitõs E, Villaverde A. Functional inclusion bodies produced in bacteria as naturally occurring nanopills for advanced cell therapies. Adv Mater. 2012;24(13):1742–7.

105. Rueda F, Gasser B, Sánchez-Chardi A, Roldán M, Villegas S, Puxbaum V, Ferrer-Miralles N, Unzueta U, Vázquez E, Garcia-Fruitós E, Mattanovich D, Villaverde A. Functional inclusion bodies produced in the yeast *Pichia pastoris*. Microb Cell Fact. 2016 Oct 1;15(1):166.

106. Rueda F, Céspedes MV, Sánchez-Chardi A, Seras-Franzoso J, Pesarrodona M, Ferrer-Miralles N, Vázquez E, Rinas U, Unzueta U, Mamat U, Mangues R, García-Fruitós E, Villaverde A. Structural and functional features of self-assembling protein nanoparticles produced in endotoxin-free *Escherichia coli*. Microb Cell Fact. 2016;15(1):1–12.

107. Li S, Lin K, Pang H, Wu Y, Xu J. Production, characterization, and application of an organic solvent-tolerant lipase present in active inclusion bodies. Appl Biochem Biotechnol. 2013;169:612–23.

108. Nahálka J, Vikartovská A, Hrabárová E. A crosslinked inclusion body process for sialic acid synthesis. J Biotechnol. 2008;134:146–53.

109. Peternel S, Komel R. Isolation of biologically active nanomaterial (inclusion bodies) from

bacterial cells. Microb Cell Fact. 2010;9:66.

110. Rodríguez-Carmona E, Cano-Garrido O, Seras-Franzoso J, Villaverde A, García-Fruitós E. Isolation of cell-free bacterial inclusion bodies. Microb Cell Fact. 2010;9:71.
111. Wang Y, Heermann R, Jung K. CipA and CipB as scaffolds to organize proteins into crystalline inclusions. ACS Synth Biol. 2017;6(5):826–36.
112. Nahálka J, Gemeiner P, Bucko M, Wang PG. Bioenergy beads: A tool for regeneration of ATP/NTP in biocatalytic synthesis. Artif Cells Blood Substit Immobil Biotechnol. 2006;34(1):515–21.
113. Nahálka J. Physiological aggregation of maltodextrin phosphorylase from *Pyrococcus furiosus* and its application in a process of batch starch degradation to alpha-D-glucose-1-phosphate. J Ind Microbiol Biotechnol. 2008;35:219–23.
114. Nahalka J, Nidetzky B. Fusion to a pull-down domain: A novel approach of producing *Trigonopsis variabilis* D-amino acid oxidase as insoluble enzyme aggregates. Biotechnol Bioeng. 2007;97(3):454–61.
115. Sun H, Gao W, Wang H, Wei D. Expression, characterization of a novel nitrilase PpL19 from *Pseudomonas psychrotolerans* with *S*-selectivity toward mandelonitrile present in active inclusion bodies. Biotechnol Lett. 2016;38(3):455–61.
116. Raghunathan G, Munussami G, Lee SG. Characterization on the aggregation of self-aggregating green fluorescent protein variant. J Ind Eng Chem. 2017;46:337–41.
117. Wang W, Sun J, Xiao W, Jiang L, Wang R, Fan J. Change of the *N*-terminal codon bias combined with tRNA supplementation outperforms the selected fusion tags for production of human D-amino acid oxidase as active inclusion bodies. Biotechnol Lett. 2017 Nov 23;39(11):1733–40.
118. Peters J, Nitsch M, Kühlmorgen B, Golbik R, Lupas A, Kellermann J, Engelhardt H, Pfander JP, Müller S, Goldie K. Tetrabrachion: A filamentous archaebacterial surface protein assembly of unusual structure and extreme stability. J Mol Biol. 1995 Jan 27;245(4):385–401.
119. Peters J, Baumeister W, Lupas A. Hyperthermostable surface layer protein tetrabrachion from the archaebacterium *Staphylothermus marinus*: Evidence for the presence of a right-handed coiled coil derived from the primary structure. J Mol Biol. 1996 Apr 19;257(5):1031–41.
120. Stetefeld J, Kammerer RA, Jenny M, Schulthess T, Landwehr R, Engel J. Crystal structure of a naturally occurring parallel right-handed coiled coil tetramer. Nat Struct Biol. 2000 Sep;7(9):772–6.
121. Diener M, Pohl M, Jaeger K-E, Krauss U. Catalytically active protein aggregates and methods for producing the same. 2017.
122. Airola M V., Watts KJ, Bilwes AM, Crane BR. Structure of concatenated HAMP comains provides a mechanism for signal transduction. Structure. 2010 Mar;18(4):436–48.
123. Wolf E, Kim PS, Berger B. MultiCoil: A program for predicting two-and three-stranded coiled

coils. Protein Sci. 1997;6(6):1179–89.

124. Pauling L, Corey RB. Compound helical configurations of polypeptide chains: Structure of proteins of the α-keratin type. Nature. 1953 Jan 10;171(4341):59–61.
125. Crick FHC. The packing of α-helices: Simple coiled-coils. Acta Crystallogr. 1953;6(8):689–97.
126. Woolfson DN, Bartlett GJ, Bruning M, Thomson AR. New currency for old rope: From coiled-coil assemblies to α-helical barrels. Curr Opin Struct Biol. 2012;22(4):432–41.
127. Lupas A, Gruber M. The structure of alpha-helical coiled coils. Adv Protein Chem. 2005;70:37–78.
128. Mason JM, Arndt KM. Coiled coil domains: Stability, specificity, and biological implications. ChemBioChem. 2004;5(2):170–6.
129. Rackham OJL, Madera M, Armstrong CT, Vincent TL, Woolfson DN, Gough J. The evolution and structure prediction of coiled coils across all genomes. J Mol Biol. 2010 Oct 29;403(3):480–93.
130. Marsden HR, Kros A. Self-assembly of coiled coils in synthetic biology: Inspiration and progress. Angew Chemie - Int Ed. 2010;49(17):2988–3005.
131. Alber T. Structure of the leucine zipper. Curr Opin Genet Dev. 1992 Apr;2(2):205–10.
132. Oshaben KM, Salari R, McCaslin DR, Chong LT, Horne WS. The native GCN4 leucine-zipper domain does not uniquely specify a dimeric oligomerization state. Biochemistry. 2012 Nov 27;51(47):9581–91.
133. Lupas AN, Bassler J. Coiled coils – A model system for the 21st century. Trends Biochem Sci. 2017;42(2):130–40.
134. Moutevelis E, Woolfson DN. A periodic table of coiled-coil protein structures. J Mol Biol. 2009 Jan 23;385(3):726–32.
135. Burkhard P, Stetefeld J, Strelkov S V. Coiled coils: A highly versatile protein folding motif. Trends Cell Biol. 2001;11(2):82–8.
136. Frank RAW, Leeper FJ, Luisi BF. Structure, mechanism and catalytic duality of thiamine-dependent enzymes. Cell Mol Life Sci. 2007 Apr;64(7–8):892–905.
137. Pohl M, Sprenger GA, Müller M. A new perspective on thiamine catalysis. Curr Opin Biotechnol. 2004 Aug;15(4):335–42.
138. Müller M, Sprenger GA, Pohl M. C-C bond formation using ThDP-dependent lyases. Curr Opin Chem Biol. 2013 Apr;17(2):261–70.
139. Vogel C, Pleiss J. The modular structure of ThDP-dependent enzymes. Proteins Struct Funct Bioinforma. 2014;(May):2523–37.
140. Widmann M, Radloff R, Pleiss J. The Thiamine diphosphate dependent Enzyme Engineering Database: A tool for the systematic analysis of sequence and structure relations. BMC Biochem. 2010 Feb 1;11(1):9.
141. Buchholz PCF, Vogel C, Reusch W, Pohl M, Rother D, Spieß AC, Pleiss J. BioCatNet: A

database aystem for the integration of enzyme sequences and biocatalytic experiments. Chembiochem. 2016 Nov 3;17(21):2093–8.

142. Muller YA, Lindqvist Y, Furey W, Schulz GE, Jordan F, Schneider G. A thiamin diphosphate binding fold revealed by comparison of the crystal structures of transketolase, pyruvate oxidase and pyruvate decarboxylase. Structure. 1993 Oct 15;1(2):95–103.
143. Duggleby RG. Domain relationships in thiamine diphosphate-dependent enzymes. Acc Chem Res. 2006;39(8):550–7.
144. Hawkins CF, Borges A, Perham RN. A common structural motif in thiamin pyrophosphate-binding enzymes. FEBS Lett. 1989 Sep;255(1):77–82.
145. Schellenberger A. Sixty years of thiamin diphosphate biochemistry. Biochim Biophys Acta - Protein Struct Mol Enzymol. 1998;1385(2):177–86.
146. Shin W, Pletcher J, Blank G, Sax M. Ring stacking interactions between thiamin and planar molecules as seen in the crystal structure of a thiamin picrolonate dihydrate complex. J Am Chem Soc. 1977 Mar;99(10):3491–9.
147. Kern D. How thiamin diphosphate is activated in enzymes. Science. 1997 Jan;275(5296):67–70.
148. Pohl M, Lingen B, Müller M. Thiamin-diphosphate-dependent enzymes: New aspects of asymmetric C-C bond formation. Chem - A Eur J. 2002;8(23):5288–95.
149. Kokova M, Zavrel M, Tittmann K, Spiess AC, Pohl M. Investigation of the carboligase activity of thiamine diphosphate-dependent enzymes using kinetic modeling and NMR spectroscopy. J Mol Catal B Enzym. 2009;61(1–2):73–9.
150. Stillger T, Pohl M, Wandrey C, Liese A. Reaction engineering of benzaldehyde lyase from *Pseudomonas fluorescens* catalyzing enantioselective C-C bond formation. Org Proc Res Dev. 2006;10(15):1172–7.
151. Zavrel M, Schmidt T, Michalik C, Ansorge-schumacher M, Marquardt W, Buchs J, Spiess A. Mechanistic kinetic model for symmetric carboligations using benzaldehyde lyase. Biotechnol Bioeng. 2008;101(1):27–38.
152. Jordan F, Nemeria NS. Progress in the experimental observation of thiamin diphosphate-bound intermediates on enzymes and mechanistic information derived from these observations. Bioorg Chem. 2014;57:251–62.
153. Janzen E, Müller M, Kolter-Jung D, Kneen MM, McLeish MJ, Pohl M. Characterization of benzaldehyde lyase from *Pseudomonas fluorescens*: A versatile enzyme for asymmetric C-C bond formation. Bioorg Chem. 2006;34:345–61.
154. González B, Vicuña R. Benzaldehyde lyase, a novel thiamine PPi-requiring enzyme, from *Pseudomonas fluorescens* biovar I. J Bacteriol. 1989 May;171(5):2401–5.
155. Gonzalez B, Merino A, Almeida M, Vicña R. Comparative growth of natural bacterial isolates on various lignin-related compounds. Appl Environ Microbiol. 1986 Dec;52(6):1428–32.

156. Harwood CS, Parales RE. The *β*-ketoadipate pathway and the biology of self-identity. Annu Rev Microbiol. 1996;50(1):553–90.

157. Mosbacher TG, Mueller M, Schulz GE. Structure and mechanism of the ThDP-dependent benzaldehyde lyase from *Pseudomonas fluorescens*. FEBS J. 2005;272:6067–76.

158. Maraite A, Schmidt T, Ansörge-Schumacher MB, Brzozowski AM, Grogan G. Structure of the ThDP-dependent enzyme benzaldehyde lyase refined to 1.65 Å resolution. Acta Crystallogr Sect F Struct Biol Cryst Commun. 2007;63(7):546–8.

159. Demir AS, Şeşenoglu Ö, Eren E, Hosrik B, Pohl M, Janzen E, Kolter D, Feldmann R, Dünkelmann P, Müller M. Enantioselective synthesis of α-hydroxy ketones via benzaldehyde lyase-catalyzed C−C bond formation reaction. Adv Synth Catal. 2002 Jan;344(1):96.

160. Demir AS, Seşenoglu O, Dünkelmann P, Müller M. Benzaldehyde lyase-catalyzed enantioselective carboligation of aromatic aldehydes with mono- and dimethoxy acetaldehyde. Org Lett. 2003 Jun 12;5(12):2047–50.

161. Dünkelmann P, Kolter-Jung D, Nitsche A, Demir AS, Siegert P, Lingen B, Baumann M, Pohl M, Müller M. Development of a donor-acceptor concept for enzymatic cross-coupling reactions of aldehydes: The first asymmetric cross-benzoin condensation. J Am Chem Soc. 2002;124(41):12084–5.

162. Sanchez-Gonzalez M, Rosazza JPN. Mixed aromatic acyloin condensations with recombinant benzaldehyde lyase: Synthesis of α-hydroxydihydrochalcones and related α-hydroxy ketones. Adv Synth Catal. 2003 Jun;345(67):819–24.

163. Janzen E. Die Benzaldehydlyase aus *Pseudomonas fluoreszens*-Biochemische Charakterisierung und die Untersuchung von Struktur-Funktionsbeziehungen, PhD thesis. 2002.

164. Müller M, Gocke D, Pohl M. Thiamin diphosphate in biological chemistry: Exploitation of diverse thiamin diphosphate-dependent enzymes for asymmetric chemoenzymatic synthesis. FEBS J. 2009;276(11):2894–904.

165. Kneen MM, Pogozheva ID, Kenyon GL, McLeish MJ. Exploring the active site of benzaldehyde lyase by modeling and mutagenesis. Biochim Biophys Acta - Proteins Proteomics. 2005;1753(2):263–71.

166. Demir AS, Pohl M, Janzen E, Müller M. Enantioselective synthesis of hydroxy ketones through cleavage and formation of acyloin linkage. Enzymatic kinetic resolution *via* C–C bond cleavage. J Chem Soc Perkin Trans 1. 2001;(7):633–5.

167. Sehl T, Maugeri Z, Rother D. Multi-step synthesis strategies towards 1,2-amino alcohols with special emphasis on phenylpropanolamines. J Mol Catal B Enzym. 2015 Apr;114(2016):65–71.

168. Goldberg K, Schroer K, Lütz S, Liese A. Biocatalytic ketone reduction—a powerful tool for the production of chiral alcohols—part II: Whole-cell reductions. Appl Microbiol Biotechnol. 2007 Jul 23;76(2):249–55.

169. Kurlemann N, Liese A. Immobilization of benzaldehyde lyase and its application as a heterogeneous catalyst in the continuous synthesis of a chiral 2-hydroxy ketone. Tetrahedron Asymmetry. 2004;15(18):2955–8.

170. Domínguez de María P, Stillger T, Pohl M, Wallert S, Drauz K, Gröger H, Trauthwein H, Liese A. Preparative enantioselective synthesis of benzoins and (*R*)-2-hydroxy-1-phenylpropanone using benzaldehyde lyase. J Mol Catal B Enzym. 2006 Jan;38(1):43–7.

171. Mikolajek RJ, Spiess AC, Pohl M, Büchs J. Propioin synthesis using thiamine diphosphate-dependent enzymes. Biotechnol Prog. 2009 Jan;25(1):132–8.

172. Hildebrand F, Kühl S, Pohl M, Vasic-Racki D, Müller M, Wandrey C, Lütz S. The production of (*R*)-2-hydroxy-1-phenyl-propan-1-one derivatives by benzaldehyde lyase from *Pseudomonas fluorescens* in a continuously operated membrane reactor. Biotechnol Bioeng. 2007 Apr 1;96(5):835–43.

173. Schwarz M. Einflussfaktoren auf die Stabilität und Aktivität der Benzaldehydlyase aus *Pseudomonas fluorescens* in Carboligasereaktionen mit aromatischen Aldehyden. Heinrich-Heine-Universität; 2010.

174. Stillger T. Enantioselektive C-C Knüpfung mit Enzymen. Rheinische Friedrich-Wilhelms-Universität Bonn; 2004.

175. Schmidt T, Zavrel M, Spieß A, Ansorge-Schumacher MB. Biochemical peculiarities of benzaldehyde lyase from *Pseudomonas fluorescens* Biovar I in the dependency on pH and cosolvent concentration. Bioorg Chem. 2009;37(3):84–9.

176. Kühl S, Zehentgruber D, Pohl M, Müller M, Lütz S. Process development for enzyme catalysed asymmetric C-C-bond formation. Chem Eng Sci. 2007;62(18–20):5201–5.

177. Shanmuganathan S, Natalia D, van den Wittenboer A, Kohlmann C, Greiner L, Domínguez de María P. Enzyme-catalyzed C–C bond formation using 2-methyltetrahydrofuran (2-MTHF) as (co)solvent: Efficient and bio-based alternative to DMSO and MTBE. Green Chem. 2010;12(12):2240.

178. Ansorge-Schumacher MB, Greiner L, Schroeper F, Mirtschin S, Hischer T. Operational concept for the improved synthesis of (*R*)-3,3'-furoin and related hydrophobic compounds with benzaldehyde lyase. Biotechnol J. 2006;1(5):564–8.

179. Carrea G. Biocatalysis in water-organic solvent two-phase systems. Trends Biotechnol. 1984 Jul;2(4):102–6.

180. van den Wittenboer A, Niemeijer B, Karmee SK, Ansorge-Schumacher MB. Systematic assessment of the stability of benzaldehyde lyase in aqueous–organic biphasic systems and its stabilization by modification with methoxy-poly(ethylene) glycol. J Mol Catal B Enzym. 2010 Dec;67(3–4):208–13.

181. Hischer T, Gocke D, Fernández M, Hoyos P, Alcántara AR, Sinisterra J V., Hartmeier W, Ansorge-Schumacher MB. Stereoselective synthesis of novel benzoins catalysed by

benzaldehyde lyase in a gel-stabilised two-phase system. Tetrahedron. 2005;61(31):7378–83.

182. van den Wittenboer A, Schmidt T, Müller P, Ansorge-Schumacher MB, Greiner L. Biphasic mini-reactor for characterization of biocatalyst performance. Biotechnol J. 2009;4(1):44–50.

183. Mikolajek R, Spiess AC, Büchs J. Feasibility of gas/solid carboligation: conversion of benzaldehyde to benzoin using thiamine diphosphate-dependent enzymes. J Biotechnol. 2007 May 10;129(4):723–5.

184. Hegeman GD. Benzoylformate decarboxylase (*Pseudomonas putida*). Methods Enzym. 1970;17A:674–8.

185. Hegeman GD. Synthesis of the enzymes of the mandelate pathway by *Pseudomonas putida*. I. Synthesis of enzymes by the wild type. J Bacteriol. 1966;91(3):1140–54.

186. Hegeman GD. Synthesis of the enzymes of the mandelate pathway by *Pseudomonas putida*. III. Isolation and properties of constitutive mutants. J Bacteriol. 1966 Mar;91(3):1161–7.

187. Henning H, Leggewie C, Pohl M, Müller M, Eggert T, Jaeger K-E. Identification of novel benzoylformate decarboxylases by growth selection. Appl Environ Microbiol. 2006 Dec 1;72(12):7510–7.

188. Saehun C, Rojanarata T, Wiyakrutta S, McLeish MJ, Meevootisom V. Isolation and characterization of a benzoylformate decarboxylase and a NAD^+/$NADP^+$-dependent benzaldehyde dehydrogenase involved in D-phenylglycine metabolism in *Pseudomonas stutzeri* ST-201. Biochim Biophys Acta - Gen Subj. 2007 Nov;1770(11):1585–92.

189. Wendorff M. Neue Benzoylformiatdecarboxylasen für die Biokatalyse. Heinrich-Heine-Universität; 2006.

190. Iding H, Dünnwald T, Greiner L, Liese A, Müller M, Siegert P, Grötzinger J, Demir AS, Pohl M. Benzoylformate decarboxylase from *Pseudomonas putida* as stable catalyst for the synthesis of chiral 2-hydroxy ketones. Chem - A Eur J. 2000 Apr 14;6(8):1483–95.

191. Siegert P, McLeish MJ, Baumann M, Iding H, Kneen MM, Kenyon GL, Pohl M. Exchanging the substrate specificities of pyruvate decarboxylase from *Zymomonas mobilis* and benzoylformate decarboxylase from *Pseudomonas putida*. Protein Eng Des Sel. 2005 Jul 1;18(7):345–57.

192. Gocke D, Walter L, Gauchenova E, Kolter G, Knoll M, Berthold CL, Schneider G, Pleiss J, Müller M, Pohl M. Rational protein design of ThDP-dependent enzymes - Engineering stereoselectivity. ChemBioChem. 2008;9(3):406–12.

193. Polovnikova ES, McLeish MJ, Sergienko EA, Burgner JT, Anderson NL, Bera AK, Jordan F, Kenyon GL, Hasson MS. Structural and kinetic analysis of catalysis by a thiamin diphosphate-dependent enzyme, benzoylformate decarboxylase. Biochemistry. 2003;42(7):1820–30.

194. Hasson MS, Muscate A, McLeish MJ, Polovnikova LS, Gerlt JA, Kenyon GL, Petsko GA, Ringe D. The crystal structure of benzoylformate decarboxylase at 1.6 Å Resolution: Diversity of catalytic residues in thiamin diphosphate-dependent enzymes. Biochemistry.

1998;37(28):9918–30.

195. Dünnwald T, Müller M. Stereoselective formation of Bis(α-hydroxy ketones) via enzymatic carboligation. J Org Chem. 2000 Dec 15;65(25):8608–12.

196. Knoll M, Müller M, Pleiss J, Pohl M. Factors mediating activity, selectivity, and substrate specificity for the thiamin diphosphate-dependent enzymes benzaldehyde lyase and benzoylformate decarboxylase. ChemBioChem. 2006 Dec 4;7(12):1928–34.

197. Lingen B, Grötzinger J, Kolter D, Kula M-R, Pohl M. Improving the carboligase activity of benzoylformate decarboxylase from *Pseudomonas putida* by a combination of directed evolution and site-directed mutagenesis. Protein Eng. 2002 Jul;15(7):585–93.

198. Lingen B, Kolter-Jung D, Dünkelmann P, Feldmann R, Grötzinger J, Pohl M, Müller M. Alteration of the substrate specificity of benzoylformate decarboxylase from *Pseudomonas putida* by directed evolution. Chembiochem. 2003 Aug 4;4(8):721–6.

199. Hilterhaus L, Minow B, Müller J, Berheide M, Quitmann H, Katzer M, Thum O, Antranikian G, Zeng AP, Liese A. Practical application of different enzymes immobilized on sepabeads. Bioprocess Biosyst Eng. 2008 Apr 1;31(3):163–71.

200. Tural B, Tarhan T, Tural S. Covalent immobilization of benzoylformate decarboxylase from *Pseudomonas putida* on magnetic epoxy support and its carboligation reactivity. J Mol Catal B Enzym. 2014 Apr;102:188–94.

201. Tural S, Tural B, Demir AS. Heterofunctional magnetic metal-chelate-epoxy supports for the purification and covalent immobilization of benzoylformate decarboxylase from *Pseudomonas putida* and its carboligation reactivity. Chirality. 2015 Sep;27(9):635–42.

202. Döbber J, Gerlach T, Offermann H, Rother D, Pohl M. Closing the gap for efficient immobilization of biocatalysts in continuous processes: HaloTag^{TM} fusion enzymes for a continuous enzymatic cascade towards a vicinal chiral diol. Green Chem. 2018;20(2):544–52.

203. Racker E. Crystalline alcohol dehydrogenase yeast. J Biol Chem. 1950;190:313–9.

204. Patel RN. Stereoselective biocatalysis. M. Dekker; 2000. 932 p.

205. Prelog V. Specification of the stereospecificity of some oxido-reductases by diamond lattice sections. Pure Appl Chem. 1964 Jan 1;9(1):119–30.

206. You KS. Stereospecificity for nicotinamide nucleotides in enzymatic and chemical hydride transfer reactions. CRC Crit Rev Biochem. 1985;17(4):313–451.

207. Rossmann MG, Moras D, Olsen KW. Chemical and biological evolution of nucleotide-binding protein. Nature. 1974 Jul 19;250(463):194–9.

208. Carugo O, Argos P. NADP-dependent enzymes. I: Conserved stereochemistry of cofactor binding. Proteins. 1997 May;28(1):10–28.

209. Lavandera I, Kern A, Ferreira-Silva B, Glieder A, De Wildeman S, Kroutil W. Stereoselective bioreduction of bulky-bulky ketones by a novel ADH from *Ralstonia sp.* J Org Chem. 2008;73:6003–5.

210. Man H, Kédziora K, Kulig J, Frank A, Lavandera I, Gotor-Fernández V, Rother D, Hart S, Turkenburg JP, Grogan G. Structures of alcohol dehydrogenases from *Ralstonia* and *Sphingobium* spp. Reveal the molecular basis for their recognition of "bulky-bulky" ketones. Top Catal. 2014;57(5):356–65.
211. Schlieben NH, Niefind K, Müller J, Riebel B, Hummel W, Schomburg D. Atomic resolution structures of *R*-specific alcohol dehydrogenase from *Lactobacillus brevis* provide the structural bases of its substrate and cosubstrate specificity. J Mol Biol. 2005;349:801–13.
212. Hummel W. Large-scale applications of NAD(P)-dependent oxidoreductases: Recent developments. Trends Biotechnol. 1999;17(12):487–92.
213. Hummel W. New alcohol dehydrogenases for the synthesis of chiral compounds. Adv Biochem Eng Biotechnol. 1997;58:145–84.
214. Filling C, Berndt KD, Benach J, Knapp S, Prozorovski T, Nordling E, Ladenstein R, Jörnvall H, Oppermann U. Critical residues for structure and catalysis in short-chain dehydrogenases/reductases. J Biol Chem. 2002 Jul 12;277(28):25677–84.
215. Oppermann U, Filling C, Hult M, Shafqat N, Wu X, Lindh M, Shafqat J, Nordling E, Kallberg Y, Persson B, Jörnvall H. Short-chain dehydrogenases/reductases (SDR): The 2002 update. Chem Biol Interact. 2003 Feb;143–144:247–53.
216. Chenault HK, Whitesides GM. Regeneration of nicotinamide cofactors for use in organic synthesis. Appl Biochem Biotechnol. 1987 Mar;14(2):147–97.
217. Wichmann R, Vasic-Racki D. Cofactor regeneration at the lab scale. Adv Biochem Eng Biotechnol. 2005 Jan 28;92(May 2014):225–60.
218. Liu W, Wang P. Cofactor regeneration for sustainable enzymatic biosynthesis. Biotechnol Adv. 2007;25(4):369–84.
219. Wong C-H, Drueckhammer DG, Sweers HM. Enzymatic vs. fermentative synthesis: Thermostable glucose dehydrogenase catalyzed regeneration of NAD(P)H for use in enzymatic synthesis. J Am Chem Soc. 1985 Jul 1;3(7):649–51.
220. Hilt W, Pfleiderer G, Fortnagel P. Glucose dehydrogenase from *Bacillus subtilis* expressed in *Escherichia coli* I: Purification, characterization and comparison with glucose dehydrogenase from *Bacillus megaterium*. Biochim Biophys Acta - Protein Struct Mol Enzymol. 1991 Jan;1076(2):298–304.
221. Peters J, Zelinski T, Minuth T, Kula M-R. Synthetic applications of the carbonyl reductases isolated from *Candida parapsilosis* and *Rhodococcus erythropolis*. Tetrahedron: Asymmetry. 1993 Jul;4(7):1683–92.
222. Müller U, Willnow P, Ruschig U, Hopner T. Formate dehydrogenase from *Pseudomonas oxalaticus*. Eur J Biochem. 1978 Feb;83(2):485–98.
223. Lavandera I, Oberdorfer G, Gross J, De Wildeman S, Kroutil W. Stereocomplementary asymmetric reduction of bulky-bulky ketones by biocatalytic hydrogen transfer. European J

Org Chem. 2008;(15):2539–43.

224. Goldberg K, Edegger K, Kroutil W, Liese A. Overcoming the thermodynamic limitation in asymmetric hydrogen transfer reactions catalyzed by whole cells. Biotechnol Bioeng. 2006 Sep 5;95(1):192–8.
225. Kara S, Spickermann D, Schrittwieser JH, Leggewie C, van Berkel WJH, Arends IWCE, Hollmann F. More efficient redox biocatalysis by utilising 1,4-butanediol as a "smart cosubstrate." Green Chem. 2013;15(Scheme 1):330–5.
226. Knaus T, Mutti FG. Biocatalytic hydrogen-borrowing cascades. Chim Oggi. 2018;35(5).
227. Schrittwieser JH, Velikogne S, Hall M, Kroutil W. Artificial biocatalytic linear cascades for preparation of organic molecules. Chem Rev. 2018 Jan 10;118(1):270–348.
228. Bisogno FR, Lavandera I, Kroutil W, Gotor V. Tandem concurrent processes: One-pot single-catalyst biohydrogen transfer for the simultaneous preparation of enantiopure secondary alcohols. J Org Chem. 2009 Feb 20;74(4):1730–2.
229. Kulig J. Stereoselective synthesis of vicinal diols with enzymatic cascade reactions. Thesis. Universität Düsseldorf; 2013.
230. Kulig J, Simon RC, Rose C a., Husain SM, Häckh M, Lüdeke S, Zeitler K, Kroutil W, Pohl M, Rother D. Stereoselective synthesis of bulky 1,2-diols with alcohol dehydrogenases. Catal Sci Technol. 2012;2:1580.
231. Choudary BM, Chowdari NS, Madhi S, Kantam ML. A trifunctional catalyst for one-pot synthesis of chiral diols via heck coupling-N-oxidation-asymmetric dihydroxylation: Application for the synthesis of diltiazem and taxol side chain. J Org Chem. 2003;68(5):1736–46.
232. Kulig J, Frese A, Kroutil W, Pohl M, Rother D. Biochemical characterization of an alcohol dehydrogenase from *Ralstonia sp.* Biotechnol Bioeng. 2013;110(7):1838–48.
233. Muschiol J, Peters C, Oberleitner N, Mihovilovic MD, Bornscheuer UT, Rudroff F. Cascade catalysis - Strategies and challenges en route to preparative synthetic biology. Chem Commun (Camb). 2015 Apr 7;51(27):5798–811.
234. Niefind K, Müller J, Riebel B, Hummel W, Schomburg D. The crystal structure of *R*-specific alcohol dehydrogenase from *Lactobacillus brevis* suggests the structural basis of its metal dependency. J Mol Biol. 2003 Mar 21;327(2):317–28.
235. Niefind K, Riebel B, Müller J, Hummel W, Schomburg D. Crystallization and preliminary characterization of crystals of *R*-alcohol dehydrogenase from *Lactobacillus brevis*. Acta Crystallogr D Biol Crystallogr. 2000 Dec;56(Pt 12):1696–8.
236. Liang P, Qin B, Mu M, Zhang X, Jia X, You S. Prelog and anti-Prelog stereoselectivity of two ketoreductases from *Candida glabrata*. Biotechnol Lett. 2013 Sep 21;35(9):1469–73.
237. Leuchs S, Greiner L. Alcohol dehydrogenase from *Lactobacillus brevis*: A versatile robust catalyst for enantioselective transformations. Chem Biochem Eng Q. 2011;25(2):267–81.

238. Rodríguez C, Borzęcka W, Sattler JH, Kroutil W, Lavandera I, Gotor V. Steric vs. electronic effects in the *Lactobacillus brevis* ADH-catalyzed bioreduction of ketones. Org Biomol Chem. 2014;12(4):673–81.

239. Kulishova L. Analysis of factors influencing enzyme activity and stability in the solid state. 2010.

240. Sanders HJ, Keag HF, McCullough HS. Acetophenone. Ind Eng Chem. 1953 Jan;45(1):2–14.

241. El-Desoky E-SI, Abozeid MA, Abdel-Rahman A-RH. Quinacetophenone: A simple precursor to privileged organic motifs. Arab J Chem. 2015 Oct;

242. Kihumbu D, Stillger T, Hummel W, Liese A. Enzymatic synthesis of all stereoisomers of 1-phenylpropane-1,2-diol. Tetrahedron Asymmetry. 2002;13(10):1069–72.

243. Schubert T, Hummel W, Kula M-R, Müller M. Enantioselective synthesis of both enantiomers of various propargylic alcohols by use of two oxidoreductases. European J Org Chem. 2001 Nov;2001(22):4181.

244. Peschke T, Skoupi M, Burgahn T, Gallus S, Ahmed I, Rabe KS, Niemeyer CM. Self-immobilizing fusion enzymes for compartmentalized biocatalysis. ACS Catal. 2017 Nov 3;7(11):7866–72.

245. Erdmann V, Mackfeld U, Rother D, Jakoblinnert A. Enantioselective, continuous (*R*)- and (*S*)-2-butanol synthesis: Achieving high space-time yields with recombinant *E. coli* cells in a micro-aqueous, solvent-free reaction system. J Biotechnol. 2014 Dec 10;191:106–12.

246. Wolberg M, Hummel W, Wandrey C, Müller M. Highly regio- and enantioselective eeduction of 3,5-dioxocarboxylates. Angew Chemie - Int Ed. 2000;39(23):4306–8.

247. Hildebrand F, Lütz S. Immobilisation of alcohol dehydrogenase from *Lactobacillus brevis* and its application in a plug-flow reactor. Tetrahedron: Asymmetry. 2006 Dec;17(23):3219–25.

248. Schroer K, Lütz S. A continuously operated bimembrane reactor process for the biocatalytic production of (2*R* ,5*R*)-hexanediol. Org Process Res Dev. 2009 Nov 20;13(6):1202–5.

249. Ferloni C, Heinemann M, Hummel W, Daussmann T, Büchs J. Optimization of enzymatic gas-phase reactions by increasing the long-term stability of the catalyst. Biotechnol Prog. 2004 Jun 4;20(3):975–8.

250. Jeromin GE. Superabsorbed alcohol dehydrogenase—a new catalyst for asymmetric reductions. Biotechnol Lett. 2009 Nov 30;31(11):1717–21.

251. Döbber J, Pohl M, Ley S V., Musio B. Rapid, selective and stable HaloTag-*Lb*ADH immobilization directly from crude cell extract for the continuous biocatalytic production of chiral alcohols and epoxides. React Chem Eng. 2018;3(1):8–12.

252. Kikuchi Y, Kojima H, Tanaka T, Takatsuka Y, Kamio Y. Characterization of a second lysine decarboxylase isolated from *Escherichia coli*. J Bacteriol. 1997;179(14):4486–92.

253. Yamamoto Y, Miwa Y, Miyoshi K, Furuyama J, Ohmori H. The *Escherichia coli ldcC* gene encodes another lysine decarboxylase, probably a constitutive enzyme. Genes Genet Syst.

1997;72(3):167–72.

254. Gale EF, Epps HM. The effect of the pH of the medium during growth on the enzymic activities of bacteria (*Escherichia coli* and *Micrococcus lysodeikticus*) and the biological significance of the changes produced. Biochem J. 1942 Sep;36(7–9):600–18.
255. Gale EF, Epps HMR. Studies on bacterial amino-acid decarboxylases: 1. L(+)-lysine decarboxylase. Biochem J. 1944;38(1):232–42.
256. Castanie-Cornet MP, Penfound TA, Smith D, Elliott JF, Foster JW. Control of acid resistance in *Escherichia coli*. J Bacteriol. 1999 Jun;181(11):3525–35.
257. Iyer R, Williams C, Miller C. Arginine-agmatine antiporter in extreme acid resistance in *Escherichia coli*. J Bacteriol. 2003 Nov;185(22):6556–61.
258. Kashiwagi K, Suzuki T, Suzuki F, Furuchi T, Kobayashi H, Igarashi K. Coexistence of the genes for putrescine transport protein and ornithine decarboxylase at 16 min on *Escherichia coli* chromosome. J Biol Chem. 1991 Nov 5;266(31):20922–7.
259. Meng SY, Bennett GN. Nucleotide sequence of the *Escherichia coli cad* operon: A system for neutralization of low extracellular pH. J Bacteriol. 1992 Apr;174(8):2659–69.
260. Soksawatmaekhin W, Kuraishi A, Sakata K, Kashiwagi K, Igarashi K. Excretion and uptake of cadaverine by CadB and its physiological functions in *Escherichia coli*. Mol Microbiol. 2004 Mar 13;51(5):1401–12.
261. Moreau PL. The lysine decarboxylase CadA protects *Escherichia coli* starved of phosphate against fermentation acids. J Bacteriol. 2007;189(6):2249–61.
262. Tabor CW, Tabor H. Polyamines. Annu Rev Biochem. 1984;(53):749–90.
263. Kanjee U. Structural and functional studies on the *Escherichia coli* inducible lysine decarboxylase: Linking the acid stress and stringent responses. University of Toronto; 2012.
264. Kanjee U, Gutsche I, Alexopoulos E, Zhao B, El Bakkouri M, Thibault G, Liu K, Ramachandran S, Snider J, Pai EF, Houry W a. Linkage between the bacterial acid stress and stringent responses: The structure of the inducible lysine decarboxylase. EMBO J. 2011;30(5):931–44.
265. Kandiah E, Carriel D, Perard J, Malet H, Bacia M, Liu K, Chan SWS, Houry WA, Ollagnier de Choudens S, Elsen S, Gutsche I. Structural insights into the *Escherichia coli* lysine decarboxylases and molecular determinants of interaction with the AAA+ ATPase RavA. Sci Rep. 2016 Jul 15;6(1):24601.
266. Alexopoulos E, Kanjee U, Snider J, Houry W a., Pai EF. Crystallization and preliminary X-ray analysis of the inducible lysine decarboxylase from *Escherichia coli*. Acta Crystallogr Sect F Struct Biol Cryst Commun. 2008;64(8):700–6.
267. Snider J, Gutsche I, Lin M, Baby S, Cox B, Butland G, Greenblatt J, Emili A, Houry WA. Formation of a distinctive complex between the inducible bacterial lysine decarboxylase and a novel AAA+ ATPase. J Biol Chem. 2006;281(3):1532–46.

268. Christen P, Mehta PK. From cofactor to enzymes. The molecular evolution of pyridoxal-5'-phosphate-dependent enzymes. Chem Rec. 2001;1(6):436–47.

269. Eliot AC, Kirsch JF. Pyridoxal phosphate enzymes: Mechanistic, structural, and evolutionary considerations. Annu Rev Biochem. 2004;73:383–415.

270. Jordan F, Patel H. Catalysis in enzymatic decarboxylations: Comparison of selected cofactor-dependent and cofactor-independent examples. ACS Catal. 2013 Jul 5;3(7):1601–17.

271. Litsanov B, Brocker M, Bott M. Toward homosuccinate fermentation: Metabolic engineering of *Corynebacterium glutamicum* for anaerobic production of succinate from glucose and formate. Appl Environ Microbiol. 2012;78(9):3325–37.

272. Okino S, Noburyu R, Suda M, Jojima T, Inui M, Yukawa H. An efficient succinic acid production process in a metabolically engineered *Corynebacterium glutamicum* strain. Appl Microbiol Biotechnol. 2008;81(3):459–64.

273. Ogunniyi DS. Castor oil: A vital industrial raw material. Bioresour Technol. 2006;97(9):1086–91.

274. Thielen M. Bio-polyamides for automotive applications. Bioplastics Mag. 2010;5:10–1.

275. Schneider J, Wendisch VF. Biotechnological production of polyamines by bacteria: Recent achievements and future perspectives. Appl Microbiol Biotechnol. 2011 Jul 7;91(1):17–30.

276. Eggeling L, Bott M. A giant market and a powerful metabolism: L-lysine provided by *Corynebacterium glutamicum*. Appl Microbiol Biotechnol. 2015;99(8):3387–94.

277. Ma W, Chen K, Li Y, Hao N, Wang X, Ouyang P. Advances in cadaverine bacterial production and its applications. Engineering. 2017;3(3):308–17.

278. Kind S, Wittmann C. Bio-based production of the platform chemical 1,5-diaminopentane. Appl Microbiol Biotechnol. 2011 Sep;91(5):1287–96.

279. Kind S, Neubauer S, Becker J, Yamamoto M, Völkert M, Abendroth G von, Zelder O, Wittmann C. From zero to hero - Production of bio-based nylon from renewable resources using engineered *Corynebacterium glutamicum*. Metab Eng. 2014 Sep;25:113–23.

280. Becker J, Zelder O, Häfner S, Schröder H, Wittmann C. From zero to hero—Design-based systems metabolic engineering of *Corynebacterium glutamicum* for L-lysine production. Metab Eng. 2011 Mar;13(2):159–68.

281. Mimitsuka T, Sawai H, Hatsu M, Yamada K. Metabolic engineering of *Corynebacterium glutamicum* for cadaverine fermentation. Biosci Biotechnol Biochem. 2007;71(9):2130–5.

282. Kind S, Jeong WK, Schröder H, Wittmann C. Systems-wide metabolic pathway engineering in *Corynebacterium glutamicum* for bio-based production of diaminopentane. Metab Eng. 2010;12(4):341–51.

283. Qian ZG, Xia XX, Lee SY. Metabolic engineering of *Escherichia coli* for the production of cadaverine: A five carbon diamine. Biotechnol Bioeng. 2011;108(1):93–103.

284. Ma W, Cao W, Zhang H, Chen K, Li Y, Ouyang P. Enhanced cadaverine production from L-

lysine using recombinant *Escherichia coli* co-overexpressing CadA and CadB. Biotechnol Lett. 2015;37(4):799–806.

285. Kind S, Kreye S, Wittmann C. Metabolic engineering of cellular transport for overproduction of the platform chemical 1,5-diaminopentane in *Corynebacterium glutamicum*. Metab Eng. 2011 Sep;13(5):617–27.
286. Li M, Li D, Huang Y, Liu M, Wang H, Tang Q, Lu F. Improving the secretion of cadaverine in *Corynebacterium glutamicum* by cadaverine-lysine antiporter. J Ind Microbiol Biotechnol. 2014 Apr 8;41(4):701–9.
287. Kind S, Jeong WK, Schröder H, Zelder O, Wittmann C. Identification and elimination of the competing *N*-acetyldiaminopentane pathway for improved production of diaminopentane by *Corynebacterium glutamicum*. Appl Environ Microbiol. 2010 Aug 1;76(15):5175–80.
288. Vrljic M, Sahm H, Eggeling L. A new type of transporter with a new type of cellular function: L-lysine export from *Corynebacterium glutamicum*. Mol Microbiol. 1996 Dec;22(5):815–26.
289. Kim HJ, Kim YH, Shin JH, Bhatia SK, Sathiyanarayanan G, Seo HM, Choi KY, Yang YH, Park K. Optimization of direct lysine decarboxylase biotransformation for cadaverine production with whole-cell biocatalysts at high lysine concentration. J Microbiol Biotechnol. 2015;25(7):1108–13.
290. Oh YH, Kang KH, Kwon MJ, Choi JW, Joo JC, Lee SH, Yang YH, Song BK, Kim IK, Yoon KH, Park K, Park SJ. Development of engineered *Escherichia coli* whole-cell biocatalysts for high-level conversion of L-lysine into cadaverine. J Ind Microbiol Biotechnol. 2015;42(11):1481–91.
291. Li N, Chou H, Yu L, Xu Y. Cadaverine production by heterologous expression of *Klebsiella oxytoca* lysine decarboxylase. Biotechnol Bioprocess Eng. 2014 Nov 16;19(6):965–72.
292. Kim J-H, Kim HJ, Kim YH, Jeon J-M, Song HS, Kim J, No S, Shin J, Choi K, Park KM, Yang Y. Functional study of lysine decarboxylases from *Klebsiella pneumoniae* in *Escherichia coli* and application of whole cell bioconversion for cadaverine production. J Microbiol Biotechnol. 2016;26(9):1586–92.
293. Kim J-H, Seo H-M, Sathiyanarayanan G, Bhatia SK, Song H-S, Kim J, Jeon J-M, Yoon J-J, Kim Y-G, Park K, Yang Y-H. Development of a continuous L-lysine bioconversion system for cadaverine production. J Ind Eng Chem. 2016;46(February):44–8.
294. Bhatia SK, Kim YH, Kim HJ, Seo HM, Kim JH, Song HS, Sathiyanarayanan G, Park SH, Park K, Yang YH. Biotransformation of lysine into cadaverine using barium alginate-immobilized *Escherichia coli* overexpressing CadA. Bioprocess Biosyst Eng. 2015;38(12):2315–22.
295. Seo H-M, Kim J-H, Jeon J-M, Song H-S, Bhatia SK, Sathiyanarayanan G, Park K, Kim KJ, Lee SH, Kim HJ, Yang Y-H. *In situ* immobilization of lysine decarboxylase on a biopolymer by fusion with phasin: Immobilization of CadA on intracellular PHA. Process Biochem. 2016 Oct;51(10):1413–9.

296. Jäger VD, Kloss R, Grünberger A, Seide S, Hahn D, Karmainski T, Piqueray M, Embruch J, Longerich S, Mackfeld U, Jaeger K-E, Wiechert W, Pohl M, Krauss U. Tailoring the properties of (catalytically)-active inclusion bodies. Microb Cell Fact. 2019;18(33):1–20.

297. Klose J, Wendt N, Kubald S, Krause E, Fechner K, Beyermann M, Bienert M, Rudolph R, Rothemund S. Hexa-histidin tag position influences disulfide structure but not binding behavior of in vitro folded N-terminal domain of rat corticotropin-releasing factor receptor type 2a. Protein Sci. 2004;13:2470–5.

298. Zhao D, Huang Z. Effect of His-tag on expression, purification, and structure of zinc finger protein, ZNF191(243-368). Bioinorg Chem Appl. 2016;2016:8206854.

299. Wachter RM, Elsliger M-A, Kallio K, Hanson GT, Remington SJ. Structural basis of spectral shifts in the yellow-emission variants of green fluorescent protein. Structure. 1998 Oct 15;6(10):1267–77.

300. Zacharias DA, Violin JD, Newton AC, Tsien RY. Partitioning of lipid-modified monomeric CFPs into membrane microdomains of live cells. Science. 2002;296(May):913–6.

301. Rokney A, Shagan M, Kessel M, Smith Y, Rosenshine I, Oppenheim AB. *E. coli* transports aggregated proteins to the poles by a specific and energy-dependent process. J Mol Biol. 2009;392(3):589–601.

302. Karmainski T. Charakterisierung katalytisch aktiver inclusion bodies am Beispiel der Benzaldehydlyase aus *Pseudomonas fluorescens*. 2017.

303. Bradford MM. A rapid and sensitive method for the quantitation of microgram quantities of protein utilizing the principle of protein-dye binding. Anal Biochem. 1976;(72):248–254.

304. Seide S. Characterization of catalytically active *Ralstonia* sp. alcohol dehydrogenase inclusion bodies. 2018.

305. Kulishova L, Dimoula K, Jordan M, Wirtz A, Hofmann D, Santiago-Schübel B, Fitter J, Pohl M, Spiess AC. Factors influencing the operational stability of NADPH-dependent alcohol dehydrogenase and an NADH-dependent variant thereof in gas/solid reactors. J Mol Catal B Enzym. 2010 Dec;67(3–4):271–83.

306. Kloss R, Karmainski T, Jäger VD, Hahn D, Grünberger A, Baumgart M, Krauss U, Jaeger K, Wiechert W, Pohl M. Tailor-made catalytically active inclusion bodies for different applications in biocatalysis. Catal Sci Technol. 2018;8(22):5816–26.

307. Allen SP, Polazzi J, Gierse JK, Easton AM. Two bovel heat shock genes encoding proteins produced in response to heterologous protein expression in *Eschenichia coli*. J Bacteriol. 1992;174(21):6938–47.

308. Carrio MM, Villaverde A. Construction and deconstruction of bacterial inclusion bodies. J Biotechnol. 2002;96:3–12.

309. Hoffmann F, Rinas U. Kinetics of heat-shock response and inclusion body formation during temperature-induced production of basic fibroblast growth factor in high-cell-density cultures

of recombinant *Escherichia coli*. Biotechnol Prog. 2000;16:1000–7.

310. Georgiou G, Valax P. Isolating inclusion bodies from bacteria. Methods Enzymol. 1999;309:48–58.
311. Ventura S, Villaverde A. Protein quality in bacterial inclusion bodies. Trends Biotechnol. 2006;24(4):179–85.
312. Krithika G, Arunachalam J, Priyanka H, Indulekha K. The two forms of lysine decarboxylase; Kinetics and effect of expression in relation to acid tolerance response in *E. coli*. J Exp Sci. 2010;1(12):10–21.
313. Kloss R, Limberg MH, Mackfeld U, Hahn D, Grünberger A, Jäger VD, Krauss U, Oldiges M, Pohl M. Catalytically active inclusion bodies of L-lysine decarboxylase from *E. coli* for 1,5-diaminopentane production. Sci Rep. 2018 Dec 11;8(1):5856.
314. Ivanova MI, Sawaya MR, Gingery M, Attinger A, Eisenberg D. An amyloid-forming segment of *β*2-microglobulin suggests a molecular model for the fibril. Proc Natl Acad Sci U S A. 2004 Jul 20;101(29):10584–9.
315. Chiti F, Stefani M, Taddei N, Ramponi G, Dobson CM. Rationalization of the effects of mutations on peptide and protein aggregation rates. Nature. 2003;424(6950):805–8.
316. Ventura S, Zurdo J, Narayanan S, Parreño M, Mangues R, Reif B, Chiti F, Giannoni E, Dobson CM, Aviles FX, Serrano L. Short amino acid stretches can mediate amyloid formation in globular proteins: The Src homology 3 (SH3) case. Proc Natl Acad Sci U S A. 2004 May 11;101(19):7258–63.
317. Kuhlman B, Baker D. Native protein sequences are close to optimal for their structures. Proc Natl Acad Sci. 2000;97(19):10383–8.
318. Rohl CA, Strauss CEM, Misura KMS, Baker D. Protein structure prediction using Rosetta. Methods Enzymol. 2004;383(2003):66–93.
319. Jacak R, Leaver-Fay A, Kuhlman B. Computational protein design with explicit consideration of surface hydrophobic patches. Proteins Struct Funct Bioinforma. 2012 Mar;80(3):825–38.
320. Ramón A, Señorale-Pose M, Marín M. Inclusion bodies: Not that bad... Front Microbiol. 2014;5(FEB):2010–5.
321. Liu L, Yang H, Shin H, Chen RR, Li J, Du G, Chen J. How to achieve high-level expression of microbial enzymes: Strategies and perspectives. Bioengineered. 2013 Jul 27;4(4):212–23.
322. de Groot NS, Ventura S. Protein activity in bacterial inclusion bodies correlates with predicted aggregation rates. J Biotechnol. 2006 Aug 20;125(1):110–3.
323. Gasteiger E, Hoogland C, Gattiker A, Duvaud S, Wilkins MR, Appel RD, Bairoch A. Protein identification and analysis tools on the ExPASy server. In: Walker JM, editor. The Proteomics Protocols Handbook. Totowa, NJ: Humana Press; 2005. p. 571–607.
324. Ogino H, Ishikawa H. Enzymes which are stable in the presence of organic solvents. J Biosci Bioeng. 2001 Jan;91(2):109–16.

325. Ghatorae AS, Bell G, Halling PJ. Inactivation of enzymes by organic solvents: New technique with well-defined interfacial area. Biotechnol Bioeng. 1994 Feb 20;43(4):331–6.

326. Pleiss J. Thermodynamic activity-based interpretation of enzyme kinetics. Trends Biotechnol. 2017 May;35(5):379–82.

327. Keilhauer C, Eggeling L, Sahm H. Isoleucine synthesis in *Corynebacterium glutamicum*: Molecular analysis of the *ilvB-ilvN-ilvC* operon. J Bacteriol. 1993 Sep;175(17):5595–603.

328. Faivre D, Schuler D. Magnetotactic bacteria and magnetosomes. Chem Rev. 2008;108(September):4875–98.

329. Matsunaga T, Kamiya S. Use of magnetic particles isolated from magnetotactic bacteria for enzyme immobilization. Appl Microbiol Biotechnol. 1987;(2):328–32.

330. Rehm FBH, Chen S, Rehm BHA. Bioengineering toward direct production of immobilized enzymes: A paradigm shift in biocatalyst design. Bioengineered. 2018 Jan 19;9(1):6–11.

331. Yan L, Da H, Zhang S, López VM, Wang W. Bacterial magnetosome and its potential application. Microbiol Res. 2017 Oct;203(March):19–28.

332. Rahmen N, Fulton A, Ihling N, Magni M, Jaeger K-E, Büchs J. Exchange of single amino acids at different positions of a recombinant protein affects metabolic burden in *Escherichia coli*. Microb Cell Fact. 2015 Jan 23;14(1):10.

333. Kunze M, Lattermann C, Diederichs S, Kroutil W, Büchs J. Minireactor-based high-throughput temperature profiling for the optimization of microbial and enzymatic processes. J Biol Eng. 2014;8(1):22.

334. Lamm R, Berg C, Jäger VD, Wandrey G, Krauss U, Jaeger K-E, Büchs J. Optimization of fluorescent inclusion body production using a high-throughput temperature profiling system. Unpubl results.

6 Appendix

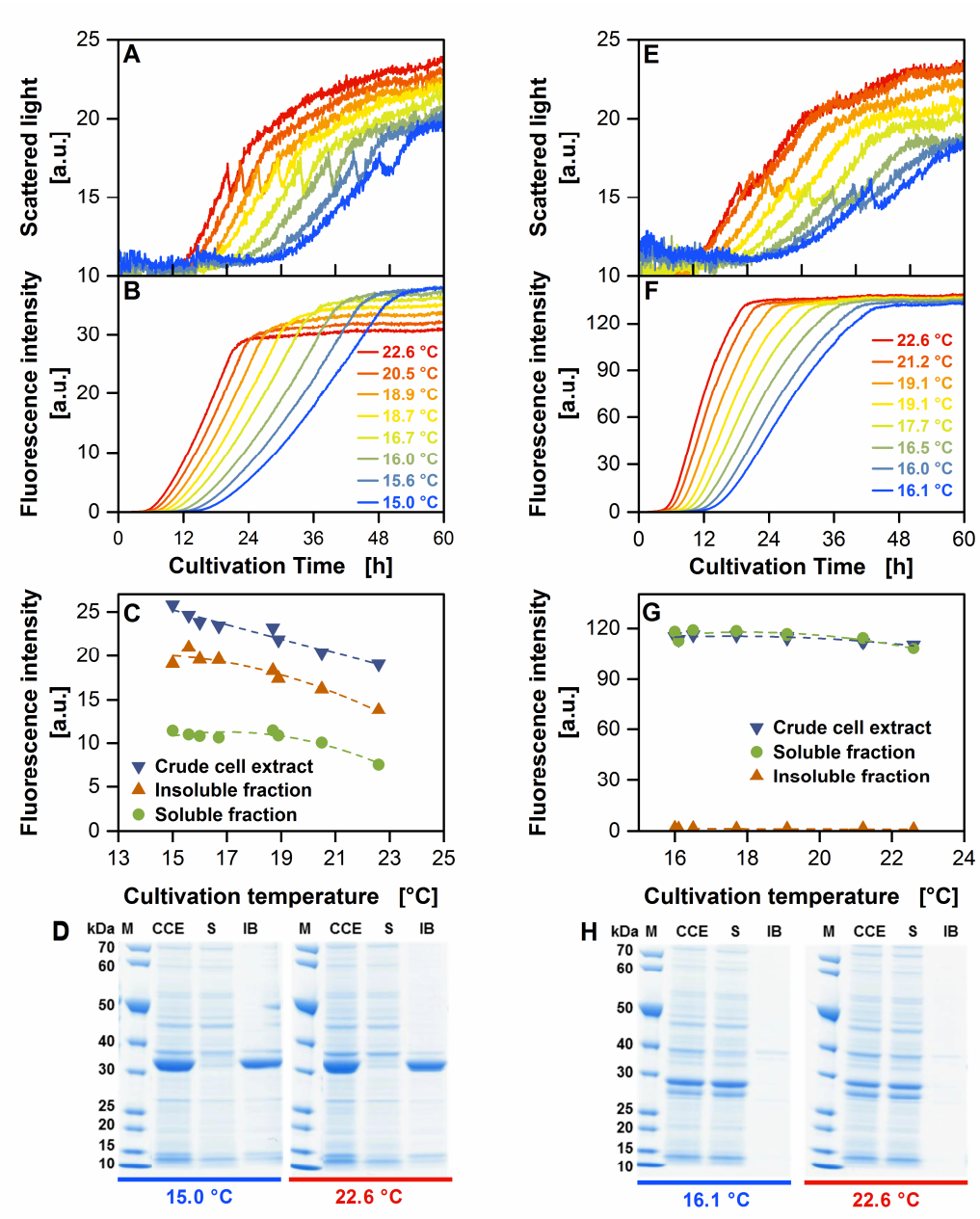

Figure 6-1 Cultivation of *E. coli* BL21(DE3) producing functional inclusion bodies (FIB) of TDoT-XaL-YFP (A-D) and the respective soluble protein XaL-YFP (E-H) by applying a constant temperature profile. Cultivation was performed in minimal Wilms MOPS autoinduction medium (0.5 g/l glucose, 2 g/l lactose, 5 g/l glycerol). Scattered light (A+E) refers to the formation of biomass and YFP fluorescence intensity (B+F) to the production and maturation of YFP fluorescence measured online in a BioLector device. (C+G) Final fluorescence intensity of crude cell extract, soluble and insoluble fraction versus the cultivation temperatures of samples taken from the cultivation. (D+H) SDS-PAGE analysis shows the protein content per sample volume at 15°C (blue) and 22.6°C (red) temperature for the crude cell extract (CCE), the soluble fraction (S) and the insoluble fraction (I) (M=protein marker). Cultivation parameters: Scattered light: λ_{ex}=650 nm λ_{em}=650 nm. Fluorescence intensity: λ_{ex}=514 nm, λ_{em}=527 nm. 48 deep-well Flowerplate with 800 µL filling volume, shaking frequency n=1000 rpm, shaking diameter d_0=3 mm. Medium consists of components summarized in the publication of Rahmen [332]. The respective temperatures were adjusted by a temperature block described elsewhere [333]. Results were taken from [334]. This cultivation profile shows clearly that a lower temperature of 15-17°C is necessary to obtain higher fluorescence intensity for the CatIBs, but is not necessary to produce the soluble enzyme.

Table 6-1 Characteristics of all CatIB constructs regarding the relative activity of the insoluble pellet-fraction compared to the crude cell extract, the initial rate activity (k_{cat}) of the lyophilized protein, residual activity compared to the soluble enzyme, the relative protein and lipid content based on the initial weight of the lyophilizate and the yield of CatIBs obtained from 100 g cells. SD refers to the standard deviation of the mean. N refers to the biological replicates. n.d. not determined. The values were taken from chapter 2.1.

		TDoT-*R*ADH	TDoT-*Pf*BAL	*Ec*LDC-TDoT	*Ec*LDC-3HAMP	3HAMP-*R*ADH	3HAMP-*Pf*BAL	3HAMP-*Lb*ADH	3HAMP-*Pp*BFD L476Q	TDoT- *Lb*ADH	TDoT-*Pp*BFD-L476Q
rel. activity insoluble fraction (%) Pellet-2	Mean	87.5	87.7	n.d.	n.d.	75.4	75.8	67	61.3	5.4	1.2
	SD	3.2	6.8	n.d.	n.d.	3.7	8	21.7	35.4	5.9	0.6
	N	4	4			4	5	3	3	3	3
yield g lyophilisate / 100 g cells (%)	Mean	9.6	8.7	12.4	7.5	3.7	4.8	8.1	6.6	2.5	1.6
	SD	1.5	1.0	3	6.5	0.5	3.5	1.3	1.4	0.4	0.7
	N	5	8	3	4	5	5	3	3	3	3
yield g protein/ 100 g cells (%)	Mean	9.04	6.6	8.4	5.9	1.6	1.8	4.5	2.1	1.1	0.5
	SD	2.16	1.2	1.8	5	0.9	1.7	1.1	0.6	0.7	0.5
	N	5	6	3	3	4	5	3	3	3	3
rel. protein content lyophilisate (%)	Mean	84.6	76.3	67.9	56.5	50.9	31.3	54.6	35.5	43.4	26.9
	SD	3.9	7.4	5.9	6.5	7.6	13.2	8	6.7	5.5	4.1
	N	5	6	3	2	4	5	3	4	3	4
lipid content (%)	Mean	14.3	16.4	12.9	17.7	30.6	30.1	34.7	27.9	25.2	19.1
	SD	0.3	1	3.2	0.6	8.3	4.7	1.36	3.7	0.73	0.8
	N	1	1	1	1	1	1	1	1	1	1
activity kcat (s^{-1})	Mean	0.054	0.77	0.71	0.80	0.33	13.9	0.332	23.4	3.63	9.2
	SD	0.008	0.12	0.07		0.02	2.9	0.019	6.1	0.9	4.7
	N	3	4	1	1	3	3	3	4	3	4
relative activity (%)	Mean	2	1	n.d.	n.d.	12	18.1	12	10.3	5.8	4.1
CatIB type		compact	compact	compact	compact	diffuse	diffuse	diffuse	diffuse	diffuse	diffuse

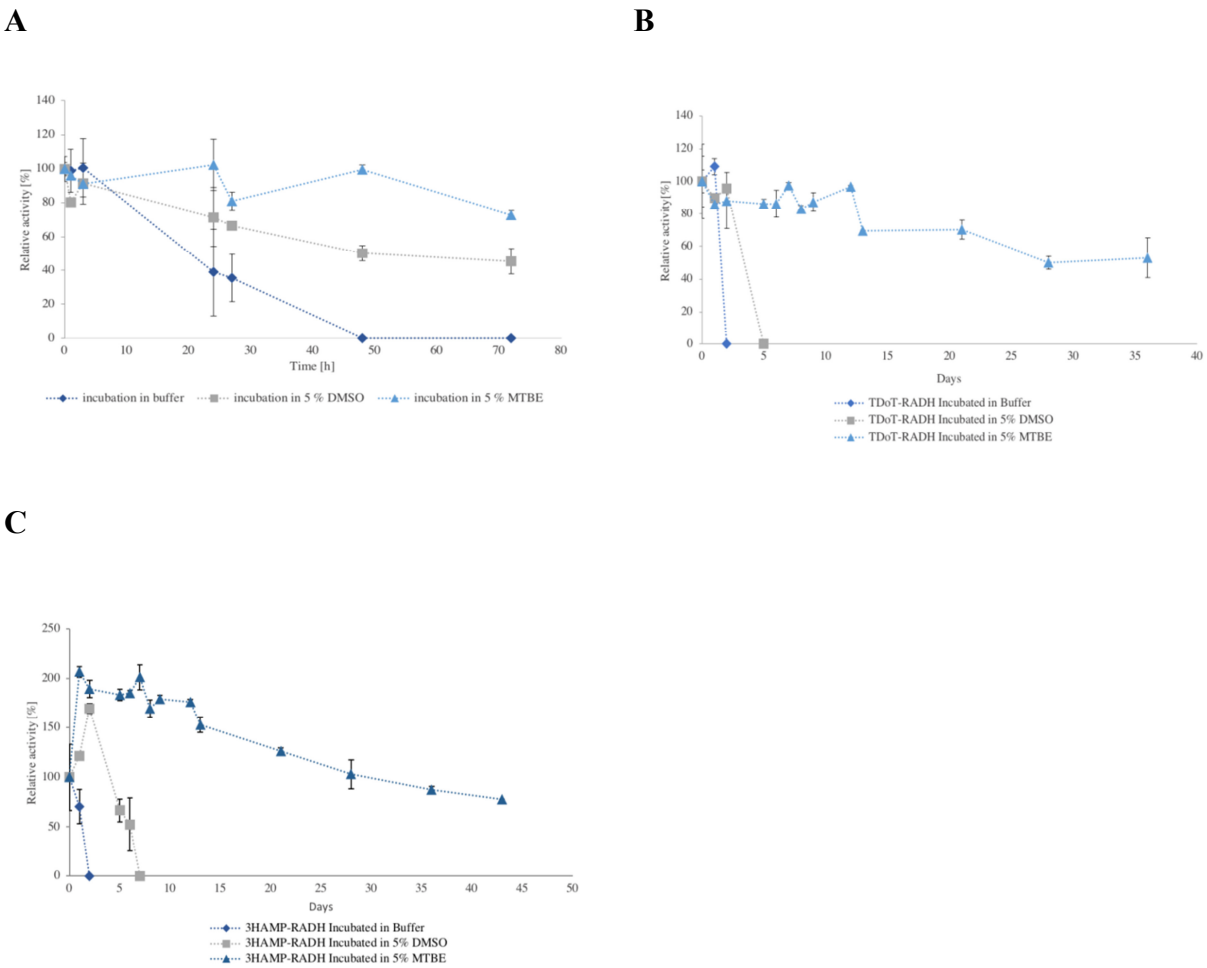

Figure 6-2 Long-term stability of soluble (A) *R*ADH, (B) TDoT-*R*ADH and (C) 3HAMP-*R*ADH (enzyme concentration 0.305 mg ml^{-1}) after incubation in 50 mM TEA-buffer (0.8 mM $CaCl_2$, pH 7.5) in the presence and absence of 5 vol% organic solvent in glass vials (total volume 2 ml) over several days at 30°C and 1000 rpm. After incubation the initial rate activity was measured via discontinuous activity assay at 30 °C, under constant shaking (1000 rpm) and in 1 ml total volume consisting of 50 mM TEA-buffer (0.8 mM $CaCl_2$, pH 7.5) 2.5 vol% organic solvent (MTBE, DMSO), 10 mM (*R*)-2-HPP, 3 mM NADPH. Enzyme concertation in the activity assay: soluble RADH: 0.305 µg ml^{-1}, TDoT-RADH: 240 µg ml^{-1}, 3HAMP-RADH: 9 µg ml^{-1}. Half-lives were deduced from the point in time where 50% of initial rate activity was reached. n = 2. Results were taken from the Master thesis of Selina Seide [304]

Danksagung

Zu Beginn meiner Danksagung möchte ich Frau Prof. Martina Pohl einen besonderen Dank für die Ermöglichung und Betreuung eines so spannenden und innovativen Promotionsthemas und für die immerwährende Unterstützung während der gesamten Zeit aussprechen. Die zahlreichen konstruktiven Diskussionen und Anregungen waren sehr hilfreich und inspirierend. Des Weiteren gilt mein Dank Herrn Prof. Wolfgang Wiechert für die Ermöglichung der Promotionsarbeit in seinem Institut. Zudem danke ich Herrn Prof. K.-E. Jäger für die Bereitschaft die Zweitbetreuung und die Funktion als Gutachter zu übernehmen.

In diesem Zusammenhang möchte ich allen Mitarbeiter des IBG-1 danken, insbesondere der Arbeitsgruppe Biokatalyse und Biosensoren für die sehr gute, freundliche und kooperative Arbeitsatmosphäre. Hier sind vor allem die Arbeitsgruppenleiterinnen Martina Pohl und Dörte Rother zu nennen, ebenso wie jedes einzelne Gruppenmitglied, die durch ihre offene Art sehr zur der angenehmen Arbeitsatmosphäre beigetragen haben.

Besonders zu erwähnen ist das Büro 125, wo ich von Saskia Bock und Alana Dreßen vor allem zu Beginn bei zahlreichen Fragen sehr gut unterstützt wurde und die mir mit hilfreichen und konstruktiven Vorschlägen zur Seite gestanden haben. Des Weiteren möchte ich mich bei Anna Baierl für viele hilfreiche Ratschläge u.a. im Bereich der Molekularbiologie bedanken und bei Victoria Steffen für die Einführung in die Fluoreszenzspektroskopie. Außerdem danke ich Zaira Maugeri und Torsten Sehl für ihre Hilfe bei der Auswertung von NMR Spektren. Neben den bereits oben genannten Personen gilt mein Dank ebenfalls Johannes Döbber, Jochen Wachtmeister, Julia Otten, Kevin Mack und Reinhard Oeggl für viele kritische Anregungen. Für die sehr gute Einarbeitung in das Thema CatIBs danke ich Martin Diener.

Mein Dank gilt ebenfalls meinen Kooperationspartnern des BioSc Projektes „CatIBs“ für die intensiven und konstruktiven Diskussionen und Ratschläge, die das Projekt sehr bereichert haben. Hier gilt mein Dank insbesondere Vera D. Jäger und Ulrich Krauss für die zahlreichen und hilfreichen Diskussionen und Anregungen, ebenso wie die Ratschläge im Bereich Molekularbiologie. Michael Limberg möchte ich ebenfalls für intensive Diskussionen und für die pragmatische Herangehensweise an das Kooperationsthema danken.

Den Bachelor- und Masterstudenten, Tobias Karmainski, Selina Seide und Jochen Embruch, die während dieser Zeit an dem Projekt mit viel Engagement mitgewirkt haben, gebührt ebenfalls mein großer Dank.

Mein Dank gilt zudem den gesamten Technikerinnen der Arbeitsgruppe Biokatalyse und Biosensoren, Frau Heike Offermann, Frau Ilona Frindi-Wosch, Frau Doris Hahn, Frau Ursula Mackfeld und Frau Lilia Arnold, ohne die eine so reibungslose Laborarbeit nicht denkbar gewesen wäre. Ihr Knowhow und die hohe Motivation hat sehr viel zu dem Gelingen dieser Promotionsarbeit beigetragen.

Für die Ermöglichung auch einen Einblick in fachfremde Themen zu erhalten, möchte ich mich sehr bedanken. Hier gilt mein Dank Frau Dr. Gina Musio für die lehrreiche Zeit bei der Einführung in die Plug-flow Reaktionstechnik und die chemische Synthese. Frau Dr. Iris von der Hocht vom ICS-5 möchte ich danken für die Einführung in die Technik der dynamischen Lichtstreuung (DLS) und die zahlreichen hilfreichen Diskussionen.

Den Teilnehmern an diversen Fahrgemeinschaften zwischen Aachen und Jülich gebührt ebenso mein Dank. Die Unterhaltungen haben auf angenehme und unterstützende Weise meine Arbeit bereichert und geholfen weitere Sichtweisen zu erlangen. Zudem haben sie die Zeiten der Fahrten subjektiv verkürzt. Hier sind zu nennen Saskia Bock, Anna Baierl, Jennifer Aschenbrenner und Christoph Westerwalbesloh.

Für die Aufnahmen mikroskopischer Bilder möchte ich mich besonders bedanken bei Prof. Alexander Grünberger und Christoph Westerwalbesloh.

Dem Brauteam JuBräu danke ich für eine sehr schöne und lustige Zeit, bei der ich das Interesse am Bierbrauen entdeckt habe. Danke an euch, Simon Unthan, Joshi Koepff, Michael Limberg, Holger Morschett, Viola Pooth, Niklas Tenhaef, Kevin Mack, Reinhard Oeggl und Julia Otten.

Mein besonderer Dank gilt meinen Freunden und meiner Familie für ihre immerwährende Unterstützung. Insbesondere möchte ich meinem Partner Dirk Moritz dafür danken, dass er mich während des gesamten Studiums und der Promotion ständig motiviert und darin bestärkt hat, meine Ziele und Wünsche zu verfolgen.

Selbstständigkeitserklärung

Hiermit versichere ich, dass die vorgelegte Dissertation von mir selbstständig und ohne unzulässige, fremde Hilfe verfasst wurde unter ausschließlicher Verwendung der angegebenen Literatur und Hilfsmittel gemäß der „Grundsätze zur Sicherung guter wissenschaftlicher Praxis an der Heinrich- Heine-Universität Düsseldorf“ erstellt wurde. Wörtliche wie inhaltliche Zitate habe ich vollständig als solche kenntlich gemacht.

Bisher habe ich keine erfolglosen Promotionsversuche unternommen und diese Dissertation an keiner anderen Fakultät vorgelegt.

Ort, Datum	Ramona Kloß